THE UNIVERSITY OF TEXAS AT AUSTIN
CENTER FOR TRANSPORTATION RESEARCH

TECHNICAL REPORT 0-6988-R2
TxDOT PROJECT NUMBER 0-6988

Development of Pavement Performance Models for Pavement Management Incorporating Treatment Type

Hongbin Xu
Moo Yeon Kim
Christian Sabillon
Lu Gao
Jorge A. Prozzi

January 2021; Published May 2021

http://library.ctr.utexas.edu/ctr-publications/0-6988-R2.pdf

Technical Report Documentation Page

1. Report No. FHWA/TX-21/0-6988-2	2. Government Accession No.	3. Recipient's Catalog No.
4. Title and Subtitle Development of Pavement Performance Models for Pavement Management Incorporating Treatment Type		5. Report Date Submitted: January 2021; Published May 2021 6. Performing Organization Code
7. Author(s) Hongbin Xu, Moo Yeon Kim, Christian Sabillon, Lu Gao, and Jorge A. Prozzi		8. Performing Organization Report No. 0-6988-2
9. Performing Organization Name and Address Center for Transportation Research The University of Texas at Austin 3925 W. Braker Lane, 4th Floor Austin, TX 78759		10. Work Unit No. (TRAIS) 11. Contract or Grant No. 0-6988
12. Sponsoring Agency Name and Address Texas Department of Transportation Research and Technology Implementation Division P.O. Box 5080 Austin, TX 78763-5080		13. Type of Report and Period Covered Technical Report September 2018–January 2021 14. Sponsoring Agency Code

15. Supplementary Notes

Project performed in cooperation with the Texas Department of Transportation.

16. Abstract

TxDOT's Pavement Management Information System (PMIS) has been recently replaced by Pavement Analyst (PA), a system for archiving, managing, and mapping data; reporting performance prediction; conducting optimization analysis for decision-making, etc. Pavement performance models comprise a key component of PA; these models quantify pavement deterioration for the planned horizon and predict the effect of maintenance and rehabilitation actions on performance. The accurate prediction of pavement performance is important for efficient management of the transportation infrastructure. By reducing the prediction error of pavement deterioration, agencies can obtain significant savings through timely intervention and accurate planning. As part of this project, the authors reviewed the current performance models, calibrated them, and updated them in a manner compatible with their implementation into PA. Extensive data analysis was conducted by using traditional and advanced data analysis techniques. Specifically, the models developed addressed the following technical objectives: 1) existing models were calibrated, correcting for biases and inefficiencies; 2) models were updated to incorporate historical construction data; 3) models were updated to incorporate the effect of maintenance and rehabilitation activities; and 4) alternative models were proposed that are free of some of the limitations of the existing models but are simple and straightforward enough to incorporate into PA.

17. Key Words Pavement management system, preventive maintenance, rehabilitation, deterioration modeling	18. Distribution Statement No restrictions. This document is available to the public through the National Technical Information Service, Springfield, Virginia 22161; www.ntis.gov.

19. Security Classif. (of report)	20. Security Classif. (of this page)	21. No. of pages	22. Price
Unclassified	Unclassified	364	

Form DOT F 1700.7 (8-72) Reproduction of completed page authorized

THE UNIVERSITY OF TEXAS AT AUSTIN
CENTER FOR TRANSPORTATION RESEARCH

Development of Pavement Performance Models for Pavement Management Incorporating Treatment Type

Hongbin Xu
Moo Yeon Kim
Christian Sabillon
Lu Gao
Jorge A. Prozzi

CTR Technical Report:	0-6988-2
Report Date:	Submitted: January 2021; Published May 2021
Project:	0-6988
Project Title:	Quantification of the Performance of Preventive Maintenance and Rehabilitation Strategies
Sponsoring Agency:	Texas Department of Transportation
Performing Agency:	Center for Transportation Research at The University of Texas at Austin

Project performed in cooperation with the Texas Department of Transportation and the Federal Highway Administration.

Disclaimers

Author's Disclaimer: The contents of this report reflect the views of the authors, who are responsible for the facts and the accuracy of the data presented herein. The contents do not necessarily reflect the official view or policies of the Federal Highway Administration or the Texas Department of Transportation (TxDOT). This report does not constitute a standard, specification, or regulation.

Patent Disclaimer: There was no invention or discovery conceived or first actually reduced to practice in the course of or under this contract, including any art, method, process, machine manufacture, design or composition of matter, or any new useful improvement thereof, or any variety of plant, which is or may be patentable under the patent laws of the United States of America or any foreign country.

Engineering Disclaimer

NOT INTENDED FOR CONSTRUCTION, BIDDING, OR PERMIT PURPOSES.

Research Supervisor: Dr. Jorge A. Prozzi

Acknowledgments

The authors want to acknowledge the support of the Texas Department of Transportation for providing access to the data and for their constant technical advice. In particular, the authors wish to express their appreciation to Dr. Jenny Li, Dr. Feng Hong, John Bilyeu, Lacy Peters, and Enad Mahmoud for their participation in the progress meetings, reviewing the technical memoranda, and providing guidance, valuable comments, and feedback.

Table of Contents

List of Tables

List of Figures

List of Terms

AADT	annual average daily traffic
ACP	asphalt concrete pavement
CRCP	continuously reinforced concrete pavement
DFO	distance from origin
DN	do-nothing
ESAL	equivalent single axle load
FM	Farm-to-Market Road
HRhb	heavy rehabilitation
IH	Interstate Highway
IRI	International Roughness Index
JCP	jointed concrete pavement
LRhb	light rehabilitation
M&R	maintenance and rehabilitation
MRhb	medium rehabilitation
NOAA	National Oceanic and Atmospheric Administration
PA	Pavement Analyst
PFA	Project Finder Algorithm
PM	preventive maintenance
PMIS	Pavement Management Information System
SH	State Highway
TACP	thick asphalt concrete pavement
TxDOT	Texas Department of Transportation
US	United States Highway

Chapter 1. Background and Introduction

1.1. Background

Recently, the Texas Department of Transportation's (TxDOT) Pavement Management Information System (PMIS) was replaced by Pavement Analyst (PA), in a joint development between TxDOT and AgileAssets. PA is capable of implementing core pavement management functions such as archiving, managing, and mapping data; reporting performance prediction; conducting optimization analysis for decision-making, etc. Furthermore, a web-based system allows any users within the TxDOT network to access pavement management data and analytics based on over 30 years of experience. Pavement performance models comprise a key component of PA; these models quantify pavement deterioration for the planned horizon and predict the effect of maintenance and rehabilitation (M&R) actions on pavement performance (Hong et al., 2017). The accurate prediction of pavement performance is important for efficient management of the transportation infrastructure (Prozzi and Madanat, 2003; Hong and Prozzi, 2013). By reducing errors in predictive models of pavement deterioration, agencies can obtain significant savings through timely intervention and accurate planning (Madanat and Prozzi, 2002). Accordingly, the current performance models, which are mostly inherited from the original performance models (Stampley et al., 1995) developed two decades ago, were in need of improvement to meet the needs of TxDOT's new PA system. The research team reviewed the current performance models, calibrated them, and updated them in a manner compatible with their implementation into PA. Extensive data analysis was conducted using traditional and advanced data analysis techniques. Specifically, the models developed addressed the following technical objectives:

- The existing models were calibrated using sound techniques and correcting for biases and inefficiencies;
- The models were updated to incorporate historical construction data;
- The models were updated to incorporate the effect of preventive maintenance (PM); light rehabilitation (LRhb), medium rehabilitation (MRhb), or heavy rehabilitation (HRhb); and
- Alternative models were proposed that are free of some of the limitations of the existing models but are simple and straightforward enough to incorporate into PA.

1.2. Pavement Performance Modeling

Pavement performance models describe changes in pavement conditions over time and are essential tools for agencies to plan cost-effective M&R actions. Based on a model assumption, pavement performance models can be divided into two types: deterministic and stochastic. Deterministic approach assumed that pavement deterioration and improvements in pavement conditions are known with complete certainty (Prozzi and Madanat, 2004). Clearly, the assumption of determinism is not reasonable in practice since pavement behavior depends on factors that are not completely known, such as environmental conditions, traffic loading and the structural properties of the pavement. On the other hand, stochastic approaches typically use Markov Decision Processes (MDP) to take into account uncertainty of pavement performance deterioration with time. The output of most MDP-based models specifies only the fraction of pavement sections in a particular state to which a certain M&R action is to be applied.

Pavement performance models also can be categorized into two groups based on an approach: empirical models and mechanistic models. In empirical models, a dependent variable is any pavement performance indicator. One or more explanatory variables representing pavement structural strength, traffic loading, age, or environmental conditions are related to the dependent variable. Mechanistic models are based on the physical representation of the pavement deterioration process. Material behavior and pavement response models are used to estimate responses such as stains, stresses, and deflections in the pavement structure under the combined actions of traffic and the environment (Aguiar and Prozzi, 2014). These responses are used to predict performance in terms of cracking, rutting, ride quality, etc. Mechanistic-empirical models use pavement responses determined by the mechanistic approach and correlations between the response and pavement performance (Hong and Prozzi, 2010).

1.3. Original PMIS Models

The original performance models in PMIS were developed in the 1990s (Stampley et al., 1995). The models do not predict performance directly but the level of distress incurred or ride quality lost (variable L_i) as a function of pavement age (variable *Age*), climate region, traffic load, and subgrade conditions. The level of distress is obtained in the original models by normalizing the rating for each distress type. The performance model for all distresses is an s-shaped curve.

Elements that affect performance models depend on pavement types, M&R types, and distress types (Prozzi and Hong, 2010). Therefore, each combination of these factors will generate a different set of model coefficients. Because field data were not sufficient at the time, engineering judgment of experts played a significant role in determining the model specification form and its parameters, which lead to the inaccurate prediction of performance, biased parameters, and inefficient estimation; therefore, their standard error is larger than what it should be. The following section summarizes efforts to recalibrate PMIS models over the course of several studies.

1.4. Recalibrated PMIS Performance Models

The original PMIS performance models were in need of improvement to predict performance and overall network conditions and to generate M&R “needs estimate” more reasonably. As part of TxDOT Project 0-6386, the researchers reviewed the original performance prediction process and concluded that the process was conceptually sound, but the models needed improvement because they over-predict distresses (Gharaibeh et al., 2012). The 0-6386 project yielded revised performance models for asphalt concrete pavements (ACP), continuously reinforced concrete pavement (CRCP), and jointed concrete pavement (JCP), produced using historical data to predict a slower rate of distress development (Gharaibeh et al., 2012). More recent studies by Prozzi and Kim for the TxDOT Maintenance Division demonstrated that the new models do not make optimal use of available data, and the parameters are biased and inefficient due to the stepwise estimation method applied.

1.4.1. ACP Models

Given the many model coefficients in the original process and a large amount of data, the 0-6386 study grouped data by categories, including climate, subgrade quality, pavement type, M&R type, traffic loading level, and distress type (Figure 1.1). Therefore, it was possible to estimate one model coefficient for each group instead of estimating model parameters separately. This approach made the parameter estimation quite simple and straightforward but resulted in biased and inefficient estimation.

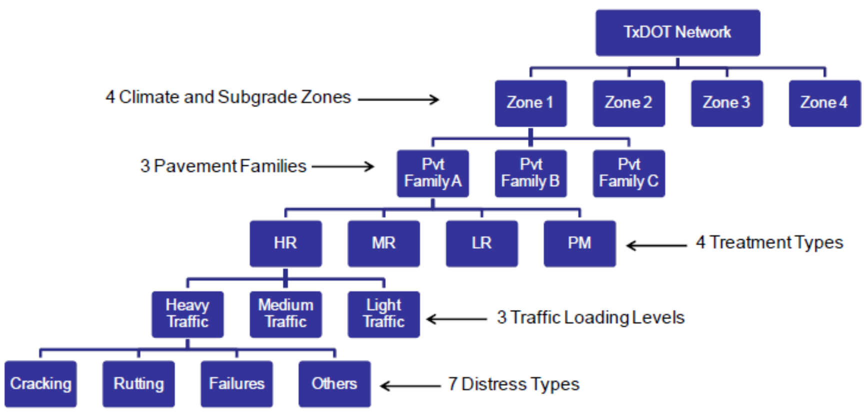

Figure 1.1 Data Grouping for ACP Models (Gharaibeh et al., 2012)

A new set of parameters was estimated by minimizing the difference between predicted and observed performance. To conduct the calibration process, the 0-6386 researchers set a constrained optimization problem with the objective function to minimize the total error and the constraints to ensure treatment types were recommended for distresses in logical order. To solve the problem, a genetic algorithm was implemented. Figure 1.2 shows one of the resulting models compared with the original model.

Based on the calibration results, the 0-6386 study concluded that its new models overcame the over-prediction issue and reduced error from 19.9 percent to 8.3 percent (Gharaibeh et al., 2012) as compared to the original models. While artificial intelligence methods (such as generic algorithms) work well for matching the data (over-fitting), they are challenging to use for predicting.

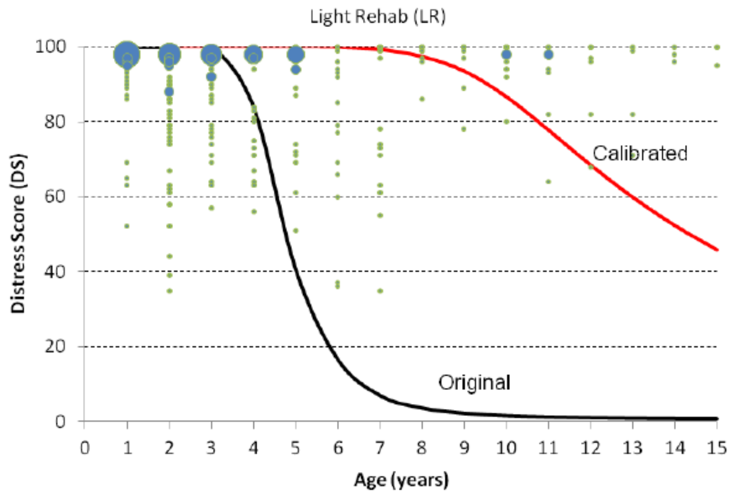

Figure 1.2 Example of the Calibrated Models on Distress Score (Gharaibeh et al., 2012)

Although the 0-6836 project yielded an improvement on the original models, these models still presented several limitations and constraints. Because of the computational complexity of the calibration process, the researchers used data from only 35 out of 254 counties. Further, the models are constrained to an s-shape and several distresses do not follow such form.

1.4.2. CRCP Models

The recalibrating process for CRCP was conducted using non-linear multi-regression across the 25 TxDOT Districts, four climate and subgrade zones, and statewide (Prozzi and Madanat, 2000). The study gathered historical data from 1993 to 2010 and conducted statistical analyses. The age of pavements for given distress was estimated by assumed rules, and then the first and fourth quartiles were filtered out to eliminate outliers. The data were artificially censored, introducing biases (Prozzi and Madanat, 2000). After conducting the regression analyses using medians for the level of distress at each age, the researchers obtained feedback on the resulting coefficients from district engineers and experts. Incorporating the experts' opinions, each model coefficient was constrained to a certain value. The researchers then recalibrated the model with the constrained coefficients. Table 1.1 presents the recalibration results across the climate-subgrade zones.

The authors concluded that the lack of data at a later deterioration stage caused by immediate repairs on CRCP makes it difficult to develop performance models. Experts' feedback was used in a later study to improve the performance models (Gharaibeh et al., 2012) but also introduced some limitations. The process is not fully data-driven because expert opinions impacted the models and introduced additional biases. Also, the models are affected by censoring bias caused by removing quartiles for outlier treatment and using only median values for regression. Furthermore, the models do not consider the effect of traffic load and treatment type. Internal evaluation of the models by TxDOT indicated that they over-predict distresses.

Table 1.1 Recalibrated Model Coefficients for CRCP Distresses

Zone	CRCP Distress	Recalibrated Performance Curve Coefficients				
		α	β	ρ	R^2-Median	R^2-Quartile
Zone 1	Spalled Cracks	3.000	230.000	9.088	0.664	0.258
	Punchouts	1.000	225.000	16.161	1.000	0.787
	ACP Patches	1.000	250.000	14.214	0.397	0.375
	PCC Patches	3.000	31.930	13.648	0.844	0.466
Zone 2	Spalled Cracks	5.000	8.994	9.463	0.778	0.429
	Punchouts	1.000	162.997	14.150	0.926	0.338
	ACP Patches	1.000	250.000	16.132	1.000	1.000
	PCC Patches	2.000	163.899	12.187	0.712	0.395
Zone 3	Spalled Cracks	2.000	200.000	9.084	0.860	0.599
	Punchouts	1.000	250.000	16.145	1.000	0.992
	ACP Patches	-	-	-	-	-
	PCC Patches	2.000	12.913	10.640	0.683	0.466
Zone 4	Spalled Cracks	1.000	200.000	9.090	0.963	0.299
	Punchouts	1.000	145.397	13.192	1.000	0.099
	ACP Patches	-	-	-	-	-
	PCC Patches	3.000	11.805	9.691	0.760	0.484

1.4.3. JCP Models

As with the ACP model process, during the 0-6386 study JCP data were grouped into two JCP types, four climatic zones, three traffic levels, and four treatment types. After aggregating groups to attain statistically significant differences in distress score and for each distress, 66 new models were generated out of 432 possible models. Boundaries for the model coefficients were determined to conform to the logical performance orders. Because information regarding pavement age and treatment types was not available, the pavement age was estimated by regression analysis with a dataset containing construction dates. The treatment types were estimated by assumptions based on distresses and distress scores in the historical data. Figure 1.3 shows models for failed joints and cracks in zone 1. As the researchers intended, the performance curves follow the logical orders—for instance, the curve for PM and high traffic predicts the worst performance over all ages. The study concluded that, in terms of root mean square error, the new models improved the original models by 27.72 percent on average (Gharaibeh et al., 2012).

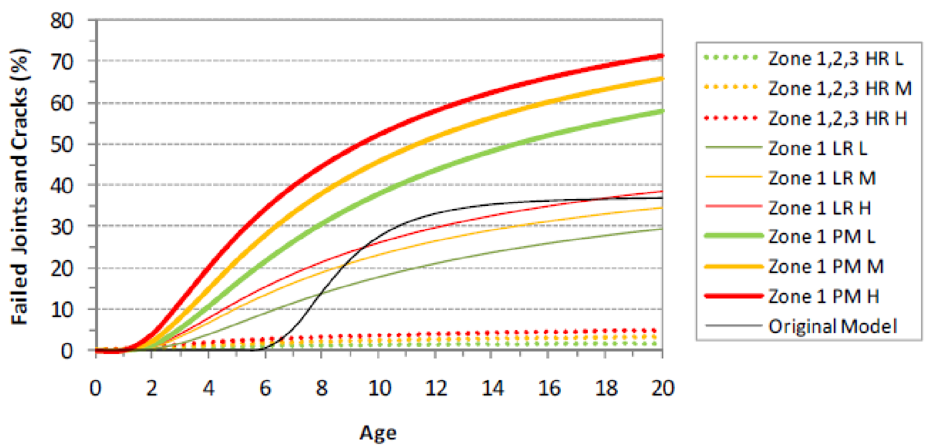

Figure 1.3 Performance Models for JCP Failed Joints and Cracks

The 0-6386 study attempted to obtain the best estimates despite missing information; however, some significant shortcomings remained. The main weakness is that the assumptions to estimate treatment types were based on average distress score per section. This estimation overlooked the effect of deterioration rate on performance.

1.5. Latest Performance Models for IRI Developed by UT Austin

Recently, researchers at the University of Texas at Austin have developed performance models for ride quality on ACP, CRCP, and JCP to be implemented into PA. This was initiated because the models developed under Project 0-6386 were over-predicting ride quality loss, resulting in low condition scores. UT Austin’s new models aimed at developing accurate performance models for predicting rooughness.

1.5.1. ACP Models

The researchers utilized fifteen years of historical PMIS data from 2002 to 2016. They determined that the s-shape curve did not capture the actual data accurately. A linear model explains roughness more accurately and produces a simpler model. As construction work history was not available, a set of rules to estimate when a treatment was applied had to be set up based on visual analysis of the data section by section. Hundreds of random samples of ACP sections showing International Roughness Index (IRI), condition score, and distress score over the years were manually inspected by multiple researchers and a TxDOT panel separately (Figure 1.4) to establish relevant criteria and the corresponding threshold values.

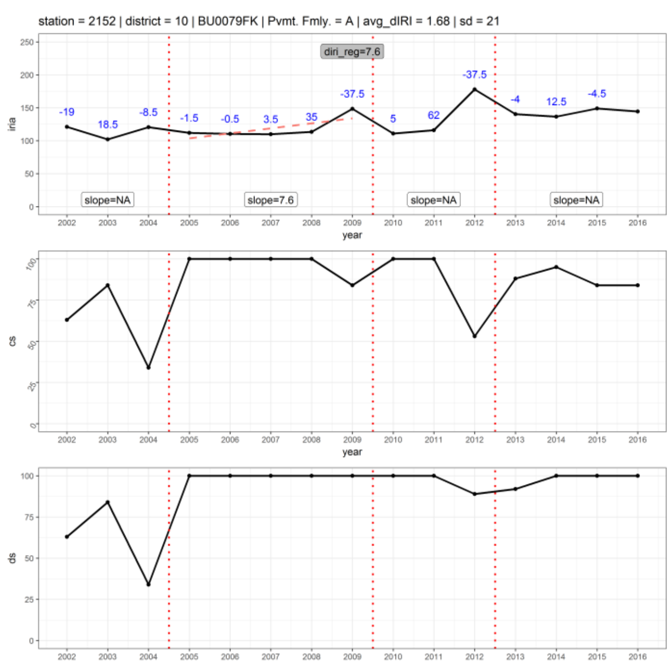

Figure 1.4 An Example of Estimation of Construction Work History

For all available sections, work history and a rate of change in IRI per year (dIRI) were estimated. The resulting dIRIs per PMIS data collection section (0.5 miles) was averaged over a project. Pavement family was categorized into four levels by ACP thickness and type. Figure 1.5 shows the comparison between predictions and observations.

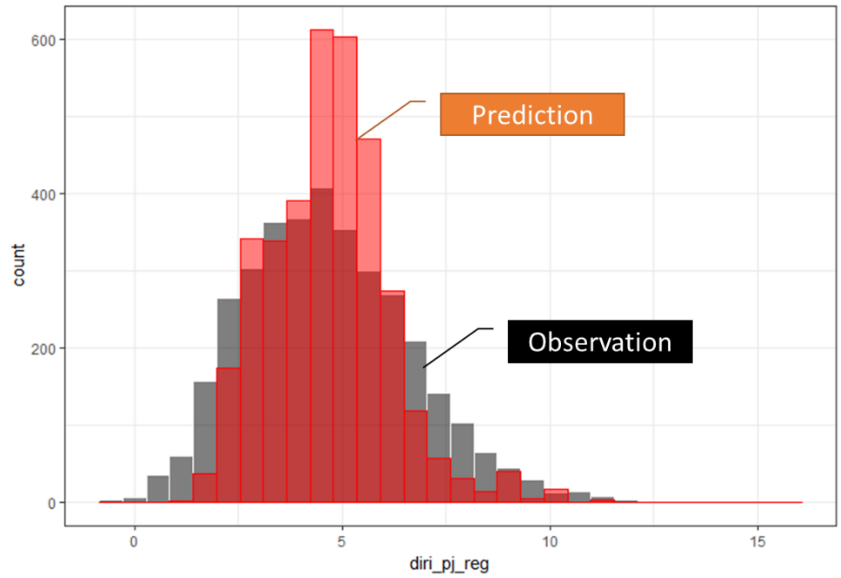

Figure 1.5 Comparison of Observations (grey) vs. Predictions (red) of the dIRI Models

1.5.2. CRCP Models

An exhaustive descriptive data analysis was conducted on CRCP data followed by the data cleaning and modeling process. dIRIs were estimated by regression analysis. The proposed CRCP models use dIRI as dependent variable and three independent variables: district, roadbed type, and highway type. Because only 15 of TxDOT's 25 districts have CRCP sections, coefficients for those 15 districts were estimated. For the other ten districts, coefficients were calculated by taking an average of neighboring districts. The models use four highway types—Interstate Highway (IH), United States Highway (US), State Highway (SH), and Farm-to-Market Road (FM)—to capture the effect of structural capacity.

1.5.3. JCP Models

The procedure used to develop IRI models for JCP was exactly the same as that for ACP. In Figure 1.6, correlations between dIRI and some explanatory variables are presented. As the left figure shows, it is unclear whether JCP type (reinforced/plain) has a significant effect on dIRI; however, the JCP type is a statistically significant factor. On the other hand, roadbed type and highway type clearly demonstrated a significant difference in dIRI, which agrees with engineering intuition. As the middle figure depicts, frontage roads tend to have greater dIRI values—that is, the IRI of frontage roads deteriorates faster in terms of roughness. As for highway types, IH is the least prone to develop roughness, but FM is the weakest type of highway. These might be attributed to factors such as traffic load, traffic speed, and pavement design.

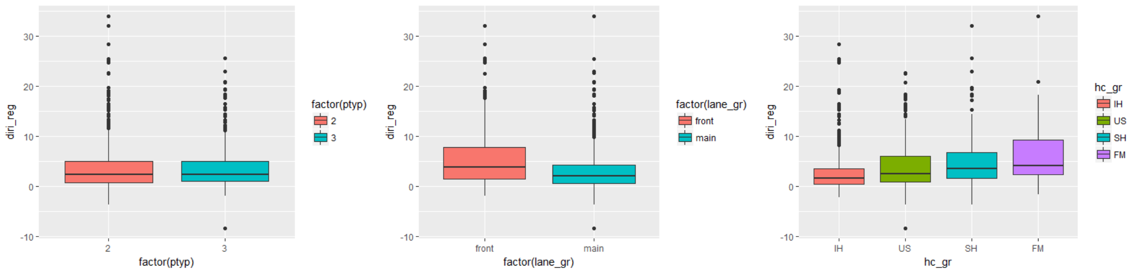

Figure 1.6 Boxplots for the Effects of Explanatory Variables on dIRI

These new models have several advantages. The linear model framework makes it easy to interpret the model parameters and predictions. For example, dIRI represents the IRI change per year. The models were derived from data without applying any constraints on the coefficients. These are preliminary models that still need to estimate the effect of treatment types. In summary, the new models developed by UT Austin achieved a series of technical objectives that could not be reached before:

- They were based on a detailed section-by-section analysis of the data to capture construction work history.
- They were estimated using linear regression, so they produced the best linear unbiased estimators for the parameters.
- The data was not grouped but pooled, so it produced estimates with minimum variance and, therefore, smaller standard errors.

1.6. Modelling Methodology: Advantages and Disadvantages

The objective of pavement performance modelling is to use the best available tools to capture as much as possible the evolution of distresses with time. The two main techniques are traditional statistical modelling and artificial intelligence. Statistical modeling is a field of mathematics that deals with finding relationships between variables to predict an outcome. Artificial intelligence is a field of computer science that builds systems capable of learning from data, instead of explicitly programmed instructions. Bayesian statistics and simulation techniques, such as Markov-Chain Monte-Carlo simulations, can be consider somewhere in between. While statistical modeling has been used for centuries, artificial intelligence—in particular machine learning—is a very recent development. It came into existence in the 1990s as advances in digitization and computing power enabled data scientists to train computers to build models, instead of having to build them manually. The volume and complexity of big data have increased the potential of machine learning.

Statistical modeling works on several assumptions (Srivastava, 2015). For instance, a linear regression (continuous variables) assumes homoscedasticity, mean of error at zero, independence of observations, etc. Similarly, choice analysis (discrete variables) comes with its own set of assumptions. Machine learning algorithms do assume a few of these things but in general are spared from most of these assumptions. The biggest advantage of using a machine learning algorithm is that there might not be any continuity of boundary. Also, we need not specify the distribution of dependent or independent variables in a machine learning algorithm.

Machine learning algorithms are wide-ranging tools. These tools are capable of learning from trillions of observations one by one. They make predictions and learn simultaneously. Machine learning does well with wide (high number of attributes) and deep (high number of observations) data sets. Statistical modeling is generally applied for smaller data sets with fewer attributes. However, statistical modeling can be controlled by developing a specification form that makes engineering sense. Machine learning (and other artificial intelligence techniques) operates as a "black box" and tends to over-fit the data. However, ultimately statistical modeling and machine learning are simply different versions of the same technique. Table 1.2 shows the terminology used by both approaches to refer to basically the same principles.

Table 1.2 Equivalent Nomenclature between Statistics and Machine Learning

Statistics	**Machine Learning**
Model	Network, graphs
Parameters	Weights
Fitting	Learning
Test set of performance	Generalization
Regression (continuous, discrete)	Supervised learning
Density estimation, clustering	Supervised learning

Even when the end goal for both machine learning and statistical modeling is same, the formulation of the two is significantly different. In a statistical model, we basically try to estimate the function as follows: Y (dependent variable) = f [Xs (dependent variables), β (parameters)] + error function. In contrast, machine learning takes away the deterministic function "f" out of the equation. It simply becomes: Output (Y) -> Input (X). It will try to find pockets of *X* in *n* dimensions (where *n* is the number of attributes), where occurrence of *Y* is significantly different.

The fewer the assumptions in a predictive model, the greater the predictive power. Machine learning needs minimal human effort and works on iterations where the computer tries to identify patterns hidden in data. Because the algorithm does this work on a comprehensive data set and is independent of all assumptions, the predictive power is generally very strong for these models. However, these models do tend to over-fit the training data set and may not be as effective at making predictions outside these training data.

Statistical models are mathematically intensive and based on coefficient estimation. The modeler must understand the relationships between variables. Therefore, statistical modeling has some clear advantages when representing phenomena that responds to well-established physical laws—e.g., greater wheel loads and higher temperatures create more rutting.

Despite these contrasting approaches, machine learning and statistical modeling have more similarities than differences. The differences have decreased significantly over past decade. Both branches have learned from each other and will likely converge further in the future.

Chapter 2. Data Compilation

2.1. Data Preparation

Data are the most important component for updating and calibrating the new pavement performance models. Therefore, the research team developed a database and performed statistical analyses of the data that was later used to develop the final models. This database combined data from the old PMIS and the new PA system, and was used to update and calibrate the current models. The team developed two sets of models: 1) updated models that follow the same specification form as the current models and 2) alternative models that conserve the same "s-shaped" specification form but correct some of the issues identified with the current models.

TxDOT historically stored, retrieved, and managed their data with PMIS, but upgraded to PA. The research team created data sets using a series of data mining techniques and processing, such as querying data tables, selecting variables, combining data sets, and so forth, to calibrate and update the models. The original data can be divided into two sets due to the change of TxDOT's measurement methodology and storage strategy. For the remainder of this report, we will refer to *PMIS data* as the data collected from 2002 to 2016 when visual surveys were carried out; the data collected from 2017 to 2019, when automatic data collection was implemented, will be referred to as *PA data*.

2.2. PMIS Data from 2002 to 2016

TxDOT provided to the research team 15 years of PMIS data in Microsoft Access format (from 2002 to 2016). To conduct the research tasks, the research team needed to combine 15 separate database files into one data set, so data could be easily utilized for modeling purposes. The research team used MS Access and R to query the necessary tables and fields, and to compile them into one data set.

The original MS Access database consists of multiple tables and each table contains various fields of information. Because not all the tables and fields were required in this project, appropriate querying was essential. Firstly, the query process was done in MS Access. Two major tables, "Data Collection Section" and "Condition Summary," which contain inventory and pavement surface data, were joined. Then, we selected necessary fields that could potentially be used as variables in the model updating. These variables include inventory variables as well as condition and performance data. The resulting query tables were exported into 15 comma-separated (csv) text files. Those files were imported into R to create a data file by combining them. The data were processed to facilitate the data analysis and were saved into a single file in R-data format, which is compatible with any version of R. Table 2.1 shows the number of half-mile roadway sections for which data was collected, per fiscal year. The list of variables included in the data set is presented in Table 2.2.

Table 2.1 Number of Roadway Sections per Fiscal Year from 2002 to 2016

Fiscal Year	*n*	Fiscal Year	*N*	Fiscal Year	*N*
2002	185,035	2007	188,110	2012	192,151
2003	185,431	2008	189,178	2013	192,939
2004	185,914	2009	189,771	2014	192,997
2005	186,733	2010	190,457	2015	193,612
2006	187,008	2011	191,248	2016	183,561

Table 2.2 Variables Included in the Compiled Data Set

No.	Variable	No.	Variable
1	FISCAL_YEAR	26	ACP_ALLIGATOR_CRACKING_PCT
2	RESPONSIBLE_DISTRICT	27	ACP_LONGITUDE_CRACKING_PCT
3	COUNTY_NBR	28	ACP_TRANSVERSE_CRACKING_QTY
4	SIGNED_HIGHWAY_RDBD_ID	29	ACP_RAVELING_CODE
5	BEG_REF_MARKER_NBR	30	ACP_FLUSHING_CODE
6	BEG_REF_MARKER_DISP	31	ACP_RUT_AUTO_SHALLOW_AVG_PCT
7	END_REF_MARKER_NBR	32	ACP_RUT_AUTO_DEEP_AVG_PCT
8	END_REF_MARKER_DISP	33	ACP_RUT_AUTO_SEVERE_AVG_PCT
9	PVMNT_TYPE_BROAD_CODE	34	ACP_RUT_AUTO_FAILURE_AVG_PCT
10	SECT_LNGTH_RDBD_NEW_MEAS	35	CRCP_SPALLED_CRACKS_QTY
11	SECT_LNGTH_RDBD_OLD_MEAS	36	CRCP_PUNCHOUT_QTY
12	CURRENT_18KIP_MEAS	37	CRCP_ACP_PATCHES_QTY
13	AADT_CURRENT	38	CRCP_PCC_PATCHES_QTY
14	SPEED_LIMIT_MAX	39	CRCP_AVG_CRACK_SPACING_QTY
15	FUNCTIONAL_SYSTEM	40	JCP_FAILED_JNTS_CRACKS_QTY
16	NUMBER_THRU_LANES	41	JCP_FAILURES_QTY
17	RURAL_URBAN_CODE	42	JCP_SHATTERED_SLABS_QTY
18	TRUCK_AADT_PCT	43	JCP_LONGITUDE_CRACKS_QTY
19	ATHWLD_100_LBS	44	JCP_PCC_PATCHES_QTY
20	DISTRESS_SCORE	45	JCP_APPARENT_JNT_SPACE_MEAS
21	CONDITION_SCORE	46	VISUAL_LANE_CODE
22	RIDE_SCORE	47	VISUAL_DATE
23	ACP_PATCHING_PCT	48	LAST_CHANGE_DATE
24	ACP_FAILURE_QTY	49	IRI_LEFT_SCORE
25	ACP_BLOCK_CRACKING_PCT	50	IRI_RIGHT_SCORE

2.3. PA Data from 2017 to 2019

Since TxDOT started outsourcing the task of measuring roughness and various pavement distresses (such as rutting and cracking) in 2017, the data sets before and after 2017 are not compatible for modeling purposes. Furthermore, more detailed information is now available because TxDOT began to store the measurements based on 0.1-mile sections rather than 0.5-mile sections. Initially the research team treated data from 2017 to 2019 separately to avoid any compatibility issues during modeling. During the first stages, PMIS data was used for model development and PA data was used for model calibration and validation. At a later stage, both datasets were combined.

2.3.1. Combining PA and PMIS Data Sets

To obtain a complete data set for the project, the researchers used the two data sets provided by TxDOT: 1) PA data and 2) PMIS data. The more detailed data from PA contains the various measurements, including roughness and pavement distresses, taken in 0.1-mile sections. The PMIS data table encompasses inventory data collected for the traditional half-mile sections. In addition, work history data, which allows users to identify which sections have experienced M&R treatments and when, was also included in the PMIS data. The work history data were not as accurate as was expected, causing some significant delays during the project. The research team encountered multiple instances where the data showed work performed that was not actually done or, alternatively, work was done but the work history file did not reflect it. The most frequent errors concerned the dates on which work was performed.

The data processing began with matching identical 0.1-mile sections for three years using the detailed data. The research team needed to connect sections from different years with location information, which was available in the form of the distance-from-origin (DFO) metric. The DFO locations where the data collection happened were recorded up to three decimals. One issue during data processing was that DFO of a 0.1-mile section did not necessarily match each year, so exact DFO locations could not be used to combine data for a section. Therefore, we developed a set of rules to merge three years of data as follows:

- Round up DFO to one decimal point, and
- Eliminate sections that were duplicated or did not match.

Using the above rules, approximately 95 percent of the sections could be joined despite the remaining mismatches. However, another issue arose in association with the vendors that collect the data. In 2017, two different vendors collected data; however, after 2018, only one vendor did. Some incompatibility between two vendors' data was found, as shown in Figure 2.1.

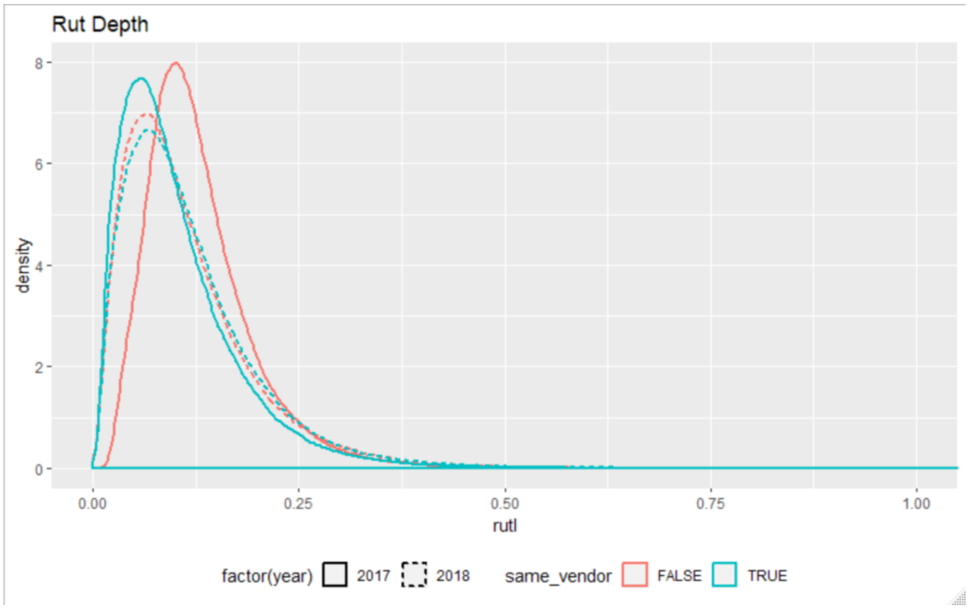

Figure 2.1 Rut Depth Incompatibility between Vendors

The blue lines in Figure 2.1 represent the density function of rut depth density of sections measured by one vendor, while the red lines represent the rut depth distribution of the sections measured by the other vendor during 2017 and 2018. The red lines have a greater gap in rut depth between 2017 and 2018, meaning the measurements of the two vendors are not compatible. Although only the rut depth is presented here, the research team recommends using caution when compiling data from different vendors.

After processing the detailed data, the inventory and the work history data were merged to complete a data set for 2017 through 2019. Note that there was inevitable discrepancy in the procedure because the data sets stored information in different section lengths (i.e., 0.1 mile versus 0.5 mile). We decided to use the middle point of the 0.1-mile sections to identify whether the section falls into a specific 0.5-mile section.

2.4. Project Finder Algorithm

The low reliability of the work history data motivated the development of the Project Finder Algorithm (PFA) to identify work performed and update current pavement performance models and other statistical models used for pavement management purposes. These models typically require the "*Age*" of the pavement as a prediction variable, where the age is the number of years since the last M&R treatment was performed. The Design and Construction Information System (DCIS) database stores work history data but was not designed to archive the history of treatments in every section; instead, it stores only the most recent work performed on a section. This limitation presents challenges when trying to analyze the historical impact of M&R treatments on pavement performance. Hence, on many occasions, visual inspection of the data was required to decide whether work has been done on a highway section, but such an approach could be overwhelming, biased, and inefficient when looking at a network as large as the one in Texas. The PFA offered a way to quickly look at large sets of data and objectively find sections where there was a high likelihood of M&R work, based on pavement performance measures and engineering judgement.

The PFA is an automated tool coded in R that identifies, flags, and reports sections within the Texas highway network that have experienced a noticeable improvement in multiple performance measures in a given year. Due to the drastic improvement within those sections over such a short period of time, the algorithm can tentatively identify M&R projects across the network using only condition data and geographical data found within the Texas PMIS.

2.4.1. Stage 1: Initial Filtering

To initiate the PFA, one must first feed it with a subset of the full pavement management database that contains inventory variables (district, county, DFO); route specific variables (route name, pavement type); performance measures (IRI, pavement scores); distress types; (rutting, cracking, flushing); traffic variables (annual average daily traffic [AADT], equivalent single axle load [ESAL]); and the fiscal year when the data were collected. Once the data are loaded onto a dedicated database, the algorithm computes the length of each section using the DFO and categorizes highways into four major groups: IH, US, SH, and FM. It should be noted that there are more highway classes but those were grouped as shown in Table 2.3.

Table 2.3 Major Highway Classification Breakdown

Major Highway Classification Group	Highway Classifications
IH	Interstate Highway (IH) Business Interstate Highway (BI)
US	United States Highway (US) Business U.S. Highway (BU) U.S. Highway Alternative Roadway (UA) U.S. Highway Spur (UP)
SH	State Highway (SH) Business State Highway (BS) State Highway Loop (SL) State Highway Spur (SS)
FM	Farm-to-Market Road (FM) Business Farm-to-Market Road (BF) Farm-to-Market Road Spurs (FS) Ranch-to-Market Road (RM) Ranch-to-Market Road Spur (RS) Ranch Road (RR)

The PFA was designed to apply to ACP; hence, it filters out any data relating to concrete or composite pavements. Once it is applied, the algorithm requires the user to select the range of years to be used in the analysis. In this case two sets of years were used: 1) from 2002 to 2016, where the method used to collect rut and IRI data is well-documented and consistent, and 2) from 2017 to 2018, once PA was implemented and data is available every 0.1 mile instead of 0.5 mile as was the case for PMIS.

Next the algorithm redefines the value of certain variables to avoid inaccuracies in the analysis. This is necessary because often when data could not be collected in a pavement section due to construction or other circumstances, a value of 0 is stored for variables such as AADT, IRI, and pavement condition scores. The algorithm changes those zeroes to a null or blank to prevent them from introducing a bias when computing averages; moreover, it is known that those variables cannot be equal to zero. Next, the algorithm sums up the lengths of every section within a highway and filters out any highway whose total length is less than 10 miles. The reason for this filtering is solely for statistical purposes, as every data point within this dataset is collected every 0.5 mile and it is desired that every highway contributes at least 20 data points to the performance models to be able to obtain robust parameter estimates. A summary of the filtering process in terms of highway mileage is presented in Table 2.4.

Table 2.4 Yearly Breakdown of Highway Mileage Before and After Initial Filtering

Fiscal Year	Mileage before filtering (in miles)	Mileage after filtering (in miles)	Percentage filtered-out (%)
2002	81,590	60,000	26.5
2003	82,010	60,210	26.6
2004	82,460	60,340	26.8
2005	82,880	60,520	27.0
2006	83,080	60,400	27.3
2007	83,866	60,890	27.4
2008	84,586	61,470	27.3
2009	85,060	61,730	27.4
2010	85,490	61,890	27.6
2011	85,980	62,150	27.7
2012	86,700	62,630	27.8
2013	87,400	63,080	27.8
2014	87,770	63,120	28.1
2015	89,050	64,090	28.0
2016	89,823	64,400	28.3
2017	89,900	64,370	28.4
2018	89,970	64,060	28.8

2.4.2. Stage 2: Section Flagging

Once the initial filtering is completed, the algorithm groups sections based on their route name, district, county, and DFO, and assigns each group of sections that share those same attributes a unique ID. Then, for every unique ID, the algorithm takes the difference of all performance and distress measures from one year to the next as per the following equation:

$$\Delta Performance = Performance_{i+1} - Performance_i$$

where *i* indicates the year of the analysis. This difference is defined such that a significant negative difference in distress measures such as rutting, IRI, or cracking is a strong indicator that M&R work was performed; in contrast, for performance measures such as the condition, distress, or ride score, significant positive differences are indicators of work performed. The probability distributions of these differences were analyzed to determine threshold values that could be used for determining when a difference was significant enough to be an indicator of work. After multiple trials and discussions with personnel from TxDOT's Maintenance Division, it was decided that the ride score should not be used as a work indicator, as it highly correlated to IRI. Furthermore, using the condition and distress scores could be considered double-counting, as they are computed using other distresses already being used as indicators. Hence, only IRI and distress measures were used as work indicators.

The threshold values that were used for each performance measure typically correspond to the lower 5th, 10th, or 15th percentile of the distribution. The decision as to which percentile is used is subjective but depends on the variance or spread of the data. Figure 2.2 shows a graphical example of the histogram that is generated by using the data on the difference in IRI on the left wheel path and the threshold value being used.

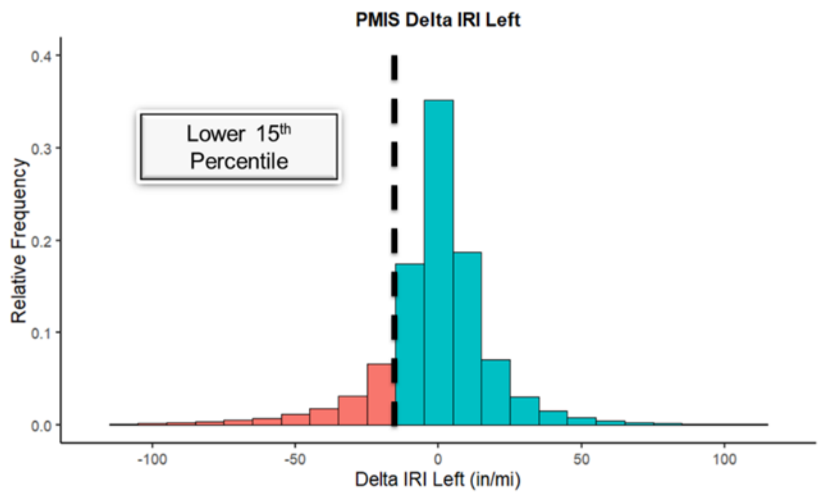

Figure 2.2 Histogram of the Difference in IRI on the Left Wheel Path over 15 Years

Something to be noted is that there are no rut depth measurements in the PA database from 2002 to 2011. Therefore, to compensate for this, a multivariate linear regression analysis was conducted using the “rut bucket” values to estimate the rut depth in inches, as per the following equation:

$$Rut\ Depth\ (in.) = \beta_1 X_1 + \beta_2 X_2 + \beta_3 X_3 + \beta_4 X_4$$

where,

$\beta_{1,2,3,4}$: parameters for shallow, deep, severe, and failure rutting, respectively.

$X_{1,2,3,4}$: rut bucket value for shallow, deep, severe, and failure rutting, respectively

Note that the regression equation was forced to explicitly have its y-intercept at zero. This is because, intuitively, if all the rut buckets have a value of zero, that implies that the pavement section has “no rutting.” In terms of rut measurements, “no rutting” implies that the average rutting in the section is less than 0.25 in. Results of the multivariate regression analysis are presented in Table 2.5. From the regression analysis it is concluded that all four regression parameters in the equation are significant in the estimation of the rut depth. This implies that the impact of the rut buckets on the prediction of average rut depth is not negligible. Furthermore, the regression does a fair job at predicting average rut depth, given that it accounts for 71.6 percent of the variability in the data.

Table 2.5 Multivariate Regression Results for the Estimation of Average Rut Depth

Parameter	Estimate	Standard error	T-statistic	P-value
□1	6.161×10−3	1.10×10−5	561	0*
β_2	4.086×10^{-3}	5.45×10^{-5}	75	0*
β_3	2.633×10^{-2}	7.10×10^{-4}	37	0*
β_4	1.937×10^{-2}	8.53×10^{-3}	2.27	0.023
Residual standard error		0.074	***Adjusted. R^2***	0.716

*** The value is so small that for practical purposes it can be assumed to be zero.***

Once the regression equation is used to estimate the rut depth for fiscal years 2002 to 2016 and all threshold values for each distress type have been established, a relative weight is assigned to each of them based on the on how reliable those measurements have been in the past to determine whether work has been done. Weights of 1.5, 1.0, and 0.5 correspond to the highest, medium, and lowest level of perceived reliability of the data. For example, IRI and rut depth measurements for either wheel path are assigned a weight of 1.5; average rut depth, number of failures, patching, and longitudinal cracking are assigned a weight of 1.0; and all other distress measures are given a weight of 0.5. However, these weights can be changed if a better-informed set of criteria could be made available.

The thresholds and weights are set into the algorithm. Once done, the algorithm searches the entire database and flags any section reporting a difference that is equal to or less than the threshold value for each performance measure. Next, the algorithm selects those sections whose total weighted score was at least four. This implies that these sections show a significant improvement in multiple performance measures over the span of one year and, therefore, have a high likelihood of having received M&R treatment. The current percentiles and threshold values for all indicators being used are shown in Table 2.6.

Table 2.6 Threshold Values Currently Used in Algorithm

Performance Measure	Percentile	PMIS Threshold Value	PA Threshold Value
IRI Left	20th	-10 in/mi	-8 in/mi
IRI Right	20th	-13 in/mi	-11 in/mi
Estimated Average Rut	15th	-0.010 in	~
Rut Left	15th	~	-0.010 in
Rut Right	15th	~	-0.019 in
Alligator Cracking	5th	-5% cracked	-5% cracked
Longitudinal Cracking	10th	-10 ft per station	-14 ft per station
Transverse Cracking	3rd	-5% cracked	-5% cracked
Block Cracking	1st	-5% cracked	-5% cracked

Performance Measure	Percentile	PMIS Threshold Value	PA Threshold Value
Number of Failures	3rd	-4 failures	-4 failures
Patching Percentage	5th	-5% patched	-5% patched
Raveling	1st	-2	-2
Flushing	5th	-2	-2

2.4.3. Stage 3: Finding Projects

In the previous stage, the algorithm selected a group of sections with a high likelihood of having received M&R work. Now, the algorithm needs to identify which of those sections are part of the same project. For the algorithm, a project is defined as a group of at least five PMIS highways sections (that is, approximately 2.5 miles in length) that are contiguous to one another and share the same route name, where contiguous means there is a distance smaller than 1.0 mile between one section and the one adjacent to it. By using this procedure, the algorithm can distinguish between groups of sections that are likely to be a project and isolated sections that happen to have spikes in their performance measures, as shown in Figure 2.3.

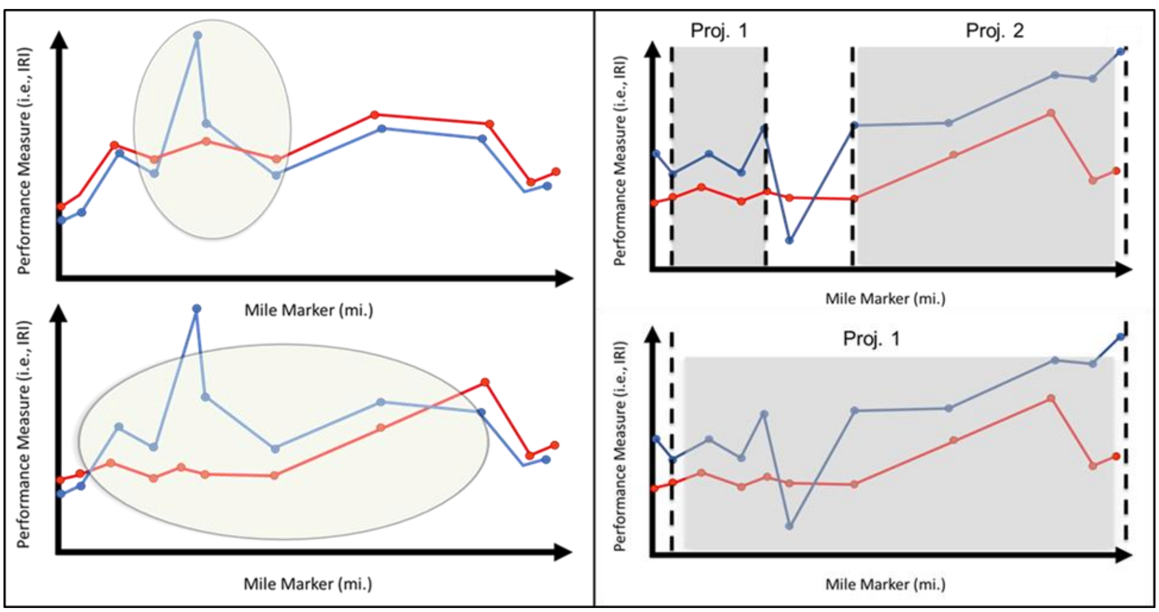

Figure 2.3 Examples of Merging Sections into Projects

However, if there is a sudden drop in the improvement of performance along the sections, using this procedure might yield cases where there are two projects that are less than 2 miles from each another. In reality, these two projects are more likely to be one long project instead of two short ones. Hence, the algorithm performs a small correction if the gap in between two projects is less than or equal to 3 miles (six data points). The algorithm will bridge the gap and treat everything as one longer project. Figure 2.3 presents a graphical example of how the algorithm bridges this gap between two projects. In Figure 2.3 it is assumed that the blue line is an arbitrary year "*i*" and the red line is the year “*i+1*”; hence, for any of the performance measures being analyzed by the algorithm, if the red line lies significantly below the blue line, then that is an indicator of work being done.

Next, the algorithm defines the project limits, computes the project length, and assigns an ID to every project. Then it outputs a table with the total highway mileage (all pavement types, treated or untreated), the total highway mileage that was treated, and the percentage of mileage treated per year. Table 2.7 shows a summary of the treated sections found by the algorithm.

Table 2.7 Yearly Breakdown of Maintenance Work Captured by Algorithm

Fiscal Year	Highway Mileage	Highway Mileage Treated	Percent Treated
2002	81,590	1,453	1.78
2003	82,010	2,806	3.42
2004	82,460	1,144	1.39
2005	82,880	1,355	1.63
2006	83,080	1,636	1.97
2007	83,866	1,308	1.56
2008	84,586	1,345	1.59
2009	85,060	1,048	1.23
2010	85,490	839	0.98
2011	85,980	1,048	1.22
2012	86,700	1,310	1.51
2013	87,400	1,211	1.39
2014	87,770	1,353	1.54
2015	89,050	1,363	1.53
2016	89,823	2,112	2.35
2017	89,900	8,978	9.99

2.4.3.1. Accuracy of the PFA

Although the algorithm was developed to be conservative for identifying potential projects, it is still possible for it to capture “false positives” or, in other words, contiguous highway sections that show significant improvement but with no record of receiving maintenance in either the work history kept by TxDOT or any other database used in previous studies with a work history database. Hence, a cross-verification process was used to check the accuracy of the algorithm by analyzing how many of the projects found by algorithm have a match in the work history databases kept by TxDOT.

The first database used was the most recent work history dataset, which stores the most recent treatment that has been performed on a given section. This work history file contains projects that range from the 1990s all the way to 2018. The second file is a database that was manually filtered to archive and show all the different projects that were performed on a large set of thick asphalt concrete pavements (TACPs). Unlike the first work history database, the second file does include the history of projects in a section spanning from the 1990s to 2018, instead of having only the most recent one.

The cross-verification consisted of matching the projects found by the algorithm against those in the two work history databases based on the year when work was done, the highway name, and project limits in terms of DFO. In this scenario, a "match" is considered any case where the project limits of the projects found by the algorithm overlap with those in the work history dataset.

The cross-verification process captures not only the number of projects that have a match in the work history, but also the mileage overlaps between the two. Once those two quantities are determined, the accuracy of the algorithm is quantified in terms of the percentage of projects that has a match and the percentage of mileage that overlaps with the work history databases.

The dates used to test the accuracy of the algorithm are the final construction date for the most recent work history and the last revision date for the TACP work history databases. However, these dates have some uncertainty associated with them given that the treatments can experience construction delays or the data that reflects the effects of the treatment is not collected until the following fiscal year. Therefore, the cross-verification was also implemented with a time buffer of ±1 and ±2 years to account for this uncertainty. A summary of the cross-verification results is provided in Tables 2.8 through 2.111. Tables 2.8 and 2.9 were generated by verifying the results from the algorithm using the PA and PMIS databases with the work history file that has only the most recent projects. Tables 2.10 and 2.11 compared the algorithm results with the work history database on solely TACPs.

Table 2.8 PMIS Algorithm Output Cross-verification with Work History Database

Algorithm and work history summary	
Number of projects found by algorithm	4,039
Mileage of projects found by algorithm (mi)	21,333
Number of projects in work history	5,224
Mileage of projects in work history (mi)	32,527
Matching with ±2-year buffer	
Projects Matched	1,122
Mileage Matched (mi)	3,962
Percent of Projects Matched	**28%**
Percent of Mileage Overlapped	**19%**
Matching with ±1-year buffer	
Projects Matched	990
Mileage Matched (mi)	3,699
Percent of Projects Matched	**25%**
Percent of Mileage Overlapped	**17%**
Matching with no buffer	
Projects Matched	561
Mileage Matched (mi)	2,000
Percent of Projects Matched	**14%**
Percent of Mileage Overlapped	**9%**

Table 2.9 PA Algorithm Output Cross-verification with Most Recent Work History Database

Algorithm and work history summary	
Number of projects found by algorithm	1,398
Mileage of projects found by algorithm (mi)	8,990
Number of projects in work history	3,512
Mileage of projects in work history	24,416
Matching with ±2-year buffer	
Projects Matched	712
Mileage Matched (mi)	1,774
Percent of Projects Matched	**51%**
Percent of Mileage Overlapped	**20%**
Matching with ±1-year buffer	
Projects Matched	712
Mileage Matched (mi)	1,774
Percent of Projects Matched	**51%**
Percent of Mileage Overlapped	**20%**
Matching with no buffer	
Projects Matched	368
Mileage Matched (mi)	724
Percent of Projects Matched	**26%**
Percent of Mileage Overlapped	**8%**

Table 2.10 PMIS Algorithm Output Cross-verification with TACP Work History Database

Algorithm and work history summary	
Number of projects found by algorithm	172
Mileage of projects found by algorithm (mi)	912
Number of projects in work history	658
Mileage of projects in work history (mi)	3,411
Matching with ±2-year buffer	
Projects Matched	92
Mileage Matched (mi)	97
Percent of Projects Matched	**53%**
Percent of Mileage Overlapped	**31%**
Matching with ±1-year buffer	
Projects Matched	64
Mileage Matched (mi)	72
Percent of Projects Matched	**37%**
Percent of Mileage Overlapped	**22%**
Matching with no buffer	
Projects Matched	30
Mileage Matched (mi)	32
Percent of Projects Matched (%)	**17%**
Percent of Mileage Overlapped (%)	**13%**

Table 2.11 PA Algorithm Output Cross-verification with TACP Work History Database

Algorithm and work history summary	
Number of projects found by algorithm	28
Mileage of projects found by algorithm (mi)	141
Number of projects in work history	374
Mileage of projects in work history (mi)	2,003
Matching with ±2-year buffer	
Projects Matched	23
Mileage Matched (mi)	19
Percent of Projects Matched	**86%**
Percent of Mileage Overlapped	**74%**
Matching with ±1-year buffer	
Projects Matched	23
Mileage Matched (mi)	19
Percent of Projects Matched	**86%**
Percent of Mileage Overlapped	**74%**
Matching with no buffer	
Projects Matched	10
Mileage Matched (mi)	8
Percent of Projects Matched	**36%**
Percent of Mileage Overlapped (%)	**25%**

It was noted that, although the algorithm captures multiple projects and mileage of treated highways, it is not accurate as it was expected. It seems that if a buffer of two years is given, the algorithm tends to have an accuracy of 50 percent in terms of projects, and close to 20 percent in terms of mileage. However, it seems that in the cases where a match is found, only a fraction of the total project mileage is captured. This phenomenon might occur because the algorithm is not sensitive enough to capture the effect of lighter PM treatments such as seal coats. Nevertheless, a visual inspection of a random sample of projects captured by the algorithm that had no match in either of the two work history databases shows that significant improvement can be visually seen in the data. An example of this shown in Figure 2.4, where the condition was improved in terms of IRI, alligator cracking, and longitudinal cracking.

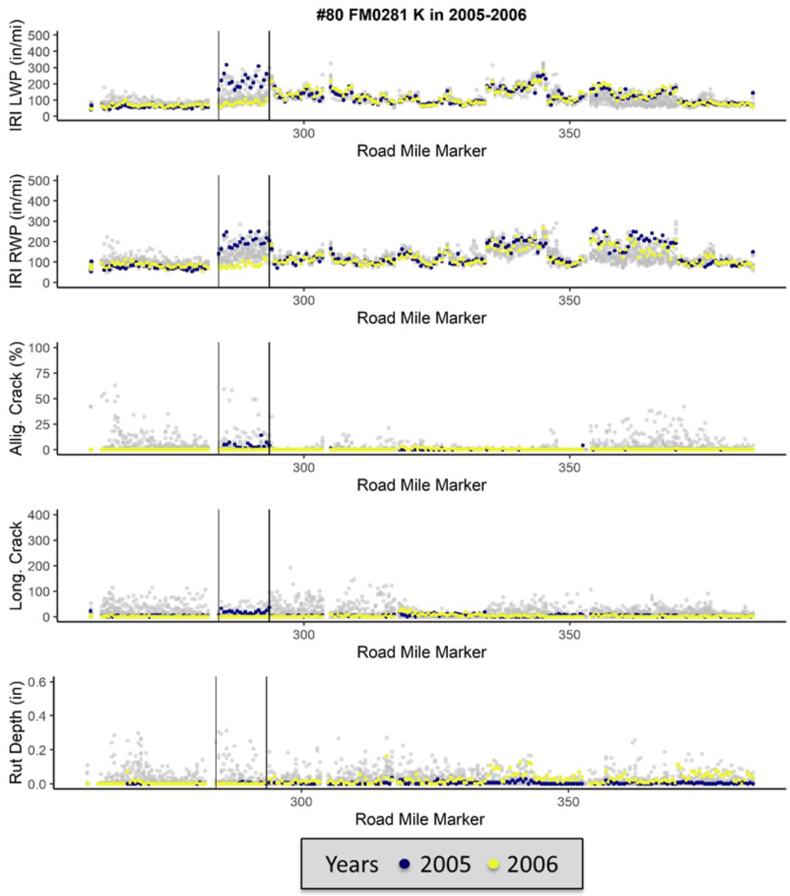

Figure 2.4 Potential Projects Found in IH 35 by Algorithm with No Match in Work History

2.5. Incorporating Treatment Type

Another issue identified with the current models was that the models for different treatment types could cross over a period of time. For example, a pavement that was subjected to HRhb could, after some years, show poorer performance—as if it had been provided with only PM. From a pavement management and a planning and programming point of view, this is not acceptable. Furthermore, this also caused some more practical issues associated with the calculation of treatment effectiveness.

In this section, we show how the different treatment types could be incorporated into the models in a manner that will ensure that higher level treatments will result in better long-term performance. The treatments considered are PM, LRhb, MRhb, and HRhb. For example, the following equation demonstrates how the various M&R activities could be incorporated into Model One (or logit model):

$$L = \frac{\beta_0}{1 + \beta_1 . exp\{-(\beta_2 + \alpha_1 PM + \alpha_2 LRhb + \alpha_3 MRhb + \alpha_4 HRhb). Age\}}$$

where,

L : distress density,

Age : independent variable that accounts for the age of the pavement section,

β_0 : asymptote parameter that captures the maximum level of distress,

β_1 : regression parameter which could be specified as a function of traffic, environmental conditions, subgrade, location, and any other relevant variables.

β_2 : regression parameter that captures the rate of the deterioration process,

$\alpha_{1,2,3,4}$: regression parameters that captures the effect of PM, LRhb, MRhb or HRhb in slowing down the deterioration process.

In this model, PM, LRhb, MRhb, and HRhb are dummy variables that capture the type of M&R work that has been performed on the specific section. By applying this model specification and the constraint that $\alpha_1 > \alpha_2 > \alpha_3 > \alpha_4$, this model ensures that the performance curves will never cross each other. Figure 2.5 represents this approach to the model.

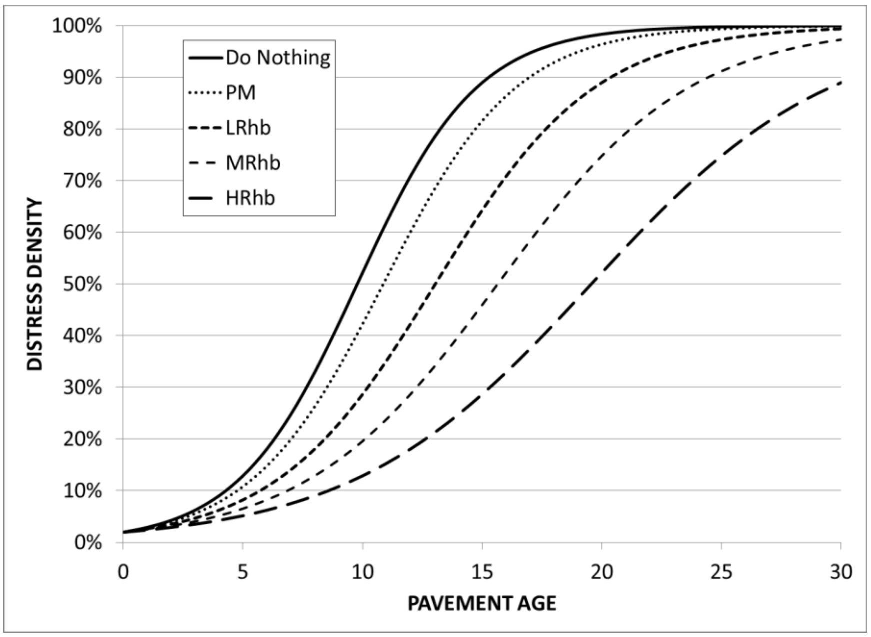

Figure 2.5 Incorporation of M&R Activities into Alternative Models

Chapter 3. Calibration and Update of Current Pavement Performance Prediction Models

3.1. Introduction

This chapter documents the updating and calibration of pavement performance models for ACP. The objective of the calibration process was to improve the current models by incorporating updated data. Performance curves were recalibrated for ACP distress types using PMIS and PA data from years from 2002 to 2019. The calibration process of the ACP performance models was conducted using nonlinear mixed effect regression with variables, such as functional class, traffic, pavement type, climate, and age. Appendix B contains the calibrated coefficients for the ACP performance prediction models developed in this project.

3.2. Development of Analysis Database

The database used for updating the models was extracted from TxDOT's PMIS and PA systems dating from 2002 to 2019. To establish an analysis data set for model development, a series of variables associated with structural and environmental factors were also extracted. Additionally, the distributions of various distresses were also investigated to assist the model estimation in the following steps.

3.2.1 Variable Preparation

Pavement deterioration is affected by various factors. In the PMIS and PA systems, variables related to functional, structural, and traffic information are stored and can be easily queried and retrieved as model variables. However, although weather conditions also play a significant role in pavement performance, only very limited environmental information is available in PA. To address this issue, the research team turned to the National Oceanic and Atmospheric Administration (NOAA) database, extracting environmental factors, including temperature and precipitation, and incorporating these factors as variables in the models. Because highway pavements deteriorate under the cumulative effect of traffic and environmental conditions, pavement age was computed as another variable to be used in the model. In the following paragraphs the model variables are introduced and described.

3.2.1.1. Functional Class

In Texas, highways are categorized into seven groups based on their function, and each group contains sub-groups. The seven main groups are numbered from 1 to 7 and stored in column "PMIS_HIGHWAY_SYSTEM" of the database, while the sub-groups can be extracted from column "ROUTE_NAME". The number of records and the corresponding percentages for different groups in the PMIS and PA databases can be found in Table 3.1. As shown, most of the highways fall into groups 2, 3, 6, and 7, which corresponds to more than 98 percent of all the records. As a result, in this project, a variable "HIGHWAY_FUN" was created that contains four levels—FM, SH, US, and IH. These four levels correspond to groups 2, 6, 7, and 3 specified in column “PMIS_HIGHWAY_SYSTEM”, respectively.

Table 3.1 Distribution of Functional Class

PMIS_HIGHWAY_SYSTEM	Description	Count	Percentage
1	BF	297	0.0%
	BS	8,277	0.3%
	BI	11,191	0.3%
	BU	22,015	0.7%
2	RS	73	0.0%
	RR	250	0.0%
	FS	2,254	0.1%
	RM	108,728	3.3%
	FM	1,409,299	43.1%
3	IH	433,262	13.2%
4	PA	1,032	0.0%
5	RE	3,002	0.1%
	PR	9,952	0.3%
6	SS	21,339	0.7%
	SL	59,372	1.8%
	SH	579,407	17.7%
7	UP	438	0.0%
	UA	9,750	0.3%
	US	591,636	18.1%

3.2.1.2. Traffic

In this project, the 20 years projected ESALs, which was stored in the column “TX_CURRENT_18KIP_MEAS”, was used to represent the traffic characteristic of each pavement section. The average 20 years projected ESALs for each pavement section was firstly computed to keep the traffic characteristic consistent across the analysis period. Next, three thresholds—200,000; 750,000; and 3,000,000—were used to divide traffic into four categories, including low, medium, high, and heavy. The distribution of the traffic and the three thresholds (vertical dash line) were plotted in Figure 3.1. Since these thresholds are selected approximately around the quartiles of the data, the number of records were roughly evenly distributed across the four traffic categories.

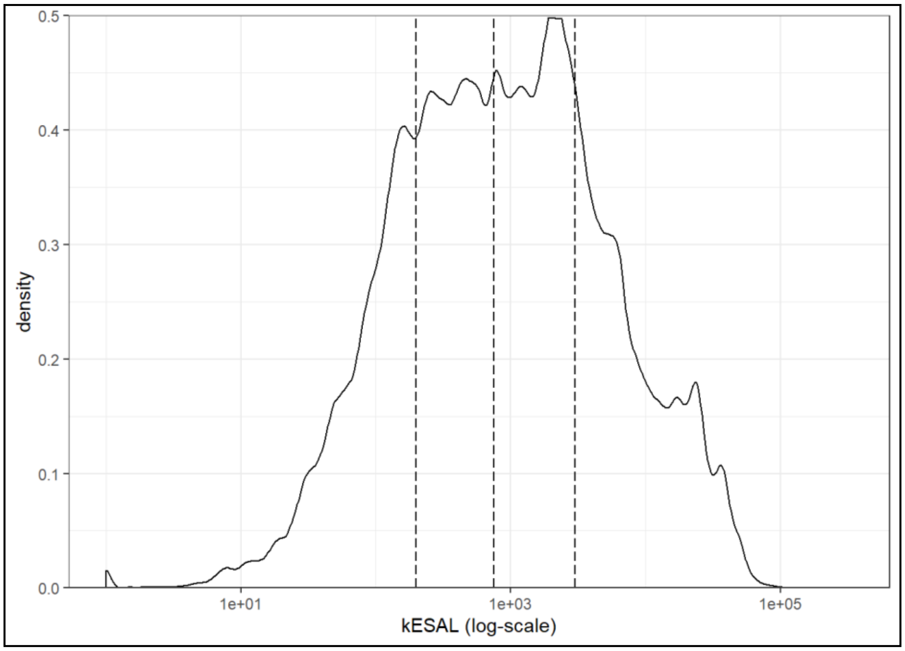

Figure 3.1 Distribution of 20 Years Projected ESALs

3.2.1.3. Pavement Type

Of the ten different types of pavements in the PA system, seven are ACPs (Table 3.2). In this project, based on the similarity of characteristics, these seven ACP types were grouped into three categories:

- Thick ACP: Type 4, PMIS Type 5, and Type 9
- Thin ACP: Type 6 and Type 10
- Composite ACP: Type 7 and Type 8

Table 3.2 Pavement Types

Pavement Type		Description
CRCP	1	Continuously Reinforced Concrete Pavement
JCP	2	Jointed Concrete Pavement-reinforced
	3	Jointed Concrete Pavement-unreinforced
ACP	4	Thick Asphalt Concrete Pavement (>5.5" thick)
	5	Intermediate Asphalt Concrete Pavement (2.5-5.5" thick)
	6	Thin Asphalt Concrete Pavement (<2.5" thick)
	7	Composite Pavement (asphalt surfaced concrete pavement)
	8	Overlaid or Widened Old Concrete Pavement
	9	Overlaid or Widened Old Flexible Pavement
	10	Thin-surfaced Flexible Base Pavement (surface treatment or seal coat)

3.2.1.4. Climate

The climate information was obtained from the NOAA database. From this database, we selected 30 years of normal annual average temperature and precipitation as representative of the climate. The NOAA data is collected from weather stations, but some counties do not have these stations. For those counties, the average information from the adjacent counties was used. For counties with multiple weather stations, the average information of these weather stations was used. After acquiring the temperature and precipitation statistics for each county, thresholds of 61.25 and 70.0 degrees for temperature and 16 and 38 inches for precipitation were used to group counties into different climate zones. After minor adjustments, a climate map with five zones was obtained, representing the west, east, north, south, and central regions.

The distributions of temperature and precipitation along with the boundaries of different climate zones are depicted in Figure 3.2. As shown, in general, an increasing trend can be found in temperature from north to south, and in precipitation from west to east. Moreover, the climate zones defined are reasonable enough to represent the general climate distribution in Texas.

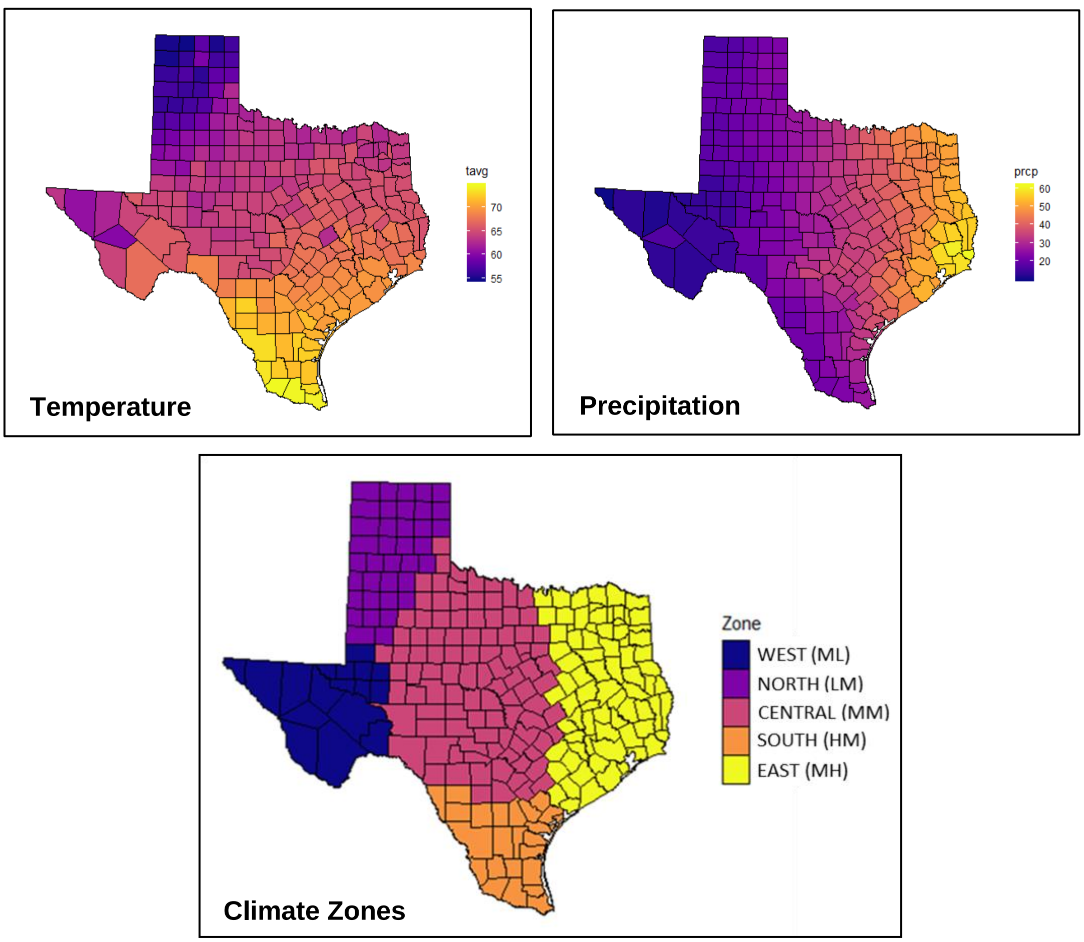

Figure 3.2 Climate Distribution and Climate Zones

3.2.1.5. Pavement Age

Pavement age plays a key role in condition score because pavement deteriorates with time even in the absence of traffic and harsh climates, simply due to the characteristics of the materials. The age of a pavement section at a specific year can be computed by computing the length of time since the last maintenance, rehabilitation, or construction work. In this project, because of the quality of the work history data, significant resources had to be diverted to the development of algorithms to identify the work history. After developing the work history, the work history data was combined with PA data to compute the age variable.

3.2.2. Identification of Correlated Variables

The design of pavement is a systematic decision process that accounts for multiple design variables including, but not limited to, structure, traffic, and environment. As a result, intrinsic correlations can be found among different variables during the development of pavement performance models. For example, for an IH with heavy traffic, normally a thick asphalt concrete surface design would prevail instead of a thin surface layer. In contrast, for FM routes with low traffic volume, agencies would be more likely to apply a thin pavement design instead of a thick pavement design. Considering this, in this project, a preliminary correlation analysis was conducted. As shown in Table 3.3, significant linear correlations could be found among the functional class, pavement type, and traffic. Therefore, a decision was made to combine these three categorical variables.

Table 3.3 Correlation Matrix

	Functional Class	**Pavement Type**	**Traffic**
Functional Class	1.00	0.35	0.57
Pavement Type	0.35	1.00	0.49
Traffic	0.57	0.49	1.00

Theoretically, four highway functional classes, three pavement types, and four traffic levels would result in 48 groups. However, due to the limited data with work history information, it was found that after combining work history data, only 19 of these 48 groups have enough data to develop performance models. For the rest of the groups, their performance models were determined from similar groups with enough data. In this regard a conservative approach was followed. For example, if a model for a specific combination of variables was missing data, the model from a "higher deterioration" was assigned.

3.2.3. Distribution of Pavement Distresses

In the TxDOT Rater's Manual, a set of maximum values have been assigned to different distresses, which is reasonable to guide raters to conduct the distress evaluation. However, in reality, when a certain type of distress reaches a certain level, maintenance or rehabilitation work is normally performed. This, in turn, generates an extremely skewed distribution for most of the distresses and leads to non-robust predictions if the deterioration models use the maximum rating values as the asymptotic value. Consequently, in this project, the distributions of various pavement distresses were investigated to elect reasonable asymptotic values for the deterioration models. In Figure 3.3, the histograms along with various percentiles for different distresses were presented together. As shown, for most of the distresses, though the maximum values of them are consistent with the maximum rating values, even the 99.9th percentiles can significantly diverge from the maximum values specified in the Rater's Manual. Accordingly, when performing model estimation, instead of using the maximum rating values in the Rater's Manual, we made corresponding adjustments of the asymptotic values based on the 99.9th percentiles for each type of distresses.

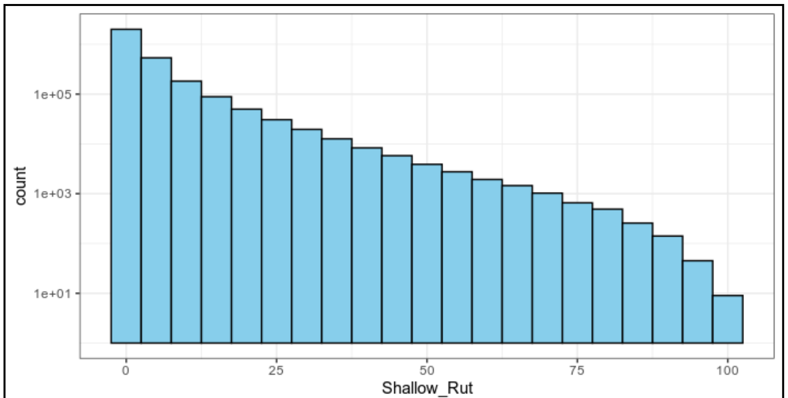

probs	10.0%	25.0%	50.0%	75.0%	95.0%	99.0%	99.9%	100.0%
percentile	0	0	1	4	17	36	66	100

(a) Shallow Rut

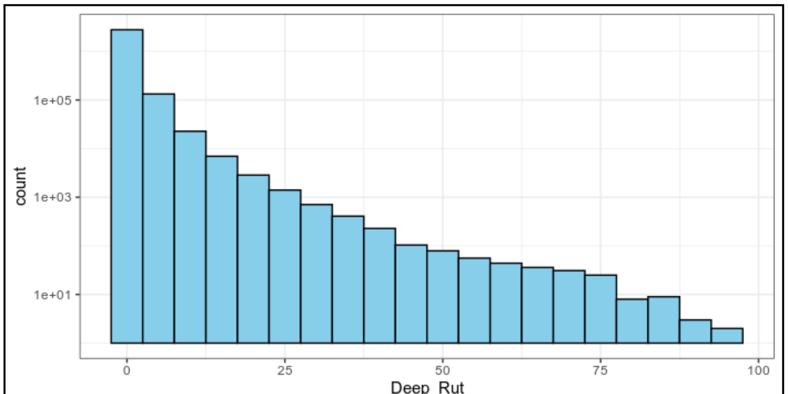

probs	10.0%	25.0%	50.0%	75.0%	95.0%	99.0%	99.9%	100.0%
percentile	0	0	0	0	3	8	23	97

(b) Deep Rut

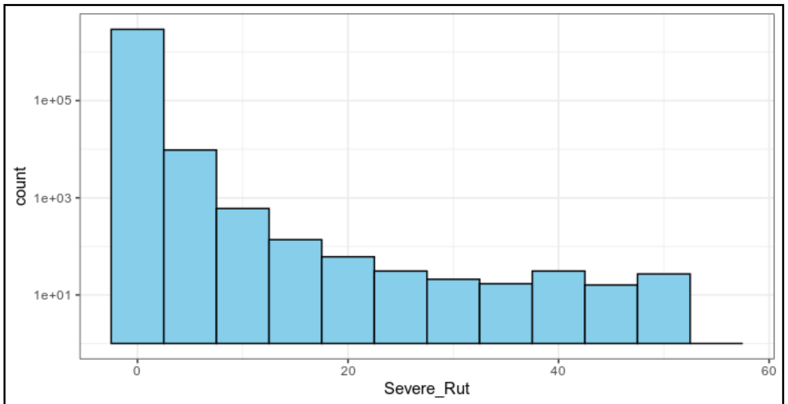

probs	10.0%	25.0%	50.0%	75.0%	95.0%	99.0%	99.9%	100.0%
percentile	0	0	0	0	0	1	5	55

(c) Severe Rut

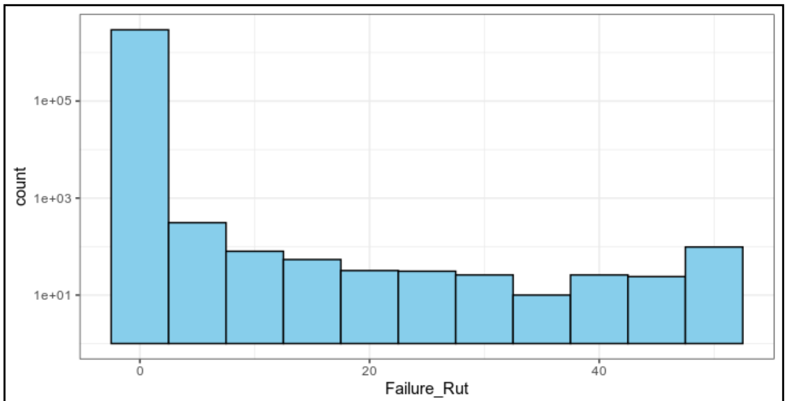

probs	10.0%	25.0%	50.0%	75.0%	95.0%	99.0%	99.9%	100.0%
percentile	0	0	0	0	0	0	1	50

(d) Failure Rut

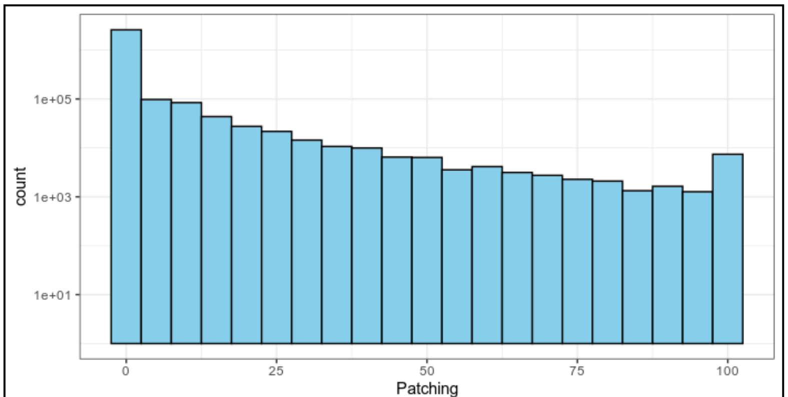

probs	10.0%	25.0%	50.0%	75.0%	95.0%	99.0%	99.9%	100.0%
percentile	0	0	0	0	15	53	100	100

(e) Patching

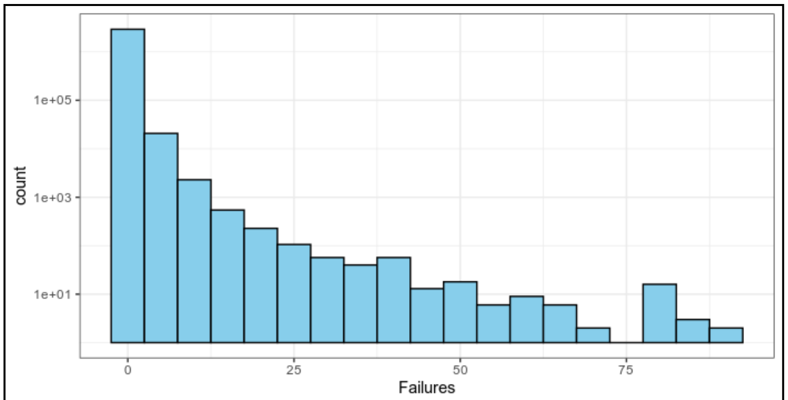

probs	10.0%	25.0%	50.0%	75.0%	95.0%	99.0%	99.9%	100.0%
percentile	0	0	0	0	0	2	8	92

(f) Failures

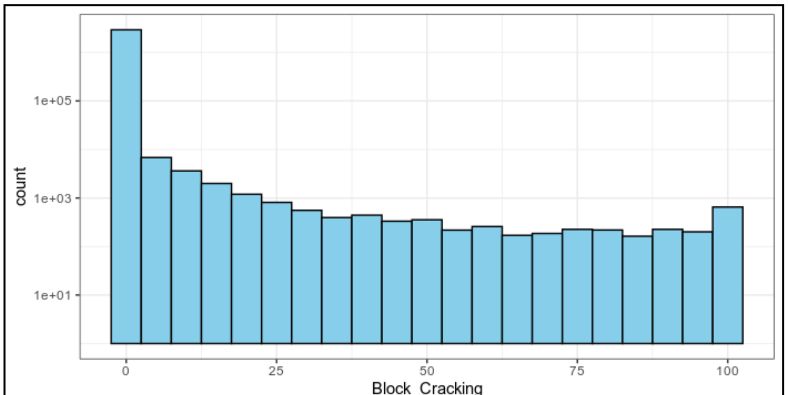

probs	10.0%	25.0%	50.0%	75.0%	95.0%	99.0%	99.9%	100.0%
percentile	0	0	0	0	0	0	46	100

(g) Block Cracking

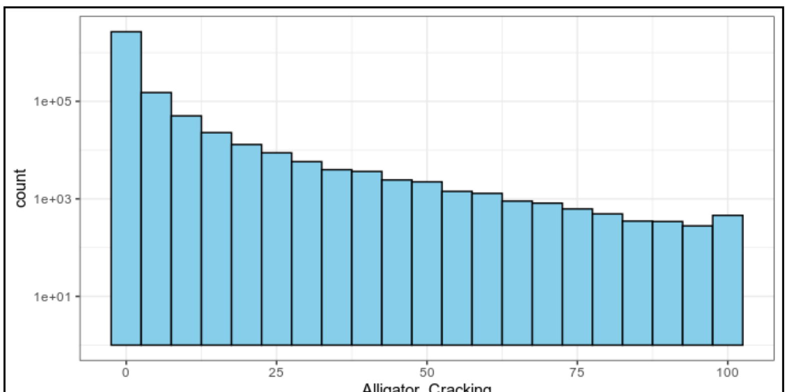

probs	10.0%	25.0%	50.0%	75.0%	95.0%	99.0%	99.9%	100.0%
percentile	0	0	0	0	6	25	70	100

(h) Alligator Cracking

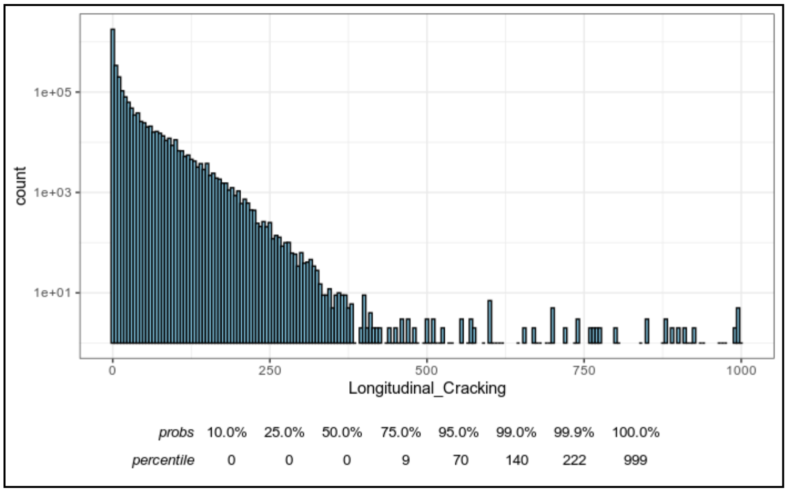

(i) Longitudinal Cracking

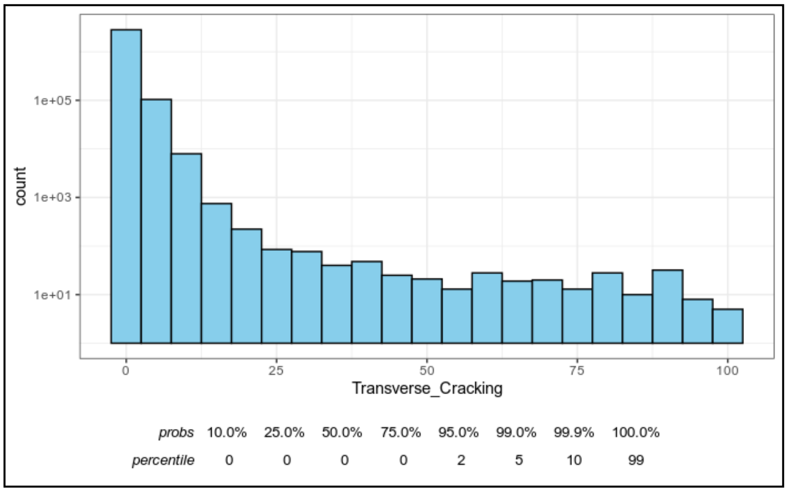

(j) Transverse Cracking

Figure 3.3 Distribution of Flexible Pavement Distresses

3.2.2 Limitations of Analysis Data

During the preparation of the database, the research team addressed many challenges, including insufficient observation length, non-increasing deterioration trends, presence of outliers, rut buckets models, and limited treatment type information. The causes of these issues included the data collection process, missing or erroneous information, or unobserved heterogeneities. To handle these issues, the following approaches were followed.

3.2.3.1. Insufficient Observation Length

A significant number of pavement sections in the database had fewer than three observations, and most of the corresponding records were aged one or two years after previous maintenance or rehabilitation work. Since at earlier ages, pavements generally exhibit extremely low severity of distresses, incorporating these sections would substantially undermine the predictions for old pavements. Consequently, in this project, 6,484 sections out of 13,378 (48 percent) with less than three years of observations were removed from the analysis data, which corresponds to 11,840 out of 54,151 records (22 percent).

3.2.3.2. Non-increasing Trend

Another issue was that between two consecutive maintenance or rehabilitation works, some distress observations exhibited lower values than preceding years, which compromised the assumption that distresses increase with time if no maintenance or rehabilitation work is applied. To address this issue, cumulative maximum adjustments were implemented for each unique pavement section. As shown in Figure 3.4 (on the left), before the adjustment, three measurements are lower than preceding measurements. Applying the cumulative maximum adjustment, which consisted of replacing a measurement at a given age by the maximum preceding measurement, yielded the results depicted in Figure 3.4 on the right.

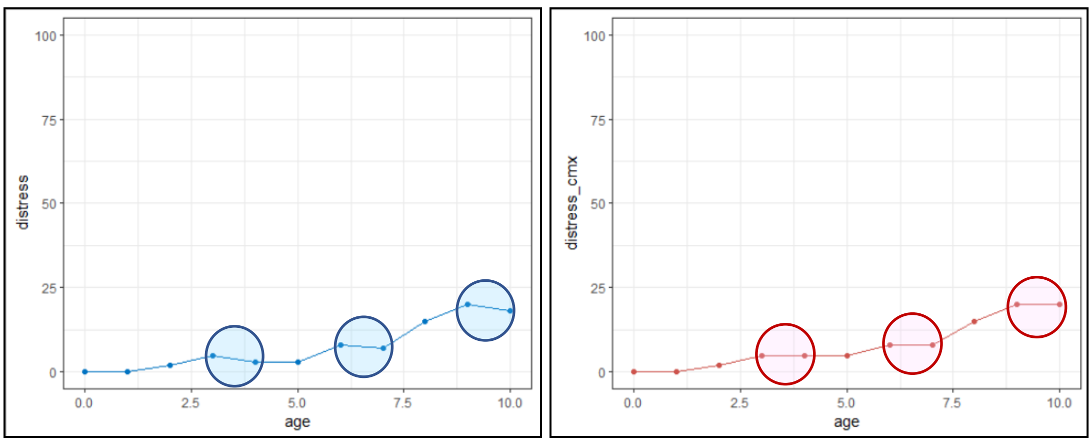

Figure 3.4 Cumulative Maximum Adjustment

To illustrate the impact of this approach, the scatter plots and boxplots of longitudinal cracking along with the deterioration curves (gray lines) for each pavement section are presented in Figure 3.5. Before the adjustment, even though there is an overall increasing trend in the data, the trend was not significant and there is a sharp decreasing trend between ages 15 and 16. This is most likely due to missing work history data. Furthermore, the deterioration curves are very scattered with no consistent increasing trend. In contrast, after the adjustment, not only does the overall increasing trend of the data get more reasonable, but also the deterioration curves exhibit increasing trends.

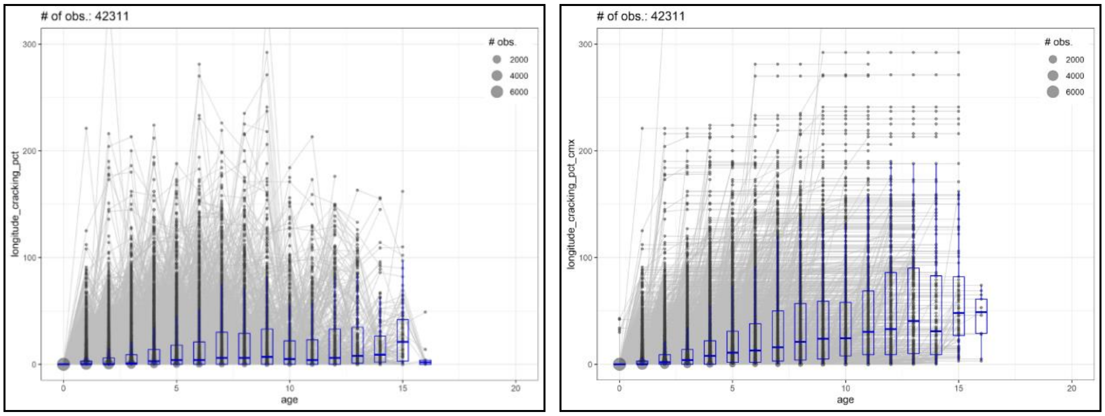

Figure 3.5 Longitudinal Cracking Distribution Before and After Adjustment

3.2.3.3. Outliers

Figure 3.6 provides an example of the change of longitudinal cracking for a set of pavement sections grouped by the same functional class, traffic, pavement type, and climate zone. As shown, outliers can be found at almost every age, most likely caused by data collection errors or inaccurate pavement M&R history information. Incorporation of these outliers into the model development could substantially hinder the model performance; therefore, when performing model estimation, outliers due to measurement error for each group of data at each age were removed.

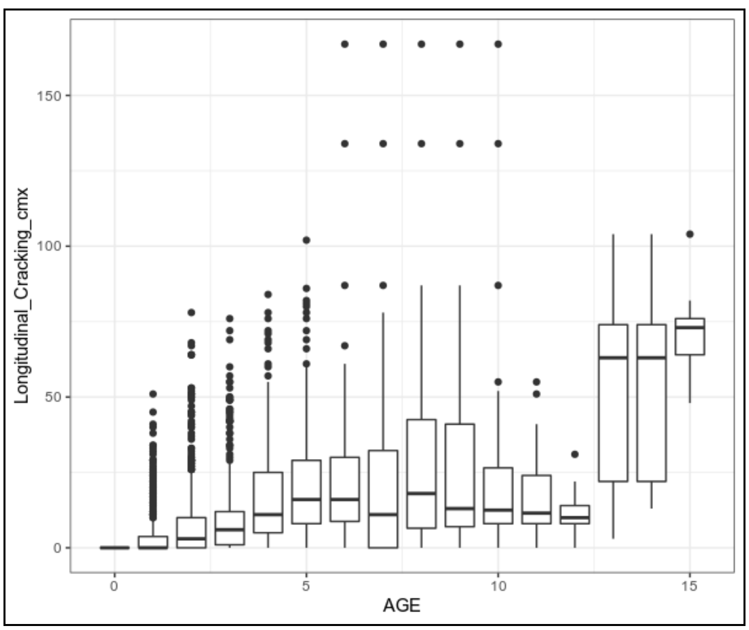

Figure 3.6 Example of Group Longitudinal Cracking Changes

3.2.3.4. Rut Bucket Models

In PA, rutting is categorized into "buckets" based on different surface rut depth ranges. These buckets are no-rut, shallow rut, deep rut, severe rut, and failure rut. Each pavement section was evaluated by the percentages of area for each rut bucket, which requires the sum of the five buckets to be 100 percent. In the current rut models, all the rut buckets were modeled as s-shape curves with asymptotic values of 100 percent. These models are physically incorrect because these rut buckets are not independent and will not increase continuously, with the exception of failure rut, which will increase all the time. For instance, starting from age zero, with the increase of rut depth, the shallow rut will increase initially. However, after a certain period, the rut depths of some locations will exceed the threshold between the shallow rut and deep rut. As a result, the shallow rut will start to decrease. This can also happen between the deep rut and severe rut, and severe rut and failure rut. Nevertheless, the current rut models do not account for these transitions, and because 100 percent was used as the asymptotic values for all the rut buckets, it is possible that at some point, the sum of predictions of rut buckets could exceed 100 percent.

Regarding the issues with the rut bucket model, the research team has proposed several alternatives to TxDOT. However, because of the constraints posed on the implementation of the models into PA, the development of rut bucket models using a formulation different from other distresses is not practical. Therefore, in this project, following TxDOT guidance only an interim approach by limiting the asymptotic values was adopted.

3.2.3.5. Limited Treatment Type Information

In Texas, based on work intensity, treatments intended to improve pavement performance are generally divided into four categories: PM, LRhb, MRhb, and HRhb. It is expected that if a pavement section receives HRhb, it will perform better than if it receives MRhb, LRhb, or PM. However, in this project, very limited information about treatment type was available and these data were highly variable and did not show any reasonable trends. For example, preliminary analysis indicated that for pavements with similar characteristics, performance curves of these four treatment types crossed each other, and in some cases, pavements treated by PM can even perform better than LRhb or even MRhb. As a result, performance models developed using this treatment type information would result in inconsistent models and induce poor M&R decisions.

Because of the high variability of treatment type information, this project adopted a probabilistic approach to supplement the treatment type information. For each group of pavement sections with the same functional class, traffic pavement type, and climate zone at each age, the bottom 25 percent of the data were assigned to HRhb, the bottom 50 percent of the data were treated as MRhb, and the bottom 70 percent of the data were assigned to LRhb. The data between 15th and 75th percentiles were allocated to PM. Moreover, all the data above 15th percentile were grouped as "do nothing" (DN). These values were adopted through a trial-and-error iterative approach so that all models representing each type of treatment was reasonable and matched the corresponding data. In this way, five separate databases for each type of distress were created and then combined to develop performance models, and it is expected that the results will follow the order of performance for different treatment types.

3.3. Model Specification

One of the main technical objectives of this project was to calibrate the current model coefficients for the existing model and to incorporate treatment type. Therefore, the research team used the same model specification as presented in the TxDOT's research study for calibrating the original models (Gharaibeh et al., 2012), which was slightly modified from the original model (Stampley, 1995). The current prediction models of the level of distress have a specification as shown in the following equation.

$$L_i = \alpha \exp\left(-\frac{A}{age}\right)^{\beta}$$

where,

L_i: level of distress in a pavement section.

α: horizontal asymptote factor that represents the maximum range of distress growth.

β: a slope factor that controls how steeply utility is lost in the middle of the curve.

A: multiplication of four parameters defined in the original model: ρ, χ, ϵ, and σ.

ρ: prolongation factor that controls the time it takes before significant increases in distress occur.

χ: the traffic weighting factor that controls the effect of an 18-k ESAL on performance.

ϵ: climate weighting factor that controls the effect of rainfall and freeze-thaw cycles on performance.

σ: subgrade weighting support factor that controls the effect of subgrade strength on performance.

age: pavement age of section, in years.

Since the four parameters on the numerator in the original model specification (ρ, χ, ϵ, and σ) cannot be estimated separately, here the parameter A replaces them and acts as a prolongation factor.

3.3.1. Model Specification for This Study

In this part of the project, the same specification of the current model was used. However, instead of parameters A and β, A^* and β^* were estimated because the research team incorporated the differences between variable groups in the parameter β^*, and incorporated the differences between treatment levels in the parameter A^*. Here, β^* is the sum of a coefficient represents all data (fixed effects β) and coefficients represent variable groups (random effects γ_k). The difference between the five treatment levels—DN, PM, LRhb, MRhb, and HRhb—were incorporated in the parameter

A^* so that there are five different coefficients for each distress. The following equation is the model specification used in the study.

$$L = \alpha \exp\left(-\frac{A^*}{age}\right)^{\beta^*}$$

with,

$$\beta^* = \beta + \gamma_k$$

where,

A^*: A_j with j = treatment levels

β: fixed effects coefficients

γ_k: random effects coefficients for variable group k

The estimation of the parameters of this specification was made possible by applying nonlinear mixed effects model and by pulling together data all instead of estimating models for each variable group with partial data. This produces a more efficient model and results in better parameter statistics. The nonlinear mixed effect model and the estimation process are explained in more details in the next section.

3.4. Model Estimation

3.4.1. Nonlinear Mixed-effects Models

The research team used nonlinear mixed effects models, also known as nonlinear multilevel models and nonlinear hierarchical models, for the calibration process. Mixed-effects models are generally used when data consist of groups of observations. The fixed-effects parameters describe the overall patterns of the data. On the other hand, random-effects parameters describe specific groups. If the model is nonlinear in the parameters, it is called a nonlinear mixed-effects model (Davidian & Giltinan, 2003).

Growth data where the change is nonlinear is a typical type of data modeled with nonlinear mixed-effect models. In this project, the level of distress increases over time (age) in a nonlinear fashion. In such a situation, the fixed effects describe the change of the level of distress for the entire network, whereas the random effects represent variability between variable groups. That is, it differentiates the effects on groups of IH, thick pavement, heavy traffic, and central climate zone from that on groups of FM road, thin pavement, low traffic, and north climate zone, and so on.

The general model for a mixed effects model is

$$y_{it} = f(z_{it}, b_{ki}) + e_{it}$$

with,

$$b_{ki} = \beta_k + r_{ki}$$

where, y_{it} is the dependent variable for individual $i = 1, \ldots, n$ measured repeatedly at times $t = 1, \ldots, T_i$, following the functional form f, which depends on the parameters b_{ki} for $k = 1, \ldots, k$ and z_{it}. The random effects, r_{ki} and the error term e_{it}, have means of 0, and are typically assumed to follow a normal distribution (Pinheiro & Bates, 2000). In this study z_{it} term is age and b_{ki} is β^* as described in the previous section.

3.4.2. Estimation Process

For estimating the nonlinear mixed models, the research team used the "nlme" package of the program language R (R Core Team, 2019; Pinheiro et al., 2017). The nlme package of R is capable of fitting nonlinear mixed effects models using an algorithm developed by Lindstrom and Bates (1990). This iterative algorithm alternates between two steps: a penalized nonlinear least squares (PNLS) step and a linear mixed effects (LME) step. In the PNLS step, the current estimate of the random effects is fixed, and the estimates of the fixed effects are obtained by minimizing the PNLS function. On the other hand, the LME step uses the current estimates of the fixed effects to estimate the random effects based on a first-order Taylor series expansion. In the LME step, a hybrid method mixing expectation-maximization (EM) algorithm and the Newton-Raphson algorithm is used. This hybrid method is beneficial because it combines the advantageous characteristics of each algorithm. The EM algorithm does not suffer from poor starting points, whereas the Newton–Raphson algorithm does but is much faster (Lindstrom & Bates, 1990).

In the estimation process, the researchers first specified the model as described in the previous section. There were three parameters to be estimated in the model specification. However, they were reduced to two parameters because the asymptote value α was estimated from data directly using the distribution of the actual data rather than a preselected level. The researchers selected 99.9 percentile of each level of distress using the entire network data from 1993 to 2019 as an α value as Table 3.3 shows. By doing so, the models excluded extreme outliers that hinder the convergence of the model estimation process.

The research team specified the fixed effects A and β and specified the random effects on β to incorporate the variability between variable groups. The researchers needed to specify the starting values for each fixed parameter. We found that the algorithm used in the nlme package was sensitive to the starting points. Therefore, if appropriate starting values were not provided, the model would either never converge or produce poor estimates. To select a proper set of starting values, the researchers followed an iterative estimation process. We first set a range of each parameter, then picked a random value from the uniform distribution of the parameter range. We estimated a model using those random selections as starting points and checked if the model converged. This process iterated for several hundred times until the models converged. In the case of multiple converging models for a distress type, Akaike Information Criterion (AIC) values were compared to evaluate the goodness-of-fit of the various models. The model with the lower AIC value among the multiple converging models was selected as the best fit model.

3.4.2.1. Treatment Level

The effect of the treatment levels was incorporated into the parameter A. Due to the lack of sufficient accurate data that contains treatment level information, the researchers determined the coefficients for each treatment level from the data following a probabilistic approach. The detailed procedure is explained in the next chapter when the alternative models are presented.

3.5. Estimation Results

As a result of the nonlinear mixed effects model estimation, the researchers estimated the model parameters for eight different distresses. The outcomes consist of fixed effects and random effects. The fixed effects outcome is shown in Table 3.4. In the table, the fixed effects model coefficients α, β, and A are presented with their standard errors and p-values.

Table 3.4 Summary of the Fixed Effects Models

Distress	alpha	effect	term	estimate	std.error	df	statistic	p.value
Shallow Rut	63	fixed	A	136.6	10.63	42222	12.8	< 0.00001
		fixed	beta	0.2453	0.0120	42222	20.4	< 0.00001
Deep Rut	23	fixed	A	1,679	349.2	42222	4.8	< 0.00001
		fixed	beta	0.2143	0.0102	42222	21.0	< 0.00001
Patching	100	fixed	A	104.8	7.417	42222	14.1	< 0.00001
		fixed	beta	0.4590	0.0196	42222	23.4	< 0.00001
Failure	10	fixed	A	21.82	0.6936	42222	31.5	< 0.00001
		fixed	beta	1.891	0.1651	42222	11.4	< 0.00001
Block Cracking	70	fixed	A	22.17	0.6495	42222	34.1	< 0.00001
		fixed	beta	3.597	0.3460	42222	10.4	< 0.00001
Alligator Cracking	73	fixed	A	23.97	0.3815	41796	62.8	< 0.00001
		fixed	beta	1.242	0.0760	41796	16.3	< 0.00001
Longitudinal Cracking	230	fixed	A	17.58	0.1905	42222	92.3	< 0.00001
		fixed	beta	0.9497	0.0871	42222	10.9	< 0.00001
Transverse Cracking	12	fixed	A	23.45	0.5030	42222	46.6	< 0.00001
		fixed	beta	1.106	0.0809	42222	13.7	< 0.00001

As for the random effects, there are 81 different estimates for each variable group. That is because in the database, we have 81 groups out of 160 possible variable combinations, i.e., highway function (4) x traffic level (4) x pavement type (2) x climate zone (4). As shown in Figure 3.7, the sample data with 81 groups has very strong correlations with population with respect to the amount of data. Thus, the researchers concluded that those 81 groups of data reasonably represent the entire network.

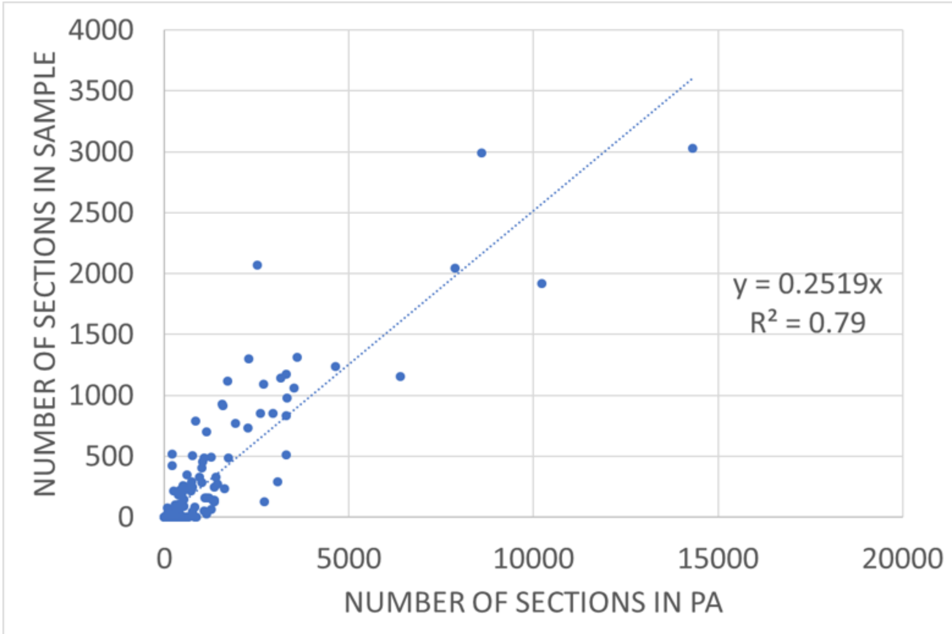

Figure 3.7 Correlation between Population and Sample in Terms of the Number of Data

In addition, the following criteria was used to obtain models for other groups for which data was not available or insufficient:

(1) If highway function, traffic class, and pavement type are the same, use the model for "central" climate zone.

(2) If highway function, pavement type, and climate zone are the same, use models for a higher traffic class.

These criteria are explained in Figure 3.8. The shaded rows indicate the 81 groups for which data were available and a model was estimated. In the case of the first five rows, none of the rows have an estimated model, so the models of the higher traffic class were assigned, following a conservative approach. In another cases, when there is no estimated model for a certain climate zone, the model of central climate zone is assigned to another climate zone group. In this manner, all the models for 160 variable groups were obtained. Appendix B contains all model coefficients for all groups and distresses.

combo	highway_fun	pavement_typ	traffic_cls	climate_zone	n	percentage	n_record
136	FM	thick	heavy	central	656	0.3%	NA
137	FM	thick	heavy	east	620	0.3%	NA
138	FM	thick	heavy	north	35	0.0%	NA
139	FM	thick	heavy	south	215	0.1%	NA
140	FM	thick	heavy	west	186	0.1%	NA
131	FM	thick	high	central	1272	0.7%	496
132	FM	thick	high	east	2511	1.3%	2070
133	FM	thick	high	north	186	0.1%	42
134	FM	thick	high	south	851	0.5%	791
135	FM	thick	high	west	96	0.1%	27
121	FM	thick	low	central	1152	0.6%	25
122	FM	thick	low	east	2718	1.4%	126
123	FM	thick	low	north	461	0.2%	6
124	FM	thick	low	south	405	0.2%	109
125	FM	thick	low	west	52	0.0%	NA

Figure 3.8 Criteria to Obtain Models for Other Groups Outside of the Sample Data

3.5.1. Figures of the Estimated Models

In this section, the resulting network level models were plotted to assess their goodness of fit visually. For each distress type, fixed effects models for the entire data set and the final models for 81 individual groups are presented in Figures 3.9 through 3.24. Note that each plot has data represented by points and boxplot, and model predictions in lines for each treatment level.

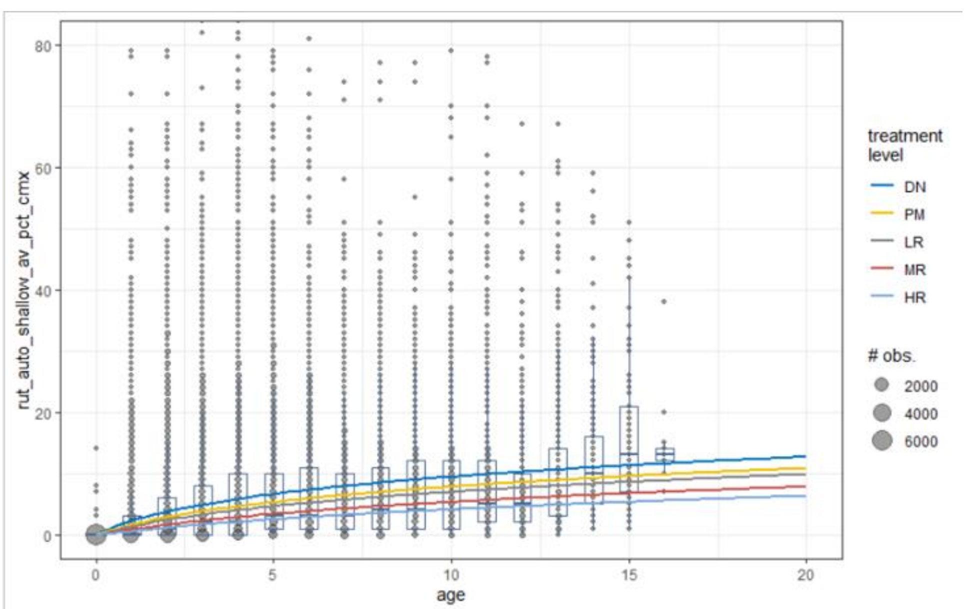

Figure 3.9 Fixed Effect Models: Shallow Rut

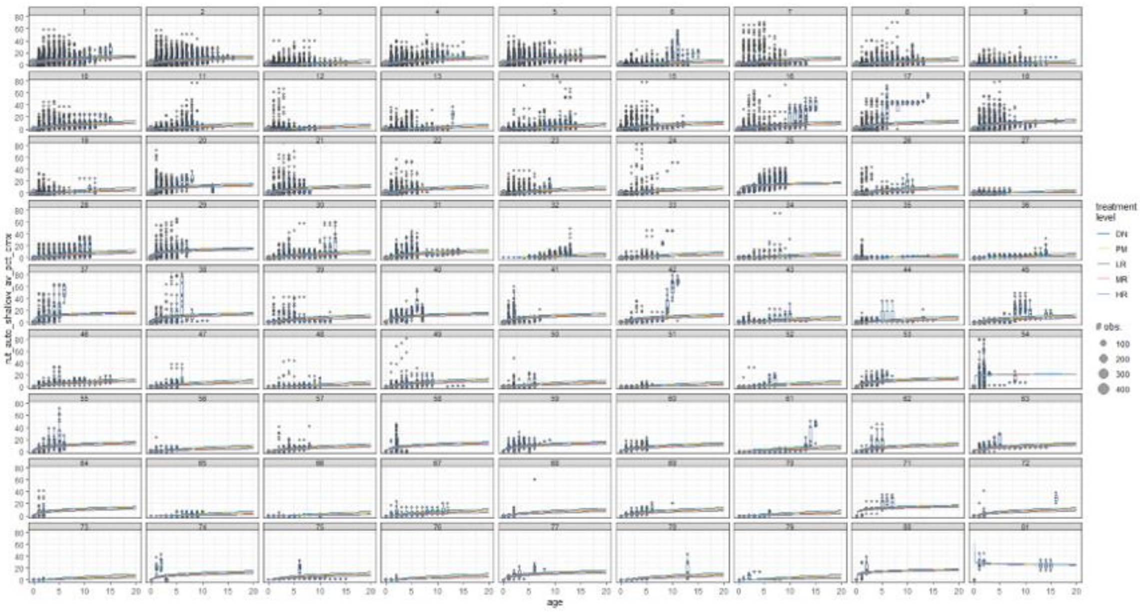

Figure 3.10 Individual Models for 81 Variable Groups: Shallow Rut

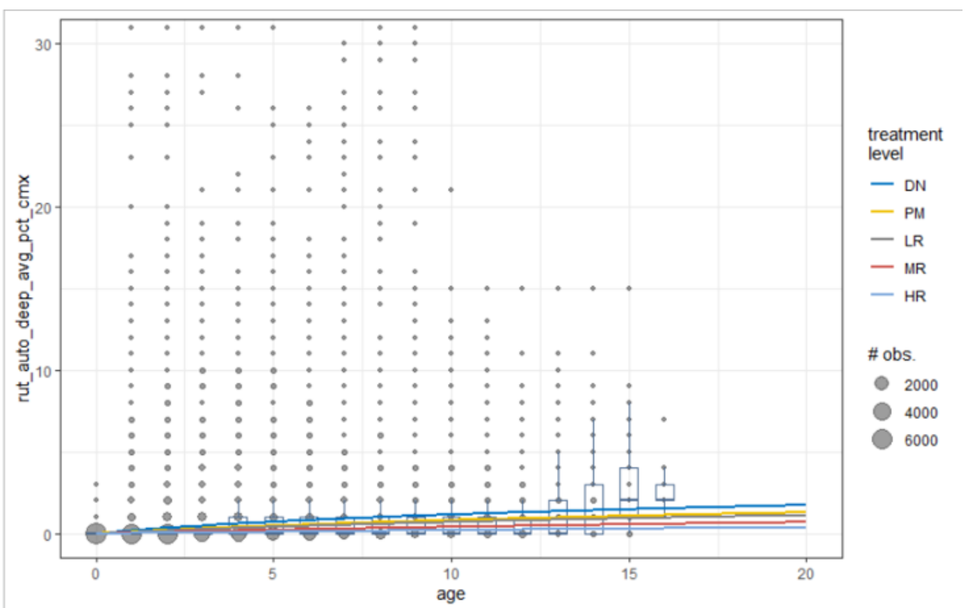

Figure 3.11 Fixed Effect Models: Deep Rut

Figure 3.12 Individual Models for 81 Variable Groups: Deep Rut

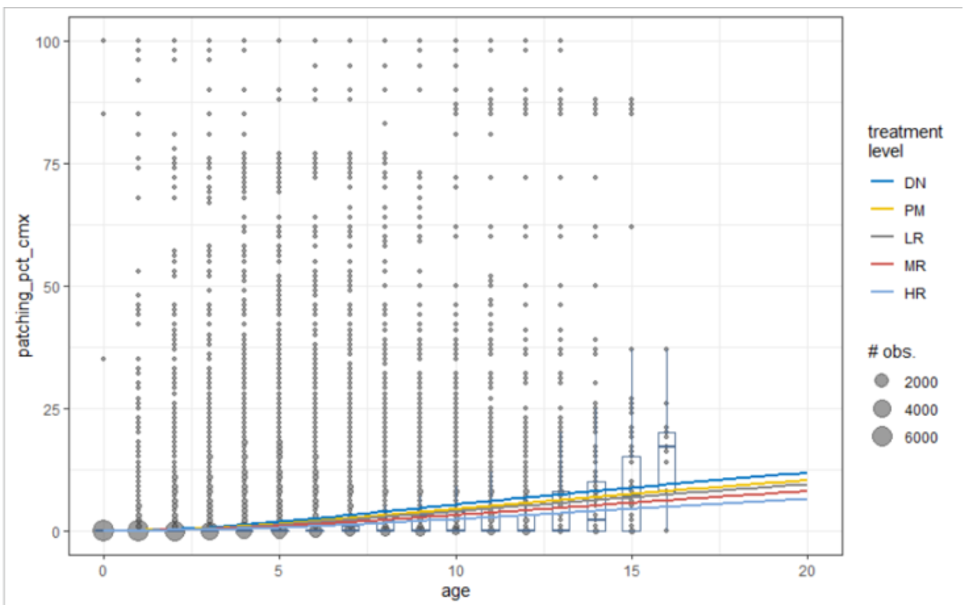

Figure 3.13 Fixed Effect Models: Patching

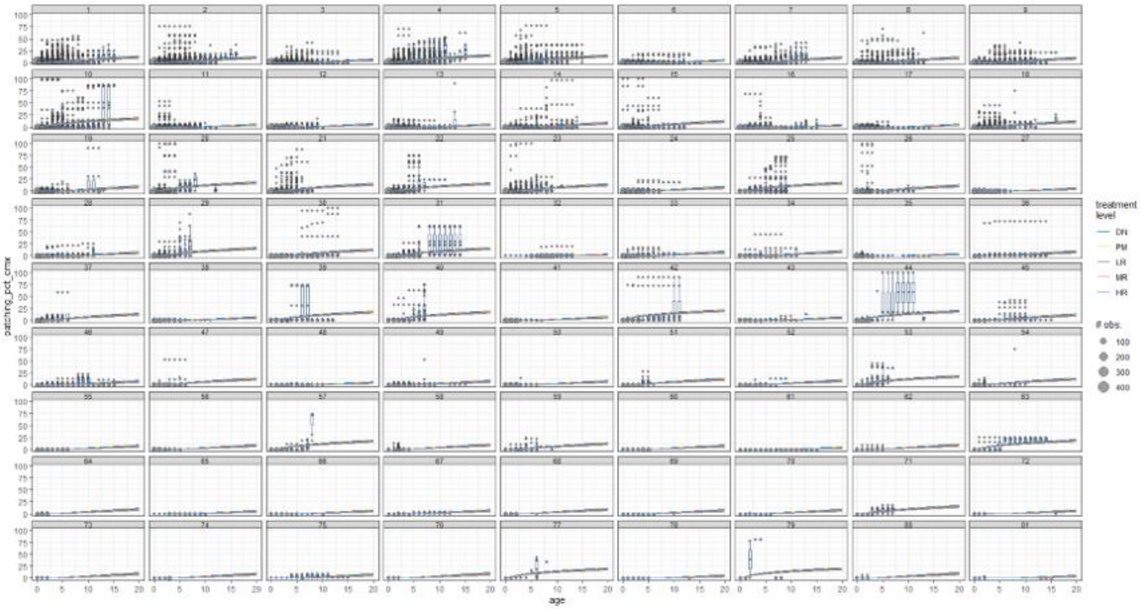

Figure 3.14 Individual Models for 81 Variable Groups: Patching

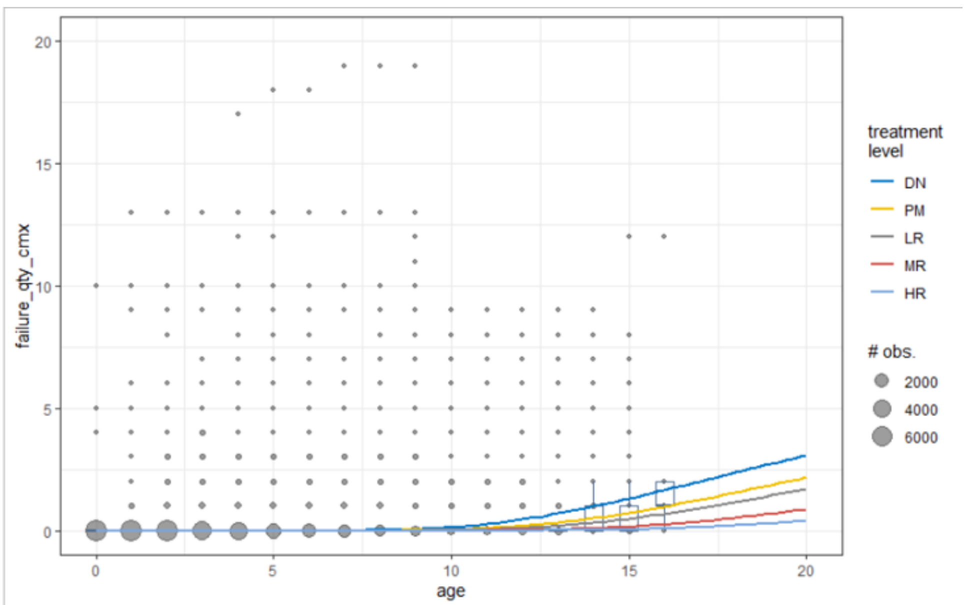

Figure 3.15 Fixed Effect Models: Failure

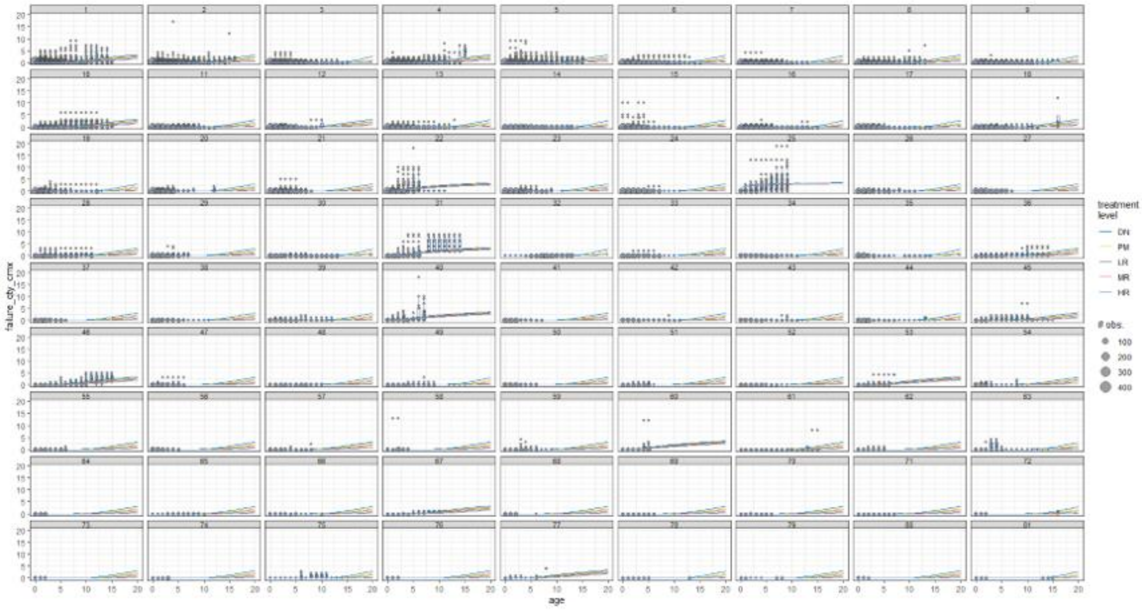

Figure 3.16 Individual Models for 81 Variable Groups: Failure

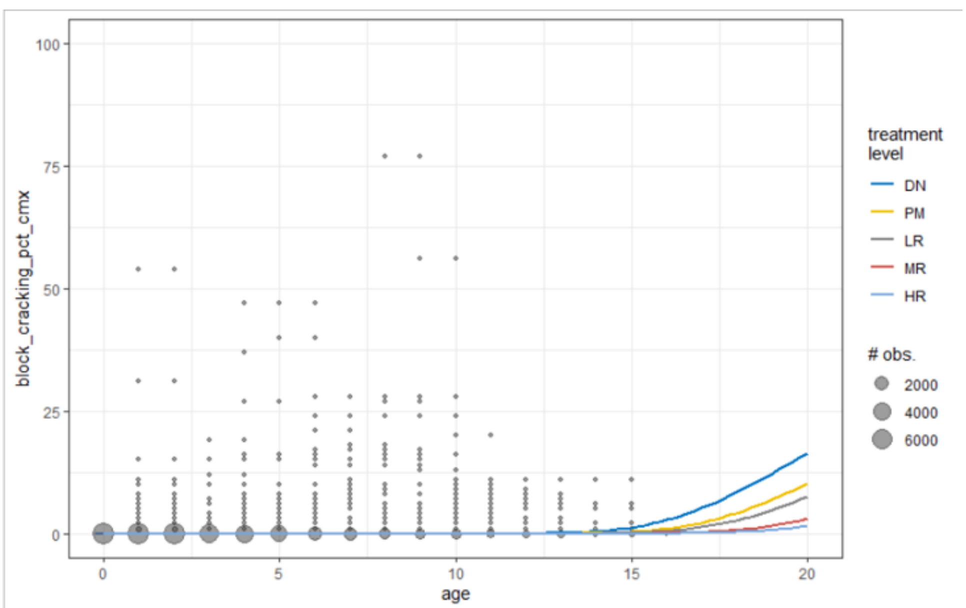

Figure 3.17 Fixed Effect Models: Block Cracking

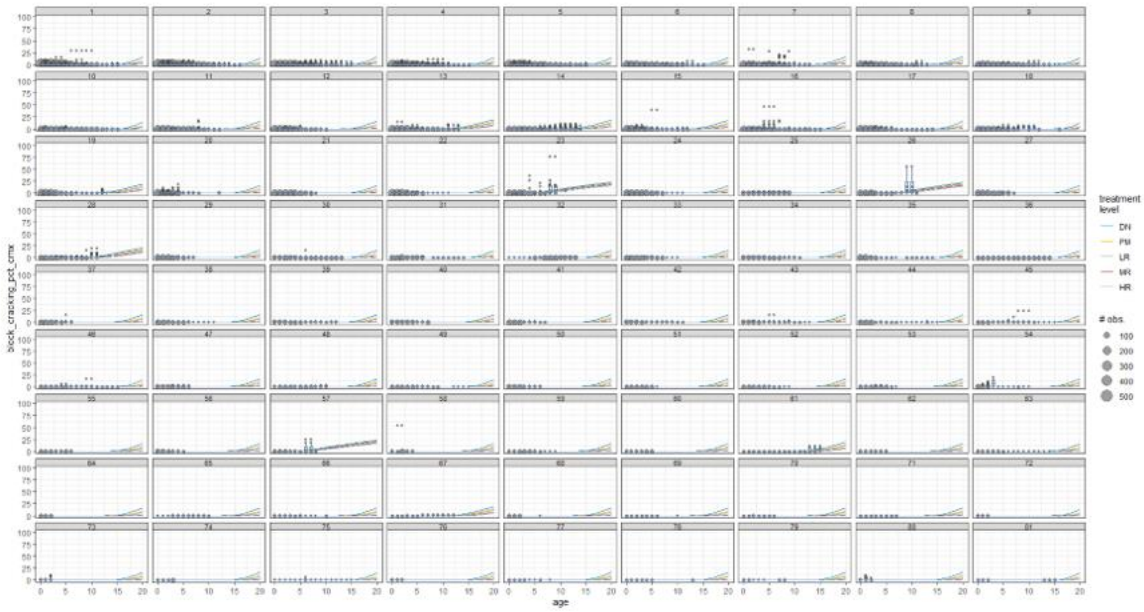

Figure 3.18 Individual Models for 81 Variable Groups: Block Cracking

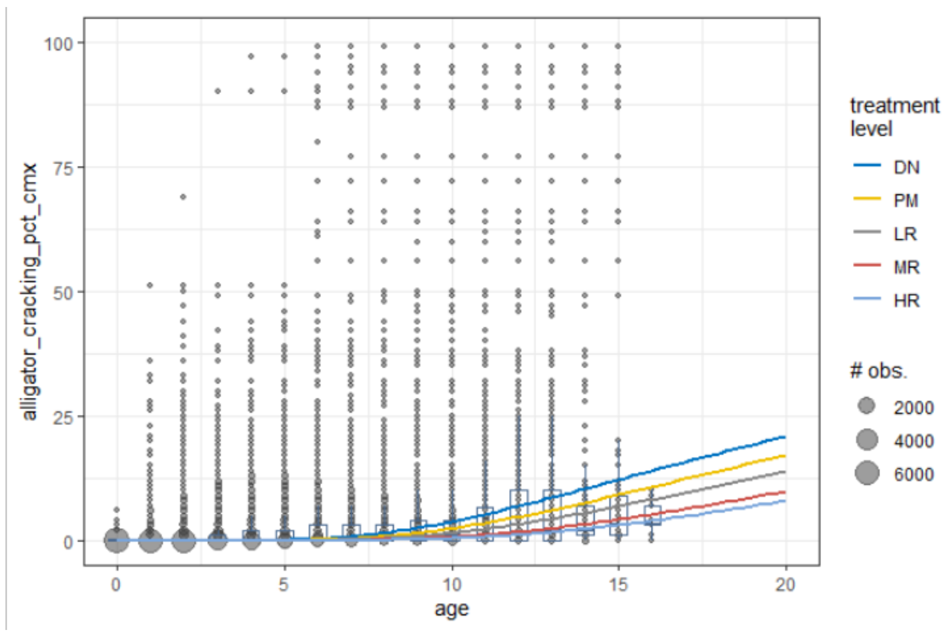

Figure 3.19 Fixed Effect Models: Alligator Cracking

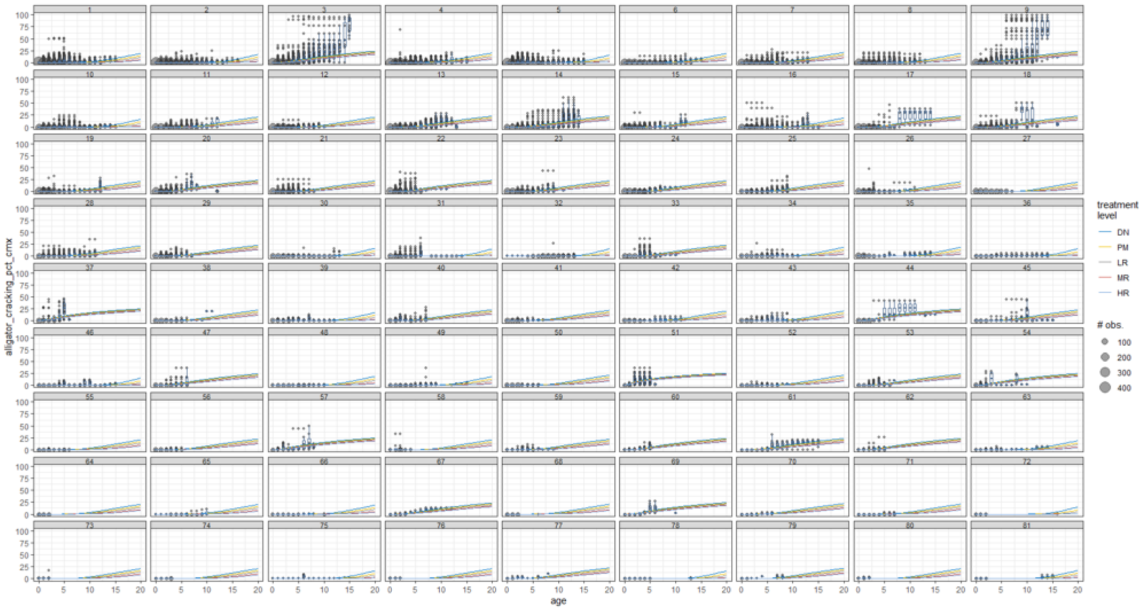

Figure 3.20 Individual Models for 81 Variable Groups: Alligator Cracking

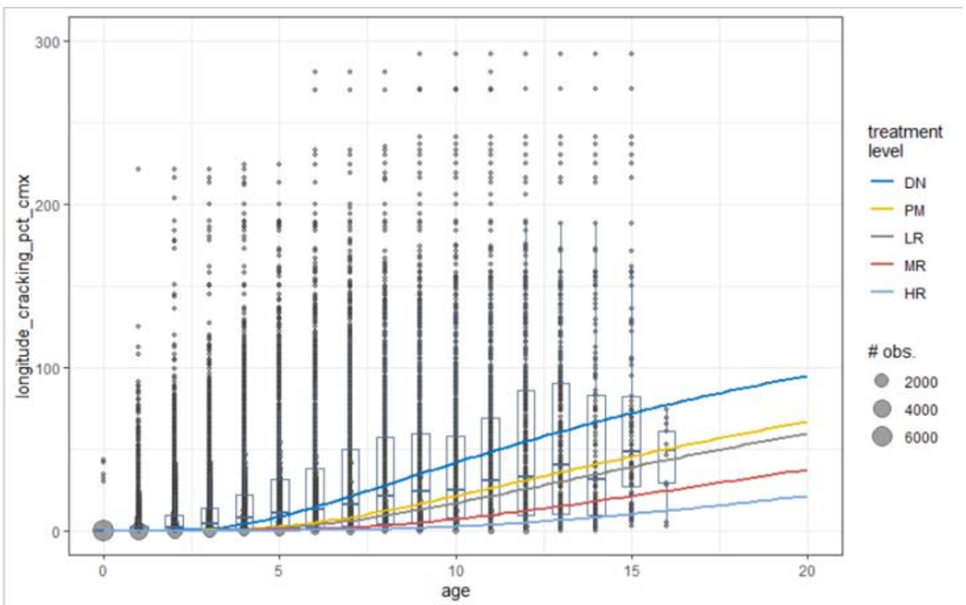

Figure 3.21 Fixed Effect Models: Longitudinal Cracking

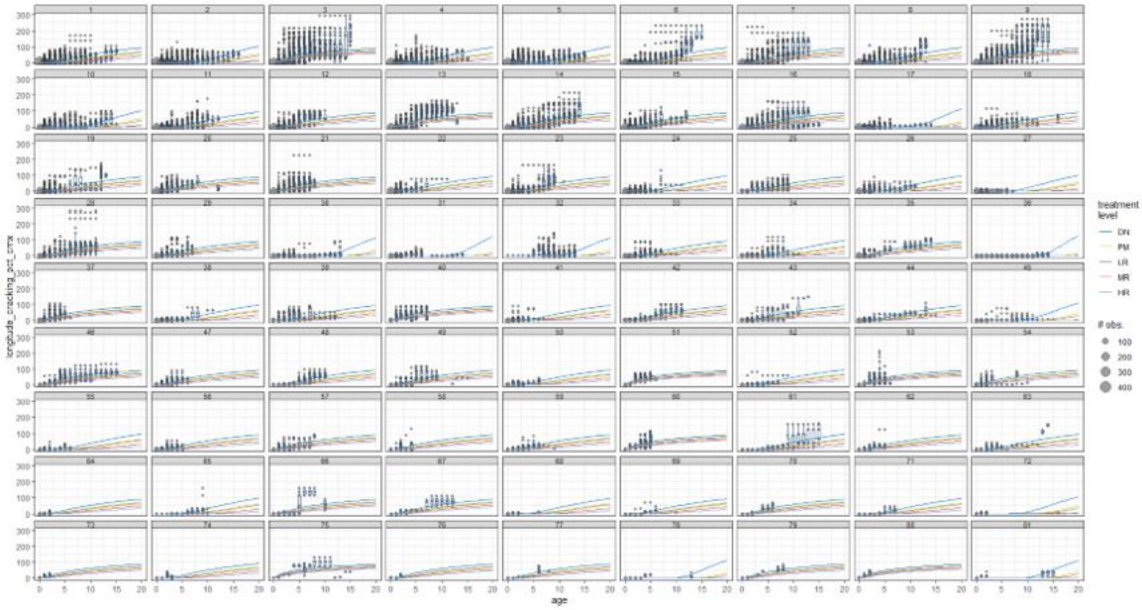

Figure 3.22 Individual Models for 81 Variable Groups: Longitudinal Cracking

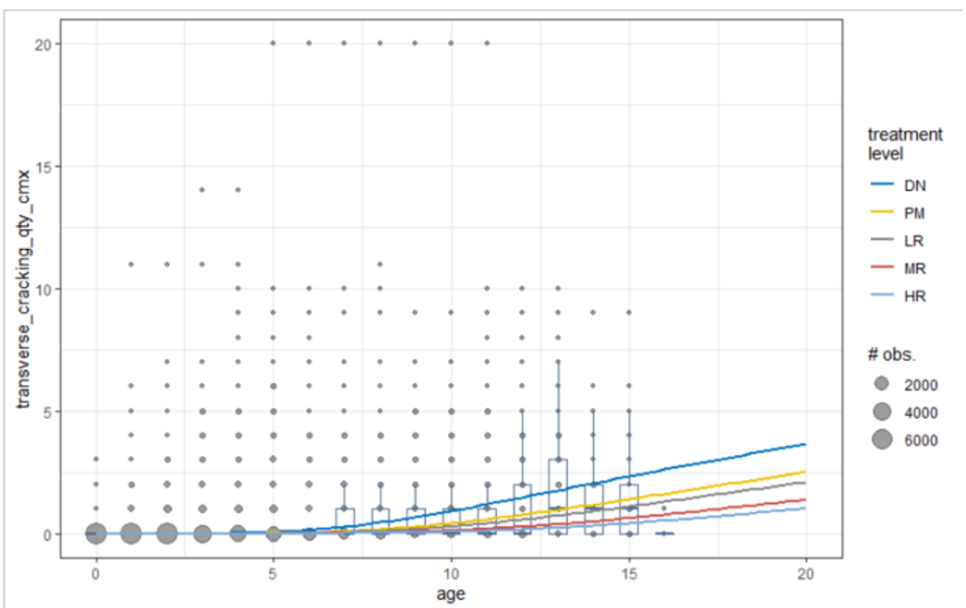

Figure 3.23 Fixed Effect Models: Transverse Cracking

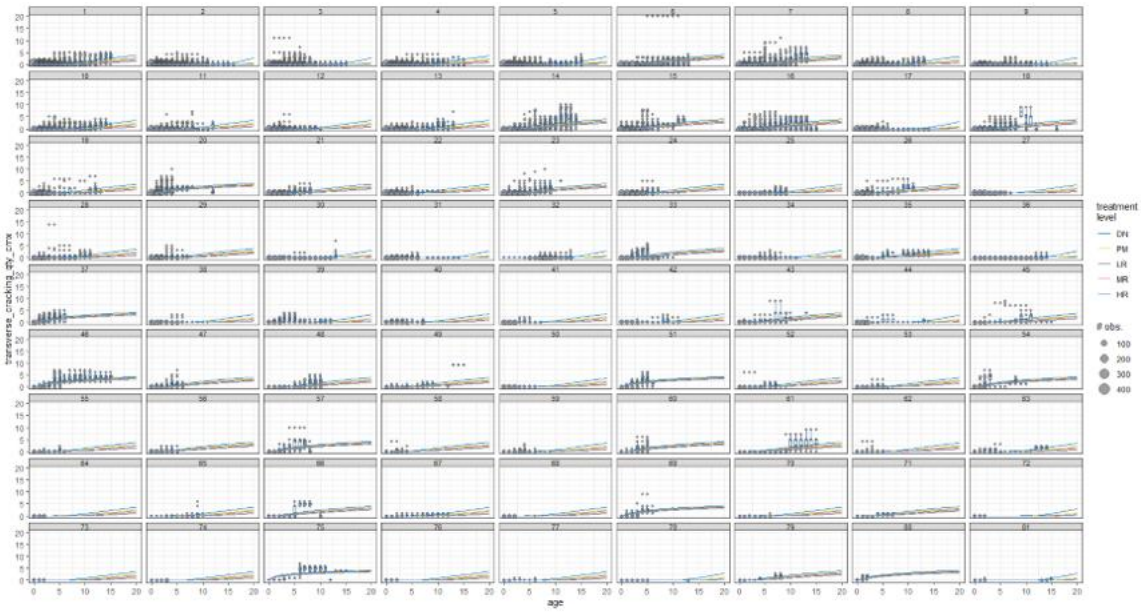

Figure 3.24 Individual Models for 81 Variable Groups: Transverse Cracking

Chapter 4. Development of Alternative Deterioration Models

In this chapter, we present the development and estimation of alternative deterioration models for flexible pavements. Firstly, a brief introduction about the alternative model specification is presented, followed by the various approaches proposed to conduct the model estimation.

4.1. Alternative Model Specification

In the current pavement deterioration models, traffic, climate, and subgrade factors were incorporated as a product in the numerator; as a result, direct estimation of these parameters is not mathematically feasible. The model parameters could be estimated only through a stratified grouping approach based on climate, pavement type, treatment type, and traffic. Although the models can perform well for each subgroup, for pavements with the same climate, pavement type, and traffic characteristics, the arrangement of the stratified group system could generate curves that cross for different types of treatments or predictions where the LRhb treatments could perform better than HRhb treatments. Additionally, another significant limitation of the current model is that the pavement age appears as a denominator; consequently, pavement distress at age zero (time of construction) cannot be estimated. In brief, due to the current model specification, the predictions from current models could be, at times, unreasonable and result in unrealistic predictions when preparing maintenance or rehabilitation plans, such as the 4-year plan. As a result, TxDOT decided to conduct a full review of the current model specifications and implement new model specifications to address these issues.

To address issues of the current models, this project report proposes three alternative s-shaped model specifications, detailed in this chapter. It should be noted that, in creating these models, the researchers were constrained by TxDOT to employing an s-shaped curve with a small number of parameters, due to practical issues related to the implementation of the potential new models into PA.

4.1.1. Alternative Models

4.1.1.1. Alternative Model One

$$L = \frac{\beta_0}{1 + \beta_1 \exp(-\beta_2 \cdot Age)}$$

where,

L : distress density,

Age : independent variable that accounts for the age of the pavement section,

β_0 : asymptotic parameter that captures the maximum level of distress as the age of the pavement section tends to infinity,

β_1, β_2 : regression parameters, which could be specified as a function of traffic, environmental conditions, subgrade, location, and any other relevant variables.

The first alternative model has three parameters. Since β_0 represents the maximum value for each type of distress, its value is predetermined for each type of distress before the model estimation, while the values of β_1, β_2 will be determined based on the data and reflect the inherent trend. The effects of β_1, β_2 on the first alternative model are illustrated in Figure 4.1. According to these plots, with the increase in β_1 or decrease in β_2, alternative Model One will predict lower distress values.

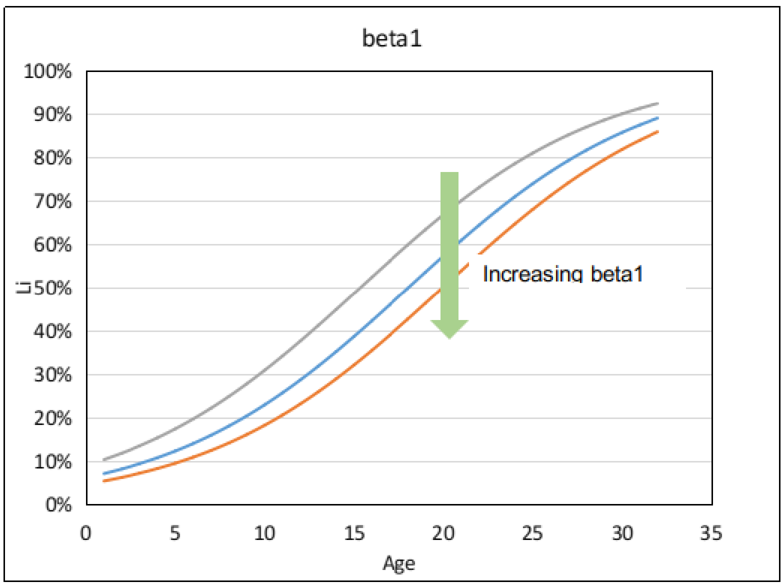

(a) beta1

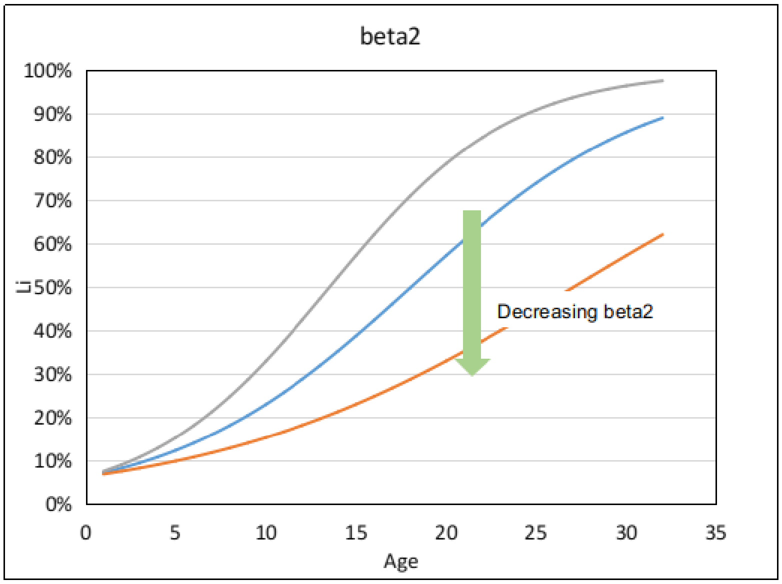

(b) beta2

Figure 4.1 Effect of Regression Parameters on Alternative Model One

In contrast to the current models, in alternative Model One, the pavement age is not in the denominator; therefore, it is easy to compute the distress at age zero:

$$L_0 = \beta_0/(1+\beta_1)$$

Moreover, for a pavement section with known distress value L_i, its corresponding age can be approximated using:

$$Age_i = \frac{1}{\beta_1} ln\left(\frac{\beta_1 L_i}{\beta_0 - L_i}\right)$$

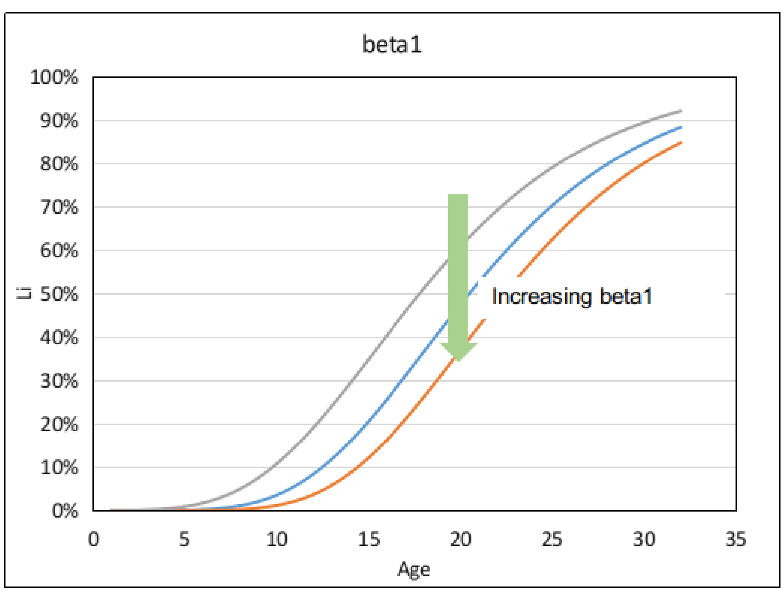

(a) beta1

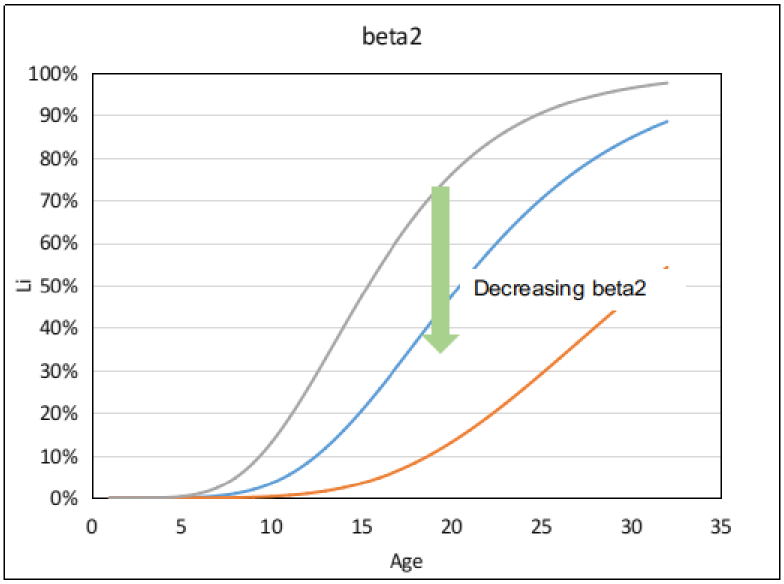

(b) beta2

Figure 4.2 Effect of Regression Parameters on Alternative Model Two

4.1.1.2. Alternative Model Two

$$L = \beta_0 \exp(-\beta_1 \cdot e^{-\beta_2 Age})$$

where,

L : distress density,

Age : independent variable that accounts for the age of the pavement section,

β_0 : asymptotic parameter that captures the maximum level of distress as the age of the pavement section tends to infinity,

β_1 : maximum drop from the final level of distress at $Age = 0$,

β_1, β_2 : regression parameters, which could be specified as a function of traffic, environmental conditions, subgrade, location, and any other relevant variables.

The second alternative model also has three parameters. Similarly, since β_0 represents the maximum value for each type of distress, its value is predetermined for each type of distress before the model estimation, while the values of β_1, β_2 will be determined based on the data and reflect the inherent trend. The effects of β_1, β_2 on alternative Model Two are illustrated in Figure 4.2. According to these plots, with the increase of β_1 or decrease in β_2, alternative Model Two will predict lower distress values.

Similar to alternative Model One, by setting Age = 0, the distress at age zero for alternative Model Two can be easily calculated as $L_0 = \beta_0 \exp(-\beta_1)$. For pavement section with known distress value L_i, its corresponding age can be approximated using:

$$Age_i = -\frac{1}{\beta_2} ln\left[ln\left(\frac{\beta_0}{L_i}\right)^{1/\beta_1}\right]$$

4.1.1.3. Alternative Model Three

$$L = \beta_0 - \beta_1 \exp(-\beta_2 \cdot Age^{\beta_3})$$

where,

L : distress density,

Age : independent variable that accounts for the age of the pavement section,

β_0 : asymptotic parameter that captures the maximum level of distress as the age of the pavement section tends to infinity,

β_1 : maximum drop from the final level of distress at $Age = 0$,

β_2, β_3 : regression parameters, which could be specified as a function of traffic, environmental conditions, subgrade, location, and any other relevant variables.

The third alternative model has four parameters. Of these, β_0 represents the maximum value for each type of distress; its value is predetermined for each type of distress before the model estimation and, together with β_1, it determines the initial distress value, $L_0 = \beta_0 - \beta_1$, after maintenance or rehabilitation works. It is evident that if a smaller β_1 were used, a higher initial distress value would be obtained, and the model would predict higher distresses. The effects of β_1, β_2 on alternative Model Three are illustrated in Figure 4.3. According to these plots, with the decrease of β_2 and β_3, alternative Model Three will predict lower distress values.

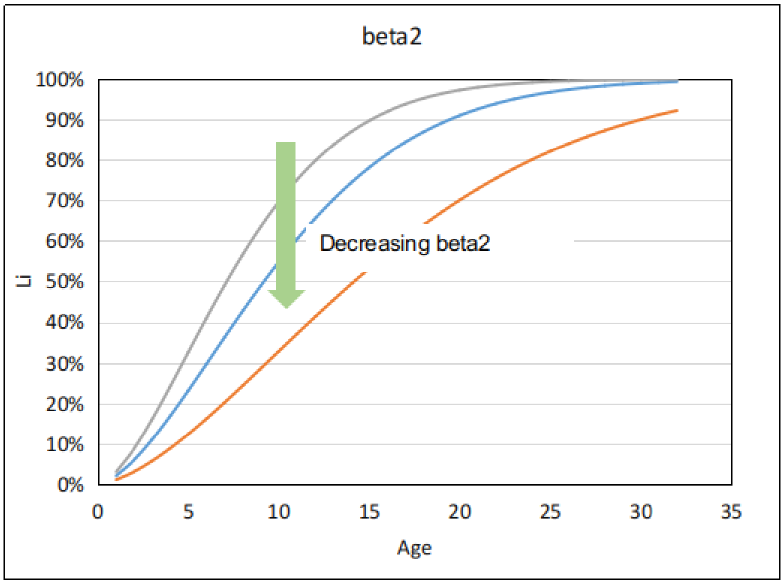

(a) beta2

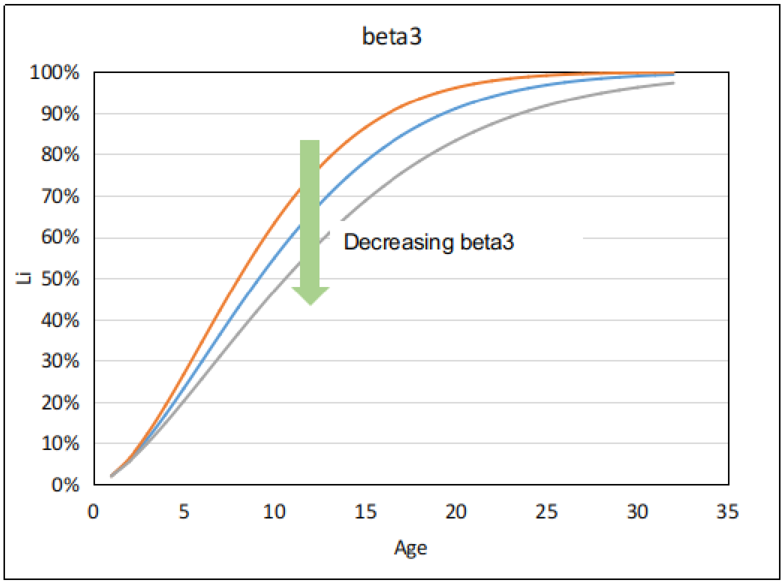

(b) beta3

Figure 4.3 Effect of Regression Parameters on Alternative Model Three

Additionally, for a pavement section with known distress value L_i, its corresponding age can be approximated using:

$$Age_i = exp\left\{\frac{1}{\beta_3} ln\left[\frac{1}{\beta_2} ln\left(\frac{\beta_1}{\beta_0 - L_i}\right)\right]\right\}$$

4.1.2. Model Selection

As presented in the previous sections, the formulations of all the three alternative models enable modelers to produce predictions at age zero and estimate model parameters directly without using any stratified grouping approaches. Of these alternative models, the initial distress values of alternative Model One and Model Two will always greater than zero, while the initial distress value of alternative Model Three can either be positive, negative, or zero. Since it was the preference of TxDOT personnel that the initial pavement distresses after treatment should be reset to zero, which might not necessarily be always the case in the field, Model Three was preferred.

Although it is possible to specify very small initial distress values by constraining the values of β_1, the goodness-of-fit might be significantly undermined for alternative Models One and Two. For alternative Model Three, zero initial distress values can be acquired by setting $\beta_1 = \beta_0$, since Model Three has four parameters, which leaves enough flexibility to model the data. In summary, since alternative Model Three can produce zero initial distress values at age zero while reserving enough flexibility to model the data, in this project, alternative Model Three was selected to develop pavement deterioration models.

4.1.3. Parameter Specification

Alternative Model Three was modified to ensure the predicted distresses at age zero will always equal to zero. The modified formula is shown below:

$$L = \beta_0 \left[1 - \exp\left(-\frac{\beta_1}{1000} \cdot Age^{\frac{\beta_2}{1000}}\right)\right]$$

As previously discussed, because of the skewness of distress distributions, the asymptotic values (β_0) used in the current models incorporated into PA are too high. Consequently, in this project, it was decided to use the 99.9th percentile for each type of distress as the asymptotic values of the deterioration models. Thus, the new models used asymptotic values based on real data rather than experts' opinion. In particular, the asymptotic values of the four rut buckets were deliberately selected to ensure the sum of predictions of these four models will never exceed 100 percent. The selected asymptotic values for each model are as follows:

- Shallow rut, percentage of wheelpath length: 66
- Deep rut, percentage of wheelpath length: 25
- Severe rut, percentage of wheelpath length: 5
- Failure rut, percentage of wheelpath length: 2
- Patching, percentage of lane area: 100
- Failures, total number: 10
- Block cracking, percentage of lane area: 50
- Alligator cracking, percentage of wheelpath length: 70
- Longitudinal cracking, length per station: 225
- Transverse cracking, number per station: 10

Since β_0 has been used to represent the asymptotic value, only the parameters β_1 and β_2 were left to incorporate different variables. Preliminary analysis indicated that β_2 has a predominant effect on the shape of deterioration curves. As a result, we decided to incorporate variables related to treatment type into β_1, while incorporating functional class, traffic, pavement type, traffic, and climate information into β_2. More specifically, the equations for β_1 and β_2 :

$$\beta_1 = \eta_0 + \eta_1 DN + \eta_2 LR + \eta_3 MR + \eta_4 HR$$

$$\beta_2 = \exp(a_0 + \sum_j a_j GROUP_j + \gamma_1 CL\_WEST + \gamma_2 CL\_EAST + \gamma_3 CL\_NORTH + \gamma_4 CL\_SOUTH)$$

4.2. Model Estimation Approach

Pavement deterioration models should be able to depict the general change of distresses under various conditions as well as produce predictions that are as close as possible to the field observations. Generally, after maintenance or rehabilitation works, pavement distresses will progressively increase without intervention until the next maintenance or rehabilitation work. For different types of M&R, it is expected that the treatment involving a higher level of work intensity, which normally corresponds to higher cost, will produce better pavement performance, i.e., lower distress and slower deterioration rate. Moreover, to facilitate plans for M&R works and the calculation of treatment effectiveness, the deterioration curves of different treatments should not cross each other. As a result, in this project, the selected specification form for the deterioration models adhere to the following principles:

- The deterioration curve should be non-decreasing—and for alternative Model Three specifically, the value of β1 and β2 should be greater than zero. Since the formulation of β2 is an exponential form, we need to constrain only β1 during the model estimation;
- The deterioration curves of different treatment types for a pavement section should not cross each other and should follow a hierarchical order by which the DN curve has the highest distress rate, followed by PM, LRhb, MRhb, and HRhb; and
- The predictions of the deterioration models should be as close as possible to the field distress measurements.

To meet the requirements above, the least-squares and a two-stage estimation approach were applied for the estimation of the model parameters.

4.2.1. Least-squares Method

The least-squares method was used to perform the model estimation. The objective function of the least-squares method is to minimize the sum of squared distance between the predictions and observations:

$$\boldsymbol{\theta} = \underset{\boldsymbol{\theta}}{\operatorname{argmin}} \sum_{i=1}^{n} (L(\boldsymbol{x}_i, \boldsymbol{\theta}) - L_i^*)^2$$

where $\boldsymbol{\theta}$ is the model parameters to be estimated, L_i^* is the distress of the ith observation in the data, and $L(\boldsymbol{x}_i, \boldsymbol{\theta})$ is the corresponding prediction from the deterioration model.

4.2.2. Two-stage Estimation

A two-stage estimation approach was used in this project primarily to ensure that the deterioration curves of different types of treatments do not cross each other and to respect the progressive order of distress, in which DN is followed by PM, LRhb, MRhb, and HRhb. The two stages are outlined here:

- Stage I: For each type of distress, without incorporating information about treatment type, conduct least-squares estimation under the constraint that β1 should be positive. In this way, a single value of β1 and a function to compute β2 for each type of distress would be obtained;
- Stage II: For each type of distress, combine the data sets of different treatment types, then incorporate treatment type information into β1 and perform least square estimation to acquire formulations for β1 while keeping the functions used to compute β2 unchanged.

4.3. Results and Discussion

The model errors of Stage I and Stage II are presented in Table 4.1 and 4.2, where the third column is the mean squared error (MSE), the fourth column is the standard error, and the last column is the normalized error with respect to the asymptotic value. As shown in the tables, for Stage I estimation, the normalized errors of all the models are below 10 percent, which indicates that the proposed alternative model can produce satisfactory results even without incorporating treatment type information. After incorporating treatment type information in Stage II, substantial decreases in the normalized errors can be observed for all the models. More remarkably, the majority of all the normalized errors are below 5 percent, except for in the shallow rut model.

Table 4.1 Model Errors for Stage I

Distress	Asymptotic Value	MSE	std_error	Normalized error
Shallow_Rut	66	36.3	6.03	9.1%
Deep_Rut	25	1.48	1.22	4.9%
Severe_Rut	5	0.02	0.15	3.0%
Failure_Rut	2	0.00	0.01	0.5%
Patching	100	15.0	3.88	3.9%
Failures	10	0.11	0.33	3.3%
Block_Cracking	50	0.25	0.50	1.0%
Alligator_Cracking	70	10.4	3.23	4.6%
Longitudinal_Cracking	225	352	18.77	8.3%
Transverse_Cracking	10	0.37	0.61	6.1%

Table 4.2 Model Errors for Stage II

Distress	Asymptotic Value	MSE	std_error	Normalized error
Shallow_Rut	66	13.6	3.69	5.6%
Deep_Rut	25	0.35	0.59	2.4%
Severe_Rut	5	0.00	0.07	1.4%
Failure_Rut	2	0.00	0.00	0.0%
Patching	100	4.10	2.02	2.0%
Failures	10	0.03	0.17	1.7%
Block_Cracking	50	0.02	0.15	0.3%
Alligator_Cracking	70	2.72	1.65	2.4%
Longitudinal_Cracking	225	115	10.72	4.8%
Transverse_Cracking	10	0.12	0.34	3.4%

The estimates of the model parameters and their corresponding statistics for Stage I and Stage II for different types of distresses are reported in Tables 4.3 to 4.21. With the exception of the failure rut model, the models' statistics suggest that the treatment type has significant effect on the deterioration of pavements. The effect of climate differs depending on distress type: climate is an insignificant factor in the propagation of severe rut, failure rut, and block cracking, but is a significant factor for other distresses. The effect of the group variable, which consists of different combinations of functional class, pavement type and traffic, is affected by the general deterioration trend of the data. For distresses with high deterioration rates (e.g., longitudinal cracking), most of the groups show a significant effect. For distresses with lower deterioration rate (e.g., failures), many groups do not show a statistically significant effect.

To visually evaluate the performance of the alternative deterioration models, the boxplots of the field measurements and the predictions from the developed models for different types of distresses are presented in Figures 4.4 to 4.23. For some group comparisons, the predictions generated by the developed models diverge from the field observation at high pavement age (e.g., as Figures 4.9 and 4.15 attest). However, in general, the deterioration models exhibit outstanding performance both at the network level and for the specific groups. The variability that appears as age increases arises because the data are not evenly distributed along the timeline: there are more data for "newer" pavements than for "old" pavements. Finally, but most importantly, it can be observed that the deterioration curves for different treatment types do not cross each other and follow the correct hierarchical order: the DN curve has the highest deterioration rate followed, in order, by PM, LRhb, MRhb, and HRhb.

4.3.1. Shallow Rut

Table 4.3 Model Estimation of Shallow Rut from Stage I

Variables	Parameter	Estimate	Std. Error	t value	p-value
-	β_1	39.4119	2.4614e-01	160.1174	0.0e+00
-	α_0	6.4655	4.4839e-03	1441.9262	0.0e+00
Group_1	α_1	-2.7472	8.1403e-01	-3.3748	3.7e-04
Group_2	α_2	-0.2988	9.5334e-02	-3.1346	8.6e-04
Group_3	α_3	0.4601	8.4791e-03	54.2660	0.0e+00
Group_4	α_4	-233.5248	1.0449e+100	0.0000	5.0e-01
Group_5	α_5	-0.3311	3.4746e-02	-9.5278	8.5e-22
Group_6	α_6	-0.1298	3.5966e-02	-3.6098	1.5e-04
Group_7	α_7	0.3960	1.7016e-02	23.2748	2.6e-119
Group_8	α_8	0.3683	2.9370e-02	12.5390	2.7e-36
Group_9	α_9	-1.7825	2.2454e-01	-7.9385	1.1e-15
Group_10	α_{10}	-1.4038	2.0935e-01	-6.7055	1.0e-11
Group_11	α_{11}	-2.7500	1.3258e+00	-2.0742	1.9e-02
Group_12	α_{12}	0.2652	1.6072e-02	16.5025	2.8e-61
Group_13	α_{13}	0.2403	4.0710e-02	5.9032	1.8e-09
Group_14	α_{14}	-1.6927	1.8621e-01	-9.0902	5.2e-20
Group_15	α_{15}	-1.2770	1.4729e-01	-8.6703	2.2e-18
Group_16	α_{16}	0.2980	3.5183e-02	8.4696	1.3e-17
Group_17	α_{17}	-0.1400	2.1922e-02	-6.3882	8.5e-11
Group_19	α_{19}	0.1035	8.6902e-03	11.9114	5.9e-33
CL_WEST	γ_1	-0.6377	4.8479e-02	-13.1541	9.8e-40
CL_EAST	γ_2	0.1288	6.8411e-03	18.8344	4.4e-79
CL_NORTH	γ_3	-0.3388	2.5191e-02	-13.4492	1.9e-41
CL_SOUTH	γ_4	0.1508	8.0075e-03	18.8339	4.4e-79

Table 4.4 Model Estimation of Shallow Rut from Stage II

Variables	Parameter	Estimate	Std. Error	t value	p-value
-	η_0	28.7388	0.0797	360.4267	0.0e+00
DN	η_1	11.6571	0.1642	70.977	0.0e+00
LR	η_2	-4.4788	0.1647	-27.1985	8.3e-163
MR	η_3	-11.0173	0.1814	-60.7295	0.0e+00
HR	η_4	-18.6942	0.2241	-83.4214	0.0e+00

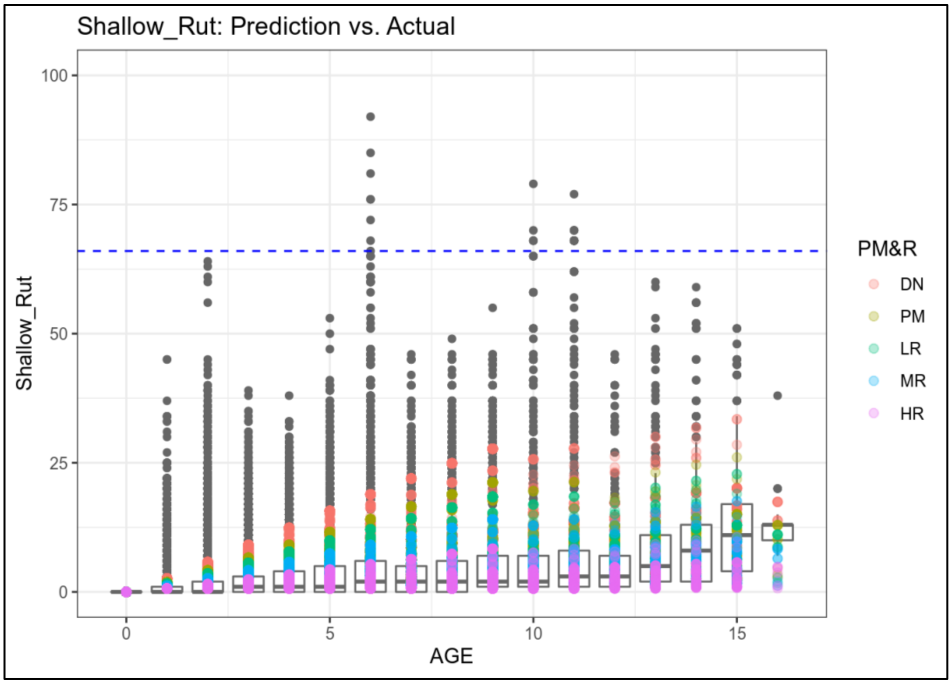

Figure 4.4 Network Performance of Shallow Rut Model

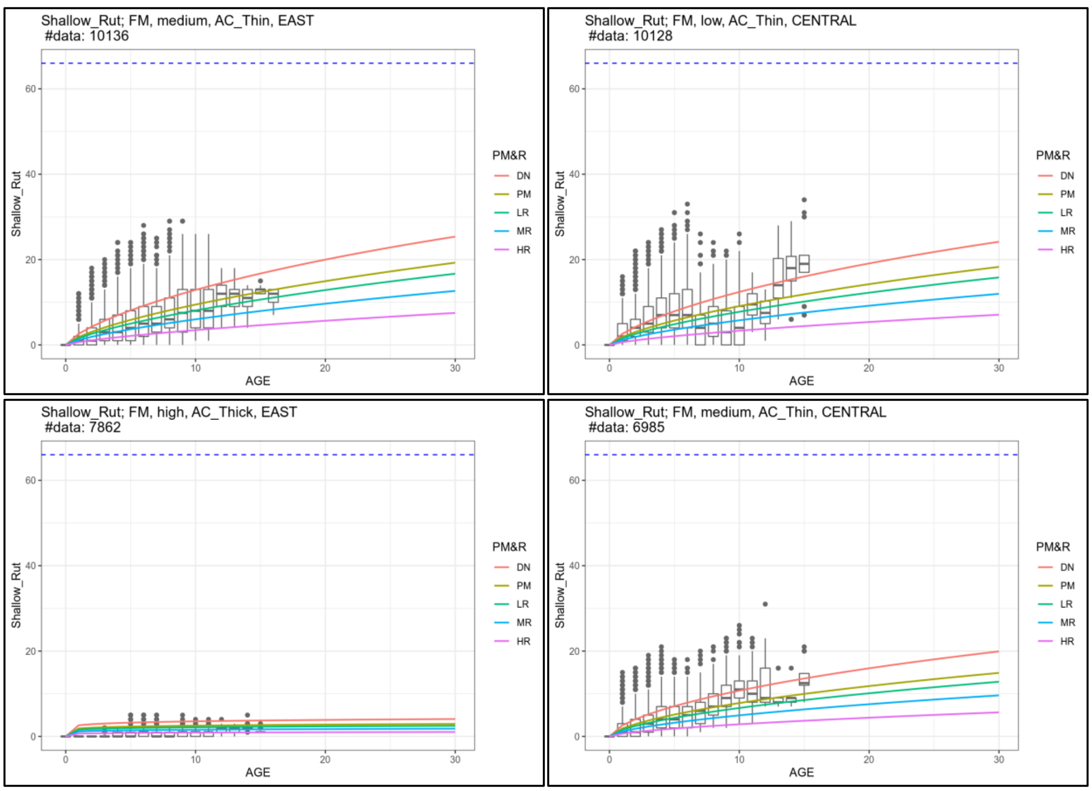

Figure 4.5 Group Performance of Shallow Rut Model

4.3.2. Deep Rut

Table 4.5 Model Estimation of Deep Rut from Stage I

Variables	Parameter	Estimate	Std. Error	t value	p-value
-	β_1	8.4996	5.7401e-02	148.0738	0.0e+00
-	α_0	6.7073	1.8467e-03	3632.0535	0.0e+00
Group_1	α_1	-17.9556	5.8495e+06	0.0000	5.0e-01
Group_2	α_2	-19.8835	7.7803e+07	0.0000	5.0e-01
Group_3	α_3	0.5647	1.9857e-03	284.3824	0.0e+00
Group_4	α_4	-18.0980	4.7006e+06	0.0000	5.0e-01
Group_5	α_5	-20.7947	9.0312e+07	0.0000	5.0e-01
Group_6	α_6	-16.1727	1.2696e+06	0.0000	5.0e-01
Group_7	α_7	-1.0460	2.9956e-01	-3.4918	2.4e-04
Group_8	α_8	0.4297	1.7089e-02	25.1418	1.1e-138
Group_9	α_9	-17.6057	3.5056e+06	0.0000	5.0e-01
Group_10	α_{10}	-20.6107	8.4929e+07	0.0000	5.0e-01
Group_11	α_{11}	-15.8676	1.1975e+06	0.0000	5.0e-01
Group_12	α_{12}	-0.5563	8.6679e-02	-6.4183	7.0e-11
Group_13	α_{13}	-15.8743	1.3375e+06	0.0000	5.0e-01
Group_14	α_{14}	-19.1104	1.3126e+07	0.0000	5.0e-01
Group_15	α_{15}	-0.9662	1.4664e-01	-6.5888	2.2e-11
Group_16	α_{16}	-0.1103	7.3677e-02	-1.4969	6.7e-02
Group_17	α_{17}	-0.6157	5.8676e-02	-10.4927	5.0e-26
Group_19	α_{19}	0.2102	5.9366e-03	35.4096	1.1e-270
CL_WEST	γ_1	-0.0940	3.2731e-02	-2.8725	2.0e-03
CL_EAST	γ_2	0.1113	6.8077e-03	16.3462	3.7e-60
CL_NORTH	γ_3	-0.0738	1.7445e-02	-4.2320	1.2e-05
CL_SOUTH	γ_4	0.4664	1.9751e-03	236.1398	0.0e+00

Table 4.6 Model Estimation of Deep Rut from Stage II

Variables	Parameter	Estimate	Std. Error	t value	p-value
-	η_0	6.1412	0.0135	455.5573	0e+00
DN	η_1	2.9379	0.0340	86.4408	0e+00
LR	η_2	-1.6197	0.0273	-59.2399	0e+00
MR	η_3	-3.2180	0.0273	-117.8413	0e+00
HR	η_4	-4.7294	0.0320	-147.9006	0e+00

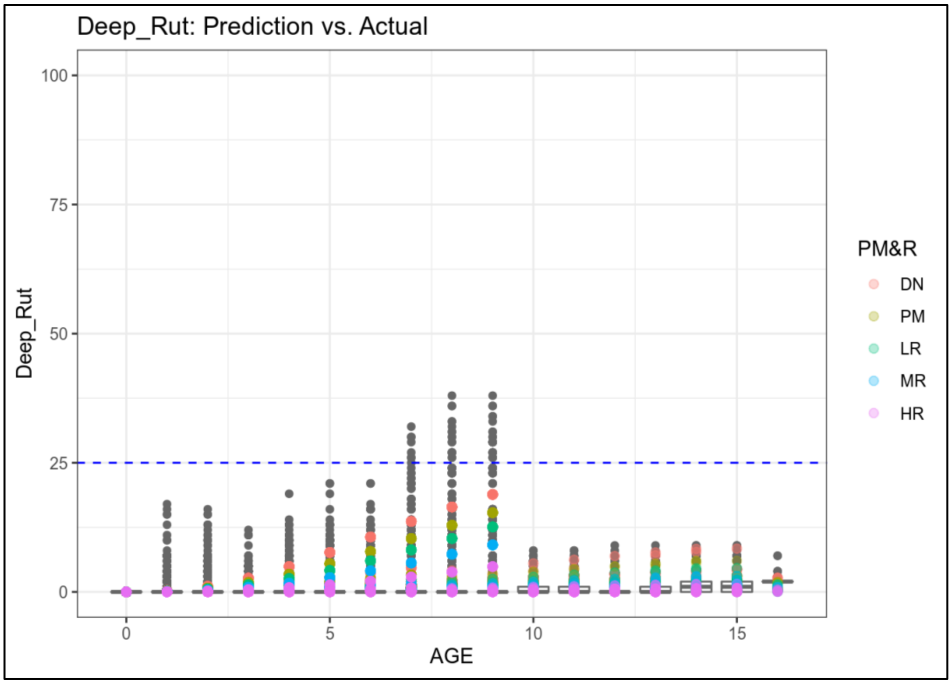

Figure 4.6 Network Performance of Deep Rut Model

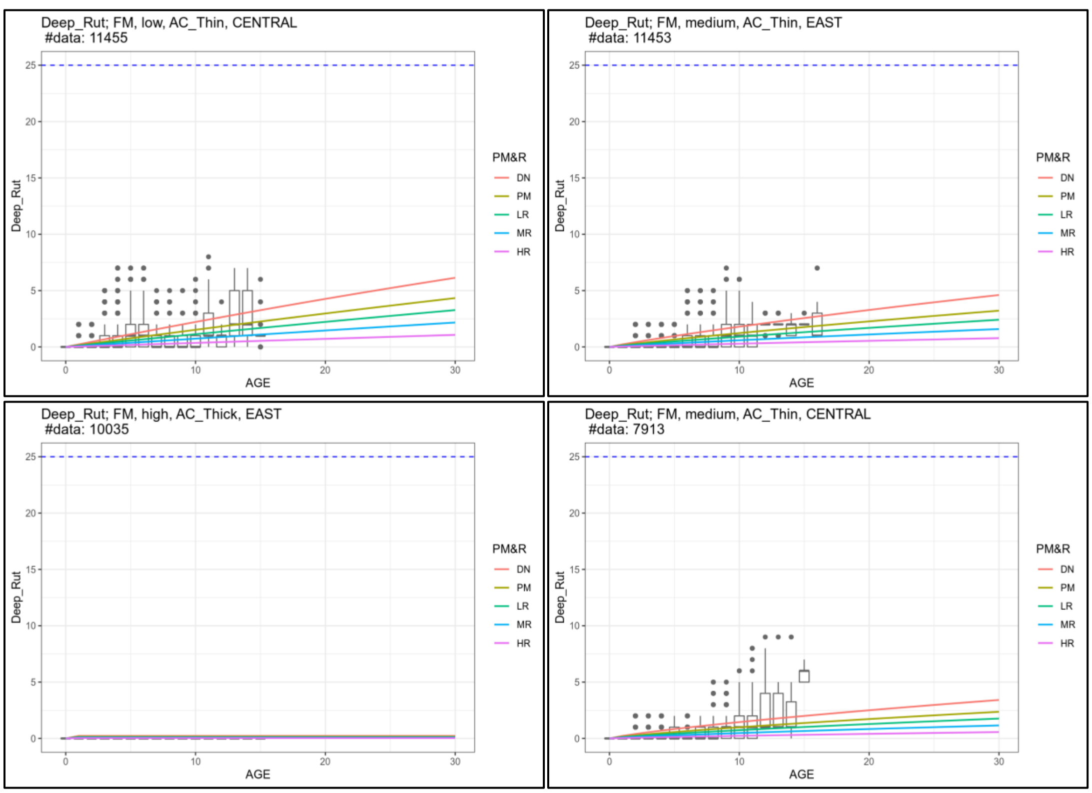

Figure 4.7 Group Performance of Deep Rut Model

4.3.3. Severe Rut

Table 4.7 Model Estimation of Severe Rut from Stage I

Variables	Parameter	Estimate	Std. Error	t value	p-value
-	β_1	0.0678	5.8868e-04	115.1465	0.0e+00
-	α_0	5.5690	9.9986e-04	5569.7614	0.0e+00
Group_1	α_1	1.6307	2.7765e-01	5.8734	2.2e-09
Group_2	α_2	0.8723	8.6717e+00	0.1006	4.6e-01
Group_3	α_3	2.3273	1.0286e-03	2262.6869	0.0e+00
Group_4	α_4	0.6917	3.1287e+00	0.2211	4.1e-01
Group_5	α_5	1.9914	5.2503e-02	37.9290	8.5e-310
Group_6	α_6	0.6178	7.3184e+00	0.0844	4.7e-01
Group_7	α_7	0.5443	1.0480e+01	0.0519	4.8e-01
Group_8	α_8	2.5259	4.5027e-03	560.9644	0.0e+00
Group_9	α_9	0.2538	8.6549e+00	0.0293	4.9e-01
Group_10	α_{10}	0.4300	8.5288e+00	0.0504	4.8e-01
Group_11	α_{11}	0.6142	7.6544e+00	0.0802	4.7e-01
Group_12	α_{12}	1.4918	2.7316e-01	5.4615	2.4e-08
Group_13	α_{13}	0.5700	1.1365e+01	0.0502	4.8e-01
Group_14	α_{14}	0.1337	9.3419e+00	0.0143	4.9e-01
Group_15	α_{15}	0.3332	9.2402e+00	0.0361	4.9e-01
Group_16	α_{16}	0.8183	9.5864e+00	0.0854	4.7e-01
Group_17	α_{17}	0.8838	1.8054e+00	0.4896	3.1e-01
Group_19	α_{19}	2.0420	1.3694e-02	149.1173	0.0e+00
CL_WEST	γ_1	-1.0729	2.7586e+00	-0.3889	3.5e-01
CL_EAST	γ_2	-0.0084	4.4912e-03	-1.8632	3.1e-02
CL_NORTH	γ_3	0.1478	1.8514e-02	7.9831	7.3e-16
CL_SOUTH	γ_4	0.4398	1.0287e-03	427.5200	0.0e+00

Table 4.8 Model Estimation of Severe Rut from Stage II

Variables	Parameter	Estimate	Std. Error	t value	p-value
-	η_0	0.0349	0.0001	290.8530	0.0e+00
DN	η_1	0.0214	0.0003	74.9768	0.0e+00
LR	η_2	-0.0050	0.0003	-19.6438	3.9e-86
MR	η_3	-0.0243	0.0003	-95.4602	0.0e+00
HR	η_4	-0.0329	0.0003	-110.3481	0.0e+00

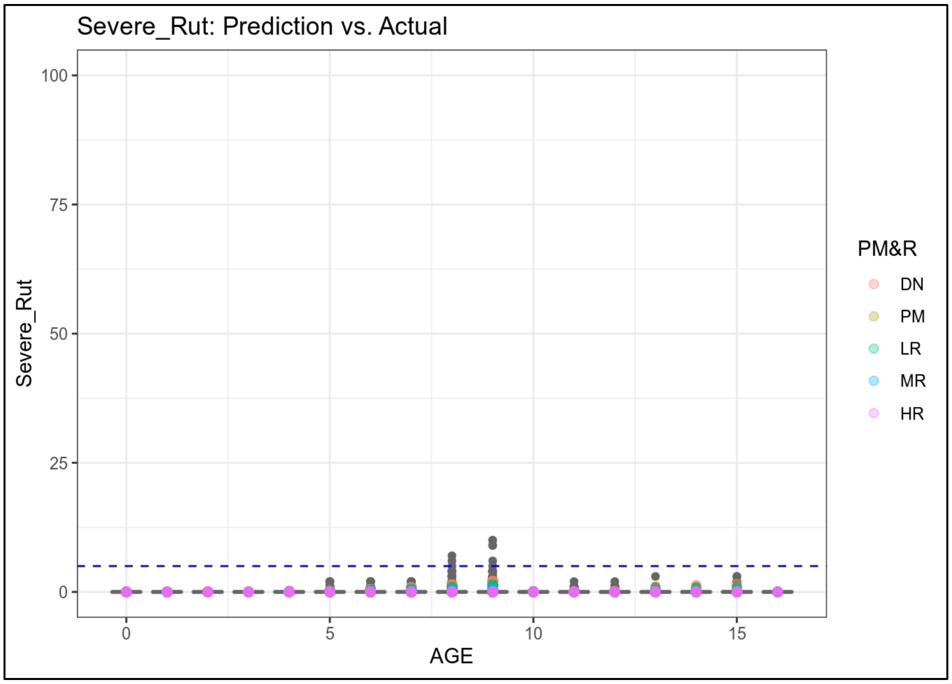

Figure 4.8 Network Performance of Severe Rut Model

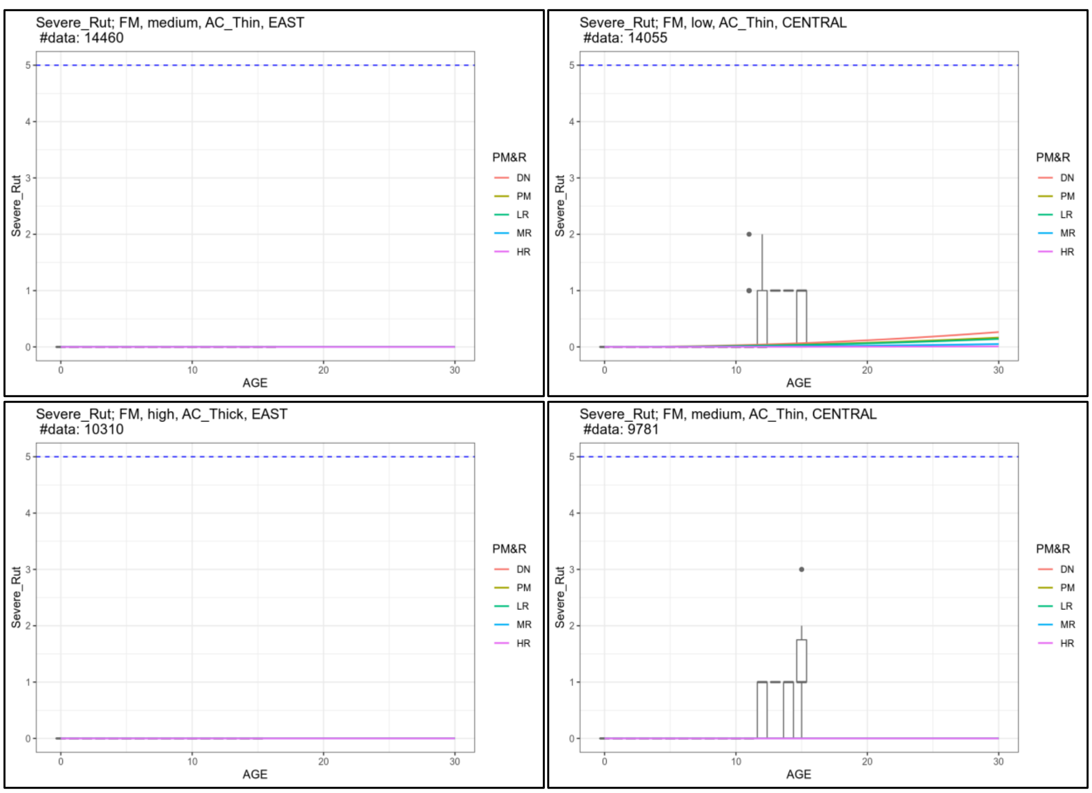

Figure 4.9 Group Performance of Severe Rut Model

4.3.4. Failure Rut

Table 4.9 Model Estimation of Failure Rut from Stage I

Variables	Parameter	Estimate	Std. Error	t value	p-value
-	β_1	0.1525	1.4261e-03	106.9608	0e+00
-	α_0	-5.2985	1.3232e-03	-4004.2753	0e+00
Group_1	α_1	0.1419	2.0781e+03	0.0001	5e-01
Group_2	α_2	0.8070	1.2350e+05	0.0000	5e-01
Group_3	α_3	0.6692	2.8329e+03	0.0002	5e-01
Group_4	α_4	-0.4884	2.0975e+03	-0.0002	5e-01
Group_5	α_5	-0.3972	2.0527e+03	-0.0002	5e-01
Group_6	α_6	0.3319	1.7373e+03	0.0002	5e-01
Group_7	α_7	7.8746	4.1807e-02	188.3563	0e+00
Group_8	α_8	8.8252	1.3239e-03	6666.2049	0e+00
Group_9	α_9	-0.5848	2.2333e+03	-0.0003	5e-01
Group_10	α_{10}	-0.1962	1.6283e+03	-0.0001	5e-01
Group_11	α_{11}	0.3281	1.7263e+03	0.0002	5e-01
Group_12	α_{12}	-0.1042	1.6222e+03	-0.0001	5e-01
Group_13	α_{13}	0.2540	1.3490e+03	0.0002	5e-01
Group_14	α_{14}	-0.9232	2.4179e+03	-0.0004	5e-01
Group_15	α_{15}	-0.5042	2.0164e+03	-0.0003	5e-01
Group_16	α_{16}	0.7222	2.1490e+03	0.0003	5e-01
Group_17	α_{17}	-0.3039	1.9323e+03	-0.0002	5e-01
Group_19	α_{19}	-1.4057	2.7882e+03	-0.0005	5e-01
CL_WEST	γ_1	-2.2843	5.4581e+02	-0.0042	5e-01
CL_EAST	γ_2	4.3647	1.3239e-03	3296.8908	0e+00
CL_NORTH	γ_3	4.6617	4.0938e-02	113.8720	0e+00
CL_SOUTH	γ_4	-0.6728	4.1179e+02	-0.0016	5e-01

Table 4.10 Model Estimation of Failure Rut from Stage II

Variables	Parameter	Estimate	Std. Error	t value	p-value
-	η_0	0.0009	0.0004	2.3591	9.2e-03
DN	η_1	0.0000	0.0008	0.0026	5.0e-01
LR	η_2	0.0000	0.0008	0.0014	5.0e-01
MR	η_3	0.0000	0.0008	0.0026	5.0e-01
HR	η_4	0.0000	0.0008	0.0026	5.0e-01

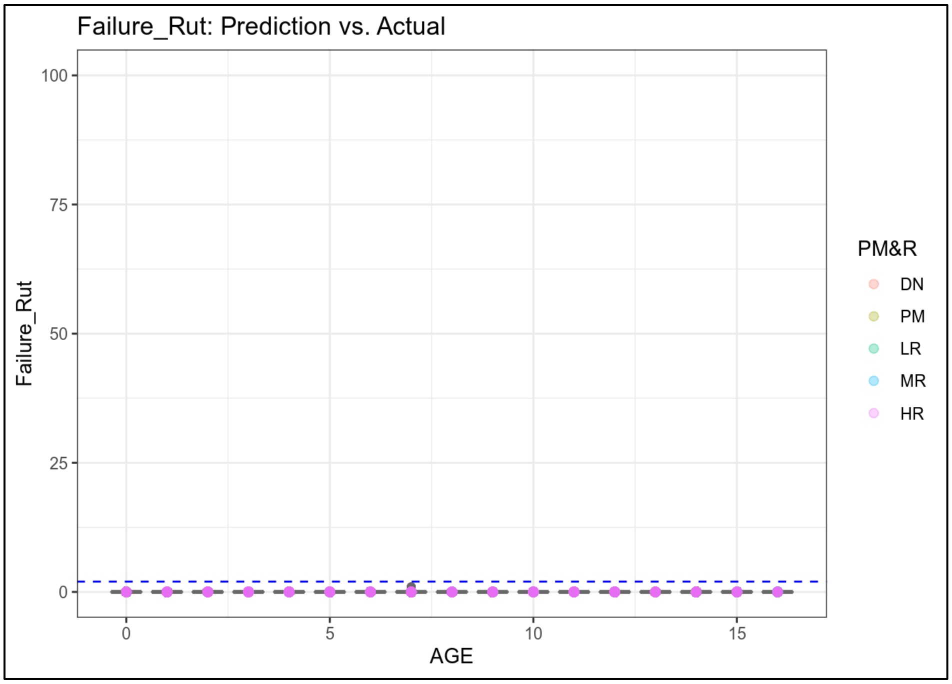

Figure 4.10 Network Performance of Failure Rut Model

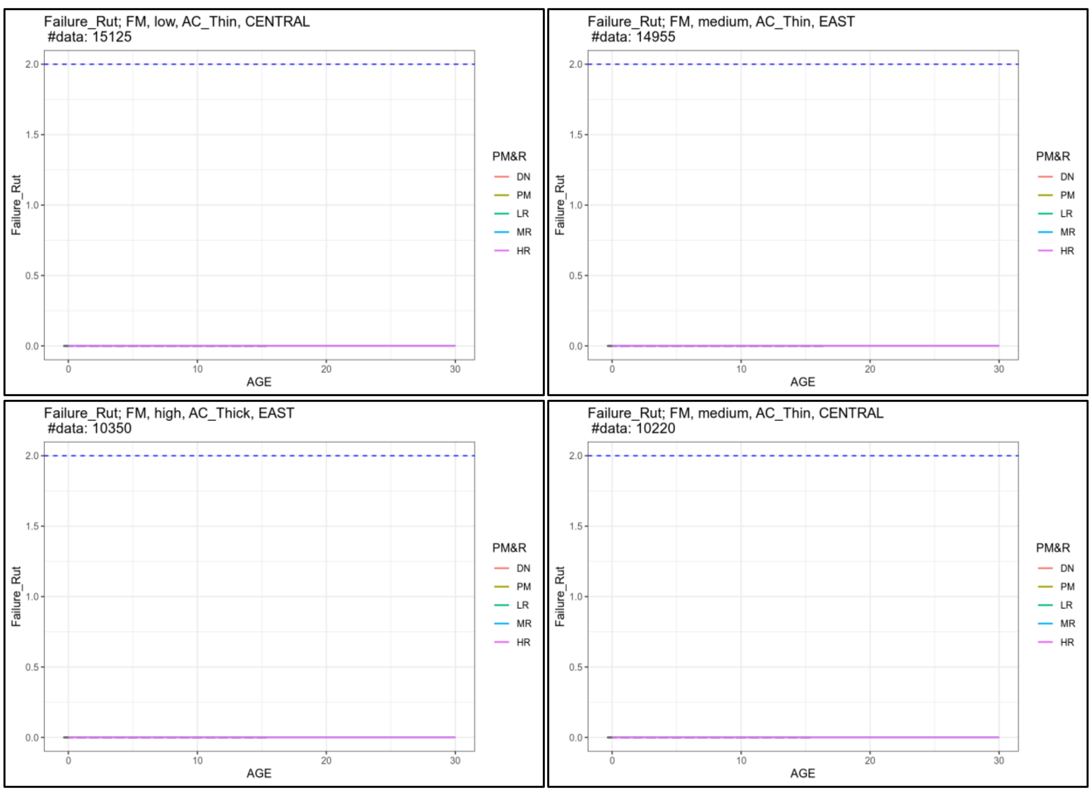

Figure 4.11 Group Performance of Failure Rut Model

4.3.5. Patching

Table 4.11 Model Estimation of Patching from Stage I

Variables	Parameter	Estimate	Std. Error	t value	p-value
-	β_1	0.3538	3.6288e-03	97.4985	0.0e+00
-	a_0	7.7809	1.7694e-03	4397.5417	0.0e+00
Group_1	a_1	-1.4047	1.0487e+00	-1.3395	9.0e-02
Group_2	a_2	-0.9177	6.2317e-01	-1.4726	7.0e-02
Group_3	a_3	-0.2984	1.3008e-02	-22.9421	5.2e-116
Group_4	a_4	-8.9754	3.8683e+03	-0.0023	5.0e-01
Group_5	a_5	-0.7117	1.7574e-01	-4.0494	2.6e-05
Group_6	a_6	-9.2416	8.8992e+03	-0.0010	5.0e-01
Group_7	a_7	-0.4111	5.7803e-02	-7.1116	5.8e-13
Group_8	a_8	-0.1127	5.4336e-02	-2.0746	1.9e-02
Group_9	a_9	-0.2133	1.7446e-02	-12.2287	1.3e-34
Group_10	a_{10}	-0.5718	7.3998e-02	-7.7276	5.6e-15
Group_11	a_{11}	-0.6474	1.2655e-01	-5.1160	1.6e-07
Group_12	a_{12}	-0.1301	5.7986e-03	-22.4404	4.1e-111
Group_13	a_{13}	-0.1379	2.0176e-02	-6.8369	4.1e-12
Group_14	a_{14}	-0.9775	3.0887e-01	-3.1647	7.8e-04
Group_15	a_{15}	-0.0512	9.2519e-03	-5.5365	1.6e-08
Group_16	a_{16}	-0.1678	5.4824e-02	-3.0606	1.1e-03
Group_17	a_{17}	-0.1909	4.3327e-03	-44.0622	0.0e+00
Group_19	a_{19}	-0.0325	2.8439e-03	-11.4270	1.7e-30
CL_WEST	γ_1	-0.3285	3.9278e-02	-8.3623	3.2e-17
CL_EAST	γ_2	-0.1482	6.4056e-03	-23.1287	7.5e-118
CL_NORTH	γ_3	0.0637	3.4420e-03	18.5158	1.6e-76
CL_SOUTH	γ_4	0.2969	2.7377e-03	108.4666	0.0e+00

Table 4.12 Model Estimation of Patching from Stage II

Variables	Parameter	Estimate	Std. Error	t value	p-value
-	η_0	0.1948	0.0010	194.0961	0.0e+00
DN	η_1	0.1383	0.0022	63.4287	0.0e+00
LR	η_2	-0.0394	0.0022	-18.2760	7.5e-75
MR	η_3	-0.0902	0.0023	-39.9155	0.0e+00
HR	η_4	-0.1213	0.0025	-49.2023	0.0e+00

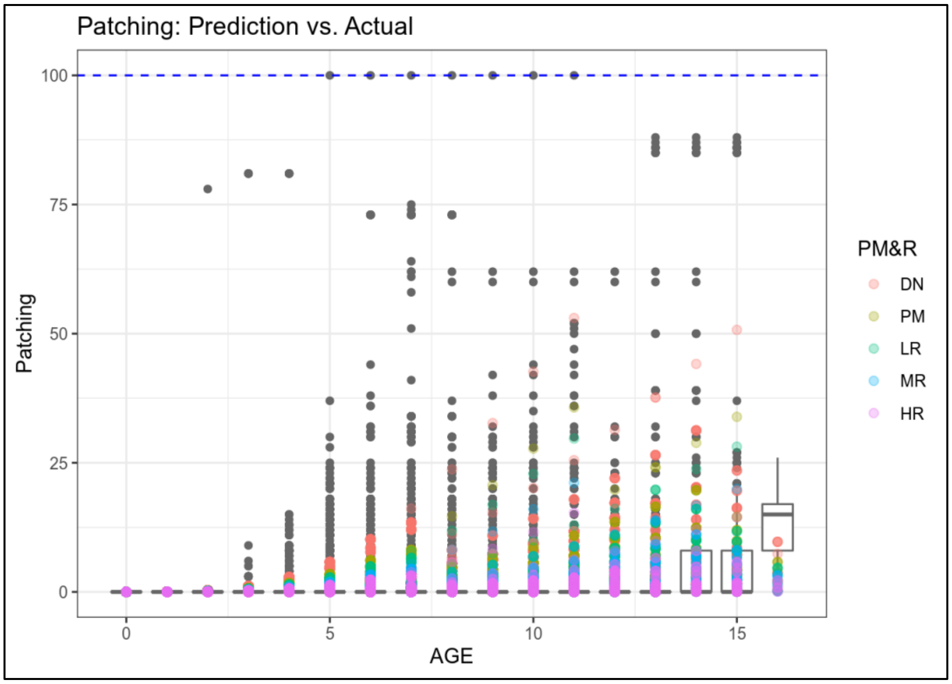

Figure 4.12 Network Performance of Patching Model

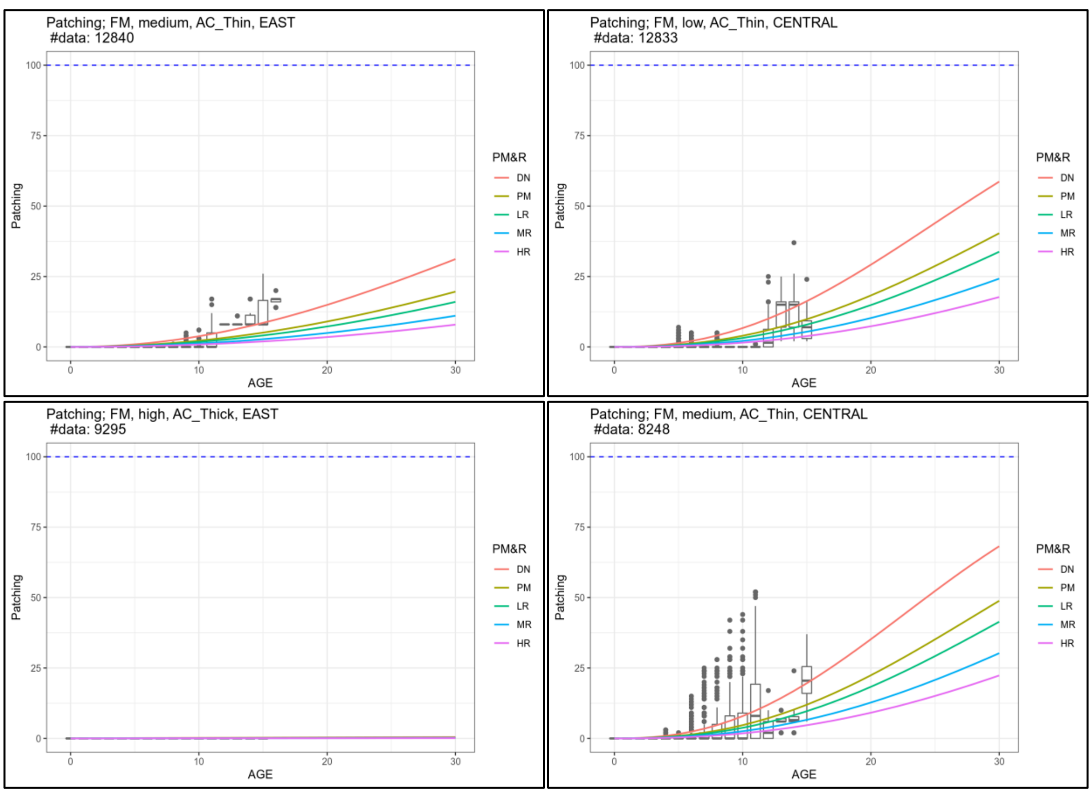

Figure 4.13 Group Performance of Patching Model

4.3.6. Failures

Table 4.13 Model Estimation of Failures from Stage I

Variables	Parameter	Estimate	Std. Error	t value	p-value
-	β_1	1.5326	1.0403e-02	147.3294	0.0e+00
-	α_0	7.1866	1.3238e-03	5428.5675	0.0e+00
Group_1	α_1	-14.3153	3.4242e+05	0.0000	5.0e-01
Group_2	α_2	-13.2899	1.8412e+05	-0.0001	5.0e-01
Group_3	α_3	0.0509	1.8077e-03	28.1687	3.3e-173
Group_4	α_4	-14.4818	2.7602e+05	-0.0001	5.0e-01
Group_5	α_5	-14.4904	3.5142e+05	0.0000	5.0e-01
Group_6	α_6	-13.6122	2.1264e+05	-0.0001	5.0e-01
Group_7	α_7	-13.6079	2.0853e+05	-0.0001	5.0e-01
Group_8	α_8	-11.3018	7.8517e+04	-0.0001	5.0e-01
Group_9	α_9	-14.5667	4.0597e+05	0.0000	5.0e-01
Group_10	α_{10}	-14.0658	2.8288e+05	0.0000	5.0e-01
Group_11	α_{11}	-0.3501	2.1686e-02	-16.1457	9.3e-59
Group_12	α_{12}	-0.6533	6.2145e-02	-10.5125	4.1e-26
Group_13	α_{13}	-12.8288	1.3628e+05	-0.0001	5.0e-01
Group_14	α_{14}	-14.7256	3.8913e+05	0.0000	5.0e-01
Group_15	α_{15}	-13.3897	1.3812e+05	-0.0001	5.0e-01
Group_16	α_{16}	-0.3669	8.1817e-02	-4.4838	3.7e-06
Group_17	α_{17}	-0.0588	2.5671e-03	-22.8870	1.7e-115
Group_19	α_{19}	0.0541	3.6150e-03	14.9643	8.6e-51
CL_WEST	γ_1	0.2670	5.7882e-03	46.1348	0.0e+00
CL_EAST	γ_2	-0.1433	1.7363e-02	-8.2523	8.0e-17
CL_NORTH	γ_3	0.0627	1.1615e-02	5.3963	3.4e-08
CL_SOUTH	γ_4	0.6546	1.3843e-03	472.9137	0.0e+00

Table 4.14 Model Estimation of Failures from Stage II

Variables	Parameter	Estimate	Std. Error	t value	p-value
-	η_0	1.0668	0.0027	398.9509	0.0e+00
DN	η_1	0.4367	0.0061	72.1155	0.0e+00
LR	η_2	-0.1127	0.0056	-20.0073	2.9e-89
MR	η_3	-0.4920	0.0059	-83.9211	0.0e+00
HR	η_4	-0.7613	0.0066	-115.7011	0.0e+00

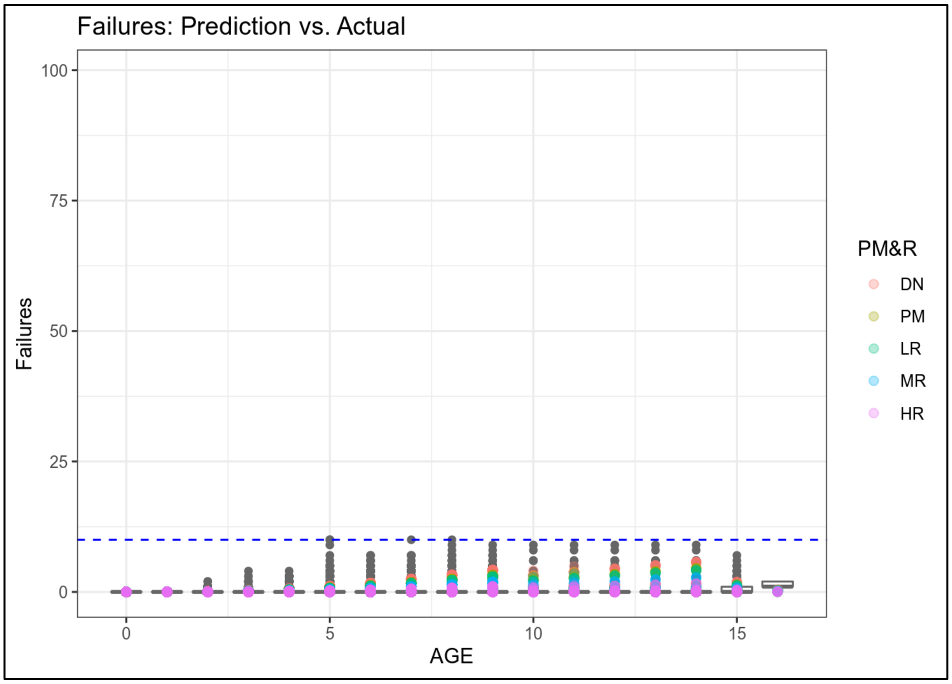

Figure 4.14 Network Performance of Failures Model

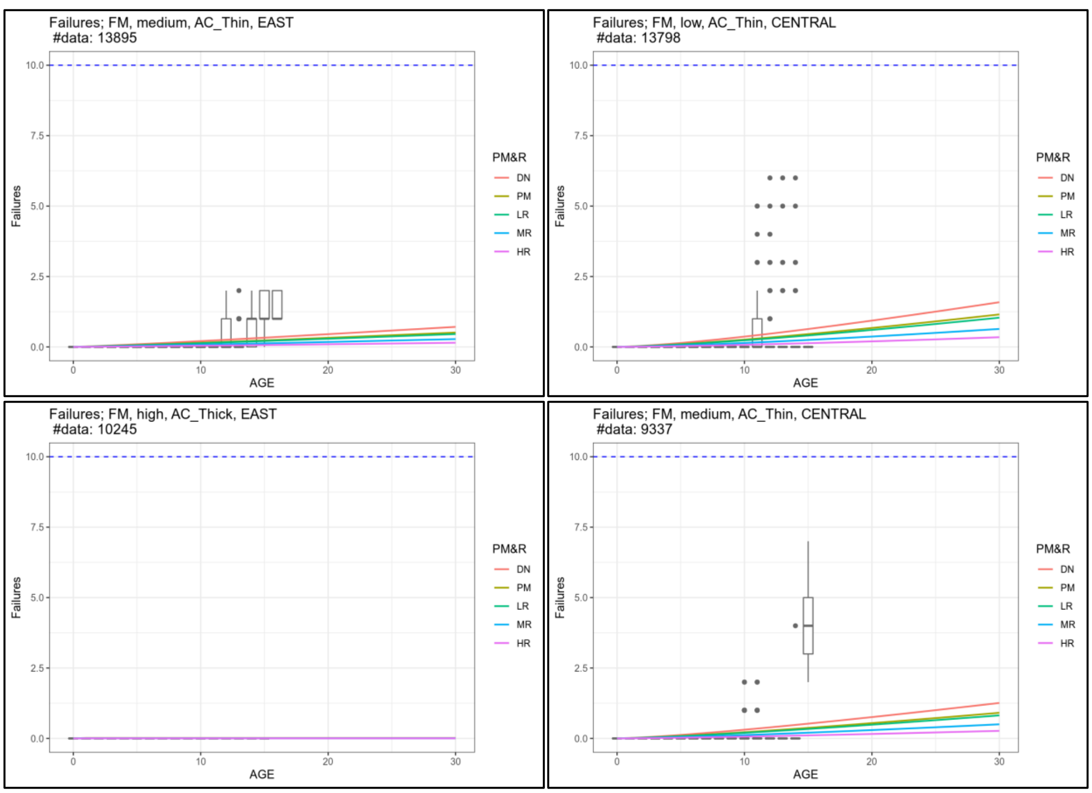

Figure 4.15 Group Performance of Failures Model

4.3.7. Block Cracking

Table 4.15 Model Estimation of Block Cracking from Stage I

Variables	Parameter	Estimate	Std. Error	t value	p-value
-	β_1	0.0114	1.3946e-04	81.8478	0.0e+00
-	α_0	2.3886	1.3488e-03	1770.9577	0.0e+00
Group_1	α_1	-2.3508	1.4113e+04	-0.0002	5.0e-01
Group_2	α_2	5.6864	5.1706e-03	1099.7445	0.0e+00
Group_3	α_3	-0.8571	9.8057e+03	-0.0001	5.0e-01
Group_4	α_4	5.3634	6.1353e-02	87.4202	0.0e+00
Group_5	α_5	4.9388	8.8821e-01	5.5604	1.4e-08
Group_6	α_6	-1.7336	1.1088e+04	-0.0002	5.0e-01
Group_7	α_7	-1.1537	6.8688e+03	-0.0002	5.0e-01
Group_8	α_8	0.1596	6.1436e+03	0.0000	5.0e-01
Group_9	α_9	-1.3324	5.1335e+03	-0.0003	5.0e-01
Group_10	α_{10}	5.9597	1.8224e-03	3270.2604	0.0e+00
Group_11	α_{11}	4.9679	1.1972e+00	4.1496	1.7e-05
Group_12	α_{12}	5.9188	2.1778e-03	2717.8486	0.0e+00
Group_13	α_{13}	-1.0381	7.2840e+03	-0.0001	5.0e-01
Group_14	α_{14}	5.2167	2.1682e-01	24.0603	2.4e-127
Group_15	α_{15}	-1.5319	1.3270e+04	-0.0001	5.0e-01
Group_16	α_{16}	5.4018	7.1973e-01	7.5053	3.1e-14
Group_17	α_{17}	4.8738	6.4259e-01	7.5846	1.7e-14
Group_19	α_{19}	5.0709	1.7212e-01	29.4620	3.8e-189
CL_WEST	γ_1	-6.6382	3.3172e+03	-0.0020	5.0e-01
CL_EAST	γ_2	-1.1002	1.0779e+00	-1.0207	1.5e-01
CL_NORTH	γ_3	-0.0744	1.3904e-02	-5.3529	4.3e-08
CL_SOUTH	γ_4	-1.1519	1.9127e+00	-0.6022	2.7e-01

Table 4.16 Model Estimation of Block Cracking from Stage II

Variables	Parameter	Estimate	Std. Error	t value	p-value
-	η_0	0.0041	0.0000	191.9726	0.0e+00
DN	η_1	0.0016	0.0000	34.3034	1.8e-257
LR	η_2	-0.0003	0.0000	-5.7067	5.8e-09
MR	η_3	-0.0035	0.0000	-72.2921	0.0e+00
HR	η_4	-0.0037	0.0000	-75.0193	0.0e+00

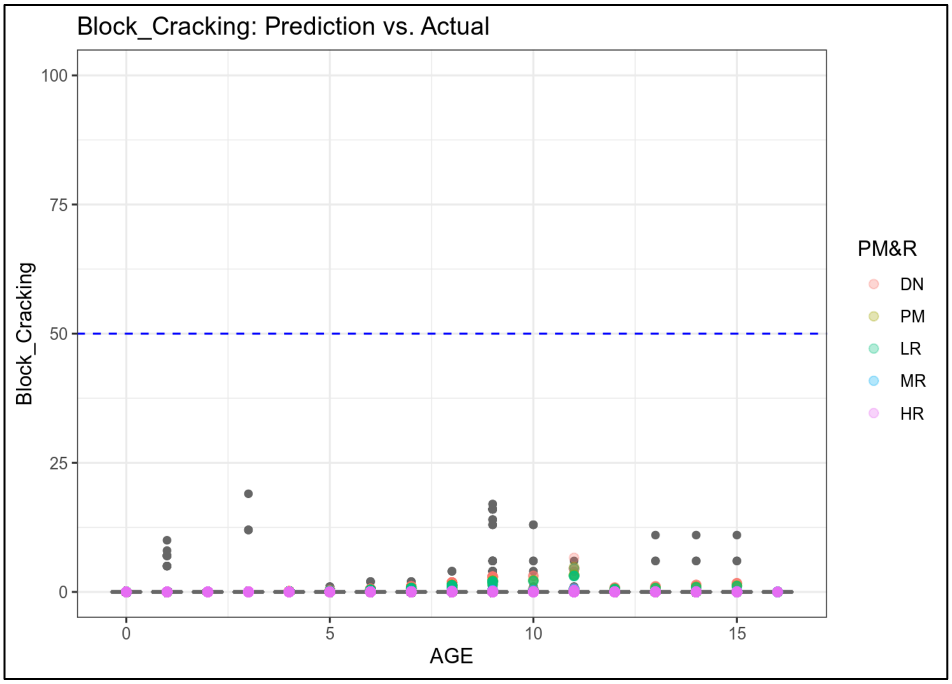

Figure 4.16 Network Performance of Block Cracking Model

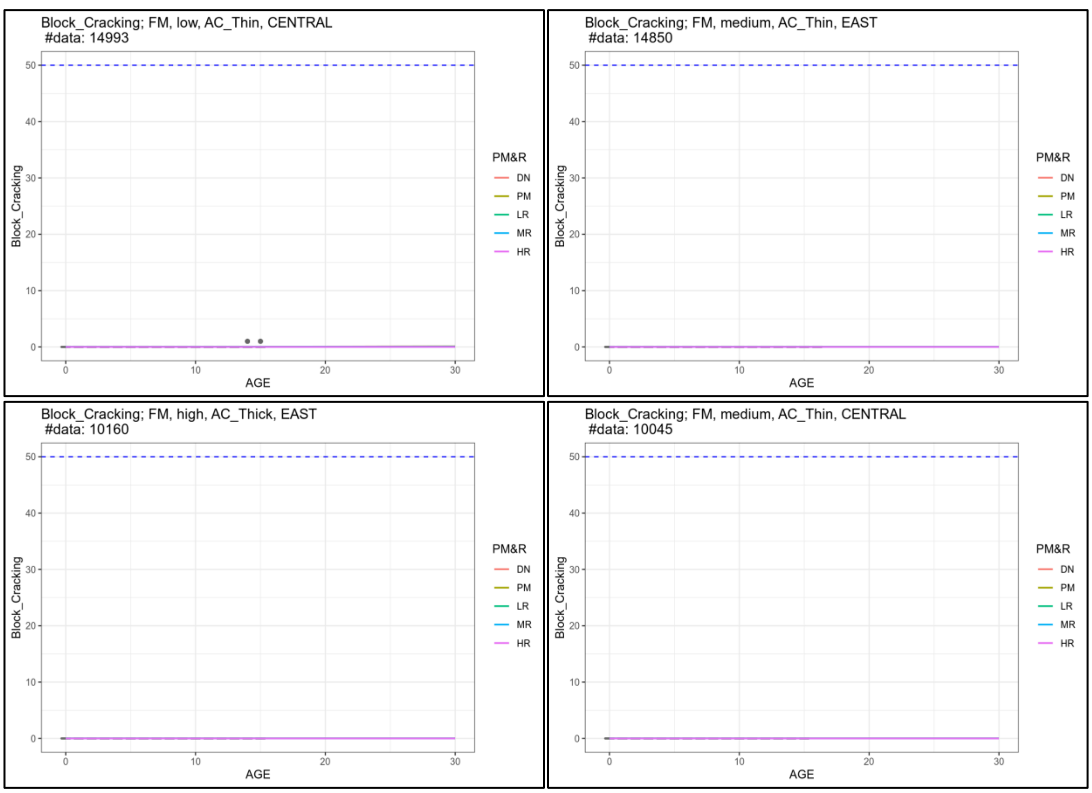

Figure 4.17 Group Performance of Block Cracking Model

4.3.8. Alligator Cracking

Table 4.16 Model Estimation of Alligator Cracking from Stage I

Variables	Parameter	Estimate	Std. Error	t value	p-value
-	β_1	0.1506	0.0010	150.7606	0.0e+00
-	a_0	7.5005	0.0009	8691.3078	0.0e+00
Group_1	a_1	0.1616	0.0242	6.6801	1.2e-11
Group_2	a_2	0.4751	0.0059	80.1436	0.0e+00
Group_3	a_3	0.3236	0.0148	21.8455	1.8e-105
Group_4	a_4	0.2705	0.0078	34.5178	1.7e-257
Group_5	a_5	0.0658	0.0146	4.5022	3.4e-06
Group_6	a_6	-0.0448	0.0941	-0.4762	3.2e-01
Group_7	a_7	-0.0262	0.0224	-1.1662	1.2e-01
Group_8	a_8	0.0201	0.0511	0.3931	3.5e-01
Group_9	a_9	0.3049	0.0024	127.6223	0.0e+00
Group_10	a_{10}	0.2571	0.0102	25.2781	3.8e-140
Group_11	a_{11}	0.1323	0.0286	4.6323	1.8e-06
Group_12	a_{12}	0.3802	0.0041	92.0548	0.0e+00
Group_13	a_{13}	-0.2345	0.1175	-1.9954	2.3e-02
Group_14	a_{14}	0.4433	0.0013	334.6230	0.0e+00
Group_15	a_{15}	0.4437	0.0015	297.4691	0.0e+00
Group_16	a_{16}	0.3165	0.0443	7.1398	4.8e-13
Group_17	a_{17}	0.2075	0.0087	23.8073	1.1e-124
Group_19	a_{19}	-0.1356	0.0203	-6.6678	1.3e-11
CL_WEST	γ_1	-0.0822	0.0156	-5.2839	6.4e-08
CL_EAST	γ_2	0.1859	0.0009	207.8160	0.0e+00
CL_NORTH	γ_3	0.2979	0.0076	38.9371	0.0e+00
CL_SOUTH	γ_4	0.0642	0.0074	8.6376	3.0e-18

Table 4.17 Model Estimation of Alligator Cracking from Stage II

Variables	Parameter	Estimate	Std. Error	t value	p-value
-	η_0	0.1179	0.0003	425.8304	0e+00
DN	η_1	0.0438	0.0007	66.4285	0e+00
LR	η_2	-0.0237	0.0006	-42.6243	0e+00
MR	η_3	-0.0483	0.0006	-83.1225	0e+00
HR	η_4	-0.0736	0.0007	-106.9000	0e+00

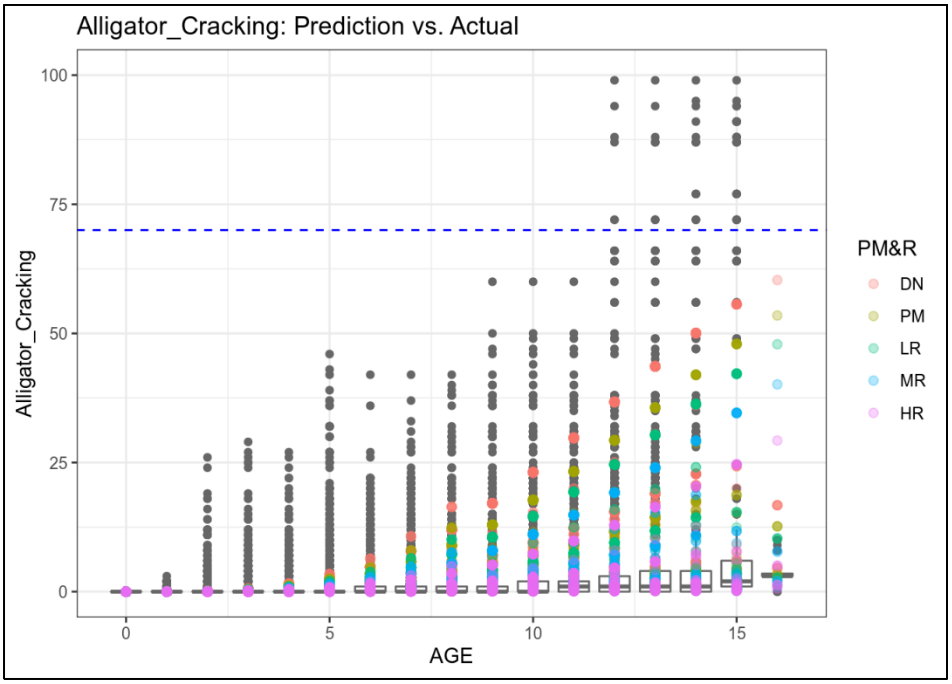

Figure 4.18 Network Performance of Alligator Cracking Model

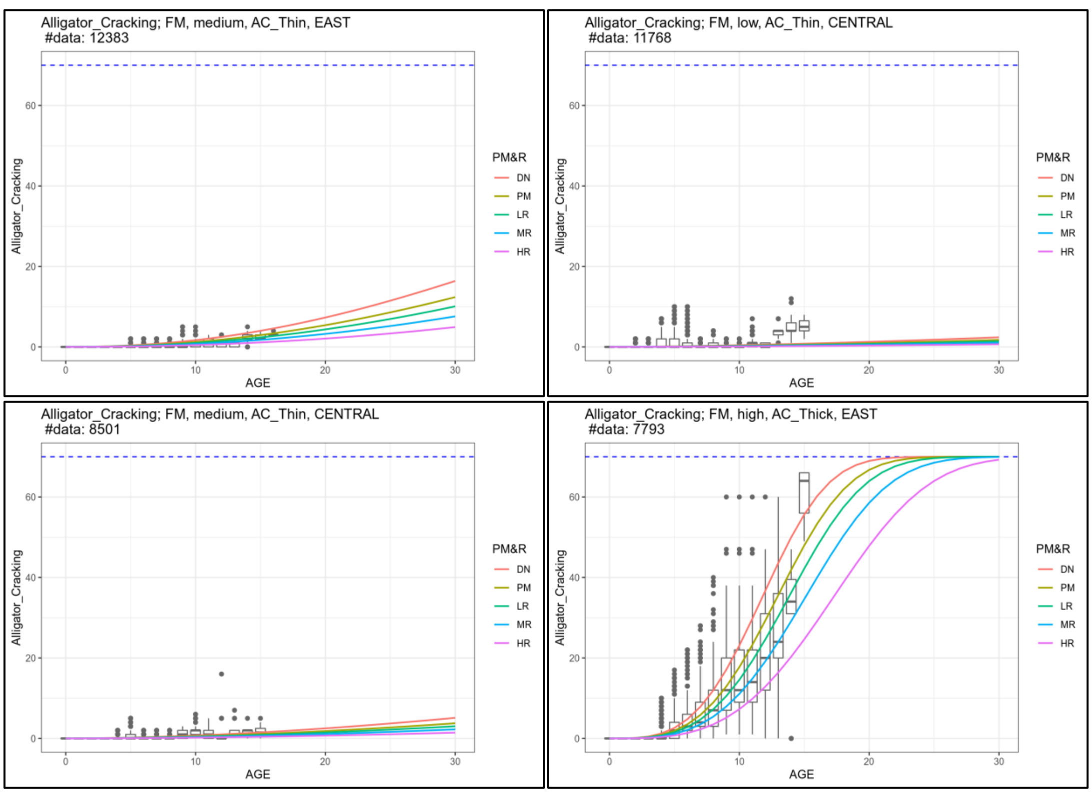

Figure 4.19 Group Performance of Alligator Cracking Model

4.3.9. Longitudinal Cracking

Table 4.18 Model Estimation of Longitudinal Cracking from Stage I

Variables	Parameter	Estimate	Std. Error	t value	p-value
-	β_1	9.5637	0.0498735	191.7583	0.0e+00
-	a_0	6.8769	0.0015927	4317.7553	0.0e+00
Group_1	a_1	0.3401	0.0086189	39.4628	0.0e+00
Group_2	a_2	0.3692	0.0160807	22.9611	3.3e-116
Group_3	a_3	0.3794	0.0135591	27.9789	6.9e-171
Group_4	a_4	0.5615	0.0040972	137.0567	0.0e+00
Group_5	a_5	0.4060	0.0072585	55.9367	0.0e+00
Group_6	a_6	-1.4520	0.6307529	-2.3020	1.1e-02
Group_7	a_7	0.4794	0.0098465	48.6867	0.0e+00
Group_8	a_8	0.0844	0.0767994	1.0992	1.4e-01
Group_9	a_9	0.4639	0.0044652	103.8904	0.0e+00
Group_10	a_{10}	0.4658	0.0091047	51.1561	0.0e+00
Group_11	a_{11}	0.2963	0.0192004	15.4327	7.1e-54
Group_12	a_{12}	0.0801	0.0346982	2.3074	1.1e-02
Group_13	a_{13}	0.1242	0.0415078	2.9911	1.4e-03
Group_14	a_{14}	0.6214	0.0030520	203.5945	0.0e+00
Group_15	a_{15}	0.6769	0.0034489	196.2645	0.0e+00
Group_16	a_{16}	0.6247	0.0202475	30.8511	7.9e-207
Group_17	a_{17}	0.1833	0.0128592	14.2530	2.8e-46
Group_19	a_{19}	0.1408	0.0090378	15.5817	7.1e-55
CL_WEST	γ_1	-0.4552	0.0212436	-21.4265	1.4e-101
CL_EAST	γ_2	-0.0471	0.0020908	-22.5390	4.4e-112
CL_NORTH	γ_3	-0.0148	0.0091565	-1.6203	5.3e-02
CL_SOUTH	γ_4	-0.0363	0.0057274	-6.3416	1.1e-10

Table 4.19 Model Estimation of Longitudinal Cracking from Stage II

Variables	Parameter	Estimate	Std. Error	t value	p-value
-	η_0	7.4525	0.0168	444.2059	0e+00
DN	η_1	2.8388	0.0362	78.4139	0e+00
LR	η_2	-1.3235	0.0337	-39.2740	0e+00
MR	η_3	-2.8318	0.0369	-76.6578	0e+00
HR	η_4	-4.3990	0.0464	-94.8703	0e+00

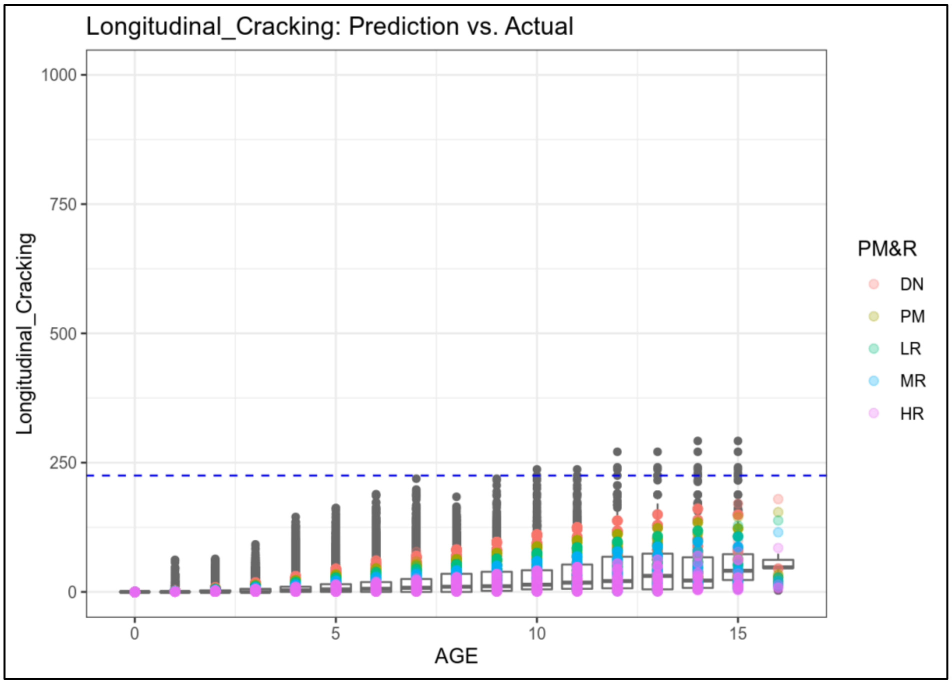

Figure 4.20 Network Performance of Longitudinal Cracking Model

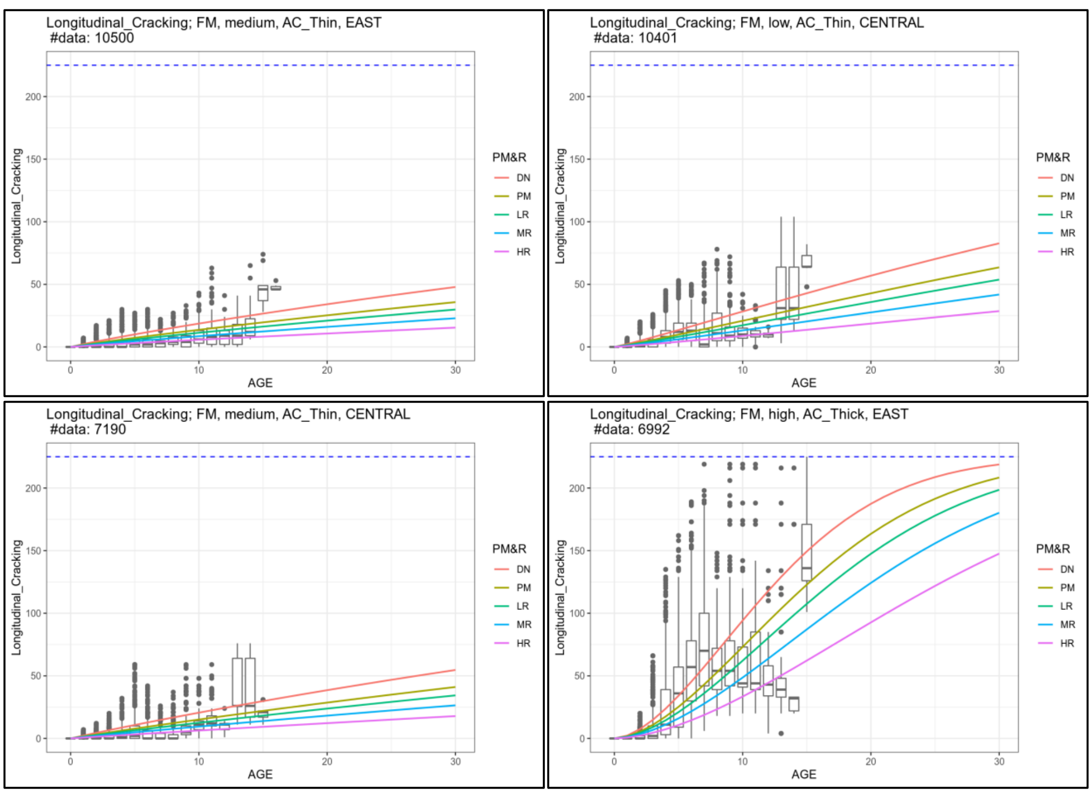

Figure 4.21 Group Performance of Longitudinal Cracking Model

4.3.10. Transverse Cracking

Table 4.20 Model Estimation of Transverse Cracking from Stage I

Variables	Parameter	Estimate	Std. Error	t value	p-value
-	β_1	1.7017	1.4143e-02	120.3264	0.0e+00
-	α_0	7.0947	1.7196e-03	4125.8409	0.0e+00
Group_1	α_1	0.3528	1.0670e-02	33.0678	6.7e-237
Group_2	α_2	0.5594	7.9938e-03	69.9853	0.0e+00
Group_3	α_3	0.1646	3.8884e-02	4.2319	1.2e-05
Group_4	α_4	-0.0531	4.5195e-02	-1.1755	1.2e-01
Group_5	α_5	0.3646	5.5447e-03	65.7504	0.0e+00
Group_6	α_6	-2.3534	5.2986e+00	-0.4442	3.3e-01
Group_7	α_7	0.0210	1.2251e-02	1.7174	4.3e-02
Group_8	α_8	-0.0229	1.1347e-01	-0.2022	4.2e-01
Group_9	α_9	0.5313	2.2918e-03	231.8076	0.0e+00
Group_10	α_{10}	0.5626	4.1715e-03	134.8732	0.0e+00
Group_11	α_{11}	0.1783	3.2445e-02	5.4947	2.0e-08
Group_12	α_{12}	0.2053	1.7380e-02	11.8119	1.9e-32
Group_13	α_{13}	-0.2211	4.6506e-02	-4.7545	1.0e-06
Group_14	α_{14}	-0.2738	7.1123e-02	-3.8492	5.9e-05
Group_15	α_{15}	-18.4044	4.1190e+07	0.0000	5.0e-01
Group_16	α_{16}	0.4374	4.1372e-02	10.5716	2.2e-26
Group_17	α_{17}	0.1947	1.3499e-02	14.4210	2.5e-47
Group_19	α_{19}	-0.0982	1.0159e-02	-9.6660	2.2e-22
CL_WEST	γ_1	-0.2466	1.9801e-02	-12.4526	7.9e-36
CL_EAST	γ_2	0.1009	2.1430e-03	47.0809	0.0e+00
CL_NORTH	γ_3	0.4434	4.5064e-03	98.3935	0.0e+00
CL_SOUTH	γ_4	0.0223	1.1150e-02	1.9980	2.3e-02

Table 4.21 Model Estimation of Transverse Cracking from Stage II

Variables	Parameter	Estimate	Std. Error	t value	p-value
-	η_0	1.2442	0.0043	291.3911	0e+00
DN	η_1	0.4915	0.0094	52.3543	0e+00
LR	η_2	-0.1493	0.0091	-16.4246	7e-61
MR	η_3	-0.4490	0.0093	-48.0259	0e+00
HR	η_4	-0.8766	0.0107	-81.8746	0e+00

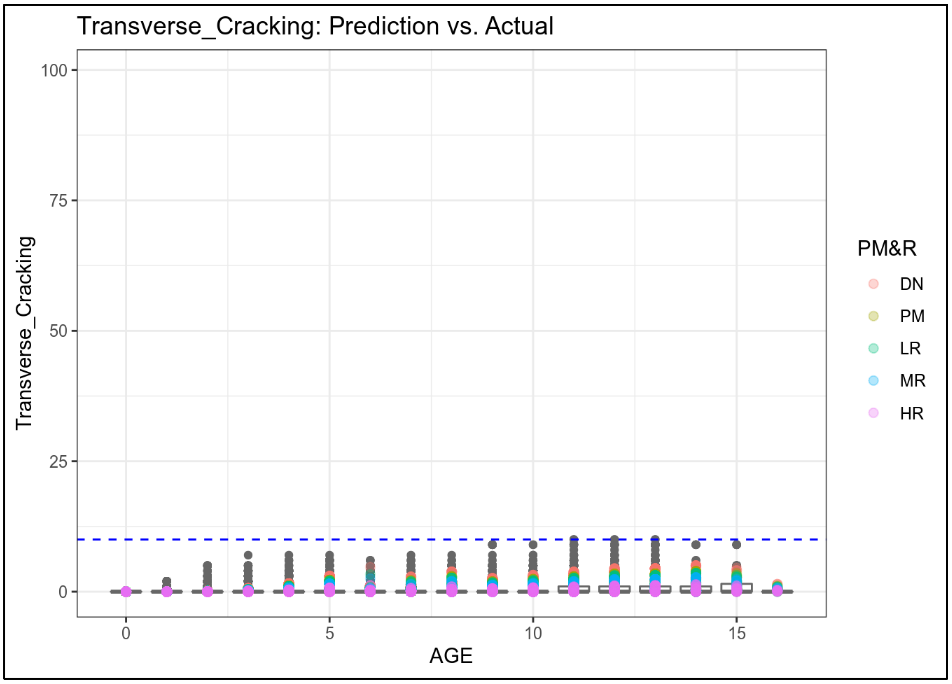

Figure 4.22 Network Performance of Transverse Cracking Model

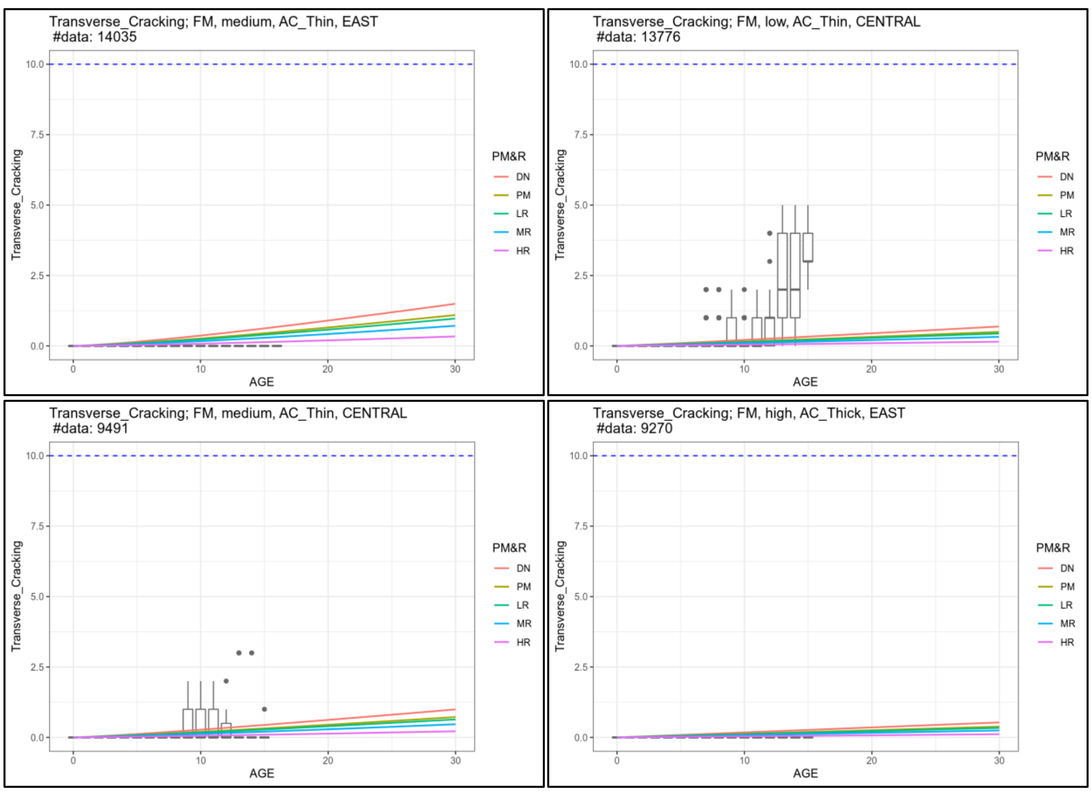

Figure 4.23 Group Performance of Transverse Cracking Model

Chapter 5. Development and Calibration of Databases and Models

This chapter presents the development of the analysis database and the calibration of performance models.

5.1. Overall Development of Analysis Database

5.1.1. Performance Data

The database used in this chapter was obtained originally from the TxDOT PMIS and PA systems dating from 2002 to 2019. To establish an analysis data set for model development, a series of variables associated with structural and environmental factors have been extracted. Additionally, the distributions of various distresses were also investigated to assist the model estimation and to have a better understanding of realistic field levels of the various distresses.

5.1.1.1. Variables

Pavement deterioration is affected by various factors. In TxDOT's PMIS and PA system, factors related to functional, structural, and traffic information have been documented and can be easily queried as model variables. Although only limited environment information is available in the PMIS and PA, the environment does play a significant role in affecting pavement performance, so environmental factors (including temperature and precipitation) were also obtained from the NOAA database. Just as for ACPs, the variables considered in the concrete pavement performance models include functional class, traffic, climate, and pavement type. Of these variables, the same definitions as those in the flexible pavement performance models have been applied to the functional class, traffic, and climate; for the pavement type, however, the concrete pavement type information stored in the PMIS was found to be not entirely accurate. Therefore, a column "pav_type_distress" was created based on the performance measurement, i.e., if a pavement section at a given year has any ratings for CRCP distresses, it is classified as CRCP at that year (it has been confirmed that a pavement section cannot have both CRCP and JCP ratings at a given year). Based on the stored pavement type information there are 191,387 data records for concrete pavements; deducting the pavement type records from performance measurement records leaves 201,606 concrete pavement data records.

5.1.1.2. Variable Correlation

The design of a pavement structure is a systematic decision process that deliberates about various factors, including but not limited to structure, traffic, and environment. As a result, intrinsic correlations are found among different variables during the development of pavement performance models. For example, IHs normally accommodate higher levels of traffic than non-interstate highways. Considering this, in this project, a preliminary correlation analysis was conducted to investigate the correlation between functional class and traffic. As shown in Figure 5.1, where the size of the marker represents the amount of available data, significant correlations can be found between the functional class and traffic for both CRCP and JCP.

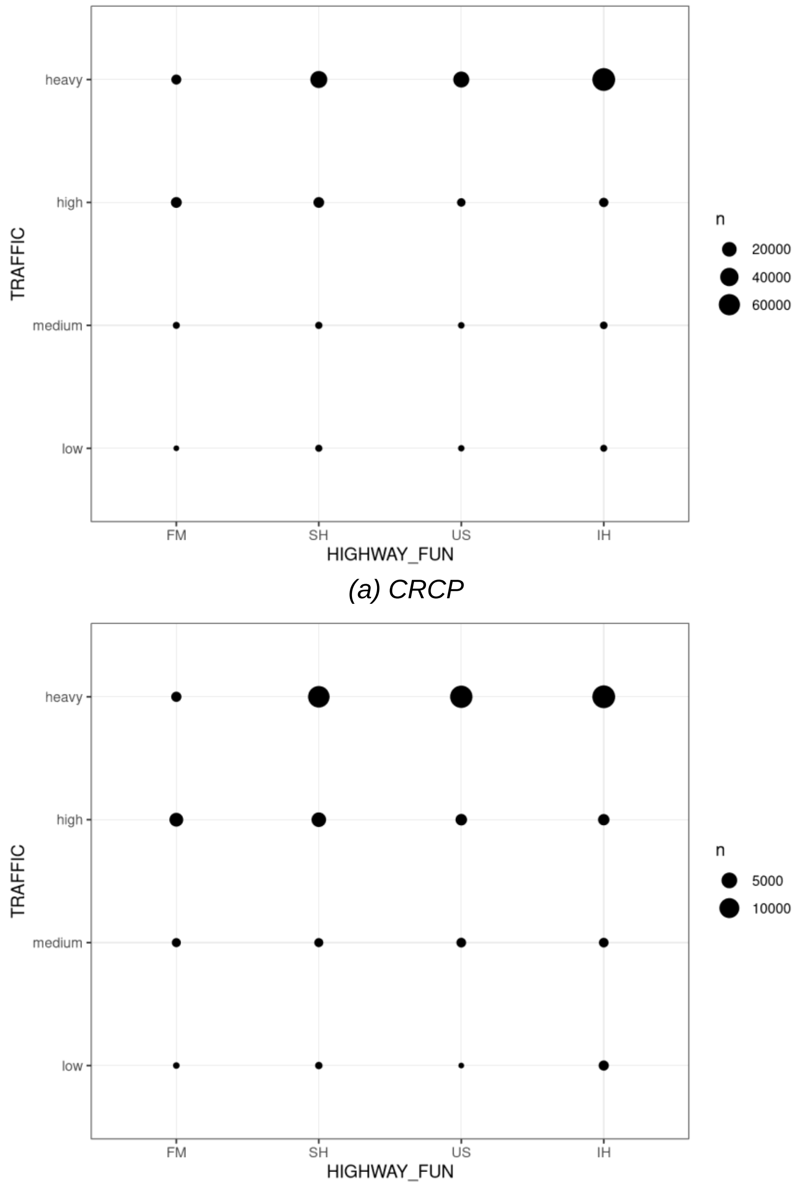

(a) CRCP

(b) JCP

Figure 5.1 Variable Correlation

5.1.1.3. Distribution of Pavement Distresses

According to the TxDOT Rater's Manual, the concrete pavement distresses for a PMIS/PA section are rated as whole numbers of distresses or distressed slabs. Since the PMIS/PA section length varies, distress ratings should be normalized first:

$$L_i = \frac{L_i'}{OFF\_TO_i - OFF\_FROM_i}$$

where L_i' is the distress rating stored in PMIS and PA, and OFF_FROM_i and OFF_TO_i are the beginning and ending DFOs of section *i*.

After normalization, the histograms (the cumulative density curves along with various percentiles for different types of CRCP and JCP distresses) were obtained and are presented together in Figure 5.2 and Figure 5.3. The maximum values proposed for different types of distresses in the TxDOT Rater's Manual are marked with vertical red dash lines. As shown, the maxima of distresses in the database may not coincide with the defined maximums, and most of the distresses exhibit extremely skewed distributions. Consequently, to ensure good performance and robust predictions, appropriate asymptotic values were selected to cover most of the data as their use prevents values that are too extreme. In this project, based on the distribution of the various distresses, when performing model estimation, the asymptotic values were selected based on the 99.9th percentiles for each type of distress.

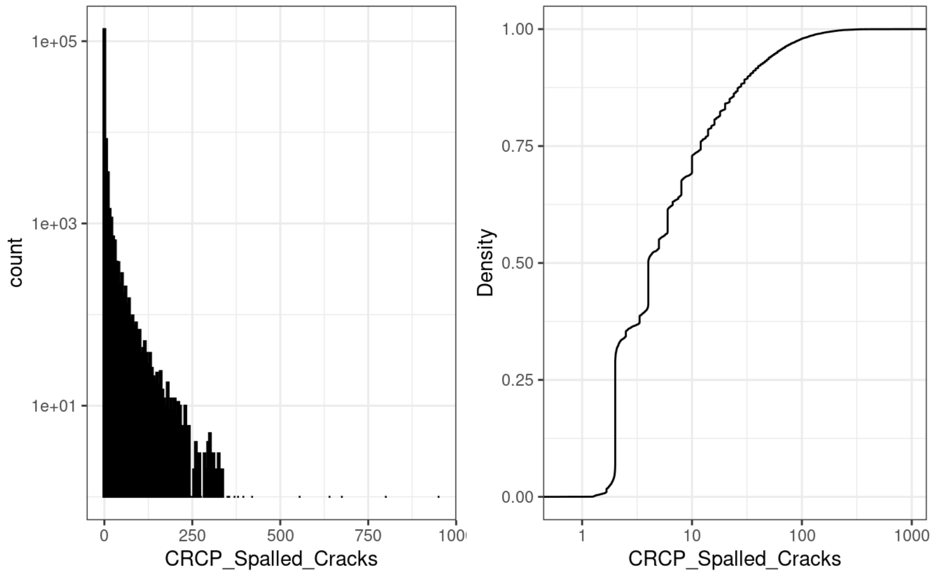

probs	10.0%	25.0%	50.0%	75.0%	95.0%	99.0%	99.9%	100.0%
percentile	0.00	0.00	0.00	0.00	11.20	57.49	182.50	950.00

(a) Spalled Cracks

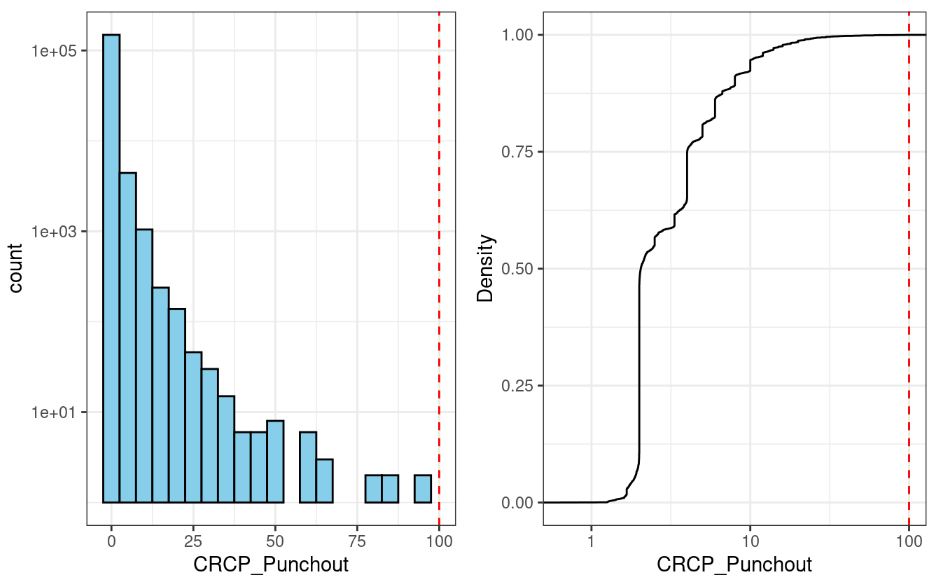

probs	10.0%	25.0%	50.0%	75.0%	95.0%	99.0%	99.9%	100.0%
percentile	0.00	0.00	0.00	0.00	2.00	7.56	22.00	100.00

(b) Punchout

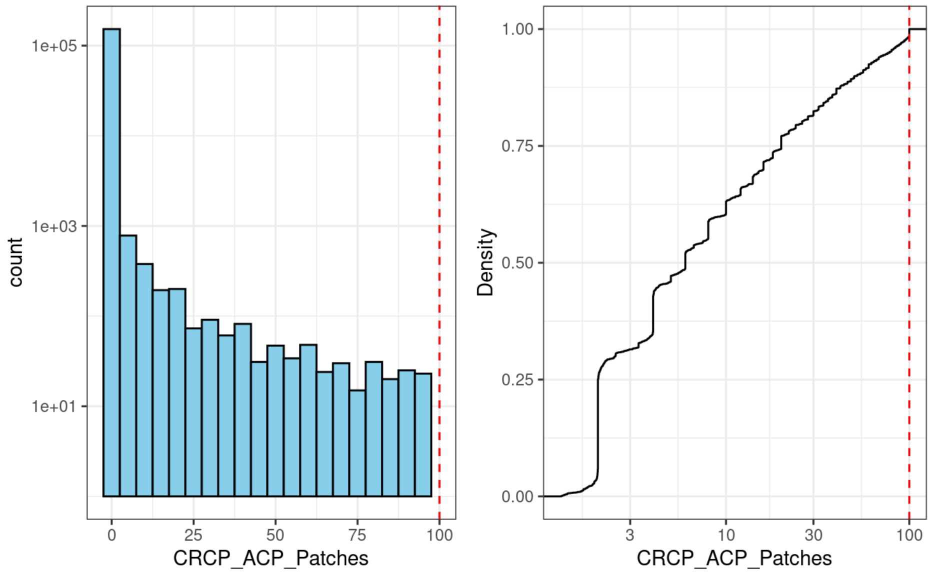

probs	10.0%	25.0%	50.0%	75.0%	95.0%	99.0%	99.9%	100.0%
percentile	0.00	0.00	0.00	0.00	0.00	6.27	81.21	149.53

(c) ACP Patches

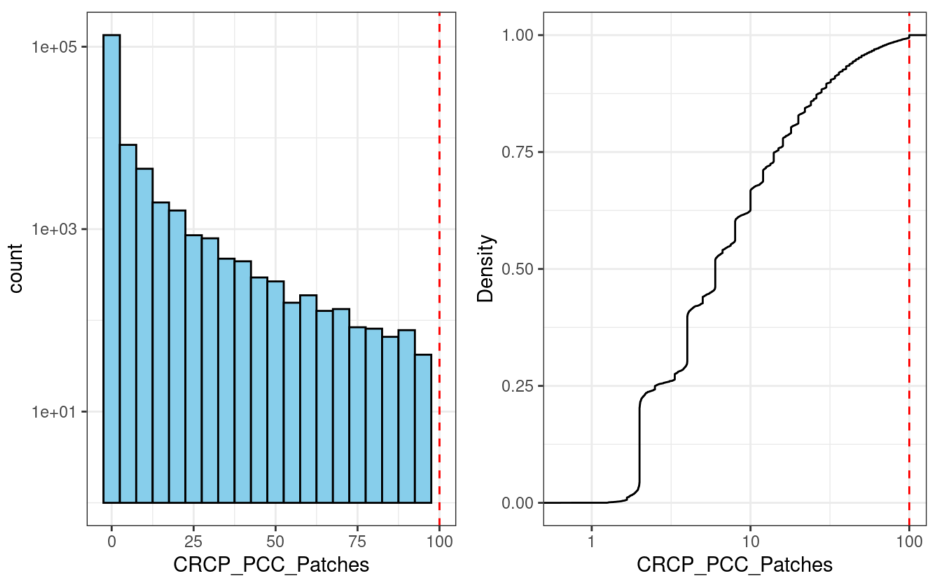

probs	10.0%	25.0%	50.0%	75.0%	95.0%	99.0%	99.9%	100.0%
percentile	0.00	0.00	0.00	0.00	13.33	46.00	100.00	132.89

(d) PCC Patches

Figure 5.2 Distribution of CRCP Distresses

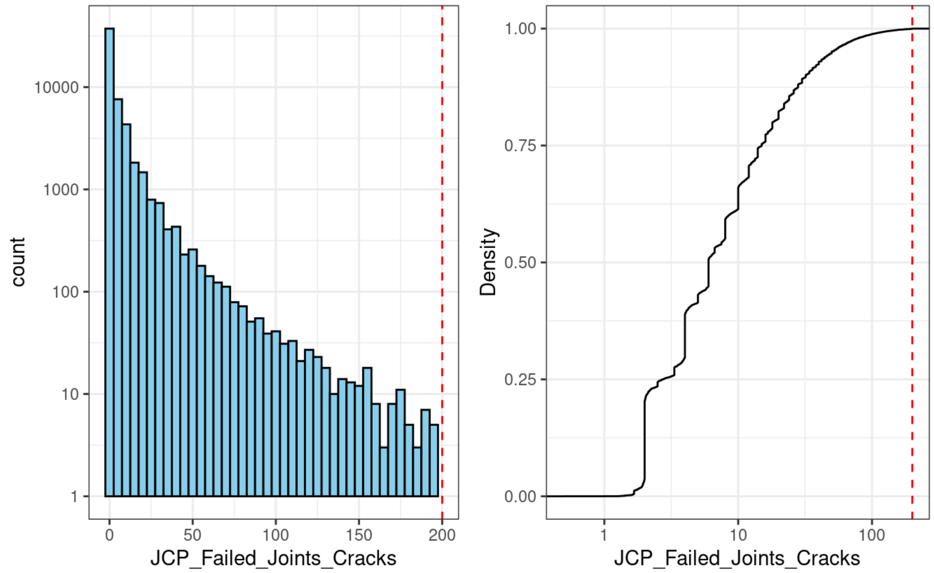

probs	10.0%	25.0%	50.0%	75.0%	95.0%	99.0%	99.9%	100.0%
percentile	0.00	0.00	0.00	5.85	30.00	76.92	172.98	397.44

(a) Failed Joints and Cracks

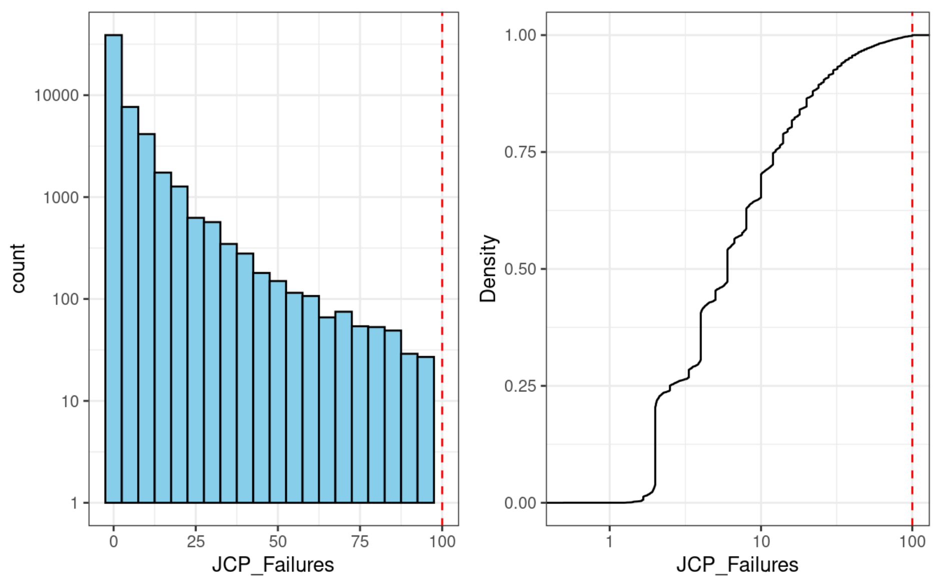

probs	10.0%	25.0%	50.0%	75.0%	95.0%	99.0%	99.9%	100.0%
percentile	0.00	0.00	0.00	4.00	23.53	61.07	147.59	665.78

(b) Failures

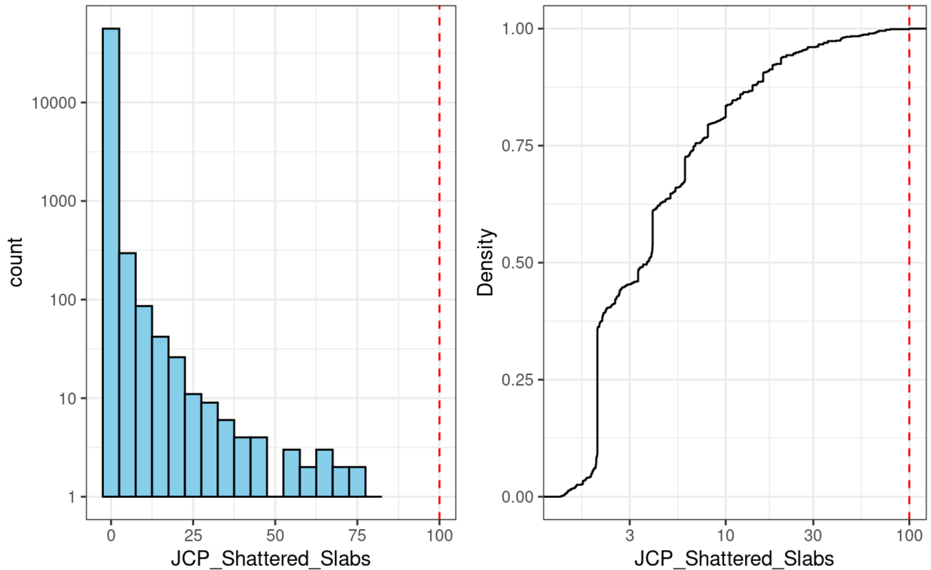

probs	10.0%	25.0%	50.0%	75.0%	95.0%	99.0%	99.9%	100.0%
percentile	0.00	0.00	0.00	0.00	0.00	2.00	23.60	351.97

(c) Shattered Slabs

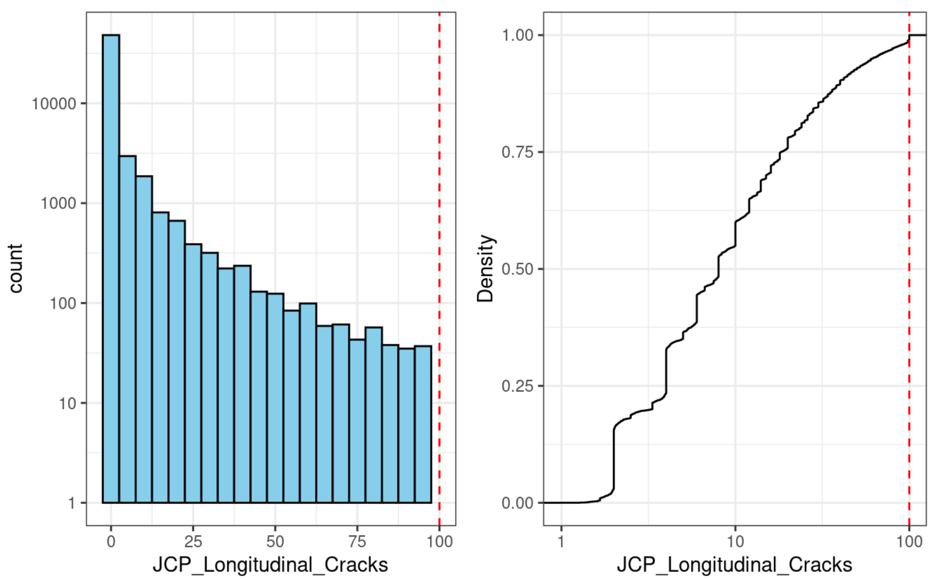

probs	10.0%	25.0%	50.0%	75.0%	95.0%	99.0%	99.9%	100.0%
percentile	0.00	0.00	0.00	0.00	17.99	65.00	101.78	147.06

(d) Longitudinal Cracks

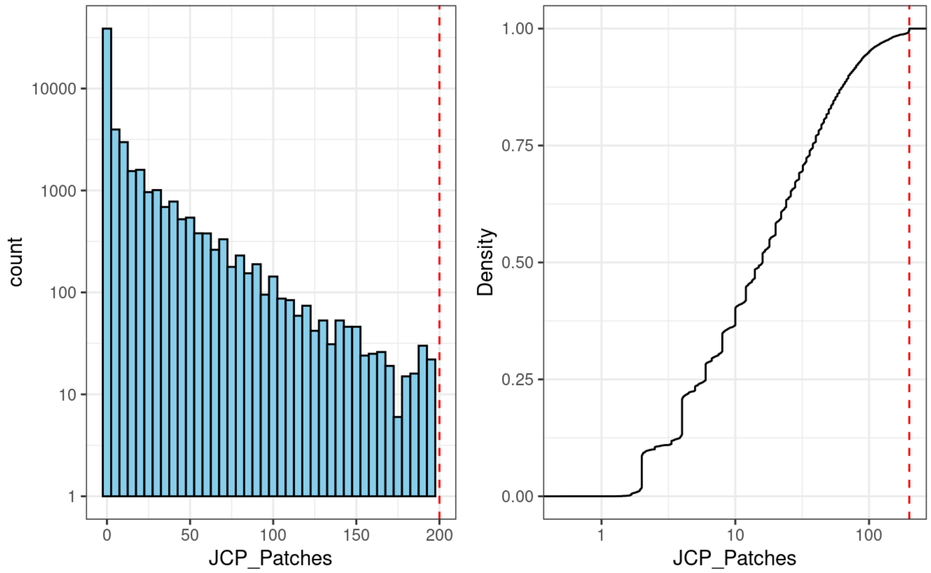

probs	10.0%	25.0%	50.0%	75.0%	95.0%	99.0%	99.9%	100.0%
percentile	0.00	0.00	0.00	6.67	59.02	136.36	203.95	442.80

(e) Patches

Figure 5.3 Distribution of JCP Distresses

5.1.2. Work History Data

In Texas, based on work intensity, treatments types intended to improve pavement condition are generally divided into four categories: PM, LRhb, MRhb, and HRhb. Since the age of the pavement (calculated as the length of time since the latest maintenance, rehabilitation, or construction work) plays a significant role in affecting the deterioration of pavement, a database documenting different M&R work is critical for developing robust performance models. In this project, the DCIS data from TxDOT was originally used to develop the work history database; however, although the DCIS data contains information about the time and location of M&R projects, most of the project records are very limited in terms of providing roadbed information and accurate treatment classification. Consequently, the developed database for performance modeling was not very accurate. For example, since HRhb generally involves much higher work intensity, a pavement section that receives HRhb is expected to perform better than those that received MRhb, LRhb, or PM. However, as shown in Figure 5.4, where the distribution of failures for JCP is plotted against pavement age, pavements treated with HRhb are revealed to have significantly more failures than those with other treatments in early ages. As a result, performance models developed using these data will result in poor predictions and induce inappropriate M&R decisions.

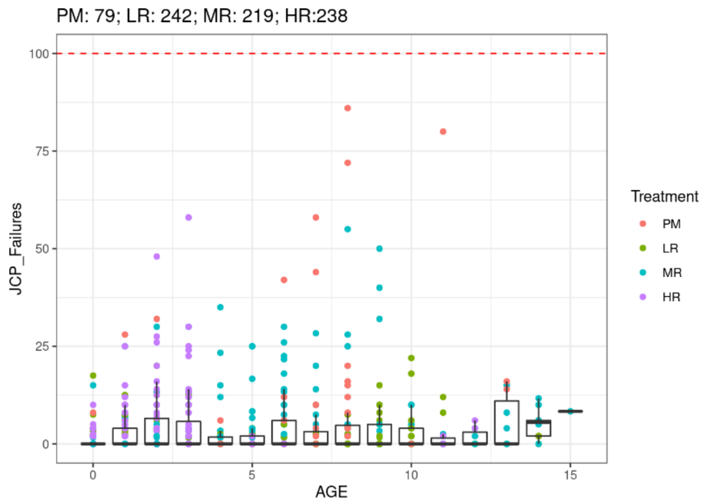

Figure 5.4 Example of Data Distribution based on DCIS Work History

Considering the relatively low accuracy of the work history based on the DCIS database, an alternative method was proposed to develop the work history data, using the following two steps:

- For each PMIS/PA section with more than four records, a linear regression was performed:

$$DS = a + b \cdot EFF\_YEAR$$

- The sections with significant non-increasing slope (b <0, p-value ≤ 0.1) were kept, and for each section, the year of the first record was treated as age 0 (year of project completion).

After obtaining the work history, the work history data was combined with the PMIS and PA data to compute the age variable and prepare a database for model development. The district distributions of all PMIS/PA data and the analysis data along with the sampling plots for CRCP and JCP are presented in Figures 5.5 to 5.8. As shown, the data prepared for model development constitute a representative sample for both CRCP and JCP concrete pavements in Texas.

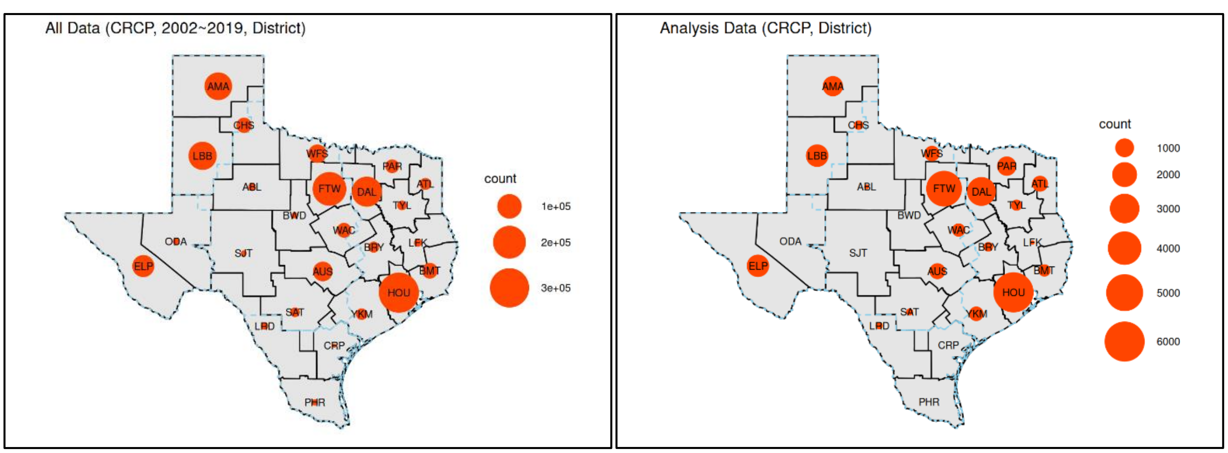

Figure 5.5 Geographic Data Distribution for CRCP

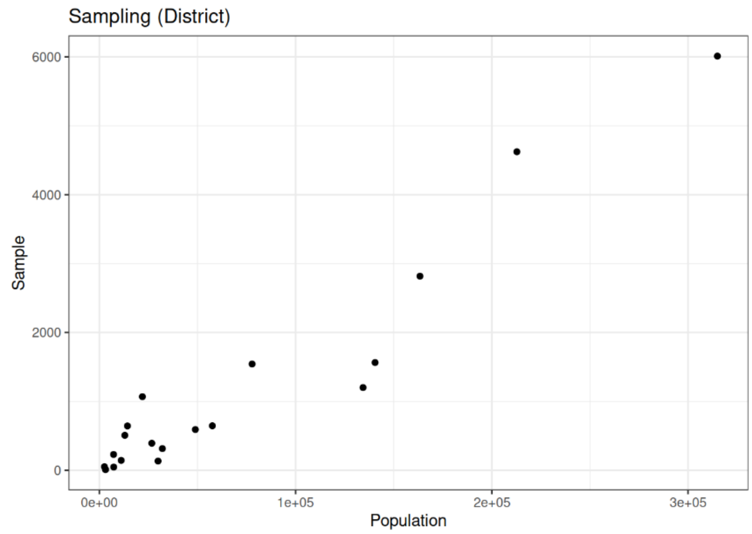

Figure 5.6 Data Sampling for CRCP

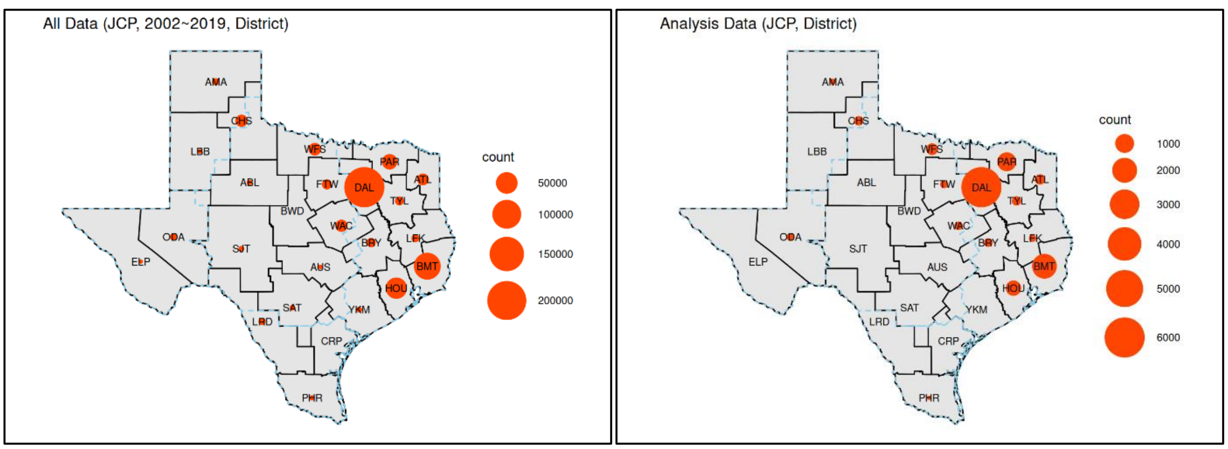

Figure 5.7 Geographic Data Distribution for JCP

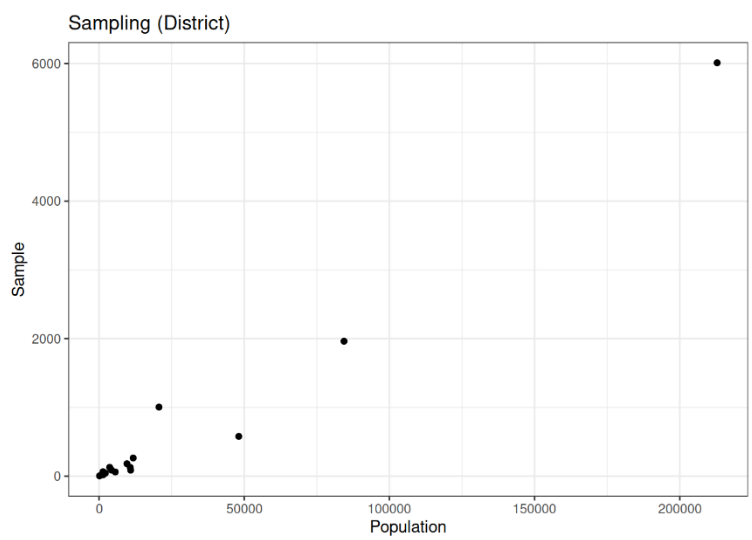

Figure 5.8 Data Sampling for JCP

As for the treatment type information, a provisional approach was adopted: for each group of pavement sections with the same traffic level and climate zone at each age, the lower 25 percent of the data were assigned to HRhb, the lower 50 percent were treated as MRhb, and the lower 70 percent of the data were assigned to LRhb, while data between 15th and 75th percentiles were allocated to PM. Moreover, all the data above the 15th percentile were grouped as DN. In this way, five separate databases for each type of distress were created and then combined to develop performance models.

5.2. Calibration of Current Performance Models for CRCPs

5.2.1. Model Specification

For the calibration of performance models for CRCPs, the current model specification used by TxDOT was used:

$$L_i = \alpha \exp[-\left(\frac{\rho\chi\epsilon\sigma}{Age}\right)^{\beta}]$$

where,

L_i: level of distress in a pavement section,

α: horizontal asymptote factor that represents the maximum range of distress growth,

β: a slope factor that controls how steeply utility is lost in the middle of the curve,

ρ: prolongation factor that controls the time it takes before significant increases in distress occur,

χ: the traffic weighting factor that controls the effect of an 18-k ESAL on performance,

ϵ: climate weighting factor that controls the effect of rainfall and freeze-thaw cycles on performance,

σ: subgrade weighting support factor that controls the effect of subgrade strength on performance, and

Age: pavement age of section, in years.

Since the parameters ρ, χ, ϵ, and σ appear in the model as a multiplication, direct estimations of them separately are impossible. Therefore, parameter A was used to replace them, which simplifies the equation as follows:

$$L_i = \alpha \exp[-\left(\frac{A}{Age}\right)^{\beta}]$$

5.2.2. Model Estimation

Based on the model specification, it can be found that when both A and β are positive, increasing A will always produce smaller L_i, while the effect of β varies depending on AGE (Figure 5.9). When $AGE < A$, larger β will produce smaller L_i; when $AGE > A$, larger β will produce larger L_i. To ensure that the effects of variables are consistent across different pavement ages, in the model estimation, the traffic, climate zone, and treatment type variables were all included into A, where γ_0 represents the parameters corresponding to medium traffic, central climate zone, and PM treatment.

$$\begin{aligned} A = {} & \gamma_0 + \gamma_1 Traffic\_Low + \gamma_2 Traffic\_High + \gamma_3 Traffic\_Heavy \\ & + \gamma_4 CL\_WEST + \gamma_5 CL\_EAST + \gamma_6 CL\_NORTH + \gamma_7 CL\_SOUTH \\ & + \gamma_8 DN + \gamma_9 LRhb + \gamma_{10} MRhb + \gamma_{11} HRhb \end{aligned}$$

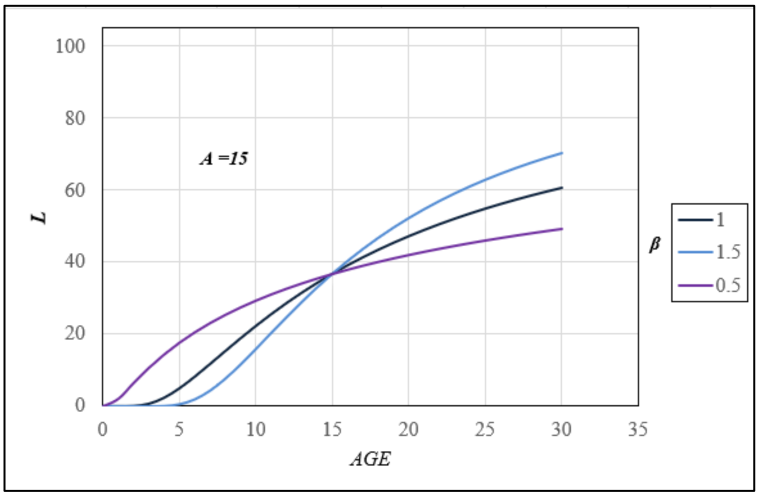

Figure 5.9 Effect of β

Pavement deterioration models should be able to depict the general change of distresses under various conditions as well as produce predictions that are as close as possible to the field observations. Generally, after maintenance or rehabilitation work, pavement distresses should progressively increase without intervention until the next maintenance or rehabilitation work. Pavement sections with higher traffic level should exhibit higher levels of distress, and for different types of M&R, it is expected that the treatment involving a higher level of work intensity, which normally corresponds to higher cost, will produce better pavement performance, i.e., lower distress and slower deterioration rate. Moreover, to facilitate plans for M&R work, and the calculation of treatment effectiveness, the deterioration curves of different treatments should not cross each other. As a result, in this project, the selected specification form for the deterioration models adhere to the following principles:

- The deterioration curve should be non-decreasing; specifically, for the current model specification, both A and β should be positive. Furthermore, based on a preliminary data analysis, the following ranges for A and β were established to guarantee the developed models are reasonable:

$$\begin{cases} 5 \le A \le 1000 \\ 1 \le \beta \le 10 \end{cases}$$

- The deterioration curves of pavement sections with different traffic level should follow an order by which the heavy traffic level has the highest distress rate followed by high, medium, and low traffic levels, which introduced the following constraints:

$$\begin{cases} \gamma_1 \ge 0 \\ \gamma_2 \le 0 \\ \gamma_3 \le 0 \\ \gamma_2 - \gamma_3 \ge 0 \end{cases}$$

- The deterioration curves of different treatment types for a pavement section should not cross each other and should follow a hierarchical order by which the DN curve has the highest distress rate followed by PM, LRhb, MRhb, and HRhb, which introduced the following constraints:

$$\begin{cases} \gamma_8 \le 0 \\ \gamma_9 \ge 0 \\ \gamma_{10} \ge 0 \\ \gamma_{11} \ge 0 \\ \gamma_9 - \gamma_{10} \le 0 \\ \gamma_{10} - \gamma_{11} \le 0 \end{cases}$$

- The predictions of the deterioration models should be as close as possible to the field measurements. In this project, to meet this requirement, the least-squares method was used to perform the model estimation. The objective function of the least-squares method is to minimize the sum of squared distance between the predictions and observations:

$$\boldsymbol{\theta} = \underset{\boldsymbol{\theta}}{\operatorname{argmin}} \sum_{i=1}^{n} (L(\boldsymbol{x}_i, \boldsymbol{\theta}) - L_i^*)^2$$

Where $\boldsymbol{\theta}$ refers to the model parameters to be estimated, L_i^* is the distress of the *i*th observation in the data, and the $L(\boldsymbol{x}_i, \boldsymbol{\theta})$ is the corresponding prediction from the deterioration model.

5.2.3. Results and Discussions

The model errors for CRCP are presented in Table 5.1, where the third column is the mean squared error (MSE), the fourth column is the standard error, and the last column is the normalized error with respect to the asymptotic value. As the table indicates, the normalized errors of all the models are below 7 percent, which indicates that the calibrated models produce robust predictions.

The summaries of the model estimations for different types of distresses are reported in Tables 5.2 to 5.5. It can be found that for all the models, the parameters for the traffic and treatment type meet the requirements specified in the previous section, which ensure that the performance models always produce higher distress for heavy traffic level followed by high, medium, and low traffic levels; smaller distress for HRhb is followed by MRhb, LRhb, PM and DN.

To visually evaluate the performance of the updated deterioration models, the boxplots of the field measurements, and the predictions from the developed models for different types of distresses are presented in Figure 5.10. As shown, in general, the deterioration models exhibit outstanding performance for different distresses. Furthermore, the deterioration curves for different treatment types follow the right hierarchical order: the DN curve has the highest deterioration rate followed in order by PM, LRhb, MRhb, and HRhb.

Table 5.1 CRCP Model Errors

Distress	Asymptotic Value	MSE	std_error	Normalized error
Spalled Cracks	183	46.1	6.79	3.7%
Punchout	22	1.00	1.00	4.6%
ACP Patches	82	5.44	2.33	2.8%
PCC Patches	100	31.5	5.61	5.6%

Table 5.2 Model Estimation for Spalled Cracks

Variable	Parameter	Estimate	std	t	p_val
-	α	183	-	-	-
-	β	1	0.05	67.35	0.00
-	γ_0	98.4	2.24	43.90	0.00
Traffic_Low	γ_1	63.8	3.86E+3	0.02	0.49
Traffic_High	γ_2	-2.18	7.26	-0.30	0.38
Traffic_Heavy	γ_3	-2.18	2.36	-0.92	0.18
CL_WEST	γ_4	24.1	58.5	0.41	0.34
CL_EAST	γ_5	-11.3	2.44	-4.63	0.00
CL_NORTH	γ_6	4.17	10.1	0.41	0.34
CL_SOUTH	γ_7	44.2	3.02E+3	0.01	0.49
DN	γ_8	-38.2	3.74	-10.20	0.00
LR	γ_9	5.62	2.03E+3	0.00	0.50
MR	γ_{10}	38.3	263	0.15	0.44
HR	γ_{11}	53.4	3.91	13.65	0.00

Table 5.3 Model Estimation for Punchout

Variable	Parameter	Estimate	std	t	p_val
-	α	22	-	-	-
-	β	1	0.01	102.59	0.00
-	γ_0	90.5	1.28	70.26	0.00
Traffic_Low	γ_1	0.0063	46.3	0.00	0.50
Traffic_High	γ_2	-2.46	4.63	-0.53	0.30
Traffic_Heavy	γ_3	-2.46	1.34	-1.83	0.03
CL_WEST	γ_4	-7.55	4.62	-1.64	0.05
CL_EAST	γ_5	-8.57	1.71	-5.01	0.00
CL_NORTH	γ_6	-8.83	2.58	-3.42	0.00
CL_SOUTH	γ_7	-23.5	14.7	-1.60	0.05
DN	γ_8	-39.1	2.62	-14.95	0.00
LR	γ_9	4.47	798	0.01	0.50
MR	γ_{10}	20.0	2.73	7.33	0.00
HR	γ_{11}	25.2	2.33	10.84	0.00

Table 5.4 Model Estimation for ACP Patches

Variable	Parameter	Estimate	std	t	p_val
-	α	82	-	-	-
-	β	6.59	0.018	356	0.00
-	γ_0	52.3	0.003	2.0E+4	0.00
Traffic_Low	γ_1	11.4	inf	0.00	0.50
Traffic_High	γ_2	-14.2	34.0	-0.42	0.34
Traffic_Heavy	γ_3	-32.0	0.003	-12437	0.00
CL_WEST	γ_4	3.07	0.007	434	0.00
CL_EAST	γ_5	20.8	3.5E+5	0.00	0.50
CL_NORTH	γ_6	9.17	0.009	1032	0.00
CL_SOUTH	γ_7	-0.565	0.029	-19.52	0.00
DN	γ_8	-2.22	6.0E+5	0.00	0.50
LR	γ_9	0.562	Inf	0.00	0.50
MR	γ_{10}	9.93	8.7E+22	0.00	0.50
HR	γ_{11}	20.6	0.003	8011	0.00

Table 5.5 Model Estimation for PCC Patches

Variable	Parameter	Estimate	std	t	p_val
-	α	100	-	-	-
-	β	1	0.004	246.14	0.00
-	γ_0	55.2	0.266	207.70	0.00
Traffic_Low	γ_1	18.2	19.8	0.92	0.18
Traffic_High	γ_2	-0.0111	0.872	-0.01	0.49
Traffic_Heavy	γ_3	-0.0114	0.280	-0.04	0.48
CL_WEST	γ_4	-2.31	1.17	-1.97	0.02
CL_EAST	γ_5	-6.80	0.328	-20.72	0.00
CL_NORTH	γ_6	-5.00	0.657	-7.62	0.00
CL_SOUTH	γ_7	-0.347	10.8	-0.03	0.49
DN	γ_8	-19.1	0.409	-46.60	0.00
LR	γ_9	3.77	17.8	0.21	0.42
MR	γ_{10}	17.4	1.85	9.43	0.00
HR	γ_{11}	40.5	0.608	66.63	0.00

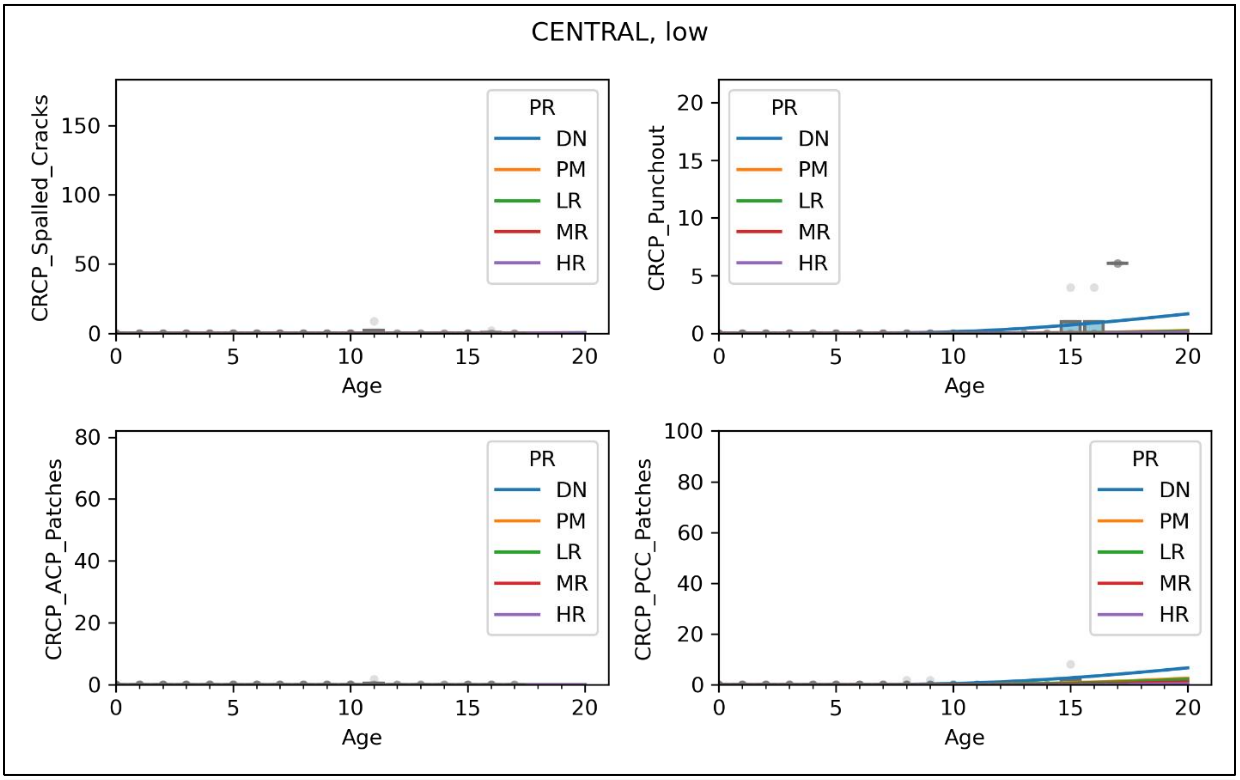
CENTRAL, low
CRCP_Spalled_Cracks
CRCP_Punchout
CRCP_ACP_Patches
CRCP_PCC_Patches
Age
PR
DN
PM
LR
MR
HR

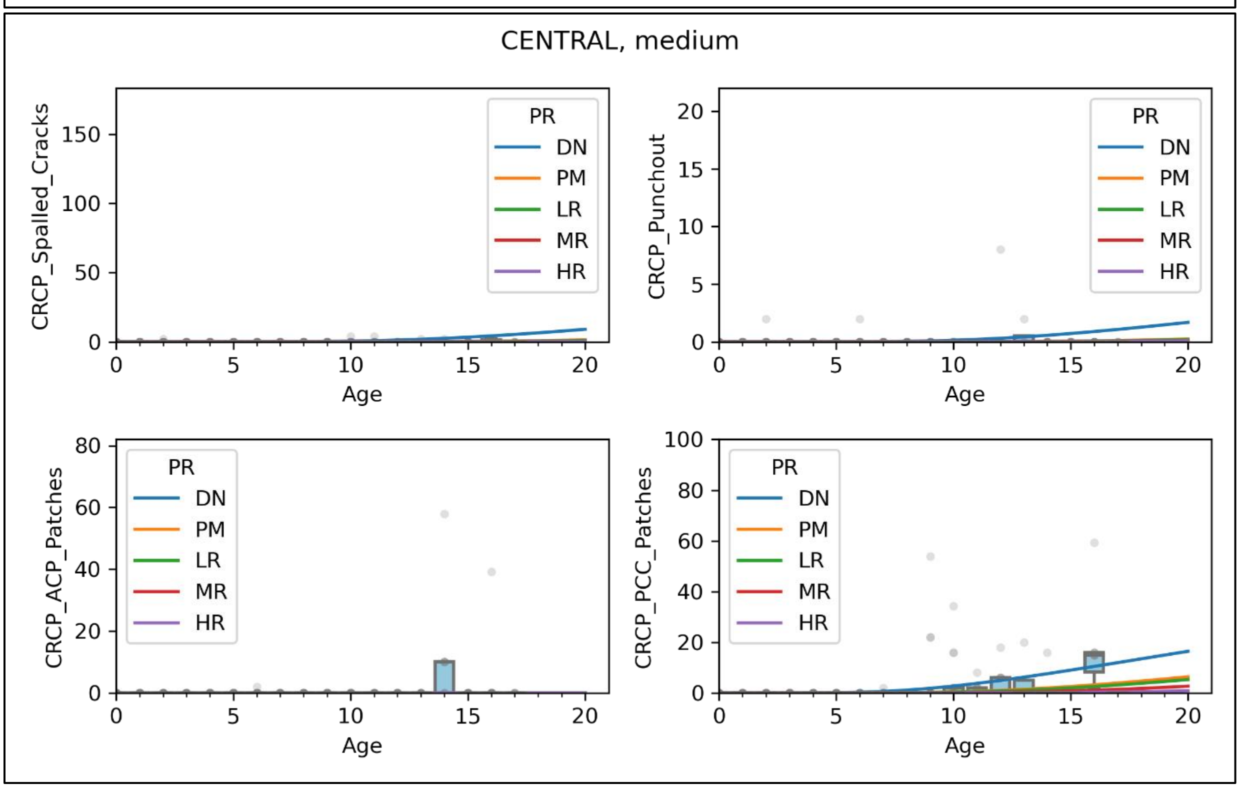
CENTRAL, medium
CRCP_Spalled_Cracks
CRCP_Punchout
CRCP_ACP_Patches
CRCP_PCC_Patches
Age
PR
DN
PM
LR
MR
HR

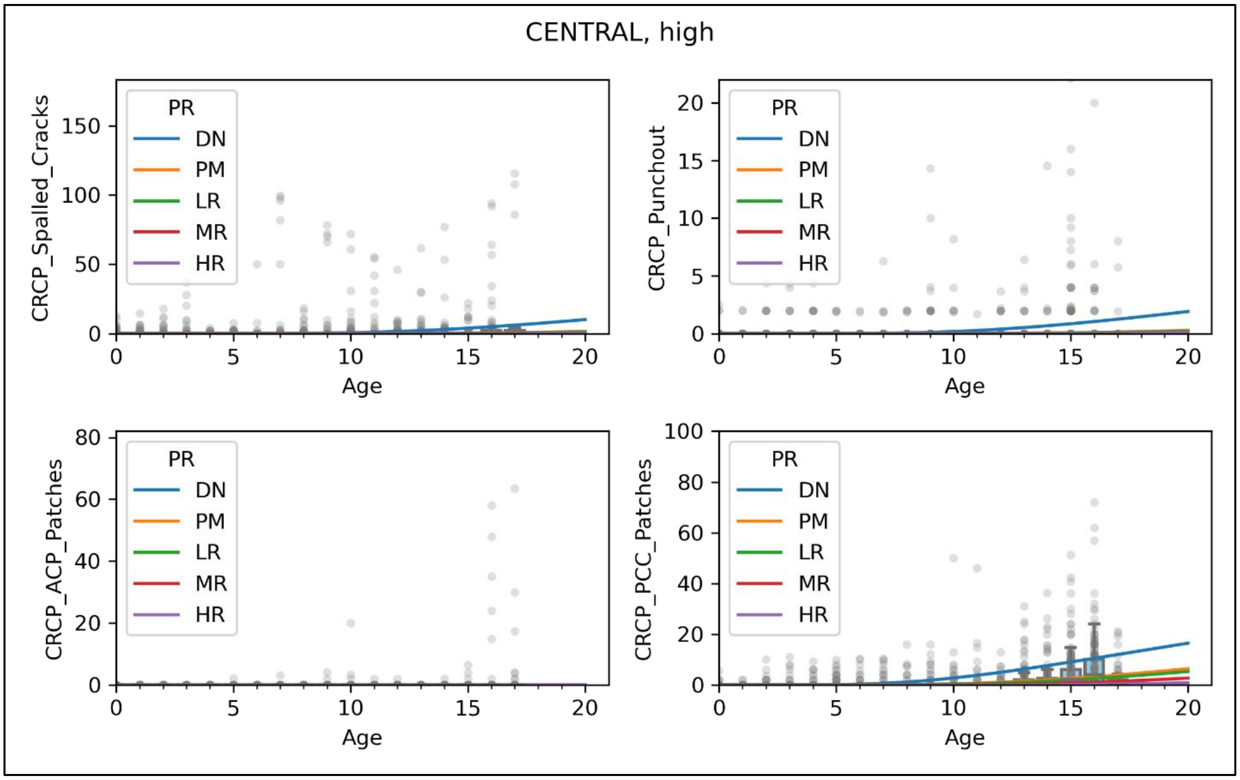
CENTRAL, high
CRCP_Spalled_Cracks
CRCP_Punchout
CRCP_ACP_Patches
CRCP_PCC_Patches
Age
PR
DN
PM
LR
MR
HR

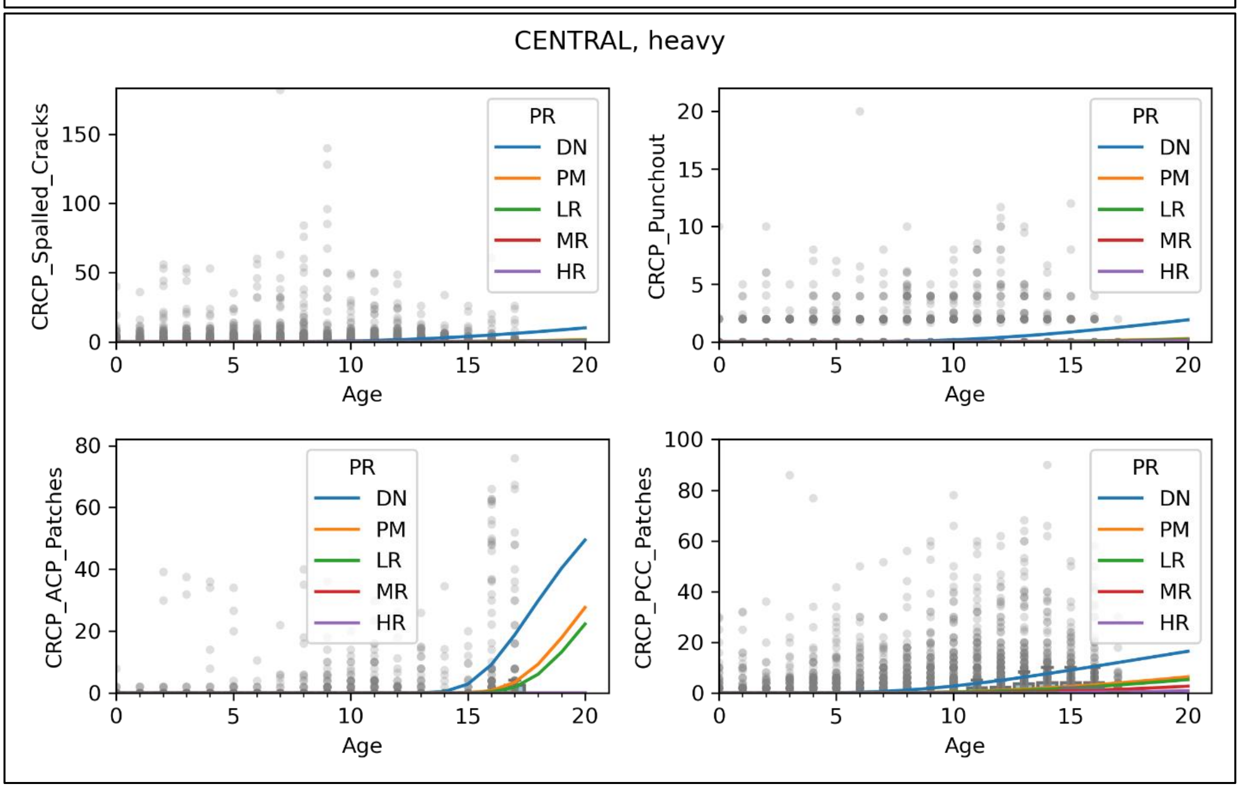
CENTRAL, heavy
CRCP_Spalled_Cracks
CRCP_Punchout
CRCP_ACP_Patches
CRCP_PCC_Patches
Age
PR
DN
PM
LR
MR
HR

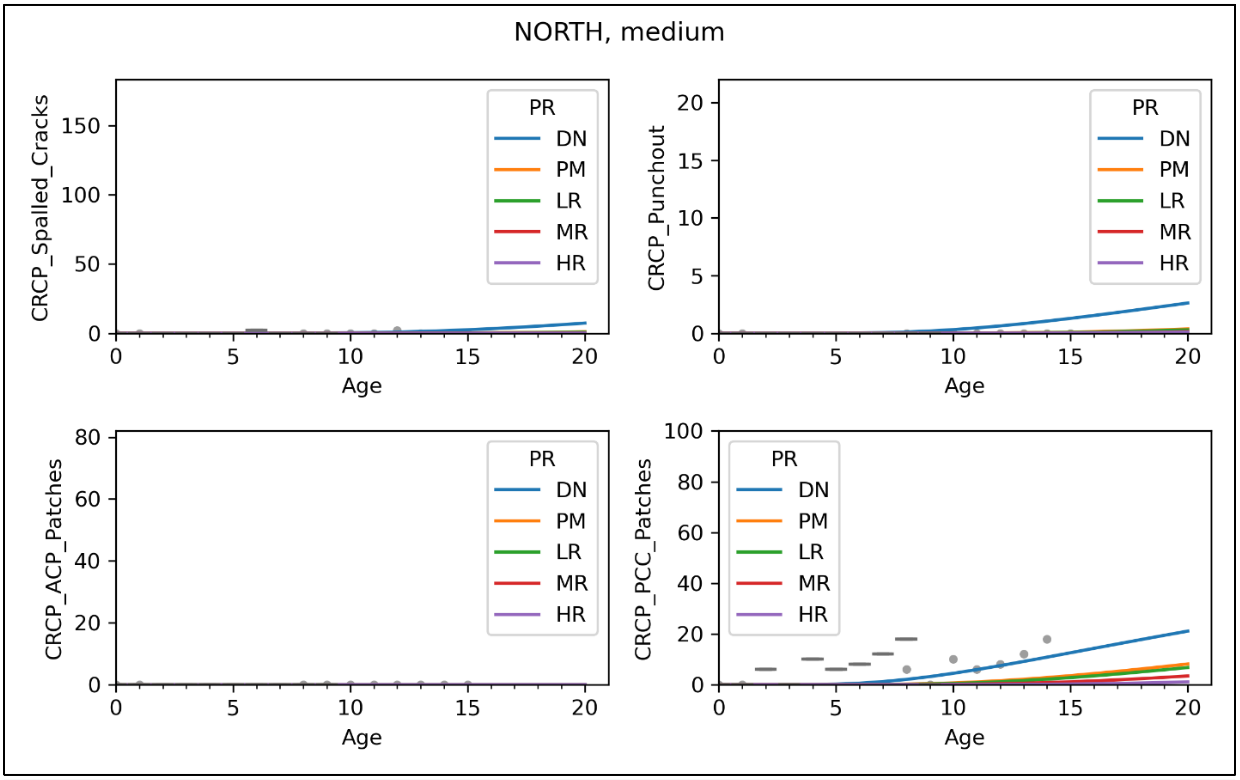
NORTH, medium
CRCP_Spalled_Cracks
CRCP_Punchout
CRCP_ACP_Patches
CRCP_PCC_Patches
Age
PR
DN
PM
LR
MR
HR

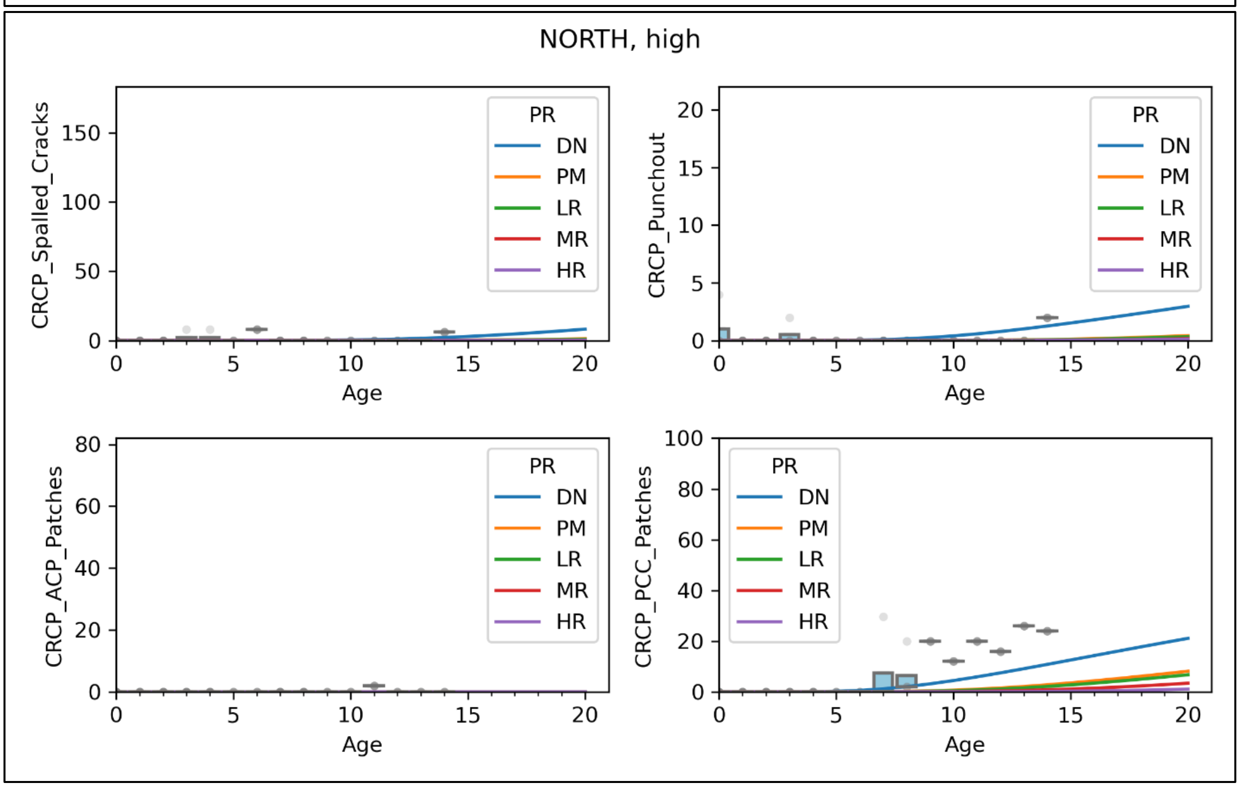
NORTH, high
CRCP_Spalled_Cracks
CRCP_Punchout
CRCP_ACP_Patches
CRCP_PCC_Patches
Age
PR
DN
PM
LR
MR
HR

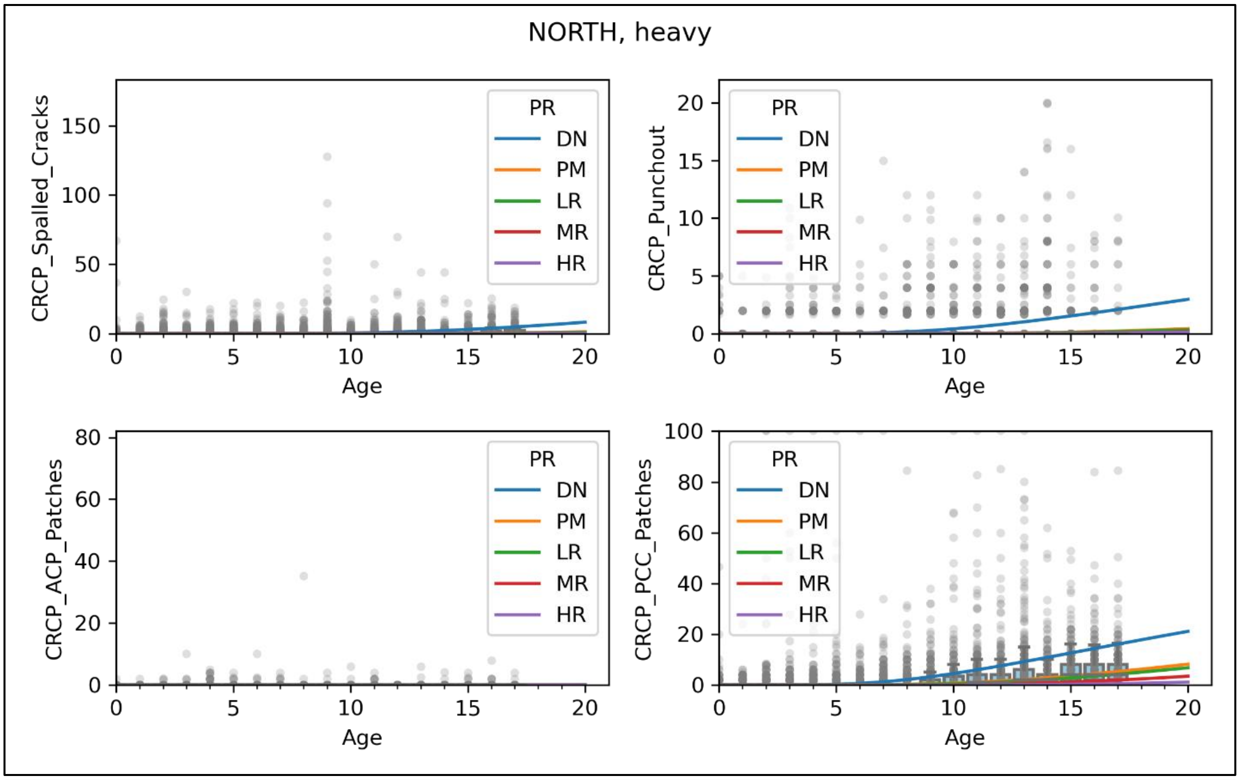
NORTH, heavy
CRCP_Spalled_Cracks
CRCP_Punchout
CRCP_ACP_Patches
CRCP_PCC_Patches
Age
PR
DN
PM
LR
MR
HR

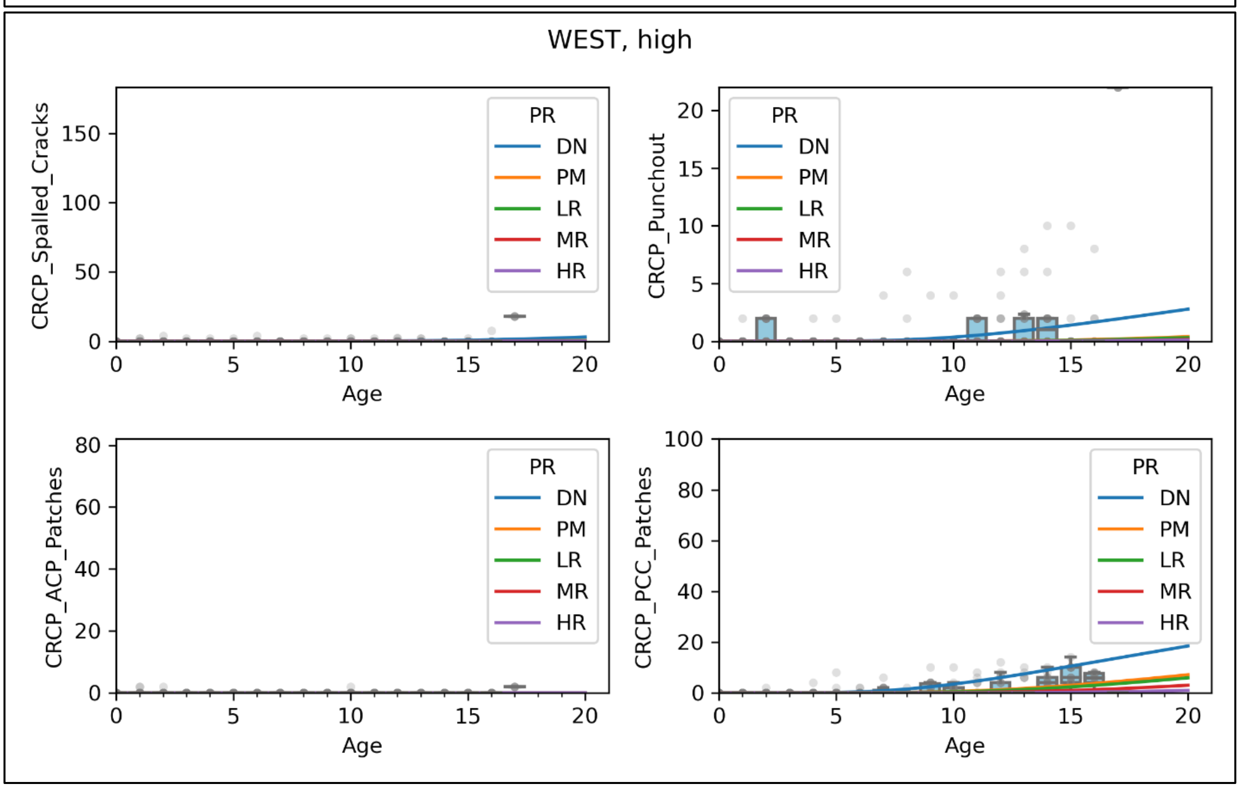
WEST, high
CRCP_Spalled_Cracks
CRCP_Punchout
CRCP_ACP_Patches
CRCP_PCC_Patches
Age
PR
DN
PM
LR
MR
HR

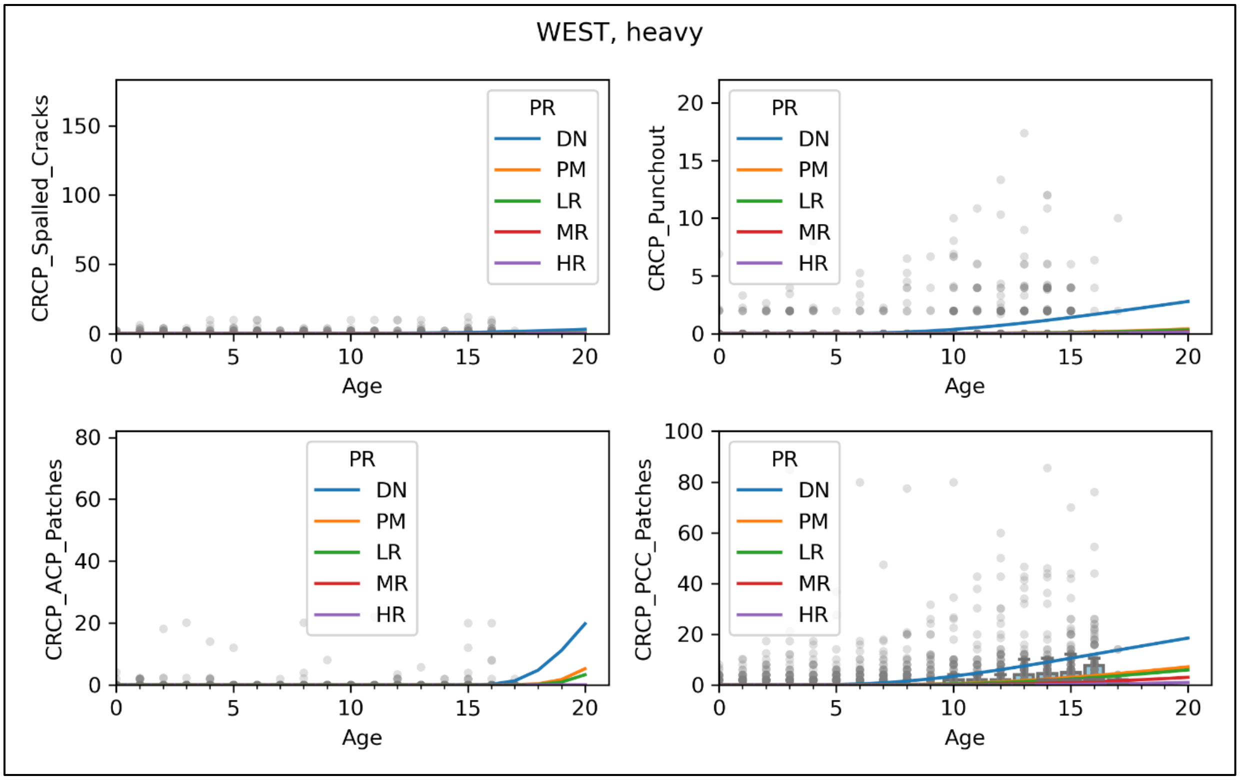
WEST, heavy
CRCP_Spalled_Cracks
CRCP_Punchout
CRCP_ACP_Patches
CRCP_PCC_Patches
Age
PR
DN
PM
LR
MR
HR

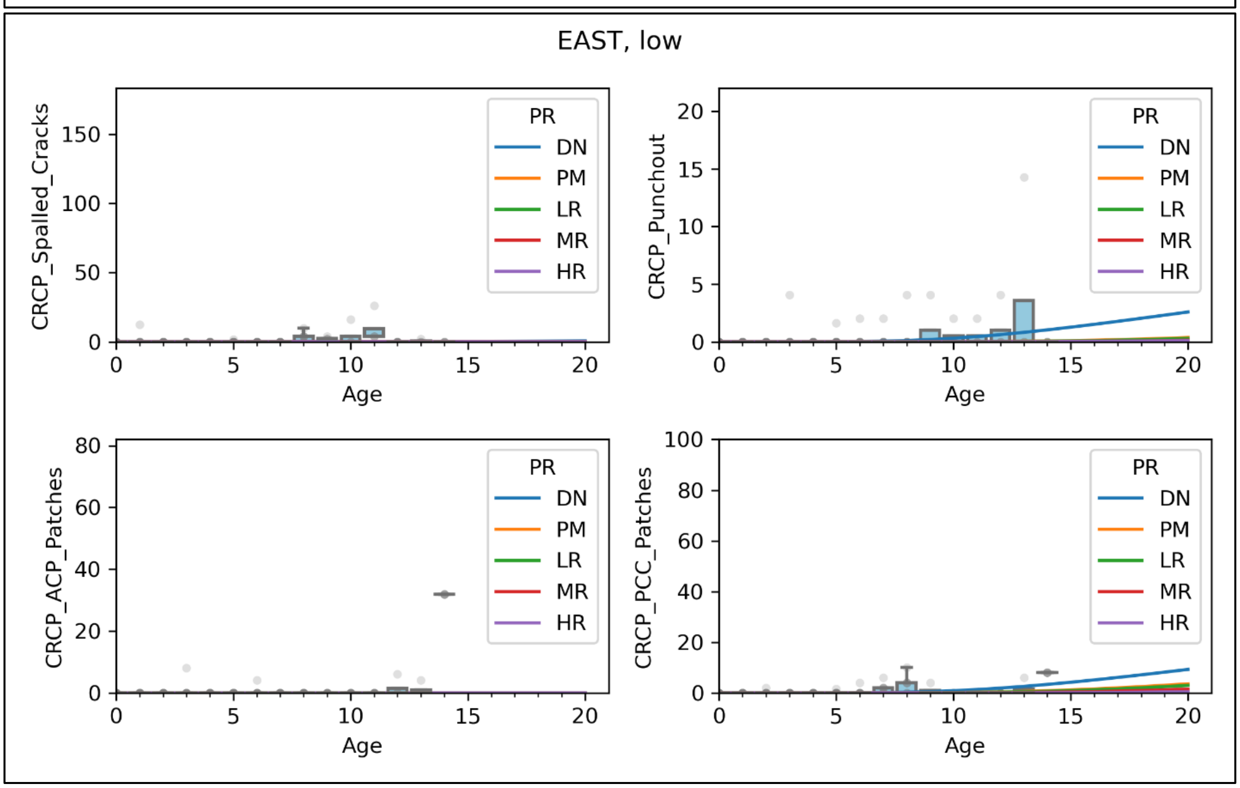
EAST, low
CRCP_Spalled_Cracks
CRCP_Punchout
CRCP_ACP_Patches
CRCP_PCC_Patches
Age
PR
DN
PM
LR
MR
HR

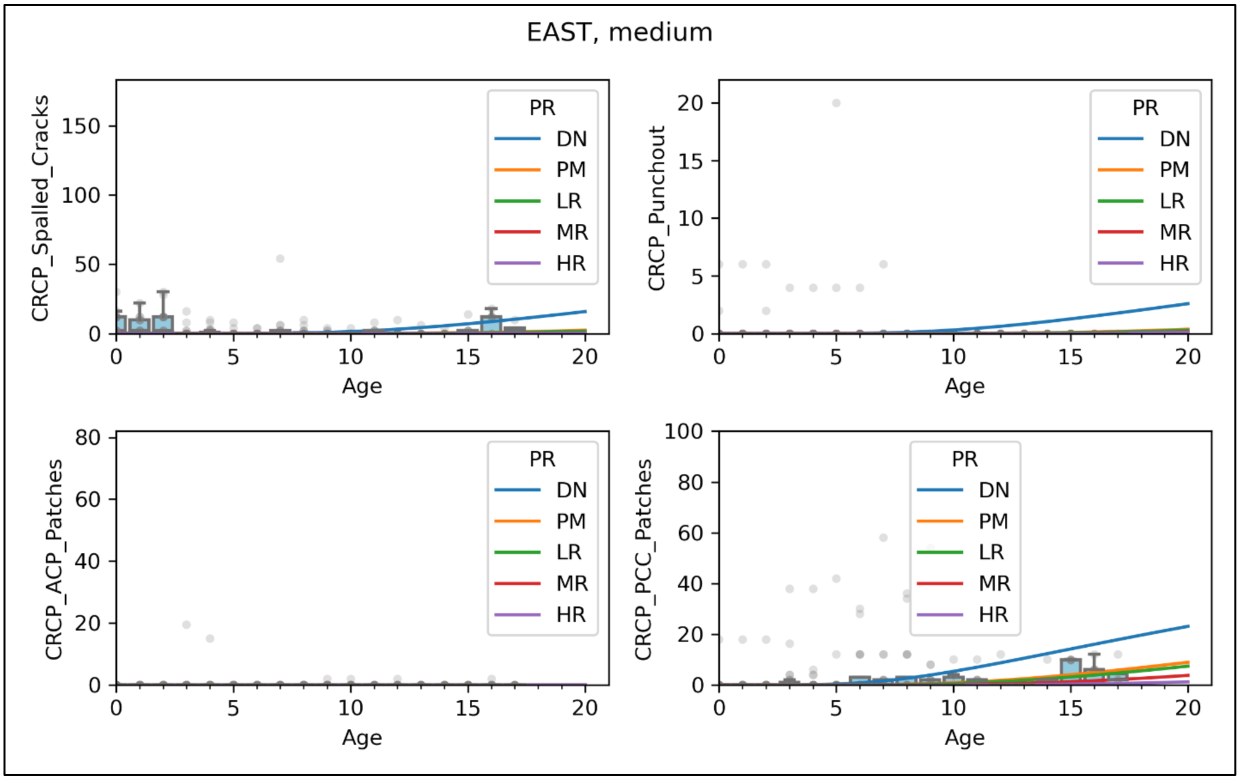
EAST, medium
CRCP_Spalled_Cracks
CRCP_Punchout
CRCP_ACP_Patches
CRCP_PCC_Patches
Age
PR
DN
PM
LR
MR
HR

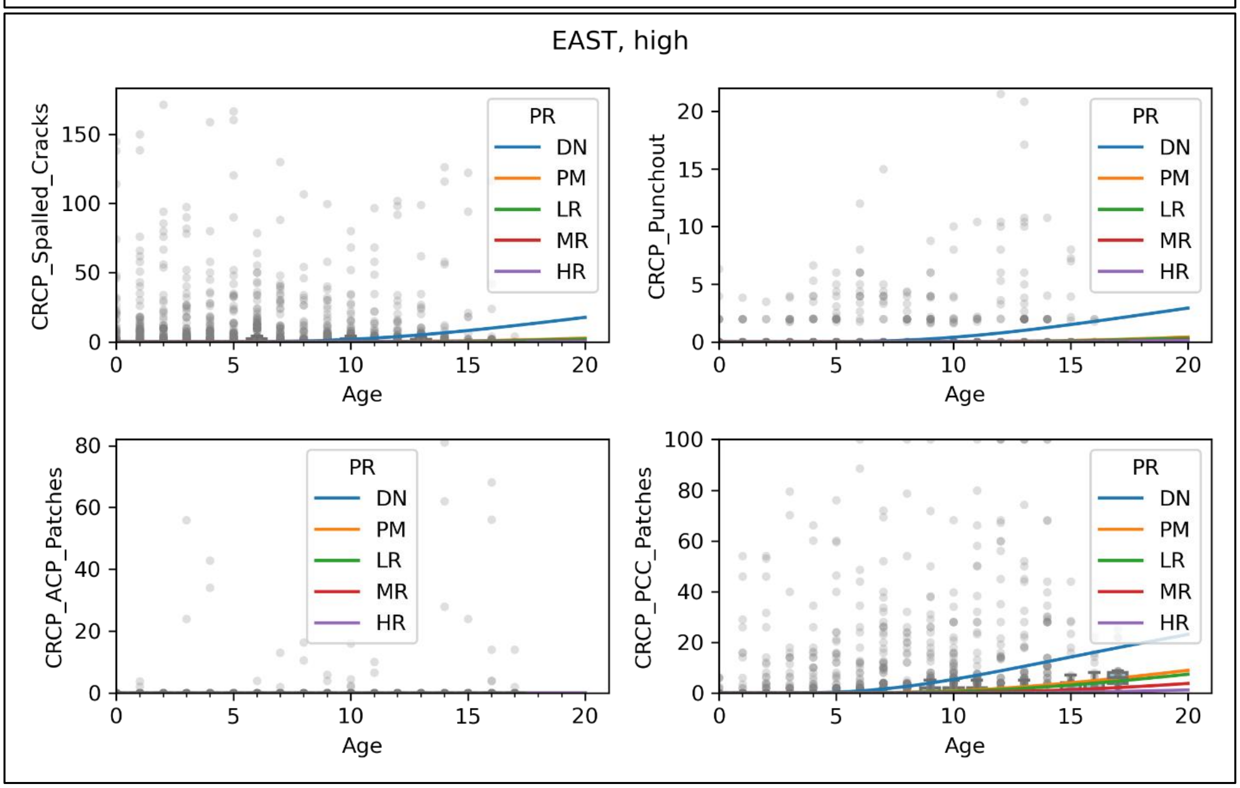
EAST, high
CRCP_Spalled_Cracks
CRCP_Punchout
CRCP_ACP_Patches
CRCP_PCC_Patches
Age
PR
DN
PM
LR
MR
HR

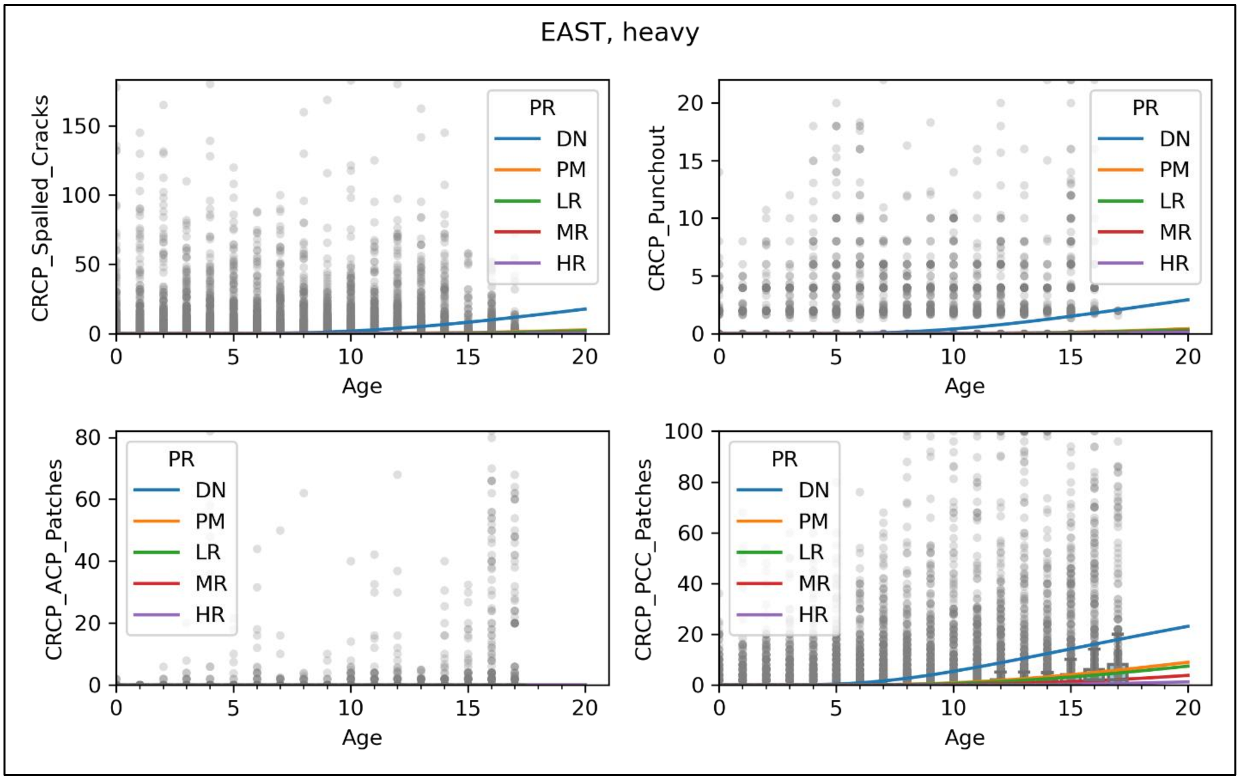

Figure 5.10 Performance of CRCP Models

5.3. Development of Analysis Database: JCP models

Developing the analysis database for JCP models required several additional procedures, as covered in this section.

5.3.1. Data Process for JCP models

In addition to the regression analysis for identifying pavement sections with significant non-increasing deterioration trends, the JCP sections were manually inspected to find any evidence of intervention that possibly increased the pavement condition in terms of distress score. This process was done to increase the data quality for JCP models by eliminating data points affected by any potential treatment at a certain time. Also, the amount of change in distresses before and after the treatment were recorded to estimate a reset value after a treatment.

Figure 5.11 shows an example plot used in this process. The distress score of this JCP section (yellow line) is decreasing as it is expected but it suddenly increases between 2016 and 2017. Therefore, this section potentially had a treatment at that time, so we only can used data from 2002 to 2016. As a result of this procedure, 638 JCP sections with various times series duration were determined to be used as the analysis database.

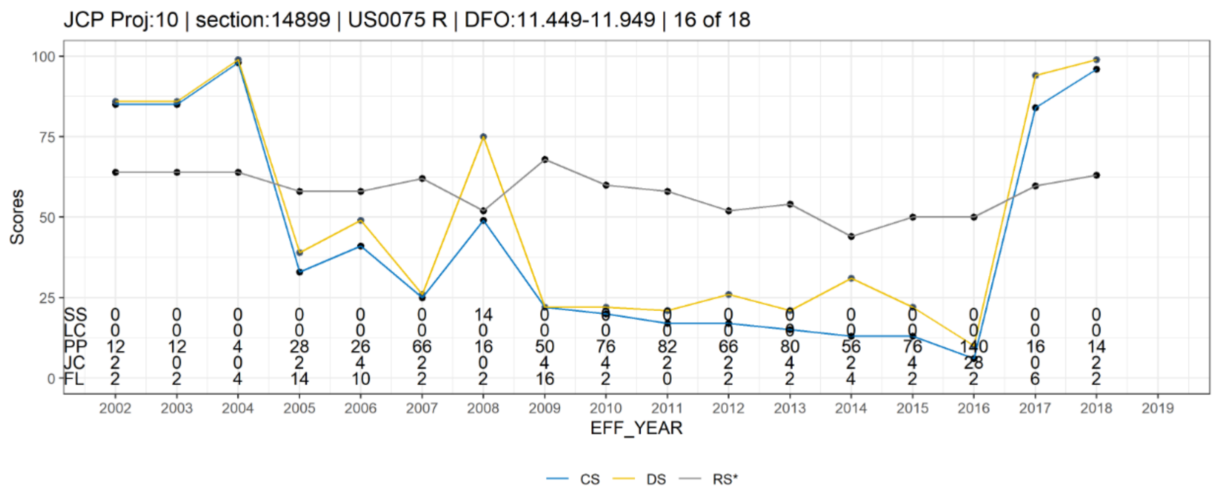

Figure 5.11 Example of Data Distribution based on DCIS Work History

5.3.2. Variable Selection for JCP models

The number of JCP sections in Texas is relatively small, and an even smaller number of sampled JCP sections were available after the data processing. A district group was used instead of climate zone as it was used in flexible pavement models. The district group for JCP sections consisted of four categories: North-East, South-East, Central, and Others. Table 5.6 shows the district groupings with the number of data points.

Table 5.6 JCP District Group

district_group	district	n
CENTRAL	DALLAS	5611
CENTRAL	WACO	181
CENTRAL	WICHITA FALLS	67
N.EAST	ATLANTA	26
N.EAST	PARIS	897
N.EAST	TYLER	99
other	CHILDRESS	44
other	ODESSA	48
S.EAST	BEAUMONT	1806
S.EAST	BRYAN	73
S.EAST	HOUSTON	108

As for the treatment type information, a probabilistic approach was adopted: for each group of pavement sections with the same traffic level and district group at each age, the lower 60 percent of the data were assigned to HRhb, the lower 70 percent of the data were treated as MRhb, the lower 80 percent of the data were assigned to LRhb, and the lower 90 percent of the data were assigned to PM, while DN models were estimated with the entire dataset.

5.4. Calibration of Current Performance Models for JCPs

5.4.1. Model Specification

For the calibration of performance models for JCPs, the current model specification used by TxDOT was used:

$$L_i = \alpha \exp[-\left(\frac{\rho\chi\epsilon\sigma}{Age}\right)^{\beta}]$$

where,

L_i: level of distress in a pavement section,

α: horizontal asymptote factor that represents the maximum range of distress growth,

β: a slope factor that controls how steeply utility is lost in the middle of the curve,

ρ: prolongation factor that controls the time it takes before significant increases in distress occur,

χ: the traffic weighting factor that controls the effect of an 18-k ESAL on performance,

ϵ: climate weighting factor that controls the effect of rainfall and freeze-thaw cycles on performance,

σ: subgrade weighting support factor that controls the effect of subgrade strength on performance, and

Age: pavement age of section, in years.

Since the parameters ρ, χ, ϵ, and σ appear in the model as a multiplication, direct estimations of them separately are not feasible. Therefore, parameter A was used to replace them, which simplifies the equation as:

$$L_i = \alpha \exp[-\left(\frac{A}{Age}\right)^{\beta}]$$

5.4.2. Model Estimation

For the estimation of the JCP models, the model specification was modified further to reduce the number of parameters to be estimated as one. This modification made the model estimation process linear, which is much simpler than non-linear estimation process. The linear estimation was possible by fixing a parameter β to a unique parameter that was estimated with the entire dataset. By linearizing the model specification, the final model was as follows:

$$\begin{aligned}
L_i &= \alpha \exp\left(-\left(\frac{A}{Age}\right)^{\beta}\right) \\
\log \frac{L_i}{\alpha} &= -\left(\frac{A}{Age}\right)^{\beta} \\
-\log \frac{L_i}{\alpha} &= \left(\frac{A}{Age}\right)^{\beta} \\
\log\left(-\log \frac{L_i}{\alpha}\right) &= \beta \log\left(\frac{A}{Age}\right) \\
\frac{\log\left(-\log \frac{L_i}{\alpha}\right)}{\beta} &= \log \frac{A}{Age} \\
\exp\left(\frac{\log\left(-\log \frac{L_i}{\alpha}\right)}{\beta}\right) &= \frac{A}{Age} \\
\exp\left(\frac{\log\left(-\log \frac{L_i}{\alpha}\right)}{\beta}\right) * Age &= A
\end{aligned}$$

The left side of the linearized equation corresponds to the dependent variable. The explanatory variables, such as traffic, district group, and treatment type, were all included in *A* as follows:

$$\begin{aligned}
A = \gamma_0 + \gamma_1 district_group_{N.EAST} + \gamma_2 district_group_{S.EAST} + \gamma_3 district_group_{CENTRAL} \\
+ \gamma_4 traffic_{medium} + \gamma_5 traffic_{high} + \gamma_6 traffic_{heavy}
\end{aligned}$$

Where γ_0 represents the parameters corresponding to other district group and low traffic.

With the linearized specification, γ parameters can be estimated using a typical linear regression procedure, then L_i can be back-calculated based on the original model specification. The fixed value for parameter β was estimated using all data based on a preliminary analysis to ensure the performance curve were non-decreasing and to fit the dataset reasonably well. Note that L_i cannot be zero due to logarithms used in the equation. Thus, all zero value of distresses were replaced by an arbitrary small value.

5.4.3. Results and Discussions

The model estimates for the five distresses of JCP are presented in Tables 5.7 through 5.12. For each distress and treatment level, there can be 16 different combinations of the categorical variables district group and traffic. However, not all combinations have data for estimation due to lack of JCP data. Therefore, the results should be used with caution for certain combinations where no back data are available. To visually evaluate the performance of the estimated models, the boxplots of the field measurements and the predictions from the developed models for different types of distresses are presented in Figures 5.12 to 5.16. As the figures illustrate, in general, the deterioration models exhibit reasonable performance for different distresses.

Table 5.7 Parameters Alpha and Beta for each JCP distress

Distress	**alpha**	**beta**
TX_JCP_FAILURES	148	1.25
TX_JCP_FAILED_JNTS_CRACKS	173	1.25
TX_JCP_PCC_PATCHES	204	1.25
TX_JCP_LONGITUDE_CRACKS	102	1.25
TX_JCP_SHATTERED_SLABS	24	1.25

Table 5.8 Model Estimation for JCP Failures

DN	parameter	estimate	std.error	statistic	p.value
Intercept	gamma0	9.5407	4.5071	2.1168	0.0343
district_groupN.EAST	gamma1	31.3370	4.6606	6.7239	0.0000
district_groupS.EAST	gamma2	39.8784	4.5942	8.6802	0.0000
district_groupCENTRAL	gamma3	31.7233	4.5607	6.9558	0.0000
traffic_levelmedium	gamma4	-8.1390	2.0982	-3.8790	0.0001
traffic_levelhigh	gamma5	-3.6639	1.2402	-2.9542	0.0031
traffic_levelheavy	gamma6	-3.6995	0.7891	-4.6885	0.0000
PM	parameter	estimate	std.error	statistic	p.value
Intercept	gamma0	12.9981	7.5194	1.7286	0.0839
district_groupN.EAST	gamma1	34.1261	1.2581	27.1254	0.0000
district_groupS.EAST	gamma2	42.0801	0.9404	44.7447	0.0000
district_groupCENTRAL	gamma3	35.2207	0.7357	47.8761	0.0000
traffic_levelmedium	gamma4	-9.5074	2.2166	-4.2891	0.0000
traffic_levelhigh	gamma5	-4.7523	1.3070	-3.6360	0.0003
traffic_levelheavy	gamma6	-4.1466	0.8366	-4.9567	0.0000
LRhb	parameter	estimate	std.error	statistic	p.value
Intercept	gamma0	15.1799	9.6143	1.5789	0.1144
district_groupN.EAST	gamma1	39.2088	1.3597	28.8368	0.0000
district_groupS.EAST	gamma2	46.2203	1.0138	45.5898	0.0000
district_groupCENTRAL	gamma3	39.8390	0.8001	49.7899	0.0000
traffic_levelmedium	gamma4	-13.0586	2.3310	-5.6022	0.0000
traffic_levelhigh	gamma5	-7.0158	1.3945	-5.0309	0.0000
traffic_levelheavy	gamma6	-6.8045	0.9040	-7.5274	0.0000
MRhb	parameter	estimate	std.error	statistic	p.value
Intercept	gamma0	19.7136	12.4671	1.5812	0.1139
district_groupN.EAST	gamma1	45.6854	1.4814	30.8388	0.0000
district_groupS.EAST	gamma2	51.1486	1.0928	46.8061	0.0000
district_groupCENTRAL	gamma3	46.2703	0.8821	52.4519	0.0000
traffic_levelmedium	gamma4	-16.5447	2.5111	-6.5886	0.0000
traffic_levelhigh	gamma5	-10.1509	1.4977	-6.7778	0.0000
traffic_levelheavy	gamma6	-10.1053	0.9873	-10.2356	0.0000
HRhb	parameter	estimate	std.error	statistic	p.value
Intercept	gamma0	22.3705	13.7216	1.6303	0.1031
district_groupN.EAST	gamma1	50.0740	1.5919	31.4555	0.0000
district_groupS.EAST	gamma2	53.8433	1.1521	46.7355	0.0000
district_groupCENTRAL	gamma3	50.1122	0.9420	53.1951	0.0000
traffic_levelmedium	gamma4	-17.9272	2.6797	-6.6901	0.0000
traffic_levelhigh	gamma5	-11.4776	1.5764	-7.2809	0.0000
traffic_levelheavy	gamma6	-11.7739	1.0507	-11.2059	0.0000

Table 5.9 Model Estimation for JCP Failed Joint Cracks

DN	parameter	estimate	std.error	statistic	p.value
Intercept	gamma0	7.2523	4.6771	1.5506	0.1210
district_groupN.EAST	gamma1	31.4685	4.8364	6.5066	0.0000
district_groupS.EAST	gamma2	36.8741	4.7675	7.7345	0.0000
district_groupCENTRAL	gamma3	35.5873	4.7327	7.5194	0.0000
traffic_levelmedium	gamma4	-10.5273	2.1773	-4.8349	0.0000
traffic_levelhigh	gamma5	-6.1471	1.2870	-4.7763	0.0000
traffic_levelheavy	gamma6	-0.3365	0.8188	-0.4110	0.6811
PM	parameter	estimate	std.error	statistic	p.value
Intercept	gamma0	7.2962	11.7415	0.6214	0.5344
district_groupN.EAST	gamma1	34.7891	1.3026	26.7068	0.0000
district_groupS.EAST	gamma2	42.2806	1.0182	41.5233	0.0000
district_groupCENTRAL	gamma3	39.1013	0.7603	51.4316	0.0000
traffic_levelmedium	gamma4	-12.3316	2.3062	-5.3471	0.0000
traffic_levelhigh	gamma5	-7.3631	1.3712	-5.3700	0.0000
traffic_levelheavy	gamma6	-1.5945	0.8710	-1.8307	0.0672
LRhb	parameter	estimate	std.error	statistic	p.value
Intercept	gamma0	8.8560	15.6932	0.5643	0.5726
district_groupN.EAST	gamma1	39.6536	1.4105	28.1140	0.0000
district_groupS.EAST	gamma2	47.0645	1.1097	42.4109	0.0000
district_groupCENTRAL	gamma3	43.3259	0.8240	52.5785	0.0000
traffic_levelmedium	gamma4	-15.2568	2.4593	-6.2036	0.0000
traffic_levelhigh	gamma5	-9.0077	1.4880	-6.0535	0.0000
traffic_levelheavy	gamma6	-3.9071	0.9410	-4.1522	0.0000
MRhb	parameter	estimate	std.error	statistic	p.value
Intercept	gamma0	11.9334	22.3799	0.5332	0.5939
district_groupN.EAST	gamma1	45.0575	1.5503	29.0642	0.0000
district_groupS.EAST	gamma2	51.6182	1.2033	42.8985	0.0000
district_groupCENTRAL	gamma3	48.5362	0.9034	53.7270	0.0000
traffic_levelmedium	gamma4	-16.6182	2.6953	-6.1656	0.0000
traffic_levelhigh	gamma5	-10.5995	1.6276	-6.5126	0.0000
traffic_levelheavy	gamma6	-6.0719	1.0258	-5.9190	0.0000
HRhb	parameter	estimate	std.error	statistic	p.value
Intercept	gamma0	11.9334	31.7045	0.3764	0.7066
district_groupN.EAST	gamma1	49.7148	1.6865	29.4776	0.0000
district_groupS.EAST	gamma2	55.6596	1.2872	43.2394	0.0000
district_groupCENTRAL	gamma3	53.4706	0.9760	54.7864	0.0000
traffic_levelmedium	gamma4	-16.9724	2.9856	-5.6847	0.0000
traffic_levelhigh	gamma5	-11.1757	1.7633	-6.3381	0.0000
traffic_levelheavy	gamma6	-7.4327	1.1044	-6.7301	0.0000

Table 5.10 Model Estimation for JCP PCC Patches

DN	parameter	estimate	std.error	statistic	p.value
Intercept	gamma0	27.6451	4.3592	6.3418	0.0000
district_groupN.EAST	gamma1	-0.9333	4.5077	-0.2070	0.8360
district_groupS.EAST	gamma2	9.6892	4.4434	2.1806	0.0292
district_groupCENTRAL	gamma3	10.6010	4.4110	2.4033	0.0163
traffic_levelmedium	gamma4	-1.0389	2.0294	-0.5120	0.6087
traffic_levelhigh	gamma5	1.8921	1.1995	1.5774	0.1147
traffic_levelheavy	gamma6	0.2157	0.7632	0.2826	0.7775
PM	parameter	estimate	std.error	statistic	p.value
Intercept	gamma0	27.6451	4.3212	6.3975	0.0000
district_groupN.EAST	gamma1	3.3960	1.2491	2.7189	0.0066
district_groupS.EAST	gamma2	12.8669	0.9218	13.9591	0.0000
district_groupCENTRAL	gamma3	13.1984	0.6904	19.1161	0.0000
traffic_levelmedium	gamma4	-3.6129	2.0281	-1.7815	0.0749
traffic_levelhigh	gamma5	1.1274	1.2327	0.9146	0.3604
traffic_levelheavy	gamma6	0.8253	0.7965	1.0361	0.3002
LRhb	parameter	estimate	std.error	statistic	p.value
Intercept	gamma0	29.1574	4.4848	6.5014	0.0000
district_groupN.EAST	gamma1	10.1026	1.3901	7.2677	0.0000
district_groupS.EAST	gamma2	18.3706	1.0143	18.1123	0.0000
district_groupCENTRAL	gamma3	16.0443	0.7278	22.0450	0.0000
traffic_levelmedium	gamma4	-6.0895	2.0737	-2.9366	0.0033
traffic_levelhigh	gamma5	1.3668	1.3138	1.0404	0.2982
traffic_levelheavy	gamma6	-0.1960	0.8468	-0.2315	0.8170
MRhb	parameter	estimate	std.error	statistic	p.value
Intercept	gamma0	32.0235	4.8354	6.6227	0.0000
district_groupN.EAST	gamma1	15.3251	1.5348	9.9852	0.0000
district_groupS.EAST	gamma2	22.9865	1.1212	20.5013	0.0000
district_groupCENTRAL	gamma3	19.5141	0.7828	24.9282	0.0000
traffic_levelmedium	gamma4	-8.3722	2.1849	-3.8318	0.0001
traffic_levelhigh	gamma5	0.1765	1.4027	0.1258	0.8999
traffic_levelheavy	gamma6	-1.6314	0.9169	-1.7792	0.0753
HRhb	parameter	estimate	std.error	statistic	p.value
Intercept	gamma0	34.3335	5.3991	6.3592	0.0000
district_groupN.EAST	gamma1	18.7161	1.6648	11.2424	0.0000
district_groupS.EAST	gamma2	25.8279	1.2109	21.3297	0.0000
district_groupCENTRAL	gamma3	22.0728	0.8442	26.1476	0.0000
traffic_levelmedium	gamma4	-10.0308	2.3157	-4.3317	0.0000
traffic_levelhigh	gamma5	-0.1846	1.5052	-0.1227	0.9024
traffic_levelheavy	gamma6	-2.9987	0.9864	-3.0402	0.0024

Table 5.11 Model Estimation for JCP Longitude Cracks

DN	parameter	estimate	std.error	statistic	p.value
Intercept	gamma0	31.8242	4.8195	6.6033	0.0000
district_groupN.EAST	gamma1	30.8252	4.9836	6.1853	0.0000
district_groupS.EAST	gamma2	31.4959	4.9126	6.4113	0.0000
district_groupCENTRAL	gamma3	19.4890	4.8768	3.9963	0.0001
traffic_levelmedium	gamma4	-10.2422	2.2436	-4.5650	0.0000
traffic_levelhigh	gamma5	-11.0153	1.3262	-8.3061	0.0000
traffic_levelheavy	gamma6	-10.2887	0.8437	-12.1942	0.0000
PM	parameter	estimate	std.error	statistic	p.value
Intercept	gamma0	31.8242	4.7471	6.7040	0.0000
district_groupN.EAST	gamma1	31.6037	1.2911	24.4772	0.0000
district_groupS.EAST	gamma2	31.4723	0.9586	32.8299	0.0000
district_groupCENTRAL	gamma3	23.5231	0.7622	30.8612	0.0000
traffic_levelmedium	gamma4	-8.6664	2.3579	-3.6755	0.0002
traffic_levelhigh	gamma5	-9.9908	1.3799	-7.2402	0.0000
traffic_levelheavy	gamma6	-9.0338	0.8678	-10.4103	0.0000
LRhb	parameter	estimate	std.error	statistic	p.value
Intercept	gamma0	31.8242	4.7529	6.6958	0.0000
district_groupN.EAST	gamma1	33.6206	1.3372	25.1422	0.0000
district_groupS.EAST	gamma2	31.9872	0.9808	32.6146	0.0000
district_groupCENTRAL	gamma3	26.5752	0.7955	33.4081	0.0000
traffic_levelmedium	gamma4	-8.5190	2.4616	-3.4607	0.0005
traffic_levelhigh	gamma5	-9.2819	1.4543	-6.3823	0.0000
traffic_levelheavy	gamma6	-8.9889	0.9035	-9.9490	0.0000
MRhb	parameter	estimate	std.error	statistic	p.value
Intercept	gamma0	31.8242	4.7697	6.6721	0.0000
district_groupN.EAST	gamma1	33.7952	1.3490	25.0513	0.0000
district_groupS.EAST	gamma2	31.9757	0.9869	32.4000	0.0000
district_groupCENTRAL	gamma3	26.8759	0.8017	33.5221	0.0000
traffic_levelmedium	gamma4	-8.5843	2.4839	-3.4559	0.0006
traffic_levelhigh	gamma5	-9.2420	1.4675	-6.2976	0.0000
traffic_levelheavy	gamma6	-8.8451	0.9113	-9.7058	0.0000
HRhb	parameter	estimate	std.error	statistic	p.value
Intercept	gamma0	31.8242	4.7757	6.6637	0.0000
district_groupN.EAST	gamma1	33.7846	1.3511	25.0061	0.0000
district_groupS.EAST	gamma2	31.9802	0.9886	32.3474	0.0000
district_groupCENTRAL	gamma3	26.8745	0.8029	33.4738	0.0000
traffic_levelmedium	gamma4	-8.5417	2.4937	-3.4254	0.0006
traffic_levelhigh	gamma5	-9.2342	1.4711	-6.2770	0.0000
traffic_levelheavy	gamma6	-8.8341	0.9130	-9.6754	0.0000

Table 5.12 Model Estimation for JCP Shattered Slabs

DN	parameter	estimate	std.error	statistic	p.value
Intercept	gamma0	26.8366	4.2950	6.2483	0.0000
district_groupN.EAST	gamma1	28.9595	4.4413	6.5206	0.0000
district_groupS.EAST	gamma2	29.4618	4.3780	6.7295	0.0000
district_groupCENTRAL	gamma3	26.1515	4.3461	6.0173	0.0000
traffic_levelmedium	gamma4	-10.1641	1.9995	-5.0834	0.0000
traffic_levelhigh	gamma5	-7.0045	1.1819	-5.9267	0.0000
traffic_levelheavy	gamma6	-6.2032	0.7519	-8.2498	0.0000
PM	**parameter**	**estimate**	**std.error**	**statistic**	**p.value**
Intercept	gamma0	28.0455	4.4342	6.3248	0.0000
district_groupN.EAST	gamma1	30.2728	1.1384	26.5935	0.0000
district_groupS.EAST	gamma2	29.8922	0.8492	35.1996	0.0000
district_groupCENTRAL	gamma3	26.4447	0.6648	39.7787	0.0000
traffic_levelmedium	gamma4	-9.6822	2.0134	-4.8088	0.0000
traffic_levelhigh	gamma5	-7.0599	1.1835	-5.9653	0.0000
traffic_levelheavy	gamma6	-6.4185	0.7524	-8.5302	0.0000
LRhb	**parameter**	**estimate**	**std.error**	**statistic**	**p.value**
Intercept	gamma0	28.0455	4.4342	6.3248	0.0000
district_groupN.EAST	gamma1	30.2728	1.1384	26.5935	0.0000
district_groupS.EAST	gamma2	29.8922	0.8492	35.1996	0.0000
district_groupCENTRAL	gamma3	26.4447	0.6648	39.7787	0.0000
traffic_levelmedium	gamma4	-9.6822	2.0134	-4.8088	0.0000
traffic_levelhigh	gamma5	-7.0599	1.1835	-5.9653	0.0000
traffic_levelheavy	gamma6	-6.4185	0.7524	-8.5302	0.0000
MRhb	**parameter**	**estimate**	**std.error**	**statistic**	**p.value**
Intercept	gamma0	28.0455	4.4342	6.3248	0.0000
district_groupN.EAST	gamma1	30.2728	1.1384	26.5935	0.0000
district_groupS.EAST	gamma2	29.8922	0.8492	35.1996	0.0000
district_groupCENTRAL	gamma3	26.4447	0.6648	39.7787	0.0000
traffic_levelmedium	gamma4	-9.6822	2.0134	-4.8088	0.0000
traffic_levelhigh	gamma5	-7.0599	1.1835	-5.9653	0.0000
traffic_levelheavy	gamma6	-6.4185	0.7524	-8.5302	0.0000
HRhb	**parameter**	**estimate**	**std.error**	**statistic**	**p.value**
Intercept	gamma0	28.0455	4.4342	6.3248	0.0000
district_groupN.EAST	gamma1	30.2728	1.1384	26.5935	0.0000
district_groupS.EAST	gamma2	29.8922	0.8492	35.1996	0.0000
district_groupCENTRAL	gamma3	26.4447	0.6648	39.7787	0.0000
traffic_levelmedium	gamma4	-9.6822	2.0134	-4.8088	0.0000
traffic_levelhigh	gamma5	-7.0599	1.1835	-5.9653	0.0000
traffic_levelheavy	gamma6	-6.4185	0.7524	-8.5302	0.0000

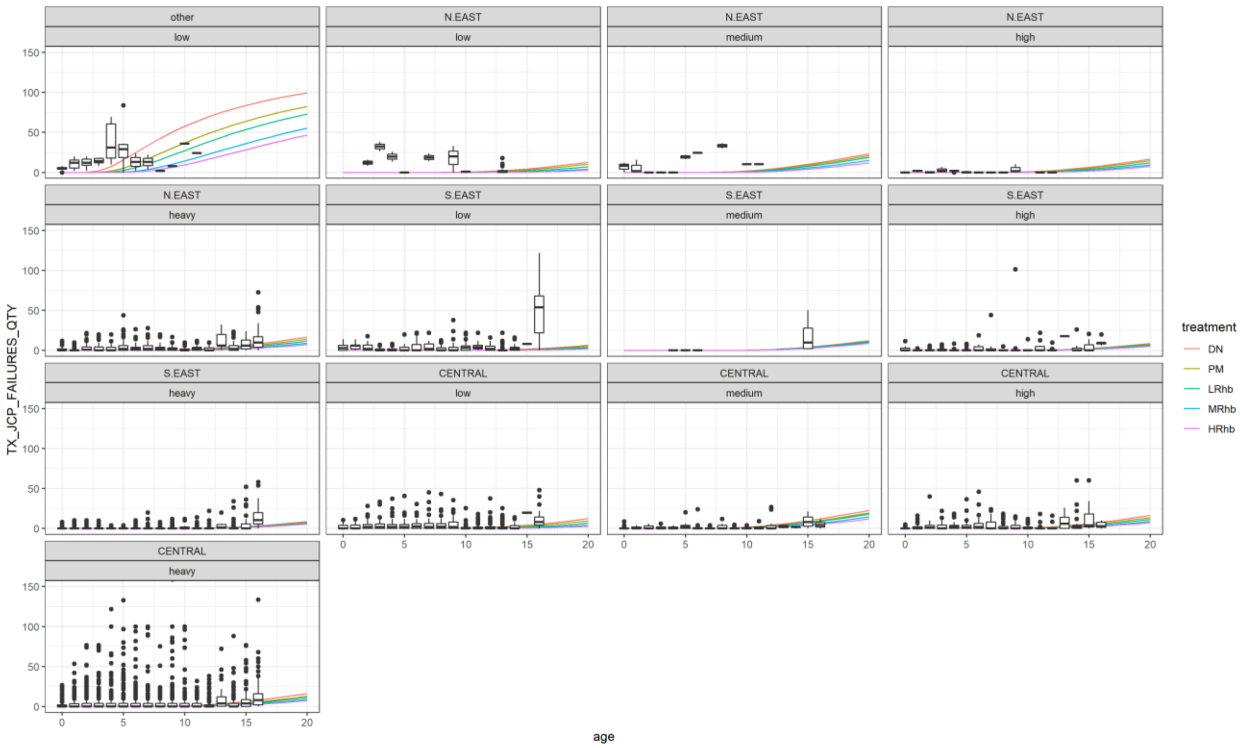

Figure 5.12 Performance of JCP Models (Failures)

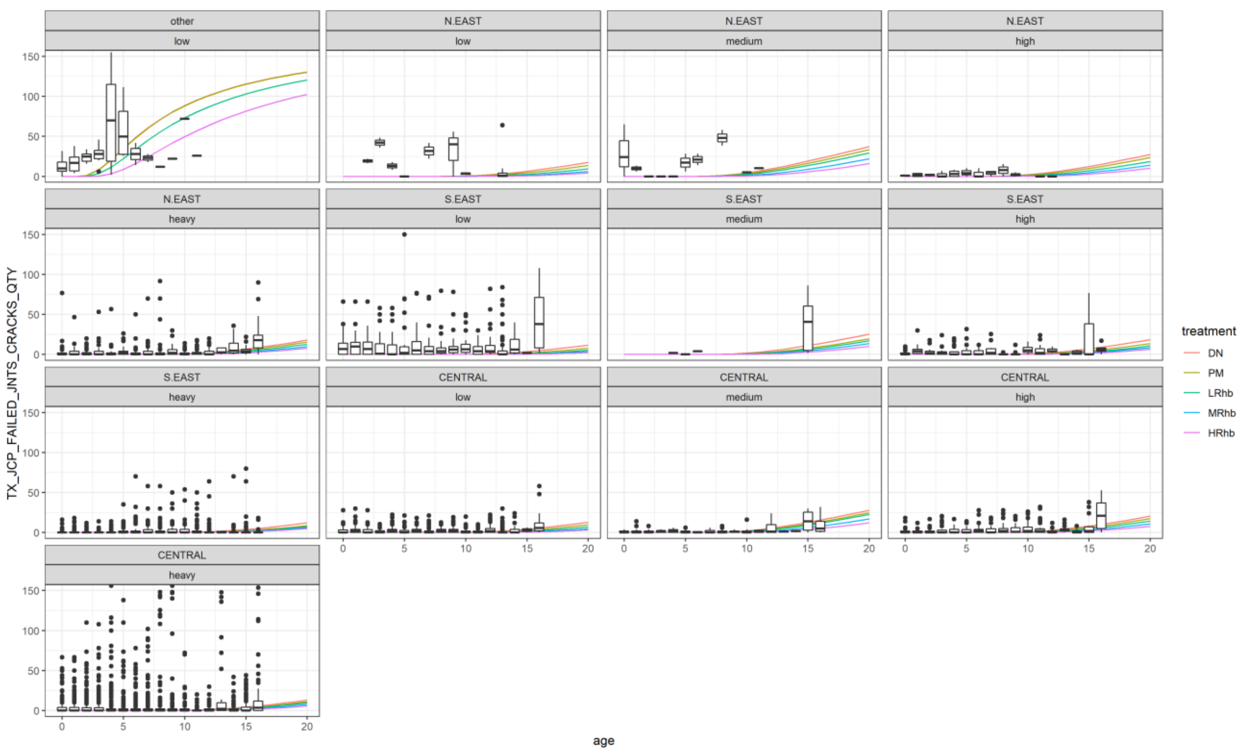

Figure 5.13 Performance of JCP Models (Failed Joint Cracks)

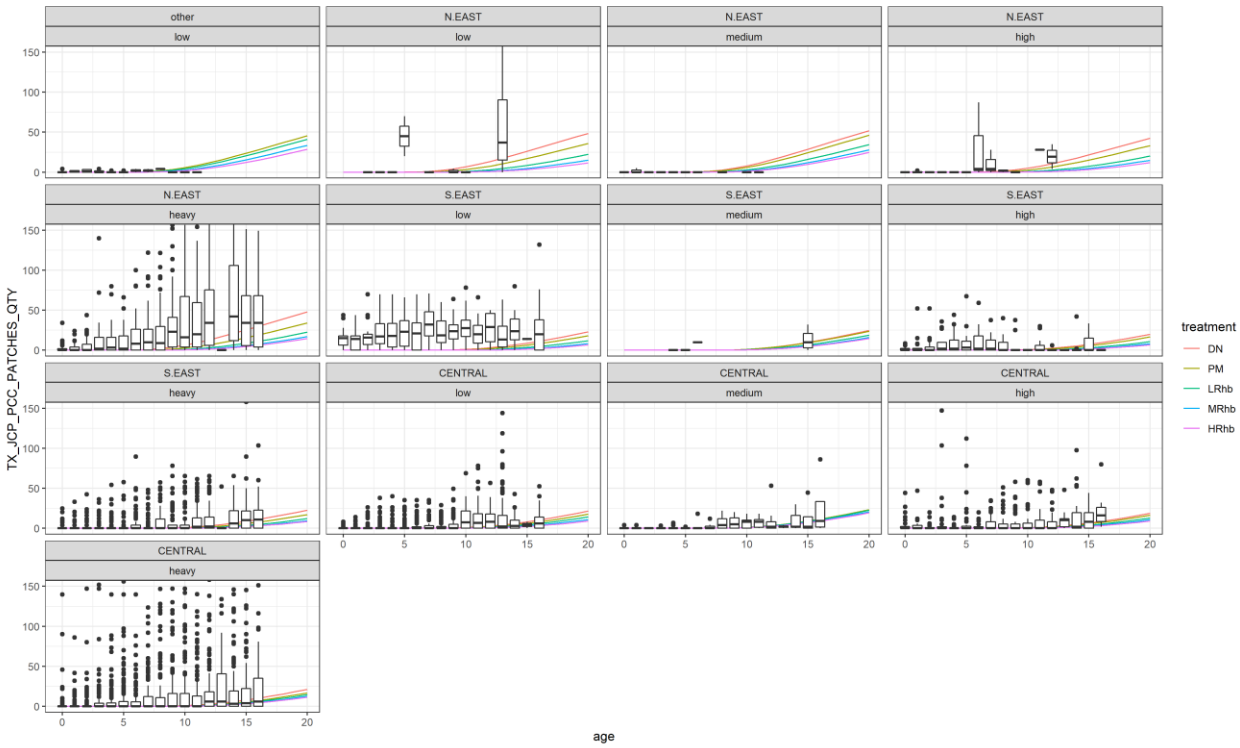

Figure 5.14 Performance of JCP Models (PCC Patches)

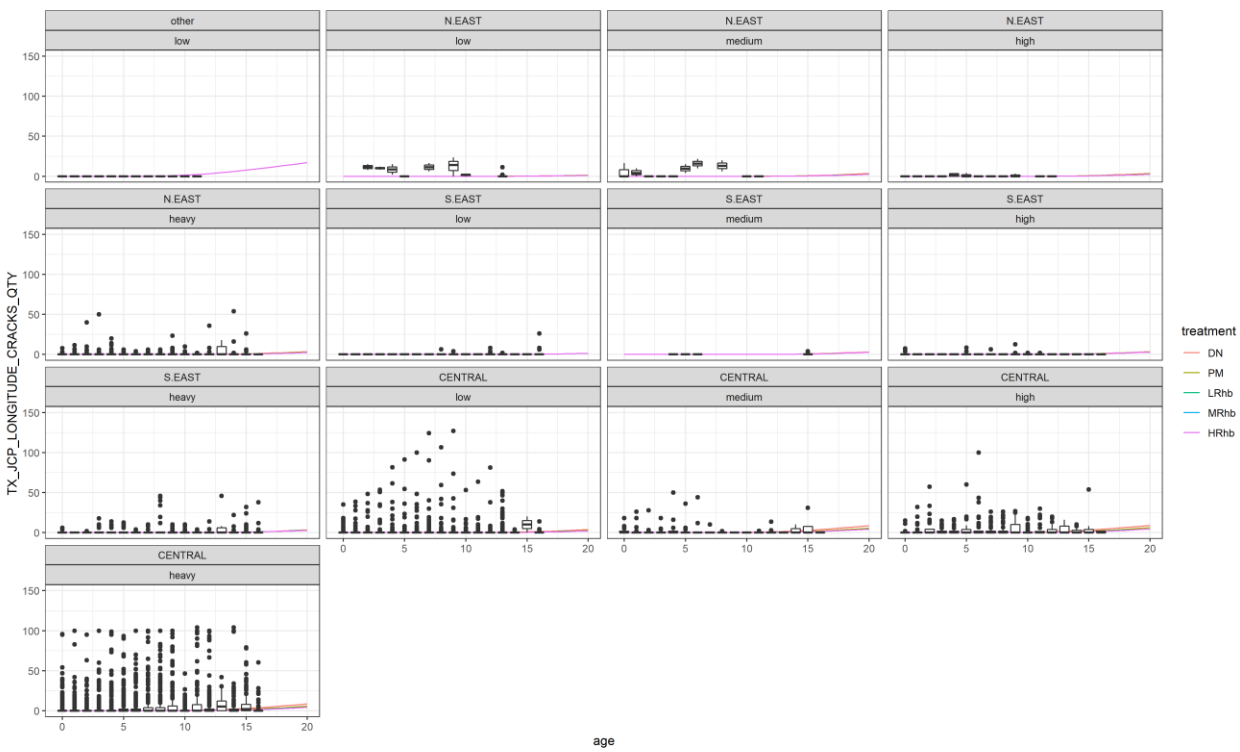

Figure 5.15 Performance of JCP Models (Longitude Cracks)

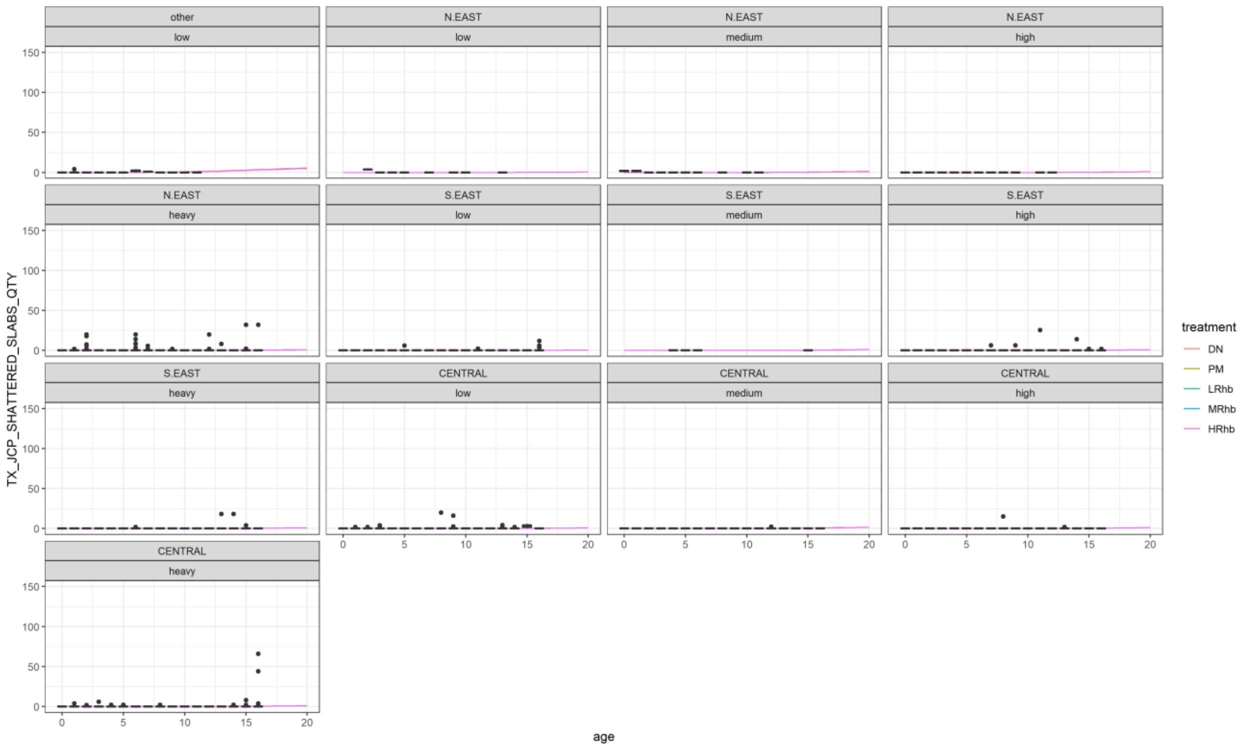

Figure 5.16 Performance of JCP Models (Shattered Slabs)

5.5. Alternative Models

This section presents the development of alternative models for CRCP and JCP. In addition, the performance of the prediction models is demonstrated by comparing the model predictions with the field measurements.

In the current pavement deterioration models, traffic, climate, and subgrade factors were incorporated as a product in the numerator. Because of this, direct estimation of these parameters is not mathematically feasible. Additionally, another significant limitation of the current model is that the pavement age appears as a denominator; consequently, pavement distress at age zero (time of construction) cannot be estimated. The specification of the age variable also makes the effect of the exponent parameter on the model prediction inconsistent at different age ranges. For example, if variables related to treatment type were incorporated into the exponent parameter, it would be impossible to guarantee that the predictions for HRhb would always be lower than MRhb, LRhb, PM, and DN. In brief, due to the current model specification, the predictions from current models could be, at times, contradictory and result in unrealistic predictions when developing maintenance or rehabilitation plans, such as the 4-year plan. As a result, TxDOT should conduct a full review of the current model specifications and implement new model specifications to address these issues.

5.5.1. Model Specification

Due to practical issues related to the implementation of the potential new models into PA, it is desirable that the performance models should be s-shaped and with a small number of parameters. In this project, considering the issues of the current models, three alternative s-shaped model specifications were proposed to TxDOT. Of these three models considered, the following model specification was selected to develop alternative pavement performance models for CRCP and JCP.

$$L = \beta_0 - \beta_1 \exp(-\beta_2 \cdot Age^{\beta_3})$$

where,

L : distress density,

Age : independent variable that accounts for the age of the pavement section,

β_0 : asymptotic parameter that captures the maximum level of distress as the age of the pavement section tends to infinity,

β_1 : maximum drop from the final level of distress at *Age* = 0, and

β_2, β_3 : regression parameters, which could be specified as a function of traffic, environmental conditions, subgrade, location, and any other relevant variables.

Of the four parameters in this model, β_0 represents the maximum value for each type of distress; its value is predetermined for each type of distress before the model estimation. Together with β_1, these two parameters determined the initial distress value, $L_0 = \beta_0 - \beta_1$, after maintenance or rehabilitation works. It is evident that if a smaller β_1 were used, a higher initial distress value would be obtained, and the model would predict higher distresses. The effects of β_1 and β_2 on the alternative model are illustrated in Figure 5.17; according to these plots, as β_2 or β_3 decrease, the alternative model predicts lower distress values.

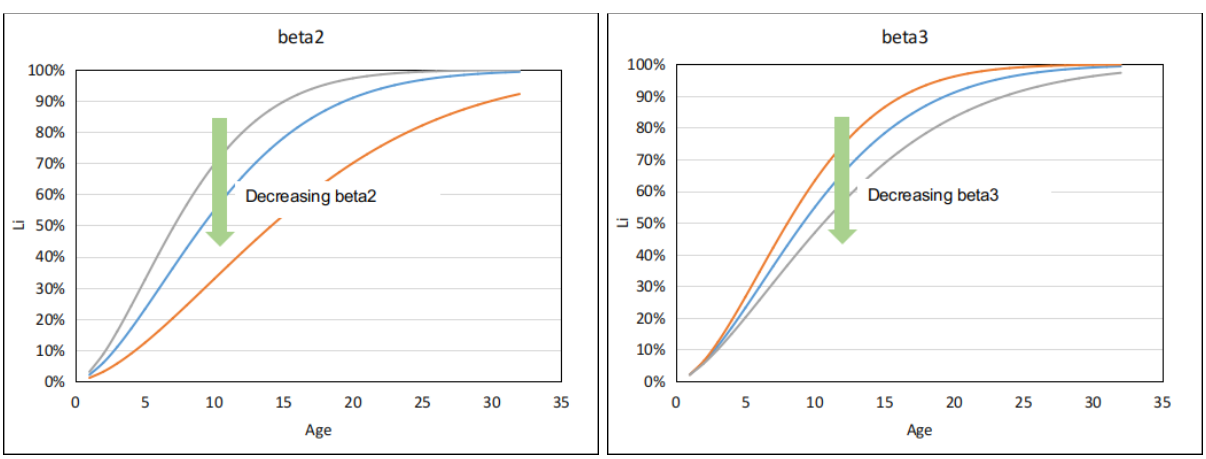

Figure 5.17 Effect of Regression Parameters on Alternative Model

Additionally, for pavement sections with a known distress level L_i, the corresponding age can be easily estimated by the following equation:

$$Age_i = exp\left\{\frac{1}{\beta_3} ln\ \left[\frac{1}{\beta_2} ln\left(\frac{\beta_1}{\beta_0 - L_i}\right)\right]\right\}$$

To ensure that the predicted distresses at age zero are always equal to zero, the alternative model was modified as follows:

$$L = \beta_0\left[1 - \exp\left(-\frac{\beta_1}{1000} \cdot Age^{\frac{\beta_2}{1000}}\right)\right]$$

Appropriate asymptotic values (β_0) are critical to warrant good model performance. In this project, based on the analysis of distress distributions, it was decided to use the 99.9th percentile for each type of distress as the asymptotic values of the deterioration model. The selected asymptotic values of different distresses for CRCP and JCP are as follows:

- CRCP Distresses
  - Spalled Cracks: 183
  - Punchouts: 22
  - Asphalt Patches: 82
  - Concrete Patches: 100
- JCP Distresses
  - Failed Joints and Cracks: 173
  - Failures: 148
  - Shattered Slabs: 24
  - Longitudinal Cracks: 102
  - Concrete Patches: 204

In the development of performance models for concrete pavements, there are four potential sets of variables: highway functional class, traffic, climate, and treatment type. Since there is a significant correlation between traffic and highway functional class, it was decided to use only traffic, climate, and treatment type as input variables for the alternative model. Based on preliminary analysis, variables related to treatment type were incorporated into β_1, while traffic and climate information were included in β_2. More specifically, the equations for β_1 and β_2 :

$$\beta_1 = \eta_0 + \eta_1 DN + \eta_2 LRhb + \eta_3 MRhb + \eta_4 HRhb$$

$$\beta_2 = \gamma_0 + \gamma_1 Traffic\_Low + \gamma_2 Traffic\_High + \gamma_3 Traffic\_Heavy$$
$$+\gamma_4 CL\_WEST + \gamma_5 CL\_EAST + \gamma_6 CL\_NORTH + \gamma_7 CL\_SOUTH$$

5.5.2. Model Estimation

To develop pavement deterioration models that can depict the general change of distresses under various conditions as well as produce reasonable predictions that are as close as possible to the field observations, this project implemented the following guidelines:

- Firstly, after maintenance or rehabilitation work, pavement distresses progressively increase without intervention until the next maintenance or rehabilitation work. This means that the deterioration curves should be non-decreasing—specifically, for the alternative model, the values of β_1 and β_2 should be positive. Moreover, concrete pavements normally deteriorate very slowly at the early ages; as a result, a lower bound of 1,000 was applied to β_2 during the model estimation.

- Secondly, pavement sections carrying heavier traffic normally deteriorate faster than the pavement sections carrying lighter traffic. Therefore, the parameters related to traffic should follow the constraints below:

$$\begin{cases} \gamma_1 \le 0 \\ \gamma_2 \ge 0 \\ \gamma_3 \ge 0 \\ \gamma_2 - \gamma_3 \le 0 \end{cases}$$

- Thirdly, for different types of pavement treatments, it is expected that the treatment involving a higher level of work intensity, which normally corresponds to higher cost, will produce better pavement performance, i.e., lower distress and slower deterioration rate. Moreover, to facilitate plans for M&R work, and the calculation of treatment effectiveness, the deterioration curves of different treatments should not cross each other. This was controlled by setting the following constraints for parameters related to treatment type:

$$\begin{cases} \eta_1 \ge 0 \\ \eta_2 \le 0 \\ \eta_3 \le 0 \\ \eta_4 \le 0 \\ \eta_2 - \eta_3 \ge 0 \\ \eta_3 - \eta_4 \ge 0 \end{cases}$$

- Finally, the predictions of the deterioration models should be as close as possible to the field distress measurements. To meet this requirement, the least-squares method was applied for the estimation of the model parameters. The objective function of the least-squares method is to minimize the sum of squared distance between the predictions and observations:

$$\boldsymbol{\theta} = \underset{\boldsymbol{\theta}}{\operatorname{argmin}} \sum_{i=1}^{n} (L(\boldsymbol{x}_i, \boldsymbol{\theta}) - L_i^*)^2$$

where $\boldsymbol{\theta}$ is the model parameters to be estimated, L_i^* is the distress of the *i*th observation in the data, and the $L(\boldsymbol{x}_i, \boldsymbol{\theta})$ is the corresponding prediction from the deterioration model.

5.5.3. Results and Discussion of Alternative Models

5.5.3.1. Alternative Models for CRCP

The alternative model errors for CRCP are presented in Table 5.13, where the third column is the mean squared error (MSE), the fourth column is the standard error, and the last column is the normalized error with respect to the asymptotic value. As shown, the normalized errors of all the models are below 6 percent, which indicates the goodness of fit of the alternative models for CRCP distresses.

The summaries of model estimation for different types of distresses are reported in Table 5.14. It can be found that for all the models, the parameters for both the traffic and treatment type meet the requirements specified in the model estimation section—i.e., pavements with heavier traffic exhibit higher distress, while pavements receiving more work-intensive treatment have lower distress. Additionally, for all the models, the effects of most variables are statistically significant.

The curves of alternative deterioration models for different types of CRCP distresses are presented together with the boxplots of the field measurements in Figure 5.18. As shown, in general, the deterioration models exhibit outstanding performance for different distresses. Furthermore, the deterioration curves for different treatment types follow the right hierarchical order: the DN curve has the highest deterioration rate followed in order by PM, LRhb, MRhb, and HRhb.

Table 5.13 CRCP Model Errors

Distress	Asymptotic Value	MSE	std_error	Normalized error
Spalled Cracks	183	44.6	6.68	3.65%
Punchout	22	0.971	0.99	4.48%
ACP Patches	82	5.22	2.28	2.79%
PCC Patches	100	31.1	5.58	5.58%

Table 5.14 Summary of Alternative Model Estimation for CRCP

Distress	Variables	Parameter	Estimate	std	t	p_val
Spalled Cracks	-	β_0	183	-	-	-
	-	γ_0	1089	<0.01	2.4E+5	0
	Traffic_Low	γ_1	-0.06243	0.10	-0.62	0.27
	Traffic_High	γ_2	0.1375	0.01	9.80	<0.01
	Traffic_Heavy	γ_3	0.2615	<0.01	54.72	0
	CL_WEST	γ_4	-89.27	0.03	-2.9E+3	0
	CL_EAST	γ_5	168.1	0.01	3.3E+4	0
	CL_NORTH	γ_6	-62.06	0.02	-3.2E+3	0
	CL_SOUTH	γ_7	32.12	0.13	245.30	0
	-	η_0	0.1411	0.01	14.91	<0.01
	DN	η_1	1.243	0.02	66.39	0
	LR	η_2	-0.06265	0.02	-2.93	<0.01
	MR	η_3	-0.1296	0.02	-5.67	<0.01
	HR	η_4	-0.1367	0.02	-5.97	<0.01
Punchout	-	β_0	22	-	-	-
	-	γ_0	1000	<0.01	2.7E+5	0
	Traffic_Low	γ_1	-0.00132	0.10	-0.01	0.49
	Traffic_High	γ_2	0.000631	0.01	0.05	0.48
	Traffic_Heavy	γ_3	0.000783	<0.01	0.20	0.42
	CL_WEST	γ_4	117.0	0.01	7.9E+3	0
	CL_EAST	γ_5	175.4	<0.01	3.7E+4	0
	CL_NORTH	γ_6	208.1	0.01	2.7E+4	0
	CL_SOUTH	γ_7	531.0	0.03	1.9E+4	0
	-	η_0	0.1593	0.01	13.19	<0.01
	DN	η_1	2.271	0.03	88.70	0
	LR	η_2	-0.06034	0.03	-2.21	0.01
	MR	η_3	-0.1367	0.03	-4.97	<0.01
	HR	η_4	-0.1429	0.03	-5.19	<0.01
ACP Patches	-	β_0	82	-	-	-
	-	γ_0	4177	<0.01	6.0E+6	0
	Traffic_Low	γ_1	-822.7	8.76	-93.95	0
	Traffic_High	γ_2	337.0	0.03	1.0E+4	0
	Traffic_Heavy	γ_3	1281.9	<0.01	1.9E+6	0
	CL_WEST	γ_4	72.50	<0.01	1.7E+4	0
	CL_EAST	γ_5	357.2	<0.01	4.9E+5	0
	CL_NORTH	γ_6	-201.3	<0.01	-4.0E+4	0
	CL_SOUTH	γ_7	125.9	0.03	3.7E+3	0
	-	η_0	2.10E-07	4.4E-08	4.76	<0.01
	DN	η_1	8.59E-06	9.6E-08	89.50	0
	LR	η_2	-8.93E-08	9.9E-08	-0.90	0.19
	MR	η_3	-2.08E-07	1.0E-07	-2.07	0.02
	HR	η_4	-2.10E-07	1.0E-07	-2.09	0.02

Distress	Variables	Parameter	Estimate	std	t	p_val
PCC Patches	-	β_0	100	-	-	-
	-	γ_0	1398	<0.01	8.2E+5	0
	Traffic_Low	γ_1	-303.1	0.11	-2.7E+3	0
	Traffic_High	γ_2	36.96	0.01	6.4E+3	0
	Traffic_Heavy	γ_3	36.98	<0.01	2.1E+4	0
	CL_WEST	γ_4	77.63	0.01	9.9E+3	0
	CL_EAST	γ_5	209.8	<0.01	1.0E+5	0
	CL_NORTH	γ_6	169.4	<0.01	4.1E+4	0
	CL_SOUTH	γ_7	77.93	0.05	1.5E+3	0
	-	η_0	0.3655	0.01	64.93	0
	DN	η_1	1.194	0.01	107.20	0
	LR	η_2	-0.08509	0.01	-7.02	<0.01
	MR	η_3	-0.2678	0.01	-19.47	<0.01
	HR	η_4	-0.3454	0.02	-22.68	<0.01

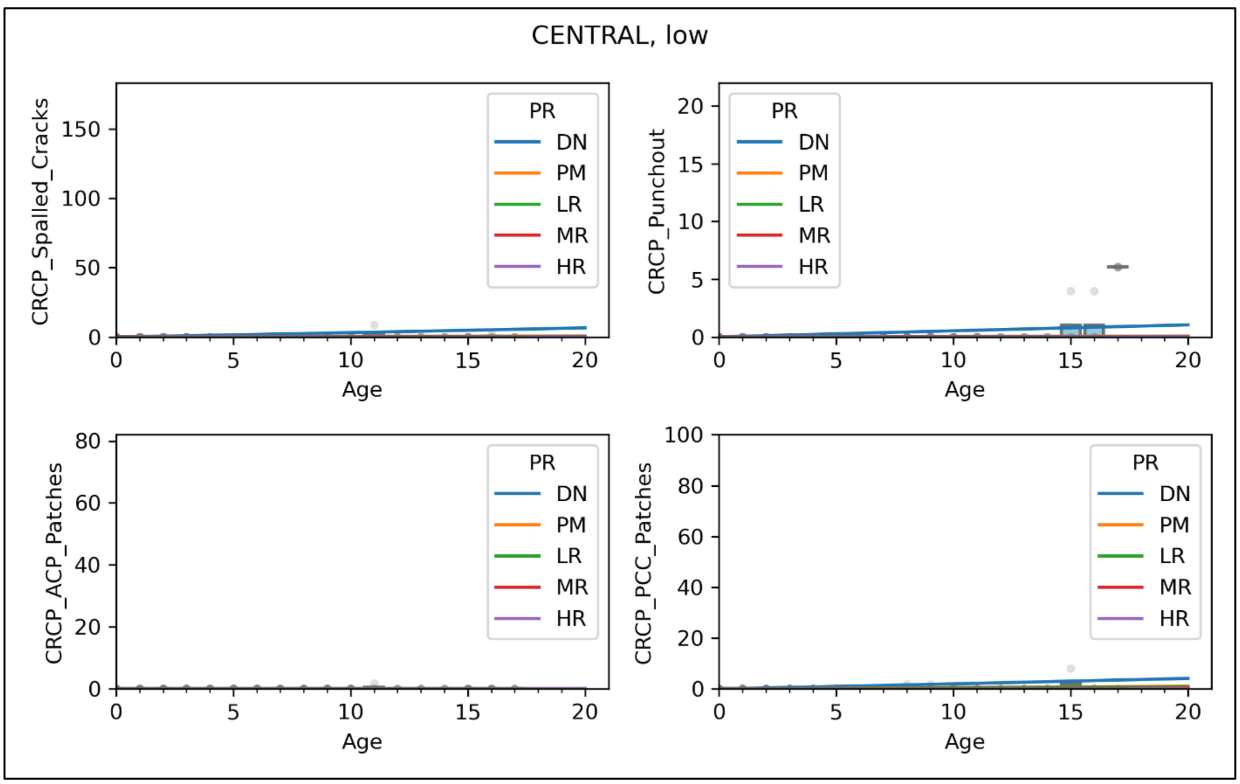

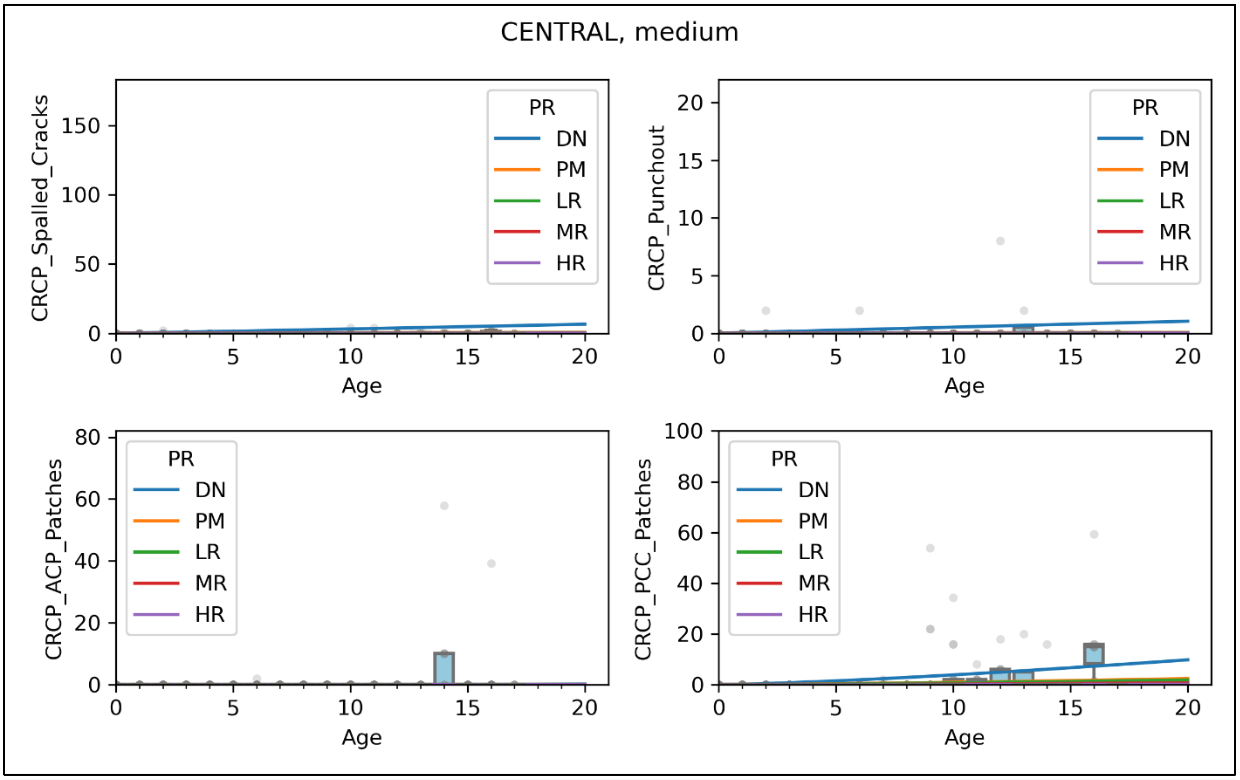
CENTRAL, medium
CRCP_Spalled_Cracks
CRCP_Punchout
CRCP_ACP_Patches
CRCP_PCC_Patches
Age
PR
DN
PM
LR
MR
HR

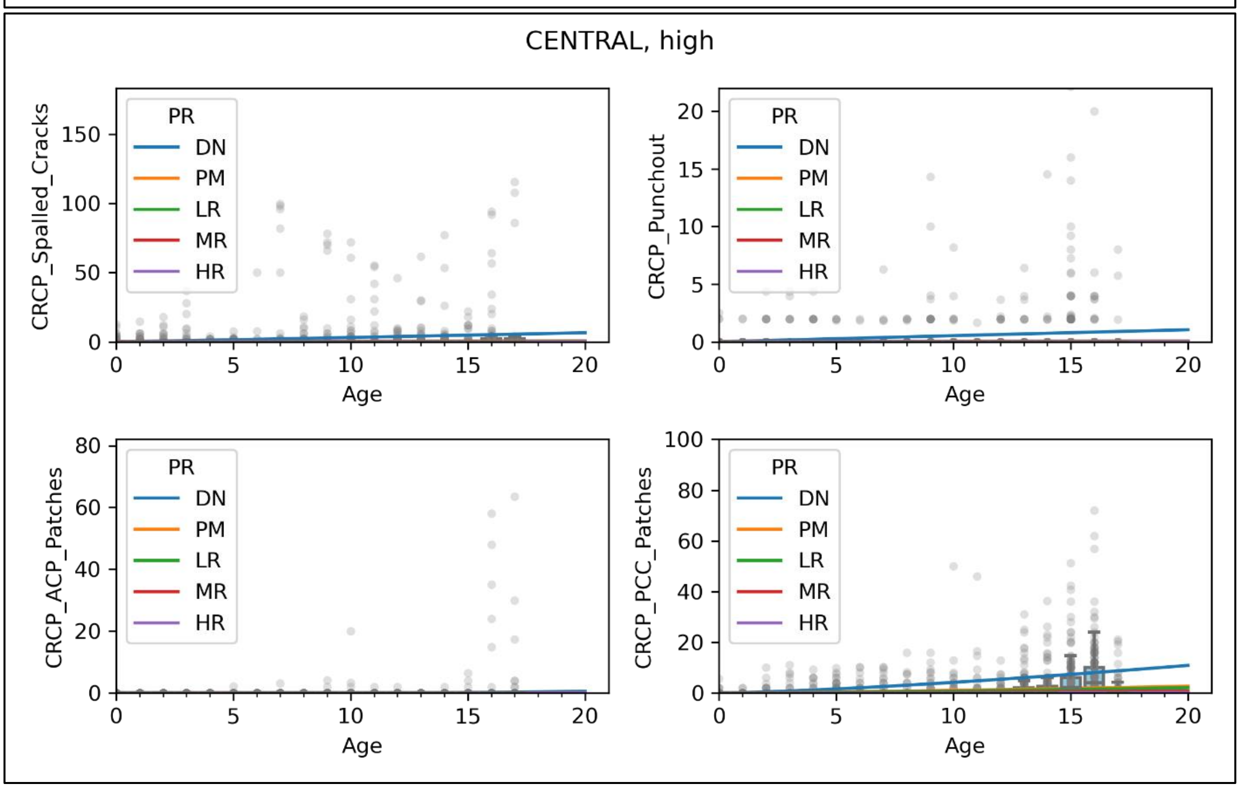
CENTRAL, high
CRCP_Spalled_Cracks
CRCP_Punchout
CRCP_ACP_Patches
CRCP_PCC_Patches
Age
PR
DN
PM
LR
MR
HR

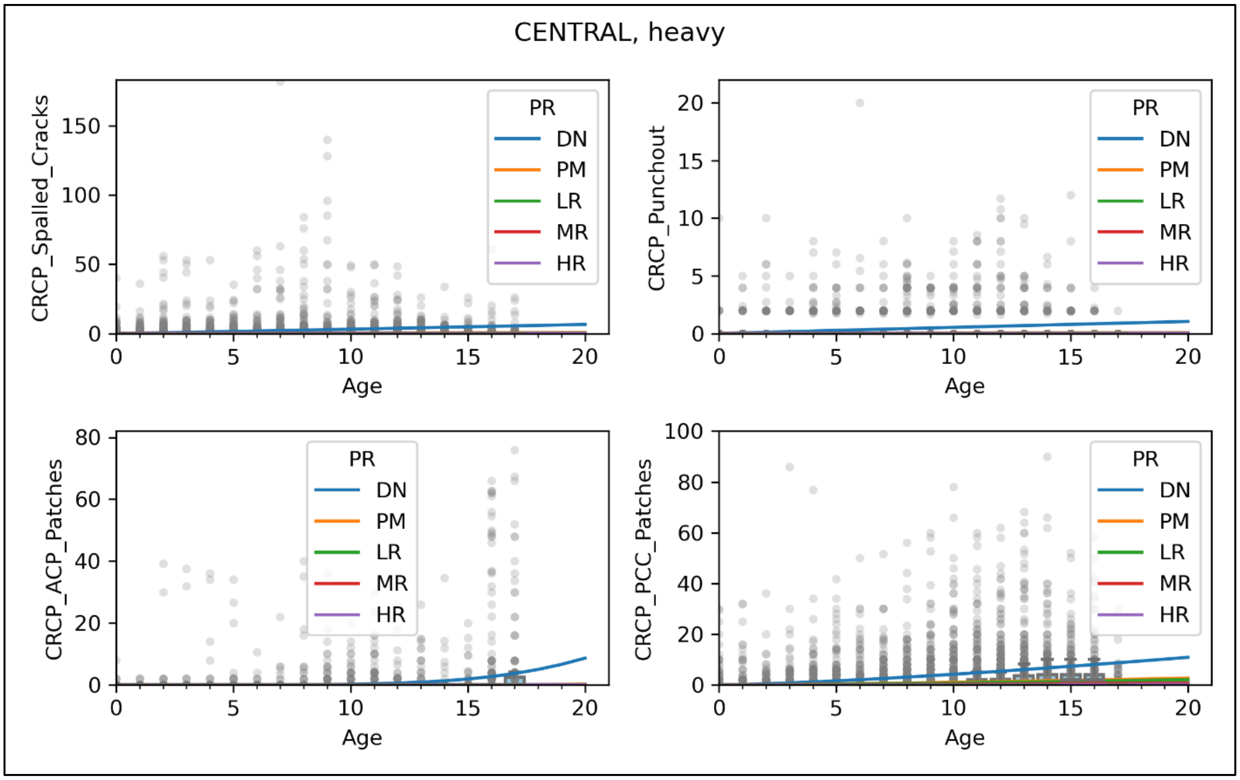
CENTRAL, heavy
CRCP_Spalled_Cracks
CRCP_Punchout
CRCP_ACP_Patches
CRCP_PCC_Patches
Age
PR
DN
PM
LR
MR
HR

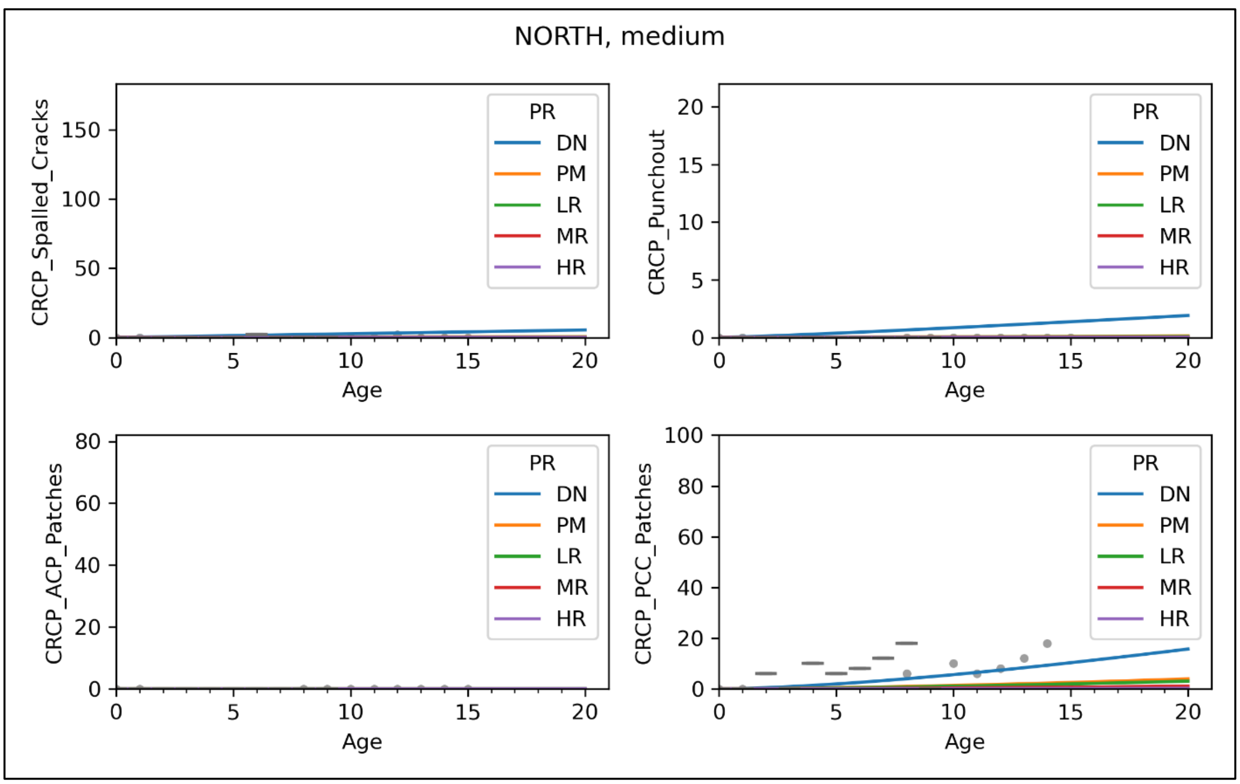
NORTH, medium
CRCP_Spalled_Cracks
CRCP_Punchout
CRCP_ACP_Patches
CRCP_PCC_Patches
Age
PR
DN
PM
LR
MR
HR

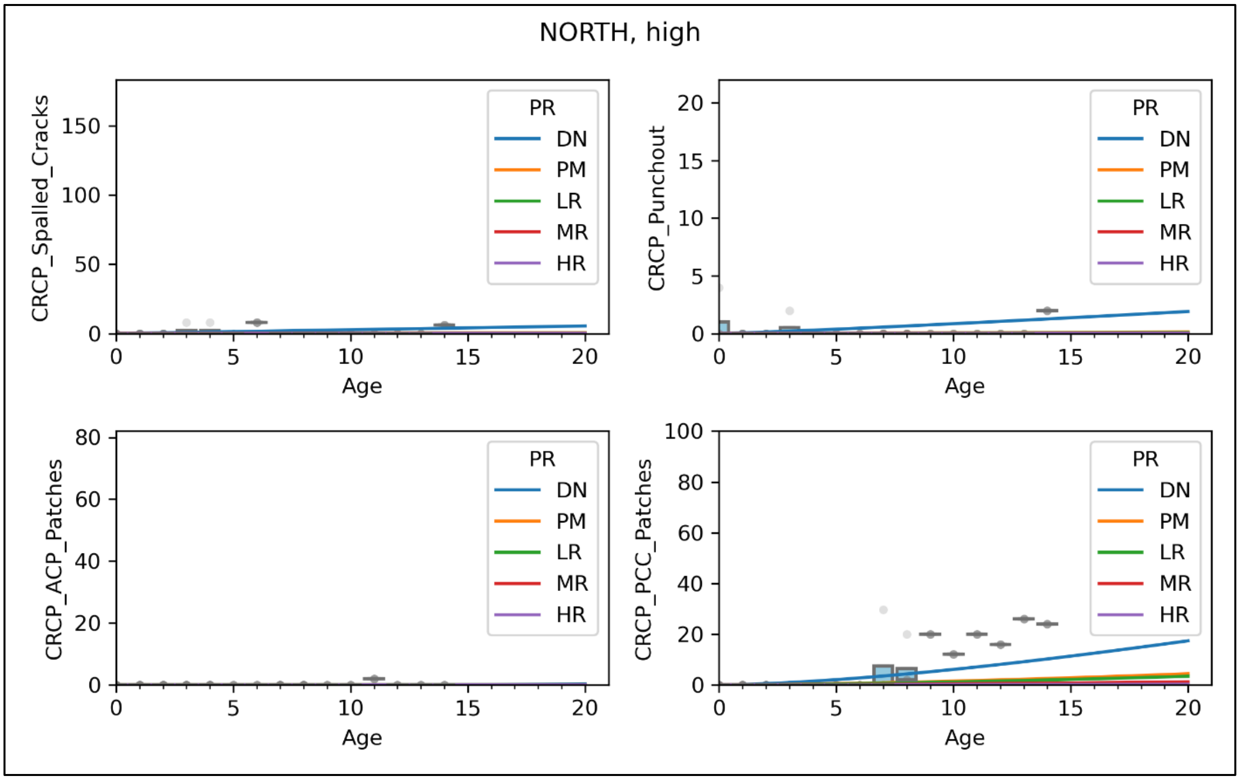
NORTH, high
CRCP_Spalled_Cracks
CRCP_Punchout
CRCP_ACP_Patches
CRCP_PCC_Patches
Age
PR
DN
PM
LR
MR
HR

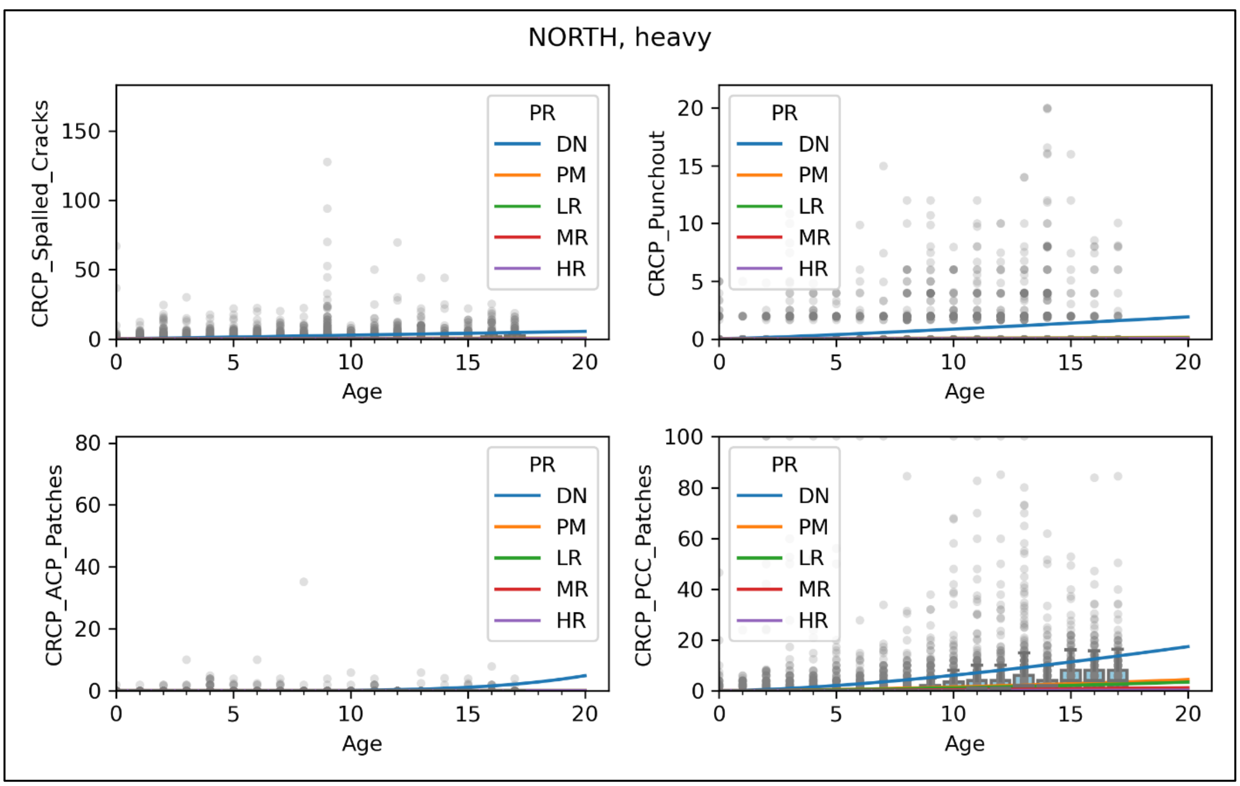
NORTH, heavy
CRCP_Spalled_Cracks
CRCP_Punchout
CRCP_ACP_Patches
CRCP_PCC_Patches
Age
PR
DN
PM
LR
MR
HR

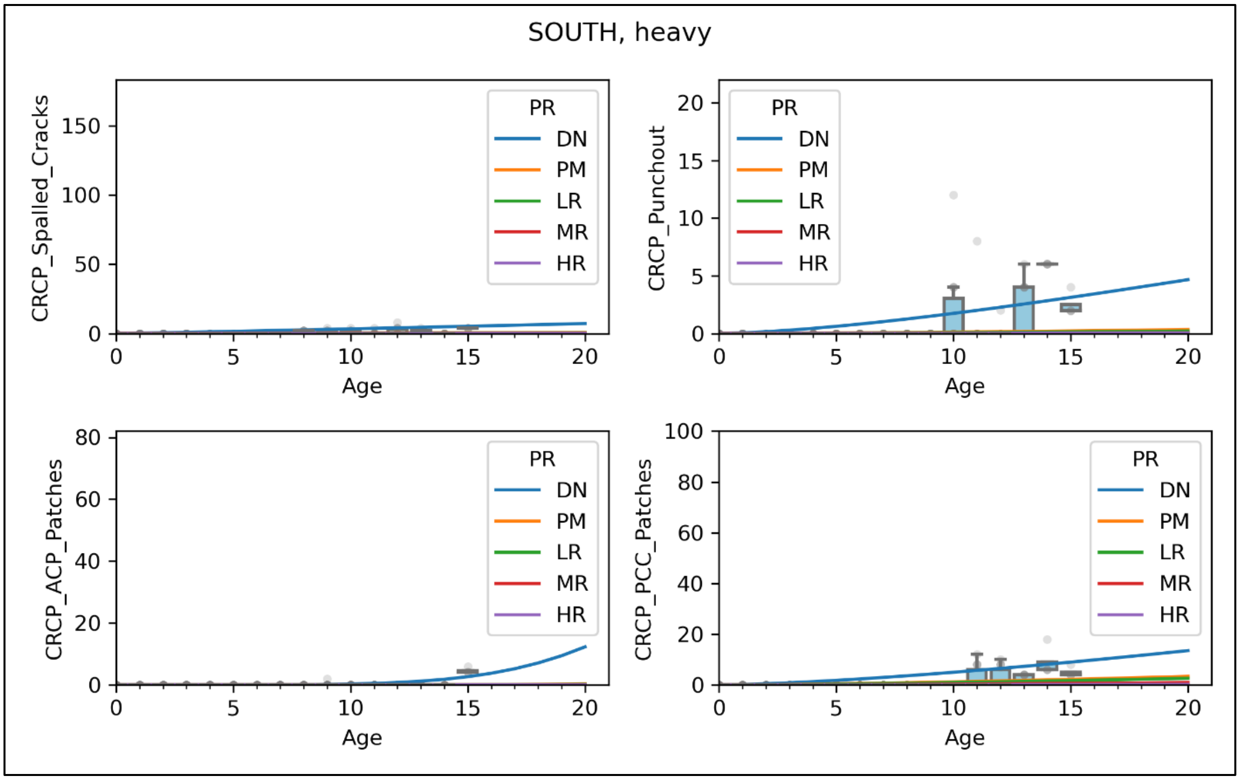
SOUTH, heavy
CRCP_Spalled_Cracks
CRCP_Punchout
CRCP_ACP_Patches
CRCP_PCC_Patches
Age
PR
DN
PM
LR
MR
HR

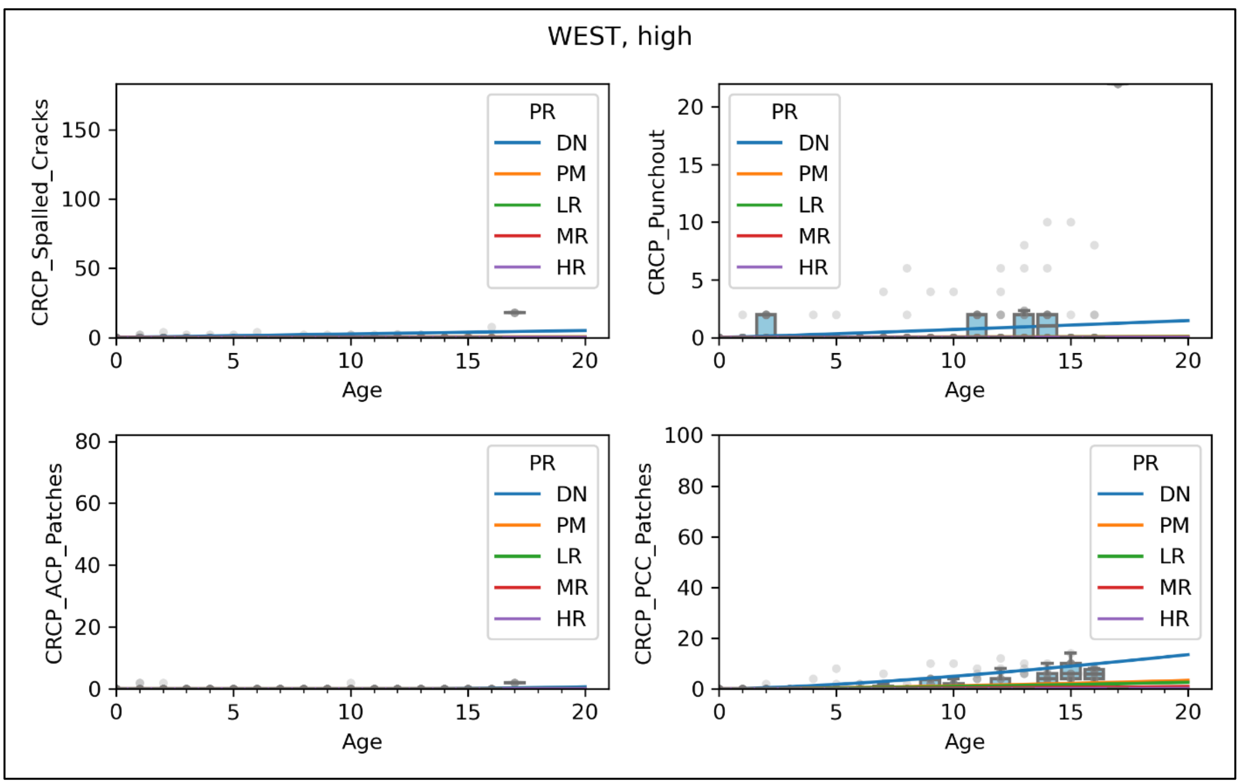
WEST, high
CRCP_Spalled_Cracks
CRCP_Punchout
CRCP_ACP_Patches
CRCP_PCC_Patches
Age
PR
DN
PM
LR
MR
HR

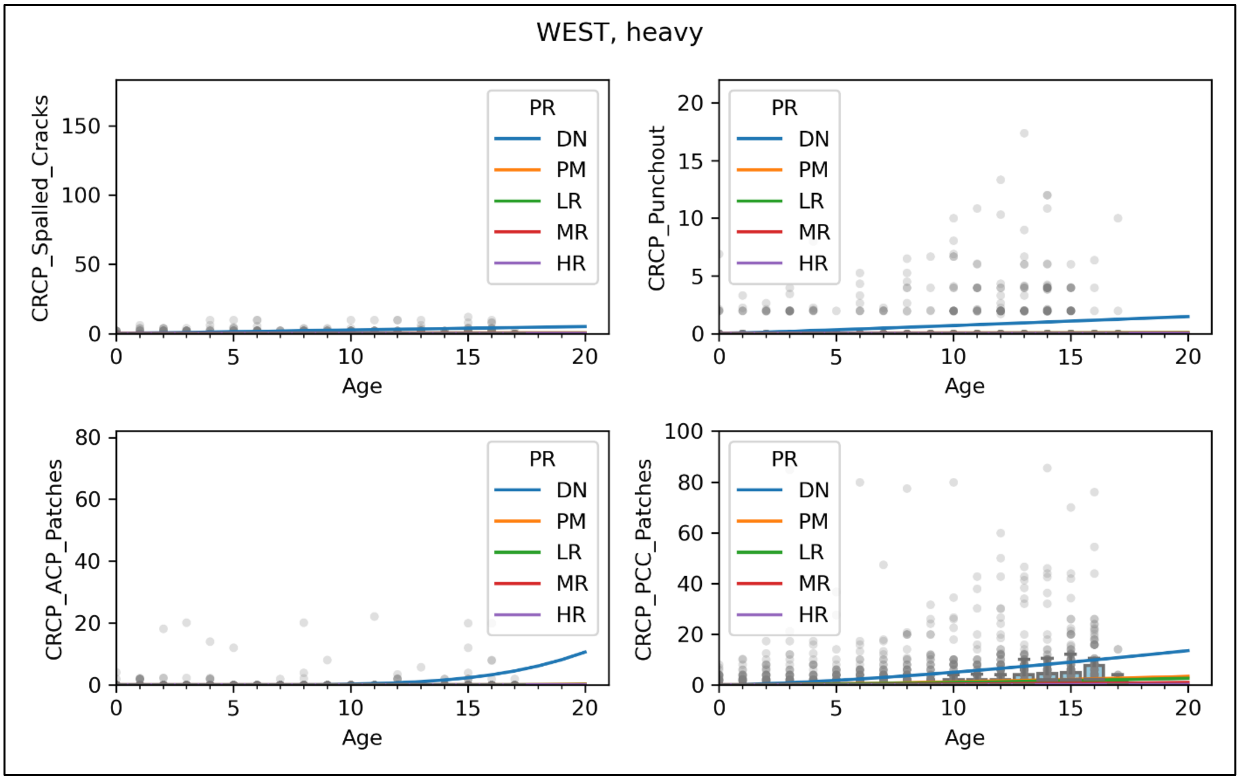
WEST, heavy
CRCP_Spalled_Cracks
CRCP_Punchout
CRCP_ACP_Patches
CRCP_PCC_Patches
Age
PR
DN
PM
LR
MR
HR

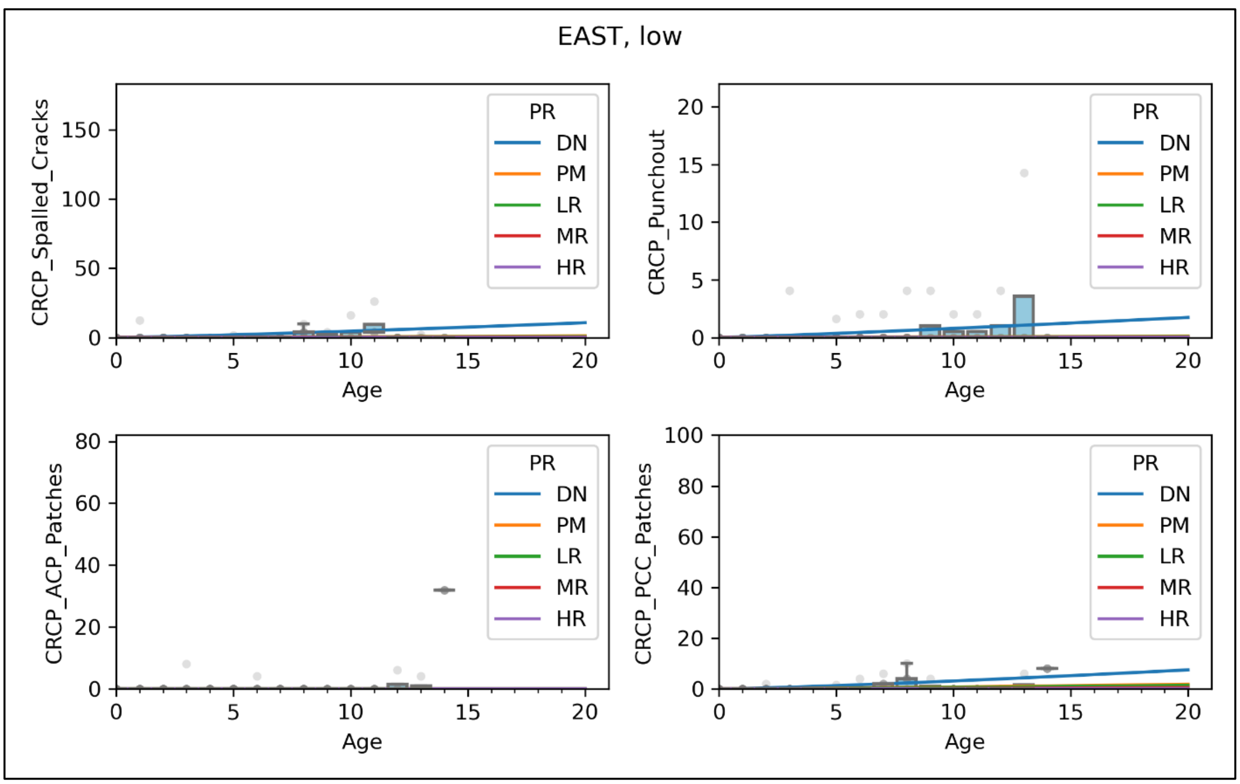
EAST, low
CRCP_Spalled_Cracks
CRCP_Punchout
CRCP_ACP_Patches
CRCP_PCC_Patches
Age
PR
DN
PM
LR
MR
HR

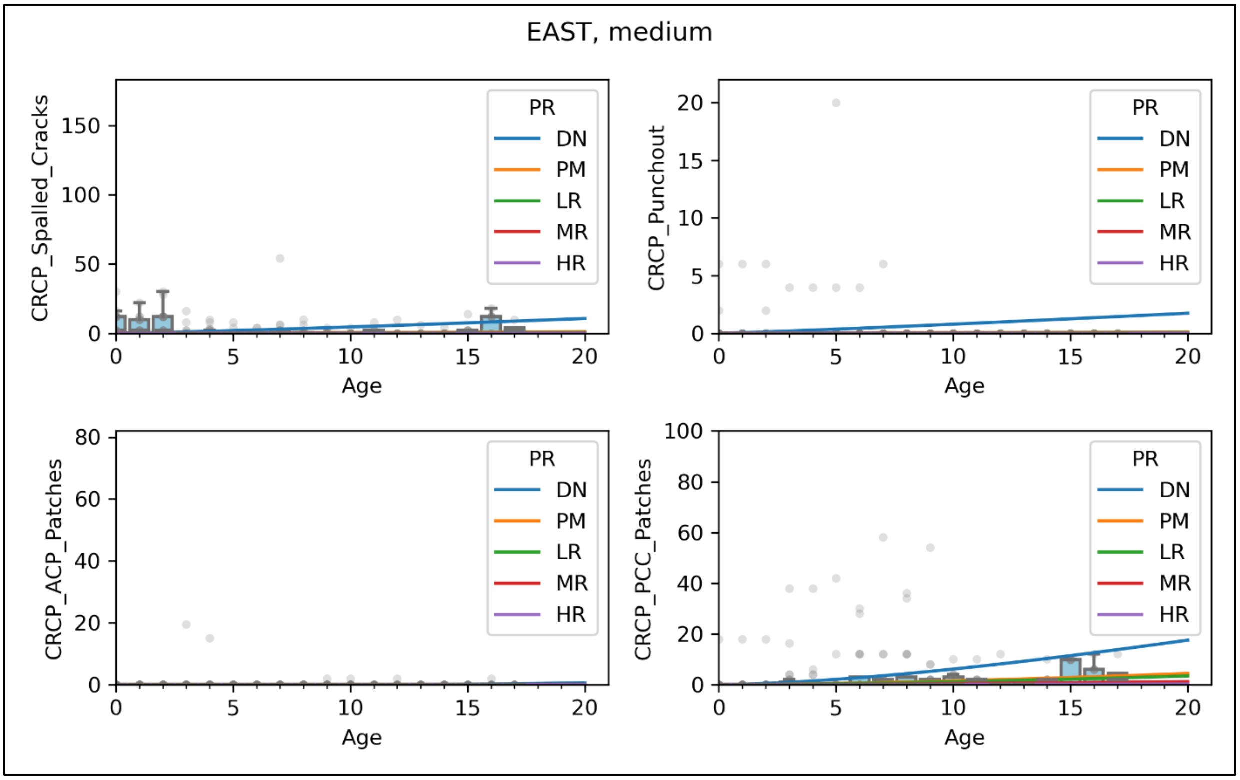
EAST, medium
CRCP_Spalled_Cracks
CRCP_Punchout
CRCP_ACP_Patches
CRCP_PCC_Patches
Age
PR
DN
PM
LR
MR
HR

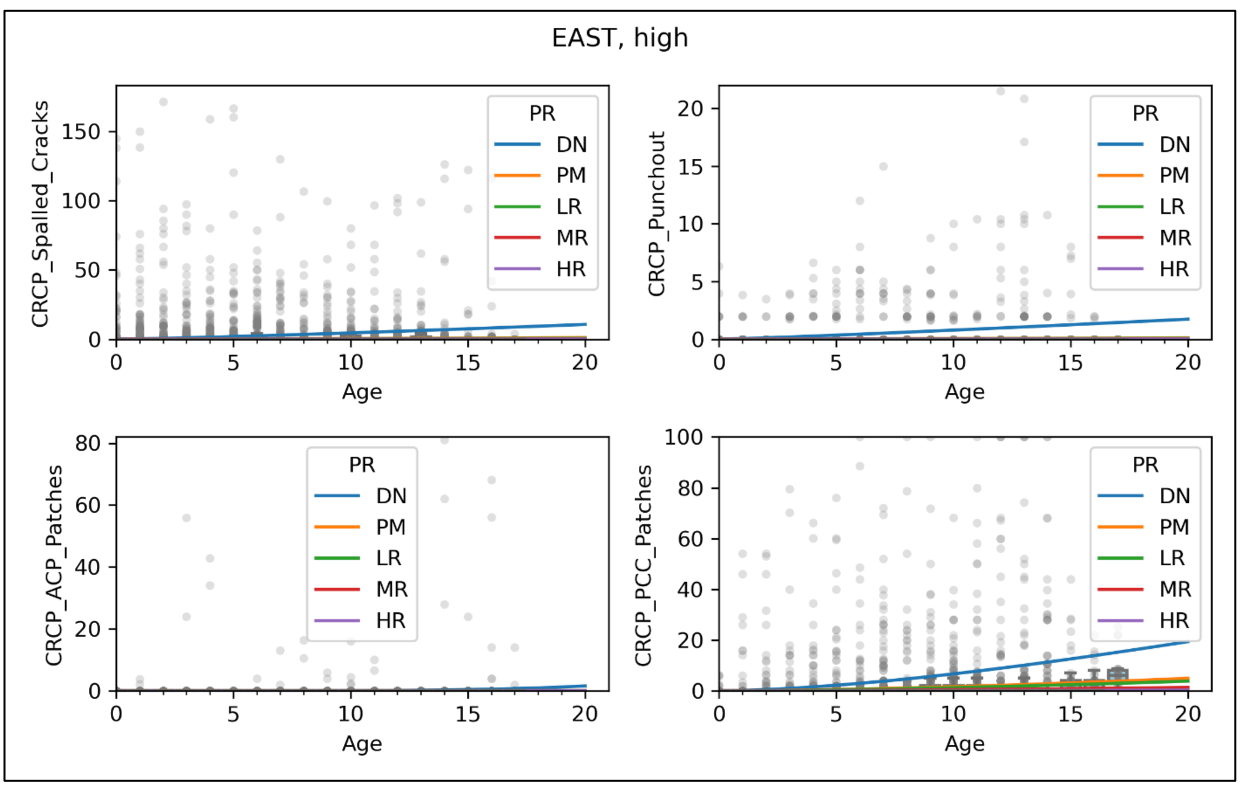
EAST, high
CRCP_Spalled_Cracks
CRCP_Punchout
CRCP_ACP_Patches
CRCP_PCC_Patches
Age
PR
DN
PM
LR
MR
HR

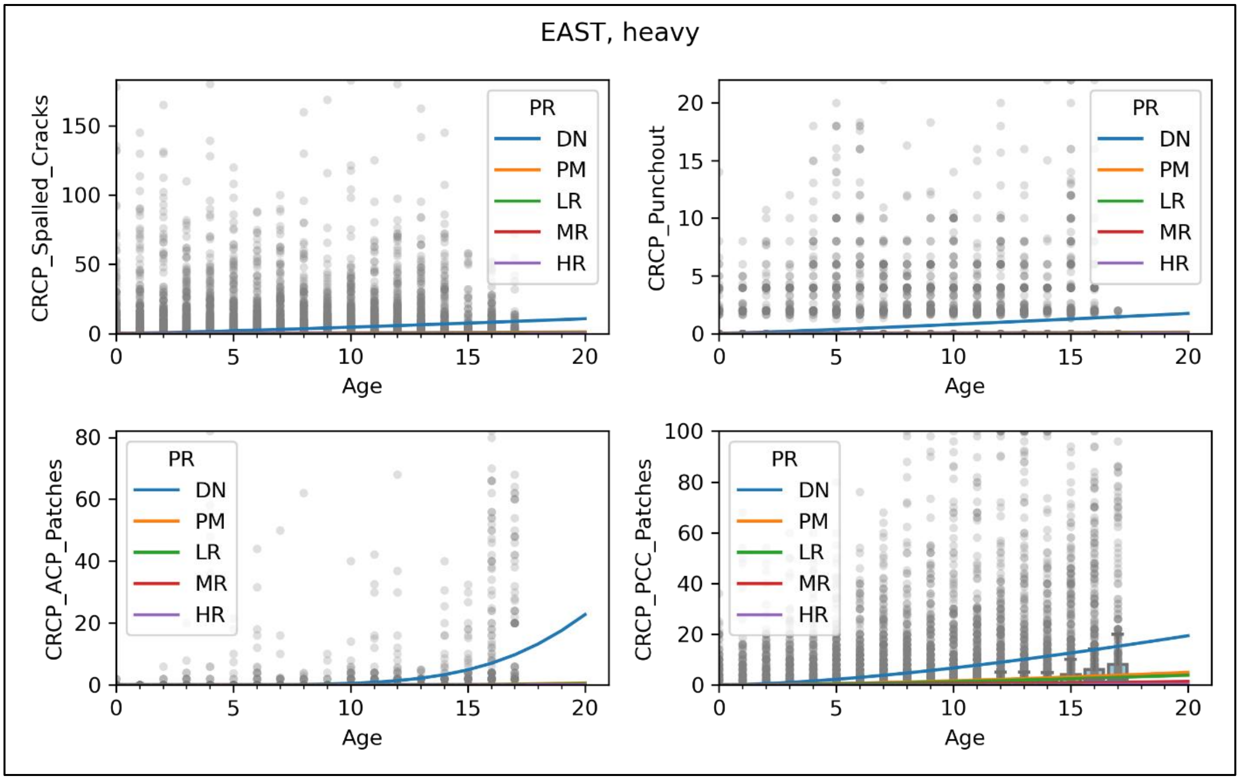

Figure 5.18 Performance of Alternative Models for CRCP

5.5.3.2. Alternative Models for JCP

The alternative model errors for JCP are presented in Table 5.15. As shown, the normalized errors of all the models are below 8 percent, suggesting that developed alternative models for JCP produce satisfactory predictions.

The results of model estimation for different JCP distresses are summarized in Table 5.16. In all the models, the effects of most variables are statistically significant. As for the previous models, the values of parameters related to the traffic and treatment type meet the requirements specified in the model estimation section—i.e., pavements with heavier traffic exhibit higher distress, while pavements receiving more work-intensive treatment show lower distress.

The performance of alternative models for JCP was also evaluated visually by comparing the boxplots of the field measurements in Figure 5.19. As can be observed, the deterioration models can capture the general trends of different distresses well. Most importantly, the deterioration curves for different treatment types follow the right hierarchical order: the DN curve has the highest deterioration rate followed in order by PM, LRhb, MRhb, and HRhb, which is essential for preparing pavement maintenance or rehabilitation plans.

Table 5.15 JCP Model Errors

Distress	Asymptotic value	MSE	std_error	Normalized error
Failed Joints and Cracks	173	74.7	8.64	5.00%
Failures	148	59.9	7.74	5.23%
Shattered Slabs	24	2.00	1.41	5.89%
Longitudinal Cracks	102	27.2	5.22	5.11%
Patches	204	207	14.4	7.05%

Table 5.16 Summary of Alternative Model Estimation for JCP

Distress	Variables	Parameter	Estimate	std	t	p_val
Failed Joints and Cracks	-	β_0	173	-	-	-
	-	γ_0	1653	<0.01	5.8E+5	0
	Traffic_Low	γ_1	-0.001210	0.01	-0.16	0.43
	Traffic_High	γ_2	0.06993	0.01	11.93	<0.01
	Traffic_Heavy	γ_3	0.1296	<0.01	34.51	<0.01
	CL_WEST	γ_4	575.0	<0.01	1.5E+5	0
	CL_EAST	γ_5	-653.3	0.01	-7.5E+4	0
	CL_NORTH	γ_6	169.0	0.01	2.2E+4	0
	CL_SOUTH	γ_7	81.55	0.59	139.29	0
	-	η_0	1.117	0.02	68.52	0
	DN	η_1	1.150	0.04	30.82	<0.01
	LR	η_2	-0.1595	0.03	-4.87	<0.01
	MR	η_3	-0.2372	0.04	-6.74	<0.01
	HR	η_4	-0.4935	0.04	-12.33	<0.01
Failures	-	β_0	148	-	-	-
	-	γ_0	5403	<0.01	7.0E+6	0
	Traffic_Low	γ_1	-0.6330	<0.01	-298.84	0
	Traffic_High	γ_2	0.3886	<0.01	197.24	0
	Traffic_Heavy	γ_3	0.5240	<0.01	558.23	0
	CL_WEST	γ_4	1138	<0.01	7.9E+5	0
	CL_EAST	γ_5	-210.8	<0.01	-2.0E+5	0
	CL_NORTH	γ_6	393.8	<0.01	1.8E+5	0
	CL_SOUTH	γ_7	-137.2	62.7	-2.19	0.01
	-	η_0	3.01E-05	<0.01	79.83	0
	DN	η_1	2.88E-05	<0.01	31.58	<0.01
	LR	η_2	-4.60E-06	<0.01	-5.94	<0.01
	MR	η_3	-6.17E-06	<0.01	-7.31	<0.01
	HR	η_4	-1.61E-05	<0.01	-20.33	<0.01
Shattered Slabs	-	β_0	24	-	-	-
	-	γ_0	3926	<0.01	9.4E+5	0
	Traffic_Low	γ_1	-451.2	0.66	-682.65	0
	Traffic_High	γ_2	619.2	0.04	1.7E+4	0

Distress	Variables	Parameter	Estimate	std	t	p_val
	Traffic_Heavy	γ_3	1162	<0.01	2.8E+5	0
	CL_WEST	γ_4	290.9	0.02	1.3E+4	0
	CL_EAST	γ_5	5.306	<0.01	1.2E+3	0
	CL_NORTH	γ_6	557.0	0.48	1.2E+3	0
	CL_SOUTH	γ_7	463.2	123	3.74	<0.01
	-	η_0	9.91E-08	<0.01	0.14	0.44
	DN	η_1	2.77E-05	<0.01	17.20	<0.01
	LR	η_2	-7.28E-08	<0.01	-0.05	0.48
	MR	η_3	-7.35E-08	<0.01	-0.05	0.48
	HR	η_4	-8.05E-08	<0.01	-0.05	0.48
Longitudinal Cracks	-	β_0	102	-	-	-
	-	γ_0	1036	0.01	1.3E+5	0
	Traffic_Low	γ_1	-0.00052	0.06	-0.01	0.50
	Traffic_High	γ_2	0.002062	0.02	0.11	0.46
	Traffic_Heavy	γ_3	0.01171	0.01	1.27	0.10
	CL_WEST	γ_4	-25.01	0.09	-283.07	0
	CL_EAST	γ_5	-35.91	0.01	-4.4E+3	0
	CL_NORTH	γ_6	-35.79	0.08	-443.47	0
	CL_SOUTH	γ_7	10.82	2.34	4.62	<0.01
	-	η_0	0.1261	0.03	4.53	<0.01
	DN	η_1	2.877	0.06	49.09	0
	LR	η_2	-0.00018	0.06	0	0.50
	MR	η_3	-0.08323	0.06	-1.31	0.10
	HR	η_4	-0.1069	0.06	-1.68	0.05
Patches	-	β_0	204	-	-	-
	-	γ_0	1089	<0.01	2.9E+5	0
	Traffic_Low	γ_1	-0.00503	0.04	-0.14	0.44
	Traffic_High	γ_2	0.001649	0.01	0.15	0.44
	Traffic_Heavy	γ_3	111.6	<0.01	2.8E+4	0
	CL_WEST	γ_4	319.2	0.02	2.0E+4	0
	CL_EAST	γ_5	-88.45	<0.01	-2.3E+4	0
	CL_NORTH	γ_6	-88.45	0.05	-1.7E+4	0
	CL_SOUTH	γ_7	42.79	0.95	45.24	0
	eta0	η_0	1.750	0.03	50.53	0
	DN	η_1	4.739	0.07	68.99	0
	LR	η_2	-0.4499	0.07	-6.05	<0.01
	MR	η_3	-1.304	0.08	-15.58	<0.01
	HR	η_4	-1.680	0.09	-17.73	<0.01

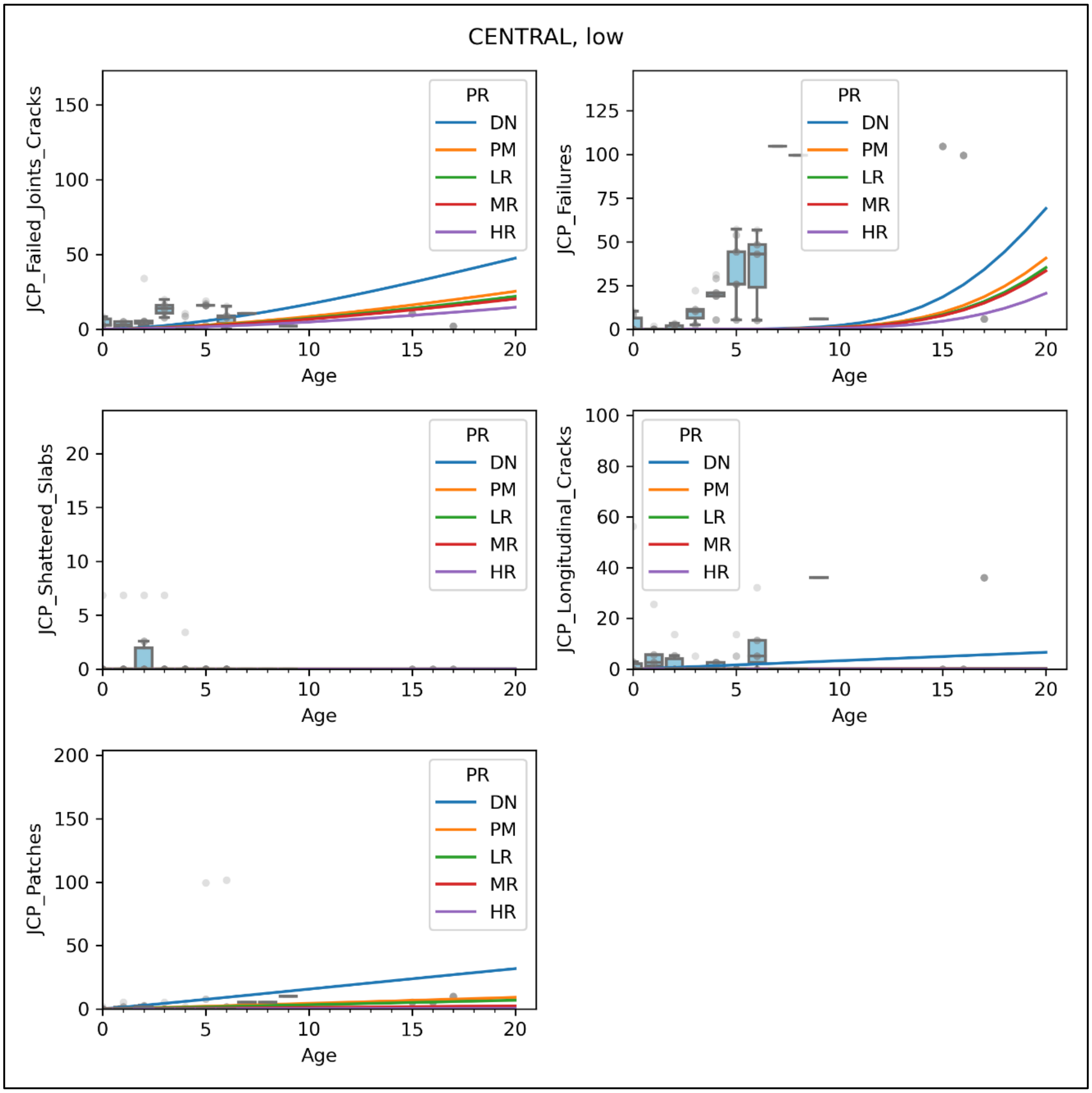

CENTRAL, low
JCP_Failed_Joints_Cracks
JCP_Failures
JCP_Shattered_Slabs
JCP_Longitudinal_Cracks
JCP_Patches
Age
PR
DN
PM
LR
MR
HR

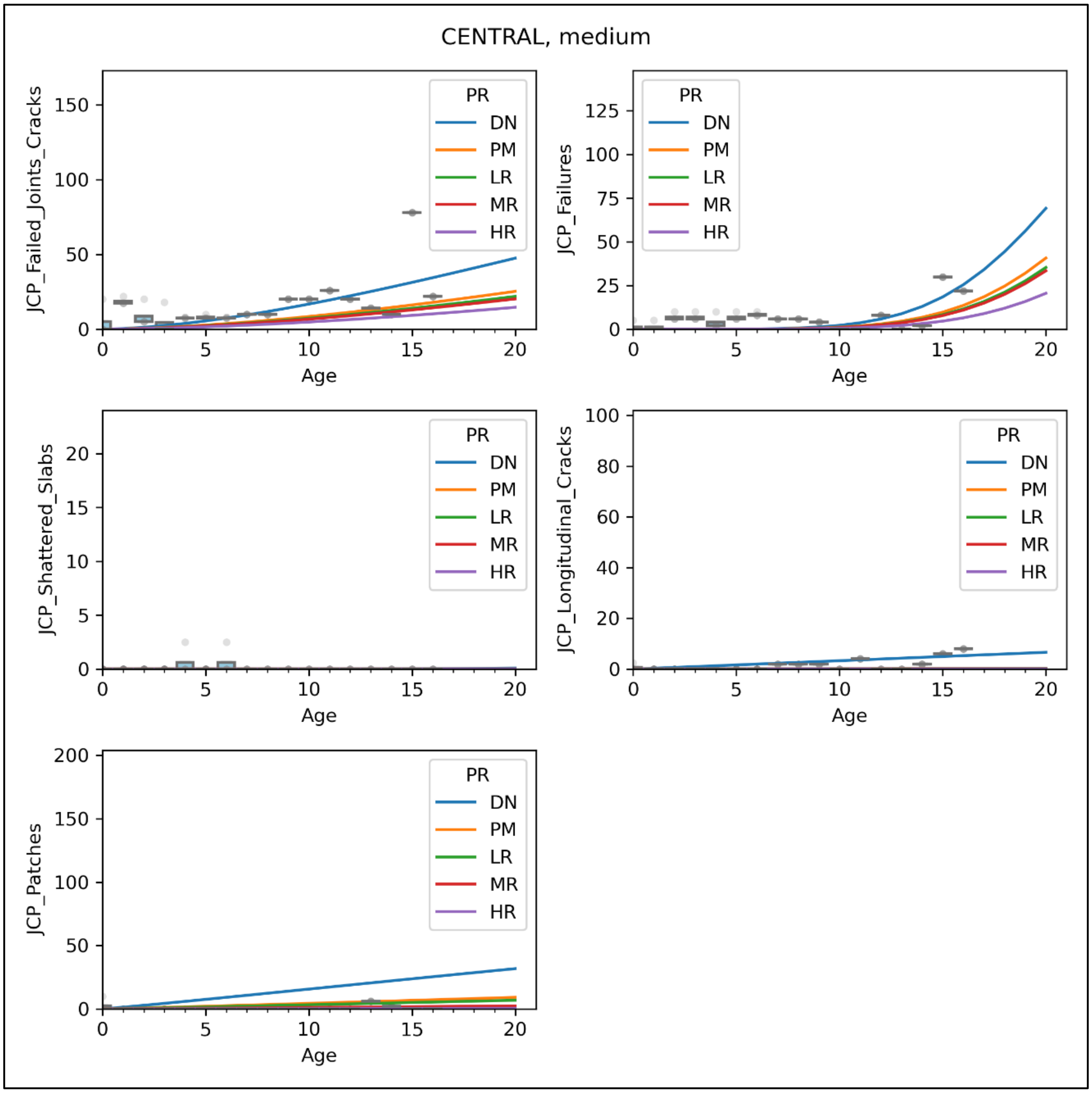
CENTRAL, medium
JCP_Failed_Joints_Cracks
JCP_Failures
JCP_Shattered_Slabs
JCP_Longitudinal_Cracks
JCP_Patches
Age
PR
DN
PM
LR
MR
HR

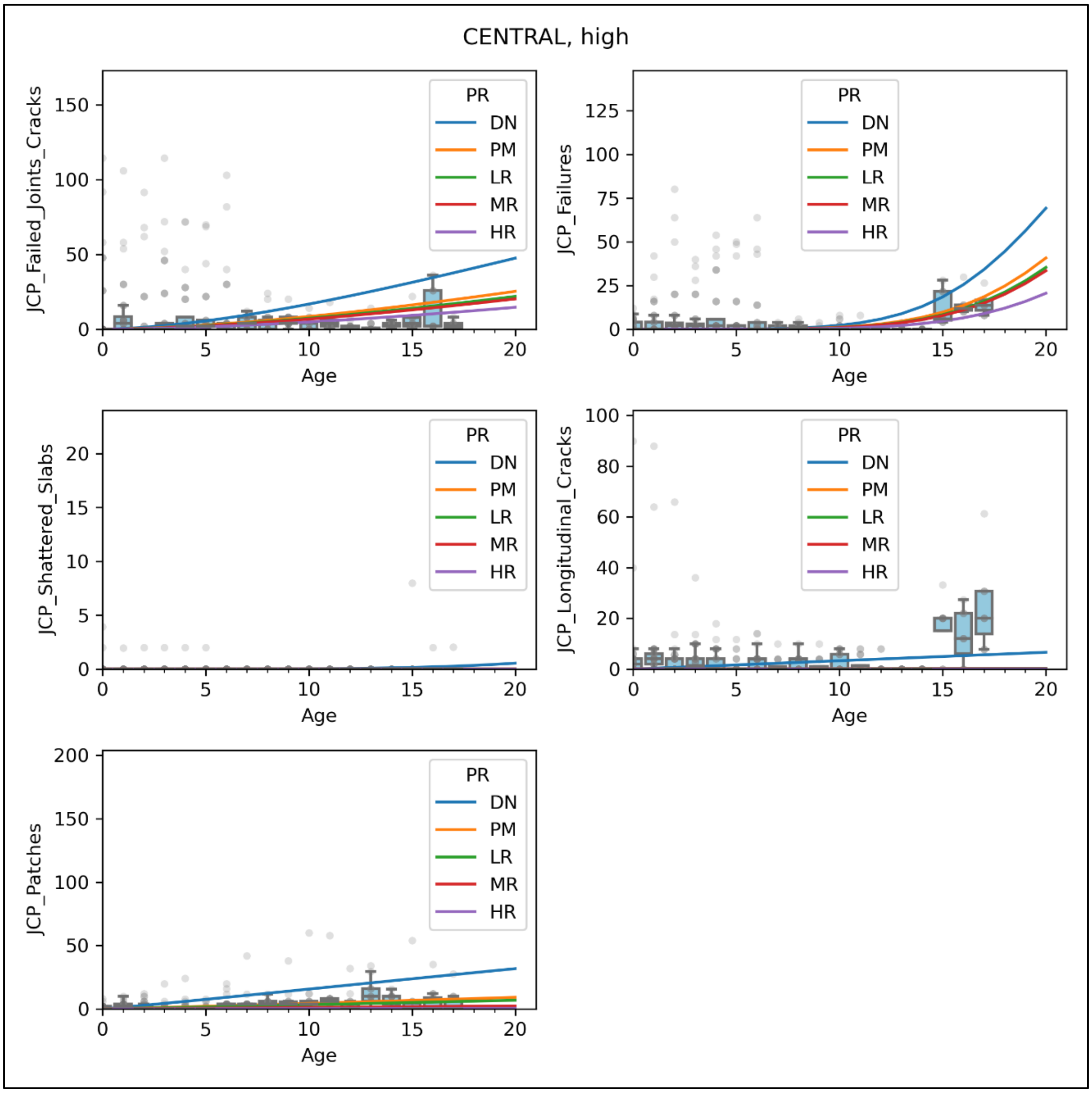

CENTRAL, high
JCP_Failed_Joints_Cracks
JCP_Failures
JCP_Shattered_Slabs
JCP_Longitudinal_Cracks
JCP_Patches
Age
PR
DN
PM
LR
MR
HR

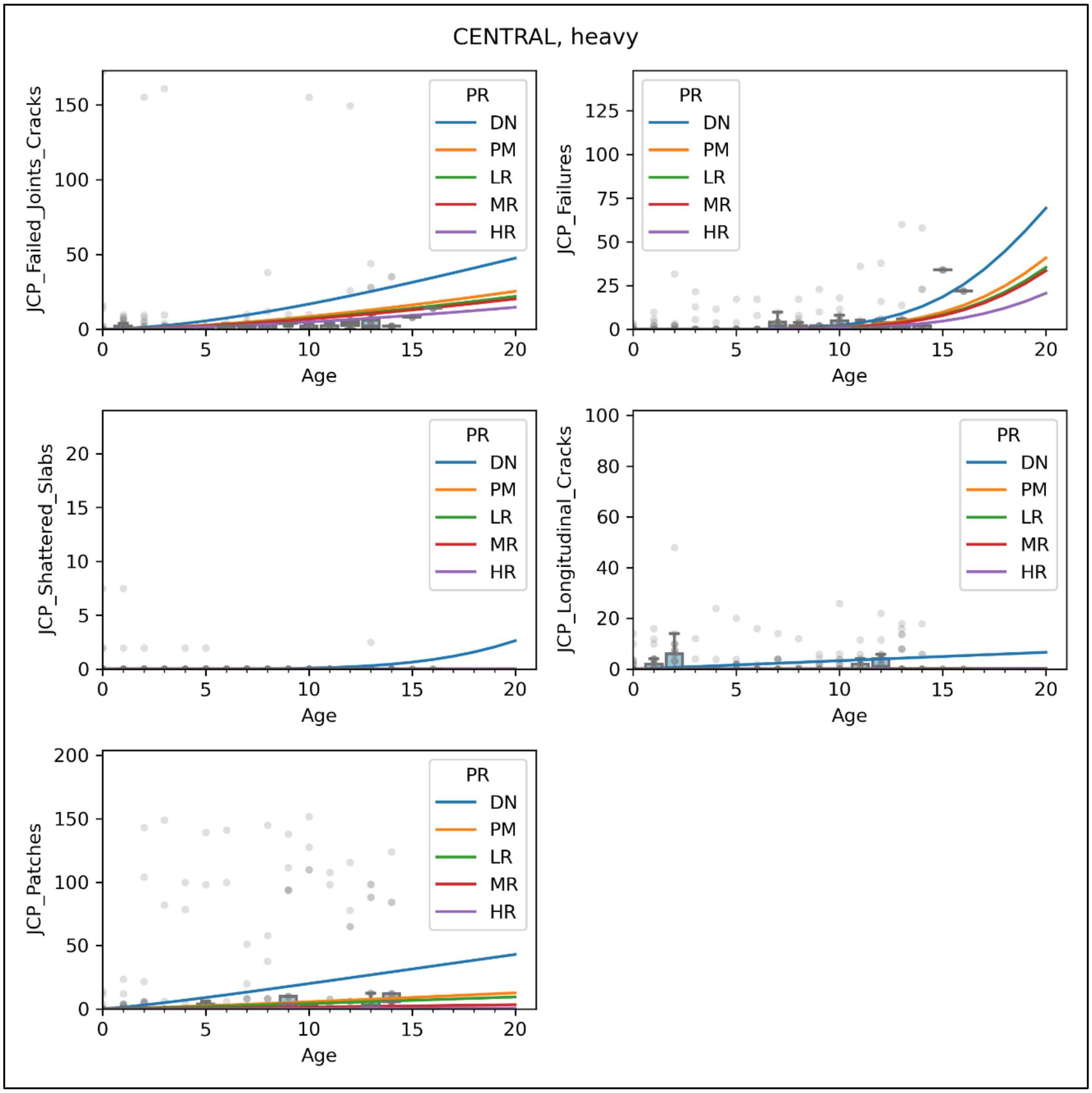

CENTRAL, heavy
JCP_Failed_Joints_Cracks
JCP_Failures
JCP_Shattered_Slabs
JCP_Longitudinal_Cracks
JCP_Patches
Age
PR
DN
PM
LR
MR
HR

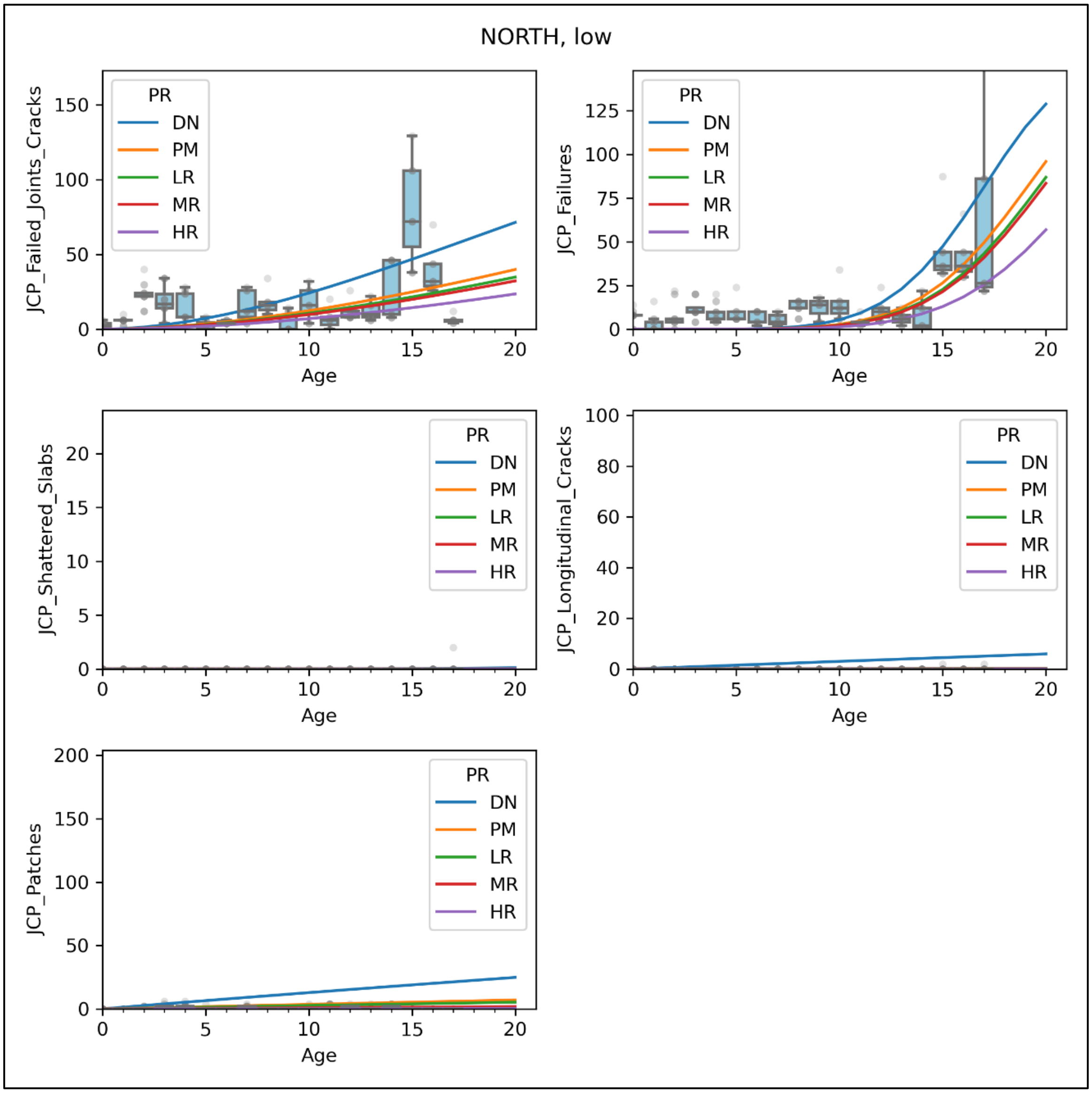

NORTH, low
PR
DN
PM
LR
MR
HR
JCP_Failed_Joints_Cracks
JCP_Failures
JCP_Shattered_Slabs
JCP_Longitudinal_Cracks
JCP_Patches
Age

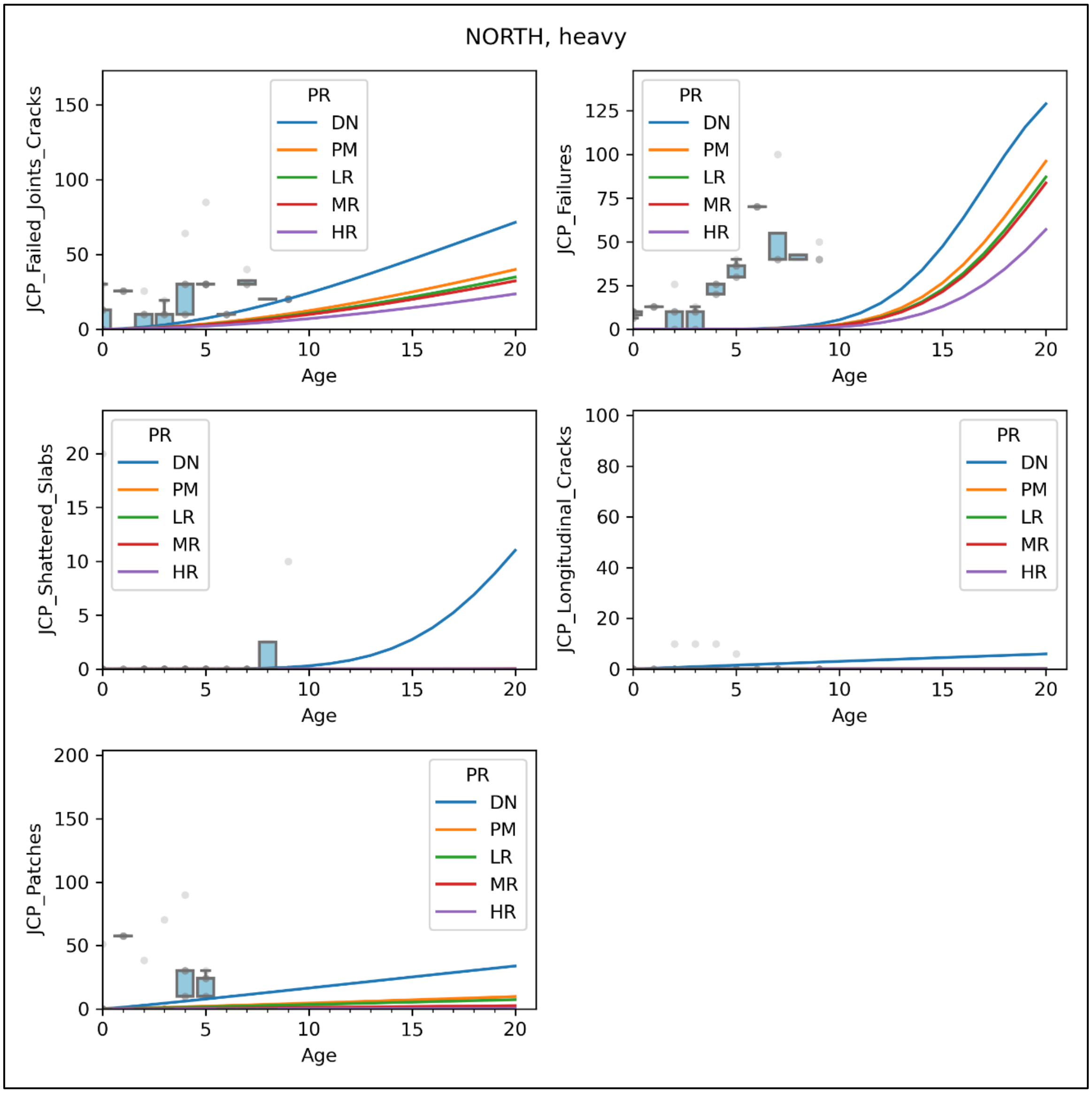
NORTH, heavy
JCP_Failed_Joints_Cracks
JCP_Failures
JCP_Shattered_Slabs
JCP_Longitudinal_Cracks
JCP_Patches
Age
PR
DN
PM
LR
MR
HR

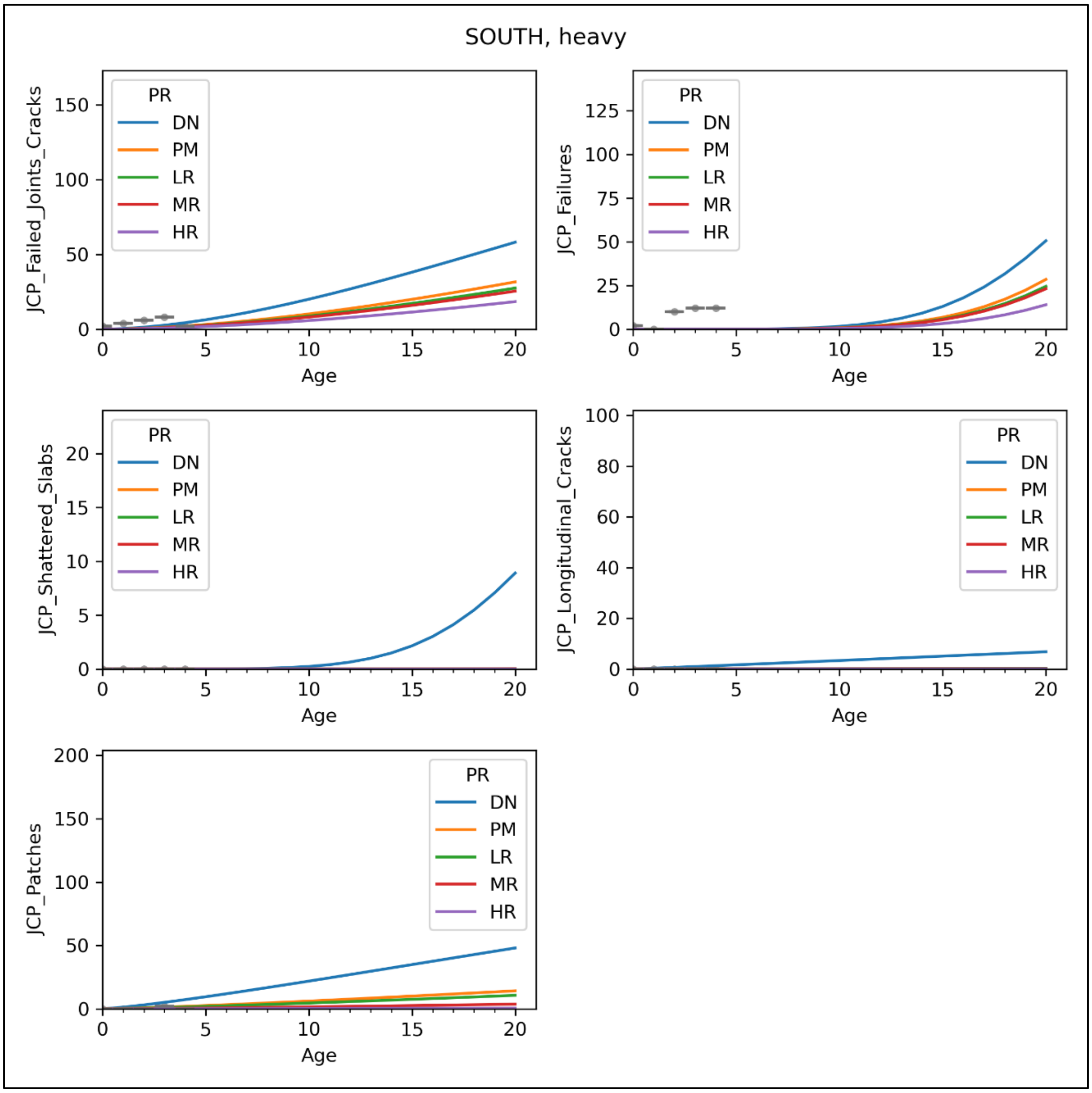

SOUTH, heavy
JCP_Failed_Joints_Cracks
JCP_Failures
JCP_Shattered_Slabs
JCP_Longitudinal_Cracks
JCP_Patches
Age
PR
DN
PM
LR
MR
HR

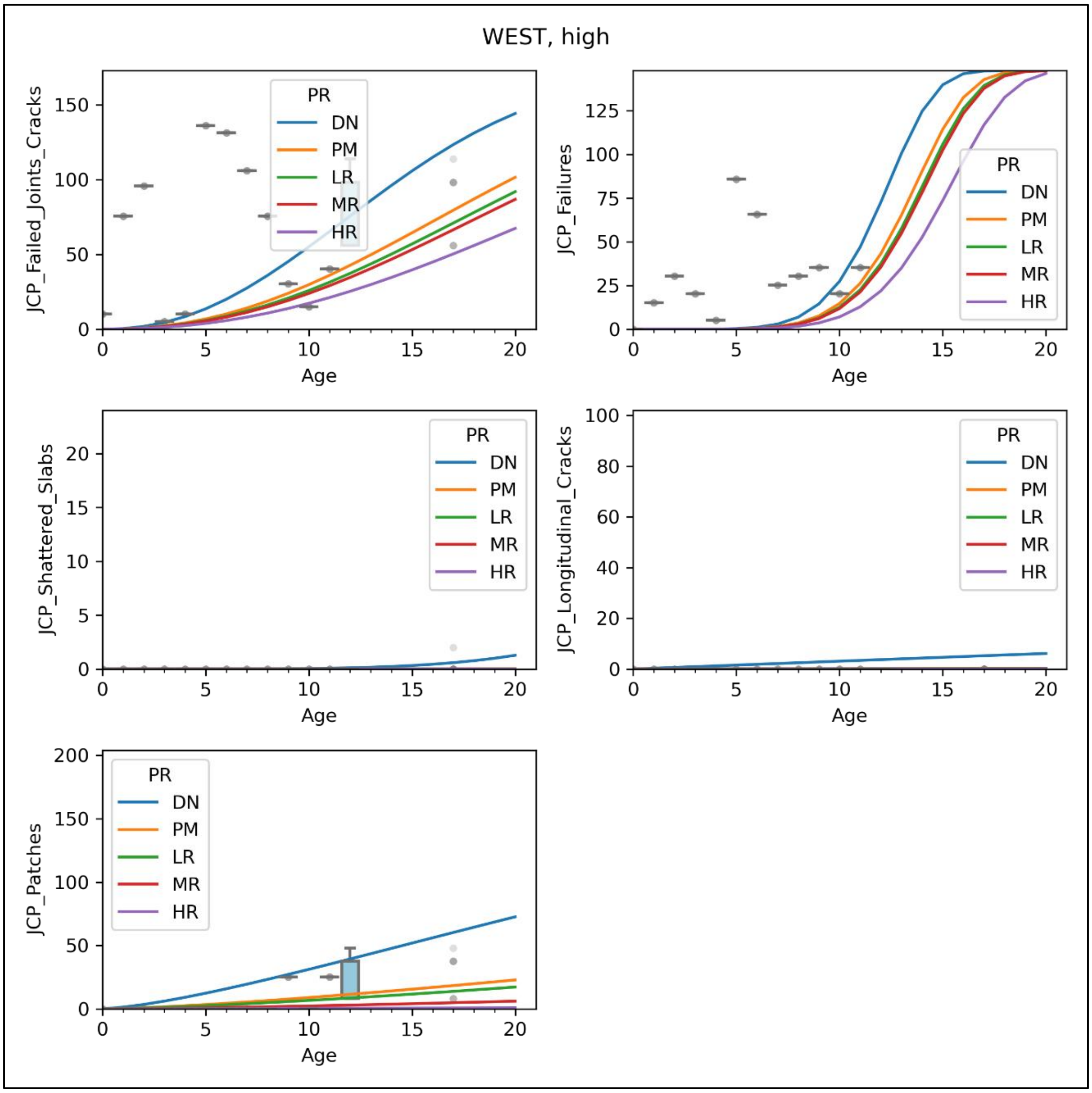
WEST, high
JCP_Failed_Joints_Cracks
JCP_Failures
JCP_Shattered_Slabs
JCP_Longitudinal_Cracks
JCP_Patches
Age
PR
DN
PM
LR
MR
HR

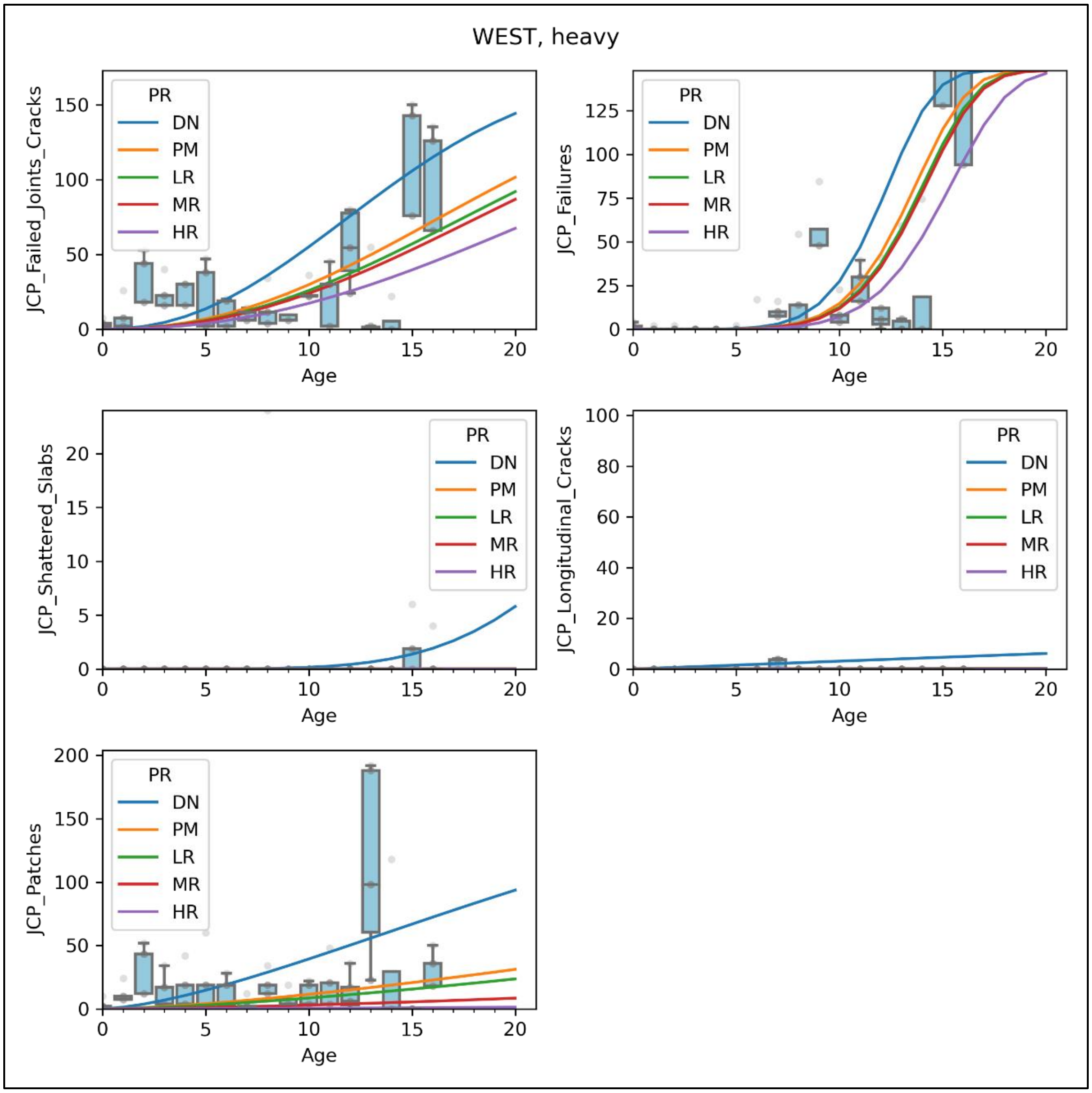

WEST, heavy
JCP_Failed_Joints_Cracks
JCP_Failures
JCP_Shattered_Slabs
JCP_Longitudinal_Cracks
JCP_Patches
Age
PR
DN
PM
LR
MR
HR

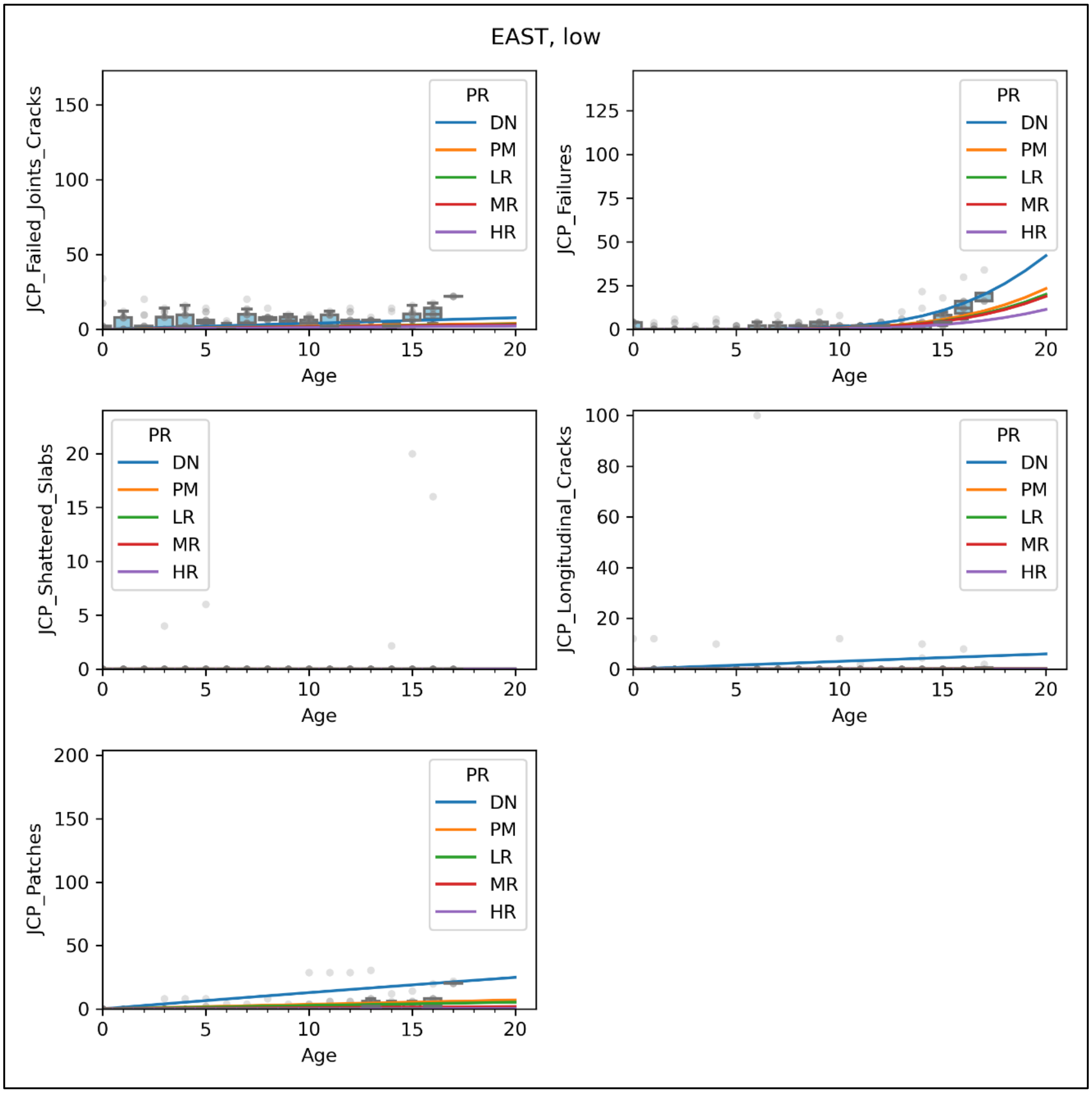

EAST, low
JCP_Failed_Joints_Cracks
JCP_Failures
JCP_Shattered_Slabs
JCP_Longitudinal_Cracks
JCP_Patches
Age
PR
DN
PM
LR
MR
HR

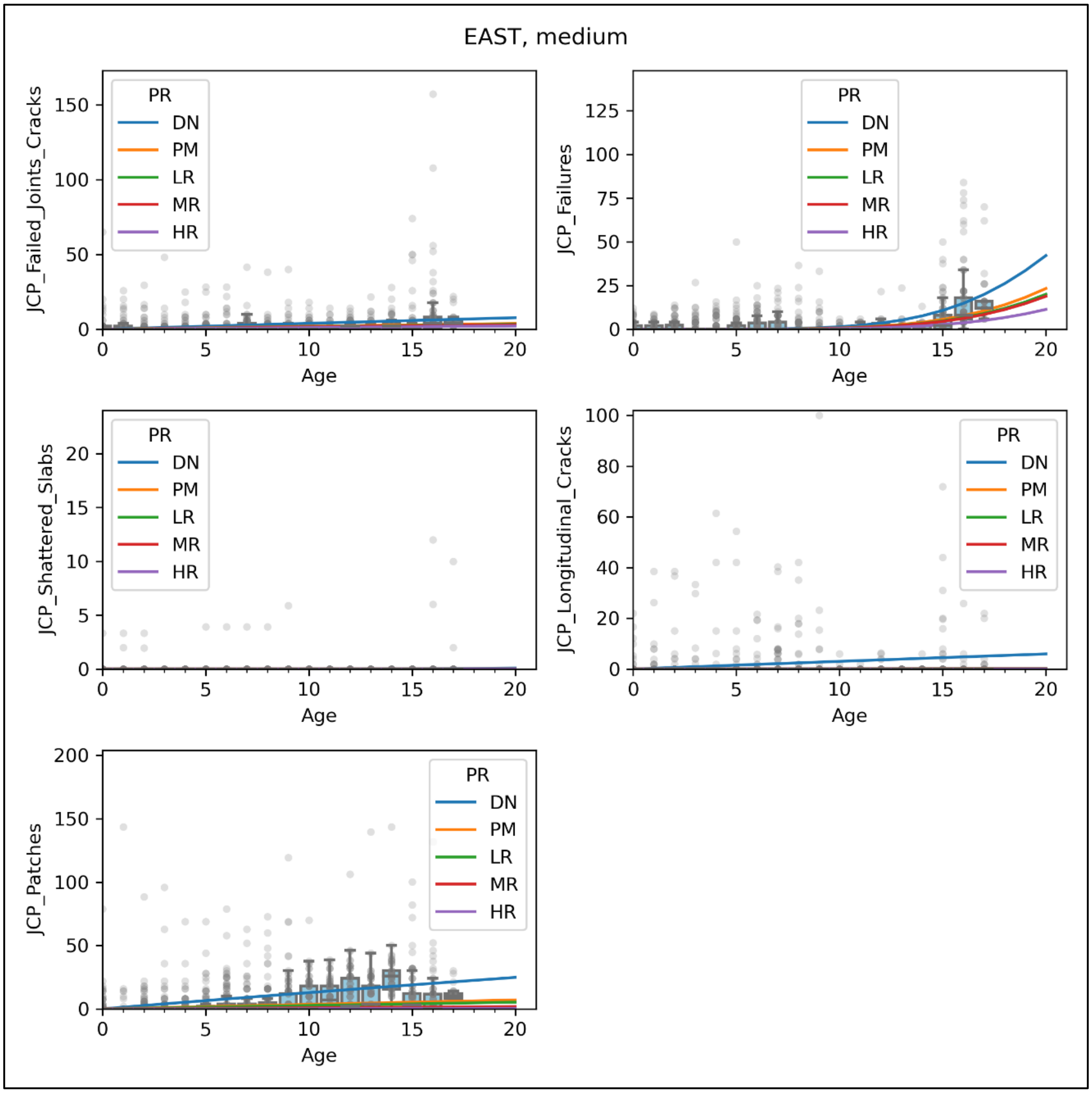
EAST, medium
JCP_Failed_Joints_Cracks
JCP_Failures
JCP_Shattered_Slabs
JCP_Longitudinal_Cracks
JCP_Patches
Age
PR
DN
PM
LR
MR
HR

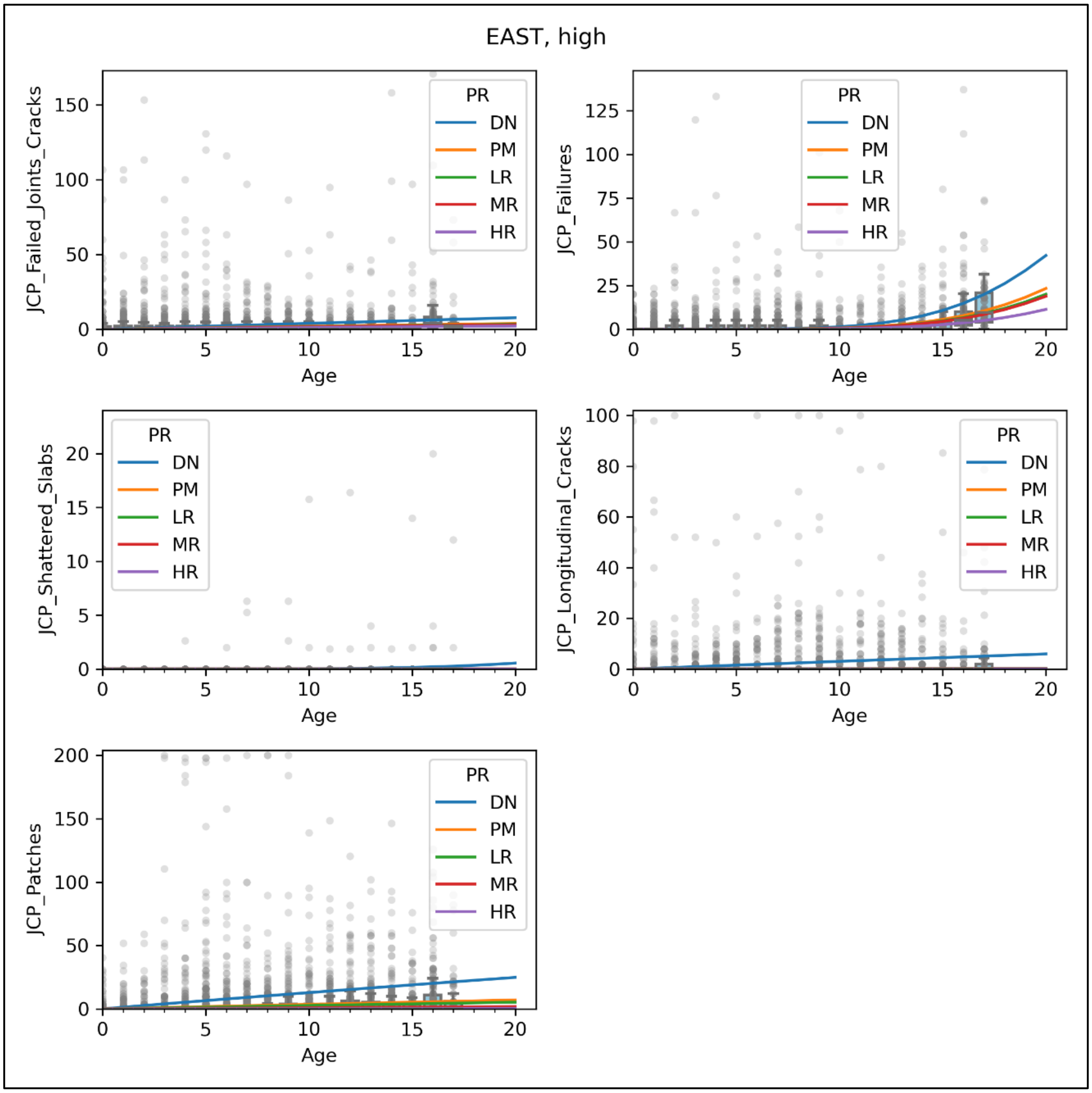
EAST, high
JCP_Failed_Joints_Cracks
JCP_Failures
JCP_Shattered_Slabs
JCP_Longitudinal_Cracks
JCP_Patches
Age
PR
DN
PM
LR
MR
HR

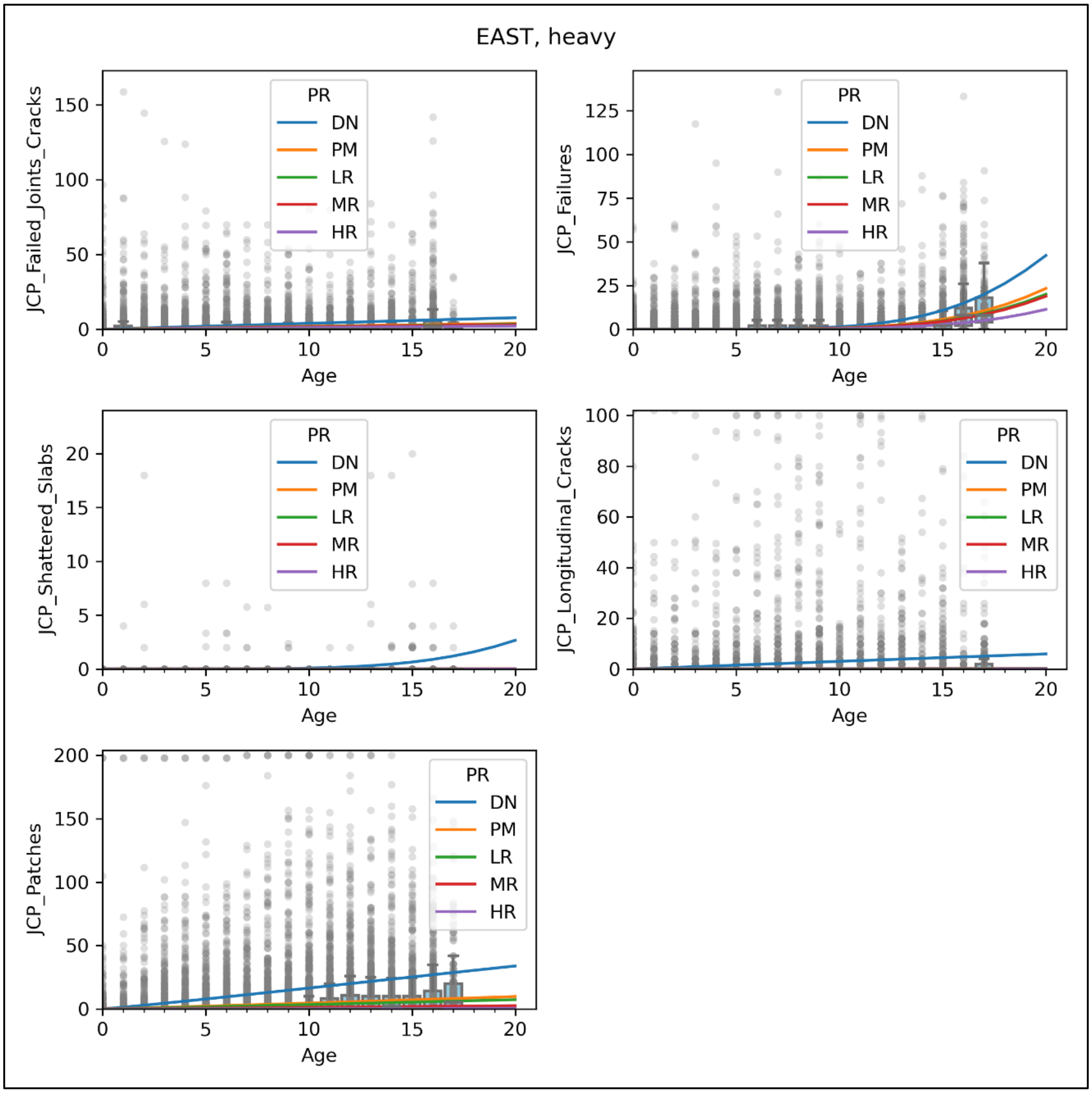

Figure 5.19 Performance of Alternative Models for JCP

Chapter 6. Summary and Conclusions

6.1. Project Summary

TxDOT's Pavement Management Information System (PMIS) was recently replaced by Pavement Analyst (PA), a system for archiving, managing, and mapping data; reporting performance prediction; conducting optimization analysis for decision-making; producing short- and medium-term M&R plans; and many other related functions. Pavement performance models comprise a key component of PA; these models quantify pavement deterioration for the planned horizon and predict the effect of M&R actions on performance. The accurate prediction of pavement performance is important for efficient management of the transportation infrastructure. By reducing errors in predictive models of pavement deterioration, agencies can obtain significant savings through timely intervention and accurate planning. As part of this project, the authors reviewed the current performance models, calibrated them, and updated them in a manner compatible with their implementation into PA. Extensive data analysis was conducted by using traditional and advanced data analysis techniques. Specifically, the models developed addressed the following technical objectives:

- The existing models were calibrated correcting for biases and inefficiencies;
- The existing models were updated incorporating historical construction data;
- The models were updated to incorporate the effect of M&R activities; and
- Alternative models were proposed that are free of some of the limitations of the existing models but are simple and straightforward enough to incorporate into PA.

6.2. Updating and Calibrating Existing Models

For the first part of this project, the researchers updated and calibrated the pavement performance models for flexible pavements based on the current model specification. In the calibration process, nonlinear mixed effects models were used to estimate the optimum model coefficients. The estimation was conducted using the statistical program R language. Since the variable "Age" is not available in PA, it had to be estimated from the work history data that was available and covered a portion of the Texas network. However, the available data provided a reliable representation of the entire Texas highway network.

The following variables and levels were considered: 4 facility types, 4 traffic classes, 2 pavement types, and 5 different environmental conditions, for a total of 160 different models. Each variable combination could be subjected to any of 5 different treatment types—do-nothing (DN), preventive maintenance (PM), light rehabilitation (LRhb), medium rehabilitation (MRhb), and heavy rehabilitation (HRhb)—and 8 different distresses were considered, so ultimately 6,400 models were actually estimated. All models are presented in Appendix B.

Because of the many models and model parameters to be estimated and given the limited data available, the research team processed the data to enhance quality of the estimation. For all eight distress types, the models converged well and showed that the model coefficients are statistically significant and representative.

One of the key differences between the updated and calibrated models created in this project and the original models is the database used in the parameter estimation. The current models were estimated using actual work history data extracted from PA. These data were used to estimate the actual "Age" after initial construction of any type of treatment was applied. This process was challenging and time-consuming, and required several assumptions. However, the results ensured that the current calibration is based on the most recently updated data available.

Another important improvement for the newly updated and calibrated models is that the performance curves representing different treatment levels do not cross each other. The model coefficients were not constrained to achieve that; instead a probabilistic approach was employed to ensure this outcome. In the models developed as part of this project, the use of the parameter A ensures this non-crossing behavior between models. Because of the data limitations, the analysis generated 81 new models, and they were then expanded to the 160 variable combinations described above. A set of conservative criteria was used for assigning models.

6.3. Alternative Models

During the second part of this project, data were compiled from PA, Design and Construction Information System (DCIS), and the National Oceanic and Atmospheric Administration (NOAA) databases. Variables such as highway function, pavement type, traffic, and climate were extracted to develop deterioration models for various types of distresses. The alternative models are provided in Appendix A. The main findings and recommendations are listed below:

- The alternative models respect the s-shape as desired by TxDOT but have several advantages over the current model:
  - They have one more parameter and, therefore, are more flexible in terms of accommodating different deterioration rates,
  - It is defined at Age = 0 so the calculation of distress can be done at any time over the life of the pavement and the equation could be easily inversed to estimate age when distress levels are available.
  - The distress at Age = 0 could be set to zero or could be estimated from the data depending on TxDOT's ultimate goal.
- The alternative models can produce reasonable and satisfactory results and have a specification form that is more flexible, to capture different distress types. Before incorporating the treatment type information, the normalized errors of all the models were below 10 percent. However, after including the treatment type information, the normalized

errors of the most models dropped below 5 percent, with the exception of the model for shallow rutting.

- The effects of different treatment types, including DN, PM, LRhb, MRhb, and HRhb, are captured by the new models in a reasonable and logical manner. The deterioration curves for different treatment types do not cross each other. Further, the deterioration curves for different treatment types follow the correct order: the DN curve shows the highest deterioration rate, followed in order by PM, LRhb, MRhb, and HRhb.

- It should be noted that a compromised approach was used to develop the models to capture the so-called "rut buckets." It is the authors' opinion that the s-shape curve should be abandoned, and its use in modeling shallow, deep, and severe rutting levels discontinued. The s-shape does not reflect the inherent dependence among these rut buckets used by TxDOT. It is strongly recommended that a configuration other than the s-shape curve be adopted by TxDOT, given that these distresses, in principle, start at zero, reach a maximum level, and then become zero again. Perhaps a better formulation is that TxDOT replaces the buckets with a rutting progression model that captures surface rut depths.

- Since limited work history information about treatment type was acquired from TxDOT and these data were highly variable, a method to exploit the distribution of the change in the distress data was used to supplement the treatment type information. It is recommended that once more accurate and extensive treatment type information is collected, another update and calibration of these models should be performed.

- It is recommended that TxDOT incorporates the full work history data into PA instead of only the most recent projects. Moreover, it is suggested that the PA database should store the date of completion for maintenance or rehabilitation, and more precisely log the date of performance measurement.

- Further research is recommended to use advance data mining and statistical techniques to further populate missing work history by looking at the change in the distresses.

References

Aguiar-Moya, J.P. and J.A. Prozzi (2014), "Accounting for Censoring and Unobserved Heterogeneity in Pavement Cracking", Journal of Infrastructure Systems, American Society of Civil Engineering.

Buddhavarapu, P., Scott, J. and Prozzi, J.A (2016), "Modeling unobserved heterogeneity using finite mixture random parameters for spatially correlated discrete count data", Transportation Research Part B: Methodological.

Davidian, M., & Giltinan, D. M. (2003). Nonlinear models for repeated measurement data: An overview and update. Journal of Agriculture, Biological, and Environmental Statistics,8, 387–419.

Gharaibeh, Nasir & Freeman, Tom & Saliminejad, Siamak & Wimsatt, Andrew & Chang-Albitres, Carlos & Nazarian, Soheil & Abdallah, Imad & Weissmann, José & Weissmann, Angela & Papagiannakis, A. (2012). 0-6386-3: Evaluation and Development of Pavement Scores, Performance Models and Needs Estimates for the Texas DOT Pavement Management Information System. 10.13140/RG.2.1.4767.3442.

Hong, F., E. Perrone, M. Mikhail, and A. Eltahan (2017), Planning Pavement Maintenance and Rehabilitation Projects in the New Pavement Management System in Texas, TRB 96th Annual Meeting.

Hong, F. and J.A. Prozzi (2006), "Estimation of Pavement Performance Deterioration using Bayesian Approach," ASCE Journal of Infrastructure Systems.

Hong, F. and J.A. Prozzi (2010), "Roughness Model Accounting for Heterogeneity based on In-Service Pavement Performance Data," ASCE Journal of Transportation Engineering.

Hong, F and J. A. Prozzi (2013), "Pavement Deterioration Model incorporating Unobserved Heterogeneity for Optimal Life-Cycle Rehabilitation Policy", ASCE Journal of Infrastructure Systems

Hong, F and J. A. Prozzi (2014), "Using Count Data to Model Infrastructure Distress Initiation and Progression", ASCE Journal of Infrastructure Systems.

Lindstrom, M. J., & Bates, D. M. (1990). Nonlinear mixed effects models for repeated measures data. Biometrics,46, 673–687.

Madanat, S.M., J.A. Prozzi, and M. Han (2002), "Effect of Performance Model Accuracy on Optimal Pavement Design," Computer-Aided Civil and Infrastructure Engineering.

Pinheiro J, Bates D, DebRoy S, Sarkar D, R Core Team (2020). nlme: Linear and Nonlinear Mixed Effects Models. R package version 3.1-148, https://CRAN.R-project.org/package=nlme.

Prozzi, J.A. and S.M. Madanat (2000), "Using Duration Models to Analyze Experimental Pavement Failure Data," Transportation Research Record: Journal of the Transportation Research Board.

Prozzi, J.A. and S.M. Madanat (2003), "Incremental Nonlinear Model for Predicting Pavement Serviceability," ASCE Journal of Transportation Engineering.

Prozzi, J.A. and S.M. Madanat (2004), "Development of Pavement Performance Models by Combining Experimental and Field Data," ASCE Journal of Infrastructure Systems.

Prozzi, J.A. and F. Hong (2010), "Average Treatment Effect for Modeling Maintenance Work," ASCE Journal of Infrastructure Systems.

R Core Team (2019). R: A language and environment for statistical computing. R Foundation for Statistical Computing, Vienna, Austria. URL https://www.R-project.org/.

Srivastava, T. (2015), "Differences Between Machine Learning and Statistical Modelling", Analytics Vidhya, www.analyticsvidhya.com, 2015.

Stampley, B., Miller, B., Smith, R., and Scullion, T. (1995). Pavement Management Information System Concepts, Equations and Analysis Models. Texas Transportation Institute, Research Report TX 96/1989-1, August.

Appendix A. Alternative Model Parameters

The group assignment for different combinations of functional class, pavement type, and traffic level is presented in Table A.1:

Table A.1 Group Assignment for Alternative Models

HIGHWAY_FUN	PAV_TYPE	TRAFFIC	Group Assignment
IH	Thick	Heavy	1
		High	1
		Medium	1
		Low	1
	Thin	Heavy	2
		High	2
		Medium	2
		Low	3
US	Thick	Heavy	4
		High	5
		Medium	5
		Low	5
	Thin	Heavy	6
		High	7
		Medium	8
		Low	8
SH	Thick	Heavy	9
		High	10
		Medium	10
		Low	10
	Thin	Heavy	11
		High	12
		Medium	13
		Low	13
FM	Thick	Heavy	14
		High	14
		Medium	15
		Low	16
	Thin	Heavy	17
		High	17
		Medium	18
		Low	19

The model coefficients for different types of distresses are reported in Table A.2 to A.11:

Shallow Rut

Table A.2 Model Parameters for Shallow Rut

Variables	Parameter	Estimate
-	a_0	6.4655
Group_1	a_1	-2.7472
Group_2	a_2	-0.2988
Group_3	a_3	0.4601
Group_4	a_4	-233.5248
Group_5	a_5	-0.3311
Group_6	a_6	-0.1298
Group_7	a_7	0.3960
Group_8	a_8	0.3683
Group_9	a_9	-1.7825
Group_10	a_{10}	-1.4038
Group_11	a_{11}	-2.7500
Group_12	a_{12}	0.2652
Group_13	a_{13}	0.2403
Group_14	a_{14}	-1.6927
Group_15	a_{15}	-1.2770
Group_16	a_{16}	0.2980
Group_17	a_{17}	-0.1400
Group_19	a_{19}	0.1035
CL_WEST	γ_1	-0.6377
CL_EAST	γ_2	0.1288
CL_NORTH	γ_3	-0.3388
CL_SOUTH	γ_4	0.1508
-	η_0	28.7388
DN	η_1	11.6571
LR	η_2	-4.4788
MR	η_3	-11.0173
HR	η_4	-18.6942

Deep Rut

Table A.3 Model Parameters for Deep Rut

Variables	Parameter	Estimate
-	a_0	6.7073
Group_1	a_1	-17.9556
Group_2	a_2	-19.8835
Group_3	a_3	0.5647
Group_4	a_4	-18.0980
Group_5	a_5	-20.7947
Group_6	a_6	-16.1727
Group_7	a_7	-1.0460
Group_8	a_8	0.4297
Group_9	a_9	-17.6057
Group_10	a_{10}	-20.6107
Group_11	a_{11}	-15.8676
Group_12	a_{12}	-0.5563
Group_13	a_{13}	-15.8743
Group_14	a_{14}	-19.1104
Group_15	a_{15}	-0.9662
Group_16	a_{16}	-0.1103
Group_17	a_{17}	-0.6157
Group_19	a_{19}	0.2102
CL_WEST	γ_1	-0.0940
CL_EAST	γ_2	0.1113
CL_NORTH	γ_3	-0.0738
CL_SOUTH	γ_4	0.4664
-	η_0	6.1412
DN	η_1	2.9379
LR	η_2	-1.6197
MR	η_3	-3.2180
HR	η_4	-4.7294

Severe Rut

Table A.4 Model Parameters for Severe Rut

Variables	Parameter	Estimate
-	a_0	5.5690
Group_1	a_1	1.6307
Group_2	a_2	0.8723
Group_3	a_3	2.3273
Group_4	a_4	0.6917
Group_5	a_5	1.9914
Group_6	a_6	0.6178
Group_7	a_7	0.5443
Group_8	a_8	2.5259
Group_9	a_9	0.2538
Group_10	a_{10}	0.4300
Group_11	a_{11}	0.6142
Group_12	a_{12}	1.4918
Group_13	a_{13}	0.5700
Group_14	a_{14}	0.1337
Group_15	a_{15}	0.3332
Group_16	a_{16}	0.8183
Group_17	a_{17}	0.8838
Group_19	a_{19}	2.0420
CL_WEST	γ_1	-1.0729
CL_EAST	γ_2	-0.0084
CL_NORTH	γ_3	0.1478
CL_SOUTH	γ_4	0.4398
-	η_0	0.0349
DN	η_1	0.0214
LR	η_2	-0.0050
MR	η_3	-0.0243
HR	η_4	-0.0329

Failure Rut

Table A.5 Model Parameters for Failure Rut

Variables	Parameter	Estimate
-	a_0	-5.2985
Group_1	a_1	0.1419
Group_2	a_2	0.8070
Group_3	a_3	0.6692
Group_4	a_4	-0.4884
Group_5	a_5	-0.3972
Group_6	a_6	0.3319
Group_7	a_7	7.8746
Group_8	a_8	8.8252
Group_9	a_9	-0.5848
Group_10	a_{10}	-0.1962
Group_11	a_{11}	0.3281
Group_12	a_{12}	-0.1042
Group_13	a_{13}	0.2540
Group_14	a_{14}	-0.9232
Group_15	a_{15}	-0.5042
Group_16	a_{16}	0.7222
Group_17	a_{17}	-0.3039
Group_19	a_{19}	-1.4057
CL_WEST	γ_1	-2.2843
CL_EAST	γ_2	4.3647
CL_NORTH	γ_3	4.6617
CL_SOUTH	γ_4	-0.6728
-	η_0	0.0009
DN	η_1	0.0000
LR	η_2	0.0000
MR	η_3	0.0000
HR	η_4	0.0000

Patching

Table A.6 Model Parameters for Patching

Variables	Parameter	Estimate
-	a_0	7.7809
Group_1	a_1	-1.4047
Group_2	a_2	-0.9177
Group_3	a_3	-0.2984
Group_4	a_4	-8.9754
Group_5	a_5	-0.7117
Group_6	a_6	-9.2416
Group_7	a_7	-0.4111
Group_8	a_8	-0.1127
Group_9	a_9	-0.2133
Group_10	a_{10}	-0.5718
Group_11	a_{11}	-0.6474
Group_12	a_{12}	-0.1301
Group_13	a_{13}	-0.1379
Group_14	a_{14}	-0.9775
Group_15	a_{15}	-0.0512
Group_16	a_{16}	-0.1678
Group_17	a_{17}	-0.1909
Group_19	a_{19}	-0.0325
CL_WEST	γ_1	-0.3285
CL_EAST	γ_2	-0.1482
CL_NORTH	γ_3	0.0637
CL_SOUTH	γ_4	0.2969
-	η_0	0.1948
DN	η_1	0.1383
LR	η_2	-0.0394
MR	η_3	-0.0902
HR	η_4	-0.1213

Failures

Table A.7 Model Parameters for Failures

Variables	Parameter	Estimate
-	a_0	7.1866
Group_1	a_1	-14.3153
Group_2	a_2	-13.2899
Group_3	a_3	0.0509
Group_4	a_4	-14.4818
Group_5	a_5	-14.4904
Group_6	a_6	-13.6122
Group_7	a_7	-13.6079
Group_8	a_8	-11.3018
Group_9	a_9	-14.5667
Group_10	a_{10}	-14.0658
Group_11	a_{11}	-0.3501
Group_12	a_{12}	-0.6533
Group_13	a_{13}	-12.8288
Group_14	a_{14}	-14.7256
Group_15	a_{15}	-13.3897
Group_16	a_{16}	-0.3669
Group_17	a_{17}	-0.0588
Group_19	a_{19}	0.0541
CL_WEST	γ_1	0.2670
CL_EAST	γ_2	-0.1433
CL_NORTH	γ_3	0.0627
CL_SOUTH	γ_4	0.6546
-	η_0	1.0668
DN	η_1	0.4367
LR	η_2	-0.1127
MR	η_3	-0.4920
HR	η_4	-0.7613

Block Cracking

Table A.8 Model Parameters for Block Cracking

Variables	Parameter	Estimate
-	a_0	2.3886
Group_1	a_1	-2.3508
Group_2	a_2	5.6864
Group_3	a_3	-0.8571
Group_4	a_4	5.3634
Group_5	a_5	4.9388
Group_6	a_6	-1.7336
Group_7	a_7	-1.1537
Group_8	a_8	0.1596
Group_9	a_9	-1.3324
Group_10	a_{10}	5.9597
Group_11	a_{11}	4.9679
Group_12	a_{12}	5.9188
Group_13	a_{13}	-1.0381
Group_14	a_{14}	5.2167
Group_15	a_{15}	-1.5319
Group_16	a_{16}	5.4018
Group_17	a_{17}	4.8738
Group_19	a_{19}	5.0709
CL_WEST	γ_1	-6.6382
CL_EAST	γ_2	-1.1002
CL_NORTH	γ_3	-0.0744
CL_SOUTH	γ_4	-1.1519
-	η_0	0.0041
DN	η_1	0.0016
LR	η_2	-0.0003
MR	η_3	-0.0035
HR	η_4	-0.0037

Alligator Cracking

Table A.9 Model Parameters for Alligator Cracking

Variables	Parameter	Estimate
-	a_0	7.5005
Group_1	a_1	0.1616
Group_2	a_2	0.4751
Group_3	a_3	0.3236
Group_4	a_4	0.2705
Group_5	a_5	0.0658
Group_6	a_6	-0.0448
Group_7	a_7	-0.0262
Group_8	a_8	0.0201
Group_9	a_9	0.3049
Group_10	a_{10}	0.2571
Group_11	a_{11}	0.1323
Group_12	a_{12}	0.3802
Group_13	a_{13}	-0.2345
Group_14	a_{14}	0.4433
Group_15	a_{15}	0.4437
Group_16	a_{16}	0.3165
Group_17	a_{17}	0.2075
Group_19	a_{19}	-0.1356
CL_WEST	γ_1	-0.0822
CL_EAST	γ_2	0.1859
CL_NORTH	γ_3	0.2979
CL_SOUTH	γ_4	0.0642
-	η_0	0.1179
DN	η_1	0.0438
LR	η_2	-0.0237
MR	η_3	-0.0483
HR	η_4	-0.0736

Longitudinal Cracking

Table A.10 Model Parameters for Longitudinal Cracking

Variables	Parameter	Estimate
-	a_0	6.8769
Group_1	a_1	0.3401
Group_2	a_2	0.3692
Group_3	a_3	0.3794
Group_4	a_4	0.5615
Group_5	a_5	0.4060
Group_6	a_6	-1.4520
Group_7	a_7	0.4794
Group_8	a_8	0.0844
Group_9	a_9	0.4639
Group_10	a_{10}	0.4658
Group_11	a_{11}	0.2963
Group_12	a_{12}	0.0801
Group_13	a_{13}	0.1242
Group_14	a_{14}	0.6214
Group_15	a_{15}	0.6769
Group_16	a_{16}	0.6247
Group_17	a_{17}	0.1833
Group_19	a_{19}	0.1408
CL_WEST	γ_1	-0.4552
CL_EAST	γ_2	-0.0471
CL_NORTH	γ_3	-0.0148
CL_SOUTH	γ_4	-0.0363
-	η_0	7.4525
DN	η_1	2.8388
LR	η_2	-1.3235
MR	η_3	-2.8318
HR	η_4	-4.3990

Transverse Cracking

Table A.11 Model Parameters for Transverse Cracking

Variables	Parameter	Estimate
-	a_0	7.0947
Group_1	a_1	0.3528
Group_2	a_2	0.5594
Group_3	a_3	0.1646
Group_4	a_4	-0.0531
Group_5	a_5	0.3646
Group_6	a_6	-2.3534
Group_7	a_7	0.0210
Group_8	a_8	-0.0229
Group_9	a_9	0.5313
Group_10	a_{10}	0.5626
Group_11	a_{11}	0.1783
Group_12	a_{12}	0.2053
Group_13	a_{13}	-0.2211
Group_14	a_{14}	-0.2738
Group_15	a_{15}	-18.4044
Group_16	a_{16}	0.4374
Group_17	a_{17}	0.1947
Group_19	a_{19}	-0.0982
CL_WEST	γ_1	-0.2466
CL_EAST	γ_2	0.1009
CL_NORTH	γ_3	0.4434
CL_SOUTH	γ_4	0.0223
-	η_0	1.2442
DN	η_1	0.4915
LR	η_2	-0.1493
MR	η_3	-0.4490
HR	η_4	-0.8766

Appendix B. Calibration of Current Models

Table B.1: Shallow Rut Model Coefficients for DN and IH

group	distress	treat_lvl	highway_fun	pavement_typ	traffic_cls	climate_zone	alpha	A_star	beta_star
1	rut_auto_shallow_av_pct	DN	IH	thick	low	central	63	136.5795	0.3490
2						east	63	136.5795	0.3102
3						north	63	136.5795	0.3490
4						south	63	136.5795	0.3153
5						west	63	136.5795	0.3613
6					medium	central	63	136.5795	0.3490
7						east	63	136.5795	0.3102
8						north	63	136.5795	0.3490
9						south	63	136.5795	0.3153
10						west	63	136.5795	0.3613
11					high	central	63	136.5795	0.3490
12						east	63	136.5795	0.3102
13						north	63	136.5795	0.3490
14						south	63	136.5795	0.3153
15						west	63	136.5795	0.3613
16					heavy	central	63	136.5795	0.3490
17						east	63	136.5795	0.3102
18						north	63	136.5795	0.3490
19						south	63	136.5795	0.3153
20						west	63	136.5795	0.3613
21				thin	low	central	63	136.5795	0.1983
22						east	63	136.5795	0.2101
23						north	63	136.5795	0.1983
24						south	63	136.5795	0.0975
25						west	63	136.5795	0.1983
26					medium	central	63	136.5795	0.3148
27						east	63	136.5795	0.3148
28						north	63	136.5795	0.3148
29						south	63	136.5795	0.3148
30						west	63	136.5795	0.2681
31					high	central	63	136.5795	0.3148
32						east	63	136.5795	0.3148
33						north	63	136.5795	0.3148
34						south	63	136.5795	0.3148
35						west	63	136.5795	0.2681
36					heavy	central	63	136.5795	0.3148
37						east	63	136.5795	0.3148
38						north	63	136.5795	0.3148
39						south	63	136.5795	0.3148
40						west	63	136.5795	0.2681

Table B.2: Shallow Rut Model Coefficients for DN and US

group	distress	treat_lvl	highway_fun	pavement_typ	traffic_cls	climate_zone	alpha	A_star	beta_star
41	rut_auto_shallow_av_pct	DN	US	thick	low	central	63	136.5795	0.3174
42						east	63	136.5795	0.2340
43						north	63	136.5795	0.3351
44						south	63	136.5795	0.2901
45						west	63	136.5795	0.3682
46					medium	central	63	136.5795	0.3174
47						east	63	136.5795	0.2340
48						north	63	136.5795	0.3351
49						south	63	136.5795	0.2901
50						west	63	136.5795	0.3682
51					high	central	63	136.5795	0.3174
52						east	63	136.5795	0.2340
53						north	63	136.5795	0.3351
54						south	63	136.5795	0.2901
55						west	63	136.5795	0.3682
56					heavy	central	63	136.5795	0.3629
57						east	63	136.5795	0.2927
58						north	63	136.5795	0.2481
59						south	63	136.5795	0.3629
60						west	63	136.5795	0.2599
61				thin	low	central	63	136.5795	0.1188
62						east	63	136.5795	-0.0456
63						north	63	136.5795	0.1188
64						south	63	136.5795	0.1188
65						west	63	136.5795	0.1717
66					medium	central	63	136.5795	0.1188
67						east	63	136.5795	0.1188
68						north	63	136.5795	0.1188
69						south	63	136.5795	0.1188
70						west	63	136.5795	0.1717
71					high	central	63	136.5795	0.1234
72						east	63	136.5795	0.2003
73						north	63	136.5795	0.4368
74						south	63	136.5795	0.3435
75						west	63	136.5795	0.4286
76					heavy	central	63	136.5795	0.2492
77						east	63	136.5795	0.1534
78						north	63	136.5795	0.1651
79						south	63	136.5795	0.1744
80						west	63	136.5795	0.2492

Table B.3: Shallow Rut Model Coefficients for DN and SH

group	distress	treat_lvl	highway_fun	pavement_typ	traffic_cls	climate_zone	alpha	A_star	beta_star
81	rut_auto_shallow_av_pct	DN	SH	thick	low	central	63	136.5795	0.2740
82						east	63	136.5795	0.2309
83						north	63	136.5795	0.3691
84						south	63	136.5795	0.2189
85						west	63	136.5795	0.3884
86					medium	central	63	136.5795	0.2740
87						east	63	136.5795	0.2309
88						north	63	136.5795	0.3691
89						south	63	136.5795	0.2189
90						west	63	136.5795	0.3884
91					high	central	63	136.5795	0.2740
92						east	63	136.5795	0.2309
93						north	63	136.5795	0.3691
94						south	63	136.5795	0.2189
95						west	63	136.5795	0.3884
96					heavy	central	63	136.5795	0.2282
97						east	63	136.5795	0.3116
98						north	63	136.5795	0.2282
99						south	63	136.5795	0.2683
100						west	63	136.5795	0.3967
101				thin	low	central	63	136.5795	0.3067
102						east	63	136.5795	0.1599
103						north	63	136.5795	0.2356
104						south	63	136.5795	0.1722
105						west	63	136.5795	0.2201
106					medium	central	63	136.5795	0.3067
107						east	63	136.5795	0.1599
108						north	63	136.5795	0.2356
109						south	63	136.5795	0.1722
110						west	63	136.5795	0.2201
111					high	central	63	136.5795	0.2451
112						east	63	136.5795	0.1882
113						north	63	136.5795	0.2457
114						south	63	136.5795	0.3068
115						west	63	136.5795	0.2385
116					heavy	central	63	136.5795	0.3088
117						east	63	136.5795	0.3400
118						north	63	136.5795	0.3088
119						south	63	136.5795	0.2781
120						west	63	136.5795	0.2235

Table B.4: Shallow Rut Model Coefficients for DN and FM

group	distress	treat_lvl	highway_fun	pavement_typ	traffic_cls	climate_zone	alpha	A_star	beta_star
121	rut_auto_shallow_av_pct	DN	FM	thick	low	central	63	136.5795	0.1552
122	rut_auto_shallow_av_pct	DN	FM	thick	low	east	63	136.5795	0.1584
123	rut_auto_shallow_av_pct	DN	FM	thick	low	north	63	136.5795	0.1552
124	rut_auto_shallow_av_pct	DN	FM	thick	low	south	63	136.5795	0.1990
125	rut_auto_shallow_av_pct	DN	FM	thick	low	west	63	136.5795	0.1552
126	rut_auto_shallow_av_pct	DN	FM	thick	medium	central	63	136.5795	0.1648
127	rut_auto_shallow_av_pct	DN	FM	thick	medium	east	63	136.5795	0.4013
128	rut_auto_shallow_av_pct	DN	FM	thick	medium	north	63	136.5795	0.0946
129	rut_auto_shallow_av_pct	DN	FM	thick	medium	south	63	136.5795	0.1326
130	rut_auto_shallow_av_pct	DN	FM	thick	medium	west	63	136.5795	0.1648
131	rut_auto_shallow_av_pct	DN	FM	thick	high	central	63	136.5795	0.2286
132	rut_auto_shallow_av_pct	DN	FM	thick	high	east	63	136.5795	0.3862
133	rut_auto_shallow_av_pct	DN	FM	thick	high	north	63	136.5795	0.3126
134	rut_auto_shallow_av_pct	DN	FM	thick	high	south	63	136.5795	0.1942
135	rut_auto_shallow_av_pct	DN	FM	thick	high	west	63	136.5795	0.2867
136	rut_auto_shallow_av_pct	DN	FM	thick	heavy	central	63	136.5795	0.2286
137	rut_auto_shallow_av_pct	DN	FM	thick	heavy	east	63	136.5795	0.3862
138	rut_auto_shallow_av_pct	DN	FM	thick	heavy	north	63	136.5795	0.3126
139	rut_auto_shallow_av_pct	DN	FM	thick	heavy	south	63	136.5795	0.1942
140	rut_auto_shallow_av_pct	DN	FM	thick	heavy	west	63	136.5795	0.2867
141	rut_auto_shallow_av_pct	DN	FM	thin	low	central	63	136.5795	0.1721
142	rut_auto_shallow_av_pct	DN	FM	thin	low	east	63	136.5795	0.1754
143	rut_auto_shallow_av_pct	DN	FM	thin	low	north	63	136.5795	0.2147
144	rut_auto_shallow_av_pct	DN	FM	thin	low	south	63	136.5795	0.1473
145	rut_auto_shallow_av_pct	DN	FM	thin	low	west	63	136.5795	0.2245
146	rut_auto_shallow_av_pct	DN	FM	thin	medium	central	63	136.5795	0.2088
147	rut_auto_shallow_av_pct	DN	FM	thin	medium	east	63	136.5795	0.1948
148	rut_auto_shallow_av_pct	DN	FM	thin	medium	north	63	136.5795	0.1494
149	rut_auto_shallow_av_pct	DN	FM	thin	medium	south	63	136.5795	0.2163
150	rut_auto_shallow_av_pct	DN	FM	thin	medium	west	63	136.5795	0.2301
151	rut_auto_shallow_av_pct	DN	FM	thin	high	central	63	136.5795	0.2687
152	rut_auto_shallow_av_pct	DN	FM	thin	high	east	63	136.5795	0.1647
153	rut_auto_shallow_av_pct	DN	FM	thin	high	north	63	136.5795	0.0308
154	rut_auto_shallow_av_pct	DN	FM	thin	high	south	63	136.5795	0.2115
155	rut_auto_shallow_av_pct	DN	FM	thin	high	west	63	136.5795	0.3790
156	rut_auto_shallow_av_pct	DN	FM	thin	heavy	central	63	136.5795	0.2687
157	rut_auto_shallow_av_pct	DN	FM	thin	heavy	east	63	136.5795	0.1647
158	rut_auto_shallow_av_pct	DN	FM	thin	heavy	north	63	136.5795	0.0308
159	rut_auto_shallow_av_pct	DN	FM	thin	heavy	south	63	136.5795	0.2115
160	rut_auto_shallow_av_pct	DN	FM	thin	heavy	west	63	136.5795	0.3790

Table B.5: Shallow Rut Model Coefficients for PM and IH

group	distress	treat_lvl	highway_fun	pavement_typ	traffic_cls	climate_zone	alpha	A_star	beta_star
1	rut_auto_shallow_av_pct	PM	IH	thick	low	central	63	200	0.3490
2						east	63	200	0.3102
3						north	63	200	0.3490
4						south	63	200	0.3153
5						west	63	200	0.3613
6					medium	central	63	200	0.3490
7						east	63	200	0.3102
8						north	63	200	0.3490
9						south	63	200	0.3153
10						west	63	200	0.3613
11					high	central	63	200	0.3490
12						east	63	200	0.3102
13						north	63	200	0.3490
14						south	63	200	0.3153
15						west	63	200	0.3613
16					heavy	central	63	200	0.3490
17						east	63	200	0.3102
18						north	63	200	0.3490
19						south	63	200	0.3153
20						west	63	200	0.3613
21				thin	low	central	63	200	0.1983
22						east	63	200	0.2101
23						north	63	200	0.1983
24						south	63	200	0.0975
25						west	63	200	0.1983
26					medium	central	63	200	0.3148
27						east	63	200	0.3148
28						north	63	200	0.3148
29						south	63	200	0.3148
30						west	63	200	0.2681
31					high	central	63	200	0.3148
32						east	63	200	0.3148
33						north	63	200	0.3148
34						south	63	200	0.3148
35						west	63	200	0.2681
36					heavy	central	63	200	0.3148
37						east	63	200	0.3148
38						north	63	200	0.3148
39						south	63	200	0.3148
40						west	63	200	0.2681

Table B.6: Shallow Rut Model Coefficients for PM and US

group	distress	treat_lvl	highway_fun	pavement_typ	traffic_cls	climate_zone	alpha	A_star	beta_star
41	rut_auto_shallow_av_pct	PM	US	thick	low	central	63	200	0.3174
42						east	63	200	0.2340
43						north	63	200	0.3351
44						south	63	200	0.2901
45						west	63	200	0.3682
46					medium	central	63	200	0.3174
47						east	63	200	0.2340
48						north	63	200	0.3351
49						south	63	200	0.2901
50						west	63	200	0.3682
51					high	central	63	200	0.3174
52						east	63	200	0.2340
53						north	63	200	0.3351
54						south	63	200	0.2901
55						west	63	200	0.3682
56					heavy	central	63	200	0.3629
57						east	63	200	0.2927
58						north	63	200	0.2481
59						south	63	200	0.3629
60						west	63	200	0.2599
61				thin	low	central	63	200	0.1188
62						east	63	200	-0.0456
63						north	63	200	0.1188
64						south	63	200	0.1188
65						west	63	200	0.1717
66					medium	central	63	200	0.1188
67						east	63	200	0.1188
68						north	63	200	0.1188
69						south	63	200	0.1188
70						west	63	200	0.1717
71					high	central	63	200	0.1234
72						east	63	200	0.2003
73						north	63	200	0.4368
74						south	63	200	0.3435
75						west	63	200	0.4286
76					heavy	central	63	200	0.2492
77						east	63	200	0.1534
78						north	63	200	0.1651
79						south	63	200	0.1744
80						west	63	200	0.2492

Table B.7: Shallow Rut Model Coefficients for PM and SH

group	distress	treat_lvl	highway_fun	pavement_typ	traffic_cls	climate_zone	alpha	A_star	beta_star
81	rut_auto_shallow_av_pct	PM	SH	thick	low	central	63	200	0.2740
82	rut_auto_shallow_av_pct	PM	SH	thick	low	east	63	200	0.2309
83	rut_auto_shallow_av_pct	PM	SH	thick	low	north	63	200	0.3691
84	rut_auto_shallow_av_pct	PM	SH	thick	low	south	63	200	0.2189
85	rut_auto_shallow_av_pct	PM	SH	thick	low	west	63	200	0.3884
86	rut_auto_shallow_av_pct	PM	SH	thick	medium	central	63	200	0.2740
87	rut_auto_shallow_av_pct	PM	SH	thick	medium	east	63	200	0.2309
88	rut_auto_shallow_av_pct	PM	SH	thick	medium	north	63	200	0.3691
89	rut_auto_shallow_av_pct	PM	SH	thick	medium	south	63	200	0.2189
90	rut_auto_shallow_av_pct	PM	SH	thick	medium	west	63	200	0.3884
91	rut_auto_shallow_av_pct	PM	SH	thick	high	central	63	200	0.2740
92	rut_auto_shallow_av_pct	PM	SH	thick	high	east	63	200	0.2309
93	rut_auto_shallow_av_pct	PM	SH	thick	high	north	63	200	0.3691
94	rut_auto_shallow_av_pct	PM	SH	thick	high	south	63	200	0.2189
95	rut_auto_shallow_av_pct	PM	SH	thick	high	west	63	200	0.3884
96	rut_auto_shallow_av_pct	PM	SH	thick	heavy	central	63	200	0.2282
97	rut_auto_shallow_av_pct	PM	SH	thick	heavy	east	63	200	0.3116
98	rut_auto_shallow_av_pct	PM	SH	thick	heavy	north	63	200	0.2282
99	rut_auto_shallow_av_pct	PM	SH	thick	heavy	south	63	200	0.2683
100	rut_auto_shallow_av_pct	PM	SH	thick	heavy	west	63	200	0.3967
101	rut_auto_shallow_av_pct	PM	SH	thin	low	central	63	200	0.3067
102	rut_auto_shallow_av_pct	PM	SH	thin	low	east	63	200	0.1599
103	rut_auto_shallow_av_pct	PM	SH	thin	low	north	63	200	0.2356
104	rut_auto_shallow_av_pct	PM	SH	thin	low	south	63	200	0.1722
105	rut_auto_shallow_av_pct	PM	SH	thin	low	west	63	200	0.2201
106	rut_auto_shallow_av_pct	PM	SH	thin	medium	central	63	200	0.3067
107	rut_auto_shallow_av_pct	PM	SH	thin	medium	east	63	200	0.1599
108	rut_auto_shallow_av_pct	PM	SH	thin	medium	north	63	200	0.2356
109	rut_auto_shallow_av_pct	PM	SH	thin	medium	south	63	200	0.1722
110	rut_auto_shallow_av_pct	PM	SH	thin	medium	west	63	200	0.2201
111	rut_auto_shallow_av_pct	PM	SH	thin	high	central	63	200	0.2451
112	rut_auto_shallow_av_pct	PM	SH	thin	high	east	63	200	0.1882
113	rut_auto_shallow_av_pct	PM	SH	thin	high	north	63	200	0.2457
114	rut_auto_shallow_av_pct	PM	SH	thin	high	south	63	200	0.3068
115	rut_auto_shallow_av_pct	PM	SH	thin	high	west	63	200	0.2385
116	rut_auto_shallow_av_pct	PM	SH	thin	heavy	central	63	200	0.3088
117	rut_auto_shallow_av_pct	PM	SH	thin	heavy	east	63	200	0.3400
118	rut_auto_shallow_av_pct	PM	SH	thin	heavy	north	63	200	0.3088
119	rut_auto_shallow_av_pct	PM	SH	thin	heavy	south	63	200	0.2781
120	rut_auto_shallow_av_pct	PM	SH	thin	heavy	west	63	200	0.2235

Table B.8: Shallow Rut Model Coefficients for PM and FM

group	distress	treat_lvl	highway_fun	pavement_typ	traffic_cls	climate_zone	alpha	A_star	beta_star
121	rut_auto_shallow_av_pct	PM	FM	thick	low	central	63	200	0.1552
122						east	63	200	0.1584
123						north	63	200	0.1552
124						south	63	200	0.1990
125						west	63	200	0.1552
126					medium	central	63	200	0.1648
127						east	63	200	0.4013
128						north	63	200	0.0946
129						south	63	200	0.1326
130						west	63	200	0.1648
131					high	central	63	200	0.2286
132						east	63	200	0.3862
133						north	63	200	0.3126
134						south	63	200	0.1942
135						west	63	200	0.2867
136					heavy	central	63	200	0.2286
137						east	63	200	0.3862
138						north	63	200	0.3126
139						south	63	200	0.1942
140						west	63	200	0.2867
141				thin	low	central	63	200	0.1721
142						east	63	200	0.1754
143						north	63	200	0.2147
144						south	63	200	0.1473
145						west	63	200	0.2245
146					medium	central	63	200	0.2088
147						east	63	200	0.1948
148						north	63	200	0.1494
149						south	63	200	0.2163
150						west	63	200	0.2301
151					high	central	63	200	0.2687
152						east	63	200	0.1647
153						north	63	200	0.0308
154						south	63	200	0.2115
155						west	63	200	0.3790
156					heavy	central	63	200	0.2687
157						east	63	200	0.1647
158						north	63	200	0.0308
159						south	63	200	0.2115
160						west	63	200	0.3790

Table B.9: Shallow Rut Model Coefficients for LR and IH

group	distress	treat_lvl	highway_fun	pavement_typ	traffic_cls	climate_zone	alpha	A_star	beta_star
1	rut_auto_shallow_av_pct	LR	IH	thick	low	central	63	250	0.3490
2						east	63	250	0.3102
3						north	63	250	0.3490
4						south	63	250	0.3153
5						west	63	250	0.3613
6					medium	central	63	250	0.3490
7						east	63	250	0.3102
8						north	63	250	0.3490
9						south	63	250	0.3153
10						west	63	250	0.3613
11					high	central	63	250	0.3490
12						east	63	250	0.3102
13						north	63	250	0.3490
14						south	63	250	0.3153
15						west	63	250	0.3613
16					heavy	central	63	250	0.3490
17						east	63	250	0.3102
18						north	63	250	0.3490
19						south	63	250	0.3153
20						west	63	250	0.3613
21				thin	low	central	63	250	0.1983
22						east	63	250	0.2101
23						north	63	250	0.1983
24						south	63	250	0.0975
25						west	63	250	0.1983
26					medium	central	63	250	0.3148
27						east	63	250	0.3148
28						north	63	250	0.3148
29						south	63	250	0.3148
30						west	63	250	0.2681
31					high	central	63	250	0.3148
32						east	63	250	0.3148
33						north	63	250	0.3148
34						south	63	250	0.3148
35						west	63	250	0.2681
36					heavy	central	63	250	0.3148
37						east	63	250	0.3148
38						north	63	250	0.3148
39						south	63	250	0.3148
40						west	63	250	0.2681

Table B.10: Shallow Rut Model Coefficients for LR and US

group	distress	treat_lvl	highway_fun	pavement_typ	traffic_cls	climate_zone	alpha	A_star	beta_star
41	rut_auto_shallow_av_pct	LR	US	thick	low	central	63	250	0.3174
42						east	63	250	0.2340
43						north	63	250	0.3351
44						south	63	250	0.2901
45						west	63	250	0.3682
46					medium	central	63	250	0.3174
47						east	63	250	0.2340
48						north	63	250	0.3351
49						south	63	250	0.2901
50						west	63	250	0.3682
51					high	central	63	250	0.3174
52						east	63	250	0.2340
53						north	63	250	0.3351
54						south	63	250	0.2901
55						west	63	250	0.3682
56					heavy	central	63	250	0.3629
57						east	63	250	0.2927
58						north	63	250	0.2481
59						south	63	250	0.3629
60						west	63	250	0.2599
61				thin	low	central	63	250	0.1188
62						east	63	250	-0.0456
63						north	63	250	0.1188
64						south	63	250	0.1188
65						west	63	250	0.1717
66					medium	central	63	250	0.1188
67						east	63	250	0.1188
68						north	63	250	0.1188
69						south	63	250	0.1188
70						west	63	250	0.1717
71					high	central	63	250	0.1234
72						east	63	250	0.2003
73						north	63	250	0.4368
74						south	63	250	0.3435
75						west	63	250	0.4286
76					heavy	central	63	250	0.2492
77						east	63	250	0.1534
78						north	63	250	0.1651
79						south	63	250	0.1744
80						west	63	250	0.2492

Table B.11: Shallow Rut Model Coefficients for LR and SH

group	distress	treat_lvl	highway_fun	pavement_typ	traffic_cls	climate_zone	alpha	A_star	beta_star
81	rut_auto_shallow_av_pct	LR	SH	thick	low	central	63	250	0.2740
82	rut_auto_shallow_av_pct	LR	SH	thick	low	east	63	250	0.2309
83	rut_auto_shallow_av_pct	LR	SH	thick	low	north	63	250	0.3691
84	rut_auto_shallow_av_pct	LR	SH	thick	low	south	63	250	0.2189
85	rut_auto_shallow_av_pct	LR	SH	thick	low	west	63	250	0.3884
86	rut_auto_shallow_av_pct	LR	SH	thick	medium	central	63	250	0.2740
87	rut_auto_shallow_av_pct	LR	SH	thick	medium	east	63	250	0.2309
88	rut_auto_shallow_av_pct	LR	SH	thick	medium	north	63	250	0.3691
89	rut_auto_shallow_av_pct	LR	SH	thick	medium	south	63	250	0.2189
90	rut_auto_shallow_av_pct	LR	SH	thick	medium	west	63	250	0.3884
91	rut_auto_shallow_av_pct	LR	SH	thick	high	central	63	250	0.2740
92	rut_auto_shallow_av_pct	LR	SH	thick	high	east	63	250	0.2309
93	rut_auto_shallow_av_pct	LR	SH	thick	high	north	63	250	0.3691
94	rut_auto_shallow_av_pct	LR	SH	thick	high	south	63	250	0.2189
95	rut_auto_shallow_av_pct	LR	SH	thick	high	west	63	250	0.3884
96	rut_auto_shallow_av_pct	LR	SH	thick	heavy	central	63	250	0.2282
97	rut_auto_shallow_av_pct	LR	SH	thick	heavy	east	63	250	0.3116
98	rut_auto_shallow_av_pct	LR	SH	thick	heavy	north	63	250	0.2282
99	rut_auto_shallow_av_pct	LR	SH	thick	heavy	south	63	250	0.2683
100	rut_auto_shallow_av_pct	LR	SH	thick	heavy	west	63	250	0.3967
101	rut_auto_shallow_av_pct	LR	SH	thin	low	central	63	250	0.3067
102	rut_auto_shallow_av_pct	LR	SH	thin	low	east	63	250	0.1599
103	rut_auto_shallow_av_pct	LR	SH	thin	low	north	63	250	0.2356
104	rut_auto_shallow_av_pct	LR	SH	thin	low	south	63	250	0.1722
105	rut_auto_shallow_av_pct	LR	SH	thin	low	west	63	250	0.2201
106	rut_auto_shallow_av_pct	LR	SH	thin	medium	central	63	250	0.3067
107	rut_auto_shallow_av_pct	LR	SH	thin	medium	east	63	250	0.1599
108	rut_auto_shallow_av_pct	LR	SH	thin	medium	north	63	250	0.2356
109	rut_auto_shallow_av_pct	LR	SH	thin	medium	south	63	250	0.1722
110	rut_auto_shallow_av_pct	LR	SH	thin	medium	west	63	250	0.2201
111	rut_auto_shallow_av_pct	LR	SH	thin	high	central	63	250	0.2451
112	rut_auto_shallow_av_pct	LR	SH	thin	high	east	63	250	0.1882
113	rut_auto_shallow_av_pct	LR	SH	thin	high	north	63	250	0.2457
114	rut_auto_shallow_av_pct	LR	SH	thin	high	south	63	250	0.3068
115	rut_auto_shallow_av_pct	LR	SH	thin	high	west	63	250	0.2385
116	rut_auto_shallow_av_pct	LR	SH	thin	heavy	central	63	250	0.3088
117	rut_auto_shallow_av_pct	LR	SH	thin	heavy	east	63	250	0.3400
118	rut_auto_shallow_av_pct	LR	SH	thin	heavy	north	63	250	0.3088
119	rut_auto_shallow_av_pct	LR	SH	thin	heavy	south	63	250	0.2781
120	rut_auto_shallow_av_pct	LR	SH	thin	heavy	west	63	250	0.2235

Table B.12: Shallow Rut Model Coefficients for LR and FM

group	distress	treat_lvl	highway_fun	pavement_typ	traffic_cls	climate_zone	alpha	A_star	beta_star
121	rut_auto_shallow_av_pct	LR	FM	thick	low	central	63	250	0.1552
122						east	63	250	0.1584
123						north	63	250	0.1552
124						south	63	250	0.1990
125						west	63	250	0.1552
126					medium	central	63	250	0.1648
127						east	63	250	0.4013
128						north	63	250	0.0946
129						south	63	250	0.1326
130						west	63	250	0.1648
131					high	central	63	250	0.2286
132						east	63	250	0.3862
133						north	63	250	0.3126
134						south	63	250	0.1942
135						west	63	250	0.2867
136					heavy	central	63	250	0.2286
137						east	63	250	0.3862
138						north	63	250	0.3126
139						south	63	250	0.1942
140						west	63	250	0.2867
141				thin	low	central	63	250	0.1721
142						east	63	250	0.1754
143						north	63	250	0.2147
144						south	63	250	0.1473
145						west	63	250	0.2245
146					medium	central	63	250	0.2088
147						east	63	250	0.1948
148						north	63	250	0.1494
149						south	63	250	0.2163
150						west	63	250	0.2301
151					high	central	63	250	0.2687
152						east	63	250	0.1647
153						north	63	250	0.0308
154						south	63	250	0.2115
155						west	63	250	0.3790
156					heavy	central	63	250	0.2687
157						east	63	250	0.1647
158						north	63	250	0.0308
159						south	63	250	0.2115
160						west	63	250	0.3790

Table B.13: Shallow Rut Model Coefficients for MR and IH

group	distress	treat_lvl	highway_fun	pavement_typ	traffic_cls	climate_zone	alpha	A_star	beta_star
1	rut_auto_shallow_av_pct	MR	IH	thick	low	central	63	400	0.3490
2						east	63	400	0.3102
3						north	63	400	0.3490
4						south	63	400	0.3153
5						west	63	400	0.3613
6					medium	central	63	400	0.3490
7						east	63	400	0.3102
8						north	63	400	0.3490
9						south	63	400	0.3153
10						west	63	400	0.3613
11					high	central	63	400	0.3490
12						east	63	400	0.3102
13						north	63	400	0.3490
14						south	63	400	0.3153
15						west	63	400	0.3613
16					heavy	central	63	400	0.3490
17						east	63	400	0.3102
18						north	63	400	0.3490
19						south	63	400	0.3153
20						west	63	400	0.3613
21				thin	low	central	63	400	0.1983
22						east	63	400	0.2101
23						north	63	400	0.1983
24						south	63	400	0.0975
25						west	63	400	0.1983
26					medium	central	63	400	0.3148
27						east	63	400	0.3148
28						north	63	400	0.3148
29						south	63	400	0.3148
30						west	63	400	0.2681
31					high	central	63	400	0.3148
32						east	63	400	0.3148
33						north	63	400	0.3148
34						south	63	400	0.3148
35						west	63	400	0.2681
36					heavy	central	63	400	0.3148
37						east	63	400	0.3148
38						north	63	400	0.3148
39						south	63	400	0.3148
40						west	63	400	0.2681

Table B.14: Shallow Rut Model Coefficients for MR and US

group	distress	treat_lvl	highway_fun	pavement_typ	traffic_cls	climate_zone	alpha	A_star	beta_star
41	rut_auto_shallow_av_pct	MR	US	thick	low	central	63	400	0.3174
42	rut_auto_shallow_av_pct	MR	US	thick	low	east	63	400	0.2340
43	rut_auto_shallow_av_pct	MR	US	thick	low	north	63	400	0.3351
44	rut_auto_shallow_av_pct	MR	US	thick	low	south	63	400	0.2901
45	rut_auto_shallow_av_pct	MR	US	thick	low	west	63	400	0.3682
46	rut_auto_shallow_av_pct	MR	US	thick	medium	central	63	400	0.3174
47	rut_auto_shallow_av_pct	MR	US	thick	medium	east	63	400	0.2340
48	rut_auto_shallow_av_pct	MR	US	thick	medium	north	63	400	0.3351
49	rut_auto_shallow_av_pct	MR	US	thick	medium	south	63	400	0.2901
50	rut_auto_shallow_av_pct	MR	US	thick	medium	west	63	400	0.3682
51	rut_auto_shallow_av_pct	MR	US	thick	high	central	63	400	0.3174
52	rut_auto_shallow_av_pct	MR	US	thick	high	east	63	400	0.2340
53	rut_auto_shallow_av_pct	MR	US	thick	high	north	63	400	0.3351
54	rut_auto_shallow_av_pct	MR	US	thick	high	south	63	400	0.2901
55	rut_auto_shallow_av_pct	MR	US	thick	high	west	63	400	0.3682
56	rut_auto_shallow_av_pct	MR	US	thick	heavy	central	63	400	0.3629
57	rut_auto_shallow_av_pct	MR	US	thick	heavy	east	63	400	0.2927
58	rut_auto_shallow_av_pct	MR	US	thick	heavy	north	63	400	0.2481
59	rut_auto_shallow_av_pct	MR	US	thick	heavy	south	63	400	0.3629
60	rut_auto_shallow_av_pct	MR	US	thick	heavy	west	63	400	0.2599
61	rut_auto_shallow_av_pct	MR	US	thin	low	central	63	400	0.1188
62	rut_auto_shallow_av_pct	MR	US	thin	low	east	63	400	-0.0456
63	rut_auto_shallow_av_pct	MR	US	thin	low	north	63	400	0.1188
64	rut_auto_shallow_av_pct	MR	US	thin	low	south	63	400	0.1188
65	rut_auto_shallow_av_pct	MR	US	thin	low	west	63	400	0.1717
66	rut_auto_shallow_av_pct	MR	US	thin	medium	central	63	400	0.1188
67	rut_auto_shallow_av_pct	MR	US	thin	medium	east	63	400	0.1188
68	rut_auto_shallow_av_pct	MR	US	thin	medium	north	63	400	0.1188
69	rut_auto_shallow_av_pct	MR	US	thin	medium	south	63	400	0.1188
70	rut_auto_shallow_av_pct	MR	US	thin	medium	west	63	400	0.1717
71	rut_auto_shallow_av_pct	MR	US	thin	high	central	63	400	0.1234
72	rut_auto_shallow_av_pct	MR	US	thin	high	east	63	400	0.2003
73	rut_auto_shallow_av_pct	MR	US	thin	high	north	63	400	0.4368
74	rut_auto_shallow_av_pct	MR	US	thin	high	south	63	400	0.3435
75	rut_auto_shallow_av_pct	MR	US	thin	high	west	63	400	0.4286
76	rut_auto_shallow_av_pct	MR	US	thin	heavy	central	63	400	0.2492
77	rut_auto_shallow_av_pct	MR	US	thin	heavy	east	63	400	0.1534
78	rut_auto_shallow_av_pct	MR	US	thin	heavy	north	63	400	0.1651
79	rut_auto_shallow_av_pct	MR	US	thin	heavy	south	63	400	0.1744
80	rut_auto_shallow_av_pct	MR	US	thin	heavy	west	63	400	0.2492

Table B.15: Shallow Rut Model Coefficients for MR and SH

group	distress	treat_lvl	highway_fun	pavement_typ	traffic_cls	climate_zone	alpha	A_star	beta_star
81	rut_auto_shallow_av_pct	MR	SH	thick	low	central	63	400	0.2740
82	rut_auto_shallow_av_pct	MR	SH	thick	low	east	63	400	0.2309
83	rut_auto_shallow_av_pct	MR	SH	thick	low	north	63	400	0.3691
84	rut_auto_shallow_av_pct	MR	SH	thick	low	south	63	400	0.2189
85	rut_auto_shallow_av_pct	MR	SH	thick	low	west	63	400	0.3884
86	rut_auto_shallow_av_pct	MR	SH	thick	medium	central	63	400	0.2740
87	rut_auto_shallow_av_pct	MR	SH	thick	medium	east	63	400	0.2309
88	rut_auto_shallow_av_pct	MR	SH	thick	medium	north	63	400	0.3691
89	rut_auto_shallow_av_pct	MR	SH	thick	medium	south	63	400	0.2189
90	rut_auto_shallow_av_pct	MR	SH	thick	medium	west	63	400	0.3884
91	rut_auto_shallow_av_pct	MR	SH	thick	high	central	63	400	0.2740
92	rut_auto_shallow_av_pct	MR	SH	thick	high	east	63	400	0.2309
93	rut_auto_shallow_av_pct	MR	SH	thick	high	north	63	400	0.3691
94	rut_auto_shallow_av_pct	MR	SH	thick	high	south	63	400	0.2189
95	rut_auto_shallow_av_pct	MR	SH	thick	high	west	63	400	0.3884
96	rut_auto_shallow_av_pct	MR	SH	thick	heavy	central	63	400	0.2282
97	rut_auto_shallow_av_pct	MR	SH	thick	heavy	east	63	400	0.3116
98	rut_auto_shallow_av_pct	MR	SH	thick	heavy	north	63	400	0.2282
99	rut_auto_shallow_av_pct	MR	SH	thick	heavy	south	63	400	0.2683
100	rut_auto_shallow_av_pct	MR	SH	thick	heavy	west	63	400	0.3967
101	rut_auto_shallow_av_pct	MR	SH	thin	low	central	63	400	0.3067
102	rut_auto_shallow_av_pct	MR	SH	thin	low	east	63	400	0.1599
103	rut_auto_shallow_av_pct	MR	SH	thin	low	north	63	400	0.2356
104	rut_auto_shallow_av_pct	MR	SH	thin	low	south	63	400	0.1722
105	rut_auto_shallow_av_pct	MR	SH	thin	low	west	63	400	0.2201
106	rut_auto_shallow_av_pct	MR	SH	thin	medium	central	63	400	0.3067
107	rut_auto_shallow_av_pct	MR	SH	thin	medium	east	63	400	0.1599
108	rut_auto_shallow_av_pct	MR	SH	thin	medium	north	63	400	0.2356
109	rut_auto_shallow_av_pct	MR	SH	thin	medium	south	63	400	0.1722
110	rut_auto_shallow_av_pct	MR	SH	thin	medium	west	63	400	0.2201
111	rut_auto_shallow_av_pct	MR	SH	thin	high	central	63	400	0.2451
112	rut_auto_shallow_av_pct	MR	SH	thin	high	east	63	400	0.1882
113	rut_auto_shallow_av_pct	MR	SH	thin	high	north	63	400	0.2457
114	rut_auto_shallow_av_pct	MR	SH	thin	high	south	63	400	0.3068
115	rut_auto_shallow_av_pct	MR	SH	thin	high	west	63	400	0.2385
116	rut_auto_shallow_av_pct	MR	SH	thin	heavy	central	63	400	0.3088
117	rut_auto_shallow_av_pct	MR	SH	thin	heavy	east	63	400	0.3400
118	rut_auto_shallow_av_pct	MR	SH	thin	heavy	north	63	400	0.3088
119	rut_auto_shallow_av_pct	MR	SH	thin	heavy	south	63	400	0.2781
120	rut_auto_shallow_av_pct	MR	SH	thin	heavy	west	63	400	0.2235

Table B.16: Shallow Rut Model Coefficients for MR and FM

group	distress	treat_lvl	highway_fun	pavement_typ	traffic_cls	climate_zone	alpha	A_star	beta_star
121	rut_auto_shallow_av_pct	MR	FM	thick	low	central	63	400	0.1552
122						east	63	400	0.1584
123						north	63	400	0.1552
124						south	63	400	0.1990
125						west	63	400	0.1552
126					medium	central	63	400	0.1648
127						east	63	400	0.4013
128						north	63	400	0.0946
129						south	63	400	0.1326
130						west	63	400	0.1648
131					high	central	63	400	0.2286
132						east	63	400	0.3862
133						north	63	400	0.3126
134						south	63	400	0.1942
135						west	63	400	0.2867
136					heavy	central	63	400	0.2286
137						east	63	400	0.3862
138						north	63	400	0.3126
139						south	63	400	0.1942
140						west	63	400	0.2867
141				thin	low	central	63	400	0.1721
142						east	63	400	0.1754
143						north	63	400	0.2147
144						south	63	400	0.1473
145						west	63	400	0.2245
146					medium	central	63	400	0.2088
147						east	63	400	0.1948
148						north	63	400	0.1494
149						south	63	400	0.2163
150						west	63	400	0.2301
151					high	central	63	400	0.2687
152						east	63	400	0.1647
153						north	63	400	0.0308
154						south	63	400	0.2115
155						west	63	400	0.3790
156					heavy	central	63	400	0.2687
157						east	63	400	0.1647
158						north	63	400	0.0308
159						south	63	400	0.2115
160						west	63	400	0.3790

Table B.17: Shallow Rut Model Coefficients for HR and IH

group	distress	treat_lvl	highway_fun	pavement_typ	traffic_cls	climate_zone	alpha	A_star	beta_star
1	rut_auto_shallow_av_pct	HR	IH	thick	low	central	63	600	0.3490
2						east	63	600	0.3102
3						north	63	600	0.3490
4						south	63	600	0.3153
5						west	63	600	0.3613
6					medium	central	63	600	0.3490
7						east	63	600	0.3102
8						north	63	600	0.3490
9						south	63	600	0.3153
10						west	63	600	0.3613
11					high	central	63	600	0.3490
12						east	63	600	0.3102
13						north	63	600	0.3490
14						south	63	600	0.3153
15						west	63	600	0.3613
16					heavy	central	63	600	0.3490
17						east	63	600	0.3102
18						north	63	600	0.3490
19						south	63	600	0.3153
20						west	63	600	0.3613
21				thin	low	central	63	600	0.1983
22						east	63	600	0.2101
23						north	63	600	0.1983
24						south	63	600	0.0975
25						west	63	600	0.1983
26					medium	central	63	600	0.3148
27						east	63	600	0.3148
28						north	63	600	0.3148
29						south	63	600	0.3148
30						west	63	600	0.2681
31					high	central	63	600	0.3148
32						east	63	600	0.3148
33						north	63	600	0.3148
34						south	63	600	0.3148
35						west	63	600	0.2681
36					heavy	central	63	600	0.3148
37						east	63	600	0.3148
38						north	63	600	0.3148
39						south	63	600	0.3148
40						west	63	600	0.2681

Table B.18: Shallow Rut Model Coefficients for HR and US

group	distress	treat_lvl	highway_fun	pavement_typ	traffic_cls	climate_zone	alpha	A_star	beta_star
41	rut_auto_shallow_av_pct	HR	US	thick	low	central	63	600	0.3174
42						east	63	600	0.2340
43						north	63	600	0.3351
44						south	63	600	0.2901
45						west	63	600	0.3682
46					medium	central	63	600	0.3174
47						east	63	600	0.2340
48						north	63	600	0.3351
49						south	63	600	0.2901
50						west	63	600	0.3682
51					high	central	63	600	0.3174
52						east	63	600	0.2340
53						north	63	600	0.3351
54						south	63	600	0.2901
55						west	63	600	0.3682
56					heavy	central	63	600	0.3629
57						east	63	600	0.2927
58						north	63	600	0.2481
59						south	63	600	0.3629
60						west	63	600	0.2599
61				thin	low	central	63	600	0.1188
62						east	63	600	-0.0456
63						north	63	600	0.1188
64						south	63	600	0.1188
65						west	63	600	0.1717
66					medium	central	63	600	0.1188
67						east	63	600	0.1188
68						north	63	600	0.1188
69						south	63	600	0.1188
70						west	63	600	0.1717
71					high	central	63	600	0.1234
72						east	63	600	0.2003
73						north	63	600	0.4368
74						south	63	600	0.3435
75						west	63	600	0.4286
76					heavy	central	63	600	0.2492
77						east	63	600	0.1534
78						north	63	600	0.1651
79						south	63	600	0.1744
80						west	63	600	0.2492

Table B.19: Shallow Rut Model Coefficients for HR and SH

group	distress	treat_lvl	highway_fun	pavement_typ	traffic_cls	climate_zone	alpha	A_star	beta_star
81	rut_auto_shallow_av_pct	HR	SH	thick	low	central	63	600	0.2740
82						east	63	600	0.2309
83						north	63	600	0.3691
84						south	63	600	0.2189
85						west	63	600	0.3884
86					medium	central	63	600	0.2740
87						east	63	600	0.2309
88						north	63	600	0.3691
89						south	63	600	0.2189
90						west	63	600	0.3884
91					high	central	63	600	0.2740
92						east	63	600	0.2309
93						north	63	600	0.3691
94						south	63	600	0.2189
95						west	63	600	0.3884
96					heavy	central	63	600	0.2282
97						east	63	600	0.3116
98						north	63	600	0.2282
99						south	63	600	0.2683
100						west	63	600	0.3967
101				thin	low	central	63	600	0.3067
102						east	63	600	0.1599
103						north	63	600	0.2356
104						south	63	600	0.1722
105						west	63	600	0.2201
106					medium	central	63	600	0.3067
107						east	63	600	0.1599
108						north	63	600	0.2356
109						south	63	600	0.1722
110						west	63	600	0.2201
111					high	central	63	600	0.2451
112						east	63	600	0.1882
113						north	63	600	0.2457
114						south	63	600	0.3068
115						west	63	600	0.2385
116					heavy	central	63	600	0.3088
117						east	63	600	0.3400
118						north	63	600	0.3088
119						south	63	600	0.2781
120						west	63	600	0.2235

Table B.20: Shallow Rut Model Coefficients for HR and FM

group	distress	treat_lvl	highway_fun	pavement_typ	traffic_cls	climate_zone	alpha	A_star	beta_star
121	rut_auto_shallow_av_pct	HR	FM	thick	low	central	63	600	0.1552
122						east	63	600	0.1584
123						north	63	600	0.1552
124						south	63	600	0.1990
125						west	63	600	0.1552
126					medium	central	63	600	0.1648
127						east	63	600	0.4013
128						north	63	600	0.0946
129						south	63	600	0.1326
130						west	63	600	0.1648
131					high	central	63	600	0.2286
132						east	63	600	0.3862
133						north	63	600	0.3126
134						south	63	600	0.1942
135						west	63	600	0.2867
136					heavy	central	63	600	0.2286
137						east	63	600	0.3862
138						north	63	600	0.3126
139						south	63	600	0.1942
140						west	63	600	0.2867
141				thin	low	central	63	600	0.1721
142						east	63	600	0.1754
143						north	63	600	0.2147
144						south	63	600	0.1473
145						west	63	600	0.2245
146					medium	central	63	600	0.2088
147						east	63	600	0.1948
148						north	63	600	0.1494
149						south	63	600	0.2163
150						west	63	600	0.2301
151					high	central	63	600	0.2687
152						east	63	600	0.1647
153						north	63	600	0.0308
154						south	63	600	0.2115
155						west	63	600	0.3790
156					heavy	central	63	600	0.2687
157						east	63	600	0.1647
158						north	63	600	0.0308
159						south	63	600	0.2115
160						west	63	600	0.3790

Table B.21: Deep Rut Model Coefficients for DN and IH

group	distress	treat_lvl	highway_fun	pavement_typ	traffic_cls	climate_zone	alpha	A_star	beta_star
1	rut_auto_deep_avg_pct	DN	IH	thick	low	central	23	1679.653	0.2829
2	rut_auto_deep_avg_pct	DN	IH	thick	low	east	23	1679.653	0.2640
3	rut_auto_deep_avg_pct	DN	IH	thick	low	north	23	1679.653	0.2829
4	rut_auto_deep_avg_pct	DN	IH	thick	low	south	23	1679.653	0.2522
5	rut_auto_deep_avg_pct	DN	IH	thick	low	west	23	1679.653	0.2634
6	rut_auto_deep_avg_pct	DN	IH	thick	medium	central	23	1679.653	0.2829
7	rut_auto_deep_avg_pct	DN	IH	thick	medium	east	23	1679.653	0.2640
8	rut_auto_deep_avg_pct	DN	IH	thick	medium	north	23	1679.653	0.2829
9	rut_auto_deep_avg_pct	DN	IH	thick	medium	south	23	1679.653	0.2522
10	rut_auto_deep_avg_pct	DN	IH	thick	medium	west	23	1679.653	0.2634
11	rut_auto_deep_avg_pct	DN	IH	thick	high	central	23	1679.653	0.2829
12	rut_auto_deep_avg_pct	DN	IH	thick	high	east	23	1679.653	0.2640
13	rut_auto_deep_avg_pct	DN	IH	thick	high	north	23	1679.653	0.2829
14	rut_auto_deep_avg_pct	DN	IH	thick	high	south	23	1679.653	0.2522
15	rut_auto_deep_avg_pct	DN	IH	thick	high	west	23	1679.653	0.2634
16	rut_auto_deep_avg_pct	DN	IH	thick	heavy	central	23	1679.653	0.2829
17	rut_auto_deep_avg_pct	DN	IH	thick	heavy	east	23	1679.653	0.2640
18	rut_auto_deep_avg_pct	DN	IH	thick	heavy	north	23	1679.653	0.2829
19	rut_auto_deep_avg_pct	DN	IH	thick	heavy	south	23	1679.653	0.2522
20	rut_auto_deep_avg_pct	DN	IH	thick	heavy	west	23	1679.653	0.2634
21	rut_auto_deep_avg_pct	DN	IH	thin	low	central	23	1679.653	0.1713
22	rut_auto_deep_avg_pct	DN	IH	thin	low	east	23	1679.653	0.1962
23	rut_auto_deep_avg_pct	DN	IH	thin	low	north	23	1679.653	0.1713
24	rut_auto_deep_avg_pct	DN	IH	thin	low	south	23	1679.653	0.0025
25	rut_auto_deep_avg_pct	DN	IH	thin	low	west	23	1679.653	0.1713
26	rut_auto_deep_avg_pct	DN	IH	thin	medium	central	23	1679.653	0.2821
27	rut_auto_deep_avg_pct	DN	IH	thin	medium	east	23	1679.653	0.2821
28	rut_auto_deep_avg_pct	DN	IH	thin	medium	north	23	1679.653	0.2821
29	rut_auto_deep_avg_pct	DN	IH	thin	medium	south	23	1679.653	0.2821
30	rut_auto_deep_avg_pct	DN	IH	thin	medium	west	23	1679.653	0.2662
31	rut_auto_deep_avg_pct	DN	IH	thin	high	central	23	1679.653	0.2821
32	rut_auto_deep_avg_pct	DN	IH	thin	high	east	23	1679.653	0.2821
33	rut_auto_deep_avg_pct	DN	IH	thin	high	north	23	1679.653	0.2821
34	rut_auto_deep_avg_pct	DN	IH	thin	high	south	23	1679.653	0.2821
35	rut_auto_deep_avg_pct	DN	IH	thin	high	west	23	1679.653	0.2662
36	rut_auto_deep_avg_pct	DN	IH	thin	heavy	central	23	1679.653	0.2821
37	rut_auto_deep_avg_pct	DN	IH	thin	heavy	east	23	1679.653	0.2821
38	rut_auto_deep_avg_pct	DN	IH	thin	heavy	north	23	1679.653	0.2821
39	rut_auto_deep_avg_pct	DN	IH	thin	heavy	south	23	1679.653	0.2821
40	rut_auto_deep_avg_pct	DN	IH	thin	heavy	west	23	1679.653	0.2662

Table B.22: Deep Rut Model Coefficients for DN and US

group	distress	treat_lvl	highway_fun	pavement_typ	traffic_cls	climate_zone	alpha	A_star	beta_star
41	rut_auto_deep_avg_pct	DN	US	thick	low	central	23	1679.653	0.2839
42						east	23	1679.653	0.2403
43						north	23	1679.653	0.2457
44						south	23	1679.653	0.2658
45						west	23	1679.653	0.2753
46					medium	central	23	1679.653	0.2839
47						east	23	1679.653	0.2403
48						north	23	1679.653	0.2457
49						south	23	1679.653	0.2658
50						west	23	1679.653	0.2753
51					high	central	23	1679.653	0.2839
52						east	23	1679.653	0.2403
53						north	23	1679.653	0.2457
54						south	23	1679.653	0.2658
55						west	23	1679.653	0.2753
56					heavy	central	23	1679.653	0.2823
57						east	23	1679.653	0.2746
58						north	23	1679.653	0.1927
59						south	23	1679.653	0.2577
60						west	23	1679.653	0.2548
61				thin	low	central	23	1679.653	0.1420
62						east	23	1679.653	0.0869
63						north	23	1679.653	0.1420
64						south	23	1679.653	0.1420
65						west	23	1679.653	0.2370
66					medium	central	23	1679.653	0.1420
67						east	23	1679.653	0.0869
68						north	23	1679.653	0.1420
69						south	23	1679.653	0.1420
70						west	23	1679.653	0.2370
71					high	central	23	1679.653	0.1547
72						east	23	1679.653	0.2160
73						north	23	1679.653	0.2685
74						south	23	1679.653	0.2530
75						west	23	1679.653	0.2403
76					heavy	central	23	1679.653	0.2297
77						east	23	1679.653	0.2353
78						north	23	1679.653	0.2465
79						south	23	1679.653	0.2591
80						west	23	1679.653	0.2297

Table B.23: Deep Rut Model Coefficients for DN and SH

group	distress	treat_lvl	highway_fun	pavement_typ	traffic_cls	climate_zone	alpha	A_star	beta_star
81	rut_auto_deep_avg_pct	DN	SH	thick	low	central	23	1679.653	0.2543
82						east	23	1679.653	0.2235
83						north	23	1679.653	0.2652
84						south	23	1679.653	0.1716
85						west	23	1679.653	0.2465
86					medium	central	23	1679.653	0.2543
87						east	23	1679.653	0.2235
88						north	23	1679.653	0.2652
89						south	23	1679.653	0.1716
90						west	23	1679.653	0.2465
91					high	central	23	1679.653	0.2543
92						east	23	1679.653	0.2235
93						north	23	1679.653	0.2652
94						south	23	1679.653	0.1716
95						west	23	1679.653	0.2465
96					heavy	central	23	1679.653	0.2292
97						east	23	1679.653	0.2832
98						north	23	1679.653	0.2292
99						south	23	1679.653	0.2410
100						west	23	1679.653	0.2641
101				thin	low	central	23	1679.653	0.2532
102						east	23	1679.653	0.2295
103						north	23	1679.653	0.2396
104						south	23	1679.653	0.1139
105						west	23	1679.653	0.2160
106					medium	central	23	1679.653	0.2532
107						east	23	1679.653	0.2295
108						north	23	1679.653	0.2396
109						south	23	1679.653	0.1139
110						west	23	1679.653	0.2160
111					high	central	23	1679.653	0.2231
112						east	23	1679.653	0.2093
113						north	23	1679.653	0.2002
114						south	23	1679.653	0.1984
115						west	23	1679.653	0.2164
116					heavy	central	23	1679.653	0.2620
117						east	23	1679.653	0.2533
118						north	23	1679.653	0.2620
119						south	23	1679.653	0.2205
120						west	23	1679.653	0.2130

Table B.24: Deep Rut Model Coefficients for DN and FM

group	distress	treat_lvl	highway_fun	pavement_typ	traffic_cls	climate_zone	alpha	A_star	beta_star
121	rut_auto_deep_avg_pct	DN	FM	thick	low	central	23	1679.653	0.1610
122						east	23	1679.653	0.1600
123						north	23	1679.653	0.1610
124						south	23	1679.653	0.1846
125						west	23	1679.653	0.1610
126					medium	central	23	1679.653	0.1509
127						east	23	1679.653	0.2896
128						north	23	1679.653	0.1736
129						south	23	1679.653	0.1539
130						west	23	1679.653	0.1509
131					high	central	23	1679.653	0.2181
132						east	23	1679.653	0.3020
133						north	23	1679.653	0.2324
134						south	23	1679.653	0.1881
135						west	23	1679.653	0.2280
136					heavy	central	23	1679.653	0.2181
137						east	23	1679.653	0.3020
138						north	23	1679.653	0.2324
139						south	23	1679.653	0.1881
140						west	23	1679.653	0.2280
141				thin	low	central	23	1679.653	0.1499
142						east	23	1679.653	0.1490
143						north	23	1679.653	0.1713
144						south	23	1679.653	0.1475
145						west	23	1679.653	0.1786
146					medium	central	23	1679.653	0.1740
147						east	23	1679.653	0.1674
148						north	23	1679.653	0.1426
149						south	23	1679.653	0.2029
150						west	23	1679.653	0.1927
151					high	central	23	1679.653	0.2264
152						east	23	1679.653	0.1864
153						north	23	1679.653	0.0561
154						south	23	1679.653	0.1996
155						west	23	1679.653	0.2196
156					heavy	central	23	1679.653	0.2264
157						east	23	1679.653	0.1864
158						north	23	1679.653	0.0561
159						south	23	1679.653	0.1996
160						west	23	1679.653	0.2196

Table B.25: Deep Rut Model Coefficients for PM and IH

group	distress	treat_lvl	highway_fun	pavement_typ	traffic_cls	climate_zone	alpha	A_star	beta_star
1	rut_auto_deep_avg_pct	PM	IH	thick	low	central	23	2800	0.2829
2						east	23	2800	0.2640
3						north	23	2800	0.2829
4						south	23	2800	0.2522
5						west	23	2800	0.2634
6					medium	central	23	2800	0.2829
7						east	23	2800	0.2640
8						north	23	2800	0.2829
9						south	23	2800	0.2522
10						west	23	2800	0.2634
11					high	central	23	2800	0.2829
12						east	23	2800	0.2640
13						north	23	2800	0.2829
14						south	23	2800	0.2522
15						west	23	2800	0.2634
16					heavy	central	23	2800	0.2829
17						east	23	2800	0.2640
18						north	23	2800	0.2829
19						south	23	2800	0.2522
20						west	23	2800	0.2634
21				thin	low	central	23	2800	0.1713
22						east	23	2800	0.1962
23						north	23	2800	0.1713
24						south	23	2800	0.0025
25						west	23	2800	0.1713
26					medium	central	23	2800	0.2821
27						east	23	2800	0.2821
28						north	23	2800	0.2821
29						south	23	2800	0.2821
30						west	23	2800	0.2662
31					high	central	23	2800	0.2821
32						east	23	2800	0.2821
33						north	23	2800	0.2821
34						south	23	2800	0.2821
35						west	23	2800	0.2662
36					heavy	central	23	2800	0.2821
37						east	23	2800	0.2821
38						north	23	2800	0.2821
39						south	23	2800	0.2821
40						west	23	2800	0.2662

Table B.26: Deep Rut Model Coefficients for PM and US

group	distress	treat_lvl	highway_fun	pavement_typ	traffic_cls	climate_zone	alpha	A_star	beta_star
41	rut_auto_deep_avg_pct	PM	US	thick	low	central	23	2800	0.2839
42						east	23	2800	0.2403
43						north	23	2800	0.2457
44						south	23	2800	0.2658
45						west	23	2800	0.2753
46					medium	central	23	2800	0.2839
47						east	23	2800	0.2403
48						north	23	2800	0.2457
49						south	23	2800	0.2658
50						west	23	2800	0.2753
51					high	central	23	2800	0.2839
52						east	23	2800	0.2403
53						north	23	2800	0.2457
54						south	23	2800	0.2658
55						west	23	2800	0.2753
56					heavy	central	23	2800	0.2823
57						east	23	2800	0.2746
58						north	23	2800	0.1927
59						south	23	2800	0.2577
60						west	23	2800	0.2548
61				thin	low	central	23	2800	0.1420
62						east	23	2800	0.0869
63						north	23	2800	0.1420
64						south	23	2800	0.1420
65						west	23	2800	0.2370
66					medium	central	23	2800	0.1420
67						east	23	2800	0.0869
68						north	23	2800	0.1420
69						south	23	2800	0.1420
70						west	23	2800	0.2370
71					high	central	23	2800	0.1547
72						east	23	2800	0.2160
73						north	23	2800	0.2685
74						south	23	2800	0.2530
75						west	23	2800	0.2403
76					heavy	central	23	2800	0.2297
77						east	23	2800	0.2353
78						north	23	2800	0.2465
79						south	23	2800	0.2591
80						west	23	2800	0.2297

Table B.27: Deep Rut Model Coefficients for PM and SH

group	distress	treat_lvl	highway_fun	pavement_typ	traffic_cls	climate_zone	alpha	A_star	beta_star
81	rut_auto_deep_avg_pct	PM	SH	thick	low	central	23	2800	0.2543
82						east	23	2800	0.2235
83						north	23	2800	0.2652
84						south	23	2800	0.1716
85						west	23	2800	0.2465
86					medium	central	23	2800	0.2543
87						east	23	2800	0.2235
88						north	23	2800	0.2652
89						south	23	2800	0.1716
90						west	23	2800	0.2465
91					high	central	23	2800	0.2543
92						east	23	2800	0.2235
93						north	23	2800	0.2652
94						south	23	2800	0.1716
95						west	23	2800	0.2465
96					heavy	central	23	2800	0.2292
97						east	23	2800	0.2832
98						north	23	2800	0.2292
99						south	23	2800	0.2410
100						west	23	2800	0.2641
101				thin	low	central	23	2800	0.2532
102						east	23	2800	0.2295
103						north	23	2800	0.2396
104						south	23	2800	0.1139
105						west	23	2800	0.2160
106					medium	central	23	2800	0.2532
107						east	23	2800	0.2295
108						north	23	2800	0.2396
109						south	23	2800	0.1139
110						west	23	2800	0.2160
111					high	central	23	2800	0.2231
112						east	23	2800	0.2093
113						north	23	2800	0.2002
114						south	23	2800	0.1984
115						west	23	2800	0.2164
116					heavy	central	23	2800	0.2620
117						east	23	2800	0.2533
118						north	23	2800	0.2620
119						south	23	2800	0.2205
120						west	23	2800	0.2130

Table B.28: Deep Rut Model Coefficients for PM and FM

group	distress	treat_lvl	highway_fun	pavement_typ	traffic_cls	climate_zone	alpha	A_star	beta_star
121	rut_auto_deep_avg_pct	PM	FM	thick	low	central	23	2800	0.1610
122						east	23	2800	0.1600
123						north	23	2800	0.1610
124						south	23	2800	0.1846
125						west	23	2800	0.1610
126					medium	central	23	2800	0.1509
127						east	23	2800	0.2896
128						north	23	2800	0.1736
129						south	23	2800	0.1539
130						west	23	2800	0.1509
131					high	central	23	2800	0.2181
132						east	23	2800	0.3020
133						north	23	2800	0.2324
134						south	23	2800	0.1881
135						west	23	2800	0.2280
136					heavy	central	23	2800	0.2181
137						east	23	2800	0.3020
138						north	23	2800	0.2324
139						south	23	2800	0.1881
140						west	23	2800	0.2280
141				thin	low	central	23	2800	0.1499
142						east	23	2800	0.1490
143						north	23	2800	0.1713
144						south	23	2800	0.1475
145						west	23	2800	0.1786
146					medium	central	23	2800	0.1740
147						east	23	2800	0.1674
148						north	23	2800	0.1426
149						south	23	2800	0.2029
150						west	23	2800	0.1927
151					high	central	23	2800	0.2264
152						east	23	2800	0.1864
153						north	23	2800	0.0561
154						south	23	2800	0.1996
155						west	23	2800	0.2196
156					heavy	central	23	2800	0.2264
157						east	23	2800	0.1864
158						north	23	2800	0.0561
159						south	23	2800	0.1996
160						west	23	2800	0.2196

Table B.29: Deep Rut Model Coefficients for LR and IH

group	distress	treat_lvl	highway_fun	pavement_typ	traffic_cls	climate_zone	alpha	A_star	beta_star
1	rut_auto_deep_avg_pct	LR	IH	thick	low	central	23	3500	0.2829
2						east	23	3500	0.2640
3						north	23	3500	0.2829
4						south	23	3500	0.2522
5						west	23	3500	0.2634
6					medium	central	23	3500	0.2829
7						east	23	3500	0.2640
8						north	23	3500	0.2829
9						south	23	3500	0.2522
10						west	23	3500	0.2634
11					high	central	23	3500	0.2829
12						east	23	3500	0.2640
13						north	23	3500	0.2829
14						south	23	3500	0.2522
15						west	23	3500	0.2634
16					heavy	central	23	3500	0.2829
17						east	23	3500	0.2640
18						north	23	3500	0.2829
19						south	23	3500	0.2522
20						west	23	3500	0.2634
21				thin	low	central	23	3500	0.1713
22						east	23	3500	0.1962
23						north	23	3500	0.1713
24						south	23	3500	0.0025
25						west	23	3500	0.1713
26					medium	central	23	3500	0.2821
27						east	23	3500	0.2821
28						north	23	3500	0.2821
29						south	23	3500	0.2821
30						west	23	3500	0.2662
31					high	central	23	3500	0.2821
32						east	23	3500	0.2821
33						north	23	3500	0.2821
34						south	23	3500	0.2821
35						west	23	3500	0.2662
36					heavy	central	23	3500	0.2821
37						east	23	3500	0.2821
38						north	23	3500	0.2821
39						south	23	3500	0.2821
40						west	23	3500	0.2662

Table B.30: Deep Rut Model Coefficients for LR and US

group	distress	treat_lvl	highway_fun	pavement_typ	traffic_cls	climate_zone	alpha	A_star	beta_star
41	rut_auto_deep_avg_pct	LR	US	thick	low	central	23	3500	0.2839
42						east	23	3500	0.2403
43						north	23	3500	0.2457
44						south	23	3500	0.2658
45						west	23	3500	0.2753
46					medium	central	23	3500	0.2839
47						east	23	3500	0.2403
48						north	23	3500	0.2457
49						south	23	3500	0.2658
50						west	23	3500	0.2753
51					high	central	23	3500	0.2839
52						east	23	3500	0.2403
53						north	23	3500	0.2457
54						south	23	3500	0.2658
55						west	23	3500	0.2753
56					heavy	central	23	3500	0.2823
57						east	23	3500	0.2746
58						north	23	3500	0.1927
59						south	23	3500	0.2577
60						west	23	3500	0.2548
61				thin	low	central	23	3500	0.1420
62						east	23	3500	0.0869
63						north	23	3500	0.1420
64						south	23	3500	0.1420
65						west	23	3500	0.2370
66					medium	central	23	3500	0.1420
67						east	23	3500	0.0869
68						north	23	3500	0.1420
69						south	23	3500	0.1420
70						west	23	3500	0.2370
71					high	central	23	3500	0.1547
72						east	23	3500	0.2160
73						north	23	3500	0.2685
74						south	23	3500	0.2530
75						west	23	3500	0.2403
76					heavy	central	23	3500	0.2297
77						east	23	3500	0.2353
78						north	23	3500	0.2465
79						south	23	3500	0.2591
80						west	23	3500	0.2297

Table B.31: Deep Rut Model Coefficients for LR and SH

group	distress	treat_lvl	highway_fun	pavement_typ	traffic_cls	climate_zone	alpha	A_star	beta_star
81	rut_auto_deep_avg_pct	LR	SH	thick	low	central	23	3500	0.2543
82						east	23	3500	0.2235
83						north	23	3500	0.2652
84						south	23	3500	0.1716
85						west	23	3500	0.2465
86					medium	central	23	3500	0.2543
87						east	23	3500	0.2235
88						north	23	3500	0.2652
89						south	23	3500	0.1716
90						west	23	3500	0.2465
91					high	central	23	3500	0.2543
92						east	23	3500	0.2235
93						north	23	3500	0.2652
94						south	23	3500	0.1716
95						west	23	3500	0.2465
96					heavy	central	23	3500	0.2292
97						east	23	3500	0.2832
98						north	23	3500	0.2292
99						south	23	3500	0.2410
100						west	23	3500	0.2641
101				thin	low	central	23	3500	0.2532
102						east	23	3500	0.2295
103						north	23	3500	0.2396
104						south	23	3500	0.1139
105						west	23	3500	0.2160
106					medium	central	23	3500	0.2532
107						east	23	3500	0.2295
108						north	23	3500	0.2396
109						south	23	3500	0.1139
110						west	23	3500	0.2160
111					high	central	23	3500	0.2231
112						east	23	3500	0.2093
113						north	23	3500	0.2002
114						south	23	3500	0.1984
115						west	23	3500	0.2164
116					heavy	central	23	3500	0.2620
117						east	23	3500	0.2533
118						north	23	3500	0.2620
119						south	23	3500	0.2205
120						west	23	3500	0.2130

Table B.32: Deep Rut Model Coefficients for LR and FM

group	distress	treat_lvl	highway_fun	pavement_typ	traffic_cls	climate_zone	alpha	A_star	beta_star
121	rut_auto_deep_avg_pct	LR	FM	thick	low	central	23	3500	0.1610
122						east	23	3500	0.1600
123						north	23	3500	0.1610
124						south	23	3500	0.1846
125						west	23	3500	0.1610
126					medium	central	23	3500	0.1509
127						east	23	3500	0.2896
128						north	23	3500	0.1736
129						south	23	3500	0.1539
130						west	23	3500	0.1509
131					high	central	23	3500	0.2181
132						east	23	3500	0.3020
133						north	23	3500	0.2324
134						south	23	3500	0.1881
135						west	23	3500	0.2280
136					heavy	central	23	3500	0.2181
137						east	23	3500	0.3020
138						north	23	3500	0.2324
139						south	23	3500	0.1881
140						west	23	3500	0.2280
141				thin	low	central	23	3500	0.1499
142						east	23	3500	0.1490
143						north	23	3500	0.1713
144						south	23	3500	0.1475
145						west	23	3500	0.1786
146					medium	central	23	3500	0.1740
147						east	23	3500	0.1674
148						north	23	3500	0.1426
149						south	23	3500	0.2029
150						west	23	3500	0.1927
151					high	central	23	3500	0.2264
152						east	23	3500	0.1864
153						north	23	3500	0.0561
154						south	23	3500	0.1996
155						west	23	3500	0.2196
156					heavy	central	23	3500	0.2264
157						east	23	3500	0.1864
158						north	23	3500	0.0561
159						south	23	3500	0.1996
160						west	23	3500	0.2196

Table B.33: Deep Rut Model Coefficients for MR and IH

group	distress	treat_lvl	highway_fun	pavement_typ	traffic_cls	climate_zone	alpha	A_star	beta_star
1	rut_auto_deep_avg_pct	MR	IH	thick	low	central	23	7000	0.2829
2						east	23	7000	0.2640
3						north	23	7000	0.2829
4						south	23	7000	0.2522
5						west	23	7000	0.2634
6					medium	central	23	7000	0.2829
7						east	23	7000	0.2640
8						north	23	7000	0.2829
9						south	23	7000	0.2522
10						west	23	7000	0.2634
11					high	central	23	7000	0.2829
12						east	23	7000	0.2640
13						north	23	7000	0.2829
14						south	23	7000	0.2522
15						west	23	7000	0.2634
16					heavy	central	23	7000	0.2829
17						east	23	7000	0.2640
18						north	23	7000	0.2829
19						south	23	7000	0.2522
20						west	23	7000	0.2634
21				thin	low	central	23	7000	0.1713
22						east	23	7000	0.1962
23						north	23	7000	0.1713
24						south	23	7000	0.0025
25						west	23	7000	0.1713
26					medium	central	23	7000	0.2821
27						east	23	7000	0.2821
28						north	23	7000	0.2821
29						south	23	7000	0.2821
30						west	23	7000	0.2662
31					high	central	23	7000	0.2821
32						east	23	7000	0.2821
33						north	23	7000	0.2821
34						south	23	7000	0.2821
35						west	23	7000	0.2662
36					heavy	central	23	7000	0.2821
37						east	23	7000	0.2821
38						north	23	7000	0.2821
39						south	23	7000	0.2821
40						west	23	7000	0.2662

Table B.34: Deep Rut Model Coefficients for MR and US

group	distress	treat_lvl	highway_fun	pavement_typ	traffic_cls	climate_zone	alpha	A_star	beta_star
41	rut_auto_deep_avg_pct	MR	US	thick	low	central	23	7000	0.2839
42						east	23	7000	0.2403
43						north	23	7000	0.2457
44						south	23	7000	0.2658
45						west	23	7000	0.2753
46					medium	central	23	7000	0.2839
47						east	23	7000	0.2403
48						north	23	7000	0.2457
49						south	23	7000	0.2658
50						west	23	7000	0.2753
51					high	central	23	7000	0.2839
52						east	23	7000	0.2403
53						north	23	7000	0.2457
54						south	23	7000	0.2658
55						west	23	7000	0.2753
56					heavy	central	23	7000	0.2823
57						east	23	7000	0.2746
58						north	23	7000	0.1927
59						south	23	7000	0.2577
60						west	23	7000	0.2548
61				thin	low	central	23	7000	0.1420
62						east	23	7000	0.0869
63						north	23	7000	0.1420
64						south	23	7000	0.1420
65						west	23	7000	0.2370
66					medium	central	23	7000	0.1420
67						east	23	7000	0.0869
68						north	23	7000	0.1420
69						south	23	7000	0.1420
70						west	23	7000	0.2370
71					high	central	23	7000	0.1547
72						east	23	7000	0.2160
73						north	23	7000	0.2685
74						south	23	7000	0.2530
75						west	23	7000	0.2403
76					heavy	central	23	7000	0.2297
77						east	23	7000	0.2353
78						north	23	7000	0.2465
79						south	23	7000	0.2591
80						west	23	7000	0.2297

Table B.35: Deep Rut Model Coefficients for MR and SH

group	distress	treat_lvl	highway_fun	pavement_typ	traffic_cls	climate_zone	alpha	A_star	beta_star
81	rut_auto_deep_avg_pct	MR	SH	thick	low	central	23	7000	0.2543
82						east	23	7000	0.2235
83						north	23	7000	0.2652
84						south	23	7000	0.1716
85						west	23	7000	0.2465
86					medium	central	23	7000	0.2543
87						east	23	7000	0.2235
88						north	23	7000	0.2652
89						south	23	7000	0.1716
90						west	23	7000	0.2465
91					high	central	23	7000	0.2543
92						east	23	7000	0.2235
93						north	23	7000	0.2652
94						south	23	7000	0.1716
95						west	23	7000	0.2465
96					heavy	central	23	7000	0.2292
97						east	23	7000	0.2832
98						north	23	7000	0.2292
99						south	23	7000	0.2410
100						west	23	7000	0.2641
101				thin	low	central	23	7000	0.2532
102						east	23	7000	0.2295
103						north	23	7000	0.2396
104						south	23	7000	0.1139
105						west	23	7000	0.2160
106					medium	central	23	7000	0.2532
107						east	23	7000	0.2295
108						north	23	7000	0.2396
109						south	23	7000	0.1139
110						west	23	7000	0.2160
111					high	central	23	7000	0.2231
112						east	23	7000	0.2093
113						north	23	7000	0.2002
114						south	23	7000	0.1984
115						west	23	7000	0.2164
116					heavy	central	23	7000	0.2620
117						east	23	7000	0.2533
118						north	23	7000	0.2620
119						south	23	7000	0.2205
120						west	23	7000	0.2130

Table B.36: Deep Rut Model Coefficients for MR and FM

group	distress	treat_lvl	highway_fun	pavement_typ	traffic_cls	climate_zone	alpha	A_star	beta_star
121	rut_auto_deep_avg_pct	MR	FM	thick	low	central	23	7000	0.1610
122						east	23	7000	0.1600
123						north	23	7000	0.1610
124						south	23	7000	0.1846
125						west	23	7000	0.1610
126					medium	central	23	7000	0.1509
127						east	23	7000	0.2896
128						north	23	7000	0.1736
129						south	23	7000	0.1539
130						west	23	7000	0.1509
131					high	central	23	7000	0.2181
132						east	23	7000	0.3020
133						north	23	7000	0.2324
134						south	23	7000	0.1881
135						west	23	7000	0.2280
136					heavy	central	23	7000	0.2181
137						east	23	7000	0.3020
138						north	23	7000	0.2324
139						south	23	7000	0.1881
140						west	23	7000	0.2280
141				thin	low	central	23	7000	0.1499
142						east	23	7000	0.1490
143						north	23	7000	0.1713
144						south	23	7000	0.1475
145						west	23	7000	0.1786
146					medium	central	23	7000	0.1740
147						east	23	7000	0.1674
148						north	23	7000	0.1426
149						south	23	7000	0.2029
150						west	23	7000	0.1927
151					high	central	23	7000	0.2264
152						east	23	7000	0.1864
153						north	23	7000	0.0561
154						south	23	7000	0.1996
155						west	23	7000	0.2196
156					heavy	central	23	7000	0.2264
157						east	23	7000	0.1864
158						north	23	7000	0.0561
159						south	23	7000	0.1996
160						west	23	7000	0.2196

Table B.37: Deep Rut Model Coefficients for HR and IH

group	distress	treat_lvl	highway_fun	pavement_typ	traffic_cls	climate_zone	alpha	A_star	beta_star
1	rut_auto_deep_avg_pct	HR	IH	thick	low	central	23	15000	0.2829
2	rut_auto_deep_avg_pct	HR	IH	thick	low	east	23	15000	0.2640
3	rut_auto_deep_avg_pct	HR	IH	thick	low	north	23	15000	0.2829
4	rut_auto_deep_avg_pct	HR	IH	thick	low	south	23	15000	0.2522
5	rut_auto_deep_avg_pct	HR	IH	thick	low	west	23	15000	0.2634
6	rut_auto_deep_avg_pct	HR	IH	thick	medium	central	23	15000	0.2829
7	rut_auto_deep_avg_pct	HR	IH	thick	medium	east	23	15000	0.2640
8	rut_auto_deep_avg_pct	HR	IH	thick	medium	north	23	15000	0.2829
9	rut_auto_deep_avg_pct	HR	IH	thick	medium	south	23	15000	0.2522
10	rut_auto_deep_avg_pct	HR	IH	thick	medium	west	23	15000	0.2634
11	rut_auto_deep_avg_pct	HR	IH	thick	high	central	23	15000	0.2829
12	rut_auto_deep_avg_pct	HR	IH	thick	high	east	23	15000	0.2640
13	rut_auto_deep_avg_pct	HR	IH	thick	high	north	23	15000	0.2829
14	rut_auto_deep_avg_pct	HR	IH	thick	high	south	23	15000	0.2522
15	rut_auto_deep_avg_pct	HR	IH	thick	high	west	23	15000	0.2634
16	rut_auto_deep_avg_pct	HR	IH	thick	heavy	central	23	15000	0.2829
17	rut_auto_deep_avg_pct	HR	IH	thick	heavy	east	23	15000	0.2640
18	rut_auto_deep_avg_pct	HR	IH	thick	heavy	north	23	15000	0.2829
19	rut_auto_deep_avg_pct	HR	IH	thick	heavy	south	23	15000	0.2522
20	rut_auto_deep_avg_pct	HR	IH	thick	heavy	west	23	15000	0.2634
21	rut_auto_deep_avg_pct	HR	IH	thin	low	central	23	15000	0.1713
22	rut_auto_deep_avg_pct	HR	IH	thin	low	east	23	15000	0.1962
23	rut_auto_deep_avg_pct	HR	IH	thin	low	north	23	15000	0.1713
24	rut_auto_deep_avg_pct	HR	IH	thin	low	south	23	15000	0.0025
25	rut_auto_deep_avg_pct	HR	IH	thin	low	west	23	15000	0.1713
26	rut_auto_deep_avg_pct	HR	IH	thin	medium	central	23	15000	0.2821
27	rut_auto_deep_avg_pct	HR	IH	thin	medium	east	23	15000	0.2821
28	rut_auto_deep_avg_pct	HR	IH	thin	medium	north	23	15000	0.2821
29	rut_auto_deep_avg_pct	HR	IH	thin	medium	south	23	15000	0.2821
30	rut_auto_deep_avg_pct	HR	IH	thin	medium	west	23	15000	0.2662
31	rut_auto_deep_avg_pct	HR	IH	thin	high	central	23	15000	0.2821
32	rut_auto_deep_avg_pct	HR	IH	thin	high	east	23	15000	0.2821
33	rut_auto_deep_avg_pct	HR	IH	thin	high	north	23	15000	0.2821
34	rut_auto_deep_avg_pct	HR	IH	thin	high	south	23	15000	0.2821
35	rut_auto_deep_avg_pct	HR	IH	thin	high	west	23	15000	0.2662
36	rut_auto_deep_avg_pct	HR	IH	thin	heavy	central	23	15000	0.2821
37	rut_auto_deep_avg_pct	HR	IH	thin	heavy	east	23	15000	0.2821
38	rut_auto_deep_avg_pct	HR	IH	thin	heavy	north	23	15000	0.2821
39	rut_auto_deep_avg_pct	HR	IH	thin	heavy	south	23	15000	0.2821
40	rut_auto_deep_avg_pct	HR	IH	thin	heavy	west	23	15000	0.2662

Table B.38: Deep Rut Model Coefficients for HR and US

group	distress	treat_lvl	highway_fun	pavement_typ	traffic_cls	climate_zone	alpha	A_star	beta_star
41	rut_auto_deep_avg_pct	HR	US	thick	low	central	23	15000	0.2839
42						east	23	15000	0.2403
43						north	23	15000	0.2457
44						south	23	15000	0.2658
45						west	23	15000	0.2753
46					medium	central	23	15000	0.2839
47						east	23	15000	0.2403
48						north	23	15000	0.2457
49						south	23	15000	0.2658
50						west	23	15000	0.2753
51					high	central	23	15000	0.2839
52						east	23	15000	0.2403
53						north	23	15000	0.2457
54						south	23	15000	0.2658
55						west	23	15000	0.2753
56					heavy	central	23	15000	0.2823
57						east	23	15000	0.2746
58						north	23	15000	0.1927
59						south	23	15000	0.2577
60						west	23	15000	0.2548
61				thin	low	central	23	15000	0.1420
62						east	23	15000	0.0869
63						north	23	15000	0.1420
64						south	23	15000	0.1420
65						west	23	15000	0.2370
66					medium	central	23	15000	0.1420
67						east	23	15000	0.0869
68						north	23	15000	0.1420
69						south	23	15000	0.1420
70						west	23	15000	0.2370
71					high	central	23	15000	0.1547
72						east	23	15000	0.2160
73						north	23	15000	0.2685
74						south	23	15000	0.2530
75						west	23	15000	0.2403
76					heavy	central	23	15000	0.2297
77						east	23	15000	0.2353
78						north	23	15000	0.2465
79						south	23	15000	0.2591
80						west	23	15000	0.2297

Table B.39: Deep Rut Model Coefficients for HR and SH

group	distress	treat_lvl	highway_fun	pavement_typ	traffic_cls	climate_zone	alpha	A_star	beta_star
81	rut_auto_deep_avg_pct	HR	SH	thick	low	central	23	15000	0.2543
82	rut_auto_deep_avg_pct	HR	SH	thick	low	east	23	15000	0.2235
83	rut_auto_deep_avg_pct	HR	SH	thick	low	north	23	15000	0.2652
84	rut_auto_deep_avg_pct	HR	SH	thick	low	south	23	15000	0.1716
85	rut_auto_deep_avg_pct	HR	SH	thick	low	west	23	15000	0.2465
86	rut_auto_deep_avg_pct	HR	SH	thick	medium	central	23	15000	0.2543
87	rut_auto_deep_avg_pct	HR	SH	thick	medium	east	23	15000	0.2235
88	rut_auto_deep_avg_pct	HR	SH	thick	medium	north	23	15000	0.2652
89	rut_auto_deep_avg_pct	HR	SH	thick	medium	south	23	15000	0.1716
90	rut_auto_deep_avg_pct	HR	SH	thick	medium	west	23	15000	0.2465
91	rut_auto_deep_avg_pct	HR	SH	thick	high	central	23	15000	0.2543
92	rut_auto_deep_avg_pct	HR	SH	thick	high	east	23	15000	0.2235
93	rut_auto_deep_avg_pct	HR	SH	thick	high	north	23	15000	0.2652
94	rut_auto_deep_avg_pct	HR	SH	thick	high	south	23	15000	0.1716
95	rut_auto_deep_avg_pct	HR	SH	thick	high	west	23	15000	0.2465
96	rut_auto_deep_avg_pct	HR	SH	thick	heavy	central	23	15000	0.2292
97	rut_auto_deep_avg_pct	HR	SH	thick	heavy	east	23	15000	0.2832
98	rut_auto_deep_avg_pct	HR	SH	thick	heavy	north	23	15000	0.2292
99	rut_auto_deep_avg_pct	HR	SH	thick	heavy	south	23	15000	0.2410
100	rut_auto_deep_avg_pct	HR	SH	thick	heavy	west	23	15000	0.2641
101	rut_auto_deep_avg_pct	HR	SH	thin	low	central	23	15000	0.2532
102	rut_auto_deep_avg_pct	HR	SH	thin	low	east	23	15000	0.2295
103	rut_auto_deep_avg_pct	HR	SH	thin	low	north	23	15000	0.2396
104	rut_auto_deep_avg_pct	HR	SH	thin	low	south	23	15000	0.1139
105	rut_auto_deep_avg_pct	HR	SH	thin	low	west	23	15000	0.2160
106	rut_auto_deep_avg_pct	HR	SH	thin	medium	central	23	15000	0.2532
107	rut_auto_deep_avg_pct	HR	SH	thin	medium	east	23	15000	0.2295
108	rut_auto_deep_avg_pct	HR	SH	thin	medium	north	23	15000	0.2396
109	rut_auto_deep_avg_pct	HR	SH	thin	medium	south	23	15000	0.1139
110	rut_auto_deep_avg_pct	HR	SH	thin	medium	west	23	15000	0.2160
111	rut_auto_deep_avg_pct	HR	SH	thin	high	central	23	15000	0.2231
112	rut_auto_deep_avg_pct	HR	SH	thin	high	east	23	15000	0.2093
113	rut_auto_deep_avg_pct	HR	SH	thin	high	north	23	15000	0.2002
114	rut_auto_deep_avg_pct	HR	SH	thin	high	south	23	15000	0.1984
115	rut_auto_deep_avg_pct	HR	SH	thin	high	west	23	15000	0.2164
116	rut_auto_deep_avg_pct	HR	SH	thin	heavy	central	23	15000	0.2620
117	rut_auto_deep_avg_pct	HR	SH	thin	heavy	east	23	15000	0.2533
118	rut_auto_deep_avg_pct	HR	SH	thin	heavy	north	23	15000	0.2620
119	rut_auto_deep_avg_pct	HR	SH	thin	heavy	south	23	15000	0.2205
120	rut_auto_deep_avg_pct	HR	SH	thin	heavy	west	23	15000	0.2130

Table B.40: Deep Rut Model Coefficients for HR and FM

group	distress	treat_lvl	highway_fun	pavement_typ	traffic_cls	climate_zone	alpha	A_star	beta_star
121	rut_auto_deep_avg_pct	HR	FM	thick	low	central	23	15000	0.1610
122						east	23	15000	0.1600
123						north	23	15000	0.1610
124						south	23	15000	0.1846
125						west	23	15000	0.1610
126					medium	central	23	15000	0.1509
127						east	23	15000	0.2896
128						north	23	15000	0.1736
129						south	23	15000	0.1539
130						west	23	15000	0.1509
131					high	central	23	15000	0.2181
132						east	23	15000	0.3020
133						north	23	15000	0.2324
134						south	23	15000	0.1881
135						west	23	15000	0.2280
136					heavy	central	23	15000	0.2181
137						east	23	15000	0.3020
138						north	23	15000	0.2324
139						south	23	15000	0.1881
140						west	23	15000	0.2280
141				thin	low	central	23	15000	0.1499
142						east	23	15000	0.1490
143						north	23	15000	0.1713
144						south	23	15000	0.1475
145						west	23	15000	0.1786
146					medium	central	23	15000	0.1740
147						east	23	15000	0.1674
148						north	23	15000	0.1426
149						south	23	15000	0.2029
150						west	23	15000	0.1927
151					high	central	23	15000	0.2264
152						east	23	15000	0.1864
153						north	23	15000	0.0561
154						south	23	15000	0.1996
155						west	23	15000	0.2196
156					heavy	central	23	15000	0.2264
157						east	23	15000	0.1864
158						north	23	15000	0.0561
159						south	23	15000	0.1996
160						west	23	15000	0.2196

Table B.41: Patching Model Coefficients for DN and IH

group	distress	treat_lvl	highway_fun	pavement_typ	traffic_cls	climate_zone	alpha	A_star	beta_star
1	patching_pct	DN	IH	thick	low	central	100	104.7756	0.6170
2						east	100	104.7756	0.5023
3						north	100	104.7756	0.6170
4						south	100	104.7756	0.4850
5						west	100	104.7756	0.6155
6					medium	central	100	104.7756	0.6170
7						east	100	104.7756	0.5023
8						north	100	104.7756	0.6170
9						south	100	104.7756	0.4850
10						west	100	104.7756	0.6155
11					high	central	100	104.7756	0.6170
12						east	100	104.7756	0.5023
13						north	100	104.7756	0.6170
14						south	100	104.7756	0.4850
15						west	100	104.7756	0.6155
16					heavy	central	100	104.7756	0.6170
17						east	100	104.7756	0.5023
18						north	100	104.7756	0.6170
19						south	100	104.7756	0.4850
20						west	100	104.7756	0.6155
21				thin	low	central	100	104.7756	0.2811
22						east	100	104.7756	0.4779
23						north	100	104.7756	0.2811
24						south	100	104.7756	0.2976
25						west	100	104.7756	0.2811
26					medium	central	100	104.7756	0.6610
27						east	100	104.7756	0.6610
28						north	100	104.7756	0.6610
29						south	100	104.7756	0.6610
30						west	100	104.7756	0.4841
31					high	central	100	104.7756	0.6610
32						east	100	104.7756	0.6610
33						north	100	104.7756	0.6610
34						south	100	104.7756	0.6610
35						west	100	104.7756	0.4841
36					heavy	central	100	104.7756	0.6610
37						east	100	104.7756	0.6610
38						north	100	104.7756	0.6610
39						south	100	104.7756	0.6610
40						west	100	104.7756	0.4841

Table B.42: Patching Model Coefficients for DN and US

group	distress	treat_lvl	highway_fun	pavement_typ	traffic_cls	climate_zone	alpha	A_star	beta_star
41	patching_pct	DN	US	thick	low	central	100	104.7756	0.4540
42	patching_pct	DN	US	thick	low	east	100	104.7756	0.6522
43	patching_pct	DN	US	thick	low	north	100	104.7756	0.2527
44	patching_pct	DN	US	thick	low	south	100	104.7756	0.5284
45	patching_pct	DN	US	thick	low	west	100	104.7756	0.6945
46	patching_pct	DN	US	thick	medium	central	100	104.7756	0.4540
47	patching_pct	DN	US	thick	medium	east	100	104.7756	0.6522
48	patching_pct	DN	US	thick	medium	north	100	104.7756	0.2527
49	patching_pct	DN	US	thick	medium	south	100	104.7756	0.5284
50	patching_pct	DN	US	thick	medium	west	100	104.7756	0.6945
51	patching_pct	DN	US	thick	high	central	100	104.7756	0.4540
52	patching_pct	DN	US	thick	high	east	100	104.7756	0.6522
53	patching_pct	DN	US	thick	high	north	100	104.7756	0.2527
54	patching_pct	DN	US	thick	high	south	100	104.7756	0.5284
55	patching_pct	DN	US	thick	high	west	100	104.7756	0.6945
56	patching_pct	DN	US	thick	heavy	central	100	104.7756	0.5998
57	patching_pct	DN	US	thick	heavy	east	100	104.7756	0.6097
58	patching_pct	DN	US	thick	heavy	north	100	104.7756	0.4731
59	patching_pct	DN	US	thick	heavy	south	100	104.7756	0.5699
60	patching_pct	DN	US	thick	heavy	west	100	104.7756	0.5871
61	patching_pct	DN	US	thin	low	central	100	104.7756	0.3333
62	patching_pct	DN	US	thin	low	east	100	104.7756	0.6118
63	patching_pct	DN	US	thin	low	north	100	104.7756	0.3333
64	patching_pct	DN	US	thin	low	south	100	104.7756	0.3333
65	patching_pct	DN	US	thin	low	west	100	104.7756	0.4781
66	patching_pct	DN	US	thin	medium	central	100	104.7756	0.3333
67	patching_pct	DN	US	thin	medium	east	100	104.7756	0.6118
68	patching_pct	DN	US	thin	medium	north	100	104.7756	0.3333
69	patching_pct	DN	US	thin	medium	south	100	104.7756	0.3333
70	patching_pct	DN	US	thin	medium	west	100	104.7756	0.4781
71	patching_pct	DN	US	thin	high	central	100	104.7756	0.3817
72	patching_pct	DN	US	thin	high	east	100	104.7756	0.2486
73	patching_pct	DN	US	thin	high	north	100	104.7756	0.6584
74	patching_pct	DN	US	thin	high	south	100	104.7756	0.5125
75	patching_pct	DN	US	thin	high	west	100	104.7756	0.5666
76	patching_pct	DN	US	thin	heavy	central	100	104.7756	0.3886
77	patching_pct	DN	US	thin	heavy	east	100	104.7756	0.5606
78	patching_pct	DN	US	thin	heavy	north	100	104.7756	0.4700
79	patching_pct	DN	US	thin	heavy	south	100	104.7756	0.5390
80	patching_pct	DN	US	thin	heavy	west	100	104.7756	0.3886

Table B.43: Patching Model Coefficients for DN and SH

group	distress	treat_lvl	highway_fun	pavement_typ	traffic_cls	climate_zone	alpha	A_star	beta_star
81	patching_pct	DN	SH	thick	low	central	100	104.7756	0.3631
82						east	100	104.7756	0.4070
83						north	100	104.7756	0.4089
84						south	100	104.7756	0.5140
85						west	100	104.7756	0.5886
86					medium	central	100	104.7756	0.3631
87						east	100	104.7756	0.4070
88						north	100	104.7756	0.4089
89						south	100	104.7756	0.5140
90						west	100	104.7756	0.5886
91					high	central	100	104.7756	0.3631
92						east	100	104.7756	0.4070
93						north	100	104.7756	0.4089
94						south	100	104.7756	0.5140
95						west	100	104.7756	0.5886
96					heavy	central	100	104.7756	0.4411
97						east	100	104.7756	0.4962
98						north	100	104.7756	0.4411
99						south	100	104.7756	0.4000
100						west	100	104.7756	0.5590
101				thin	low	central	100	104.7756	0.5013
102						east	100	104.7756	0.5314
103						north	100	104.7756	0.2973
104						south	100	104.7756	0.4620
105						west	100	104.7756	0.5235
106					medium	central	100	104.7756	0.5013
107						east	100	104.7756	0.5314
108						north	100	104.7756	0.2973
109						south	100	104.7756	0.4620
110						west	100	104.7756	0.5235
111					high	central	100	104.7756	0.4104
112						east	100	104.7756	0.6136
113						north	100	104.7756	0.3028
114						south	100	104.7756	0.2690
115						west	100	104.7756	0.4175
116					heavy	central	100	104.7756	0.5687
117						east	100	104.7756	0.4774
118						north	100	104.7756	0.5687
119						south	100	104.7756	0.5382
120						west	100	104.7756	0.5486

Table B.44: Patching Model Coefficients for DN and FM

group	distress	treat_lvl	highway_fun	pavement_typ	traffic_cls	climate_zone	alpha	A_star	beta_star
121	patching_pct	DN	FM	thick	low	central	100	104.7756	0.2618
122						east	100	104.7756	0.4043
123						north	100	104.7756	0.2618
124						south	100	104.7756	0.5229
125						west	100	104.7756	0.2618
126					medium	central	100	104.7756	0.2951
127						east	100	104.7756	0.4707
128						north	100	104.7756	0.4513
129						south	100	104.7756	0.3274
130						west	100	104.7756	0.2951
131					high	central	100	104.7756	0.5335
132						east	100	104.7756	0.5676
133						north	100	104.7756	0.4625
134						south	100	104.7756	0.3426
135						west	100	104.7756	0.4611
136					heavy	central	100	104.7756	0.5335
137						east	100	104.7756	0.5676
138						north	100	104.7756	0.4625
139						south	100	104.7756	0.3426
140						west	100	104.7756	0.4611
141				thin	low	central	100	104.7756	0.4098
142						east	100	104.7756	0.3640
143						north	100	104.7756	0.2868
144						south	100	104.7756	0.2967
145						west	100	104.7756	0.5213
146					medium	central	100	104.7756	0.3437
147						east	100	104.7756	0.4351
148						north	100	104.7756	0.2826
149						south	100	104.7756	0.3160
150						west	100	104.7756	0.5106
151					high	central	100	104.7756	0.4460
152						east	100	104.7756	0.4175
153						north	100	104.7756	0.3996
154						south	100	104.7756	0.3322
155						west	100	104.7756	0.4848
156					heavy	central	100	104.7756	0.4460
157						east	100	104.7756	0.4175
158						north	100	104.7756	0.3996
159						south	100	104.7756	0.3322
160						west	100	104.7756	0.4848

Table B.45: Patching Model Coefficients for PM and IH

group	distress	treat_lvl	highway_fun	pavement_typ	traffic_cls	climate_zone	alpha	A_star	beta_star
1	patching_pct	PM	IH	thick	low	central	100	120	0.6170
2						east	100	120	0.5023
3						north	100	120	0.6170
4						south	100	120	0.4850
5						west	100	120	0.6155
6					medium	central	100	120	0.6170
7						east	100	120	0.5023
8						north	100	120	0.6170
9						south	100	120	0.4850
10						west	100	120	0.6155
11					high	central	100	120	0.6170
12						east	100	120	0.5023
13						north	100	120	0.6170
14						south	100	120	0.4850
15						west	100	120	0.6155
16					heavy	central	100	120	0.6170
17						east	100	120	0.5023
18						north	100	120	0.6170
19						south	100	120	0.4850
20						west	100	120	0.6155
21				thin	low	central	100	120	0.2811
22						east	100	120	0.4779
23						north	100	120	0.2811
24						south	100	120	0.2976
25						west	100	120	0.2811
26					medium	central	100	120	0.6610
27						east	100	120	0.6610
28						north	100	120	0.6610
29						south	100	120	0.6610
30						west	100	120	0.4841
31					high	central	100	120	0.6610
32						east	100	120	0.6610
33						north	100	120	0.6610
34						south	100	120	0.6610
35						west	100	120	0.4841
36					heavy	central	100	120	0.6610
37						east	100	120	0.6610
38						north	100	120	0.6610
39						south	100	120	0.6610
40						west	100	120	0.4841

Table B.46: Patching Model Coefficients for PM and US

group	distress	treat_lvl	highway_fun	pavement_typ	traffic_cls	climate_zone	alpha	A_star	beta_star
41	patching_pct	PM	US	thick	low	central	100	120	0.4540
42						east	100	120	0.6522
43						north	100	120	0.2527
44						south	100	120	0.5284
45						west	100	120	0.6945
46					medium	central	100	120	0.4540
47						east	100	120	0.6522
48						north	100	120	0.2527
49						south	100	120	0.5284
50						west	100	120	0.6945
51					high	central	100	120	0.4540
52						east	100	120	0.6522
53						north	100	120	0.2527
54						south	100	120	0.5284
55						west	100	120	0.6945
56					heavy	central	100	120	0.5998
57						east	100	120	0.6097
58						north	100	120	0.4731
59						south	100	120	0.5699
60						west	100	120	0.5871
61				thin	low	central	100	120	0.3333
62						east	100	120	0.6118
63						north	100	120	0.3333
64						south	100	120	0.3333
65						west	100	120	0.4781
66					medium	central	100	120	0.3333
67						east	100	120	0.6118
68						north	100	120	0.3333
69						south	100	120	0.3333
70						west	100	120	0.4781
71					high	central	100	120	0.3817
72						east	100	120	0.2486
73						north	100	120	0.6584
74						south	100	120	0.5125
75						west	100	120	0.5666
76					heavy	central	100	120	0.3886
77						east	100	120	0.5606
78						north	100	120	0.4700
79						south	100	120	0.5390
80						west	100	120	0.3886

Table B.47: Patching Model Coefficients for PM and SH

group	distress	treat_lvl	highway_fun	pavement_typ	traffic_cls	climate_zone	alpha	A_star	beta_star
81	patching_pct	PM	SH	thick	low	central	100	120	0.3631
82						east	100	120	0.4070
83						north	100	120	0.4089
84						south	100	120	0.5140
85						west	100	120	0.5886
86					medium	central	100	120	0.3631
87						east	100	120	0.4070
88						north	100	120	0.4089
89						south	100	120	0.5140
90						west	100	120	0.5886
91					high	central	100	120	0.3631
92						east	100	120	0.4070
93						north	100	120	0.4089
94						south	100	120	0.5140
95						west	100	120	0.5886
96					heavy	central	100	120	0.4411
97						east	100	120	0.4962
98						north	100	120	0.4411
99						south	100	120	0.4000
100						west	100	120	0.5590
101				thin	low	central	100	120	0.5013
102						east	100	120	0.5314
103						north	100	120	0.2973
104						south	100	120	0.4620
105						west	100	120	0.5235
106					medium	central	100	120	0.5013
107						east	100	120	0.5314
108						north	100	120	0.2973
109						south	100	120	0.4620
110						west	100	120	0.5235
111					high	central	100	120	0.4104
112						east	100	120	0.6136
113						north	100	120	0.3028
114						south	100	120	0.2690
115						west	100	120	0.4175
116					heavy	central	100	120	0.5687
117						east	100	120	0.4774
118						north	100	120	0.5687
119						south	100	120	0.5382
120						west	100	120	0.5486

Table B.48: Patching Model Coefficients for PM and FM

group	distress	treat_lvl	highway_fun	pavement_typ	traffic_cls	climate_zone	alpha	A_star	beta_star
121	patching_pct	PM	FM	thick	low	central	100	120	0.2618
122						east	100	120	0.4043
123						north	100	120	0.2618
124						south	100	120	0.5229
125						west	100	120	0.2618
126					medium	central	100	120	0.2951
127						east	100	120	0.4707
128						north	100	120	0.4513
129						south	100	120	0.3274
130						west	100	120	0.2951
131					high	central	100	120	0.5335
132						east	100	120	0.5676
133						north	100	120	0.4625
134						south	100	120	0.3426
135						west	100	120	0.4611
136					heavy	central	100	120	0.5335
137						east	100	120	0.5676
138						north	100	120	0.4625
139						south	100	120	0.3426
140						west	100	120	0.4611
141				thin	low	central	100	120	0.4098
142						east	100	120	0.3640
143						north	100	120	0.2868
144						south	100	120	0.2967
145						west	100	120	0.5213
146					medium	central	100	120	0.3437
147						east	100	120	0.4351
148						north	100	120	0.2826
149						south	100	120	0.3160
150						west	100	120	0.5106
151					high	central	100	120	0.4460
152						east	100	120	0.4175
153						north	100	120	0.3996
154						south	100	120	0.3322
155						west	100	120	0.4848
156					heavy	central	100	120	0.4460
157						east	100	120	0.4175
158						north	100	120	0.3996
159						south	100	120	0.3322
160						west	100	120	0.4848

Table B.49: Patching Model Coefficients for LR and IH

group	distress	treat_lvl	highway_fun	pavement_typ	traffic_cls	climate_zone	alpha	A_star	beta_star
1	patching_pct	LR	IH	thick	low	central	100	130	0.6170
2						east	100	130	0.5023
3						north	100	130	0.6170
4						south	100	130	0.4850
5						west	100	130	0.6155
6					medium	central	100	130	0.6170
7						east	100	130	0.5023
8						north	100	130	0.6170
9						south	100	130	0.4850
10						west	100	130	0.6155
11					high	central	100	130	0.6170
12						east	100	130	0.5023
13						north	100	130	0.6170
14						south	100	130	0.4850
15						west	100	130	0.6155
16					heavy	central	100	130	0.6170
17						east	100	130	0.5023
18						north	100	130	0.6170
19						south	100	130	0.4850
20						west	100	130	0.6155
21				thin	low	central	100	130	0.2811
22						east	100	130	0.4779
23						north	100	130	0.2811
24						south	100	130	0.2976
25						west	100	130	0.2811
26					medium	central	100	130	0.6610
27						east	100	130	0.6610
28						north	100	130	0.6610
29						south	100	130	0.6610
30						west	100	130	0.4841
31					high	central	100	130	0.6610
32						east	100	130	0.6610
33						north	100	130	0.6610
34						south	100	130	0.6610
35						west	100	130	0.4841
36					heavy	central	100	130	0.6610
37						east	100	130	0.6610
38						north	100	130	0.6610
39						south	100	130	0.6610
40						west	100	130	0.4841

Table B.50: Patching Model Coefficients for LR and US

group	distress	treat_lvl	highway_fun	pavement_typ	traffic_cls	climate_zone	alpha	A_star	beta_star
41	patching_pct	LR	US	thick	low	central	100	130	0.4540
42						east	100	130	0.6522
43						north	100	130	0.2527
44						south	100	130	0.5284
45						west	100	130	0.6945
46					medium	central	100	130	0.4540
47						east	100	130	0.6522
48						north	100	130	0.2527
49						south	100	130	0.5284
50						west	100	130	0.6945
51					high	central	100	130	0.4540
52						east	100	130	0.6522
53						north	100	130	0.2527
54						south	100	130	0.5284
55						west	100	130	0.6945
56					heavy	central	100	130	0.5998
57						east	100	130	0.6097
58						north	100	130	0.4731
59						south	100	130	0.5699
60						west	100	130	0.5871
61				thin	low	central	100	130	0.3333
62						east	100	130	0.6118
63						north	100	130	0.3333
64						south	100	130	0.3333
65						west	100	130	0.4781
66					medium	central	100	130	0.3333
67						east	100	130	0.6118
68						north	100	130	0.3333
69						south	100	130	0.3333
70						west	100	130	0.4781
71					high	central	100	130	0.3817
72						east	100	130	0.2486
73						north	100	130	0.6584
74						south	100	130	0.5125
75						west	100	130	0.5666
76					heavy	central	100	130	0.3886
77						east	100	130	0.5606
78						north	100	130	0.4700
79						south	100	130	0.5390
80						west	100	130	0.3886

Table B.51: Patching Model Coefficients for LR and SH

group	distress	treat_lvl	highway_fun	pavement_typ	traffic_cls	climate_zone	alpha	A_star	beta_star
81	patching_pct	LR	SH	thick	low	central	100	130	0.3631
82						east	100	130	0.4070
83						north	100	130	0.4089
84						south	100	130	0.5140
85						west	100	130	0.5886
86					medium	central	100	130	0.3631
87						east	100	130	0.4070
88						north	100	130	0.4089
89						south	100	130	0.5140
90						west	100	130	0.5886
91					high	central	100	130	0.3631
92						east	100	130	0.4070
93						north	100	130	0.4089
94						south	100	130	0.5140
95						west	100	130	0.5886
96					heavy	central	100	130	0.4411
97						east	100	130	0.4962
98						north	100	130	0.4411
99						south	100	130	0.4000
100						west	100	130	0.5590
101				thin	low	central	100	130	0.5013
102						east	100	130	0.5314
103						north	100	130	0.2973
104						south	100	130	0.4620
105						west	100	130	0.5235
106					medium	central	100	130	0.5013
107						east	100	130	0.5314
108						north	100	130	0.2973
109						south	100	130	0.4620
110						west	100	130	0.5235
111					high	central	100	130	0.4104
112						east	100	130	0.6136
113						north	100	130	0.3028
114						south	100	130	0.2690
115						west	100	130	0.4175
116					heavy	central	100	130	0.5687
117						east	100	130	0.4774
118						north	100	130	0.5687
119						south	100	130	0.5382
120						west	100	130	0.5486

Table B.52: Patching Model Coefficients for LR and FM

group	distress	treat_lvl	highway_fun	pavement_typ	traffic_cls	climate_zone	alpha	A_star	beta_star
121	patching_pct	LR	FM	thick	low	central	100	130	0.2618
122						east	100	130	0.4043
123						north	100	130	0.2618
124						south	100	130	0.5229
125						west	100	130	0.2618
126					medium	central	100	130	0.2951
127						east	100	130	0.4707
128						north	100	130	0.4513
129						south	100	130	0.3274
130						west	100	130	0.2951
131					high	central	100	130	0.5335
132						east	100	130	0.5676
133						north	100	130	0.4625
134						south	100	130	0.3426
135						west	100	130	0.4611
136					heavy	central	100	130	0.5335
137						east	100	130	0.5676
138						north	100	130	0.4625
139						south	100	130	0.3426
140						west	100	130	0.4611
141				thin	low	central	100	130	0.4098
142						east	100	130	0.3640
143						north	100	130	0.2868
144						south	100	130	0.2967
145						west	100	130	0.5213
146					medium	central	100	130	0.3437
147						east	100	130	0.4351
148						north	100	130	0.2826
149						south	100	130	0.3160
150						west	100	130	0.5106
151					high	central	100	130	0.4460
152						east	100	130	0.4175
153						north	100	130	0.3996
154						south	100	130	0.3322
155						west	100	130	0.4848
156					heavy	central	100	130	0.4460
157						east	100	130	0.4175
158						north	100	130	0.3996
159						south	100	130	0.3322
160						west	100	130	0.4848

Table B.53: Patching Model Coefficients for MR and IH

group	distress	treat_lvl	highway_fun	pavement_typ	traffic_cls	climate_zone	alpha	A_star	beta_star
1	patching_pct	MR	IH	thick	low	central	100	150	0.6170
2						east	100	150	0.5023
3						north	100	150	0.6170
4						south	100	150	0.4850
5						west	100	150	0.6155
6					medium	central	100	150	0.6170
7						east	100	150	0.5023
8						north	100	150	0.6170
9						south	100	150	0.4850
10						west	100	150	0.6155
11					high	central	100	150	0.6170
12						east	100	150	0.5023
13						north	100	150	0.6170
14						south	100	150	0.4850
15						west	100	150	0.6155
16					heavy	central	100	150	0.6170
17						east	100	150	0.5023
18						north	100	150	0.6170
19						south	100	150	0.4850
20						west	100	150	0.6155
21				thin	low	central	100	150	0.2811
22						east	100	150	0.4779
23						north	100	150	0.2811
24						south	100	150	0.2976
25						west	100	150	0.2811
26					medium	central	100	150	0.6610
27						east	100	150	0.6610
28						north	100	150	0.6610
29						south	100	150	0.6610
30						west	100	150	0.4841
31					high	central	100	150	0.6610
32						east	100	150	0.6610
33						north	100	150	0.6610
34						south	100	150	0.6610
35						west	100	150	0.4841
36					heavy	central	100	150	0.6610
37						east	100	150	0.6610
38						north	100	150	0.6610
39						south	100	150	0.6610
40						west	100	150	0.4841

Table B.54: Patching Model Coefficients for MR and US

group	distress	treat_lvl	highway_fun	pavement_typ	traffic_cls	climate_zone	alpha	A_star	beta_star
41	patching_pct	MR	US	thick	low	central	100	150	0.4540
42						east	100	150	0.6522
43						north	100	150	0.2527
44						south	100	150	0.5284
45						west	100	150	0.6945
46					medium	central	100	150	0.4540
47						east	100	150	0.6522
48						north	100	150	0.2527
49						south	100	150	0.5284
50						west	100	150	0.6945
51					high	central	100	150	0.4540
52						east	100	150	0.6522
53						north	100	150	0.2527
54						south	100	150	0.5284
55						west	100	150	0.6945
56					heavy	central	100	150	0.5998
57						east	100	150	0.6097
58						north	100	150	0.4731
59						south	100	150	0.5699
60						west	100	150	0.5871
61				thin	low	central	100	150	0.3333
62						east	100	150	0.6118
63						north	100	150	0.3333
64						south	100	150	0.3333
65						west	100	150	0.4781
66					medium	central	100	150	0.3333
67						east	100	150	0.6118
68						north	100	150	0.3333
69						south	100	150	0.3333
70						west	100	150	0.4781
71					high	central	100	150	0.3817
72						east	100	150	0.2486
73						north	100	150	0.6584
74						south	100	150	0.5125
75						west	100	150	0.5666
76					heavy	central	100	150	0.3886
77						east	100	150	0.5606
78						north	100	150	0.4700
79						south	100	150	0.5390
80						west	100	150	0.3886

Table B.55: Patching Model Coefficients for MR and SH

group	distress	treat_lvl	highway_fun	pavement_typ	traffic_cls	climate_zone	alpha	A_star	beta_star
81	patching_pct	MR	SH	thick	low	central	100	150	0.3631
82						east	100	150	0.4070
83						north	100	150	0.4089
84						south	100	150	0.5140
85						west	100	150	0.5886
86					medium	central	100	150	0.3631
87						east	100	150	0.4070
88						north	100	150	0.4089
89						south	100	150	0.5140
90						west	100	150	0.5886
91					high	central	100	150	0.3631
92						east	100	150	0.4070
93						north	100	150	0.4089
94						south	100	150	0.5140
95						west	100	150	0.5886
96					heavy	central	100	150	0.4411
97						east	100	150	0.4962
98						north	100	150	0.4411
99						south	100	150	0.4000
100						west	100	150	0.5590
101				thin	low	central	100	150	0.5013
102						east	100	150	0.5314
103						north	100	150	0.2973
104						south	100	150	0.4620
105						west	100	150	0.5235
106					medium	central	100	150	0.5013
107						east	100	150	0.5314
108						north	100	150	0.2973
109						south	100	150	0.4620
110						west	100	150	0.5235
111					high	central	100	150	0.4104
112						east	100	150	0.6136
113						north	100	150	0.3028
114						south	100	150	0.2690
115						west	100	150	0.4175
116					heavy	central	100	150	0.5687
117						east	100	150	0.4774
118						north	100	150	0.5687
119						south	100	150	0.5382
120						west	100	150	0.5486

Table B.56: Patching Model Coefficients for MR and FM

group	distress	treat_lvl	highway_fun	pavement_typ	traffic_cls	climate_zone	alpha	A_star	beta_star
121	patching_pct	MR	FM	thick	low	central	100	150	0.2618
122						east	100	150	0.4043
123						north	100	150	0.2618
124						south	100	150	0.5229
125						west	100	150	0.2618
126					medium	central	100	150	0.2951
127						east	100	150	0.4707
128						north	100	150	0.4513
129						south	100	150	0.3274
130						west	100	150	0.2951
131					high	central	100	150	0.5335
132						east	100	150	0.5676
133						north	100	150	0.4625
134						south	100	150	0.3426
135						west	100	150	0.4611
136					heavy	central	100	150	0.5335
137						east	100	150	0.5676
138						north	100	150	0.4625
139						south	100	150	0.3426
140						west	100	150	0.4611
141				thin	low	central	100	150	0.4098
142						east	100	150	0.3640
143						north	100	150	0.2868
144						south	100	150	0.2967
145						west	100	150	0.5213
146					medium	central	100	150	0.3437
147						east	100	150	0.4351
148						north	100	150	0.2826
149						south	100	150	0.3160
150						west	100	150	0.5106
151					high	central	100	150	0.4460
152						east	100	150	0.4175
153						north	100	150	0.3996
154						south	100	150	0.3322
155						west	100	150	0.4848
156					heavy	central	100	150	0.4460
157						east	100	150	0.4175
158						north	100	150	0.3996
159						south	100	150	0.3322
160						west	100	150	0.4848

Table B.57: Patching Model Coefficients for HR and IH

group	distress	treat_lvl	highway_fun	pavement_typ	traffic_cls	climate_zone	alpha	A_star	beta_star
1	patching_pct	HR	IH	thick	low	central	100	180	0.6170
2						east	100	180	0.5023
3						north	100	180	0.6170
4						south	100	180	0.4850
5						west	100	180	0.6155
6					medium	central	100	180	0.6170
7						east	100	180	0.5023
8						north	100	180	0.6170
9						south	100	180	0.4850
10						west	100	180	0.6155
11					high	central	100	180	0.6170
12						east	100	180	0.5023
13						north	100	180	0.6170
14						south	100	180	0.4850
15						west	100	180	0.6155
16					heavy	central	100	180	0.6170
17						east	100	180	0.5023
18						north	100	180	0.6170
19						south	100	180	0.4850
20						west	100	180	0.6155
21				thin	low	central	100	180	0.2811
22						east	100	180	0.4779
23						north	100	180	0.2811
24						south	100	180	0.2976
25						west	100	180	0.2811
26					medium	central	100	180	0.6610
27						east	100	180	0.6610
28						north	100	180	0.6610
29						south	100	180	0.6610
30						west	100	180	0.4841
31					high	central	100	180	0.6610
32						east	100	180	0.6610
33						north	100	180	0.6610
34						south	100	180	0.6610
35						west	100	180	0.4841
36					heavy	central	100	180	0.6610
37						east	100	180	0.6610
38						north	100	180	0.6610
39						south	100	180	0.6610
40						west	100	180	0.4841

Table B.58: Patching Model Coefficients for HR and US

group	distress	treat_lvl	highway_fun	pavement_typ	traffic_cls	climate_zone	alpha	A_star	beta_star
41	patching_pct	HR	US	thick	low	central	100	180	0.4540
42						east	100	180	0.6522
43						north	100	180	0.2527
44						south	100	180	0.5284
45						west	100	180	0.6945
46					medium	central	100	180	0.4540
47						east	100	180	0.6522
48						north	100	180	0.2527
49						south	100	180	0.5284
50						west	100	180	0.6945
51					high	central	100	180	0.4540
52						east	100	180	0.6522
53						north	100	180	0.2527
54						south	100	180	0.5284
55						west	100	180	0.6945
56					heavy	central	100	180	0.5998
57						east	100	180	0.6097
58						north	100	180	0.4731
59						south	100	180	0.5699
60						west	100	180	0.5871
61				thin	low	central	100	180	0.3333
62						east	100	180	0.6118
63						north	100	180	0.3333
64						south	100	180	0.3333
65						west	100	180	0.4781
66					medium	central	100	180	0.3333
67						east	100	180	0.6118
68						north	100	180	0.3333
69						south	100	180	0.3333
70						west	100	180	0.4781
71					high	central	100	180	0.3817
72						east	100	180	0.2486
73						north	100	180	0.6584
74						south	100	180	0.5125
75						west	100	180	0.5666
76					heavy	central	100	180	0.3886
77						east	100	180	0.5606
78						north	100	180	0.4700
79						south	100	180	0.5390
80						west	100	180	0.3886

Table B.59: Patching Model Coefficients for HR and SH

group	distress	treat_lvl	highway_fun	pavement_typ	traffic_cls	climate_zone	alpha	A_star	beta_star
81	patching_pct	HR	SH	thick	low	central	100	180	0.3631
82						east	100	180	0.4070
83						north	100	180	0.4089
84						south	100	180	0.5140
85						west	100	180	0.5886
86					medium	central	100	180	0.3631
87						east	100	180	0.4070
88						north	100	180	0.4089
89						south	100	180	0.5140
90						west	100	180	0.5886
91					high	central	100	180	0.3631
92						east	100	180	0.4070
93						north	100	180	0.4089
94						south	100	180	0.5140
95						west	100	180	0.5886
96					heavy	central	100	180	0.4411
97						east	100	180	0.4962
98						north	100	180	0.4411
99						south	100	180	0.4000
100						west	100	180	0.5590
101				thin	low	central	100	180	0.5013
102						east	100	180	0.5314
103						north	100	180	0.2973
104						south	100	180	0.4620
105						west	100	180	0.5235
106					medium	central	100	180	0.5013
107						east	100	180	0.5314
108						north	100	180	0.2973
109						south	100	180	0.4620
110						west	100	180	0.5235
111					high	central	100	180	0.4104
112						east	100	180	0.6136
113						north	100	180	0.3028
114						south	100	180	0.2690
115						west	100	180	0.4175
116					heavy	central	100	180	0.5687
117						east	100	180	0.4774
118						north	100	180	0.5687
119						south	100	180	0.5382
120						west	100	180	0.5486

Table B.60: Patching Model Coefficients for HR and FM

group	distress	treat_lvl	highway_fun	pavement_typ	traffic_cls	climate_zone	alpha	A_star	beta_star
121	patching_pct	HR	FM	thick	low	central	100	180	0.2618
122						east	100	180	0.4043
123						north	100	180	0.2618
124						south	100	180	0.5229
125						west	100	180	0.2618
126					medium	central	100	180	0.2951
127						east	100	180	0.4707
128						north	100	180	0.4513
129						south	100	180	0.3274
130						west	100	180	0.2951
131					high	central	100	180	0.5335
132						east	100	180	0.5676
133						north	100	180	0.4625
134						south	100	180	0.3426
135						west	100	180	0.4611
136					heavy	central	100	180	0.5335
137						east	100	180	0.5676
138						north	100	180	0.4625
139						south	100	180	0.3426
140						west	100	180	0.4611
141				thin	low	central	100	180	0.4098
142						east	100	180	0.3640
143						north	100	180	0.2868
144						south	100	180	0.2967
145						west	100	180	0.5213
146					medium	central	100	180	0.3437
147						east	100	180	0.4351
148						north	100	180	0.2826
149						south	100	180	0.3160
150						west	100	180	0.5106
151					high	central	100	180	0.4460
152						east	100	180	0.4175
153						north	100	180	0.3996
154						south	100	180	0.3322
155						west	100	180	0.4848
156					heavy	central	100	180	0.4460
157						east	100	180	0.4175
158						north	100	180	0.3996
159						south	100	180	0.3322
160						west	100	180	0.4848

Table B.61: Failure Model Coefficients for DN and IH

group	distress	treat_lvl	highway_fun	pavement_typ	traffic_cls	climate_zone	alpha	A_star	beta_star
1	failure_qty	DN	IH	thick	low	central	10	21.8229	2.3327
2	failure_qty	DN	IH	thick	low	east	10	21.8229	1.9422
3	failure_qty	DN	IH	thick	low	north	10	21.8229	2.3327
4	failure_qty	DN	IH	thick	low	south	10	21.8229	1.8975
5	failure_qty	DN	IH	thick	low	west	10	21.8229	2.0496
6	failure_qty	DN	IH	thick	medium	central	10	21.8229	2.3327
7	failure_qty	DN	IH	thick	medium	east	10	21.8229	1.9422
8	failure_qty	DN	IH	thick	medium	north	10	21.8229	2.3327
9	failure_qty	DN	IH	thick	medium	south	10	21.8229	1.8975
10	failure_qty	DN	IH	thick	medium	west	10	21.8229	2.0496
11	failure_qty	DN	IH	thick	high	central	10	21.8229	2.3327
12	failure_qty	DN	IH	thick	high	east	10	21.8229	1.9422
13	failure_qty	DN	IH	thick	high	north	10	21.8229	2.3327
14	failure_qty	DN	IH	thick	high	south	10	21.8229	1.8975
15	failure_qty	DN	IH	thick	high	west	10	21.8229	2.0496
16	failure_qty	DN	IH	thick	heavy	central	10	21.8229	2.3327
17	failure_qty	DN	IH	thick	heavy	east	10	21.8229	1.9422
18	failure_qty	DN	IH	thick	heavy	north	10	21.8229	2.3327
19	failure_qty	DN	IH	thick	heavy	south	10	21.8229	1.8975
20	failure_qty	DN	IH	thick	heavy	west	10	21.8229	2.0496
21	failure_qty	DN	IH	thin	low	central	10	21.8229	2.4684
22	failure_qty	DN	IH	thin	low	east	10	21.8229	1.8912
23	failure_qty	DN	IH	thin	low	north	10	21.8229	2.4684
24	failure_qty	DN	IH	thin	low	south	10	21.8229	0.1414
25	failure_qty	DN	IH	thin	low	west	10	21.8229	2.4684
26	failure_qty	DN	IH	thin	medium	central	10	21.8229	1.9248
27	failure_qty	DN	IH	thin	medium	east	10	21.8229	1.9248
28	failure_qty	DN	IH	thin	medium	north	10	21.8229	1.9248
29	failure_qty	DN	IH	thin	medium	south	10	21.8229	1.9248
30	failure_qty	DN	IH	thin	medium	west	10	21.8229	1.9680
31	failure_qty	DN	IH	thin	high	central	10	21.8229	1.9248
32	failure_qty	DN	IH	thin	high	east	10	21.8229	1.9248
33	failure_qty	DN	IH	thin	high	north	10	21.8229	1.9248
34	failure_qty	DN	IH	thin	high	south	10	21.8229	1.9248
35	failure_qty	DN	IH	thin	high	west	10	21.8229	1.9680
36	failure_qty	DN	IH	thin	heavy	central	10	21.8229	1.9248
37	failure_qty	DN	IH	thin	heavy	east	10	21.8229	1.9248
38	failure_qty	DN	IH	thin	heavy	north	10	21.8229	1.9248
39	failure_qty	DN	IH	thin	heavy	south	10	21.8229	1.9248
40	failure_qty	DN	IH	thin	heavy	west	10	21.8229	1.9680

Table B.62: Failure Model Coefficients for DN and US

group	distress	treat_lvl	highway_fun	pavement_typ	traffic_cls	climate_zone	alpha	A_star	beta_star
41	failure_qty	DN	US	thick	low	central	10	21.8229	2.1809
42	failure_qty	DN	US	thick	low	east	10	21.8229	3.0163
43	failure_qty	DN	US	thick	low	north	10	21.8229	1.8952
44	failure_qty	DN	US	thick	low	south	10	21.8229	1.8912
45	failure_qty	DN	US	thick	low	west	10	21.8229	2.8298
46	failure_qty	DN	US	thick	medium	central	10	21.8229	2.1809
47	failure_qty	DN	US	thick	medium	east	10	21.8229	3.0163
48	failure_qty	DN	US	thick	medium	north	10	21.8229	1.8952
49	failure_qty	DN	US	thick	medium	south	10	21.8229	1.8912
50	failure_qty	DN	US	thick	medium	west	10	21.8229	2.8298
51	failure_qty	DN	US	thick	high	central	10	21.8229	2.1809
52	failure_qty	DN	US	thick	high	east	10	21.8229	3.0163
53	failure_qty	DN	US	thick	high	north	10	21.8229	1.8952
54	failure_qty	DN	US	thick	high	south	10	21.8229	1.8912
55	failure_qty	DN	US	thick	high	west	10	21.8229	2.8298
56	failure_qty	DN	US	thick	heavy	central	10	21.8229	2.2628
57	failure_qty	DN	US	thick	heavy	east	10	21.8229	2.1761
58	failure_qty	DN	US	thick	heavy	north	10	21.8229	1.8912
59	failure_qty	DN	US	thick	heavy	south	10	21.8229	1.5104
60	failure_qty	DN	US	thick	heavy	west	10	21.8229	2.4561
61	failure_qty	DN	US	thin	low	central	10	21.8229	1.8913
62	failure_qty	DN	US	thin	low	east	10	21.8229	2.7977
63	failure_qty	DN	US	thin	low	north	10	21.8229	1.8913
64	failure_qty	DN	US	thin	low	south	10	21.8229	1.8913
65	failure_qty	DN	US	thin	low	west	10	21.8229	1.8912
66	failure_qty	DN	US	thin	medium	central	10	21.8229	1.8913
67	failure_qty	DN	US	thin	medium	east	10	21.8229	2.7977
68	failure_qty	DN	US	thin	medium	north	10	21.8229	1.8913
69	failure_qty	DN	US	thin	medium	south	10	21.8229	1.8913
70	failure_qty	DN	US	thin	medium	west	10	21.8229	1.8912
71	failure_qty	DN	US	thin	high	central	10	21.8229	1.8912
72	failure_qty	DN	US	thin	high	east	10	21.8229	2.0964
73	failure_qty	DN	US	thin	high	north	10	21.8229	2.7619
74	failure_qty	DN	US	thin	high	south	10	21.8229	1.8912
75	failure_qty	DN	US	thin	high	west	10	21.8229	1.8913
76	failure_qty	DN	US	thin	heavy	central	10	21.8229	2.7217
77	failure_qty	DN	US	thin	heavy	east	10	21.8229	1.9753
78	failure_qty	DN	US	thin	heavy	north	10	21.8229	1.8912
79	failure_qty	DN	US	thin	heavy	south	10	21.8229	1.8914
80	failure_qty	DN	US	thin	heavy	west	10	21.8229	2.7217

Table B.63: Failure Model Coefficients for DN and SH

group	distress	treat_lvl	highway_fun	pavement_typ	traffic_cls	climate_zone	alpha	A_star	beta_star
81	failure_qty	DN	SH	thick	low	central	10	21.8229	1.9322
82						east	10	21.8229	2.3244
83						north	10	21.8229	1.8912
84						south	10	21.8229	2.4845
85						west	10	21.8229	1.9761
86					medium	central	10	21.8229	1.9322
87						east	10	21.8229	2.3244
88						north	10	21.8229	1.8912
89						south	10	21.8229	2.4845
90						west	10	21.8229	1.9761
91					high	central	10	21.8229	1.9322
92						east	10	21.8229	2.3244
93						north	10	21.8229	1.8912
94						south	10	21.8229	2.4845
95						west	10	21.8229	1.9761
96					heavy	central	10	21.8229	2.6038
97						east	10	21.8229	3.0106
98						north	10	21.8229	2.6038
99						south	10	21.8229	1.8886
100						west	10	21.8229	1.9882
101				thin	low	central	10	21.8229	1.8912
102						east	10	21.8229	1.8904
103						north	10	21.8229	2.1803
104						south	10	21.8229	1.8912
105						west	10	21.8229	1.9167
106					medium	central	10	21.8229	1.8912
107						east	10	21.8229	1.8904
108						north	10	21.8229	2.1803
109						south	10	21.8229	1.8912
110						west	10	21.8229	1.9167
111					high	central	10	21.8229	2.0930
112						east	10	21.8229	2.5608
113						north	10	21.8229	1.6425
114						south	10	21.8229	2.2414
115						west	10	21.8229	1.3115
116					heavy	central	10	21.8229	2.1555
117						east	10	21.8229	2.1543
118						north	10	21.8229	2.1555
119						south	10	21.8229	1.0433
120						west	10	21.8229	2.4626

Table B.64: Failure Model Coefficients for DN and FM

group	distress	treat_lvl	highway_fun	pavement_typ	traffic_cls	climate_zone	alpha	A_star	beta_star
121	failure_qty	DN	FM	thick	low	central	10	21.8229	0.8731
122						east	10	21.8229	1.8960
123						north	10	21.8229	0.8731
124						south	10	21.8229	0.6207
125						west	10	21.8229	0.8731
126					medium	central	10	21.8229	0.7647
127						east	10	21.8229	2.6847
128						north	10	21.8229	1.8912
129						south	10	21.8229	1.8627
130						west	10	21.8229	0.7647
131					high	central	10	21.8229	1.6804
132						east	10	21.8229	3.2255
133						north	10	21.8229	1.8912
134						south	10	21.8229	1.8845
135						west	10	21.8229	1.8912
136					heavy	central	10	21.8229	1.6804
137						east	10	21.8229	3.2255
138						north	10	21.8229	1.8912
139						south	10	21.8229	1.8845
140						west	10	21.8229	1.8912
141				thin	low	central	10	21.8229	1.0510
142						east	10	21.8229	1.7830
143						north	10	21.8229	1.1485
144						south	10	21.8229	0.5287
145						west	10	21.8229	0.8932
146					medium	central	10	21.8229	1.2995
147						east	10	21.8229	1.6562
148						north	10	21.8229	1.9928
149						south	10	21.8229	0.4330
150						west	10	21.8229	2.3226
151					high	central	10	21.8229	1.8017
152						east	10	21.8229	1.6053
153						north	10	21.8229	1.6198
154						south	10	21.8229	0.4793
155						west	10	21.8229	1.5564
156					heavy	central	10	21.8229	1.8017
157						east	10	21.8229	1.6053
158						north	10	21.8229	1.6198
159						south	10	21.8229	0.4793
160						west	10	21.8229	1.5564

Table B.65: Failure Model Coefficients for PM and IH

group	distress	treat_lvl	highway_fun	pavement_typ	traffic_cls	climate_zone	alpha	A_star	beta_star
1	failure_qty	PM	IH	thick	low	central	10	25	2.3327
2	failure_qty	PM	IH	thick	low	east	10	25	1.9422
3	failure_qty	PM	IH	thick	low	north	10	25	2.3327
4	failure_qty	PM	IH	thick	low	south	10	25	1.8975
5	failure_qty	PM	IH	thick	low	west	10	25	2.0496
6	failure_qty	PM	IH	thick	medium	central	10	25	2.3327
7	failure_qty	PM	IH	thick	medium	east	10	25	1.9422
8	failure_qty	PM	IH	thick	medium	north	10	25	2.3327
9	failure_qty	PM	IH	thick	medium	south	10	25	1.8975
10	failure_qty	PM	IH	thick	medium	west	10	25	2.0496
11	failure_qty	PM	IH	thick	high	central	10	25	2.3327
12	failure_qty	PM	IH	thick	high	east	10	25	1.9422
13	failure_qty	PM	IH	thick	high	north	10	25	2.3327
14	failure_qty	PM	IH	thick	high	south	10	25	1.8975
15	failure_qty	PM	IH	thick	high	west	10	25	2.0496
16	failure_qty	PM	IH	thick	heavy	central	10	25	2.3327
17	failure_qty	PM	IH	thick	heavy	east	10	25	1.9422
18	failure_qty	PM	IH	thick	heavy	north	10	25	2.3327
19	failure_qty	PM	IH	thick	heavy	south	10	25	1.8975
20	failure_qty	PM	IH	thick	heavy	west	10	25	2.0496
21	failure_qty	PM	IH	thin	low	central	10	25	2.4684
22	failure_qty	PM	IH	thin	low	east	10	25	1.8912
23	failure_qty	PM	IH	thin	low	north	10	25	2.4684
24	failure_qty	PM	IH	thin	low	south	10	25	0.1414
25	failure_qty	PM	IH	thin	low	west	10	25	2.4684
26	failure_qty	PM	IH	thin	medium	central	10	25	1.9248
27	failure_qty	PM	IH	thin	medium	east	10	25	1.9248
28	failure_qty	PM	IH	thin	medium	north	10	25	1.9248
29	failure_qty	PM	IH	thin	medium	south	10	25	1.9248
30	failure_qty	PM	IH	thin	medium	west	10	25	1.9680
31	failure_qty	PM	IH	thin	high	central	10	25	1.9248
32	failure_qty	PM	IH	thin	high	east	10	25	1.9248
33	failure_qty	PM	IH	thin	high	north	10	25	1.9248
34	failure_qty	PM	IH	thin	high	south	10	25	1.9248
35	failure_qty	PM	IH	thin	high	west	10	25	1.9680
36	failure_qty	PM	IH	thin	heavy	central	10	25	1.9248
37	failure_qty	PM	IH	thin	heavy	east	10	25	1.9248
38	failure_qty	PM	IH	thin	heavy	north	10	25	1.9248
39	failure_qty	PM	IH	thin	heavy	south	10	25	1.9248
40	failure_qty	PM	IH	thin	heavy	west	10	25	1.9680

Table B.66: Failure Model Coefficients for PM and US

group	distress	treat_lvl	highway_fun	pavement_typ	traffic_cls	climate_zone	alpha	A_star	beta_star
41	failure_qty	PM	US	thick	low	central	10	25	2.1809
42						east	10	25	3.0163
43						north	10	25	1.8952
44						south	10	25	1.8912
45						west	10	25	2.8298
46					medium	central	10	25	2.1809
47						east	10	25	3.0163
48						north	10	25	1.8952
49						south	10	25	1.8912
50						west	10	25	2.8298
51					high	central	10	25	2.1809
52						east	10	25	3.0163
53						north	10	25	1.8952
54						south	10	25	1.8912
55						west	10	25	2.8298
56					heavy	central	10	25	2.2628
57						east	10	25	2.1761
58						north	10	25	1.8912
59						south	10	25	1.5104
60						west	10	25	2.4561
61				thin	low	central	10	25	1.8913
62						east	10	25	2.7977
63						north	10	25	1.8913
64						south	10	25	1.8913
65						west	10	25	1.8912
66					medium	central	10	25	1.8913
67						east	10	25	2.7977
68						north	10	25	1.8913
69						south	10	25	1.8913
70						west	10	25	1.8912
71					high	central	10	25	1.8912
72						east	10	25	2.0964
73						north	10	25	2.7619
74						south	10	25	1.8912
75						west	10	25	1.8913
76					heavy	central	10	25	2.7217
77						east	10	25	1.9753
78						north	10	25	1.8912
79						south	10	25	1.8914
80						west	10	25	2.7217

Table B.67: Failure Model Coefficients for PM and SH

group	distress	treat_lvl	highway_fun	pavement_typ	traffic_cls	climate_zone	alpha	A_star	beta_star
81	failure_qty	PM	SH	thick	low	central	10	25	1.9322
82						east	10	25	2.3244
83						north	10	25	1.8912
84						south	10	25	2.4845
85						west	10	25	1.9761
86					medium	central	10	25	1.9322
87						east	10	25	2.3244
88						north	10	25	1.8912
89						south	10	25	2.4845
90						west	10	25	1.9761
91					high	central	10	25	1.9322
92						east	10	25	2.3244
93						north	10	25	1.8912
94						south	10	25	2.4845
95						west	10	25	1.9761
96					heavy	central	10	25	2.6038
97						east	10	25	3.0106
98						north	10	25	2.6038
99						south	10	25	1.8886
100						west	10	25	1.9882
101				thin	low	central	10	25	1.8912
102						east	10	25	1.8904
103						north	10	25	2.1803
104						south	10	25	1.8912
105						west	10	25	1.9167
106					medium	central	10	25	1.8912
107						east	10	25	1.8904
108						north	10	25	2.1803
109						south	10	25	1.8912
110						west	10	25	1.9167
111					high	central	10	25	2.0930
112						east	10	25	2.5608
113						north	10	25	1.6425
114						south	10	25	2.2414
115						west	10	25	1.3115
116					heavy	central	10	25	2.1555
117						east	10	25	2.1543
118						north	10	25	2.1555
119						south	10	25	1.0433
120						west	10	25	2.4626

Table B.68: Failure Model Coefficients for PM and FM

group	distress	treat_lvl	highway_fun	pavement_typ	traffic_cls	climate_zone	alpha	A_star	beta_star
121	failure_qty	PM	FM	thick	low	central	10	25	0.8731
122	failure_qty	PM	FM	thick	low	east	10	25	1.8960
123	failure_qty	PM	FM	thick	low	north	10	25	0.8731
124	failure_qty	PM	FM	thick	low	south	10	25	0.6207
125	failure_qty	PM	FM	thick	low	west	10	25	0.8731
126	failure_qty	PM	FM	thick	medium	central	10	25	0.7647
127	failure_qty	PM	FM	thick	medium	east	10	25	2.6847
128	failure_qty	PM	FM	thick	medium	north	10	25	1.8912
129	failure_qty	PM	FM	thick	medium	south	10	25	1.8627
130	failure_qty	PM	FM	thick	medium	west	10	25	0.7647
131	failure_qty	PM	FM	thick	high	central	10	25	1.6804
132	failure_qty	PM	FM	thick	high	east	10	25	3.2255
133	failure_qty	PM	FM	thick	high	north	10	25	1.8912
134	failure_qty	PM	FM	thick	high	south	10	25	1.8845
135	failure_qty	PM	FM	thick	high	west	10	25	1.8912
136	failure_qty	PM	FM	thick	heavy	central	10	25	1.6804
137	failure_qty	PM	FM	thick	heavy	east	10	25	3.2255
138	failure_qty	PM	FM	thick	heavy	north	10	25	1.8912
139	failure_qty	PM	FM	thick	heavy	south	10	25	1.8845
140	failure_qty	PM	FM	thick	heavy	west	10	25	1.8912
141	failure_qty	PM	FM	thin	low	central	10	25	1.0510
142	failure_qty	PM	FM	thin	low	east	10	25	1.7830
143	failure_qty	PM	FM	thin	low	north	10	25	1.1485
144	failure_qty	PM	FM	thin	low	south	10	25	0.5287
145	failure_qty	PM	FM	thin	low	west	10	25	0.8932
146	failure_qty	PM	FM	thin	medium	central	10	25	1.2995
147	failure_qty	PM	FM	thin	medium	east	10	25	1.6562
148	failure_qty	PM	FM	thin	medium	north	10	25	1.9928
149	failure_qty	PM	FM	thin	medium	south	10	25	0.4330
150	failure_qty	PM	FM	thin	medium	west	10	25	2.3226
151	failure_qty	PM	FM	thin	high	central	10	25	1.8017
152	failure_qty	PM	FM	thin	high	east	10	25	1.6053
153	failure_qty	PM	FM	thin	high	north	10	25	1.6198
154	failure_qty	PM	FM	thin	high	south	10	25	0.4793
155	failure_qty	PM	FM	thin	high	west	10	25	1.5564
156	failure_qty	PM	FM	thin	heavy	central	10	25	1.8017
157	failure_qty	PM	FM	thin	heavy	east	10	25	1.6053
158	failure_qty	PM	FM	thin	heavy	north	10	25	1.6198
159	failure_qty	PM	FM	thin	heavy	south	10	25	0.4793
160	failure_qty	PM	FM	thin	heavy	west	10	25	1.5564

Table B.69: Failure Model Coefficients for LR and IH

group	distress	treat_lvl	highway_fun	pavement_typ	traffic_cls	climate_zone	alpha	A_star	beta_star
1	failure_qty	LR	IH	thick	low	central	10	27	2.3327
2						east	10	27	1.9422
3						north	10	27	2.3327
4						south	10	27	1.8975
5						west	10	27	2.0496
6					medium	central	10	27	2.3327
7						east	10	27	1.9422
8						north	10	27	2.3327
9						south	10	27	1.8975
10						west	10	27	2.0496
11					high	central	10	27	2.3327
12						east	10	27	1.9422
13						north	10	27	2.3327
14						south	10	27	1.8975
15						west	10	27	2.0496
16					heavy	central	10	27	2.3327
17						east	10	27	1.9422
18						north	10	27	2.3327
19						south	10	27	1.8975
20						west	10	27	2.0496
21				thin	low	central	10	27	2.4684
22						east	10	27	1.8912
23						north	10	27	2.4684
24						south	10	27	0.1414
25						west	10	27	2.4684
26					medium	central	10	27	1.9248
27						east	10	27	1.9248
28						north	10	27	1.9248
29						south	10	27	1.9248
30						west	10	27	1.9680
31					high	central	10	27	1.9248
32						east	10	27	1.9248
33						north	10	27	1.9248
34						south	10	27	1.9248
35						west	10	27	1.9680
36					heavy	central	10	27	1.9248
37						east	10	27	1.9248
38						north	10	27	1.9248
39						south	10	27	1.9248
40						west	10	27	1.9680

Table B.70: Failure Model Coefficients for LR and US

group	distress	treat_lvl	highway_fun	pavement_typ	traffic_cls	climate_zone	alpha	A_star	beta_star
41	failure_qty	LR	US	thick	low	central	10	27	2.1809
42						east	10	27	3.0163
43						north	10	27	1.8952
44						south	10	27	1.8912
45						west	10	27	2.8298
46					medium	central	10	27	2.1809
47						east	10	27	3.0163
48						north	10	27	1.8952
49						south	10	27	1.8912
50						west	10	27	2.8298
51					high	central	10	27	2.1809
52						east	10	27	3.0163
53						north	10	27	1.8952
54						south	10	27	1.8912
55						west	10	27	2.8298
56					heavy	central	10	27	2.2628
57						east	10	27	2.1761
58						north	10	27	1.8912
59						south	10	27	1.5104
60						west	10	27	2.4561
61				thin	low	central	10	27	1.8913
62						east	10	27	2.7977
63						north	10	27	1.8913
64						south	10	27	1.8913
65						west	10	27	1.8912
66					medium	central	10	27	1.8913
67						east	10	27	2.7977
68						north	10	27	1.8913
69						south	10	27	1.8913
70						west	10	27	1.8912
71					high	central	10	27	1.8912
72						east	10	27	2.0964
73						north	10	27	2.7619
74						south	10	27	1.8912
75						west	10	27	1.8913
76					heavy	central	10	27	2.7217
77						east	10	27	1.9753
78						north	10	27	1.8912
79						south	10	27	1.8914
80						west	10	27	2.7217

Table B.71: Failure Model Coefficients for LR and SH

group	distress	treat_lvl	highway_fun	pavement_typ	traffic_cls	climate_zone	alpha	A_star	beta_star
81	failure_qty	LR	SH	thick	low	central	10	27	1.9322
82						east	10	27	2.3244
83						north	10	27	1.8912
84						south	10	27	2.4845
85						west	10	27	1.9761
86					medium	central	10	27	1.9322
87						east	10	27	2.3244
88						north	10	27	1.8912
89						south	10	27	2.4845
90						west	10	27	1.9761
91					high	central	10	27	1.9322
92						east	10	27	2.3244
93						north	10	27	1.8912
94						south	10	27	2.4845
95						west	10	27	1.9761
96					heavy	central	10	27	2.6038
97						east	10	27	3.0106
98						north	10	27	2.6038
99						south	10	27	1.8886
100						west	10	27	1.9882
101				thin	low	central	10	27	1.8912
102						east	10	27	1.8904
103						north	10	27	2.1803
104						south	10	27	1.8912
105						west	10	27	1.9167
106					medium	central	10	27	1.8912
107						east	10	27	1.8904
108						north	10	27	2.1803
109						south	10	27	1.8912
110						west	10	27	1.9167
111					high	central	10	27	2.0930
112						east	10	27	2.5608
113						north	10	27	1.6425
114						south	10	27	2.2414
115						west	10	27	1.3115
116					heavy	central	10	27	2.1555
117						east	10	27	2.1543
118						north	10	27	2.1555
119						south	10	27	1.0433
120						west	10	27	2.4626

Table B.72: Failure Model Coefficients for LR and FM

group	distress	treat_lvl	highway_fun	pavement_typ	traffic_cls	climate_zone	alpha	A_star	beta_star
121	failure_qty	LR	FM	thick	low	central	10	27	0.8731
122						east	10	27	1.8960
123						north	10	27	0.8731
124						south	10	27	0.6207
125						west	10	27	0.8731
126					medium	central	10	27	0.7647
127						east	10	27	2.6847
128						north	10	27	1.8912
129						south	10	27	1.8627
130						west	10	27	0.7647
131					high	central	10	27	1.6804
132						east	10	27	3.2255
133						north	10	27	1.8912
134						south	10	27	1.8845
135						west	10	27	1.8912
136					heavy	central	10	27	1.6804
137						east	10	27	3.2255
138						north	10	27	1.8912
139						south	10	27	1.8845
140						west	10	27	1.8912
141				thin	low	central	10	27	1.0510
142						east	10	27	1.7830
143						north	10	27	1.1485
144						south	10	27	0.5287
145						west	10	27	0.8932
146					medium	central	10	27	1.2995
147						east	10	27	1.6562
148						north	10	27	1.9928
149						south	10	27	0.4330
150						west	10	27	2.3226
151					high	central	10	27	1.8017
152						east	10	27	1.6053
153						north	10	27	1.6198
154						south	10	27	0.4793
155						west	10	27	1.5564
156					heavy	central	10	27	1.8017
157						east	10	27	1.6053
158						north	10	27	1.6198
159						south	10	27	0.4793
160						west	10	27	1.5564

Table B.73: Failure Model Coefficients for MR and IH

group	distress	treat_lvl	highway_fun	pavement_typ	traffic_cls	climate_zone	alpha	A_star	beta_star
1	failure_qty	MR	IH	thick	low	central	10	32	2.3327
2						east	10	32	1.9422
3						north	10	32	2.3327
4						south	10	32	1.8975
5						west	10	32	2.0496
6					medium	central	10	32	2.3327
7						east	10	32	1.9422
8						north	10	32	2.3327
9						south	10	32	1.8975
10						west	10	32	2.0496
11					high	central	10	32	2.3327
12						east	10	32	1.9422
13						north	10	32	2.3327
14						south	10	32	1.8975
15						west	10	32	2.0496
16					heavy	central	10	32	2.3327
17						east	10	32	1.9422
18						north	10	32	2.3327
19						south	10	32	1.8975
20						west	10	32	2.0496
21				thin	low	central	10	32	2.4684
22						east	10	32	1.8912
23						north	10	32	2.4684
24						south	10	32	0.1414
25						west	10	32	2.4684
26					medium	central	10	32	1.9248
27						east	10	32	1.9248
28						north	10	32	1.9248
29						south	10	32	1.9248
30						west	10	32	1.9680
31					high	central	10	32	1.9248
32						east	10	32	1.9248
33						north	10	32	1.9248
34						south	10	32	1.9248
35						west	10	32	1.9680
36					heavy	central	10	32	1.9248
37						east	10	32	1.9248
38						north	10	32	1.9248
39						south	10	32	1.9248
40						west	10	32	1.9680

Table B.74: Failure Model Coefficients for MR and US

group	distress	treat_lvl	highway_fun	pavement_typ	traffic_cls	climate_zone	alpha	A_star	beta_star
41	failure_qty	MR	US	thick	low	central	10	32	2.1809
42						east	10	32	3.0163
43						north	10	32	1.8952
44						south	10	32	1.8912
45						west	10	32	2.8298
46					medium	central	10	32	2.1809
47						east	10	32	3.0163
48						north	10	32	1.8952
49						south	10	32	1.8912
50						west	10	32	2.8298
51					high	central	10	32	2.1809
52						east	10	32	3.0163
53						north	10	32	1.8952
54						south	10	32	1.8912
55						west	10	32	2.8298
56					heavy	central	10	32	2.2628
57						east	10	32	2.1761
58						north	10	32	1.8912
59						south	10	32	1.5104
60						west	10	32	2.4561
61				thin	low	central	10	32	1.8913
62						east	10	32	2.7977
63						north	10	32	1.8913
64						south	10	32	1.8913
65						west	10	32	1.8912
66					medium	central	10	32	1.8913
67						east	10	32	2.7977
68						north	10	32	1.8913
69						south	10	32	1.8913
70						west	10	32	1.8912
71					high	central	10	32	1.8912
72						east	10	32	2.0964
73						north	10	32	2.7619
74						south	10	32	1.8912
75						west	10	32	1.8913
76					heavy	central	10	32	2.7217
77						east	10	32	1.9753
78						north	10	32	1.8912
79						south	10	32	1.8914
80						west	10	32	2.7217

Table B.75: Failure Model Coefficients for MR and SH

group	distress	treat_lvl	highway_fun	pavement_typ	traffic_cls	climate_zone	alpha	A_star	beta_star
81	failure_qty	MR	SH	thick	low	central	10	32	1.9322
82						east	10	32	2.3244
83						north	10	32	1.8912
84						south	10	32	2.4845
85						west	10	32	1.9761
86					medium	central	10	32	1.9322
87						east	10	32	2.3244
88						north	10	32	1.8912
89						south	10	32	2.4845
90						west	10	32	1.9761
91					high	central	10	32	1.9322
92						east	10	32	2.3244
93						north	10	32	1.8912
94						south	10	32	2.4845
95						west	10	32	1.9761
96					heavy	central	10	32	2.6038
97						east	10	32	3.0106
98						north	10	32	2.6038
99						south	10	32	1.8886
100						west	10	32	1.9882
101				thin	low	central	10	32	1.8912
102						east	10	32	1.8904
103						north	10	32	2.1803
104						south	10	32	1.8912
105						west	10	32	1.9167
106					medium	central	10	32	1.8912
107						east	10	32	1.8904
108						north	10	32	2.1803
109						south	10	32	1.8912
110						west	10	32	1.9167
111					high	central	10	32	2.0930
112						east	10	32	2.5608
113						north	10	32	1.6425
114						south	10	32	2.2414
115						west	10	32	1.3115
116					heavy	central	10	32	2.1555
117						east	10	32	2.1543
118						north	10	32	2.1555
119						south	10	32	1.0433
120						west	10	32	2.4626

Table B.76: Failure Model Coefficients for MR and FM

group	distress	treat_lvl	highway_fun	pavement_typ	traffic_cls	climate_zone	alpha	A_star	beta_star
121	failure_qty	MR	FM	thick	low	central	10	32	0.8731
122	failure_qty	MR	FM	thick	low	east	10	32	1.8960
123	failure_qty	MR	FM	thick	low	north	10	32	0.8731
124	failure_qty	MR	FM	thick	low	south	10	32	0.6207
125	failure_qty	MR	FM	thick	low	west	10	32	0.8731
126	failure_qty	MR	FM	thick	medium	central	10	32	0.7647
127	failure_qty	MR	FM	thick	medium	east	10	32	2.6847
128	failure_qty	MR	FM	thick	medium	north	10	32	1.8912
129	failure_qty	MR	FM	thick	medium	south	10	32	1.8627
130	failure_qty	MR	FM	thick	medium	west	10	32	0.7647
131	failure_qty	MR	FM	thick	high	central	10	32	1.6804
132	failure_qty	MR	FM	thick	high	east	10	32	3.2255
133	failure_qty	MR	FM	thick	high	north	10	32	1.8912
134	failure_qty	MR	FM	thick	high	south	10	32	1.8845
135	failure_qty	MR	FM	thick	high	west	10	32	1.8912
136	failure_qty	MR	FM	thick	heavy	central	10	32	1.6804
137	failure_qty	MR	FM	thick	heavy	east	10	32	3.2255
138	failure_qty	MR	FM	thick	heavy	north	10	32	1.8912
139	failure_qty	MR	FM	thick	heavy	south	10	32	1.8845
140	failure_qty	MR	FM	thick	heavy	west	10	32	1.8912
141	failure_qty	MR	FM	thin	low	central	10	32	1.0510
142	failure_qty	MR	FM	thin	low	east	10	32	1.7830
143	failure_qty	MR	FM	thin	low	north	10	32	1.1485
144	failure_qty	MR	FM	thin	low	south	10	32	0.5287
145	failure_qty	MR	FM	thin	low	west	10	32	0.8932
146	failure_qty	MR	FM	thin	medium	central	10	32	1.2995
147	failure_qty	MR	FM	thin	medium	east	10	32	1.6562
148	failure_qty	MR	FM	thin	medium	north	10	32	1.9928
149	failure_qty	MR	FM	thin	medium	south	10	32	0.4330
150	failure_qty	MR	FM	thin	medium	west	10	32	2.3226
151	failure_qty	MR	FM	thin	high	central	10	32	1.8017
152	failure_qty	MR	FM	thin	high	east	10	32	1.6053
153	failure_qty	MR	FM	thin	high	north	10	32	1.6198
154	failure_qty	MR	FM	thin	high	south	10	32	0.4793
155	failure_qty	MR	FM	thin	high	west	10	32	1.5564
156	failure_qty	MR	FM	thin	heavy	central	10	32	1.8017
157	failure_qty	MR	FM	thin	heavy	east	10	32	1.6053
158	failure_qty	MR	FM	thin	heavy	north	10	32	1.6198
159	failure_qty	MR	FM	thin	heavy	south	10	32	0.4793
160	failure_qty	MR	FM	thin	heavy	west	10	32	1.5564

Table B.77: Failure Model Coefficients for HR and IH

group	distress	treat_lvl	highway_fun	pavement_typ	traffic_cls	climate_zone	alpha	A_star	beta_star
1	failure_qty	HR	IH	thick	low	central	10	37	2.3327
2						east	10	37	1.9422
3						north	10	37	2.3327
4						south	10	37	1.8975
5						west	10	37	2.0496
6					medium	central	10	37	2.3327
7						east	10	37	1.9422
8						north	10	37	2.3327
9						south	10	37	1.8975
10						west	10	37	2.0496
11					high	central	10	37	2.3327
12						east	10	37	1.9422
13						north	10	37	2.3327
14						south	10	37	1.8975
15						west	10	37	2.0496
16					heavy	central	10	37	2.3327
17						east	10	37	1.9422
18						north	10	37	2.3327
19						south	10	37	1.8975
20						west	10	37	2.0496
21				thin	low	central	10	37	2.4684
22						east	10	37	1.8912
23						north	10	37	2.4684
24						south	10	37	0.1414
25						west	10	37	2.4684
26					medium	central	10	37	1.9248
27						east	10	37	1.9248
28						north	10	37	1.9248
29						south	10	37	1.9248
30						west	10	37	1.9680
31					high	central	10	37	1.9248
32						east	10	37	1.9248
33						north	10	37	1.9248
34						south	10	37	1.9248
35						west	10	37	1.9680
36					heavy	central	10	37	1.9248
37						east	10	37	1.9248
38						north	10	37	1.9248
39						south	10	37	1.9248
40						west	10	37	1.9680

Table B.78: Failure Model Coefficients for HR and US

group	distress	treat_lvl	highway_fun	pavement_typ	traffic_cls	climate_zone	alpha	A_star	beta_star
41	failure_qty	HR	US	thick	low	central	10	37	2.1809
42						east	10	37	3.0163
43						north	10	37	1.8952
44						south	10	37	1.8912
45						west	10	37	2.8298
46					medium	central	10	37	2.1809
47						east	10	37	3.0163
48						north	10	37	1.8952
49						south	10	37	1.8912
50						west	10	37	2.8298
51					high	central	10	37	2.1809
52						east	10	37	3.0163
53						north	10	37	1.8952
54						south	10	37	1.8912
55						west	10	37	2.8298
56					heavy	central	10	37	2.2628
57						east	10	37	2.1761
58						north	10	37	1.8912
59						south	10	37	1.5104
60						west	10	37	2.4561
61				thin	low	central	10	37	1.8913
62						east	10	37	2.7977
63						north	10	37	1.8913
64						south	10	37	1.8913
65						west	10	37	1.8912
66					medium	central	10	37	1.8913
67						east	10	37	2.7977
68						north	10	37	1.8913
69						south	10	37	1.8913
70						west	10	37	1.8912
71					high	central	10	37	1.8912
72						east	10	37	2.0964
73						north	10	37	2.7619
74						south	10	37	1.8912
75						west	10	37	1.8913
76					heavy	central	10	37	2.7217
77						east	10	37	1.9753
78						north	10	37	1.8912
79						south	10	37	1.8914
80						west	10	37	2.7217

Table B.79: Failure Model Coefficients for HR and SH

group	distress	treat_lvl	highway_fun	pavement_typ	traffic_cls	climate_zone	alpha	A_star	beta_star
81	failure_qty	HR	SH	thick	low	central	10	37	1.9322
82						east	10	37	2.3244
83						north	10	37	1.8912
84						south	10	37	2.4845
85						west	10	37	1.9761
86					medium	central	10	37	1.9322
87						east	10	37	2.3244
88						north	10	37	1.8912
89						south	10	37	2.4845
90						west	10	37	1.9761
91					high	central	10	37	1.9322
92						east	10	37	2.3244
93						north	10	37	1.8912
94						south	10	37	2.4845
95						west	10	37	1.9761
96					heavy	central	10	37	2.6038
97						east	10	37	3.0106
98						north	10	37	2.6038
99						south	10	37	1.8886
100						west	10	37	1.9882
101				thin	low	central	10	37	1.8912
102						east	10	37	1.8904
103						north	10	37	2.1803
104						south	10	37	1.8912
105						west	10	37	1.9167
106					medium	central	10	37	1.8912
107						east	10	37	1.8904
108						north	10	37	2.1803
109						south	10	37	1.8912
110						west	10	37	1.9167
111					high	central	10	37	2.0930
112						east	10	37	2.5608
113						north	10	37	1.6425
114						south	10	37	2.2414
115						west	10	37	1.3115
116					heavy	central	10	37	2.1555
117						east	10	37	2.1543
118						north	10	37	2.1555
119						south	10	37	1.0433
120						west	10	37	2.4626

Table B.80: Failure Model Coefficients for HR and FM

group	distress	treat_lvl	highway_fun	pavement_typ	traffic_cls	climate_zone	alpha	A_star	beta_star
121	failure_qty	HR	FM	thick	low	central	10	37	0.8731
122						east	10	37	1.8960
123						north	10	37	0.8731
124						south	10	37	0.6207
125						west	10	37	0.8731
126					medium	central	10	37	0.7647
127						east	10	37	2.6847
128						north	10	37	1.8912
129						south	10	37	1.8627
130						west	10	37	0.7647
131					high	central	10	37	1.6804
132						east	10	37	3.2255
133						north	10	37	1.8912
134						south	10	37	1.8845
135						west	10	37	1.8912
136					heavy	central	10	37	1.6804
137						east	10	37	3.2255
138						north	10	37	1.8912
139						south	10	37	1.8845
140						west	10	37	1.8912
141				thin	low	central	10	37	1.0510
142						east	10	37	1.7830
143						north	10	37	1.1485
144						south	10	37	0.5287
145						west	10	37	0.8932
146					medium	central	10	37	1.2995
147						east	10	37	1.6562
148						north	10	37	1.9928
149						south	10	37	0.4330
150						west	10	37	2.3226
151					high	central	10	37	1.8017
152						east	10	37	1.6053
153						north	10	37	1.6198
154						south	10	37	0.4793
155						west	10	37	1.5564
156					heavy	central	10	37	1.8017
157						east	10	37	1.6053
158						north	10	37	1.6198
159						south	10	37	0.4793
160						west	10	37	1.5564

Table B.81: Block Cracking Model Coefficients for DN and IH

group	distress	treat_lvl	highway_fun	pavement_typ	traffic_cls	climate_zone	alpha	A_star	beta_star
1	block_cracking_pct	DN	IH	thick	low	central	70	22.1735	4.2769
2	block_cracking_pct	DN	IH	thick	low	east	70	22.1735	3.5972
3	block_cracking_pct	DN	IH	thick	low	north	70	22.1735	4.2769
4	block_cracking_pct	DN	IH	thick	low	south	70	22.1735	3.5972
5	block_cracking_pct	DN	IH	thick	low	west	70	22.1735	3.5972
6	block_cracking_pct	DN	IH	thick	medium	central	70	22.1735	4.2769
7	block_cracking_pct	DN	IH	thick	medium	east	70	22.1735	3.5972
8	block_cracking_pct	DN	IH	thick	medium	north	70	22.1735	4.2769
9	block_cracking_pct	DN	IH	thick	medium	south	70	22.1735	3.5972
10	block_cracking_pct	DN	IH	thick	medium	west	70	22.1735	3.5972
11	block_cracking_pct	DN	IH	thick	high	central	70	22.1735	4.2769
12	block_cracking_pct	DN	IH	thick	high	east	70	22.1735	3.5972
13	block_cracking_pct	DN	IH	thick	high	north	70	22.1735	4.2769
14	block_cracking_pct	DN	IH	thick	high	south	70	22.1735	3.5972
15	block_cracking_pct	DN	IH	thick	high	west	70	22.1735	3.5972
16	block_cracking_pct	DN	IH	thick	heavy	central	70	22.1735	4.2769
17	block_cracking_pct	DN	IH	thick	heavy	east	70	22.1735	3.5972
18	block_cracking_pct	DN	IH	thick	heavy	north	70	22.1735	4.2769
19	block_cracking_pct	DN	IH	thick	heavy	south	70	22.1735	3.5972
20	block_cracking_pct	DN	IH	thick	heavy	west	70	22.1735	3.5972
21	block_cracking_pct	DN	IH	thin	low	central	70	22.1735	3.8438
22	block_cracking_pct	DN	IH	thin	low	east	70	22.1735	3.5972
23	block_cracking_pct	DN	IH	thin	low	north	70	22.1735	3.8438
24	block_cracking_pct	DN	IH	thin	low	south	70	22.1735	3.5972
25	block_cracking_pct	DN	IH	thin	low	west	70	22.1735	3.8438
26	block_cracking_pct	DN	IH	thin	medium	central	70	22.1735	2.5134
27	block_cracking_pct	DN	IH	thin	medium	east	70	22.1735	2.5134
28	block_cracking_pct	DN	IH	thin	medium	north	70	22.1735	2.5134
29	block_cracking_pct	DN	IH	thin	medium	south	70	22.1735	2.5134
30	block_cracking_pct	DN	IH	thin	medium	west	70	22.1735	3.5972
31	block_cracking_pct	DN	IH	thin	high	central	70	22.1735	2.5134
32	block_cracking_pct	DN	IH	thin	high	east	70	22.1735	2.5134
33	block_cracking_pct	DN	IH	thin	high	north	70	22.1735	2.5134
34	block_cracking_pct	DN	IH	thin	high	south	70	22.1735	2.5134
35	block_cracking_pct	DN	IH	thin	high	west	70	22.1735	3.5972
36	block_cracking_pct	DN	IH	thin	heavy	central	70	22.1735	2.5134
37	block_cracking_pct	DN	IH	thin	heavy	east	70	22.1735	2.5134
38	block_cracking_pct	DN	IH	thin	heavy	north	70	22.1735	2.5134
39	block_cracking_pct	DN	IH	thin	heavy	south	70	22.1735	2.5134
40	block_cracking_pct	DN	IH	thin	heavy	west	70	22.1735	3.5972

Table B.82: Block Cracking Model Coefficients for DN and US

group	distress	treat_lvl	highway_fun	pavement_typ	traffic_cls	climate_zone	alpha	A_star	beta_star
41	block_cracking_pct	DN	US	thick	low	central	70	22.1735	2.2781
42						east	70	22.1735	4.4768
43						north	70	22.1735	3.5972
44						south	70	22.1735	3.5972
45						west	70	22.1735	3.7981
46					medium	central	70	22.1735	2.2781
47						east	70	22.1735	4.4768
48						north	70	22.1735	3.5972
49						south	70	22.1735	3.5972
50						west	70	22.1735	3.7981
51					high	central	70	22.1735	2.2781
52						east	70	22.1735	4.4768
53						north	70	22.1735	3.5972
54						south	70	22.1735	3.5972
55						west	70	22.1735	3.7981
56					heavy	central	70	22.1735	2.2484
57						east	70	22.1735	3.5983
58						north	70	22.1735	3.5972
59						south	70	22.1735	3.5972
60						west	70	22.1735	3.6856
61				thin	low	central	70	22.1735	3.5972
62						east	70	22.1735	4.3168
63						north	70	22.1735	3.5972
64						south	70	22.1735	3.5972
65						west	70	22.1735	3.5972
66					medium	central	70	22.1735	3.5972
67						east	70	22.1735	4.3168
68						north	70	22.1735	3.5972
69						south	70	22.1735	3.5972
70						west	70	22.1735	3.5972
71					high	central	70	22.1735	3.5972
72						east	70	22.1735	3.5972
73						north	70	22.1735	3.9937
74						south	70	22.1735	3.5972
75						west	70	22.1735	3.5972
76					heavy	central	70	22.1735	3.7568
77						east	70	22.1735	3.5972
78						north	70	22.1735	3.5972
79						south	70	22.1735	3.5972
80						west	70	22.1735	3.7568

Table B.83: Block Cracking Model Coefficients for DN and SH

group	distress	treat_lvl	highway_fun	pavement_typ	traffic_cls	climate_zone	alpha	A_star	beta_star
81	block_cracking_pct	DN	SH	thick	low	central	70	22.1735	0.9252
82						east	70	22.1735	2.8684
83						north	70	22.1735	3.5972
84						south	70	22.1735	4.1136
85						west	70	22.1735	3.5972
86					medium	central	70	22.1735	0.9252
87						east	70	22.1735	2.8684
88						north	70	22.1735	3.5972
89						south	70	22.1735	4.1136
90						west	70	22.1735	3.5972
91					high	central	70	22.1735	0.9252
92						east	70	22.1735	2.8684
93						north	70	22.1735	3.5972
94						south	70	22.1735	4.1136
95						west	70	22.1735	3.5972
96					heavy	central	70	22.1735	3.7128
97						east	70	22.1735	2.6262
98						north	70	22.1735	3.7128
99						south	70	22.1735	3.5972
100						west	70	22.1735	3.5972
101				thin	low	central	70	22.1735	3.5972
102						east	70	22.1735	3.5972
103						north	70	22.1735	3.6005
104						south	70	22.1735	3.5972
105						west	70	22.1735	3.5972
106					medium	central	70	22.1735	3.5972
107						east	70	22.1735	3.5972
108						north	70	22.1735	3.6005
109						south	70	22.1735	3.5972
110						west	70	22.1735	3.5972
111					high	central	70	22.1735	1.1189
112						east	70	22.1735	3.8900
113						north	70	22.1735	0.9691
114						south	70	22.1735	4.0780
115						west	70	22.1735	4.2408
116					heavy	central	70	22.1735	3.6178
117						east	70	22.1735	3.5972
118						north	70	22.1735	3.6178
119						south	70	22.1735	2.4297
120						west	70	22.1735	4.7926

Table B.84: Block Cracking Model Coefficients for DN and FM

group	distress	treat_lvl	highway_fun	pavement_typ	traffic_cls	climate_zone	alpha	A_star	beta_star
121	block_cracking_pct	DN	FM	thick	low	central	70	22.1735	3.5972
122						east	70	22.1735	3.5972
123						north	70	22.1735	3.5972
124						south	70	22.1735	3.5972
125						west	70	22.1735	3.5972
126					medium	central	70	22.1735	3.5972
127						east	70	22.1735	4.6222
128						north	70	22.1735	3.5972
129						south	70	22.1735	3.5972
130						west	70	22.1735	3.5972
131					high	central	70	22.1735	1.6559
132						east	70	22.1735	4.0611
133						north	70	22.1735	3.5972
134						south	70	22.1735	3.5972
135						west	70	22.1735	3.5972
136					heavy	central	70	22.1735	1.6559
137						east	70	22.1735	4.0611
138						north	70	22.1735	3.5972
139						south	70	22.1735	3.5972
140						west	70	22.1735	3.5972
141				thin	low	central	70	22.1735	4.0025
142						east	70	22.1735	4.5652
143						north	70	22.1735	4.4206
144						south	70	22.1735	3.5972
145						west	70	22.1735	4.4768
146					medium	central	70	22.1735	4.4477
147						east	70	22.1735	5.0932
148						north	70	22.1735	3.6032
149						south	70	22.1735	3.5972
150						west	70	22.1735	4.1136
151					high	central	70	22.1735	3.5420
152						east	70	22.1735	4.9818
153						north	70	22.1735	3.5972
154						south	70	22.1735	3.9937
155						west	70	22.1735	4.1363
156					heavy	central	70	22.1735	3.5420
157						east	70	22.1735	4.9818
158						north	70	22.1735	3.5972
159						south	70	22.1735	3.9937
160						west	70	22.1735	4.1363

Table B.85: Block Cracking Model Coefficients for PM and IH

group	distress	treat_lvl	highway_fun	pavement_typ	traffic_cls	climate_zone	alpha	A_star	beta_star
1	block_cracking_pct	PM	IH	thick	low	central	70	24	4.2769
2						east	70	24	3.5972
3						north	70	24	4.2769
4						south	70	24	3.5972
5						west	70	24	3.5972
6					medium	central	70	24	4.2769
7						east	70	24	3.5972
8						north	70	24	4.2769
9						south	70	24	3.5972
10						west	70	24	3.5972
11					high	central	70	24	4.2769
12						east	70	24	3.5972
13						north	70	24	4.2769
14						south	70	24	3.5972
15						west	70	24	3.5972
16					heavy	central	70	24	4.2769
17						east	70	24	3.5972
18						north	70	24	4.2769
19						south	70	24	3.5972
20						west	70	24	3.5972
21				thin	low	central	70	24	3.8438
22						east	70	24	3.5972
23						north	70	24	3.8438
24						south	70	24	3.5972
25						west	70	24	3.8438
26					medium	central	70	24	2.5134
27						east	70	24	2.5134
28						north	70	24	2.5134
29						south	70	24	2.5134
30						west	70	24	3.5972
31					high	central	70	24	2.5134
32						east	70	24	2.5134
33						north	70	24	2.5134
34						south	70	24	2.5134
35						west	70	24	3.5972
36					heavy	central	70	24	2.5134
37						east	70	24	2.5134
38						north	70	24	2.5134
39						south	70	24	2.5134
40						west	70	24	3.5972

Table B.86: Block Cracking Model Coefficients for PM and US

group	distress	treat_lvl	highway_fun	pavement_typ	traffic_cls	climate_zone	alpha	A_star	beta_star
41	block_cracking_pct	PM	US	thick	low	central	70	24	2.2781
42	block_cracking_pct	PM	US	thick	low	east	70	24	4.4768
43	block_cracking_pct	PM	US	thick	low	north	70	24	3.5972
44	block_cracking_pct	PM	US	thick	low	south	70	24	3.5972
45	block_cracking_pct	PM	US	thick	low	west	70	24	3.7981
46	block_cracking_pct	PM	US	thick	medium	central	70	24	2.2781
47	block_cracking_pct	PM	US	thick	medium	east	70	24	4.4768
48	block_cracking_pct	PM	US	thick	medium	north	70	24	3.5972
49	block_cracking_pct	PM	US	thick	medium	south	70	24	3.5972
50	block_cracking_pct	PM	US	thick	medium	west	70	24	3.7981
51	block_cracking_pct	PM	US	thick	high	central	70	24	2.2781
52	block_cracking_pct	PM	US	thick	high	east	70	24	4.4768
53	block_cracking_pct	PM	US	thick	high	north	70	24	3.5972
54	block_cracking_pct	PM	US	thick	high	south	70	24	3.5972
55	block_cracking_pct	PM	US	thick	high	west	70	24	3.7981
56	block_cracking_pct	PM	US	thick	heavy	central	70	24	2.2484
57	block_cracking_pct	PM	US	thick	heavy	east	70	24	3.5983
58	block_cracking_pct	PM	US	thick	heavy	north	70	24	3.5972
59	block_cracking_pct	PM	US	thick	heavy	south	70	24	3.5972
60	block_cracking_pct	PM	US	thick	heavy	west	70	24	3.6856
61	block_cracking_pct	PM	US	thin	low	central	70	24	3.5972
62	block_cracking_pct	PM	US	thin	low	east	70	24	4.3168
63	block_cracking_pct	PM	US	thin	low	north	70	24	3.5972
64	block_cracking_pct	PM	US	thin	low	south	70	24	3.5972
65	block_cracking_pct	PM	US	thin	low	west	70	24	3.5972
66	block_cracking_pct	PM	US	thin	medium	central	70	24	3.5972
67	block_cracking_pct	PM	US	thin	medium	east	70	24	4.3168
68	block_cracking_pct	PM	US	thin	medium	north	70	24	3.5972
69	block_cracking_pct	PM	US	thin	medium	south	70	24	3.5972
70	block_cracking_pct	PM	US	thin	medium	west	70	24	3.5972
71	block_cracking_pct	PM	US	thin	high	central	70	24	3.5972
72	block_cracking_pct	PM	US	thin	high	east	70	24	3.5972
73	block_cracking_pct	PM	US	thin	high	north	70	24	3.9937
74	block_cracking_pct	PM	US	thin	high	south	70	24	3.5972
75	block_cracking_pct	PM	US	thin	high	west	70	24	3.5972
76	block_cracking_pct	PM	US	thin	heavy	central	70	24	3.7568
77	block_cracking_pct	PM	US	thin	heavy	east	70	24	3.5972
78	block_cracking_pct	PM	US	thin	heavy	north	70	24	3.5972
79	block_cracking_pct	PM	US	thin	heavy	south	70	24	3.5972
80	block_cracking_pct	PM	US	thin	heavy	west	70	24	3.7568

Table B.87: Block Cracking Model Coefficients for PM and SH

group	distress	treat_lvl	highway_fun	pavement_typ	traffic_cls	climate_zone	alpha	A_star	beta_star
81	block_cracking_pct	PM	SH	thick	low	central	70	24	0.9252
82						east	70	24	2.8684
83						north	70	24	3.5972
84						south	70	24	4.1136
85						west	70	24	3.5972
86					medium	central	70	24	0.9252
87						east	70	24	2.8684
88						north	70	24	3.5972
89						south	70	24	4.1136
90						west	70	24	3.5972
91					high	central	70	24	0.9252
92						east	70	24	2.8684
93						north	70	24	3.5972
94						south	70	24	4.1136
95						west	70	24	3.5972
96					heavy	central	70	24	3.7128
97						east	70	24	2.6262
98						north	70	24	3.7128
99						south	70	24	3.5972
100						west	70	24	3.5972
101				thin	low	central	70	24	3.5972
102						east	70	24	3.5972
103						north	70	24	3.6005
104						south	70	24	3.5972
105						west	70	24	3.5972
106					medium	central	70	24	3.5972
107						east	70	24	3.5972
108						north	70	24	3.6005
109						south	70	24	3.5972
110						west	70	24	3.5972
111					high	central	70	24	1.1189
112						east	70	24	3.8900
113						north	70	24	0.9691
114						south	70	24	4.0780
115						west	70	24	4.2408
116					heavy	central	70	24	3.6178
117						east	70	24	3.5972
118						north	70	24	3.6178
119						south	70	24	2.4297
120						west	70	24	4.7926

Table B.88: Block Cracking Model Coefficients for PM and FM

group	distress	treat_lvl	highway_fun	pavement_typ	traffic_cls	climate_zone	alpha	A_star	beta_star
121	block_cracking_pct	PM	FM	thick	low	central	70	24	3.5972
122						east	70	24	3.5972
123						north	70	24	3.5972
124						south	70	24	3.5972
125						west	70	24	3.5972
126					medium	central	70	24	3.5972
127						east	70	24	4.6222
128						north	70	24	3.5972
129						south	70	24	3.5972
130						west	70	24	3.5972
131					high	central	70	24	1.6559
132						east	70	24	4.0611
133						north	70	24	3.5972
134						south	70	24	3.5972
135						west	70	24	3.5972
136					heavy	central	70	24	1.6559
137						east	70	24	4.0611
138						north	70	24	3.5972
139						south	70	24	3.5972
140						west	70	24	3.5972
141				thin	low	central	70	24	4.0025
142						east	70	24	4.5652
143						north	70	24	4.4206
144						south	70	24	3.5972
145						west	70	24	4.4768
146					medium	central	70	24	4.4477
147						east	70	24	5.0932
148						north	70	24	3.6032
149						south	70	24	3.5972
150						west	70	24	4.1136
151					high	central	70	24	3.5420
152						east	70	24	4.9818
153						north	70	24	3.5972
154						south	70	24	3.9937
155						west	70	24	4.1363
156					heavy	central	70	24	3.5420
157						east	70	24	4.9818
158						north	70	24	3.5972
159						south	70	24	3.9937
160						west	70	24	4.1363

Table B.89: Block Cracking Model Coefficients for LR and IH

group	distress	treat_lvl	highway_fun	pavement_typ	traffic_cls	climate_zone	alpha	A_star	beta_star
1	block_cracking_pct	LR	IH	thick	low	central	70	25	4.2769
2						east	70	25	3.5972
3						north	70	25	4.2769
4						south	70	25	3.5972
5						west	70	25	3.5972
6					medium	central	70	25	4.2769
7						east	70	25	3.5972
8						north	70	25	4.2769
9						south	70	25	3.5972
10						west	70	25	3.5972
11					high	central	70	25	4.2769
12						east	70	25	3.5972
13						north	70	25	4.2769
14						south	70	25	3.5972
15						west	70	25	3.5972
16					heavy	central	70	25	4.2769
17						east	70	25	3.5972
18						north	70	25	4.2769
19						south	70	25	3.5972
20						west	70	25	3.5972
21				thin	low	central	70	25	3.8438
22						east	70	25	3.5972
23						north	70	25	3.8438
24						south	70	25	3.5972
25						west	70	25	3.8438
26					medium	central	70	25	2.5134
27						east	70	25	2.5134
28						north	70	25	2.5134
29						south	70	25	2.5134
30						west	70	25	3.5972
31					high	central	70	25	2.5134
32						east	70	25	2.5134
33						north	70	25	2.5134
34						south	70	25	2.5134
35						west	70	25	3.5972
36					heavy	central	70	25	2.5134
37						east	70	25	2.5134
38						north	70	25	2.5134
39						south	70	25	2.5134
40						west	70	25	3.5972

Table B.90: Block Cracking Model Coefficients for LR and US

group	distress	treat_lvl	highway_fun	pavement_typ	traffic_cls	climate_zone	alpha	A_star	beta_star
41	block_cracking_pct	LR	US	thick	low	central	70	25	2.2781
42	block_cracking_pct	LR	US	thick	low	east	70	25	4.4768
43	block_cracking_pct	LR	US	thick	low	north	70	25	3.5972
44	block_cracking_pct	LR	US	thick	low	south	70	25	3.5972
45	block_cracking_pct	LR	US	thick	low	west	70	25	3.7981
46	block_cracking_pct	LR	US	thick	medium	central	70	25	2.2781
47	block_cracking_pct	LR	US	thick	medium	east	70	25	4.4768
48	block_cracking_pct	LR	US	thick	medium	north	70	25	3.5972
49	block_cracking_pct	LR	US	thick	medium	south	70	25	3.5972
50	block_cracking_pct	LR	US	thick	medium	west	70	25	3.7981
51	block_cracking_pct	LR	US	thick	high	central	70	25	2.2781
52	block_cracking_pct	LR	US	thick	high	east	70	25	4.4768
53	block_cracking_pct	LR	US	thick	high	north	70	25	3.5972
54	block_cracking_pct	LR	US	thick	high	south	70	25	3.5972
55	block_cracking_pct	LR	US	thick	high	west	70	25	3.7981
56	block_cracking_pct	LR	US	thick	heavy	central	70	25	2.2484
57	block_cracking_pct	LR	US	thick	heavy	east	70	25	3.5983
58	block_cracking_pct	LR	US	thick	heavy	north	70	25	3.5972
59	block_cracking_pct	LR	US	thick	heavy	south	70	25	3.5972
60	block_cracking_pct	LR	US	thick	heavy	west	70	25	3.6856
61	block_cracking_pct	LR	US	thin	low	central	70	25	3.5972
62	block_cracking_pct	LR	US	thin	low	east	70	25	4.3168
63	block_cracking_pct	LR	US	thin	low	north	70	25	3.5972
64	block_cracking_pct	LR	US	thin	low	south	70	25	3.5972
65	block_cracking_pct	LR	US	thin	low	west	70	25	3.5972
66	block_cracking_pct	LR	US	thin	medium	central	70	25	3.5972
67	block_cracking_pct	LR	US	thin	medium	east	70	25	4.3168
68	block_cracking_pct	LR	US	thin	medium	north	70	25	3.5972
69	block_cracking_pct	LR	US	thin	medium	south	70	25	3.5972
70	block_cracking_pct	LR	US	thin	medium	west	70	25	3.5972
71	block_cracking_pct	LR	US	thin	high	central	70	25	3.5972
72	block_cracking_pct	LR	US	thin	high	east	70	25	3.5972
73	block_cracking_pct	LR	US	thin	high	north	70	25	3.9937
74	block_cracking_pct	LR	US	thin	high	south	70	25	3.5972
75	block_cracking_pct	LR	US	thin	high	west	70	25	3.5972
76	block_cracking_pct	LR	US	thin	heavy	central	70	25	3.7568
77	block_cracking_pct	LR	US	thin	heavy	east	70	25	3.5972
78	block_cracking_pct	LR	US	thin	heavy	north	70	25	3.5972
79	block_cracking_pct	LR	US	thin	heavy	south	70	25	3.5972
80	block_cracking_pct	LR	US	thin	heavy	west	70	25	3.7568

Table B.91: Block Cracking Model Coefficients for LR and SH

group	distress	treat_lvl	highway_fun	pavement_typ	traffic_cls	climate_zone	alpha	A_star	beta_star
81	block_cracking_pct	LR	SH	thick	low	central	70	25	0.9252
82						east	70	25	2.8684
83						north	70	25	3.5972
84						south	70	25	4.1136
85						west	70	25	3.5972
86					medium	central	70	25	0.9252
87						east	70	25	2.8684
88						north	70	25	3.5972
89						south	70	25	4.1136
90						west	70	25	3.5972
91					high	central	70	25	0.9252
92						east	70	25	2.8684
93						north	70	25	3.5972
94						south	70	25	4.1136
95						west	70	25	3.5972
96					heavy	central	70	25	3.7128
97						east	70	25	2.6262
98						north	70	25	3.7128
99						south	70	25	3.5972
100						west	70	25	3.5972
101				thin	low	central	70	25	3.5972
102						east	70	25	3.5972
103						north	70	25	3.6005
104						south	70	25	3.5972
105						west	70	25	3.5972
106					medium	central	70	25	3.5972
107						east	70	25	3.5972
108						north	70	25	3.6005
109						south	70	25	3.5972
110						west	70	25	3.5972
111					high	central	70	25	1.1189
112						east	70	25	3.8900
113						north	70	25	0.9691
114						south	70	25	4.0780
115						west	70	25	4.2408
116					heavy	central	70	25	3.6178
117						east	70	25	3.5972
118						north	70	25	3.6178
119						south	70	25	2.4297
120						west	70	25	4.7926

Table B.92: Block Cracking Model Coefficients for LR and FM

group	distress	treat_lvl	highway_fun	pavement_typ	traffic_cls	climate_zone	alpha	A_star	beta_star
121	block_cracking_pct	LR	FM	thick	low	central	70	25	3.5972
122						east	70	25	3.5972
123						north	70	25	3.5972
124						south	70	25	3.5972
125						west	70	25	3.5972
126					medium	central	70	25	3.5972
127						east	70	25	4.6222
128						north	70	25	3.5972
129						south	70	25	3.5972
130						west	70	25	3.5972
131					high	central	70	25	1.6559
132						east	70	25	4.0611
133						north	70	25	3.5972
134						south	70	25	3.5972
135						west	70	25	3.5972
136					heavy	central	70	25	1.6559
137						east	70	25	4.0611
138						north	70	25	3.5972
139						south	70	25	3.5972
140						west	70	25	3.5972
141				thin	low	central	70	25	4.0025
142						east	70	25	4.5652
143						north	70	25	4.4206
144						south	70	25	3.5972
145						west	70	25	4.4768
146					medium	central	70	25	4.4477
147						east	70	25	5.0932
148						north	70	25	3.6032
149						south	70	25	3.5972
150						west	70	25	4.1136
151					high	central	70	25	3.5420
152						east	70	25	4.9818
153						north	70	25	3.5972
154						south	70	25	3.9937
155						west	70	25	4.1363
156					heavy	central	70	25	3.5420
157						east	70	25	4.9818
158						north	70	25	3.5972
159						south	70	25	3.9937
160						west	70	25	4.1363

Table B.93: Block Cracking Model Coefficients for MR and IH

group	distress	treat_lvl	highway_fun	pavement_typ	traffic_cls	climate_zone	alpha	A_star	beta_star
1	block_cracking_pct	MR	IH	thick	low	central	70	27.5	4.2769
2						east	70	27.5	3.5972
3						north	70	27.5	4.2769
4						south	70	27.5	3.5972
5						west	70	27.5	3.5972
6					medium	central	70	27.5	4.2769
7						east	70	27.5	3.5972
8						north	70	27.5	4.2769
9						south	70	27.5	3.5972
10						west	70	27.5	3.5972
11					high	central	70	27.5	4.2769
12						east	70	27.5	3.5972
13						north	70	27.5	4.2769
14						south	70	27.5	3.5972
15						west	70	27.5	3.5972
16					heavy	central	70	27.5	4.2769
17						east	70	27.5	3.5972
18						north	70	27.5	4.2769
19						south	70	27.5	3.5972
20						west	70	27.5	3.5972
21				thin	low	central	70	27.5	3.8438
22						east	70	27.5	3.5972
23						north	70	27.5	3.8438
24						south	70	27.5	3.5972
25						west	70	27.5	3.8438
26					medium	central	70	27.5	2.5134
27						east	70	27.5	2.5134
28						north	70	27.5	2.5134
29						south	70	27.5	2.5134
30						west	70	27.5	3.5972
31					high	central	70	27.5	2.5134
32						east	70	27.5	2.5134
33						north	70	27.5	2.5134
34						south	70	27.5	2.5134
35						west	70	27.5	3.5972
36					heavy	central	70	27.5	2.5134
37						east	70	27.5	2.5134
38						north	70	27.5	2.5134
39						south	70	27.5	2.5134
40						west	70	27.5	3.5972

Table B.94: Block Cracking Model Coefficients for MR and US

group	distress	treat_lvl	highway_fun	pavement_typ	traffic_cls	climate_zone	alpha	A_star	beta_star
41	block_cracking_pct	MR	US	thick	low	central	70	27.5	2.2781
42						east	70	27.5	4.4768
43						north	70	27.5	3.5972
44						south	70	27.5	3.5972
45						west	70	27.5	3.7981
46					medium	central	70	27.5	2.2781
47						east	70	27.5	4.4768
48						north	70	27.5	3.5972
49						south	70	27.5	3.5972
50						west	70	27.5	3.7981
51					high	central	70	27.5	2.2781
52						east	70	27.5	4.4768
53						north	70	27.5	3.5972
54						south	70	27.5	3.5972
55						west	70	27.5	3.7981
56					heavy	central	70	27.5	2.2484
57						east	70	27.5	3.5983
58						north	70	27.5	3.5972
59						south	70	27.5	3.5972
60						west	70	27.5	3.6856
61				thin	low	central	70	27.5	3.5972
62						east	70	27.5	4.3168
63						north	70	27.5	3.5972
64						south	70	27.5	3.5972
65						west	70	27.5	3.5972
66					medium	central	70	27.5	3.5972
67						east	70	27.5	4.3168
68						north	70	27.5	3.5972
69						south	70	27.5	3.5972
70						west	70	27.5	3.5972
71					high	central	70	27.5	3.5972
72						east	70	27.5	3.5972
73						north	70	27.5	3.9937
74						south	70	27.5	3.5972
75						west	70	27.5	3.5972
76					heavy	central	70	27.5	3.7568
77						east	70	27.5	3.5972
78						north	70	27.5	3.5972
79						south	70	27.5	3.5972
80						west	70	27.5	3.7568

Table B.95: Block Cracking Model Coefficients for MR and SH

group	distress	treat_lvl	highway_fun	pavement_typ	traffic_cls	climate_zone	alpha	A_star	beta_star
81	block_cracking_pct	MR	SH	thick	low	central	70	27.5	0.9252
82						east	70	27.5	2.8684
83						north	70	27.5	3.5972
84						south	70	27.5	4.1136
85						west	70	27.5	3.5972
86					medium	central	70	27.5	0.9252
87						east	70	27.5	2.8684
88						north	70	27.5	3.5972
89						south	70	27.5	4.1136
90						west	70	27.5	3.5972
91					high	central	70	27.5	0.9252
92						east	70	27.5	2.8684
93						north	70	27.5	3.5972
94						south	70	27.5	4.1136
95						west	70	27.5	3.5972
96					heavy	central	70	27.5	3.7128
97						east	70	27.5	2.6262
98						north	70	27.5	3.7128
99						south	70	27.5	3.5972
100						west	70	27.5	3.5972
101				thin	low	central	70	27.5	3.5972
102						east	70	27.5	3.5972
103						north	70	27.5	3.6005
104						south	70	27.5	3.5972
105						west	70	27.5	3.5972
106					medium	central	70	27.5	3.5972
107						east	70	27.5	3.5972
108						north	70	27.5	3.6005
109						south	70	27.5	3.5972
110						west	70	27.5	3.5972
111					high	central	70	27.5	1.1189
112						east	70	27.5	3.8900
113						north	70	27.5	0.9691
114						south	70	27.5	4.0780
115						west	70	27.5	4.2408
116					heavy	central	70	27.5	3.6178
117						east	70	27.5	3.5972
118						north	70	27.5	3.6178
119						south	70	27.5	2.4297
120						west	70	27.5	4.7926

Table B.96: Block Cracking Model Coefficients for MR and FM

group	distress	treat_lvl	highway_fun	pavement_typ	traffic_cls	climate_zone	alpha	A_star	beta_star
121	block_cracking_pct	MR	FM	thick	low	central	70	27.5	3.5972
122	block_cracking_pct	MR	FM	thick	low	east	70	27.5	3.5972
123	block_cracking_pct	MR	FM	thick	low	north	70	27.5	3.5972
124	block_cracking_pct	MR	FM	thick	low	south	70	27.5	3.5972
125	block_cracking_pct	MR	FM	thick	low	west	70	27.5	3.5972
126	block_cracking_pct	MR	FM	thick	medium	central	70	27.5	3.5972
127	block_cracking_pct	MR	FM	thick	medium	east	70	27.5	4.6222
128	block_cracking_pct	MR	FM	thick	medium	north	70	27.5	3.5972
129	block_cracking_pct	MR	FM	thick	medium	south	70	27.5	3.5972
130	block_cracking_pct	MR	FM	thick	medium	west	70	27.5	3.5972
131	block_cracking_pct	MR	FM	thick	high	central	70	27.5	1.6559
132	block_cracking_pct	MR	FM	thick	high	east	70	27.5	4.0611
133	block_cracking_pct	MR	FM	thick	high	north	70	27.5	3.5972
134	block_cracking_pct	MR	FM	thick	high	south	70	27.5	3.5972
135	block_cracking_pct	MR	FM	thick	high	west	70	27.5	3.5972
136	block_cracking_pct	MR	FM	thick	heavy	central	70	27.5	1.6559
137	block_cracking_pct	MR	FM	thick	heavy	east	70	27.5	4.0611
138	block_cracking_pct	MR	FM	thick	heavy	north	70	27.5	3.5972
139	block_cracking_pct	MR	FM	thick	heavy	south	70	27.5	3.5972
140	block_cracking_pct	MR	FM	thick	heavy	west	70	27.5	3.5972
141	block_cracking_pct	MR	FM	thin	low	central	70	27.5	4.0025
142	block_cracking_pct	MR	FM	thin	low	east	70	27.5	4.5652
143	block_cracking_pct	MR	FM	thin	low	north	70	27.5	4.4206
144	block_cracking_pct	MR	FM	thin	low	south	70	27.5	3.5972
145	block_cracking_pct	MR	FM	thin	low	west	70	27.5	4.4768
146	block_cracking_pct	MR	FM	thin	medium	central	70	27.5	4.4477
147	block_cracking_pct	MR	FM	thin	medium	east	70	27.5	5.0932
148	block_cracking_pct	MR	FM	thin	medium	north	70	27.5	3.6032
149	block_cracking_pct	MR	FM	thin	medium	south	70	27.5	3.5972
150	block_cracking_pct	MR	FM	thin	medium	west	70	27.5	4.1136
151	block_cracking_pct	MR	FM	thin	high	central	70	27.5	3.5420
152	block_cracking_pct	MR	FM	thin	high	east	70	27.5	4.9818
153	block_cracking_pct	MR	FM	thin	high	north	70	27.5	3.5972
154	block_cracking_pct	MR	FM	thin	high	south	70	27.5	3.9937
155	block_cracking_pct	MR	FM	thin	high	west	70	27.5	4.1363
156	block_cracking_pct	MR	FM	thin	heavy	central	70	27.5	3.5420
157	block_cracking_pct	MR	FM	thin	heavy	east	70	27.5	4.9818
158	block_cracking_pct	MR	FM	thin	heavy	north	70	27.5	3.5972
159	block_cracking_pct	MR	FM	thin	heavy	south	70	27.5	3.9937
160	block_cracking_pct	MR	FM	thin	heavy	west	70	27.5	4.1363

Table B.97: Block Cracking Model Coefficients for HR and IH

group	distress	treat_lvl	highway_fun	pavement_typ	traffic_cls	climate_zone	alpha	A_star	beta_star
1	block_cracking_pct	HR	IH	thick	low	central	70	29	4.2769
2						east	70	29	3.5972
3						north	70	29	4.2769
4						south	70	29	3.5972
5						west	70	29	3.5972
6					medium	central	70	29	4.2769
7						east	70	29	3.5972
8						north	70	29	4.2769
9						south	70	29	3.5972
10						west	70	29	3.5972
11					high	central	70	29	4.2769
12						east	70	29	3.5972
13						north	70	29	4.2769
14						south	70	29	3.5972
15						west	70	29	3.5972
16					heavy	central	70	29	4.2769
17						east	70	29	3.5972
18						north	70	29	4.2769
19						south	70	29	3.5972
20						west	70	29	3.5972
21				thin	low	central	70	29	3.8438
22						east	70	29	3.5972
23						north	70	29	3.8438
24						south	70	29	3.5972
25						west	70	29	3.8438
26					medium	central	70	29	2.5134
27						east	70	29	2.5134
28						north	70	29	2.5134
29						south	70	29	2.5134
30						west	70	29	3.5972
31					high	central	70	29	2.5134
32						east	70	29	2.5134
33						north	70	29	2.5134
34						south	70	29	2.5134
35						west	70	29	3.5972
36					heavy	central	70	29	2.5134
37						east	70	29	2.5134
38						north	70	29	2.5134
39						south	70	29	2.5134
40						west	70	29	3.5972

Table B.98: Block Cracking Model Coefficients for HR and US

group	distress	treat_lvl	highway_fun	pavement_typ	traffic_cls	climate_zone	alpha	A_star	beta_star
41	block_cracking_pct	HR	US	thick	low	central	70	29	2.2781
42						east	70	29	4.4768
43						north	70	29	3.5972
44						south	70	29	3.5972
45						west	70	29	3.7981
46					medium	central	70	29	2.2781
47						east	70	29	4.4768
48						north	70	29	3.5972
49						south	70	29	3.5972
50						west	70	29	3.7981
51					high	central	70	29	2.2781
52						east	70	29	4.4768
53						north	70	29	3.5972
54						south	70	29	3.5972
55						west	70	29	3.7981
56					heavy	central	70	29	2.2484
57						east	70	29	3.5983
58						north	70	29	3.5972
59						south	70	29	3.5972
60						west	70	29	3.6856
61				thin	low	central	70	29	3.5972
62						east	70	29	4.3168
63						north	70	29	3.5972
64						south	70	29	3.5972
65						west	70	29	3.5972
66					medium	central	70	29	3.5972
67						east	70	29	4.3168
68						north	70	29	3.5972
69						south	70	29	3.5972
70						west	70	29	3.5972
71					high	central	70	29	3.5972
72						east	70	29	3.5972
73						north	70	29	3.9937
74						south	70	29	3.5972
75						west	70	29	3.5972
76					heavy	central	70	29	3.7568
77						east	70	29	3.5972
78						north	70	29	3.5972
79						south	70	29	3.5972
80						west	70	29	3.7568

Table B.99: Block Cracking Model Coefficients for HR and SH

group	distress	treat_lvl	highway_fun	pavement_typ	traffic_cls	climate_zone	alpha	A_star	beta_star
81	block_cracking_pct	HR	SH	thick	low	central	70	29	0.9252
82	block_cracking_pct	HR	SH	thick	low	east	70	29	2.8684
83	block_cracking_pct	HR	SH	thick	low	north	70	29	3.5972
84	block_cracking_pct	HR	SH	thick	low	south	70	29	4.1136
85	block_cracking_pct	HR	SH	thick	low	west	70	29	3.5972
86	block_cracking_pct	HR	SH	thick	medium	central	70	29	0.9252
87	block_cracking_pct	HR	SH	thick	medium	east	70	29	2.8684
88	block_cracking_pct	HR	SH	thick	medium	north	70	29	3.5972
89	block_cracking_pct	HR	SH	thick	medium	south	70	29	4.1136
90	block_cracking_pct	HR	SH	thick	medium	west	70	29	3.5972
91	block_cracking_pct	HR	SH	thick	high	central	70	29	0.9252
92	block_cracking_pct	HR	SH	thick	high	east	70	29	2.8684
93	block_cracking_pct	HR	SH	thick	high	north	70	29	3.5972
94	block_cracking_pct	HR	SH	thick	high	south	70	29	4.1136
95	block_cracking_pct	HR	SH	thick	high	west	70	29	3.5972
96	block_cracking_pct	HR	SH	thick	heavy	central	70	29	3.7128
97	block_cracking_pct	HR	SH	thick	heavy	east	70	29	2.6262
98	block_cracking_pct	HR	SH	thick	heavy	north	70	29	3.7128
99	block_cracking_pct	HR	SH	thick	heavy	south	70	29	3.5972
100	block_cracking_pct	HR	SH	thick	heavy	west	70	29	3.5972
101	block_cracking_pct	HR	SH	thin	low	central	70	29	3.5972
102	block_cracking_pct	HR	SH	thin	low	east	70	29	3.5972
103	block_cracking_pct	HR	SH	thin	low	north	70	29	3.6005
104	block_cracking_pct	HR	SH	thin	low	south	70	29	3.5972
105	block_cracking_pct	HR	SH	thin	low	west	70	29	3.5972
106	block_cracking_pct	HR	SH	thin	medium	central	70	29	3.5972
107	block_cracking_pct	HR	SH	thin	medium	east	70	29	3.5972
108	block_cracking_pct	HR	SH	thin	medium	north	70	29	3.6005
109	block_cracking_pct	HR	SH	thin	medium	south	70	29	3.5972
110	block_cracking_pct	HR	SH	thin	medium	west	70	29	3.5972
111	block_cracking_pct	HR	SH	thin	high	central	70	29	1.1189
112	block_cracking_pct	HR	SH	thin	high	east	70	29	3.8900
113	block_cracking_pct	HR	SH	thin	high	north	70	29	0.9691
114	block_cracking_pct	HR	SH	thin	high	south	70	29	4.0780
115	block_cracking_pct	HR	SH	thin	high	west	70	29	4.2408
116	block_cracking_pct	HR	SH	thin	heavy	central	70	29	3.6178
117	block_cracking_pct	HR	SH	thin	heavy	east	70	29	3.5972
118	block_cracking_pct	HR	SH	thin	heavy	north	70	29	3.6178
119	block_cracking_pct	HR	SH	thin	heavy	south	70	29	2.4297
120	block_cracking_pct	HR	SH	thin	heavy	west	70	29	4.7926

Table B.100: Block Cracking Model Coefficients for HR and FM

group	distress	treat_lvl	highway_fun	pavement_typ	traffic_cls	climate_zone	alpha	A_star	beta_star
121	block_cracking_pct	HR	FM	thick	low	central	70	29	3.5972
122						east	70	29	3.5972
123						north	70	29	3.5972
124						south	70	29	3.5972
125						west	70	29	3.5972
126					medium	central	70	29	3.5972
127						east	70	29	4.6222
128						north	70	29	3.5972
129						south	70	29	3.5972
130						west	70	29	3.5972
131					high	central	70	29	1.6559
132						east	70	29	4.0611
133						north	70	29	3.5972
134						south	70	29	3.5972
135						west	70	29	3.5972
136					heavy	central	70	29	1.6559
137						east	70	29	4.0611
138						north	70	29	3.5972
139						south	70	29	3.5972
140						west	70	29	3.5972
141				thin	low	central	70	29	4.0025
142						east	70	29	4.5652
143						north	70	29	4.4206
144						south	70	29	3.5972
145						west	70	29	4.4768
146					medium	central	70	29	4.4477
147						east	70	29	5.0932
148						north	70	29	3.6032
149						south	70	29	3.5972
150						west	70	29	4.1136
151					high	central	70	29	3.5420
152						east	70	29	4.9818
153						north	70	29	3.5972
154						south	70	29	3.9937
155						west	70	29	4.1363
156					heavy	central	70	29	3.5420
157						east	70	29	4.9818
158						north	70	29	3.5972
159						south	70	29	3.9937
160						west	70	29	4.1363

Table B.101: Alligator Cracking Model Coefficients for DN and IH

group	distress	treat_lvl	highway_fun	pavement_typ	traffic_cls	climate_zone	alpha	A_star	beta_star
1	alligator_cracking_pct	DN	IH	thick	low	central	73	23.9679	1.5855
2						east	73	23.9679	0.7799
3						north	73	23.9679	1.5855
4						south	73	23.9679	1.2511
5						west	73	23.9679	1.7599
6					medium	central	73	23.9679	1.5855
7						east	73	23.9679	0.7799
8						north	73	23.9679	1.5855
9						south	73	23.9679	1.2511
10						west	73	23.9679	1.7599
11					high	central	73	23.9679	1.5855
12						east	73	23.9679	0.7799
13						north	73	23.9679	1.5855
14						south	73	23.9679	1.2511
15						west	73	23.9679	1.7599
16					heavy	central	73	23.9679	1.5855
17						east	73	23.9679	0.7799
18						north	73	23.9679	1.5855
19						south	73	23.9679	1.2511
20						west	73	23.9679	1.7599
21				thin	low	central	73	23.9679	1.6448
22						east	73	23.9679	0.6460
23						north	73	23.9679	1.6448
24						south	73	23.9679	0.9596
25						west	73	23.9679	1.6448
26					medium	central	73	23.9679	0.7343
27						east	73	23.9679	0.7343
28						north	73	23.9679	0.7343
29						south	73	23.9679	0.7343
30						west	73	23.9679	0.8488
31					high	central	73	23.9679	0.7343
32						east	73	23.9679	0.7343
33						north	73	23.9679	0.7343
34						south	73	23.9679	0.7343
35						west	73	23.9679	0.8488
36					heavy	central	73	23.9679	0.7343
37						east	73	23.9679	0.7343
38						north	73	23.9679	0.7343
39						south	73	23.9679	0.7343
40						west	73	23.9679	0.8488

Table B.102: Alligator Cracking Model Coefficients for DN and US

group	distress	treat_lvl	highway_fun	pavement_typ	traffic_cls	climate_zone	alpha	A_star	beta_star
41	alligator_cracking_pct	DN	US	thick	low	central	73	23.9679	1.0741
42						east	73	23.9679	1.6171
43						north	73	23.9679	1.0450
44						south	73	23.9679	1.2148
45						west	73	23.9679	2.4274
46					medium	central	73	23.9679	1.0741
47						east	73	23.9679	1.6171
48						north	73	23.9679	1.0450
49						south	73	23.9679	1.2148
50						west	73	23.9679	2.4274
51					high	central	73	23.9679	1.0741
52						east	73	23.9679	1.6171
53						north	73	23.9679	1.0450
54						south	73	23.9679	1.2148
55						west	73	23.9679	2.4274
56					heavy	central	73	23.9679	0.8196
57						east	73	23.9679	1.1417
58						north	73	23.9679	1.2542
59						south	73	23.9679	1.2011
60						west	73	23.9679	2.1708
61				thin	low	central	73	23.9679	1.1633
62						east	73	23.9679	1.9891
63						north	73	23.9679	1.1633
64						south	73	23.9679	1.1633
65						west	73	23.9679	1.2420
66					medium	central	73	23.9679	1.1633
67						east	73	23.9679	1.9891
68						north	73	23.9679	1.1633
69						south	73	23.9679	1.1633
70						west	73	23.9679	1.2420
71					high	central	73	23.9679	0.4393
72						east	73	23.9679	1.3330
73						north	73	23.9679	1.7277
74						south	73	23.9679	0.9494
75						west	73	23.9679	1.3806
76					heavy	central	73	23.9679	2.1566
77						east	73	23.9679	0.9981
78						north	73	23.9679	1.2425
79						south	73	23.9679	1.0675
80						west	73	23.9679	2.1566

Table B.103: Alligator Cracking Model Coefficients for DN and SH

group	distress	treat_lvl	highway_fun	pavement_typ	traffic_cls	climate_zone	alpha	A_star	beta_star
81	alligator_cracking_pct	DN	SH	thick	low	central	73	23.9679	0.8932
82						east	73	23.9679	1.0364
83						north	73	23.9679	0.3469
84						south	73	23.9679	1.7733
85						west	73	23.9679	1.3986
86					medium	central	73	23.9679	0.8932
87						east	73	23.9679	1.0364
88						north	73	23.9679	0.3469
89						south	73	23.9679	1.7733
90						west	73	23.9679	1.3986
91					high	central	73	23.9679	0.8932
92						east	73	23.9679	1.0364
93						north	73	23.9679	0.3469
94						south	73	23.9679	1.7733
95						west	73	23.9679	1.3986
96					heavy	central	73	23.9679	1.1917
97						east	73	23.9679	0.7555
98						north	73	23.9679	1.1917
99						south	73	23.9679	0.6468
100						west	73	23.9679	1.6691
101				thin	low	central	73	23.9679	0.9324
102						east	73	23.9679	1.2864
103						north	73	23.9679	2.0631
104						south	73	23.9679	1.2422
105						west	73	23.9679	0.5386
106					medium	central	73	23.9679	0.9324
107						east	73	23.9679	1.2864
108						north	73	23.9679	2.0631
109						south	73	23.9679	1.2422
110						west	73	23.9679	0.5386
111					high	central	73	23.9679	1.2034
112						east	73	23.9679	0.7215
113						north	73	23.9679	0.5041
114						south	73	23.9679	0.4943
115						west	73	23.9679	0.9468
116					heavy	central	73	23.9679	1.3942
117						east	73	23.9679	1.7323
118						north	73	23.9679	1.3942
119						south	73	23.9679	0.6745
120						west	73	23.9679	2.4412

Table B.104: Alligator Cracking Model Coefficients for DN and FM

group	distress	treat_lvl	highway_fun	pavement_typ	traffic_cls	climate_zone	alpha	A_star	beta_star
121	alligator_cracking_pct	DN	FM	thick	low	central	73	23.9679	0.8798
122	alligator_cracking_pct	DN	FM	thick	low	east	73	23.9679	0.9931
123	alligator_cracking_pct	DN	FM	thick	low	north	73	23.9679	0.8798
124	alligator_cracking_pct	DN	FM	thick	low	south	73	23.9679	0.6108
125	alligator_cracking_pct	DN	FM	thick	low	west	73	23.9679	0.8798
126	alligator_cracking_pct	DN	FM	thick	medium	central	73	23.9679	0.7473
127	alligator_cracking_pct	DN	FM	thick	medium	east	73	23.9679	0.6731
128	alligator_cracking_pct	DN	FM	thick	medium	north	73	23.9679	1.2422
129	alligator_cracking_pct	DN	FM	thick	medium	south	73	23.9679	0.8490
130	alligator_cracking_pct	DN	FM	thick	medium	west	73	23.9679	0.7473
131	alligator_cracking_pct	DN	FM	thick	high	central	73	23.9679	1.0545
132	alligator_cracking_pct	DN	FM	thick	high	east	73	23.9679	0.5986
133	alligator_cracking_pct	DN	FM	thick	high	north	73	23.9679	1.2422
134	alligator_cracking_pct	DN	FM	thick	high	south	73	23.9679	0.9035
135	alligator_cracking_pct	DN	FM	thick	high	west	73	23.9679	1.2422
136	alligator_cracking_pct	DN	FM	thick	heavy	central	73	23.9679	1.0545
137	alligator_cracking_pct	DN	FM	thick	heavy	east	73	23.9679	0.5986
138	alligator_cracking_pct	DN	FM	thick	heavy	north	73	23.9679	1.2422
139	alligator_cracking_pct	DN	FM	thick	heavy	south	73	23.9679	0.9035
140	alligator_cracking_pct	DN	FM	thick	heavy	west	73	23.9679	1.2422
141	alligator_cracking_pct	DN	FM	thin	low	central	73	23.9679	1.5896
142	alligator_cracking_pct	DN	FM	thin	low	east	73	23.9679	2.3028
143	alligator_cracking_pct	DN	FM	thin	low	north	73	23.9679	2.1168
144	alligator_cracking_pct	DN	FM	thin	low	south	73	23.9679	0.8458
145	alligator_cracking_pct	DN	FM	thin	low	west	73	23.9679	2.4845
146	alligator_cracking_pct	DN	FM	thin	medium	central	73	23.9679	1.3637
147	alligator_cracking_pct	DN	FM	thin	medium	east	73	23.9679	2.0325
148	alligator_cracking_pct	DN	FM	thin	medium	north	73	23.9679	0.6478
149	alligator_cracking_pct	DN	FM	thin	medium	south	73	23.9679	0.6653
150	alligator_cracking_pct	DN	FM	thin	medium	west	73	23.9679	2.1024
151	alligator_cracking_pct	DN	FM	thin	high	central	73	23.9679	1.5257
152	alligator_cracking_pct	DN	FM	thin	high	east	73	23.9679	0.7738
153	alligator_cracking_pct	DN	FM	thin	high	north	73	23.9679	0.5222
154	alligator_cracking_pct	DN	FM	thin	high	south	73	23.9679	2.4882
155	alligator_cracking_pct	DN	FM	thin	high	west	73	23.9679	2.3684
156	alligator_cracking_pct	DN	FM	thin	heavy	central	73	23.9679	1.5257
157	alligator_cracking_pct	DN	FM	thin	heavy	east	73	23.9679	0.7738
158	alligator_cracking_pct	DN	FM	thin	heavy	north	73	23.9679	0.5222
159	alligator_cracking_pct	DN	FM	thin	heavy	south	73	23.9679	2.4882
160	alligator_cracking_pct	DN	FM	thin	heavy	west	73	23.9679	2.3684

Table B.105: Alligator Cracking Model Coefficients for PM and IH

group	distress	treat_lvl	highway_fun	pavement_typ	traffic_cls	climate_zone	alpha	A_star	beta_star
1	alligator_cracking_pct	PM	IH	thick	low	central	73	27	1.5855
2						east	73	27	0.7799
3						north	73	27	1.5855
4						south	73	27	1.2511
5						west	73	27	1.7599
6					medium	central	73	27	1.5855
7						east	73	27	0.7799
8						north	73	27	1.5855
9						south	73	27	1.2511
10						west	73	27	1.7599
11					high	central	73	27	1.5855
12						east	73	27	0.7799
13						north	73	27	1.5855
14						south	73	27	1.2511
15						west	73	27	1.7599
16					heavy	central	73	27	1.5855
17						east	73	27	0.7799
18						north	73	27	1.5855
19						south	73	27	1.2511
20						west	73	27	1.7599
21				thin	low	central	73	27	1.6448
22						east	73	27	0.6460
23						north	73	27	1.6448
24						south	73	27	0.9596
25						west	73	27	1.6448
26					medium	central	73	27	0.7343
27						east	73	27	0.7343
28						north	73	27	0.7343
29						south	73	27	0.7343
30						west	73	27	0.8488
31					high	central	73	27	0.7343
32						east	73	27	0.7343
33						north	73	27	0.7343
34						south	73	27	0.7343
35						west	73	27	0.8488
36					heavy	central	73	27	0.7343
37						east	73	27	0.7343
38						north	73	27	0.7343
39						south	73	27	0.7343
40						west	73	27	0.8488

Table B.106: Alligator Cracking Model Coefficients for PM and US

group	distress	treat_lvl	highway_fun	pavement_typ	traffic_cls	climate_zone	alpha	A_star	beta_star
41	alligator_cracking_pct	PM	US	thick	low	central	73	27	1.0741
42						east	73	27	1.6171
43						north	73	27	1.0450
44						south	73	27	1.2148
45						west	73	27	2.4274
46					medium	central	73	27	1.0741
47						east	73	27	1.6171
48						north	73	27	1.0450
49						south	73	27	1.2148
50						west	73	27	2.4274
51					high	central	73	27	1.0741
52						east	73	27	1.6171
53						north	73	27	1.0450
54						south	73	27	1.2148
55						west	73	27	2.4274
56					heavy	central	73	27	0.8196
57						east	73	27	1.1417
58						north	73	27	1.2542
59						south	73	27	1.2011
60						west	73	27	2.1708
61				thin	low	central	73	27	1.1633
62						east	73	27	1.9891
63						north	73	27	1.1633
64						south	73	27	1.1633
65						west	73	27	1.2420
66					medium	central	73	27	1.1633
67						east	73	27	1.9891
68						north	73	27	1.1633
69						south	73	27	1.1633
70						west	73	27	1.2420
71					high	central	73	27	0.4393
72						east	73	27	1.3330
73						north	73	27	1.7277
74						south	73	27	0.9494
75						west	73	27	1.3806
76					heavy	central	73	27	2.1566
77						east	73	27	0.9981
78						north	73	27	1.2425
79						south	73	27	1.0675
80						west	73	27	2.1566

Table B.107: Alligator Cracking Model Coefficients for PM and SH

group	distress	treat_lvl	highway_fun	pavement_typ	traffic_cls	climate_zone	alpha	A_star	beta_star
81	alligator_cracking_pct	PM	SH	thick	low	central	73	27	0.8932
82						east	73	27	1.0364
83						north	73	27	0.3469
84						south	73	27	1.7733
85						west	73	27	1.3986
86					medium	central	73	27	0.8932
87						east	73	27	1.0364
88						north	73	27	0.3469
89						south	73	27	1.7733
90						west	73	27	1.3986
91					high	central	73	27	0.8932
92						east	73	27	1.0364
93						north	73	27	0.3469
94						south	73	27	1.7733
95						west	73	27	1.3986
96					heavy	central	73	27	1.1917
97						east	73	27	0.7555
98						north	73	27	1.1917
99						south	73	27	0.6468
100						west	73	27	1.6691
101				thin	low	central	73	27	0.9324
102						east	73	27	1.2864
103						north	73	27	2.0631
104						south	73	27	1.2422
105						west	73	27	0.5386
106					medium	central	73	27	0.9324
107						east	73	27	1.2864
108						north	73	27	2.0631
109						south	73	27	1.2422
110						west	73	27	0.5386
111					high	central	73	27	1.2034
112						east	73	27	0.7215
113						north	73	27	0.5041
114						south	73	27	0.4943
115						west	73	27	0.9468
116					heavy	central	73	27	1.3942
117						east	73	27	1.7323
118						north	73	27	1.3942
119						south	73	27	0.6745
120						west	73	27	2.4412

Table B.108: Alligator Cracking Model Coefficients for PM and FM

group	distress	treat_lvl	highway_fun	pavement_typ	traffic_cls	climate_zone	alpha	A_star	beta_star
121	alligator_cracking_pct	PM	FM	thick	low	central	73	27	0.8798
122						east	73	27	0.9931
123						north	73	27	0.8798
124						south	73	27	0.6108
125						west	73	27	0.8798
126					medium	central	73	27	0.7473
127						east	73	27	0.6731
128						north	73	27	1.2422
129						south	73	27	0.8490
130						west	73	27	0.7473
131					high	central	73	27	1.0545
132						east	73	27	0.5986
133						north	73	27	1.2422
134						south	73	27	0.9035
135						west	73	27	1.2422
136					heavy	central	73	27	1.0545
137						east	73	27	0.5986
138						north	73	27	1.2422
139						south	73	27	0.9035
140						west	73	27	1.2422
141				thin	low	central	73	27	1.5896
142						east	73	27	2.3028
143						north	73	27	2.1168
144						south	73	27	0.8458
145						west	73	27	2.4845
146					medium	central	73	27	1.3637
147						east	73	27	2.0325
148						north	73	27	0.6478
149						south	73	27	0.6653
150						west	73	27	2.1024
151					high	central	73	27	1.5257
152						east	73	27	0.7738
153						north	73	27	0.5222
154						south	73	27	2.4882
155						west	73	27	2.3684
156					heavy	central	73	27	1.5257
157						east	73	27	0.7738
158						north	73	27	0.5222
159						south	73	27	2.4882
160						west	73	27	2.3684

Table B.109: Alligator Cracking Model Coefficients for LR and IH

group	distress	treat_lvl	highway_fun	pavement_typ	traffic_cls	climate_zone	alpha	A_star	beta_star
1	alligator_cracking_pct	LR	IH	thick	low	central	73	30	1.5855
2	alligator_cracking_pct	LR	IH	thick	low	east	73	30	0.7799
3	alligator_cracking_pct	LR	IH	thick	low	north	73	30	1.5855
4	alligator_cracking_pct	LR	IH	thick	low	south	73	30	1.2511
5	alligator_cracking_pct	LR	IH	thick	low	west	73	30	1.7599
6	alligator_cracking_pct	LR	IH	thick	medium	central	73	30	1.5855
7	alligator_cracking_pct	LR	IH	thick	medium	east	73	30	0.7799
8	alligator_cracking_pct	LR	IH	thick	medium	north	73	30	1.5855
9	alligator_cracking_pct	LR	IH	thick	medium	south	73	30	1.2511
10	alligator_cracking_pct	LR	IH	thick	medium	west	73	30	1.7599
11	alligator_cracking_pct	LR	IH	thick	high	central	73	30	1.5855
12	alligator_cracking_pct	LR	IH	thick	high	east	73	30	0.7799
13	alligator_cracking_pct	LR	IH	thick	high	north	73	30	1.5855
14	alligator_cracking_pct	LR	IH	thick	high	south	73	30	1.2511
15	alligator_cracking_pct	LR	IH	thick	high	west	73	30	1.7599
16	alligator_cracking_pct	LR	IH	thick	heavy	central	73	30	1.5855
17	alligator_cracking_pct	LR	IH	thick	heavy	east	73	30	0.7799
18	alligator_cracking_pct	LR	IH	thick	heavy	north	73	30	1.5855
19	alligator_cracking_pct	LR	IH	thick	heavy	south	73	30	1.2511
20	alligator_cracking_pct	LR	IH	thick	heavy	west	73	30	1.7599
21	alligator_cracking_pct	LR	IH	thin	low	central	73	30	1.6448
22	alligator_cracking_pct	LR	IH	thin	low	east	73	30	0.6460
23	alligator_cracking_pct	LR	IH	thin	low	north	73	30	1.6448
24	alligator_cracking_pct	LR	IH	thin	low	south	73	30	0.9596
25	alligator_cracking_pct	LR	IH	thin	low	west	73	30	1.6448
26	alligator_cracking_pct	LR	IH	thin	medium	central	73	30	0.7343
27	alligator_cracking_pct	LR	IH	thin	medium	east	73	30	0.7343
28	alligator_cracking_pct	LR	IH	thin	medium	north	73	30	0.7343
29	alligator_cracking_pct	LR	IH	thin	medium	south	73	30	0.7343
30	alligator_cracking_pct	LR	IH	thin	medium	west	73	30	0.8488
31	alligator_cracking_pct	LR	IH	thin	high	central	73	30	0.7343
32	alligator_cracking_pct	LR	IH	thin	high	east	73	30	0.7343
33	alligator_cracking_pct	LR	IH	thin	high	north	73	30	0.7343
34	alligator_cracking_pct	LR	IH	thin	high	south	73	30	0.7343
35	alligator_cracking_pct	LR	IH	thin	high	west	73	30	0.8488
36	alligator_cracking_pct	LR	IH	thin	heavy	central	73	30	0.7343
37	alligator_cracking_pct	LR	IH	thin	heavy	east	73	30	0.7343
38	alligator_cracking_pct	LR	IH	thin	heavy	north	73	30	0.7343
39	alligator_cracking_pct	LR	IH	thin	heavy	south	73	30	0.7343
40	alligator_cracking_pct	LR	IH	thin	heavy	west	73	30	0.8488

Table B.110: Alligator Cracking Model Coefficients for LR and US

group	distress	treat_lvl	highway_fun	pavement_typ	traffic_cls	climate_zone	alpha	A_star	beta_star
41	alligator_cracking_pct	LR	US	thick	low	central	73	30	1.0741
42						east	73	30	1.6171
43						north	73	30	1.0450
44						south	73	30	1.2148
45						west	73	30	2.4274
46					medium	central	73	30	1.0741
47						east	73	30	1.6171
48						north	73	30	1.0450
49						south	73	30	1.2148
50						west	73	30	2.4274
51					high	central	73	30	1.0741
52						east	73	30	1.6171
53						north	73	30	1.0450
54						south	73	30	1.2148
55						west	73	30	2.4274
56					heavy	central	73	30	0.8196
57						east	73	30	1.1417
58						north	73	30	1.2542
59						south	73	30	1.2011
60						west	73	30	2.1708
61				thin	low	central	73	30	1.1633
62						east	73	30	1.9891
63						north	73	30	1.1633
64						south	73	30	1.1633
65						west	73	30	1.2420
66					medium	central	73	30	1.1633
67						east	73	30	1.9891
68						north	73	30	1.1633
69						south	73	30	1.1633
70						west	73	30	1.2420
71					high	central	73	30	0.4393
72						east	73	30	1.3330
73						north	73	30	1.7277
74						south	73	30	0.9494
75						west	73	30	1.3806
76					heavy	central	73	30	2.1566
77						east	73	30	0.9981
78						north	73	30	1.2425
79						south	73	30	1.0675
80						west	73	30	2.1566

Table B.111: Alligator Cracking Model Coefficients for LR and SH

group	distress	treat_lvl	highway_fun	pavement_typ	traffic_cls	climate_zone	alpha	A_star	beta_star
81	alligator_cracking_pct	LR	SH	thick	low	central	73	30	0.8932
82						east	73	30	1.0364
83						north	73	30	0.3469
84						south	73	30	1.7733
85						west	73	30	1.3986
86					medium	central	73	30	0.8932
87						east	73	30	1.0364
88						north	73	30	0.3469
89						south	73	30	1.7733
90						west	73	30	1.3986
91					high	central	73	30	0.8932
92						east	73	30	1.0364
93						north	73	30	0.3469
94						south	73	30	1.7733
95						west	73	30	1.3986
96					heavy	central	73	30	1.1917
97						east	73	30	0.7555
98						north	73	30	1.1917
99						south	73	30	0.6468
100						west	73	30	1.6691
101				thin	low	central	73	30	0.9324
102						east	73	30	1.2864
103						north	73	30	2.0631
104						south	73	30	1.2422
105						west	73	30	0.5386
106					medium	central	73	30	0.9324
107						east	73	30	1.2864
108						north	73	30	2.0631
109						south	73	30	1.2422
110						west	73	30	0.5386
111					high	central	73	30	1.2034
112						east	73	30	0.7215
113						north	73	30	0.5041
114						south	73	30	0.4943
115						west	73	30	0.9468
116					heavy	central	73	30	1.3942
117						east	73	30	1.7323
118						north	73	30	1.3942
119						south	73	30	0.6745
120						west	73	30	2.4412

Table B.112: Alligator Cracking Model Coefficients for LR and FM

group	distress	treat_lvl	highway_fun	pavement_typ	traffic_cls	climate_zone	alpha	A_star	beta_star
121	alligator_cracking_pct	LR	FM	thick	low	central	73	30	0.8798
122						east	73	30	0.9931
123						north	73	30	0.8798
124						south	73	30	0.6108
125						west	73	30	0.8798
126					medium	central	73	30	0.7473
127						east	73	30	0.6731
128						north	73	30	1.2422
129						south	73	30	0.8490
130						west	73	30	0.7473
131					high	central	73	30	1.0545
132						east	73	30	0.5986
133						north	73	30	1.2422
134						south	73	30	0.9035
135						west	73	30	1.2422
136					heavy	central	73	30	1.0545
137						east	73	30	0.5986
138						north	73	30	1.2422
139						south	73	30	0.9035
140						west	73	30	1.2422
141				thin	low	central	73	30	1.5896
142						east	73	30	2.3028
143						north	73	30	2.1168
144						south	73	30	0.8458
145						west	73	30	2.4845
146					medium	central	73	30	1.3637
147						east	73	30	2.0325
148						north	73	30	0.6478
149						south	73	30	0.6653
150						west	73	30	2.1024
151					high	central	73	30	1.5257
152						east	73	30	0.7738
153						north	73	30	0.5222
154						south	73	30	2.4882
155						west	73	30	2.3684
156					heavy	central	73	30	1.5257
157						east	73	30	0.7738
158						north	73	30	0.5222
159						south	73	30	2.4882
160						west	73	30	2.3684

Table B.113: Alligator Cracking Model Coefficients for MR and IH

group	distress	treat_lvl	highway_fun	pavement_typ	traffic_cls	climate_zone	alpha	A_star	beta_star
1	alligator_cracking_pct	MR	IH	thick	low	central	73	35	1.5855
2	alligator_cracking_pct	MR	IH	thick	low	east	73	35	0.7799
3	alligator_cracking_pct	MR	IH	thick	low	north	73	35	1.5855
4	alligator_cracking_pct	MR	IH	thick	low	south	73	35	1.2511
5	alligator_cracking_pct	MR	IH	thick	low	west	73	35	1.7599
6	alligator_cracking_pct	MR	IH	thick	medium	central	73	35	1.5855
7	alligator_cracking_pct	MR	IH	thick	medium	east	73	35	0.7799
8	alligator_cracking_pct	MR	IH	thick	medium	north	73	35	1.5855
9	alligator_cracking_pct	MR	IH	thick	medium	south	73	35	1.2511
10	alligator_cracking_pct	MR	IH	thick	medium	west	73	35	1.7599
11	alligator_cracking_pct	MR	IH	thick	high	central	73	35	1.5855
12	alligator_cracking_pct	MR	IH	thick	high	east	73	35	0.7799
13	alligator_cracking_pct	MR	IH	thick	high	north	73	35	1.5855
14	alligator_cracking_pct	MR	IH	thick	high	south	73	35	1.2511
15	alligator_cracking_pct	MR	IH	thick	high	west	73	35	1.7599
16	alligator_cracking_pct	MR	IH	thick	heavy	central	73	35	1.5855
17	alligator_cracking_pct	MR	IH	thick	heavy	east	73	35	0.7799
18	alligator_cracking_pct	MR	IH	thick	heavy	north	73	35	1.5855
19	alligator_cracking_pct	MR	IH	thick	heavy	south	73	35	1.2511
20	alligator_cracking_pct	MR	IH	thick	heavy	west	73	35	1.7599
21	alligator_cracking_pct	MR	IH	thin	low	central	73	35	1.6448
22	alligator_cracking_pct	MR	IH	thin	low	east	73	35	0.6460
23	alligator_cracking_pct	MR	IH	thin	low	north	73	35	1.6448
24	alligator_cracking_pct	MR	IH	thin	low	south	73	35	0.9596
25	alligator_cracking_pct	MR	IH	thin	low	west	73	35	1.6448
26	alligator_cracking_pct	MR	IH	thin	medium	central	73	35	0.7343
27	alligator_cracking_pct	MR	IH	thin	medium	east	73	35	0.7343
28	alligator_cracking_pct	MR	IH	thin	medium	north	73	35	0.7343
29	alligator_cracking_pct	MR	IH	thin	medium	south	73	35	0.7343
30	alligator_cracking_pct	MR	IH	thin	medium	west	73	35	0.8488
31	alligator_cracking_pct	MR	IH	thin	high	central	73	35	0.7343
32	alligator_cracking_pct	MR	IH	thin	high	east	73	35	0.7343
33	alligator_cracking_pct	MR	IH	thin	high	north	73	35	0.7343
34	alligator_cracking_pct	MR	IH	thin	high	south	73	35	0.7343
35	alligator_cracking_pct	MR	IH	thin	high	west	73	35	0.8488
36	alligator_cracking_pct	MR	IH	thin	heavy	central	73	35	0.7343
37	alligator_cracking_pct	MR	IH	thin	heavy	east	73	35	0.7343
38	alligator_cracking_pct	MR	IH	thin	heavy	north	73	35	0.7343
39	alligator_cracking_pct	MR	IH	thin	heavy	south	73	35	0.7343
40	alligator_cracking_pct	MR	IH	thin	heavy	west	73	35	0.8488

Table B.114: Alligator Cracking Model Coefficients for MR and US

group	distress	treat_lvl	highway_fun	pavement_typ	traffic_cls	climate_zone	alpha	A_star	beta_star
41	alligator_cracking_pct	MR	US	thick	low	central	73	35	1.0741
42						east	73	35	1.6171
43						north	73	35	1.0450
44						south	73	35	1.2148
45						west	73	35	2.4274
46					medium	central	73	35	1.0741
47						east	73	35	1.6171
48						north	73	35	1.0450
49						south	73	35	1.2148
50						west	73	35	2.4274
51					high	central	73	35	1.0741
52						east	73	35	1.6171
53						north	73	35	1.0450
54						south	73	35	1.2148
55						west	73	35	2.4274
56					heavy	central	73	35	0.8196
57						east	73	35	1.1417
58						north	73	35	1.2542
59						south	73	35	1.2011
60						west	73	35	2.1708
61				thin	low	central	73	35	1.1633
62						east	73	35	1.9891
63						north	73	35	1.1633
64						south	73	35	1.1633
65						west	73	35	1.2420
66					medium	central	73	35	1.1633
67						east	73	35	1.9891
68						north	73	35	1.1633
69						south	73	35	1.1633
70						west	73	35	1.2420
71					high	central	73	35	0.4393
72						east	73	35	1.3330
73						north	73	35	1.7277
74						south	73	35	0.9494
75						west	73	35	1.3806
76					heavy	central	73	35	2.1566
77						east	73	35	0.9981
78						north	73	35	1.2425
79						south	73	35	1.0675
80						west	73	35	2.1566

Table B.115: Alligator Cracking Model Coefficients for MR and SH

group	distress	treat_lvl	highway_fun	pavement_typ	traffic_cls	climate_zone	alpha	A_star	beta_star
81	alligator_cracking_pct	MR	SH	thick	low	central	73	35	0.8932
82						east	73	35	1.0364
83						north	73	35	0.3469
84						south	73	35	1.7733
85						west	73	35	1.3986
86					medium	central	73	35	0.8932
87						east	73	35	1.0364
88						north	73	35	0.3469
89						south	73	35	1.7733
90						west	73	35	1.3986
91					high	central	73	35	0.8932
92						east	73	35	1.0364
93						north	73	35	0.3469
94						south	73	35	1.7733
95						west	73	35	1.3986
96					heavy	central	73	35	1.1917
97						east	73	35	0.7555
98						north	73	35	1.1917
99						south	73	35	0.6468
100						west	73	35	1.6691
101				thin	low	central	73	35	0.9324
102						east	73	35	1.2864
103						north	73	35	2.0631
104						south	73	35	1.2422
105						west	73	35	0.5386
106					medium	central	73	35	0.9324
107						east	73	35	1.2864
108						north	73	35	2.0631
109						south	73	35	1.2422
110						west	73	35	0.5386
111					high	central	73	35	1.2034
112						east	73	35	0.7215
113						north	73	35	0.5041
114						south	73	35	0.4943
115						west	73	35	0.9468
116					heavy	central	73	35	1.3942
117						east	73	35	1.7323
118						north	73	35	1.3942
119						south	73	35	0.6745
120						west	73	35	2.4412

Table B.116: Alligator Cracking Model Coefficients for MR and FM

group	distress	treat_lvl	highway_fun	pavement_typ	traffic_cls	climate_zone	alpha	A_star	beta_star
121	alligator_cracking_pct	MR	FM	thick	low	central	73	35	0.8798
122						east	73	35	0.9931
123						north	73	35	0.8798
124						south	73	35	0.6108
125						west	73	35	0.8798
126					medium	central	73	35	0.7473
127						east	73	35	0.6731
128						north	73	35	1.2422
129						south	73	35	0.8490
130						west	73	35	0.7473
131					high	central	73	35	1.0545
132						east	73	35	0.5986
133						north	73	35	1.2422
134						south	73	35	0.9035
135						west	73	35	1.2422
136					heavy	central	73	35	1.0545
137						east	73	35	0.5986
138						north	73	35	1.2422
139						south	73	35	0.9035
140						west	73	35	1.2422
141				thin	low	central	73	35	1.5896
142						east	73	35	2.3028
143						north	73	35	2.1168
144						south	73	35	0.8458
145						west	73	35	2.4845
146					medium	central	73	35	1.3637
147						east	73	35	2.0325
148						north	73	35	0.6478
149						south	73	35	0.6653
150						west	73	35	2.1024
151					high	central	73	35	1.5257
152						east	73	35	0.7738
153						north	73	35	0.5222
154						south	73	35	2.4882
155						west	73	35	2.3684
156					heavy	central	73	35	1.5257
157						east	73	35	0.7738
158						north	73	35	0.5222
159						south	73	35	2.4882
160						west	73	35	2.3684

Table B.117: Alligator Cracking Model Coefficients for HR and IH

group	distress	treat_lvl	highway_fun	pavement_typ	traffic_cls	climate_zone	alpha	A_star	beta_star
1	alligator_cracking_pct	HR	IH	thick	low	central	73	38	1.5855
2						east	73	38	0.7799
3						north	73	38	1.5855
4						south	73	38	1.2511
5						west	73	38	1.7599
6					medium	central	73	38	1.5855
7						east	73	38	0.7799
8						north	73	38	1.5855
9						south	73	38	1.2511
10						west	73	38	1.7599
11					high	central	73	38	1.5855
12						east	73	38	0.7799
13						north	73	38	1.5855
14						south	73	38	1.2511
15						west	73	38	1.7599
16					heavy	central	73	38	1.5855
17						east	73	38	0.7799
18						north	73	38	1.5855
19						south	73	38	1.2511
20						west	73	38	1.7599
21				thin	low	central	73	38	1.6448
22						east	73	38	0.6460
23						north	73	38	1.6448
24						south	73	38	0.9596
25						west	73	38	1.6448
26					medium	central	73	38	0.7343
27						east	73	38	0.7343
28						north	73	38	0.7343
29						south	73	38	0.7343
30						west	73	38	0.8488
31					high	central	73	38	0.7343
32						east	73	38	0.7343
33						north	73	38	0.7343
34						south	73	38	0.7343
35						west	73	38	0.8488
36					heavy	central	73	38	0.7343
37						east	73	38	0.7343
38						north	73	38	0.7343
39						south	73	38	0.7343
40						west	73	38	0.8488

Table B.118: Alligator Cracking Model Coefficients for HR and US

group	distress	treat_lvl	highway_fun	pavement_typ	traffic_cls	climate_zone	alpha	A_star	beta_star
41	alligator_cracking_pct	HR	US	thick	low	central	73	38	1.0741
42						east	73	38	1.6171
43						north	73	38	1.0450
44						south	73	38	1.2148
45						west	73	38	2.4274
46					medium	central	73	38	1.0741
47						east	73	38	1.6171
48						north	73	38	1.0450
49						south	73	38	1.2148
50						west	73	38	2.4274
51					high	central	73	38	1.0741
52						east	73	38	1.6171
53						north	73	38	1.0450
54						south	73	38	1.2148
55						west	73	38	2.4274
56					heavy	central	73	38	0.8196
57						east	73	38	1.1417
58						north	73	38	1.2542
59						south	73	38	1.2011
60						west	73	38	2.1708
61				thin	low	central	73	38	1.1633
62						east	73	38	1.9891
63						north	73	38	1.1633
64						south	73	38	1.1633
65						west	73	38	1.2420
66					medium	central	73	38	1.1633
67						east	73	38	1.9891
68						north	73	38	1.1633
69						south	73	38	1.1633
70						west	73	38	1.2420
71					high	central	73	38	0.4393
72						east	73	38	1.3330
73						north	73	38	1.7277
74						south	73	38	0.9494
75						west	73	38	1.3806
76					heavy	central	73	38	2.1566
77						east	73	38	0.9981
78						north	73	38	1.2425
79						south	73	38	1.0675
80						west	73	38	2.1566

Table B.119: Alligator Cracking Model Coefficients for HR and SH

group	distress	treat_lvl	highway_fun	pavement_typ	traffic_cls	climate_zone	alpha	A_star	beta_star
81	alligator_cracking_pct	HR	SH	thick	low	central	73	38	0.8932
82						east	73	38	1.0364
83						north	73	38	0.3469
84						south	73	38	1.7733
85						west	73	38	1.3986
86					medium	central	73	38	0.8932
87						east	73	38	1.0364
88						north	73	38	0.3469
89						south	73	38	1.7733
90						west	73	38	1.3986
91					high	central	73	38	0.8932
92						east	73	38	1.0364
93						north	73	38	0.3469
94						south	73	38	1.7733
95						west	73	38	1.3986
96					heavy	central	73	38	1.1917
97						east	73	38	0.7555
98						north	73	38	1.1917
99						south	73	38	0.6468
100						west	73	38	1.6691
101				thin	low	central	73	38	0.9324
102						east	73	38	1.2864
103						north	73	38	2.0631
104						south	73	38	1.2422
105						west	73	38	0.5386
106					medium	central	73	38	0.9324
107						east	73	38	1.2864
108						north	73	38	2.0631
109						south	73	38	1.2422
110						west	73	38	0.5386
111					high	central	73	38	1.2034
112						east	73	38	0.7215
113						north	73	38	0.5041
114						south	73	38	0.4943
115						west	73	38	0.9468
116					heavy	central	73	38	1.3942
117						east	73	38	1.7323
118						north	73	38	1.3942
119						south	73	38	0.6745
120						west	73	38	2.4412

Table B.120: Alligator Cracking Model Coefficients for HR and FM

group	distress	treat_lvl	highway_fun	pavement_typ	traffic_cls	climate_zone	alpha	A_star	beta_star
121	alligator_cracking_pct	HR	FM	thick	low	central	73	38	0.8798
122						east	73	38	0.9931
123						north	73	38	0.8798
124						south	73	38	0.6108
125						west	73	38	0.8798
126					medium	central	73	38	0.7473
127						east	73	38	0.6731
128						north	73	38	1.2422
129						south	73	38	0.8490
130						west	73	38	0.7473
131					high	central	73	38	1.0545
132						east	73	38	0.5986
133						north	73	38	1.2422
134						south	73	38	0.9035
135						west	73	38	1.2422
136					heavy	central	73	38	1.0545
137						east	73	38	0.5986
138						north	73	38	1.2422
139						south	73	38	0.9035
140						west	73	38	1.2422
141				thin	low	central	73	38	1.5896
142						east	73	38	2.3028
143						north	73	38	2.1168
144						south	73	38	0.8458
145						west	73	38	2.4845
146					medium	central	73	38	1.3637
147						east	73	38	2.0325
148						north	73	38	0.6478
149						south	73	38	0.6653
150						west	73	38	2.1024
151					high	central	73	38	1.5257
152						east	73	38	0.7738
153						north	73	38	0.5222
154						south	73	38	2.4882
155						west	73	38	2.3684
156					heavy	central	73	38	1.5257
157						east	73	38	0.7738
158						north	73	38	0.5222
159						south	73	38	2.4882
160						west	73	38	2.3684

Table B.121: Longitudinal Cracking Model Coefficients for DN and IH

group	distress	treat_lvl	highway_fun	pavement_typ	traffic_cls	climate_zone	alpha	A_star	beta_star
1	longitude_cracking_pct	DN	IH	thick	low	central	230	17.5793	0.8662
2						east	230	17.5793	0.8095
3						north	230	17.5793	0.8662
4						south	230	17.5793	0.8355
5						west	230	17.5793	0.6807
6					medium	central	230	17.5793	0.8662
7						east	230	17.5793	0.8095
8						north	230	17.5793	0.8662
9						south	230	17.5793	0.8355
10						west	230	17.5793	0.6807
11					high	central	230	17.5793	0.8662
12						east	230	17.5793	0.8095
13						north	230	17.5793	0.8662
14						south	230	17.5793	0.8355
15						west	230	17.5793	0.6807
16					heavy	central	230	17.5793	0.8662
17						east	230	17.5793	0.8095
18						north	230	17.5793	0.8662
19						south	230	17.5793	0.8355
20						west	230	17.5793	0.6807
21				thin	low	central	230	17.5793	0.8218
22						east	230	17.5793	0.5933
23						north	230	17.5793	0.8218
24						south	230	17.5793	0.6921
25						west	230	17.5793	0.8218
26					medium	central	230	17.5793	0.9249
27						east	230	17.5793	0.9249
28						north	230	17.5793	0.9249
29						south	230	17.5793	0.9249
30						west	230	17.5793	1.0898
31					high	central	230	17.5793	0.9249
32						east	230	17.5793	0.9249
33						north	230	17.5793	0.9249
34						south	230	17.5793	0.9249
35						west	230	17.5793	1.0898
36					heavy	central	230	17.5793	0.9249
37						east	230	17.5793	0.9249
38						north	230	17.5793	0.9249
39						south	230	17.5793	0.9249
40						west	230	17.5793	1.0898

Table B.122: Longitudinal Cracking Model Coefficients for DN and US

group	distress	treat_lvl	highway_fun	pavement_typ	traffic_cls	climate_zone	alpha	A_star	beta_star
41	longitude_cracking_pct	DN	US	thick	low	central	230	17.5793	0.6761
42						east	230	17.5793	0.5874
43						north	230	17.5793	0.4482
44						south	230	17.5793	0.8057
45						west	230	17.5793	2.6308
46					medium	central	230	17.5793	0.6761
47						east	230	17.5793	0.5874
48						north	230	17.5793	0.4482
49						south	230	17.5793	0.8057
50						west	230	17.5793	2.6308
51					high	central	230	17.5793	0.6761
52						east	230	17.5793	0.5874
53						north	230	17.5793	0.4482
54						south	230	17.5793	0.8057
55						west	230	17.5793	2.6308
56					heavy	central	230	17.5793	0.3994
57						east	230	17.5793	0.9315
58						north	230	17.5793	1.0218
59						south	230	17.5793	0.5910
60						west	230	17.5793	2.6996
61				thin	low	central	230	17.5793	0.9331
62						east	230	17.5793	2.4483
63						north	230	17.5793	0.9331
64						south	230	17.5793	0.9331
65						west	230	17.5793	0.7334
66					medium	central	230	17.5793	0.9331
67						east	230	17.5793	2.4483
68						north	230	17.5793	0.9331
69						south	230	17.5793	0.9331
70						west	230	17.5793	0.7334
71					high	central	230	17.5793	0.4555
72						east	230	17.5793	0.6417
73						north	230	17.5793	0.5362
74						south	230	17.5793	0.5584
75						west	230	17.5793	1.5218
76					heavy	central	230	17.5793	2.6868
77						east	230	17.5793	1.0194
78						north	230	17.5793	0.5795
79						south	230	17.5793	0.9306
80						west	230	17.5793	2.6868

Table B.123: Longitudinal Cracking Model Coefficients for DN and SH

group	distress	treat_lvl	highway_fun	pavement_typ	traffic_cls	climate_zone	alpha	A_star	beta_star
81	longitude_cracking_pct	DN	SH	thick	low	central	230	17.5793	0.6819
82						east	230	17.5793	0.6245
83						north	230	17.5793	0.3282
84						south	230	17.5793	0.5449
85						west	230	17.5793	1.1688
86					medium	central	230	17.5793	0.6819
87						east	230	17.5793	0.6245
88						north	230	17.5793	0.3282
89						south	230	17.5793	0.5449
90						west	230	17.5793	1.1688
91					high	central	230	17.5793	0.6819
92						east	230	17.5793	0.6245
93						north	230	17.5793	0.3282
94						south	230	17.5793	0.5449
95						west	230	17.5793	1.1688
96					heavy	central	230	17.5793	0.5937
97						east	230	17.5793	0.5947
98						north	230	17.5793	0.5937
99						south	230	17.5793	0.5195
100						west	230	17.5793	0.4869
101				thin	low	central	230	17.5793	0.6629
102						east	230	17.5793	1.0440
103						north	230	17.5793	0.8039
104						south	230	17.5793	0.6712
105						west	230	17.5793	0.8065
106					medium	central	230	17.5793	0.6629
107						east	230	17.5793	1.0440
108						north	230	17.5793	0.8039
109						south	230	17.5793	0.6712
110						west	230	17.5793	0.8065
111					high	central	230	17.5793	1.0892
112						east	230	17.5793	2.7368
113						north	230	17.5793	0.4806
114						south	230	17.5793	0.7693
115						west	230	17.5793	2.2689
116					heavy	central	230	17.5793	0.6509
117						east	230	17.5793	1.1347
118						north	230	17.5793	0.6509
119						south	230	17.5793	0.5634
120						west	230	17.5793	1.9888

Table B.124: Longitudinal Cracking Model Coefficients for DN and FM

group	distress	treat_lvl	highway_fun	pavement_typ	traffic_cls	climate_zone	alpha	A_star	beta_star
121	longitude_cracking_pct	DN	FM	thick	low	central	230	17.5793	0.5454
122						east	230	17.5793	0.6849
123						north	230	17.5793	0.5454
124						south	230	17.5793	0.3642
125						west	230	17.5793	0.5454
126					medium	central	230	17.5793	0.3974
127						east	230	17.5793	0.3786
128						north	230	17.5793	0.3452
129						south	230	17.5793	0.5699
130						west	230	17.5793	0.3974
131					high	central	230	17.5793	0.4917
132						east	230	17.5793	0.3498
133						north	230	17.5793	0.4539
134						south	230	17.5793	0.4637
135						west	230	17.5793	0.5154
136					heavy	central	230	17.5793	0.4917
137						east	230	17.5793	0.3498
138						north	230	17.5793	0.4539
139						south	230	17.5793	0.4637
140						west	230	17.5793	0.5154
141				thin	low	central	230	17.5793	0.7692
142						east	230	17.5793	1.5124
143						north	230	17.5793	1.7322
144						south	230	17.5793	0.4114
145						west	230	17.5793	0.4629
146					medium	central	230	17.5793	1.1263
147						east	230	17.5793	1.6214
148						north	230	17.5793	0.5110
149						south	230	17.5793	0.7611
150						west	230	17.5793	0.3000
151					high	central	230	17.5793	0.9063
152						east	230	17.5793	0.8100
153						north	230	17.5793	0.4700
154						south	230	17.5793	3.4893
155						west	230	17.5793	4.1200
156					heavy	central	230	17.5793	0.9063
157						east	230	17.5793	0.8100
158						north	230	17.5793	0.4700
159						south	230	17.5793	3.4893
160						west	230	17.5793	4.1200

Table B.125: Longitudinal Cracking Model Coefficients for PM and IH

group	distress	treat_lvl	highway_fun	pavement_typ	traffic_cls	climate_zone	alpha	A_star	beta_star
1	longitude_cracking_pct	PM	IH	thick	low	central	230	25	0.8662
2						east	230	25	0.8095
3						north	230	25	0.8662
4						south	230	25	0.8355
5						west	230	25	0.6807
6					medium	central	230	25	0.8662
7						east	230	25	0.8095
8						north	230	25	0.8662
9						south	230	25	0.8355
10						west	230	25	0.6807
11					high	central	230	25	0.8662
12						east	230	25	0.8095
13						north	230	25	0.8662
14						south	230	25	0.8355
15						west	230	25	0.6807
16					heavy	central	230	25	0.8662
17						east	230	25	0.8095
18						north	230	25	0.8662
19						south	230	25	0.8355
20						west	230	25	0.6807
21				thin	low	central	230	25	0.8218
22						east	230	25	0.5933
23						north	230	25	0.8218
24						south	230	25	0.6921
25						west	230	25	0.8218
26					medium	central	230	25	0.9249
27						east	230	25	0.9249
28						north	230	25	0.9249
29						south	230	25	0.9249
30						west	230	25	1.0898
31					high	central	230	25	0.9249
32						east	230	25	0.9249
33						north	230	25	0.9249
34						south	230	25	0.9249
35						west	230	25	1.0898
36					heavy	central	230	25	0.9249
37						east	230	25	0.9249
38						north	230	25	0.9249
39						south	230	25	0.9249
40						west	230	25	1.0898

Table B.126: Longitudinal Cracking Model Coefficients for PM and US

group	distress	treat_lvl	highway_fun	pavement_typ	traffic_cls	climate_zone	alpha	A_star	beta_star
41	longitude_cracking_pct	PM	US	thick	low	central	230	25	0.6761
42						east	230	25	0.5874
43						north	230	25	0.4482
44						south	230	25	0.8057
45						west	230	25	2.6308
46					medium	central	230	25	0.6761
47						east	230	25	0.5874
48						north	230	25	0.4482
49						south	230	25	0.8057
50						west	230	25	2.6308
51					high	central	230	25	0.6761
52						east	230	25	0.5874
53						north	230	25	0.4482
54						south	230	25	0.8057
55						west	230	25	2.6308
56					heavy	central	230	25	0.3994
57						east	230	25	0.9315
58						north	230	25	1.0218
59						south	230	25	0.5910
60						west	230	25	2.6996
61				thin	low	central	230	25	0.9331
62						east	230	25	2.4483
63						north	230	25	0.9331
64						south	230	25	0.9331
65						west	230	25	0.7334
66					medium	central	230	25	0.9331
67						east	230	25	2.4483
68						north	230	25	0.9331
69						south	230	25	0.9331
70						west	230	25	0.7334
71					high	central	230	25	0.4555
72						east	230	25	0.6417
73						north	230	25	0.5362
74						south	230	25	0.5584
75						west	230	25	1.5218
76					heavy	central	230	25	2.6868
77						east	230	25	1.0194
78						north	230	25	0.5795
79						south	230	25	0.9306
80						west	230	25	2.6868

Table B.127: Longitudinal Cracking Model Coefficients for PM and SH

group	distress	treat_lvl	highway_fun	pavement_typ	traffic_cls	climate_zone	alpha	A_star	beta_star
81	longitude_cracking_pct	PM	SH	thick	low	central	230	25	0.6819
82						east	230	25	0.6245
83						north	230	25	0.3282
84						south	230	25	0.5449
85						west	230	25	1.1688
86					medium	central	230	25	0.6819
87						east	230	25	0.6245
88						north	230	25	0.3282
89						south	230	25	0.5449
90						west	230	25	1.1688
91					high	central	230	25	0.6819
92						east	230	25	0.6245
93						north	230	25	0.3282
94						south	230	25	0.5449
95						west	230	25	1.1688
96					heavy	central	230	25	0.5937
97						east	230	25	0.5947
98						north	230	25	0.5937
99						south	230	25	0.5195
100						west	230	25	0.4869
101				thin	low	central	230	25	0.6629
102						east	230	25	1.0440
103						north	230	25	0.8039
104						south	230	25	0.6712
105						west	230	25	0.8065
106					medium	central	230	25	0.6629
107						east	230	25	1.0440
108						north	230	25	0.8039
109						south	230	25	0.6712
110						west	230	25	0.8065
111					high	central	230	25	1.0892
112						east	230	25	2.7368
113						north	230	25	0.4806
114						south	230	25	0.7693
115						west	230	25	2.2689
116					heavy	central	230	25	0.6509
117						east	230	25	1.1347
118						north	230	25	0.6509
119						south	230	25	0.5634
120						west	230	25	1.9888

Table B.128: Longitudinal Cracking Model Coefficients for PM and FM

group	distress	treat_lvl	highway_fun	pavement_typ	traffic_cls	climate_zone	alpha	A_star	beta_star
121	longitude_cracking_pct	PM	FM	thick	low	central	230	25	0.5454
122						east	230	25	0.6849
123						north	230	25	0.5454
124						south	230	25	0.3642
125						west	230	25	0.5454
126					medium	central	230	25	0.3974
127						east	230	25	0.3786
128						north	230	25	0.3452
129						south	230	25	0.5699
130						west	230	25	0.3974
131					high	central	230	25	0.4917
132						east	230	25	0.3498
133						north	230	25	0.4539
134						south	230	25	0.4637
135						west	230	25	0.5154
136					heavy	central	230	25	0.4917
137						east	230	25	0.3498
138						north	230	25	0.4539
139						south	230	25	0.4637
140						west	230	25	0.5154
141				thin	low	central	230	25	0.7692
142						east	230	25	1.5124
143						north	230	25	1.7322
144						south	230	25	0.4114
145						west	230	25	0.4629
146					medium	central	230	25	1.1263
147						east	230	25	1.6214
148						north	230	25	0.5110
149						south	230	25	0.7611
150						west	230	25	0.3000
151					high	central	230	25	0.9063
152						east	230	25	0.8100
153						north	230	25	0.4700
154						south	230	25	3.4893
155						west	230	25	4.1200
156					heavy	central	230	25	0.9063
157						east	230	25	0.8100
158						north	230	25	0.4700
159						south	230	25	3.4893
160						west	230	25	4.1200

Table B.129: Longitudinal Cracking Model Coefficients for LR and IH

group	distress	treat_lvl	highway_fun	pavement_typ	traffic_cls	climate_zone	alpha	A_star	beta_star
1	longitude_cracking_pct	LR	IH	thick	low	central	230	27.5	0.8662
2						east	230	27.5	0.8095
3						north	230	27.5	0.8662
4						south	230	27.5	0.8355
5						west	230	27.5	0.6807
6					medium	central	230	27.5	0.8662
7						east	230	27.5	0.8095
8						north	230	27.5	0.8662
9						south	230	27.5	0.8355
10						west	230	27.5	0.6807
11					high	central	230	27.5	0.8662
12						east	230	27.5	0.8095
13						north	230	27.5	0.8662
14						south	230	27.5	0.8355
15						west	230	27.5	0.6807
16					heavy	central	230	27.5	0.8662
17						east	230	27.5	0.8095
18						north	230	27.5	0.8662
19						south	230	27.5	0.8355
20						west	230	27.5	0.6807
21				thin	low	central	230	27.5	0.8218
22						east	230	27.5	0.5933
23						north	230	27.5	0.8218
24						south	230	27.5	0.6921
25						west	230	27.5	0.8218
26					medium	central	230	27.5	0.9249
27						east	230	27.5	0.9249
28						north	230	27.5	0.9249
29						south	230	27.5	0.9249
30						west	230	27.5	1.0898
31					high	central	230	27.5	0.9249
32						east	230	27.5	0.9249
33						north	230	27.5	0.9249
34						south	230	27.5	0.9249
35						west	230	27.5	1.0898
36					heavy	central	230	27.5	0.9249
37						east	230	27.5	0.9249
38						north	230	27.5	0.9249
39						south	230	27.5	0.9249
40						west	230	27.5	1.0898

Table B.130: Longitudinal Cracking Model Coefficients for LR and US

group	distress	treat_lvl	highway_fun	pavement_typ	traffic_cls	climate_zone	alpha	A_star	beta_star
41	longitude_cracking_pct	LR	US	thick	low	central	230	27.5	0.6761
42						east	230	27.5	0.5874
43						north	230	27.5	0.4482
44						south	230	27.5	0.8057
45						west	230	27.5	2.6308
46					medium	central	230	27.5	0.6761
47						east	230	27.5	0.5874
48						north	230	27.5	0.4482
49						south	230	27.5	0.8057
50						west	230	27.5	2.6308
51					high	central	230	27.5	0.6761
52						east	230	27.5	0.5874
53						north	230	27.5	0.4482
54						south	230	27.5	0.8057
55						west	230	27.5	2.6308
56					heavy	central	230	27.5	0.3994
57						east	230	27.5	0.9315
58						north	230	27.5	1.0218
59						south	230	27.5	0.5910
60						west	230	27.5	2.6996
61				thin	low	central	230	27.5	0.9331
62						east	230	27.5	2.4483
63						north	230	27.5	0.9331
64						south	230	27.5	0.9331
65						west	230	27.5	0.7334
66					medium	central	230	27.5	0.9331
67						east	230	27.5	2.4483
68						north	230	27.5	0.9331
69						south	230	27.5	0.9331
70						west	230	27.5	0.7334
71					high	central	230	27.5	0.4555
72						east	230	27.5	0.6417
73						north	230	27.5	0.5362
74						south	230	27.5	0.5584
75						west	230	27.5	1.5218
76					heavy	central	230	27.5	2.6868
77						east	230	27.5	1.0194
78						north	230	27.5	0.5795
79						south	230	27.5	0.9306
80						west	230	27.5	2.6868

Table B.131: Longitudinal Cracking Model Coefficients for LR and SH

group	distress	treat_lvl	highway_fun	pavement_typ	traffic_cls	climate_zone	alpha	A_star	beta_star
81	longitude_cracking_pct	LR	SH	thick	low	central	230	27.5	0.6819
82						east	230	27.5	0.6245
83						north	230	27.5	0.3282
84						south	230	27.5	0.5449
85						west	230	27.5	1.1688
86					medium	central	230	27.5	0.6819
87						east	230	27.5	0.6245
88						north	230	27.5	0.3282
89						south	230	27.5	0.5449
90						west	230	27.5	1.1688
91					high	central	230	27.5	0.6819
92						east	230	27.5	0.6245
93						north	230	27.5	0.3282
94						south	230	27.5	0.5449
95						west	230	27.5	1.1688
96					heavy	central	230	27.5	0.5937
97						east	230	27.5	0.5947
98						north	230	27.5	0.5937
99						south	230	27.5	0.5195
100						west	230	27.5	0.4869
101				thin	low	central	230	27.5	0.6629
102						east	230	27.5	1.0440
103						north	230	27.5	0.8039
104						south	230	27.5	0.6712
105						west	230	27.5	0.8065
106					medium	central	230	27.5	0.6629
107						east	230	27.5	1.0440
108						north	230	27.5	0.8039
109						south	230	27.5	0.6712
110						west	230	27.5	0.8065
111					high	central	230	27.5	1.0892
112						east	230	27.5	2.7368
113						north	230	27.5	0.4806
114						south	230	27.5	0.7693
115						west	230	27.5	2.2689
116					heavy	central	230	27.5	0.6509
117						east	230	27.5	1.1347
118						north	230	27.5	0.6509
119						south	230	27.5	0.5634
120						west	230	27.5	1.9888

Table B.132: Longitudinal Cracking Model Coefficients for LR and FM

group	distress	treat_lvl	highway_fun	pavement_typ	traffic_cls	climate_zone	alpha	A_star	beta_star
121	longitude_cracking_pct	LR	FM	thick	low	central	230	27.5	0.5454
122						east	230	27.5	0.6849
123						north	230	27.5	0.5454
124						south	230	27.5	0.3642
125						west	230	27.5	0.5454
126					medium	central	230	27.5	0.3974
127						east	230	27.5	0.3786
128						north	230	27.5	0.3452
129						south	230	27.5	0.5699
130						west	230	27.5	0.3974
131					high	central	230	27.5	0.4917
132						east	230	27.5	0.3498
133						north	230	27.5	0.4539
134						south	230	27.5	0.4637
135						west	230	27.5	0.5154
136					heavy	central	230	27.5	0.4917
137						east	230	27.5	0.3498
138						north	230	27.5	0.4539
139						south	230	27.5	0.4637
140						west	230	27.5	0.5154
141				thin	low	central	230	27.5	0.7692
142						east	230	27.5	1.5124
143						north	230	27.5	1.7322
144						south	230	27.5	0.4114
145						west	230	27.5	0.4629
146					medium	central	230	27.5	1.1263
147						east	230	27.5	1.6214
148						north	230	27.5	0.5110
149						south	230	27.5	0.7611
150						west	230	27.5	0.3000
151					high	central	230	27.5	0.9063
152						east	230	27.5	0.8100
153						north	230	27.5	0.4700
154						south	230	27.5	3.4893
155						west	230	27.5	4.1200
156					heavy	central	230	27.5	0.9063
157						east	230	27.5	0.8100
158						north	230	27.5	0.4700
159						south	230	27.5	3.4893
160						west	230	27.5	4.1200

Table B.133: Longitudinal Cracking Model Coefficients for MR and IH

group	distress	treat_lvl	highway_fun	pavement_typ	traffic_cls	climate_zone	alpha	A_star	beta_star
1	longitude_cracking_pct	MR	IH	thick	low	central	230	37.5	0.8662
2						east	230	37.5	0.8095
3						north	230	37.5	0.8662
4						south	230	37.5	0.8355
5						west	230	37.5	0.6807
6					medium	central	230	37.5	0.8662
7						east	230	37.5	0.8095
8						north	230	37.5	0.8662
9						south	230	37.5	0.8355
10						west	230	37.5	0.6807
11					high	central	230	37.5	0.8662
12						east	230	37.5	0.8095
13						north	230	37.5	0.8662
14						south	230	37.5	0.8355
15						west	230	37.5	0.6807
16					heavy	central	230	37.5	0.8662
17						east	230	37.5	0.8095
18						north	230	37.5	0.8662
19						south	230	37.5	0.8355
20						west	230	37.5	0.6807
21				thin	low	central	230	37.5	0.8218
22						east	230	37.5	0.5933
23						north	230	37.5	0.8218
24						south	230	37.5	0.6921
25						west	230	37.5	0.8218
26					medium	central	230	37.5	0.9249
27						east	230	37.5	0.9249
28						north	230	37.5	0.9249
29						south	230	37.5	0.9249
30						west	230	37.5	1.0898
31					high	central	230	37.5	0.9249
32						east	230	37.5	0.9249
33						north	230	37.5	0.9249
34						south	230	37.5	0.9249
35						west	230	37.5	1.0898
36					heavy	central	230	37.5	0.9249
37						east	230	37.5	0.9249
38						north	230	37.5	0.9249
39						south	230	37.5	0.9249
40						west	230	37.5	1.0898

Table B.134: Longitudinal Cracking Model Coefficients for MR and US

group	distress	treat_lvl	highway_fun	pavement_typ	traffic_cls	climate_zone	alpha	A_star	beta_star
41	longitude_cracking_pct	MR	US	thick	low	central	230	37.5	0.6761
42						east	230	37.5	0.5874
43						north	230	37.5	0.4482
44						south	230	37.5	0.8057
45						west	230	37.5	2.6308
46					medium	central	230	37.5	0.6761
47						east	230	37.5	0.5874
48						north	230	37.5	0.4482
49						south	230	37.5	0.8057
50						west	230	37.5	2.6308
51					high	central	230	37.5	0.6761
52						east	230	37.5	0.5874
53						north	230	37.5	0.4482
54						south	230	37.5	0.8057
55						west	230	37.5	2.6308
56					heavy	central	230	37.5	0.3994
57						east	230	37.5	0.9315
58						north	230	37.5	1.0218
59						south	230	37.5	0.5910
60						west	230	37.5	2.6996
61				thin	low	central	230	37.5	0.9331
62						east	230	37.5	2.4483
63						north	230	37.5	0.9331
64						south	230	37.5	0.9331
65						west	230	37.5	0.7334
66					medium	central	230	37.5	0.9331
67						east	230	37.5	2.4483
68						north	230	37.5	0.9331
69						south	230	37.5	0.9331
70						west	230	37.5	0.7334
71					high	central	230	37.5	0.4555
72						east	230	37.5	0.6417
73						north	230	37.5	0.5362
74						south	230	37.5	0.5584
75						west	230	37.5	1.5218
76					heavy	central	230	37.5	2.6868
77						east	230	37.5	1.0194
78						north	230	37.5	0.5795
79						south	230	37.5	0.9306
80						west	230	37.5	2.6868

Table B.135: Longitudinal Cracking Model Coefficients for MR and SH

group	distress	treat_lvl	highway_fun	pavement_typ	traffic_cls	climate_zone	alpha	A_star	beta_star
81	longitude_cracking_pct	MR	SH	thick	low	central	230	37.5	0.6819
82						east	230	37.5	0.6245
83						north	230	37.5	0.3282
84						south	230	37.5	0.5449
85						west	230	37.5	1.1688
86					medium	central	230	37.5	0.6819
87						east	230	37.5	0.6245
88						north	230	37.5	0.3282
89						south	230	37.5	0.5449
90						west	230	37.5	1.1688
91					high	central	230	37.5	0.6819
92						east	230	37.5	0.6245
93						north	230	37.5	0.3282
94						south	230	37.5	0.5449
95						west	230	37.5	1.1688
96					heavy	central	230	37.5	0.5937
97						east	230	37.5	0.5947
98						north	230	37.5	0.5937
99						south	230	37.5	0.5195
100						west	230	37.5	0.4869
101				thin	low	central	230	37.5	0.6629
102						east	230	37.5	1.0440
103						north	230	37.5	0.8039
104						south	230	37.5	0.6712
105						west	230	37.5	0.8065
106					medium	central	230	37.5	0.6629
107						east	230	37.5	1.0440
108						north	230	37.5	0.8039
109						south	230	37.5	0.6712
110						west	230	37.5	0.8065
111					high	central	230	37.5	1.0892
112						east	230	37.5	2.7368
113						north	230	37.5	0.4806
114						south	230	37.5	0.7693
115						west	230	37.5	2.2689
116					heavy	central	230	37.5	0.6509
117						east	230	37.5	1.1347
118						north	230	37.5	0.6509
119						south	230	37.5	0.5634
120						west	230	37.5	1.9888

Table B.136: Longitudinal Cracking Model Coefficients for MR and FM

group	distress	treat_lvl	highway_fun	pavement_typ	traffic_cls	climate_zone	alpha	A_star	beta_star
121	longitude_cracking_pct	MR	FM	thick	low	central	230	37.5	0.5454
122						east	230	37.5	0.6849
123						north	230	37.5	0.5454
124						south	230	37.5	0.3642
125						west	230	37.5	0.5454
126					medium	central	230	37.5	0.3974
127						east	230	37.5	0.3786
128						north	230	37.5	0.3452
129						south	230	37.5	0.5699
130						west	230	37.5	0.3974
131					high	central	230	37.5	0.4917
132						east	230	37.5	0.3498
133						north	230	37.5	0.4539
134						south	230	37.5	0.4637
135						west	230	37.5	0.5154
136					heavy	central	230	37.5	0.4917
137						east	230	37.5	0.3498
138						north	230	37.5	0.4539
139						south	230	37.5	0.4637
140						west	230	37.5	0.5154
141				thin	low	central	230	37.5	0.7692
142						east	230	37.5	1.5124
143						north	230	37.5	1.7322
144						south	230	37.5	0.4114
145						west	230	37.5	0.4629
146					medium	central	230	37.5	1.1263
147						east	230	37.5	1.6214
148						north	230	37.5	0.5110
149						south	230	37.5	0.7611
150						west	230	37.5	0.3000
151					high	central	230	37.5	0.9063
152						east	230	37.5	0.8100
153						north	230	37.5	0.4700
154						south	230	37.5	3.4893
155						west	230	37.5	4.1200
156					heavy	central	230	37.5	0.9063
157						east	230	37.5	0.8100
158						north	230	37.5	0.4700
159						south	230	37.5	3.4893
160						west	230	37.5	4.1200

Table B.137: Longitudinal Cracking Model Coefficients for HR and IH

group	distress	treat_lvl	highway_fun	pavement_typ	traffic_cls	climate_zone	alpha	A_star	beta_star
1	longitude_cracking_pct	HR	IH	thick	low	central	230	50	0.8662
2						east	230	50	0.8095
3						north	230	50	0.8662
4						south	230	50	0.8355
5						west	230	50	0.6807
6					medium	central	230	50	0.8662
7						east	230	50	0.8095
8						north	230	50	0.8662
9						south	230	50	0.8355
10						west	230	50	0.6807
11					high	central	230	50	0.8662
12						east	230	50	0.8095
13						north	230	50	0.8662
14						south	230	50	0.8355
15						west	230	50	0.6807
16					heavy	central	230	50	0.8662
17						east	230	50	0.8095
18						north	230	50	0.8662
19						south	230	50	0.8355
20						west	230	50	0.6807
21				thin	low	central	230	50	0.8218
22						east	230	50	0.5933
23						north	230	50	0.8218
24						south	230	50	0.6921
25						west	230	50	0.8218
26					medium	central	230	50	0.9249
27						east	230	50	0.9249
28						north	230	50	0.9249
29						south	230	50	0.9249
30						west	230	50	1.0898
31					high	central	230	50	0.9249
32						east	230	50	0.9249
33						north	230	50	0.9249
34						south	230	50	0.9249
35						west	230	50	1.0898
36					heavy	central	230	50	0.9249
37						east	230	50	0.9249
38						north	230	50	0.9249
39						south	230	50	0.9249
40						west	230	50	1.0898

Table B.138: Longitudinal Cracking Model Coefficients for HR and US

group	distress	treat_lvl	highway_fun	pavement_typ	traffic_cls	climate_zone	alpha	A_star	beta_star
41	longitude_cracking_pct	HR	US	thick	low	central	230	50	0.6761
42						east	230	50	0.5874
43						north	230	50	0.4482
44						south	230	50	0.8057
45						west	230	50	2.6308
46					medium	central	230	50	0.6761
47						east	230	50	0.5874
48						north	230	50	0.4482
49						south	230	50	0.8057
50						west	230	50	2.6308
51					high	central	230	50	0.6761
52						east	230	50	0.5874
53						north	230	50	0.4482
54						south	230	50	0.8057
55						west	230	50	2.6308
56					heavy	central	230	50	0.3994
57						east	230	50	0.9315
58						north	230	50	1.0218
59						south	230	50	0.5910
60						west	230	50	2.6996
61				thin	low	central	230	50	0.9331
62						east	230	50	2.4483
63						north	230	50	0.9331
64						south	230	50	0.9331
65						west	230	50	0.7334
66					medium	central	230	50	0.9331
67						east	230	50	2.4483
68						north	230	50	0.9331
69						south	230	50	0.9331
70						west	230	50	0.7334
71					high	central	230	50	0.4555
72						east	230	50	0.6417
73						north	230	50	0.5362
74						south	230	50	0.5584
75						west	230	50	1.5218
76					heavy	central	230	50	2.6868
77						east	230	50	1.0194
78						north	230	50	0.5795
79						south	230	50	0.9306
80						west	230	50	2.6868

Table B.139: Longitudinal Cracking Model Coefficients for HR and SH

group	distress	treat_lvl	highway_fun	pavement_typ	traffic_cls	climate_zone	alpha	A_star	beta_star
81	longitude_cracking_pct	HR	SH	thick	low	central	230	50	0.6819
82						east	230	50	0.6245
83						north	230	50	0.3282
84						south	230	50	0.5449
85						west	230	50	1.1688
86					medium	central	230	50	0.6819
87						east	230	50	0.6245
88						north	230	50	0.3282
89						south	230	50	0.5449
90						west	230	50	1.1688
91					high	central	230	50	0.6819
92						east	230	50	0.6245
93						north	230	50	0.3282
94						south	230	50	0.5449
95						west	230	50	1.1688
96					heavy	central	230	50	0.5937
97						east	230	50	0.5947
98						north	230	50	0.5937
99						south	230	50	0.5195
100						west	230	50	0.4869
101				thin	low	central	230	50	0.6629
102						east	230	50	1.0440
103						north	230	50	0.8039
104						south	230	50	0.6712
105						west	230	50	0.8065
106					medium	central	230	50	0.6629
107						east	230	50	1.0440
108						north	230	50	0.8039
109						south	230	50	0.6712
110						west	230	50	0.8065
111					high	central	230	50	1.0892
112						east	230	50	2.7368
113						north	230	50	0.4806
114						south	230	50	0.7693
115						west	230	50	2.2689
116					heavy	central	230	50	0.6509
117						east	230	50	1.1347
118						north	230	50	0.6509
119						south	230	50	0.5634
120						west	230	50	1.9888

Table B.140: Longitudinal Cracking Model Coefficients for HR and FM

group	distress	treat_lvl	highway_fun	pavement_typ	traffic_cls	climate_zone	alpha	A_star	beta_star
121	longitude_cracking_pct	HR	FM	thick	low	central	230	50	0.5454
122						east	230	50	0.6849
123						north	230	50	0.5454
124						south	230	50	0.3642
125						west	230	50	0.5454
126					medium	central	230	50	0.3974
127						east	230	50	0.3786
128						north	230	50	0.3452
129						south	230	50	0.5699
130						west	230	50	0.3974
131					high	central	230	50	0.4917
132						east	230	50	0.3498
133						north	230	50	0.4539
134						south	230	50	0.4637
135						west	230	50	0.5154
136					heavy	central	230	50	0.4917
137						east	230	50	0.3498
138						north	230	50	0.4539
139						south	230	50	0.4637
140						west	230	50	0.5154
141				thin	low	central	230	50	0.7692
142						east	230	50	1.5124
143						north	230	50	1.7322
144						south	230	50	0.4114
145						west	230	50	0.4629
146					medium	central	230	50	1.1263
147						east	230	50	1.6214
148						north	230	50	0.5110
149						south	230	50	0.7611
150						west	230	50	0.3000
151					high	central	230	50	0.9063
152						east	230	50	0.8100
153						north	230	50	0.4700
154						south	230	50	3.4893
155						west	230	50	4.1200
156					heavy	central	230	50	0.9063
157						east	230	50	0.8100
158						north	230	50	0.4700
159						south	230	50	3.4893
160						west	230	50	4.1200

Table B.141: Transverse Cracking Model Coefficients for DN and IH

group	distress	treat_lvl	highway_fun	pavement_typ	traffic_cls	climate_zone	alpha	A_star	beta_star
1	transverse_cracking_qty	DN	IH	thick	low	central	12	23.4507	0.6029
2						east	12	23.4507	0.5714
3						north	12	23.4507	0.6029
4						south	12	23.4507	0.8755
5						west	12	23.4507	0.7812
6					medium	central	12	23.4507	0.6029
7						east	12	23.4507	0.5714
8						north	12	23.4507	0.6029
9						south	12	23.4507	0.8755
10						west	12	23.4507	0.7812
11					high	central	12	23.4507	0.6029
12						east	12	23.4507	0.5714
13						north	12	23.4507	0.6029
14						south	12	23.4507	0.8755
15						west	12	23.4507	0.7812
16					heavy	central	12	23.4507	0.6029
17						east	12	23.4507	0.5714
18						north	12	23.4507	0.6029
19						south	12	23.4507	0.8755
20						west	12	23.4507	0.7812
21				thin	low	central	12	23.4507	1.4061
22						east	12	23.4507	1.1357
23						north	12	23.4507	1.4061
24						south	12	23.4507	1.1494
25						west	12	23.4507	1.4061
26					medium	central	12	23.4507	0.7408
27						east	12	23.4507	0.7408
28						north	12	23.4507	0.7408
29						south	12	23.4507	0.7408
30						west	12	23.4507	0.9063
31					high	central	12	23.4507	0.7408
32						east	12	23.4507	0.7408
33						north	12	23.4507	0.7408
34						south	12	23.4507	0.7408
35						west	12	23.4507	0.9063
36					heavy	central	12	23.4507	0.7408
37						east	12	23.4507	0.7408
38						north	12	23.4507	0.7408
39						south	12	23.4507	0.7408
40						west	12	23.4507	0.9063

Table B.142: Transverse Cracking Model Coefficients for DN and US

group	distress	treat_lvl	highway_fun	pavement_typ	traffic_cls	climate_zone	alpha	A_star	beta_star
41	transverse_cracking_qty	DN	US	thick	low	central	12	23.4507	0.9490
42						east	12	23.4507	0.6067
43						north	12	23.4507	0.6018
44						south	12	23.4507	1.2272
45						west	12	23.4507	2.1883
46					medium	central	12	23.4507	0.9490
47						east	12	23.4507	0.6067
48						north	12	23.4507	0.6018
49						south	12	23.4507	1.2272
50						west	12	23.4507	2.1883
51					high	central	12	23.4507	0.9490
52						east	12	23.4507	0.6067
53						north	12	23.4507	0.6018
54						south	12	23.4507	1.2272
55						west	12	23.4507	2.1883
56					heavy	central	12	23.4507	1.1814
57						east	12	23.4507	1.1978
58						north	12	23.4507	1.1328
59						south	12	23.4507	1.2622
60						west	12	23.4507	2.0201
61				thin	low	central	12	23.4507	0.7125
62						east	12	23.4507	2.1411
63						north	12	23.4507	0.7125
64						south	12	23.4507	0.7125
65						west	12	23.4507	1.1063
66					medium	central	12	23.4507	0.7125
67						east	12	23.4507	2.1411
68						north	12	23.4507	0.7125
69						south	12	23.4507	0.7125
70						west	12	23.4507	1.1063
71					high	central	12	23.4507	0.3739
72						east	12	23.4507	1.3153
73						north	12	23.4507	0.8192
74						south	12	23.4507	1.1105
75						west	12	23.4507	1.3067
76					heavy	central	12	23.4507	1.8693
77						east	12	23.4507	1.4567
78						north	12	23.4507	0.8709
79						south	12	23.4507	1.2431
80						west	12	23.4507	1.8693

Table B.143: Transverse Cracking Model Coefficients for DN and SH

group	distress	treat_lvl	highway_fun	pavement_typ	traffic_cls	climate_zone	alpha	A_star	beta_star
81	transverse_cracking_qty	DN	SH	thick	low	central	12	23.4507	0.5983
82						east	12	23.4507	0.5671
83						north	12	23.4507	0.2991
84						south	12	23.4507	0.8504
85						west	12	23.4507	1.1167
86					medium	central	12	23.4507	0.5983
87						east	12	23.4507	0.5671
88						north	12	23.4507	0.2991
89						south	12	23.4507	0.8504
90						west	12	23.4507	1.1167
91					high	central	12	23.4507	0.5983
92						east	12	23.4507	0.5671
93						north	12	23.4507	0.2991
94						south	12	23.4507	0.8504
95						west	12	23.4507	1.1167
96					heavy	central	12	23.4507	0.6875
97						east	12	23.4507	0.5879
98						north	12	23.4507	0.6875
99						south	12	23.4507	0.5993
100						west	12	23.4507	0.5425
101				thin	low	central	12	23.4507	0.6719
102						east	12	23.4507	0.9480
103						north	12	23.4507	1.6240
104						south	12	23.4507	1.1062
105						west	12	23.4507	0.3227
106					medium	central	12	23.4507	0.6719
107						east	12	23.4507	0.9480
108						north	12	23.4507	1.6240
109						south	12	23.4507	1.1062
110						west	12	23.4507	0.3227
111					high	central	12	23.4507	0.7490
112						east	12	23.4507	2.1135
113						north	12	23.4507	0.4091
114						south	12	23.4507	1.9568
115						west	12	23.4507	0.8834
116					heavy	central	12	23.4507	0.6497
117						east	12	23.4507	1.7612
118						north	12	23.4507	0.6497
119						south	12	23.4507	1.2464
120						west	12	23.4507	2.0840

Table B.144: Transverse Cracking Model Coefficients for DN and FM

group	distress	treat_lvl	highway_fun	pavement_typ	traffic_cls	climate_zone	alpha	A_star	beta_star
121	transverse_cracking_qty	DN	FM	thick	low	central	12	23.4507	1.1854
122						east	12	23.4507	1.2750
123						north	12	23.4507	1.1854
124						south	12	23.4507	0.4629
125						west	12	23.4507	1.1854
126					medium	central	12	23.4507	0.9582
127						east	12	23.4507	2.2878
128						north	12	23.4507	0.3227
129						south	12	23.4507	0.8189
130						west	12	23.4507	0.9582
131					high	central	12	23.4507	1.1232
132						east	12	23.4507	2.5368
133						north	12	23.4507	1.1062
134						south	12	23.4507	0.8201
135						west	12	23.4507	1.1062
136					heavy	central	12	23.4507	1.1232
137						east	12	23.4507	2.5368
138						north	12	23.4507	1.1062
139						south	12	23.4507	0.8201
140						west	12	23.4507	1.1062
141				thin	low	central	12	23.4507	0.9766
142						east	12	23.4507	1.8648
143						north	12	23.4507	1.2128
144						south	12	23.4507	1.2689
145						west	12	23.4507	0.3269
146					medium	central	12	23.4507	1.2878
147						east	12	23.4507	2.6700
148						north	12	23.4507	0.3859
149						south	12	23.4507	0.9944
150						west	12	23.4507	0.2330
151					high	central	12	23.4507	1.4098
152						east	12	23.4507	0.6948
153						north	12	23.4507	0.3855
154						south	12	23.4507	2.3136
155						west	12	23.4507	2.3389
156					heavy	central	12	23.4507	1.4098
157						east	12	23.4507	0.6948
158						north	12	23.4507	0.3855
159						south	12	23.4507	2.3136
160						west	12	23.4507	2.3389

Table B.145: Transverse Cracking Model Coefficients for PM and IH

group	distress	treat_lvl	highway_fun	pavement_typ	traffic_cls	climate_zone	alpha	A_star	beta_star
1	transverse_cracking_qty	PM	IH	thick	low	central	12	30	0.6029
2	transverse_cracking_qty	PM	IH	thick	low	east	12	30	0.5714
3	transverse_cracking_qty	PM	IH	thick	low	north	12	30	0.6029
4	transverse_cracking_qty	PM	IH	thick	low	south	12	30	0.8755
5	transverse_cracking_qty	PM	IH	thick	low	west	12	30	0.7812
6	transverse_cracking_qty	PM	IH	thick	medium	central	12	30	0.6029
7	transverse_cracking_qty	PM	IH	thick	medium	east	12	30	0.5714
8	transverse_cracking_qty	PM	IH	thick	medium	north	12	30	0.6029
9	transverse_cracking_qty	PM	IH	thick	medium	south	12	30	0.8755
10	transverse_cracking_qty	PM	IH	thick	medium	west	12	30	0.7812
11	transverse_cracking_qty	PM	IH	thick	high	central	12	30	0.6029
12	transverse_cracking_qty	PM	IH	thick	high	east	12	30	0.5714
13	transverse_cracking_qty	PM	IH	thick	high	north	12	30	0.6029
14	transverse_cracking_qty	PM	IH	thick	high	south	12	30	0.8755
15	transverse_cracking_qty	PM	IH	thick	high	west	12	30	0.7812
16	transverse_cracking_qty	PM	IH	thick	heavy	central	12	30	0.6029
17	transverse_cracking_qty	PM	IH	thick	heavy	east	12	30	0.5714
18	transverse_cracking_qty	PM	IH	thick	heavy	north	12	30	0.6029
19	transverse_cracking_qty	PM	IH	thick	heavy	south	12	30	0.8755
20	transverse_cracking_qty	PM	IH	thick	heavy	west	12	30	0.7812
21	transverse_cracking_qty	PM	IH	thin	low	central	12	30	1.4061
22	transverse_cracking_qty	PM	IH	thin	low	east	12	30	1.1357
23	transverse_cracking_qty	PM	IH	thin	low	north	12	30	1.4061
24	transverse_cracking_qty	PM	IH	thin	low	south	12	30	1.1494
25	transverse_cracking_qty	PM	IH	thin	low	west	12	30	1.4061
26	transverse_cracking_qty	PM	IH	thin	medium	central	12	30	0.7408
27	transverse_cracking_qty	PM	IH	thin	medium	east	12	30	0.7408
28	transverse_cracking_qty	PM	IH	thin	medium	north	12	30	0.7408
29	transverse_cracking_qty	PM	IH	thin	medium	south	12	30	0.7408
30	transverse_cracking_qty	PM	IH	thin	medium	west	12	30	0.9063
31	transverse_cracking_qty	PM	IH	thin	high	central	12	30	0.7408
32	transverse_cracking_qty	PM	IH	thin	high	east	12	30	0.7408
33	transverse_cracking_qty	PM	IH	thin	high	north	12	30	0.7408
34	transverse_cracking_qty	PM	IH	thin	high	south	12	30	0.7408
35	transverse_cracking_qty	PM	IH	thin	high	west	12	30	0.9063
36	transverse_cracking_qty	PM	IH	thin	heavy	central	12	30	0.7408
37	transverse_cracking_qty	PM	IH	thin	heavy	east	12	30	0.7408
38	transverse_cracking_qty	PM	IH	thin	heavy	north	12	30	0.7408
39	transverse_cracking_qty	PM	IH	thin	heavy	south	12	30	0.7408
40	transverse_cracking_qty	PM	IH	thin	heavy	west	12	30	0.9063

Table B.146: Transverse Cracking Model Coefficients for PM and US

group	distress	treat_lvl	highway_fun	pavement_typ	traffic_cls	climate_zone	alpha	A_star	beta_star
41	transverse_cracking_qty	PM	US	thick	low	central	12	30	0.9490
42						east	12	30	0.6067
43						north	12	30	0.6018
44						south	12	30	1.2272
45						west	12	30	2.1883
46					medium	central	12	30	0.9490
47						east	12	30	0.6067
48						north	12	30	0.6018
49						south	12	30	1.2272
50						west	12	30	2.1883
51					high	central	12	30	0.9490
52						east	12	30	0.6067
53						north	12	30	0.6018
54						south	12	30	1.2272
55						west	12	30	2.1883
56					heavy	central	12	30	1.1814
57						east	12	30	1.1978
58						north	12	30	1.1328
59						south	12	30	1.2622
60						west	12	30	2.0201
61				thin	low	central	12	30	0.7125
62						east	12	30	2.1411
63						north	12	30	0.7125
64						south	12	30	0.7125
65						west	12	30	1.1063
66					medium	central	12	30	0.7125
67						east	12	30	2.1411
68						north	12	30	0.7125
69						south	12	30	0.7125
70						west	12	30	1.1063
71					high	central	12	30	0.3739
72						east	12	30	1.3153
73						north	12	30	0.8192
74						south	12	30	1.1105
75						west	12	30	1.3067
76					heavy	central	12	30	1.8693
77						east	12	30	1.4567
78						north	12	30	0.8709
79						south	12	30	1.2431
80						west	12	30	1.8693

Table B.147: Transverse Cracking Model Coefficients for PM and SH

group	distress	treat_lvl	highway_fun	pavement_typ	traffic_cls	climate_zone	alpha	A_star	beta_star
81	transverse_cracking_qty	PM	SH	thick	low	central	12	30	0.5983
82						east	12	30	0.5671
83						north	12	30	0.2991
84						south	12	30	0.8504
85						west	12	30	1.1167
86					medium	central	12	30	0.5983
87						east	12	30	0.5671
88						north	12	30	0.2991
89						south	12	30	0.8504
90						west	12	30	1.1167
91					high	central	12	30	0.5983
92						east	12	30	0.5671
93						north	12	30	0.2991
94						south	12	30	0.8504
95						west	12	30	1.1167
96					heavy	central	12	30	0.6875
97						east	12	30	0.5879
98						north	12	30	0.6875
99						south	12	30	0.5993
100						west	12	30	0.5425
101				thin	low	central	12	30	0.6719
102						east	12	30	0.9480
103						north	12	30	1.6240
104						south	12	30	1.1062
105						west	12	30	0.3227
106					medium	central	12	30	0.6719
107						east	12	30	0.9480
108						north	12	30	1.6240
109						south	12	30	1.1062
110						west	12	30	0.3227
111					high	central	12	30	0.7490
112						east	12	30	2.1135
113						north	12	30	0.4091
114						south	12	30	1.9568
115						west	12	30	0.8834
116					heavy	central	12	30	0.6497
117						east	12	30	1.7612
118						north	12	30	0.6497
119						south	12	30	1.2464
120						west	12	30	2.0840

Table B.148: Transverse Cracking Model Coefficients for PM and FM

group	distress	treat_lvl	highway_fun	pavement_typ	traffic_cls	climate_zone	alpha	A_star	beta_star
121	transverse_cracking_qty	PM	FM	thick	low	central	12	30	1.1854
122						east	12	30	1.2750
123						north	12	30	1.1854
124						south	12	30	0.4629
125						west	12	30	1.1854
126					medium	central	12	30	0.9582
127						east	12	30	2.2878
128						north	12	30	0.3227
129						south	12	30	0.8189
130						west	12	30	0.9582
131					high	central	12	30	1.1232
132						east	12	30	2.5368
133						north	12	30	1.1062
134						south	12	30	0.8201
135						west	12	30	1.1062
136					heavy	central	12	30	1.1232
137						east	12	30	2.5368
138						north	12	30	1.1062
139						south	12	30	0.8201
140						west	12	30	1.1062
141				thin	low	central	12	30	0.9766
142						east	12	30	1.8648
143						north	12	30	1.2128
144						south	12	30	1.2689
145						west	12	30	0.3269
146					medium	central	12	30	1.2878
147						east	12	30	2.6700
148						north	12	30	0.3859
149						south	12	30	0.9944
150						west	12	30	0.2330
151					high	central	12	30	1.4098
152						east	12	30	0.6948
153						north	12	30	0.3855
154						south	12	30	2.3136
155						west	12	30	2.3389
156					heavy	central	12	30	1.4098
157						east	12	30	0.6948
158						north	12	30	0.3855
159						south	12	30	2.3136
160						west	12	30	2.3389

Table B.149: Transverse Cracking Model Coefficients for LR and IH

group	distress	treat_lvl	highway_fun	pavement_typ	traffic_cls	climate_zone	alpha	A_star	beta_star
1	transverse_cracking_qty	LR	IH	thick	low	central	12	33	0.6029
2						east	12	33	0.5714
3						north	12	33	0.6029
4						south	12	33	0.8755
5						west	12	33	0.7812
6					medium	central	12	33	0.6029
7						east	12	33	0.5714
8						north	12	33	0.6029
9						south	12	33	0.8755
10						west	12	33	0.7812
11					high	central	12	33	0.6029
12						east	12	33	0.5714
13						north	12	33	0.6029
14						south	12	33	0.8755
15						west	12	33	0.7812
16					heavy	central	12	33	0.6029
17						east	12	33	0.5714
18						north	12	33	0.6029
19						south	12	33	0.8755
20						west	12	33	0.7812
21				thin	low	central	12	33	1.4061
22						east	12	33	1.1357
23						north	12	33	1.4061
24						south	12	33	1.1494
25						west	12	33	1.4061
26					medium	central	12	33	0.7408
27						east	12	33	0.7408
28						north	12	33	0.7408
29						south	12	33	0.7408
30						west	12	33	0.9063
31					high	central	12	33	0.7408
32						east	12	33	0.7408
33						north	12	33	0.7408
34						south	12	33	0.7408
35						west	12	33	0.9063
36					heavy	central	12	33	0.7408
37						east	12	33	0.7408
38						north	12	33	0.7408
39						south	12	33	0.7408
40						west	12	33	0.9063

Table B.150: Transverse Cracking Model Coefficients for LR and US

group	distress	treat_lvl	highway_fun	pavement_typ	traffic_cls	climate_zone	alpha	A_star	beta_star
41	transverse_cracking_qty	LR	US	thick	low	central	12	33	0.9490
42						east	12	33	0.6067
43						north	12	33	0.6018
44						south	12	33	1.2272
45						west	12	33	2.1883
46					medium	central	12	33	0.9490
47						east	12	33	0.6067
48						north	12	33	0.6018
49						south	12	33	1.2272
50						west	12	33	2.1883
51					high	central	12	33	0.9490
52						east	12	33	0.6067
53						north	12	33	0.6018
54						south	12	33	1.2272
55						west	12	33	2.1883
56					heavy	central	12	33	1.1814
57						east	12	33	1.1978
58						north	12	33	1.1328
59						south	12	33	1.2622
60						west	12	33	2.0201
61				thin	low	central	12	33	0.7125
62						east	12	33	2.1411
63						north	12	33	0.7125
64						south	12	33	0.7125
65						west	12	33	1.1063
66					medium	central	12	33	0.7125
67						east	12	33	2.1411
68						north	12	33	0.7125
69						south	12	33	0.7125
70						west	12	33	1.1063
71					high	central	12	33	0.3739
72						east	12	33	1.3153
73						north	12	33	0.8192
74						south	12	33	1.1105
75						west	12	33	1.3067
76					heavy	central	12	33	1.8693
77						east	12	33	1.4567
78						north	12	33	0.8709
79						south	12	33	1.2431
80						west	12	33	1.8693

Table B.151: Transverse Cracking Model Coefficients for LR and SH

group	distress	treat_lvl	highway_fun	pavement_typ	traffic_cls	climate_zone	alpha	A_star	beta_star
81	transverse_cracking_qty	LR	SH	thick	low	central	12	33	0.5983
82						east	12	33	0.5671
83						north	12	33	0.2991
84						south	12	33	0.8504
85						west	12	33	1.1167
86					medium	central	12	33	0.5983
87						east	12	33	0.5671
88						north	12	33	0.2991
89						south	12	33	0.8504
90						west	12	33	1.1167
91					high	central	12	33	0.5983
92						east	12	33	0.5671
93						north	12	33	0.2991
94						south	12	33	0.8504
95						west	12	33	1.1167
96					heavy	central	12	33	0.6875
97						east	12	33	0.5879
98						north	12	33	0.6875
99						south	12	33	0.5993
100						west	12	33	0.5425
101				thin	low	central	12	33	0.6719
102						east	12	33	0.9480
103						north	12	33	1.6240
104						south	12	33	1.1062
105						west	12	33	0.3227
106					medium	central	12	33	0.6719
107						east	12	33	0.9480
108						north	12	33	1.6240
109						south	12	33	1.1062
110						west	12	33	0.3227
111					high	central	12	33	0.7490
112						east	12	33	2.1135
113						north	12	33	0.4091
114						south	12	33	1.9568
115						west	12	33	0.8834
116					heavy	central	12	33	0.6497
117						east	12	33	1.7612
118						north	12	33	0.6497
119						south	12	33	1.2464
120						west	12	33	2.0840

Table B.152: Transverse Cracking Model Coefficients for LR and FM

group	distress	treat_lvl	highway_fun	pavement_typ	traffic_cls	climate_zone	alpha	A_star	beta_star
121	transverse_cracking_qty	LR	FM	thick	low	central	12	33	1.1854
122						east	12	33	1.2750
123						north	12	33	1.1854
124						south	12	33	0.4629
125						west	12	33	1.1854
126					medium	central	12	33	0.9582
127						east	12	33	2.2878
128						north	12	33	0.3227
129						south	12	33	0.8189
130						west	12	33	0.9582
131					high	central	12	33	1.1232
132						east	12	33	2.5368
133						north	12	33	1.1062
134						south	12	33	0.8201
135						west	12	33	1.1062
136					heavy	central	12	33	1.1232
137						east	12	33	2.5368
138						north	12	33	1.1062
139						south	12	33	0.8201
140						west	12	33	1.1062
141				thin	low	central	12	33	0.9766
142						east	12	33	1.8648
143						north	12	33	1.2128
144						south	12	33	1.2689
145						west	12	33	0.3269
146					medium	central	12	33	1.2878
147						east	12	33	2.6700
148						north	12	33	0.3859
149						south	12	33	0.9944
150						west	12	33	0.2330
151					high	central	12	33	1.4098
152						east	12	33	0.6948
153						north	12	33	0.3855
154						south	12	33	2.3136
155						west	12	33	2.3389
156					heavy	central	12	33	1.4098
157						east	12	33	0.6948
158						north	12	33	0.3855
159						south	12	33	2.3136
160						west	12	33	2.3389

Table B.153: Transverse Cracking Model Coefficients for MR and IH

group	distress	treat_lvl	highway_fun	pavement_typ	traffic_cls	climate_zone	alpha	A_star	beta_star
1	transverse_cracking_qty	MR	IH	thick	low	central	12	40	0.6029
2						east	12	40	0.5714
3						north	12	40	0.6029
4						south	12	40	0.8755
5						west	12	40	0.7812
6					medium	central	12	40	0.6029
7						east	12	40	0.5714
8						north	12	40	0.6029
9						south	12	40	0.8755
10						west	12	40	0.7812
11					high	central	12	40	0.6029
12						east	12	40	0.5714
13						north	12	40	0.6029
14						south	12	40	0.8755
15						west	12	40	0.7812
16					heavy	central	12	40	0.6029
17						east	12	40	0.5714
18						north	12	40	0.6029
19						south	12	40	0.8755
20						west	12	40	0.7812
21				thin	low	central	12	40	1.4061
22						east	12	40	1.1357
23						north	12	40	1.4061
24						south	12	40	1.1494
25						west	12	40	1.4061
26					medium	central	12	40	0.7408
27						east	12	40	0.7408
28						north	12	40	0.7408
29						south	12	40	0.7408
30						west	12	40	0.9063
31					high	central	12	40	0.7408
32						east	12	40	0.7408
33						north	12	40	0.7408
34						south	12	40	0.7408
35						west	12	40	0.9063
36					heavy	central	12	40	0.7408
37						east	12	40	0.7408
38						north	12	40	0.7408
39						south	12	40	0.7408
40						west	12	40	0.9063

Table B.154: Transverse Cracking Model Coefficients for MR and US

group	distress	treat_lvl	highway_fun	pavement_typ	traffic_cls	climate_zone	alpha	A_star	beta_star
41	transverse_cracking_qty	MR	US	thick	low	central	12	40	0.9490
42						east	12	40	0.6067
43						north	12	40	0.6018
44						south	12	40	1.2272
45						west	12	40	2.1883
46					medium	central	12	40	0.9490
47						east	12	40	0.6067
48						north	12	40	0.6018
49						south	12	40	1.2272
50						west	12	40	2.1883
51					high	central	12	40	0.9490
52						east	12	40	0.6067
53						north	12	40	0.6018
54						south	12	40	1.2272
55						west	12	40	2.1883
56					heavy	central	12	40	1.1814
57						east	12	40	1.1978
58						north	12	40	1.1328
59						south	12	40	1.2622
60						west	12	40	2.0201
61				thin	low	central	12	40	0.7125
62						east	12	40	2.1411
63						north	12	40	0.7125
64						south	12	40	0.7125
65						west	12	40	1.1063
66					medium	central	12	40	0.7125
67						east	12	40	2.1411
68						north	12	40	0.7125
69						south	12	40	0.7125
70						west	12	40	1.1063
71					high	central	12	40	0.3739
72						east	12	40	1.3153
73						north	12	40	0.8192
74						south	12	40	1.1105
75						west	12	40	1.3067
76					heavy	central	12	40	1.8693
77						east	12	40	1.4567
78						north	12	40	0.8709
79						south	12	40	1.2431
80						west	12	40	1.8693

Table B.155: Transverse Cracking Model Coefficients for MR and SH

group	distress	treat_lvl	highway_fun	pavement_typ	traffic_cls	climate_zone	alpha	A_star	beta_star
81	transverse_cracking_qty	MR	SH	thick	low	central	12	40	0.5983
82						east	12	40	0.5671
83						north	12	40	0.2991
84						south	12	40	0.8504
85						west	12	40	1.1167
86					medium	central	12	40	0.5983
87						east	12	40	0.5671
88						north	12	40	0.2991
89						south	12	40	0.8504
90						west	12	40	1.1167
91					high	central	12	40	0.5983
92						east	12	40	0.5671
93						north	12	40	0.2991
94						south	12	40	0.8504
95						west	12	40	1.1167
96					heavy	central	12	40	0.6875
97						east	12	40	0.5879
98						north	12	40	0.6875
99						south	12	40	0.5993
100						west	12	40	0.5425
101				thin	low	central	12	40	0.6719
102						east	12	40	0.9480
103						north	12	40	1.6240
104						south	12	40	1.1062
105						west	12	40	0.3227
106					medium	central	12	40	0.6719
107						east	12	40	0.9480
108						north	12	40	1.6240
109						south	12	40	1.1062
110						west	12	40	0.3227
111					high	central	12	40	0.7490
112						east	12	40	2.1135
113						north	12	40	0.4091
114						south	12	40	1.9568
115						west	12	40	0.8834
116					heavy	central	12	40	0.6497
117						east	12	40	1.7612
118						north	12	40	0.6497
119						south	12	40	1.2464
120						west	12	40	2.0840

Table B.156: Transverse Cracking Model Coefficients for MR and FM

group	distress	treat_lvl	highway_fun	pavement_typ	traffic_cls	climate_zone	alpha	A_star	beta_star
121	transverse_cracking_qty	MR	FM	thick	low	central	12	40	1.1854
122						east	12	40	1.2750
123						north	12	40	1.1854
124						south	12	40	0.4629
125						west	12	40	1.1854
126					medium	central	12	40	0.9582
127						east	12	40	2.2878
128						north	12	40	0.3227
129						south	12	40	0.8189
130						west	12	40	0.9582
131					high	central	12	40	1.1232
132						east	12	40	2.5368
133						north	12	40	1.1062
134						south	12	40	0.8201
135						west	12	40	1.1062
136					heavy	central	12	40	1.1232
137						east	12	40	2.5368
138						north	12	40	1.1062
139						south	12	40	0.8201
140						west	12	40	1.1062
141				thin	low	central	12	40	0.9766
142						east	12	40	1.8648
143						north	12	40	1.2128
144						south	12	40	1.2689
145						west	12	40	0.3269
146					medium	central	12	40	1.2878
147						east	12	40	2.6700
148						north	12	40	0.3859
149						south	12	40	0.9944
150						west	12	40	0.2330
151					high	central	12	40	1.4098
152						east	12	40	0.6948
153						north	12	40	0.3855
154						south	12	40	2.3136
155						west	12	40	2.3389
156					heavy	central	12	40	1.4098
157						east	12	40	0.6948
158						north	12	40	0.3855
159						south	12	40	2.3136
160						west	12	40	2.3389

Table B.157: Transverse Cracking Model Coefficients for HR and IH

group	distress	treat_lvl	highway_fun	pavement_typ	traffic_cls	climate_zone	alpha	A_star	beta_star
1	transverse_cracking_qty	HR	IH	thick	low	central	12	45	0.6029
2						east	12	45	0.5714
3						north	12	45	0.6029
4						south	12	45	0.8755
5						west	12	45	0.7812
6					medium	central	12	45	0.6029
7						east	12	45	0.5714
8						north	12	45	0.6029
9						south	12	45	0.8755
10						west	12	45	0.7812
11					high	central	12	45	0.6029
12						east	12	45	0.5714
13						north	12	45	0.6029
14						south	12	45	0.8755
15						west	12	45	0.7812
16					heavy	central	12	45	0.6029
17						east	12	45	0.5714
18						north	12	45	0.6029
19						south	12	45	0.8755
20						west	12	45	0.7812
21				thin	low	central	12	45	1.4061
22						east	12	45	1.1357
23						north	12	45	1.4061
24						south	12	45	1.1494
25						west	12	45	1.4061
26					medium	central	12	45	0.7408
27						east	12	45	0.7408
28						north	12	45	0.7408
29						south	12	45	0.7408
30						west	12	45	0.9063
31					high	central	12	45	0.7408
32						east	12	45	0.7408
33						north	12	45	0.7408
34						south	12	45	0.7408
35						west	12	45	0.9063
36					heavy	central	12	45	0.7408
37						east	12	45	0.7408
38						north	12	45	0.7408
39						south	12	45	0.7408
40						west	12	45	0.9063

Table B.158: Transverse Cracking Model Coefficients for HR and US

group	distress	treat_lvl	highway_fun	pavement_typ	traffic_cls	climate_zone	alpha	A_star	beta_star
41	transverse_cracking_qty	HR	US	thick	low	central	12	45	0.9490
42						east	12	45	0.6067
43						north	12	45	0.6018
44						south	12	45	1.2272
45						west	12	45	2.1883
46					medium	central	12	45	0.9490
47						east	12	45	0.6067
48						north	12	45	0.6018
49						south	12	45	1.2272
50						west	12	45	2.1883
51					high	central	12	45	0.9490
52						east	12	45	0.6067
53						north	12	45	0.6018
54						south	12	45	1.2272
55						west	12	45	2.1883
56					heavy	central	12	45	1.1814
57						east	12	45	1.1978
58						north	12	45	1.1328
59						south	12	45	1.2622
60						west	12	45	2.0201
61				thin	low	central	12	45	0.7125
62						east	12	45	2.1411
63						north	12	45	0.7125
64						south	12	45	0.7125
65						west	12	45	1.1063
66					medium	central	12	45	0.7125
67						east	12	45	2.1411
68						north	12	45	0.7125
69						south	12	45	0.7125
70						west	12	45	1.1063
71					high	central	12	45	0.3739
72						east	12	45	1.3153
73						north	12	45	0.8192
74						south	12	45	1.1105
75						west	12	45	1.3067
76					heavy	central	12	45	1.8693
77						east	12	45	1.4567
78						north	12	45	0.8709
79						south	12	45	1.2431
80						west	12	45	1.8693

Table B.159: Transverse Cracking Model Coefficients for HR and SH

group	distress	treat_lvl	highway_fun	pavement_typ	traffic_cls	climate_zone	alpha	A_star	beta_star
81	transverse_cracking_qty	HR	SH	thick	low	central	12	45	0.5983
82						east	12	45	0.5671
83						north	12	45	0.2991
84						south	12	45	0.8504
85						west	12	45	1.1167
86					medium	central	12	45	0.5983
87						east	12	45	0.5671
88						north	12	45	0.2991
89						south	12	45	0.8504
90						west	12	45	1.1167
91					high	central	12	45	0.5983
92						east	12	45	0.5671
93						north	12	45	0.2991
94						south	12	45	0.8504
95						west	12	45	1.1167
96					heavy	central	12	45	0.6875
97						east	12	45	0.5879
98						north	12	45	0.6875
99						south	12	45	0.5993
100						west	12	45	0.5425
101				thin	low	central	12	45	0.6719
102						east	12	45	0.9480
103						north	12	45	1.6240
104						south	12	45	1.1062
105						west	12	45	0.3227
106					medium	central	12	45	0.6719
107						east	12	45	0.9480
108						north	12	45	1.6240
109						south	12	45	1.1062
110						west	12	45	0.3227
111					high	central	12	45	0.7490
112						east	12	45	2.1135
113						north	12	45	0.4091
114						south	12	45	1.9568
115						west	12	45	0.8834
116					heavy	central	12	45	0.6497
117						east	12	45	1.7612
118						north	12	45	0.6497
119						south	12	45	1.2464
120						west	12	45	2.0840

Table B.160: Transverse Cracking Model Coefficients for HR and FM

group	distress	treat_lvl	highway_fun	pavement_typ	traffic_cls	climate_zone	alpha	A_star	beta_star
121	transverse_cracking_qty	HR	FM	thick	low	central	12	45	1.1854
122						east	12	45	1.2750
123						north	12	45	1.1854
124						south	12	45	0.4629
125						west	12	45	1.1854
126					medium	central	12	45	0.9582
127						east	12	45	2.2878
128						north	12	45	0.3227
129						south	12	45	0.8189
130						west	12	45	0.9582
131					high	central	12	45	1.1232
132						east	12	45	2.5368
133						north	12	45	1.1062
134						south	12	45	0.8201
135						west	12	45	1.1062
136					heavy	central	12	45	1.1232
137						east	12	45	2.5368
138						north	12	45	1.1062
139						south	12	45	0.8201
140						west	12	45	1.1062
141				thin	low	central	12	45	0.9766
142						east	12	45	1.8648
143						north	12	45	1.2128
144						south	12	45	1.2689
145						west	12	45	0.3269
146					medium	central	12	45	1.2878
147						east	12	45	2.6700
148						north	12	45	0.3859
149						south	12	45	0.9944
150						west	12	45	0.2330
151					high	central	12	45	1.4098
152						east	12	45	0.6948
153						north	12	45	0.3855
154						south	12	45	2.3136
155						west	12	45	2.3389
156					heavy	central	12	45	1.4098
157						east	12	45	0.6948
158						north	12	45	0.3855
159						south	12	45	2.3136
160						west	12	45	2.3389

Appendix C. Reset Values

Reset Values for Asphalt Concrete Pavement

Shallow Rut

Table C.1 Pre and Post Treatment Shallow Rut

Distress	Percent of Zeros	min	max	Percentiles		
				25%	50%	75%
pre_Shallow_Rut	16.24%	0	38	1	4	9
post_Shallow_Rut	29.95%	0	47	0	3	11

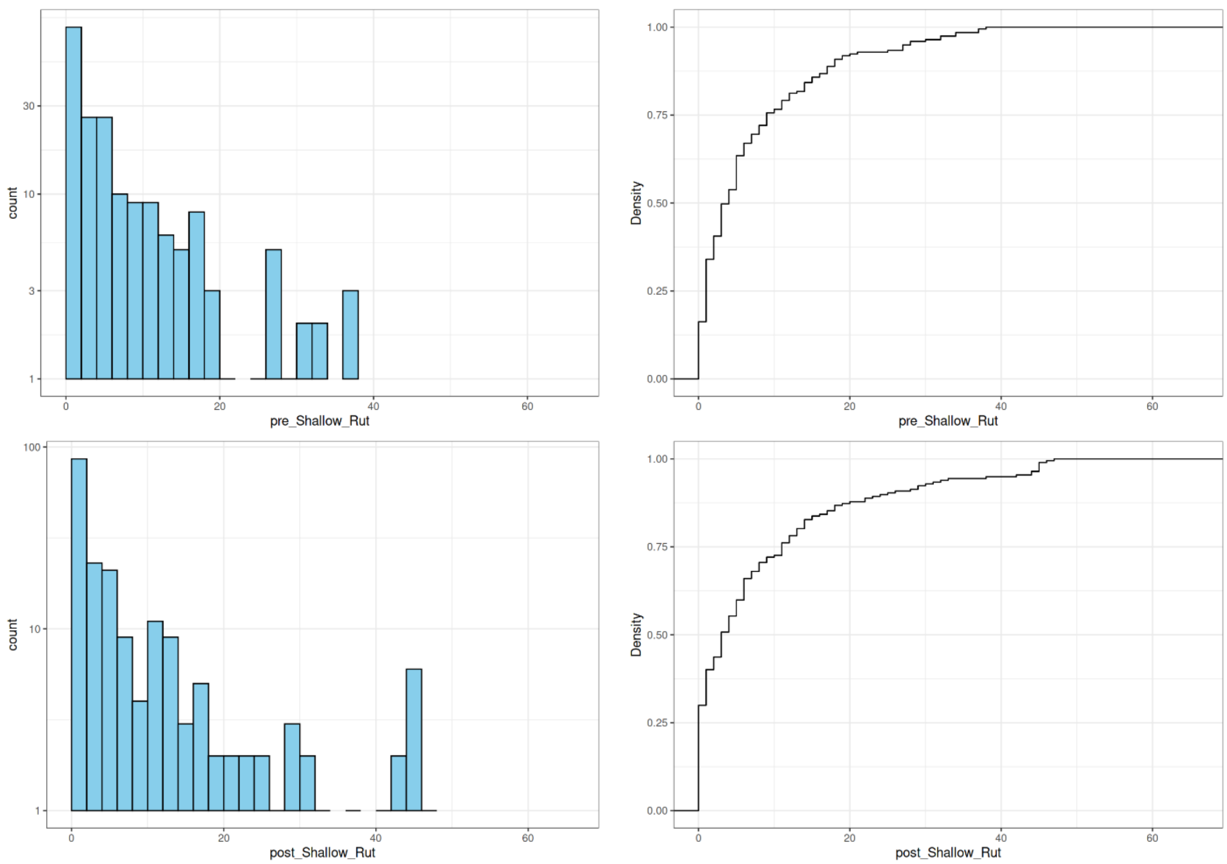

Figure C.1 Pre and Post Treatment Shallow Rut

In the case of shallow rutting on asphalt pavements, it is recommended that for PM, the percentage should be re-set to 10 percent while for LRhb, MRhb, and HRhb, the reset value should be zero.

Deep Rut

Table C.2 Pre and Post Treatment Deep Rut

Distress	Percent of Zeros	min	max	Percentiles		
				25%	50%	75%
pre_Deep_Rut	70.05%	0	13	0	0	1
post_Deep_Rut	69.54%	0	14	0	0	1

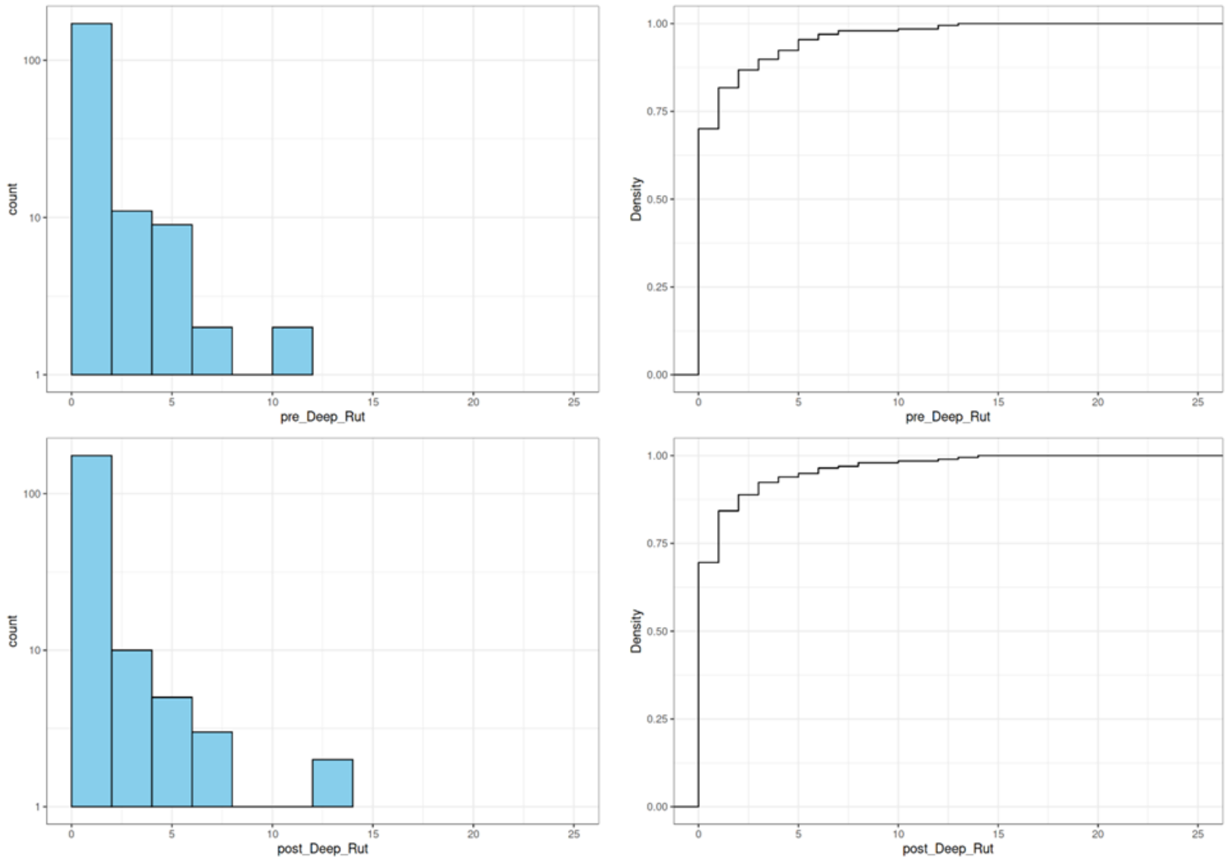

Figure C.2 Pre and Post Treatment Deep Rut

In the case of deep rutting on asphalt pavements, it is recommended that for PM, LRhb, MRhb, and HRhb, the reset value should be set to zero. When deep rutting if found, only high-intensity M&R work should be carried out.

Longitudinal Cracking

Table C.3 Pre and Post Treatment Longitudinal Cracking

Distress	Percent of Zeros	min	max	Percentiles		
				25%	50%	75%
pre_Longitudinal_Cracking	30.96%	0	150	0	12	35
post_Longitudinal_Cracking	64.97%	0	207	0	0	3

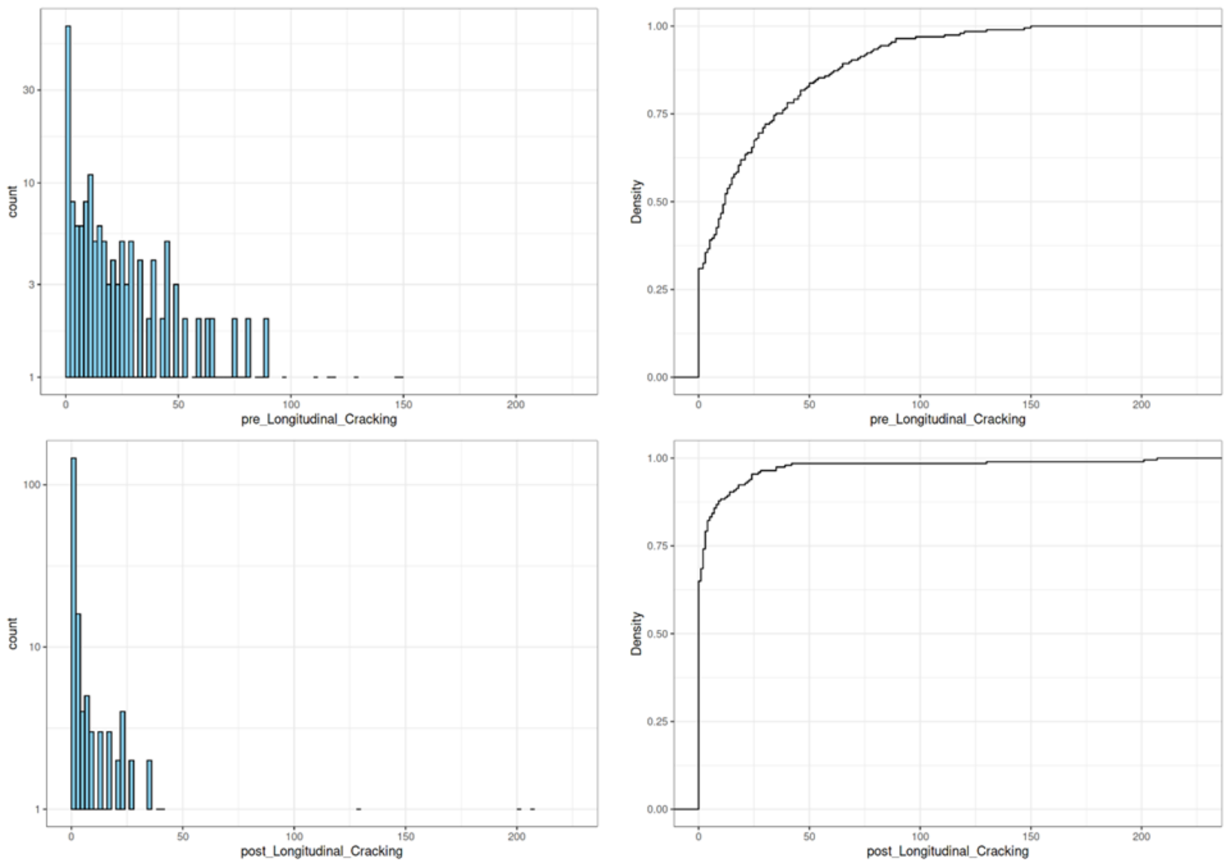

Figure C.3 Pre and Post Treatment Longitudinal Cracking

In the case of longitudinal cracking on asphalt pavements, it is recommended that for MRhb and HRhb, the reset value should be zero with the understanding that good maintenance and rehabilitation (M&R) practices are applied so PM and LRhb should not be applied in these cases. However, data shows that a number of sections still show this type of distress after M&R.

Transverse Cracking

Table C.4 Pre and Post Treatment Transverse Cracking

Distress	Percent of Zeros	min	max	Percentiles		
				25%	50%	75%
pre_Transverse_Cracking	74.62%	0	6	0	0	1
post_Transverse_Cracking	96.95%	0	2	0	0	0

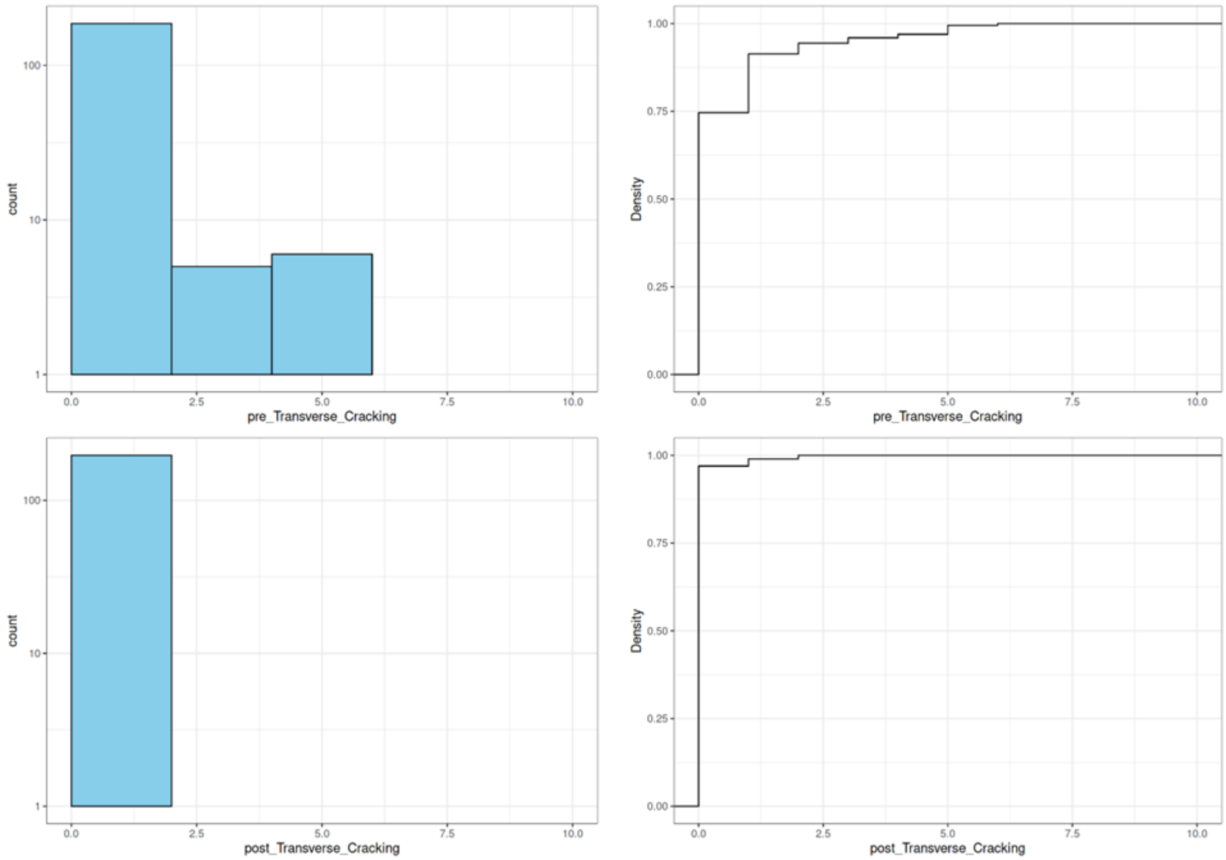

Figure C.4 Pre and Post Treatment Transverse Cracking

In the case of transverse cracking on asphalt pavements, it is recommended that for MRhb and HRhb, the reset value should be zero with the understanding that good maintenance and rehabilitation practices are applied so PM and LRhb should not be applied in these cases.

Alligator Cracking

Table C.5 Pre and Post Treatment Alligator Cracking

Distress	Percent of Zeros	min	max	Percentiles		
				25%	50%	75%
pre_Alligator_Cracking	56.35%	0	44	0	0	4
post_Alligator_Cracking	83.76%	0	23	0	0	0

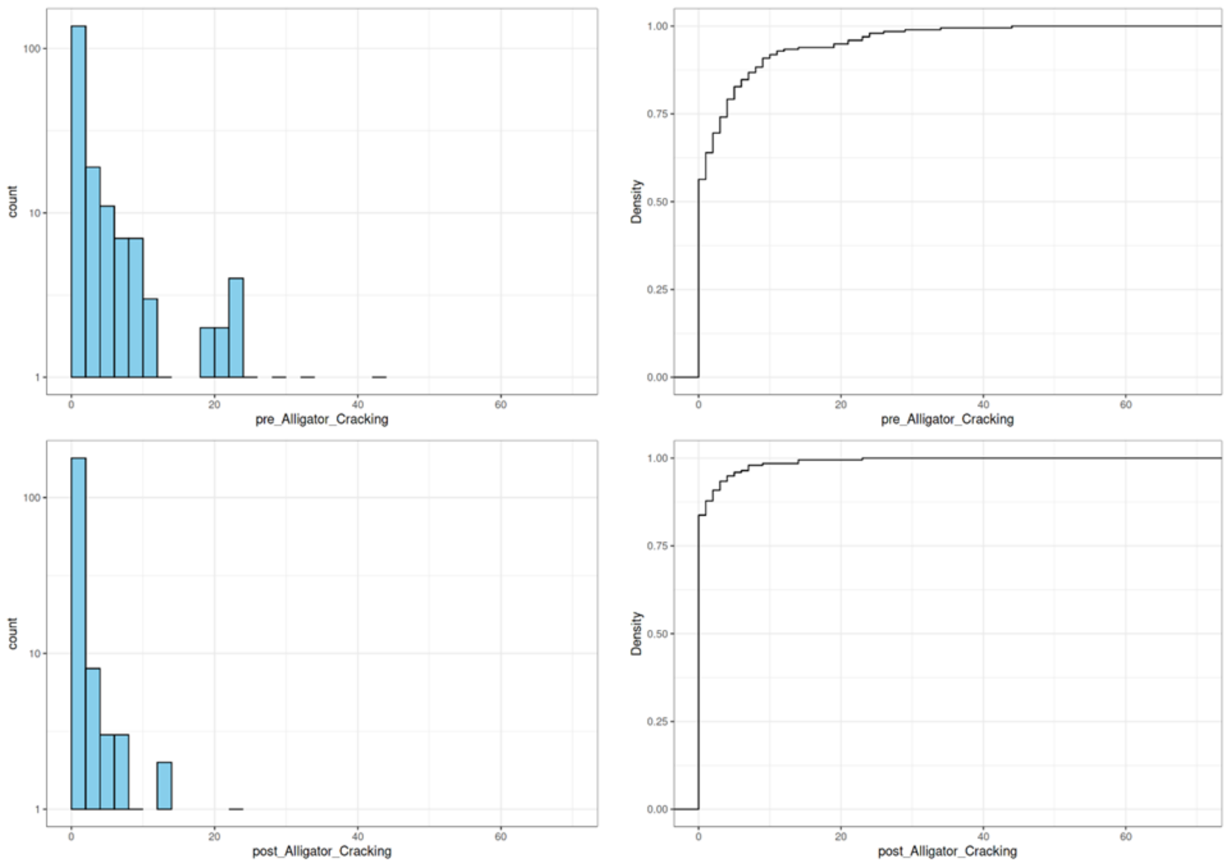

Figure C.5 Pre and Post Treatment Alligator Cracking

In the case of alligator cracking on asphalt pavements, it is recommended that for all treatment types (PM, LRhb, MRhb, and HRhb), the reset value should be zero. PM and LRhb should not be applied in these cases, as they will mask the distress but fail to address the problem effectively.

Block Cracking

Table C.6 Pre and Post Treatment Block Cracking

Distress	Percent of Zeros	min	max	Percentiles		
				25%	50%	75%
pre_Block_Cracking	99.49%	0	5	0	0	0
post_Block_Cracking	100%	0	0	0	0	0

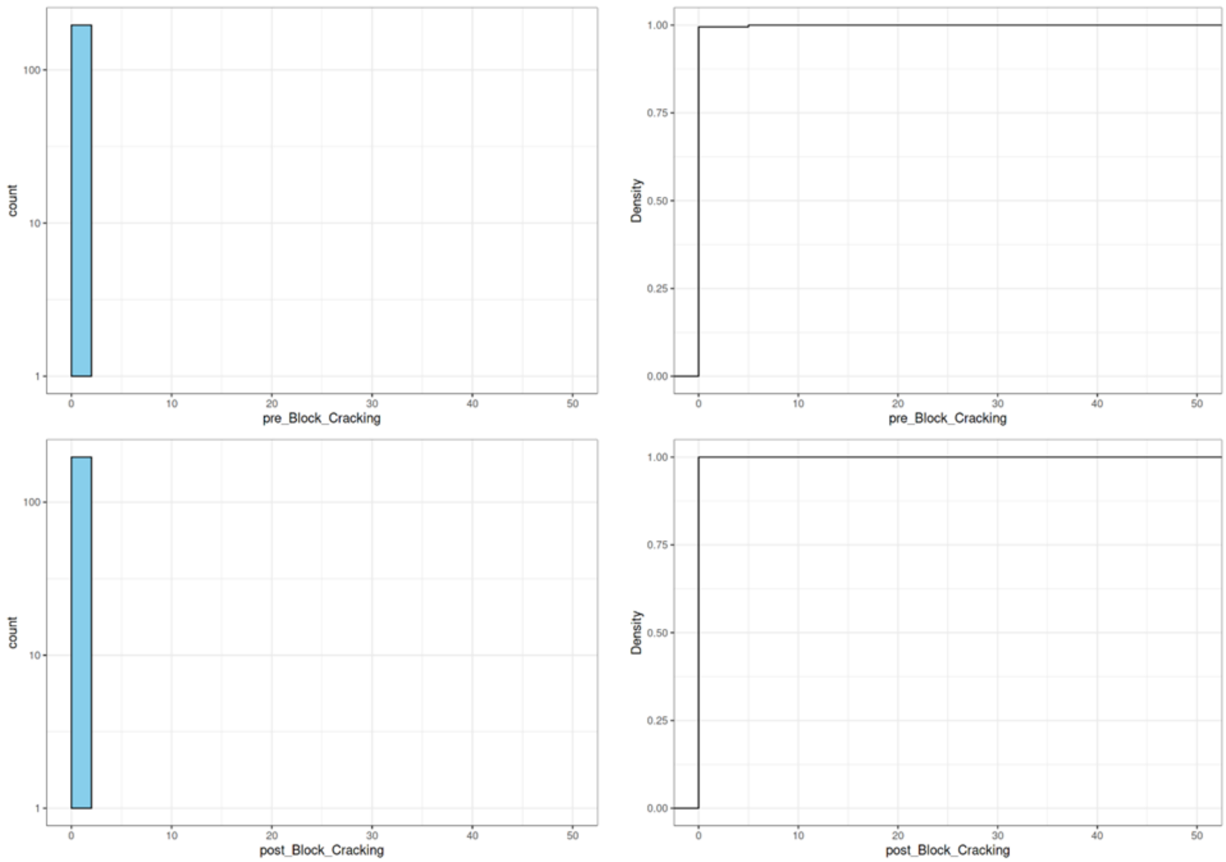

Figure C.6 Pre and Post Treatment Block Cracking

Almost no block cracking was observed in the data analyzed. For that reason, it is recommended that for all treatment types (PM, LRhb, MRhb and HRhb), the reset value should be zero.

Patching

Table C.7 Pre and Post Treatment Patching

Distress	Percent of Zeros	min	max	Percentiles		
				25%	50%	75%
pre_Patching	68.02%	0	100	0	0	5
post_Patching	95.43%	0	44	0	0	0

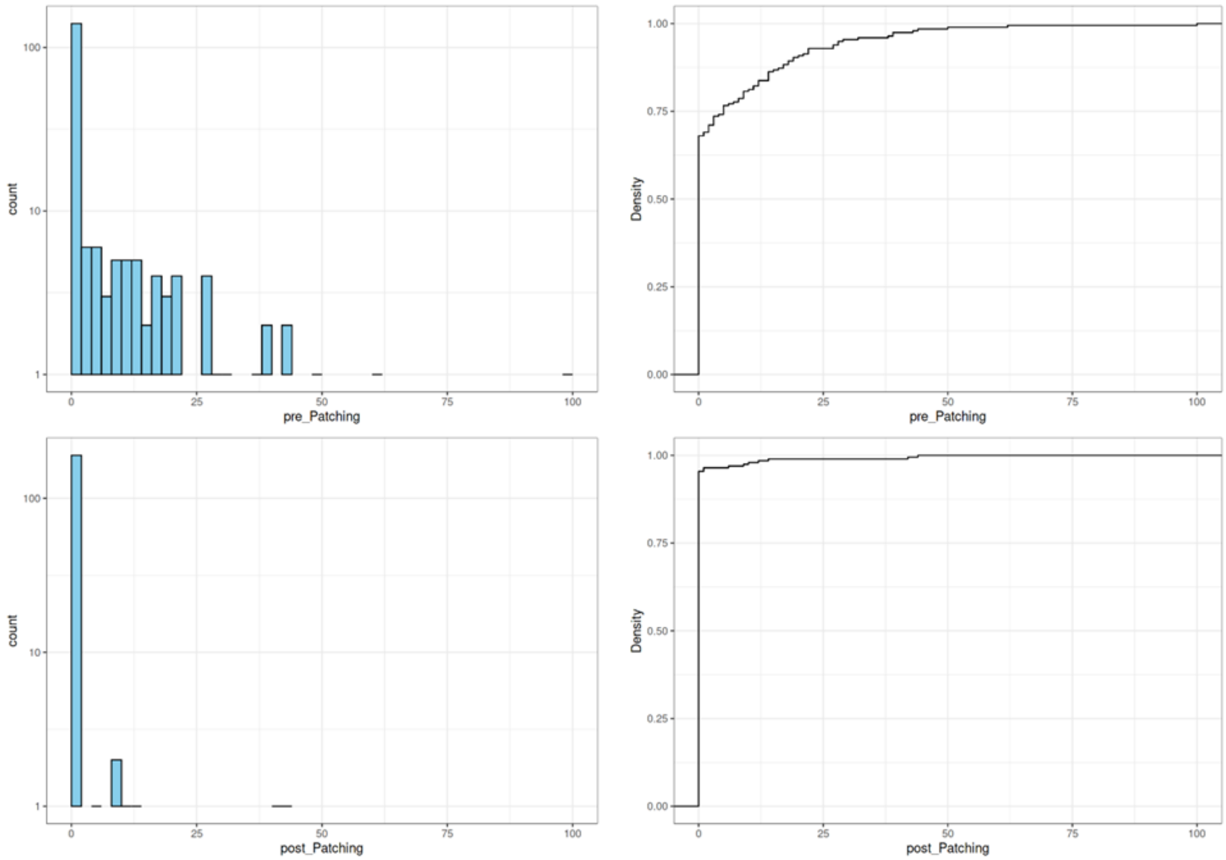

Figure C.7 Pre and Post Treatment Patching

After all type of treatments, little to no patching was observed in the analyzed database. Therefore, it is recommended that for all treatment types (PM, LRhb, MRhb, and HRhb), the reset value should be zero.

Failures

Table C.8 Pre and Post Treatment Failures

Distress	Percent of Zeros	min	max	Percentiles		
				25%	50%	75%
pre_Failures	94.42%	0	5	0	0	0
post_Failures	98.48%	0	1	0	0	0

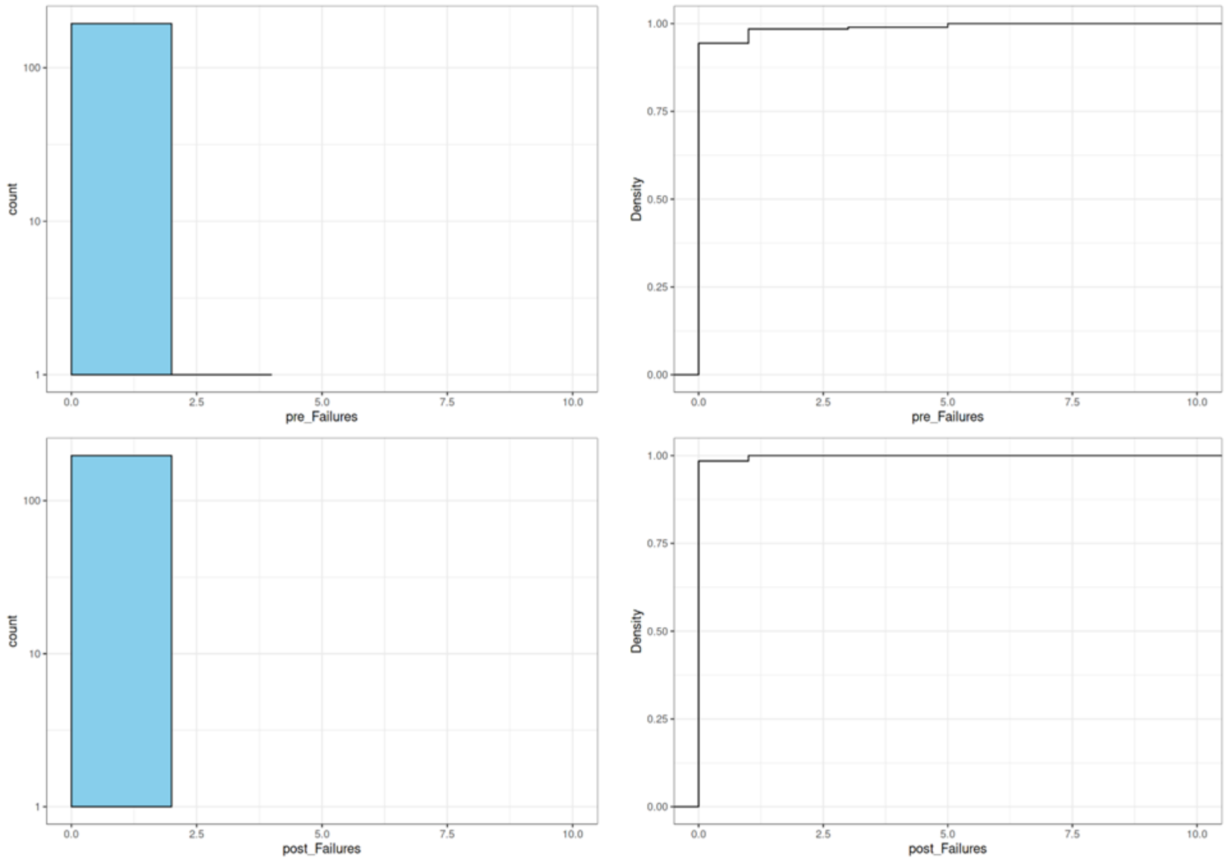

Figure C.8 Pre and Post Treatment Failures

Very few failures were observed in the analyzed database as TxDOT addresses failures with high priority and no delays. Therefore, it is recommended that for all treatment types (PM, LRhb, MRhb, and HRhb), the reset value for failures should be zero. However, the right treatment should be applied in each case depending on the failure type.

Reset Values for Continuously Reinforced Concrete Pavement

Spalled Cracks

Table C.9 Pre and Post Treatment Spalled Cracks

Distress	Percent of Zeros	min	max	Percentiles		
				25%	50%	75%
pre_Spalled_Cracks	0.95%	0	642	2	5	14
post_Spalled_Cracks	78.90%	0	160	0	0	0

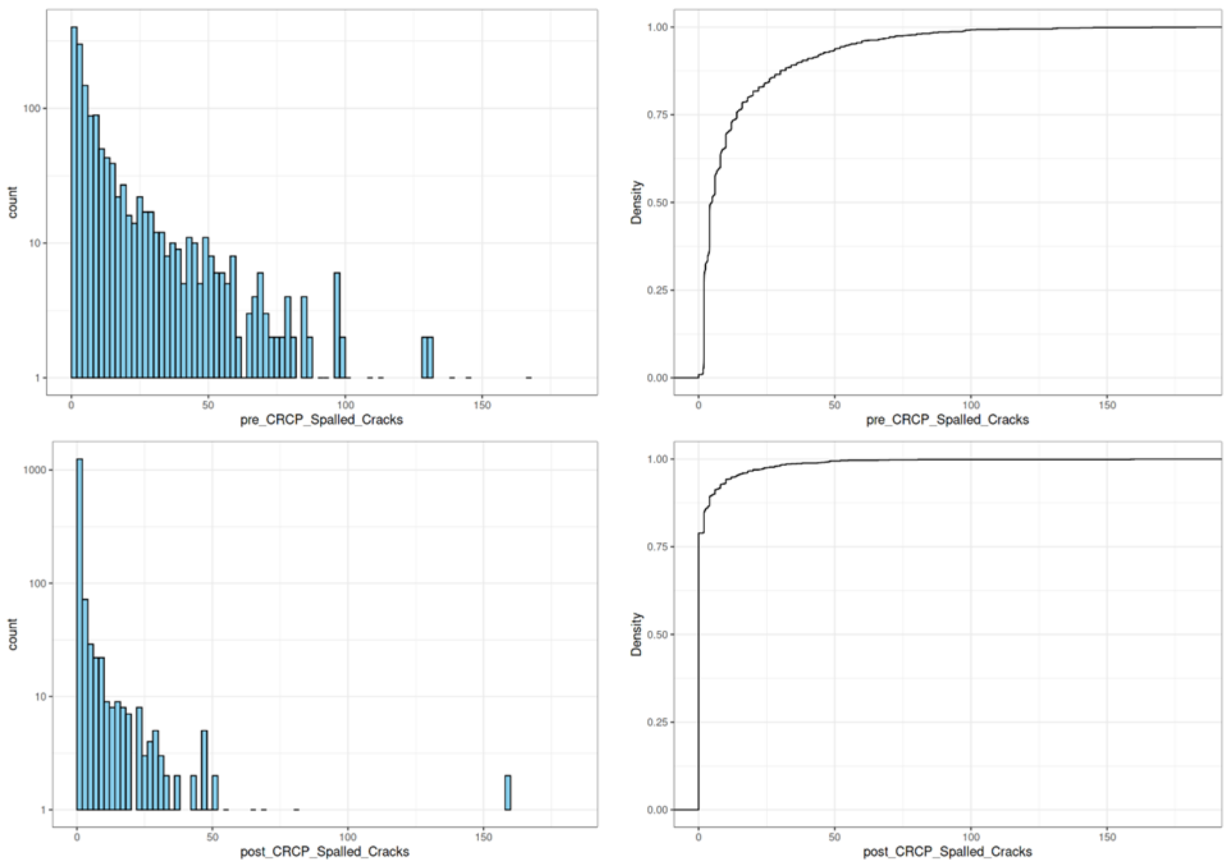

Figure C.9 Pre and Post Treatment Spalled Cracks

The database demonstrated that M&R activities on rigid pavements are carried out in a different manner than on flexible pavements. Some of the distresses are corrected immediately and addressing one type of distress often shows as an increase on the level of another distress. However, when it comes to specific distresses, the reset value is generally zero. In the case of spalled cracks, it is recommended that for all types of treatments, the reset value should be zero.

Punchouts

Table C.10 Pre and Post Treatment Punchouts

Distress	Percent of Zeros	min	max	Percentiles		
				25%	50%	75%
pre_Punchouts	1.94%	0	37	2	3	6
post_Punchouts	92.85%	0	18	0	0	0

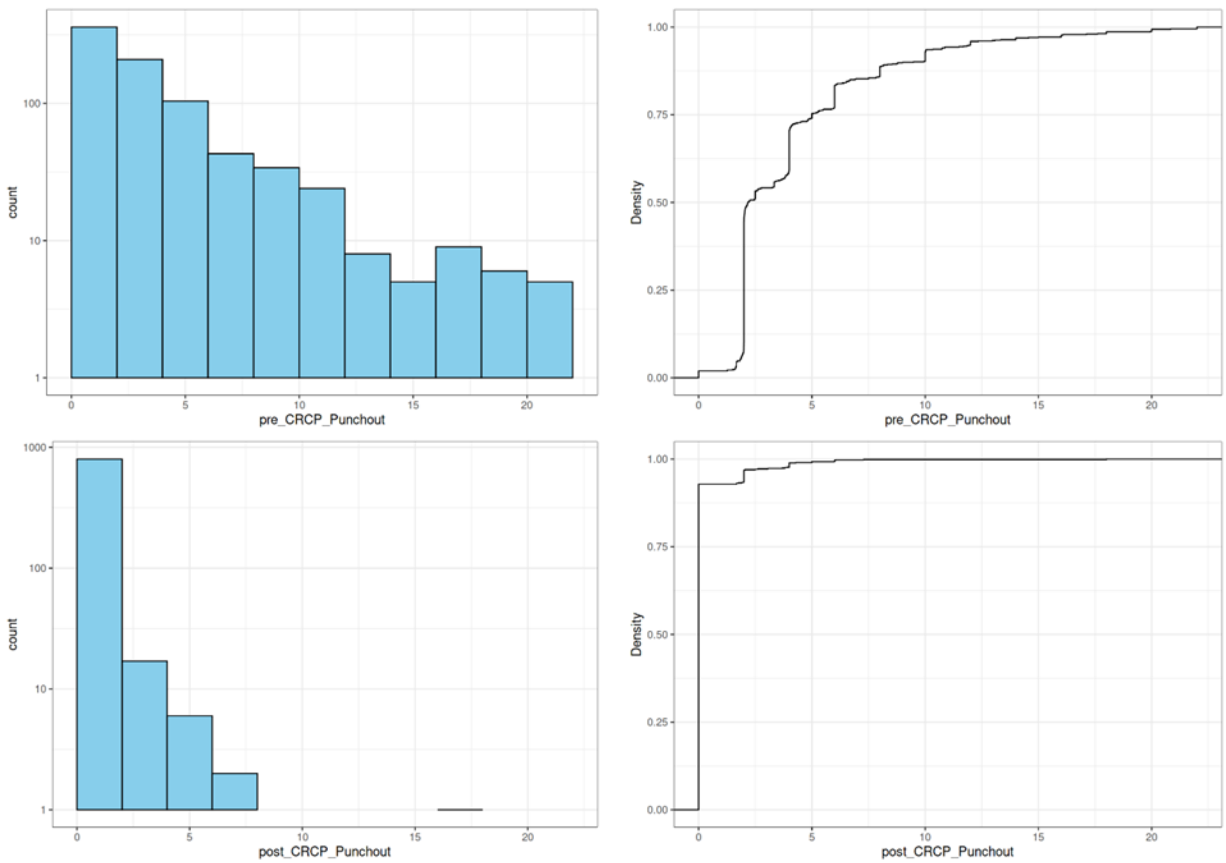

Figure C.10 Pre and Post Treatment Punchouts

As the data shows, punchouts should be always reset to zero. TxDOT is very efficient in fixing punchouts; however, many instances of this work could not be found in the work history database.

Asphalt Patches

Table C.11 Pre and Post Treatment Asphalt Patches

Distress	Percent of Zeros	min	max	Percentiles		
				25%	50%	75%
pre_ACP_Patches	3.52%	0	98	2	4	9
post_ACP_Patches	91.55%	0	27	0	0	0

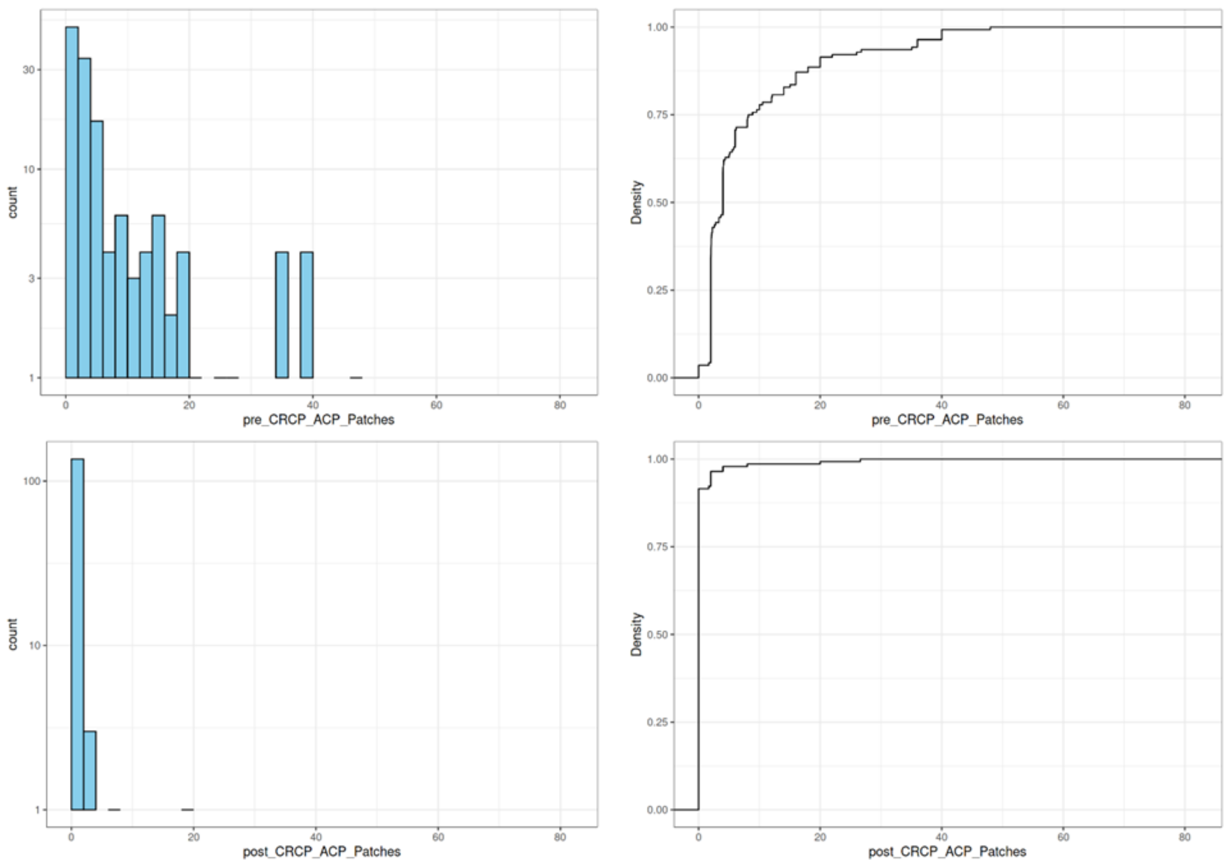

Figure C.11 Pre and Post Treatment Asphalt Patches

As with punchouts, ACP patches should be always reset to zero. Also, as in the previous distress, TxDOT is very efficient in fixing ACP patches but much of this information was not available in the work history database.

Concrete Patches

Table C.12 Pre and Post Treatment Concrete Patches

Distress	Percent of Zeros	min	max	Percentiles		
				25%	50%	75%
pre_PCC_Patches	2.22%	0	102	4	7	18
post_PCC_Patches	66.10%	0	72	0	0	2

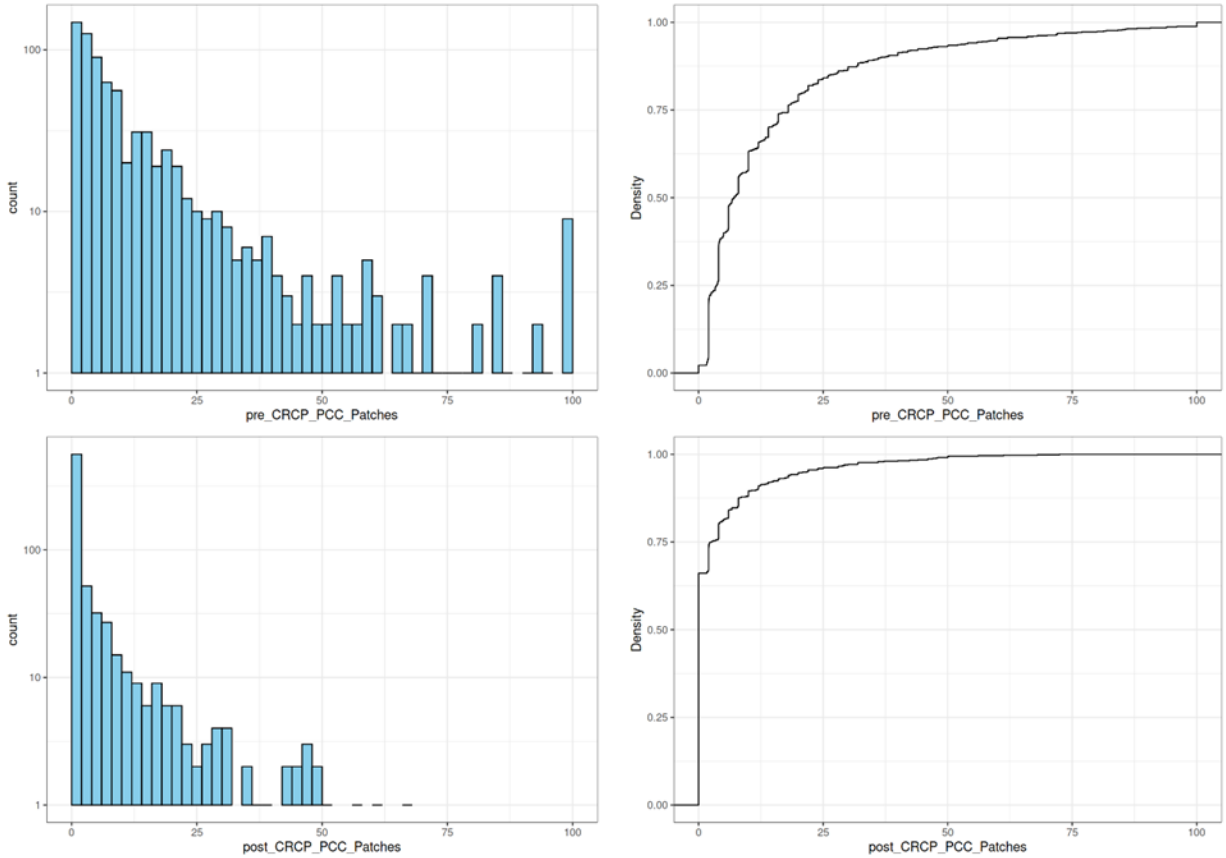

Figure C.12 Pre and Post Treatment Concrete Patches

In the case of concrete patches, it is recommended that for PM and LRhb the reset value should be 2, while for more intensive rehabilitation work, such as MRhb and HRhb, the reset value should be zero.

Reset Values for Jointed Concrete Pavement

Failures

Table C.13 Pre and Post Treatment Failures

Distress	Percent of Zeros	min	max	Percentiles		
				25%	50%	75%
pre_JCP_FAILURES	34.33%	0	100	0	4	14
post_JCP_FAILURES	69.09%	0	36	0	0	2

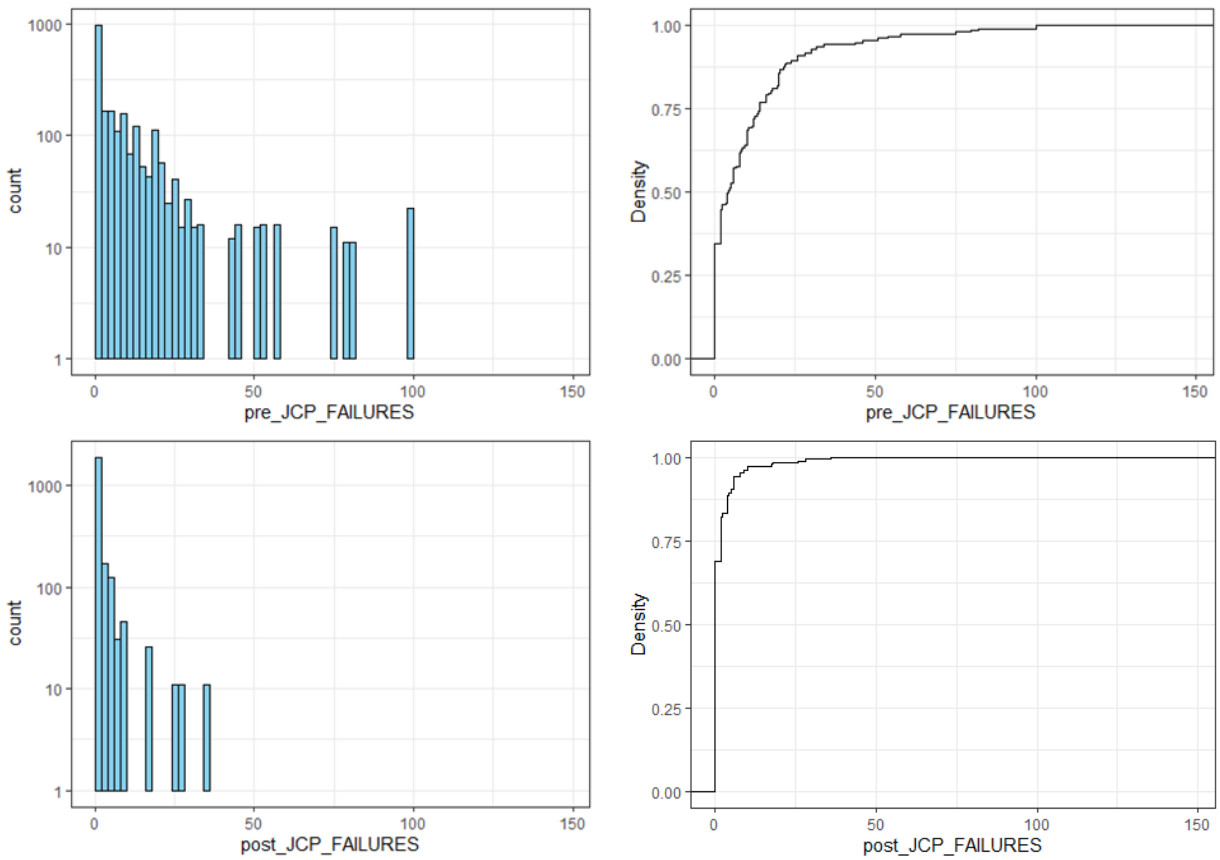

Figure C.13 Pre and Post Treatment Failures

The data for failures for JCP is similar to that of concrete patches for CRCP. Therefore, it is recommended that for PM and LRhb the reset value should be 2, while for MRhb and HRhb, the reset value should be zero.

Failed Joints and Cracks

Table C.14 Pre and Post Treatment Failed Joints and Cracks

Distress	Percent of Zeros	min	max	Percentiles		
				25%	50%	75%
pre_JCP_FAILED_JNTS_CRACKS	41.79%	0	200	0	2	8
post_JCP_FAILED_JNTS_CRACKS	70.00%	0	98	0	0	2

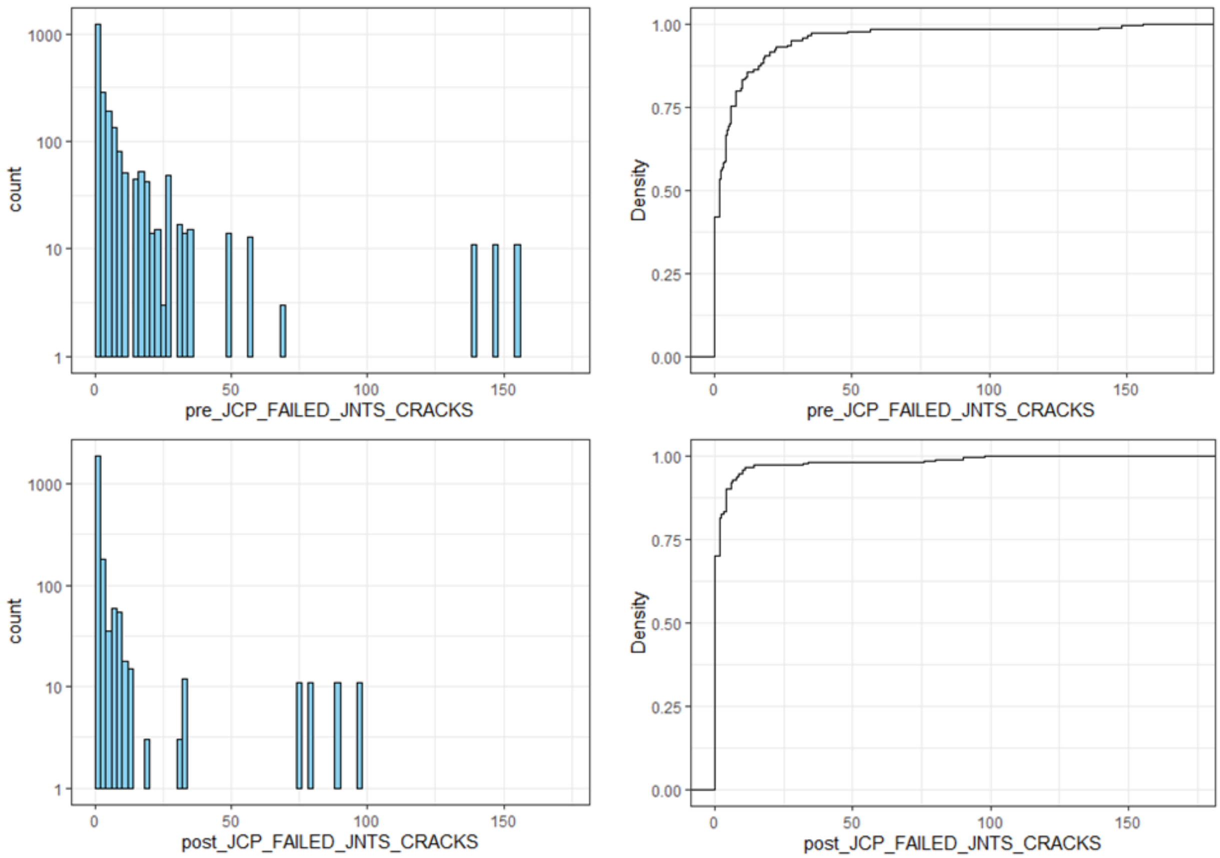

Figure C.14 Pre and Post Treatment Failed Joints and Cracks

For failed joints and cracks on JCP, it is recommended that for PM and LRhb work, the reset value should be 2, while for more intensive rehabilitation work (MRhb and HRhb) the reset value should be zero.

Concrete Patches

Table C.15 Pre and Post Treatment Concrete Patches

Distress	Percent of Zeros	min	max	Percentiles		
				25%	50%	75%
pre_JCP_PCC_PATCHES	35.11%	0	200	0	10	24
post_JCP_PCC_PATCHES	64.54%	0	96	0	0	4

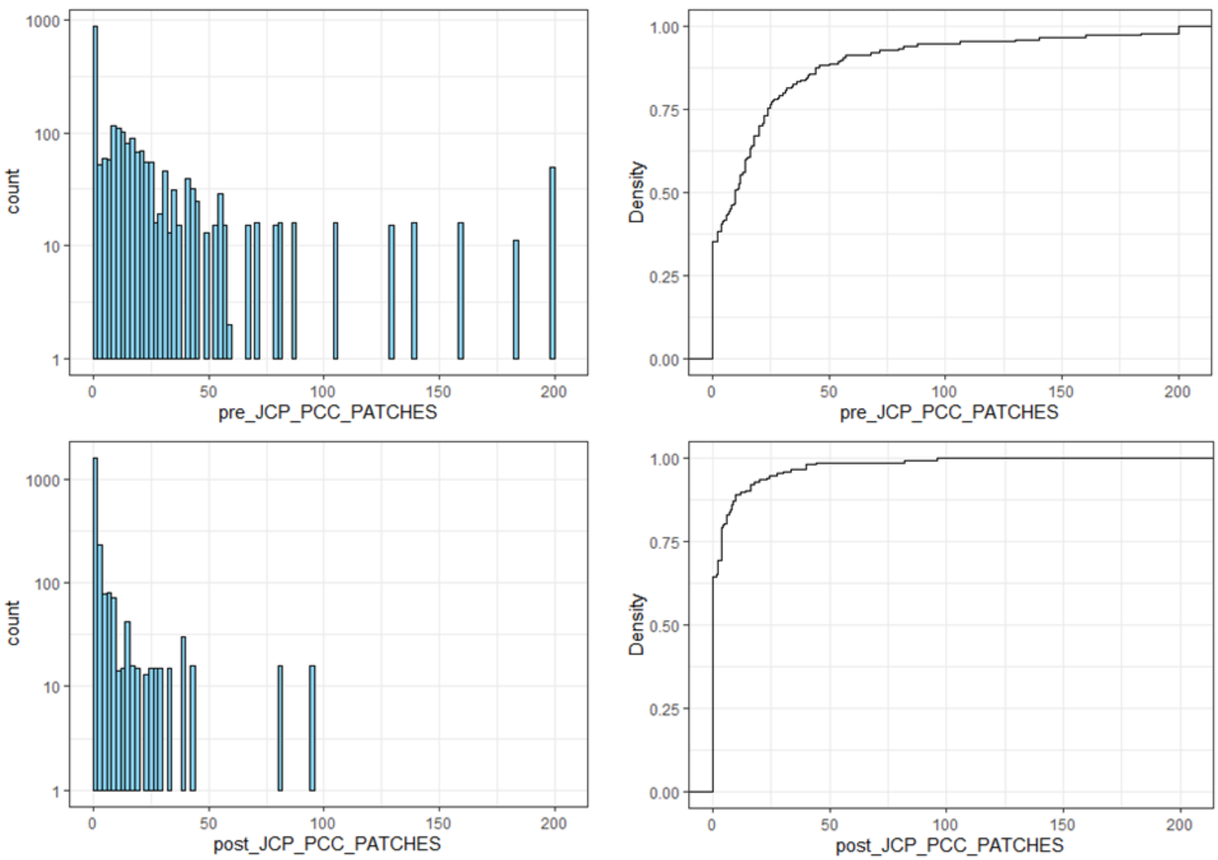

Figure C.15 Pre and Post Treatment Concrete Patches

The data shows that concrete patches in JCP follow a similar pattern than concrete patches in CRCP. Therefore, it is recommended the reset value should be zero for HRhb and MRhb but a value of 2 should be used for LRhb and PM work.

Slabs with Longitudinal Cracks

Table C.16 Pre and Post Treatment Slabs with Longitudinal Cracks

Distress	Percent of Zeros	min	max	Percentiles		
				25%	50%	75%
pre_JCP_LONGITUDE_CRACKS	60.64%	0	100	0	0	10
post_JCP_LONGITUDE_CRACKS	80.88%	0	37	0	0	0

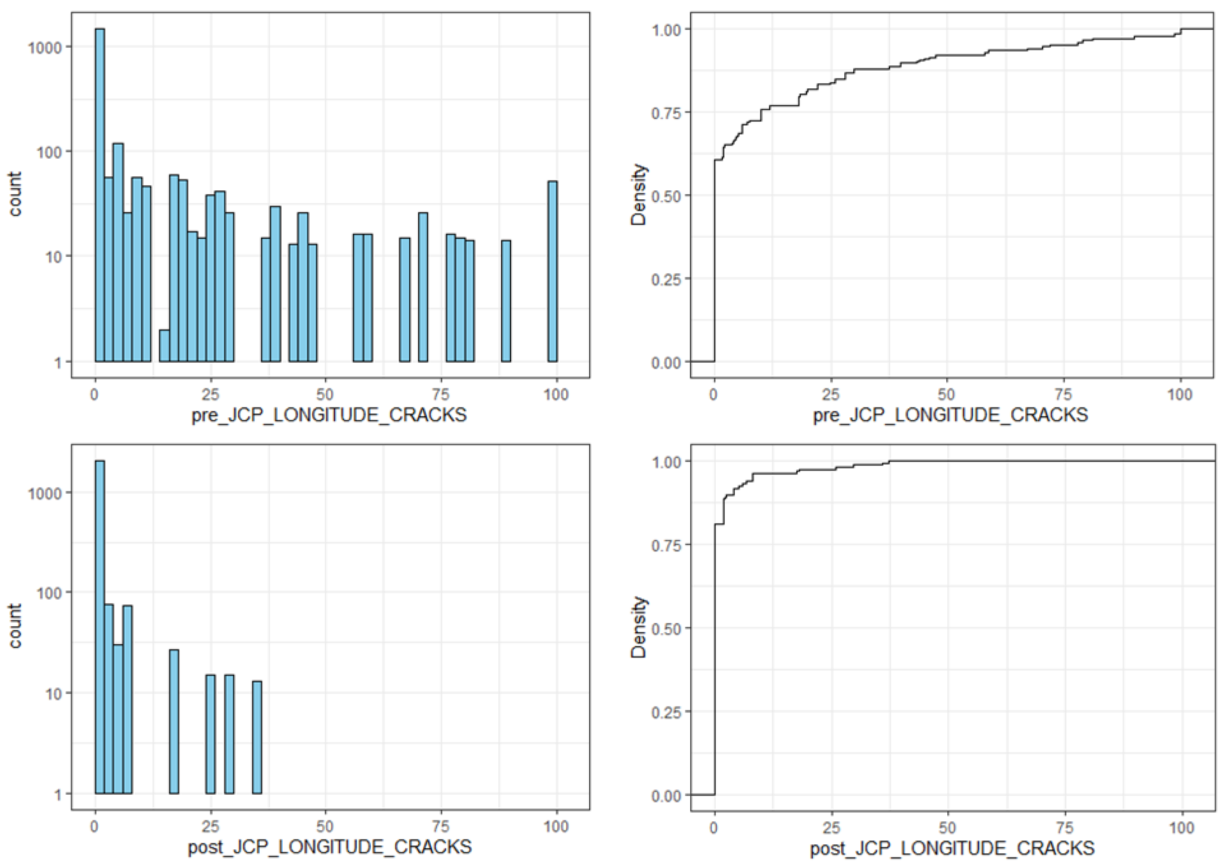

Figure C.16 Pre and Post Treatment Slabs with Longitudinal Cracks

When the longitudinal cracks on JCP are repaired, the reset value should be set to zero as the data shows.

Shattered Slabs

Table C.17 Pre and Post Treatment Shattered Slabs

Distress	Percent of Zeros	min	max	Percentiles		
				25%	50%	75%
pre_JCP_SHATTERED_SLABS	98.05%	0	14	0	0	0
post_JCP_SHATTERED_SLABS	99.35%	0	4	0	0	0

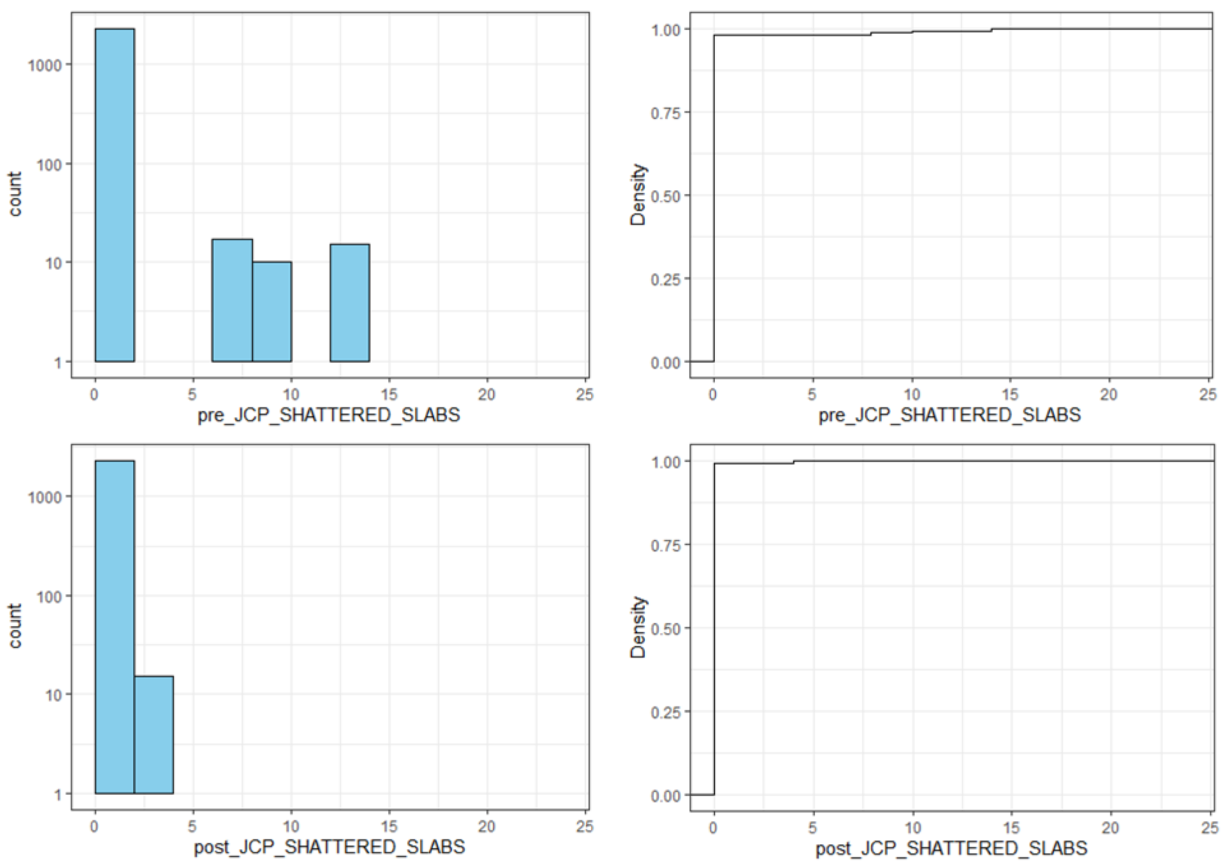

Figure C.17 Pre and Post Treatment Shattered Slabs

Very few and localized shattered slabs were found in the database. When the shattered slabs of JCP are repaired, the reset value should be set to zero as the data shows.

Appendix D. Project 0-6988: Value of Research

Introduction

TxDOT Research Project 0-6988, *Quantification of the Performance of Preventive Maintenance and Rehabilitation Strategies*, was performed to address two main technical objectives. The first objective was to calibrate the current performance models that were incorporated into Pavement Analyst (PA) from the TxDOT's Pavement Management Information System (PMIS), while, at the same time, incorporating the effect of maintenance and rehabilitation activities. The calibrated models were to incorporate the effect of expected performance of preventive maintenance (PM) and light (LRhb), medium (MRhb), and heavy rehabilitation (HRhb) treatments.

The second objective was to provide an alternative specification form that respected the original s-shape of the performance curve, could also be easily implemented into PA, and addressed some of the shortcomings and limitations of the current specification. Some of the limitations included the fact that the current specification form is not defined at age zero and that performance curves corresponding to different level of treatments cross each other, which is unreasonable.

A non-linear estimation approach using panel data analysis (Greene, 1993) was utilized for the development of performance models for flexible asphalt concrete pavement, jointed concrete pavement, and continuously reinforced concrete pavement (CRCP). This approach is consistent with previous work conducted by Madanat and Mishalani (1998) and Prozzi and Madanat (2000) that revealed the importance of the panel data approach as it allows the modelers to account for issues such as correlation between variables, censored data, endogeneity, and unobserved heterogeneity.

Another significant improvement over the previous performance models is that the current models were updated and calibrated with actual performance data from PA; therefore, the models fit the data very well and have significant smaller prediction errors than do the existing models. For example, the normalized errors for CRCP distresses range from 2.8 to 5.6%. As highlighted by Madanat et al. (2002), a reduction in the prediction error is not only a statistical improvement but also translates into significant agency savings when incorporated into a pavement management system. In practical terms, this implies that the newly calibrated models will be more accurate in predicting distress levels and, therefore, the estimation for the time of maintenance and rehabilitation can be estimated more accurately (Prozzi and Madanat, 2000). In the next sections, we estimate the overall benefit of better estimating the time of rehabilitation by just one year using well-established economic literature.

Economic Models

To quantify the value of research (VoR) of the current project, a simplified economic model was used. This model was originally proposed by Small and Winston (1988). The model considers a section of highway of width L (where L is the number of lanes) that is subjected to an annual traffic load T (where T is given by the 20-year design number of ESALs). The pavement strength, S, is a simplified measure of the total pavement structural capacity. Such a measure could be interpreted as the structural number for a flexible pavement, or the slab thickness (D) for a rigid pavement. Everything else equal, we are assuming that traffic loading is the dominant cause of pavement deterioration. The effects of aging, weathering, extreme events, and environmental factors are not considered in the model as their effect will only increase the cost. Therefore, we are following a very conservative approach when estimating the savings.

We use ρ(*S*) to denote the number of ESALs that causes the pavement to deteriorate from an initial condition after new construction or rehabilitation to a terminal condition, which depends on the distress being considered. At that point, LRhb, MRhb, or HRhb is required. We labeled this component ρ(*S*) because it is assumed that the pavement performance is a function of the pavement strength. Following this reasoning, the time between rehabilitation events, *R*(ρ), is then given by:

$$R(\rho) = \frac{\rho(S)}{\gamma T} \quad \text{(D.1)}$$

Where γ is the lane distribution factor, which represents the percentage of annual loading *T* that occurs in the outer lane. The time between rehabilitation events (also referred to as performance period), *R*(ρ), is assumed to be constant for a given pavement strength, which is a reasonable assumption under steady-state conditions.

To account for costs, a simple cost model proposed by Madanat et al. (2002) was adopted. Through this model, which consists of initial capital costs and maintenance costs (including preventive and routine maintenance) for an infinite horizon, the optimal pavement strengths that yield the minimum discounted total pavement costs were determined. As expected, both initial capital and maintenance costs are functions of design pavement strength. It should be noted that there is a tradeoff between initial capital and future maintenance; everything else being equal, as pavement strength increases so does the initial capital cost—but expected maintenance costs decrease.

The capital cost per mile of constructing a new highway, *K* (*L*, *S*), increases approximately linearly with both highway width, *L*, and structural strength, *S*. It can be represented by fixed cost k_0 (which includes mobilization and preparation cost), a cost component proportional to the highway width (*L*), and a term for the cost of construction and materials, which is proportional to the highway width (*L*) and the structural strength (*S*). Therefore, the capital cost per mile can be expressed as:

$$K(L, S) = k_0 + k_1.L + k_2.L.S \quad \text{(D.2)}$$

The cost of rehabilitation per mile of pavement is denoted as *M* (*T*, *L*, *S*) and it is a function of the design traffic (*T*), the width (*L*), and the strength (*S*). The rehabilitation cost is accrued every *R*(ρ) years and it is the dominant component. For this analysis, we are not accounting for the PM costs and we consider only one type of rehabilitation cost, which is an average of the LRhb, MRhb, and HRhb costs. Therefore, the net present value (NPV) of all future rehabilitation costs is given by:

$$M(T, L, S) = \frac{C(L)}{e^{r.R(\rho)} - 1} \quad \text{(D.3)}$$

Which is the NPV of an infinite sequence of payments, *C*(*L*), made every *R*(ρ) years. Recall that *R*(ρ) is proportional to the pavement strength. Finally, the total pavement cost is the sum of *K* (*L*, *S*) and *M* (*T*, *L*, *S*):

$$TPC = k_0 + k_1.L + k_2.L.S + \frac{C(L)}{e^{r.R(\rho)} - 1} \tag{D.4}$$

Dropping those terms that do not include pavement strength and dividing by the number of lanes yields the objective function we wish to minimize. Then the discounted lifecycle cost per lane-mile becomes:

$$TPC_0 = k_2.S + \frac{C(L)/L}{e^{r.R(\rho)} - 1} \tag{D.5}$$

Where $C(L)/L$ is the average cost of rehabilitation of one lane-mile of pavement. Though the cost model is fully defined at this point, the relationship between pavement life and structural capacity, $\rho(S)$, must be determined through a deterioration models before the objective function can be optimized. Therefore, for each distress under consideration, $\rho(S)$ is represented by the deterioration model developed as part of this project.

Data and Analysis

TxDOT maintains a network of approximately 72,985 center-lane miles, which translates into approximately 197,438 lane-miles. On average, about 12% of the highway network receives some type of maintenance or rehabilitation work done on any given year. Of this work, about 80% is PM and the remaining 20% is classified as LRhb, MRhb, or HRhb work (TxDOT, 2018a). Therefore, it could be established that approximately 4,740 lane-miles receive some type of rehabilitation (not including PM work).

For the calculation of the total annual discounted lifecycle cost, an average pavement designed for 2,000,000 ESALs was used. The average initial construction cost per unit of strength was $35,707, which was adopted from Madanat et al. (2002) and adjusted to 2020 dollars. The average unitary rehabilitation cost, $C(L)/L$, was also adopted and updated from the same reference as $163,142. Based on these assumptions, the discounted lifecycle cost for an average pavement was calculated for performance periods of 7, 9, 10 and 15 years. The results of these analyses are presented in Figure 1.

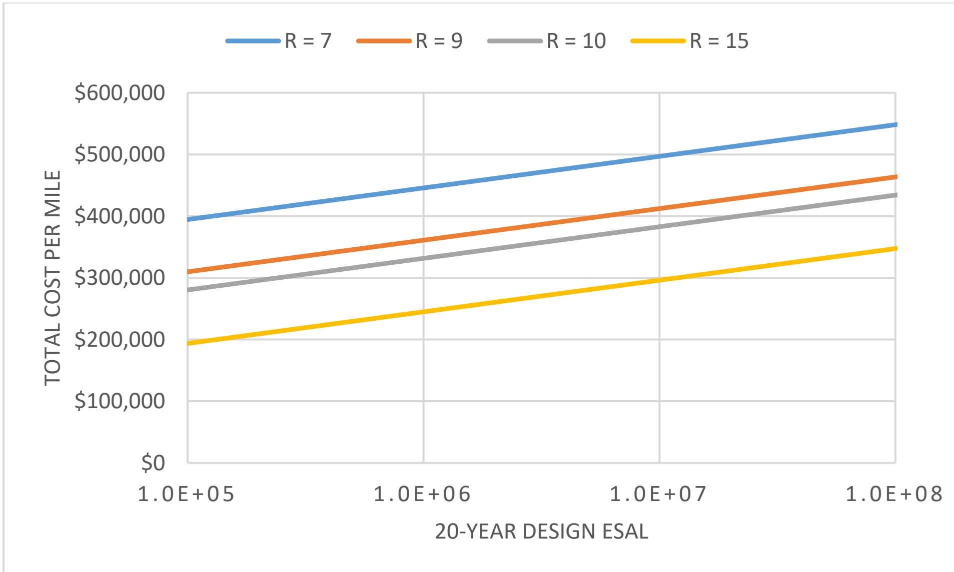

Figure D.1 Discounted Total Lifecycle Pavement Costs

As expected, the total cost per mile increases as the pavement strength increases and decreases significantly as the time between rehabilitation increases. The distance between the lines in Figure 1 could be interpreted as the additional cost incurred by not rehabilitating a given pavement at the optimal time.

Calculation of Benefit/Cost Ratio

To properly account for the discounted cost of construction and maintenance of all pavements in Texas, one would have to conduct a design-by-design evaluation and integrate all costs. In this project, we selected an average representative pavement and extrapolated the results to the entire TxDOT-maintained network. It should be noted that the effects of local conditions on pavement performance have been ignored and, therefore, the saving calculation are somewhat conservative.

To represent the construction and maintenance activities in the state for the economic calculations, a pavement designed for Central Texas for 2,000,000 ESALs was selected. Furthermore, we are assuming that an average LRhb treatment lasts about 9.5 years (TxDOT, 2018b).

To arrive at the benefit/cost calculation, we incorporate the effect of the improved accuracy of the newly calibrated models. The increased accuracy translates into a better estimate of the time required between rehabilitation events. For example, for a given reliability level, the original performance model predicts that a given section is in need of rehabilitation by year 9, while the most accurate model developed as part of this research project indicates that the rehabilitation work will not be necessary until year 10. Under the assumption described in this document (refer to Figure 1), this updated estimate will translate into a savings of $29,409 per mile for the life of the pavement. On average, TxDOT performs rehabilitation work on approximately 4,740 miles. Thus, the potential savings at a state level is approximately $139,403,400. The total budget for performing TxDOT Research Project 0-6988 was $448,370, which yields a conservative estimate of the benefit/cost ratio of 311.

References for VOR

Greene, W. (1993), Econometric Analysis, MacMillan, New York, NY.

Madanat, S. and R. Mishalani (1998), Selectivity bias in modeling highway pavement maintenance activity effectiveness, ASCE Journal of Infrastructure Systems, 4(3), 134–137.

Madanat, S., J.A. Prozzi, and M. Han (2002), Effect of performance model accuracy on optimal pavement design, Computer-Aided Civil and Infrastructure Engineering, Vol. 17, Issue 1, pp. 22-30.

Prozzi, J. A. and S. Madanat (2000), Analysis of experimental pavement failure data using probabilistic duration models, Transportation Research Record 1699, TRB, National Research Council, Washington, D.C.

Small, K. and C. Winston (1988), Optimal highway durability, Academic Economic Review, 78(3), 560–9.

TxDOT (2018a), 4-Year Pavement Management Plan (FY2019-FY2022), Maintenance Division, Texas Department of Transportation, Austin, TX,

TxDOT (2018b), FY 2018 Lifetime Cost Analysis for TACP, Maintenance Division, Texas Department of Transportation, Austin, TX,